

Silvia Nair Goyanes
Norma Beatriz D'Accorso *Editors*

Industrial Applications of Renewable Biomass Products

Past, Present and Future

 Springer

Industrial Applications of Renewable Biomass Products

Silvia Nair Goyanes • Norma Beatriz D'Accorso
Editors

Industrial Applications of Renewable Biomass Products

Past, Present and Future

 Springer

Editors

Silvia Nair Goyanes
Facultad de Ciencias Exactas y Naturales
Departamento de Física
Laboratorio de Polímeros y Materiales
Compuestos (LPM&C)
Universidad de Buenos Aires
Buenos Aires, Argentina
Consejo Nacional de Investigaciones
Científicas y Técnicas (CONICET)-UBA
Instituto de Física de Buenos Aires (IFIBA)
Buenos Aires, Argentina

Norma Beatriz D'Accorso
Facultad de Ciencias Exactas y Naturales
Departamento de Química Orgánica
Universidad de Buenos Aires
Buenos Aires, Argentina
Consejo Nacional de Investigaciones
científicas y Técnicas (CONICET)
Centro de Investigaciones en Hidratos
de Carbono (CIHIDECAR)
Buenos Aires, Argentina

ISBN 978-3-319-61287-4

ISBN 978-3-319-61288-1 (eBook)

DOI 10.1007/978-3-319-61288-1

Library of Congress Control Number: 2017948732

© Springer International Publishing AG 2017

This work is subject to copyright. All rights are reserved by the Publisher, whether the whole or part of the material is concerned, specifically the rights of translation, reprinting, reuse of illustrations, recitation, broadcasting, reproduction on microfilms or in any other physical way, and transmission or information storage and retrieval, electronic adaptation, computer software, or by similar or dissimilar methodology now known or hereafter developed.

The use of general descriptive names, registered names, trademarks, service marks, etc. in this publication does not imply, even in the absence of a specific statement, that such names are exempt from the relevant protective laws and regulations and therefore free for general use.

The publisher, the authors and the editors are safe to assume that the advice and information in this book are believed to be true and accurate at the date of publication. Neither the publisher nor the authors or the editors give a warranty, express or implied, with respect to the material contained herein or for any errors or omissions that may have been made. The publisher remains neutral with regard to jurisdictional claims in published maps and institutional affiliations.

Printed on acid-free paper

This Springer imprint is published by Springer Nature

The registered company is Springer International Publishing AG

The registered company address is: Gewerbestrasse 11, 6330 Cham, Switzerland

Preface

For decades, chemical industry has relied heavily on the fossil oil sector. In recent years, rapidly increasing oil prices, unstable supply, and potential fuel shortages have significantly increased interest in alternative resources. On the other hand, the environmental impact produced by chemical manufacturers led to a critical rethinking of chemical and energy technologies. Replacing fossil fuels, a primary source of synthetic chemicals, with renewable sources to produce polymeric materials is a big challenge.

Worldwide sustainable technologies are gradually introduced to produce “renewable” energy and to replace petrochemical products by resources provided from the renewable biomass. In this sense, the use of this kind of products is in rapid expansion, as it would allow obtaining cheaper and environmentally friendly methodologies.

In this context, biodegradable polymers have become a top research topic nowadays. These materials can be grouped into two large categories, agro-polymers, such as polysaccharides and proteins, which are directly derived from biomass, and biodegradable polyesters, like polyhydroxyalkanoates, which are those derived from microorganisms or synthetically made from either naturally or synthetic monomers. Biodegradable polymers have been proposed for a wide range of applications, from medicinal chemistry to agricultural industry and packaging. On the other hand, the introduction of synthesis alternatives using raw materials from the renewable biomass results in more sustainable routes for the production of chemicals, materials, energy, as well as products with medicinal applications.

Among biomolecules, polysaccharides are the most abundant in nature and are essential elements in a wide range of processes of living systems. These molecules produced by plants are a basic component of human and animal diets and serve as essential ingredients in many manufacturing processes. They are used to recognize proteins and other biological entities, tumor genesis and progression, immune responses, fertilization, apoptosis, and infection. Increasing the total carbohydrate yield is a major goal in biotechnology agriculture.

Starch and cellulose are the most commercially important carbohydrates. They are composed of glucose units with different chemical structures that grant them particular characteristic. Among a large number of applications, we can find the synthesis of polyurethanes with biomedical use, the development of additives to improve polymeric and cement matrix properties, and the fabrication of systems for oil recovery and pollutant removal.

Other polysaccharides include glycosaminoglycans, which are complex molecules ubiquitously present in the extracellular matrix of mammalian tissues and have very important medicinal applications; chitosan, which is made by treating the chitin shells of shrimp and other crustaceans and has a wide range of applications, from tissue engineering to environmental remediation; seaweed polymers, which have been investigated for their strong biological activities (antiviral, antitumor, anticoagulant, etc.); and guar gums, which are obtained from beans and are used in different fields such as oil industry.

On the other hand, proteins such as collagen and silk have been applied in different biomedical applications, from tissue engineering to drug delivery. In particular hydrogels based in proteins have been developed as suitable systems for sustained and targeted drug delivery.

In the field of biodegradable polyesters, the poly(lactic acid) is the one most currently applied in the market. It can be synthesized from fossil resources, but main productions are obtained from renewable resources. Thanks to the ability to process it through a variety of technologies and its excellent compostability, it has been applied to different fields, like sustainable food packaging material or nanofibrous membranes for pollutant removal.

Other important biodegradable polyesters are polyhydroxyalkanoates. These are produced in nature by bacterial fermentation of sugar or lipids and have shown excellent biocompatibility, which makes them perfect candidates for biomedical applications, such as bone tissue engineering.

This book aims to associate the latest scientific advances with current technological applications of polymers from renewable biomass. It features authors' contributions from academic ambit as well as private industry, allowing the reader to find topics that are not developed in related bibliographies and addressed in such diverse areas as, for example, the use in food packaging, medicinal products, energy production, and cosmetics industry as well as in environmental remediation.

Contents

Synthesis and Applications of Carbohydrate-Based Polyurethanes	1
Verónica E. Manzano, Adriana A. Kolender, and Oscar Varela	
Part I Medical Applications	
Biodegradable Polymers for Bone Tissue Engineering	47
M. Susana Cortizo and M. Soledad Belluzo	
Seaweed Polysaccharides: Structure and Applications	75
Vanina A. Cosenza, Diego A. Navarro, Nora M.A. Ponce, and Carlos A. Stortz	
Innovative Systems from Clickable Biopolymer-Based Hydrogels for Drug Delivery	117
C. García-Astrain, L. Martín, M.A. Corcuera, A. Eceiza, and N. Gabilondo	
Applications of Glycosaminoglycans in the Medical, Veterinary, Pharmaceutical, and Cosmetic Fields	135
José Kovensky, Eric Grand, and María Laura Uhrig	
Bacterial Cellulose Nanoribbons: A New Bioengineering Additive for Biomedical and Food Applications.....	165
M. Osorio, C. Castro, J. Velásquez-Cock, L. Vélez-Acosta, L. Cáracamo, S. Sierra, R. Klaiss, D. Avendaño, C. Correa, C. Gómez, R. Zuluaga, D. Builes, and P. Gañán	
Part II Oil Industry	
Biobased Additives in Oilwell Cement	179
A. Vázquez and T.M. Pique	
Polymers from Biomass Widely Spread in the Oil Industry	199
Isabel Natalia Vega and María Isabel Hernández	

Modified Starches Used as Additives in Enhanced Oil Recovery (EOR)	227
Olivia V. López, Luciana A. Castillo, Mario D. Ninago, Andrés E. Ciolino, and Marcelo A. Villar	
Part III Other Applications Related to Environmental Care	
Chitosan: From Organic Pollutants to High-Value Polymeric Materials	251
María I. Errea, Ezequiel Rossi, Silvia Nair Goyanes, and Norma Beatriz D'Accorso	
PLA-Based Nanocomposites Reinforced with CNC for Food Packaging Applications: From Synthesis to Biodegradation	265
M.P. Arrieta, M.A. Peltzer, J. López, and L. Peponi	
Removal of Pollutants Using Electrospun Nanofiber Membranes	301
Laura G. Ribba, Jonathan D. Cimadoro, Norma Beatriz D'Accorso, and Silvia Nair Goyanes	
Index	325

Synthesis and Applications of Carbohydrate-Based Polyurethanes

Verónica E. Manzano, Adriana A. Kolender, and Oscar Varela

1 Introduction

The most recent advances in polymer research have been focused on the replacement of petro-based monomers with analogs derived from renewable sources, because of the increased demand and limited supply of petroleum feedstocks. Furthermore, the petroleum-derived polymers are resistant to microbial degradation; therefore, these materials tend to accumulate in the environment leading to pollution. Modern medicine and chemistry are also paying special attention to the use of renewable resources for the design and production of new polymers, since those derived from natural products are expected to be biodegradable, biocompatible, and nontoxic. The biodegradation of polymers involves the hydrolytic or enzymatic cleavage of sensitive bonds in the chain that leads to polymer erosion. It is believed that the introduction of hydrophilic units into the polymer chain facilitates water attack, increasing the hydrolytic degradation. Materials which are able to replace or restore biological functions and exhibit a pronounced compatibility with the biological environment are known as *biomaterials* (Drotleff et al. 2004). Nowadays, a biomaterial (for medical devices, prosthesis, or implants) should satisfy a number of criteria and requirements (Langer et al. 1990; Drotleff et al. 2004), such as biocompatibility; sterilizability; biostability; biofunctionality during the implantation; mechanical, electrical, and physical compatibility; morphological or topographical aspects; and adequate manufacturing (Parisi et al. 2015).

V.E. Manzano • A.A. Kolender • O. Varela (✉)

Universidad de Buenos Aires, Facultad de Ciencias Exactas y Naturales, Departamento de Química Orgánica, Pabellón 2, Ciudad Universitaria, C1428EHA Buenos Aires, Argentina

Consejo Nacional de Investigaciones Científicas y Técnicas (CONICET)-UBA, Centro de Investigación en Hidratos de Carbono (CIHIDECAR), Buenos Aires, Argentina

e-mail: varela@qo.fcen.uba.ar

By biocompatibility it is understood that the substance itself and its degradation products should not induce any deleterious reactions or disturb the biological environment.

One of the most important and widespread types of polymers is the polyurethanes (PUs). Because of their versatile properties, they are widely used in modern life. In addition to their use as thermoplastic elastomers, as flexible or rigid foams, as coating, and as adhesives (paints, varnishes, glue, binders), among other applications (Szycher 2013; Król 2009), PUs are considered one of the most bio- and blood-compatible materials (Fernández et al. 2010). Therefore, they are being widely studied in the field of biomedicine, mainly when contact with biological fluids is required. Nowadays, PUs played a major role in the development of many medical devices, such as blood bags, vascular catheters, stents, blood oxygenators, scaffolds for tissue engineering, cardiac valves, internal lining of artificial hearts, membranes for wound dressings, drug delivery systems, and vascular grafts, among others (Zdrahala and Zdrahala 1999; Alves et al. 2012). Biodegradable PUs are being used as nonpermanent devices because of their excellent biocompatibility and low thrombogenicity. For instance, they are employed in the preparation of biodegradable endoprosthesis (Marín et al. 2009), and biodegradable PUs that contain degradable segments of poly- ϵ -caprolactone are used as implants for tissue repair and as drug delivery systems (Sun et al. 2011).

2 Classification of Polyurethanes: Thermoplastic or Thermosetting

The properties of the PUs can be tailored by selecting the proper building blocks in order to get a material with special physical–mechanical behavior and characteristics such as bio-identity, biocompatibility, and biodegradability (Campiñez et al. 2013; Cherng et al. 2013). All these properties of the PUs are highly dependent on the composition of the polymer. Based on the composition, the PUs are classified into two major groups: *thermoplastic* and *thermosetting* (Fig. 1). The *thermoplastic* PUs are elastomers with linear and flexible chains, composed of a hard segment (HS) and a soft segment (SS). The HS generally combines a diisocyanate and a chain extender (usually a low molecular weight diamine or diol). The most common

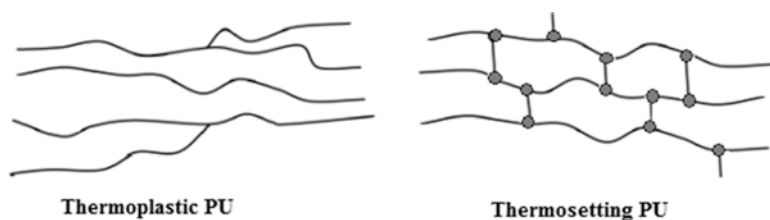


Fig. 1 Thermoplastic and thermosetting polyurethanes

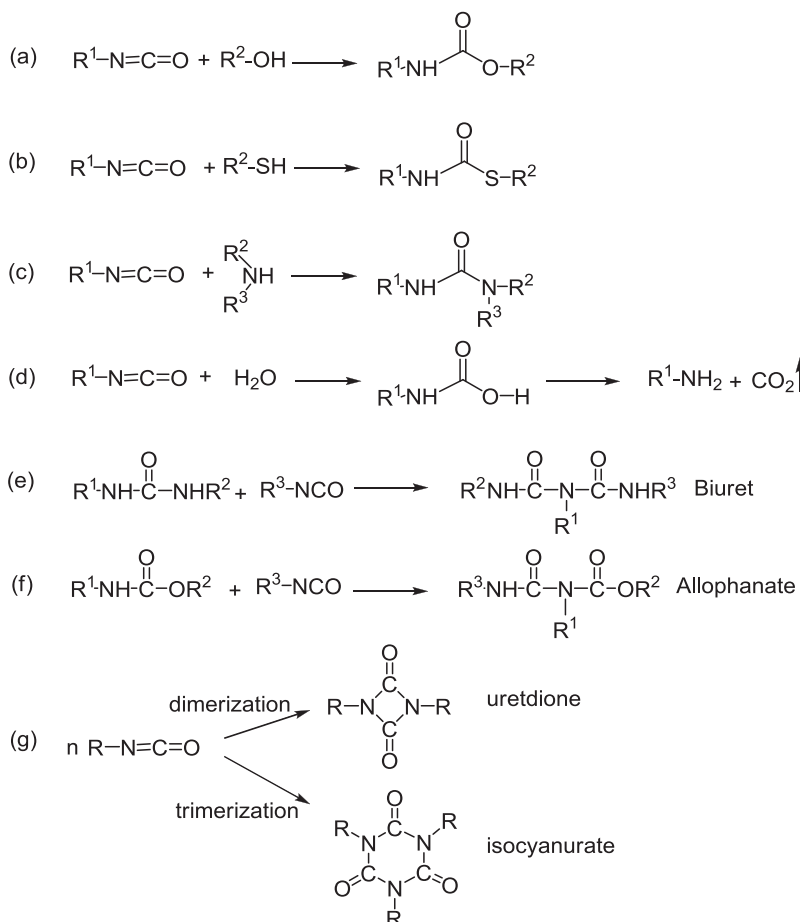
compounds used in the HS are 4,4'-diphenylmethane diisocyanate (MDI) and 1,4-butanediol or 1,2-ethylene diamine (Zdrahala and Zdrahala 1999). The SS is usually a polyol (polyester, polyether, polycarbonate, etc.). The SS has usually a low glass transition temperature (T_g), which provides elastomeric properties, while the HS typically presents a high T_g value, which provides mechanical strength to the material. This difference between the segments is highly relevant to explain the physical properties of a PU and its effect in properties such as biocompatibility (Alves et al. 2012). The HS and SS tend to separate into the respective domains. The extent of separation depends on the composition and the molecular weight of both segments. Thermodynamic immiscibility between hard and soft segments induces phase separation and generates a two-phase morphology in these segmented block copolymers. Phase separation in segmented polyurethanes is an important phenomenon, which affects the properties of the material (Velankar and Cooper 1998, 2000a, b; Furukawa et al. 2005).

The *thermosetting* PUs are chemically cross-linked polymers (networks), either in the hard or soft segments or in both. In this case, a lesser extent of phase separation is expected. As mentioned before, the grade of phase separation (mechanical resistance from the HS and elastomeric behavior from the SS) can be tailored by choosing the proper intermediates in order to get the desired property. The different hardness/softness properties should be taken into account in order to use polyurethanes in medical devices, so as to have the desired response (Zdrahala and Zdrahala 1999).

3 Synthesis of Polyurethanes: Formation of the Urethane Linkage

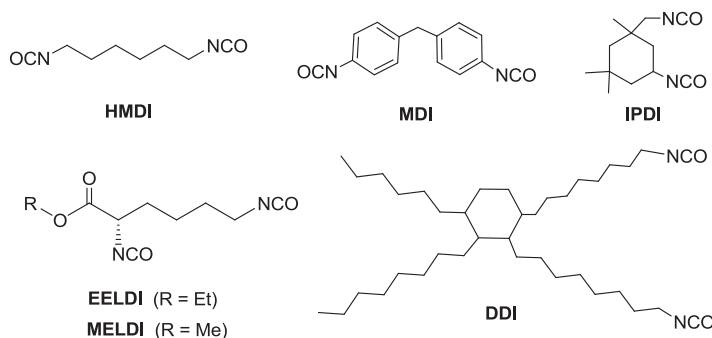
The classical procedure for the synthesis of PUs is the polyaddition reaction between the hydroxyl group of a diol or polyol and a diisocyanate. It should be mentioned that the chemistry of the isocyanate group is rather complex, as it comprises varied reactions with other single functions (alcohol, amines, thiols, etc.) as well as self-additions and trans-condensations (Delebecq et al. 2013). Some common reactions used in polyurethane chemistry are shown in Scheme 1.

The electrophilic carbon of isocyanate undergoes nucleophilic attack by the hydroxyl group of an alcohol to yield a urethane (a), with a thiol to give a thio-urethane (b) or with an amine to produce a urea (c). The reaction with water (d) leads to an unstable carbamic acid, which decomposes into carbon dioxide and a primary amine. This last reaction can lead to the formation of urea bonds when water is present during the synthesis of a PU. Furthermore, the isocyanate can also react with reactive hydrogen-containing compounds, such as urethane or urea functions, to give, respectively, biuret (e) or allophanate (f) by-products. In addition to the previous reactions, isocyanates can also undergo homodimerization or homotrimerization (g), depending on the catalyst employed.



Scheme 1 Some common reactions in polyurethane chemistry

As already mentioned, in recent years, an increased interest is devoted to the use of biomolecules as precursors of polymers. Renewable-based polyurethane building blocks have been developed from sugars, fatty acids, amino acids, etc. as more sustainable alternatives for fossil fuel-based raw materials (Donnelly et al. 1993; Abraham et al. 2006; van Haveren et al. 2008). Among the biomolecules employed as precursors of PUs, the use of carbohydrates has gained attention owing to the rich functionality, varied stereochemistry, and renewable production of carbohydrates on an impressive scale ($\sim 10^{14}$ kg/year). The progress in the development of polymers from natural resources (Hu et al. 2014; Gandini et al. 2016; Noreen et al. 2016), and specifically from carbohydrates (Galbis et al. 2016), has been recently reviewed.



Scheme 2 Common diisocyanates

The synthesis of polyurethanes from sugar-based monomers is a topic of current research because these materials are able to mimic the structure and function of biological polymers. The incorporation of a carbohydrate unit could improve biodegradability and biocompatibility, which may also present enhanced hydrolytic degradability. Particularly, the numerous hydroxyl groups present in natural sugars make these molecules suitable for the synthesis of monomers that are precursors of polyhydroxyurethanes (PHUs), an increasingly important group of polymers.

In the area of carbohydrate-based polyurethanes, some of these types of materials are entirely derived from carbohydrates, while others are prepared by combination of natural biopolymers with synthetic monomers or polymers. Also, the development of PUs with carbohydrates as pendant groups or as constituents of the soft part of the polymer chain has been reported. All these topics, as well as the properties and applications of the resulting PUs, are discussed in this chapter.

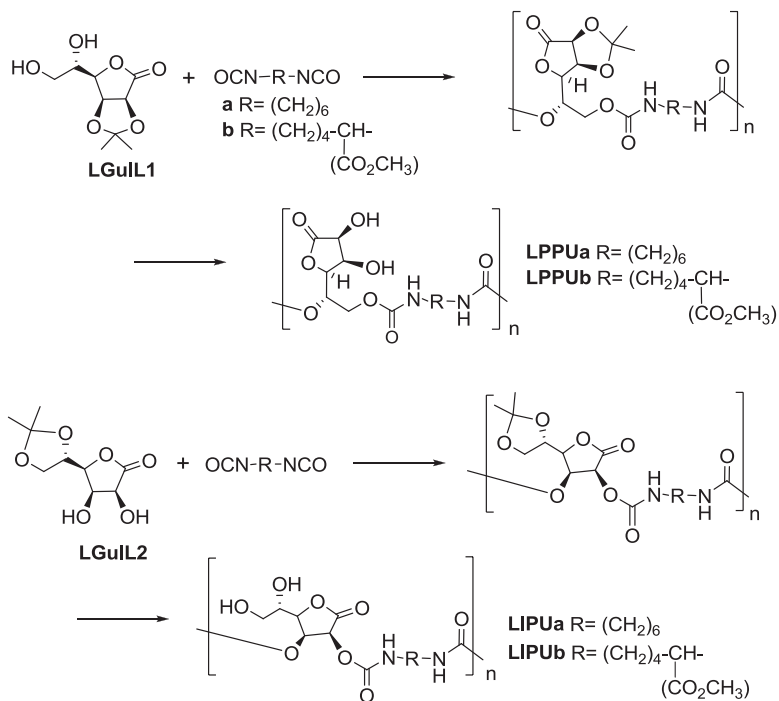
In spite of the limitations of the polycondensation reaction between diols and diisocyanates to afford $[m,n]$ -polyurethanes (also called $[AA, BB]$ -polyurethanes), this type of polymerization has been widely applied to carbohydrate-derived monomers. A variety of selectively protected sugars having two reactive hydroxyl groups have been used as diol monomers, which reacted with diisocyanates. The more commonly used diisocyanates are 1,6-hexamethylene diisocyanate (HMDI) and 4,4'-diphenylmethane diisocyanate (MDI) (Scheme 2). Both isocyanate groups in these bifunctional monomers have the same reactivity. However, some diisocyanates exhibit a different reactivity for each isocyanate group. For example, the methyl or ethyl esters of L-lysine diisocyanate (MELDI or EELDI, respectively) are biomass-based molecules derived from the amino acid L-lysine. The asymmetric aliphatic structure may facilitate the formation of PUs with an amorphous structure. One of the isocyanate groups of MELDI or EELDI, the α -NCO, is attached to a secondary carbon atom, while the ϵ -NCO is attached to a primary carbon atom. The α -isocyanate group may experience steric hindrance from the ester group attached to the secondary carbon (Sanda et al. 1995). On the other hand, this adjacent carboxyl group has an electron-withdrawing character that induces an enhanced

positive charge on the isocyanate carbon atom, increasing its reactivity. The combined effect of these two factors determines the overall reactivity.

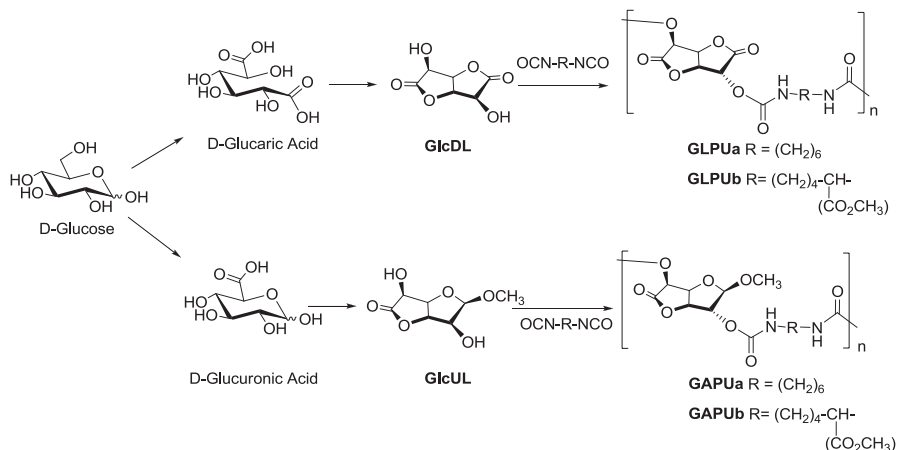
Other commonly used biomass-based diisocyanates are the symmetric dimer fatty acid-based diisocyanate (DDI) and the alicyclic isophorone diisocyanate (IPDI). DDI is obtained from C36 dimer fatty acids (the dimerization products of C18 unsaturated fatty acids). Its approximate molecular structure is shown in Scheme 2. This diisocyanate has the advantage of its high UV stability, as well as its highly nonpolar character and flexibility. On the other hand, IPDI exists as two stereoisomers, *cis* and *trans*, which have similar reactivity. Due to the absence of insaturations in its structure, IPDI is resistant to abrasion and degradation by UV light and is commonly used in coating formulations based on PU, such as paints or varnishes.

The aliphatic diisocyanate HMDI (**a**) and the lysine-derived diisocyanate MELDI (**b**) have been employed as precursors of carbohydrate-derived PUs. Thus, Yamanaka and Hashimoto (2002) prepared PUs with pendant lactone groups (LPPU) or with such groups incorporated into the polymer chain (LIPU), using partially protected L-gulonolactone derivatives **LGulL1** and **LGulL2** as the diol monomer (Scheme 3).

The hydrolytic stability of **LPPUa,b** and **LIPUa,b** was studied and compared with that of the analog PUs **GLPUa** and **GAPUa,b** (Scheme 4). These PUs had



Scheme 3 Polyurethanes derived from L-gulonolactone derivatives

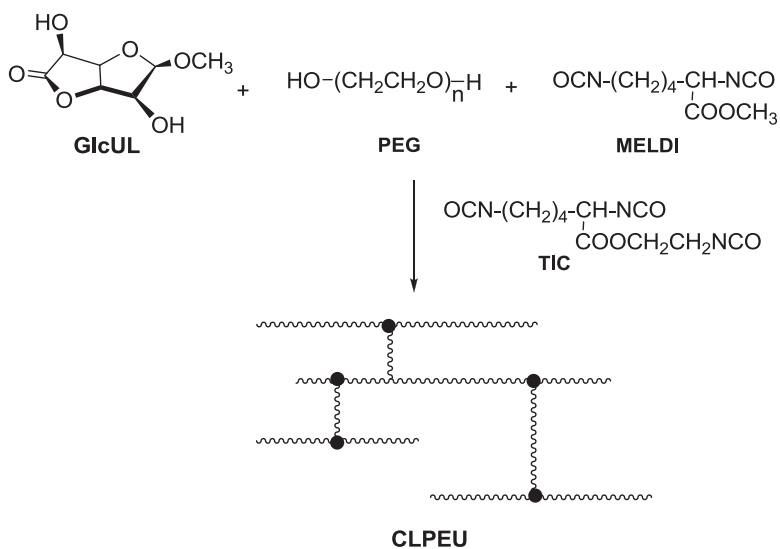


Scheme 4 Polyurethanes derived from glucaric or glucuronic acids

been previously synthesized, respectively, from glucaric or glucuronic acids, via the corresponding lactones **GlcDL** or **GlcUL**, and the same diisocyanates (Hashimoto et al. 1990, 1992, 1993a, b; Wibullucksanakul et al. 1996a, b, 1997). An increased hydrolyzability was observed when the lactone ring was introduced into the main chain of the polymer. This was explained by a ring-opening mechanism of the lactone, followed by breaking of the urethane linkage.

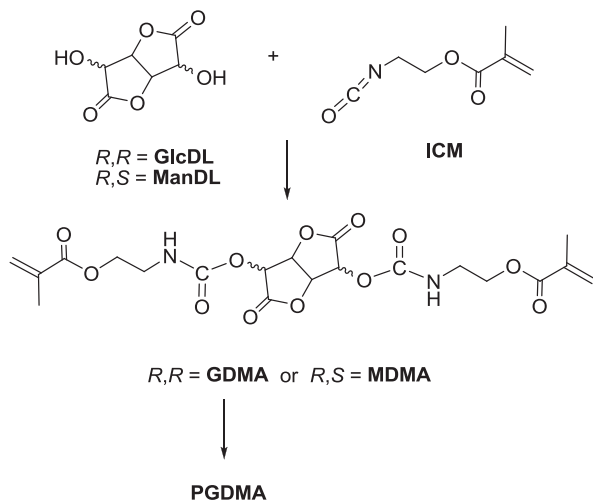
Hydrolyzable poly(ether urethane) gels (**CLPEU**) bearing a saccharide and an amino acid have been prepared. The polymer **CLPEU** was synthesized by the dibutyltin dilaurate-catalyzed polycondensation of methyl β -D-glucofuranosidurono-3,6-lactone (**GlcUL**) and poly(ethylene glycol) (PEG) with the lysine diisocyanate (MELDI) and using a lysine-derived triisocyanate (TIC) as a cross-linking agent (Scheme 5) (Wibullucksanakul et al. 1996b). The swelling ratio and rate of hydrolysis of the polymer increased with the content of PEG and with the pH. This research group also studied the release of 5(6)-carboxyfluorescein (CF) and magnesium 8-anilino-1-naphthalenesulfonate (ANS) from these gels, showing that the hydrophilic compound (CF) was released faster than the hydrophobic one (ANS).

The sugar-derived dilactones glucarodilactone (**GlcDL**) and mannarodilactone (**ManDL**) contain both diol groups to install polymerizable vinyl moieties (i.e., methacrylates) and a ring system susceptible to further functionalization (Scheme 6). Dimethacrylate monomers are ubiquitous and utilized in coatings, adhesives, chromatography packing, and biomaterials (i.e., dental composites) (Kloosterboer 1988; Sideridou et al. 2006; Vlakh and Tennikova 2009). Gallagher et al. (2014) developed the synthesis of two new dimethacrylate feedstocks, glucarodilactone methacrylate (**GDMA**) and mannarodilactone methacrylate (**MDMA**), that contain rigid core structures derived from glucose and mannose. Thermal initiated free radical polymerization of **GDMA** at 135 °C, in the presence of dicumyl peroxide as an initiator, formed highly cross-linked thermosets (**PGDMA**) with

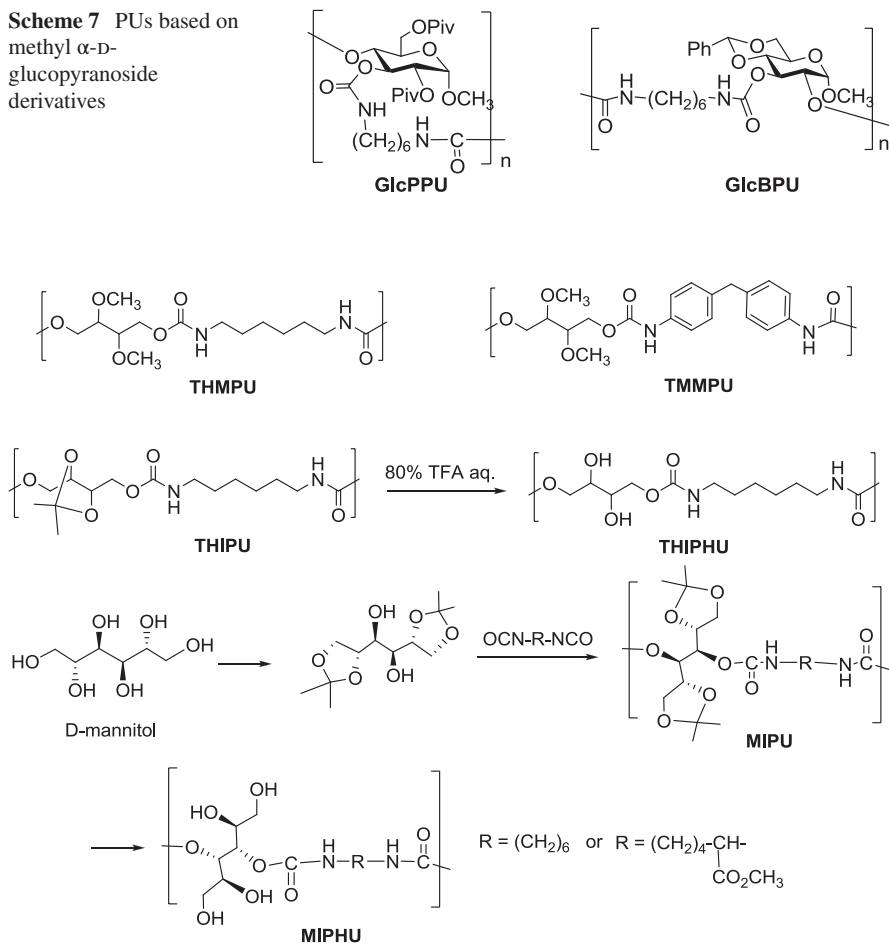


Scheme 5 Hydrolyzable poly(ether urethane) gels obtained from methyl β-D-glucopyranosiduronate-3,6-lactone

Scheme 6 Thermoset PUs derived from aldarolactones



mechanical properties comparable to those reported for commercially available stiff poly (dimethacrylates). Materials derived from these structures, while stable in aqueous neutral and acidic conditions, rapidly degrade in aqueous basic conditions, offering a potential-triggered degradation pathway. In addition, these monomers formed clear film and monodisperse microgel particles, supporting the utility of these sugar dilactone feedstock platforms for a variety of sustainable applications.

Scheme 7 PUs based on methyl α -D-glucopyranoside derivatives**Scheme 8** PUs and PHUs based on alditols

The polymerization reaction of methyl α -D-glucopyranoside derivatives, having a 3,4- or 2,3-diol systems, with HMDI afforded polymers **GlcPPU** and **GlcBPU** (Scheme 7), with hexopyranosyl rings included in the chain (Garçon et al. 2001). No studies on the degradation of the polymers have been conducted.

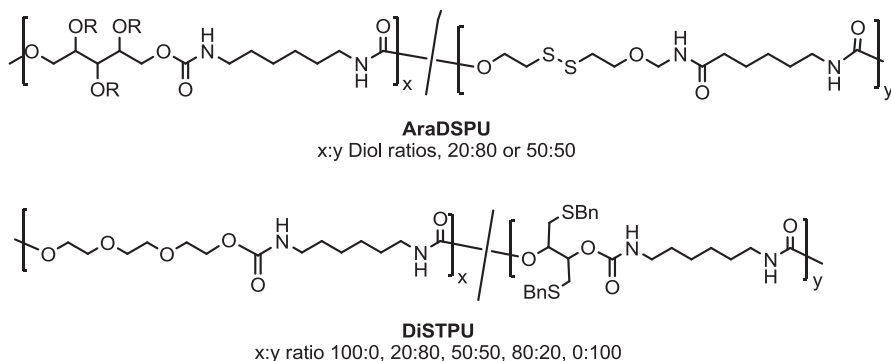
The groups of Galbis and Muñoz-Guerra prepared sets of linear $[m,n]$ -PUs by polycondensation of alditol derivatives with HMDI or MDI. Thus, diol monomers of threitol, arabinitol, and xylitol, bearing the secondary hydroxyl groups protected as methyl ethers, were polycondensed with HMDI or MDI to give PUs of the type of **THMPU** or **TMMPU** (Scheme 8) as amorphous materials with T_g being highly dependent on the aliphatic (HMDI) or aromatic (MDI) nature of the diisocyanate used but scarcely depending on the structure of the alditol (de Paz et al. 2007).

Similarly, 2,3-acetalized derivatives of threitol were polymerized with HMDI or MDI to afford the acetalized PUs **THIPU**, which on treatment under acid conditions underwent removal of the acetal groups to give polyhydroxyurethanes (PHUs) like **THIPHU** (Marín and Muñoz-Guerra 2008). Also, linear PUs containing benzyl groups as substituents of the secondary hydroxyl groups of the starting alditols have been synthesized. On hydrogenolysis of the benzyl ethers, PHUs were obtained (Marin et al. 2009). Hexitols having the *D-gluco*, *D-galacto*, and *D-manno* configurations, with the secondary hydroxyl functions protected as bicyclic acetals, were used as 1,6-diol monomers in the polyaddition to HMDI or MDI. The resulting PUs were conformationally restricted because of the presence of acetal rings in the alditol units. These materials showed thermal stability and T_g values higher than those of their acyclic analogs (Begines et al. 2012). The hydrolytic stability of all these PUs has been determined, and many of them were degraded significantly in a buffer at pH = 10 and 37 °C.

In line with the previous reports on PUs derived from alditols, Hashimoto et al. (2011) reported the synthesis of four biobased polyurethanes bearing pendant hydroxy groups. Derivatives of *D*-mannitol and *D,L*-erythritol were employed as monomeric diols (1,2:5,6-di-*O*-isopropylidene-*D*-mannitol and 1,2-*O*-isopropylidene-*D,L*-erythritol) for the condensation with hexamethylene diisocyanate (HMDI) and methyl (*S*)-2,6-diisocyanatohexanoate (MELDI), to afford PUs of the type of **MIPU**. The following deprotection of the isopropylidene groups led to PHU like **MIPHU**, bearing hydroxyl groups in the pendants. These products showed enhanced hydrolyzability.

In order to increase the degradation rates of the materials, many researches focused their studies in the design of PUs with hydrolyzable linkages in addition to the urethane bonds. Thus, Galbis et al. (de Paz et al. 2010) suggested that the introduction of a hydrolyzable disulfide group could improve the biodegradability, taking into account that the disulfide bond could be cleaved by the action of the natural peptide glutathione. Therefore, copolymers of the type of **AraDSPU** (Scheme 9) were synthesized by reaction of two different diols: 2,2'-dithiodiethanol (DiT) and derivatives of *L*-arabinitol [2,3,4-tri-*O*-benzyl-*L*-arabinitol ($R = \text{Bn}$) or 2,3,4-tri-*O*-methyl-*L*-arabinitol ($R = \text{Me}$)]. These copolymers were thermally stable and the introduction of a sugar-based diol in the PU backbone led to reduction of the crystallinity. Chemically and enzymatically catalyzed hydrolysis of these macromolecules has been tested. Copolyurethanes of the type of **AraDSPU** proved to be biodegradable under physiological conditions (pH 7.02 and 37 °C) in the presence of glutathione, which promotes the breaking of the disulfide linkage. The degradation pattern depended not only on the presence of dithiodiethanol but also on the crystallinity of the final macromolecule.

Homo- and copolyurethanes of the type of **DiSTPU** have been obtained by reaction of a sugar diol (1,4-di-*S*-benzyl-*D,L*-dithiothreitol), triethylene glycol, and HMDI (Ferris et al. 2010). The degree of crystallinity of the copolymers decreased with the proportion of dithiothreitol moiety, with an increase of the stiffness. The homo- and copolymers synthesized showed degradation temperatures above 250 °C, and they were hydrolytically degraded at different pH and temperatures. However,



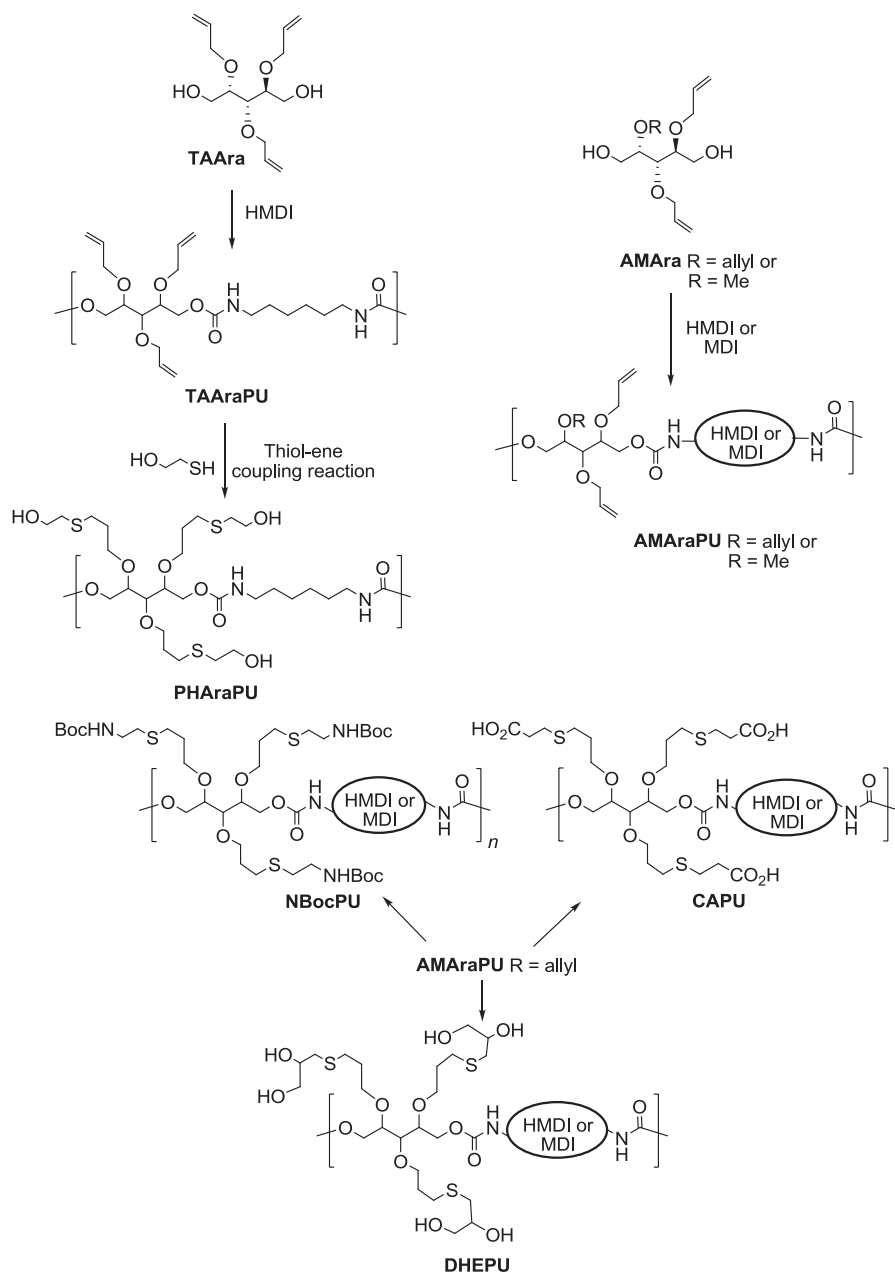
Scheme 9 Homo- and copolyurethanes based on arabinitol derivatives or 1,4-di-S-benzyl-D, L-dithiothreitol

the dithiothreitol-based PUs did not exhibit a significant degradation at neutral or basic pH at 37 °C.

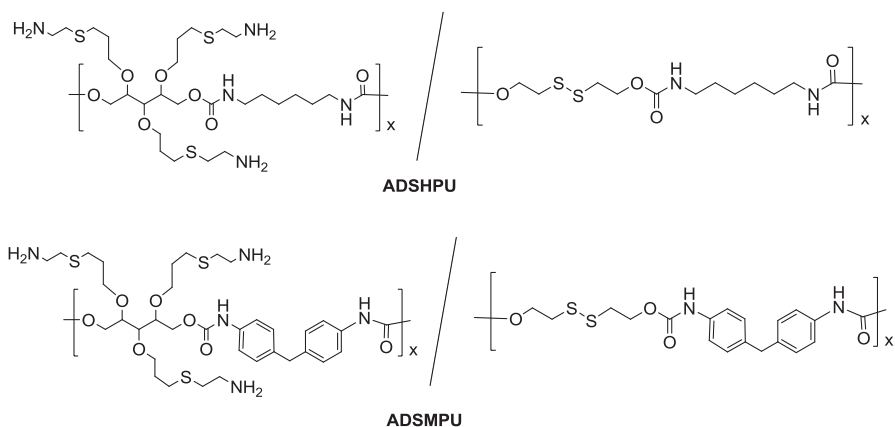
The polyurethane **TAARA**PU, with multiple pendant allyl groups, was prepared by polyaddition of 2,3,4-tri-*O*-allyl-L-arabinitol (**TAARA**) with HMDI and then functionalized with 2-thioethanol by the thiol-ene reaction (Scheme 10) (Ferris et al. 2011). The thiol-ene “click” reaction took place in every allyl group of the macromolecule to give the highly functionalized **PHARA**PU. Other PUs like **AMARA**PU, with varied degree of allyl substitution, have also been prepared using derivatives of L-arabinitol (**AMARA**) as monomers. The allyl groups took part in thiol-ene reactions to afford greatly diverse materials. Thus, highly substituted polymers with NHBOC (**NBoc**PU), carboxylic acid (**CAPU**), and 1,2-dihydroxyethyl groups (**DHEPU**) have been obtained through click chemistry (Ferris et al. 2012).

Another achievement of Galbis’s group was the synthesis of biodegradable polyurethanes containing allyl or amine residues useful as carriers of anionic drugs (at physiological pH) or gene materials (Ferris et al. 2014). Polymers of the type of **ADSHPU** or **ADSM**PU (Scheme 11) combined two interesting aspects, functionalization of the PU backbone by the thiol-ene reaction and biodegradation, necessary for use as carry systems for drug delivery in the colon. As mentioned before, an increased degradability was achieved by the introduction of a disulfide linkage in the polymer chain. The morphology of the PUs and the biodegradation process in reductive environments were studied by atomic force microscopy (AFM). It is interesting to note that polymers with amine residues presented lower thermal stability than those bearing allyloxy pendant groups.

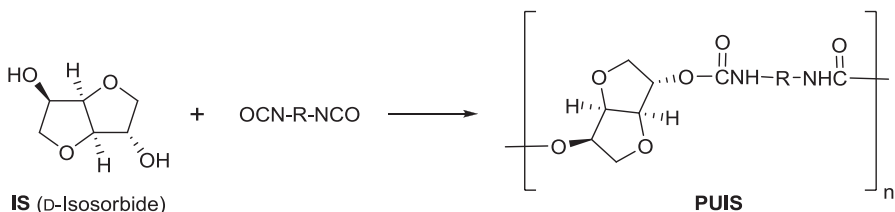
Polyurethane hard segment is not limited to the structure of diisocyanate and the attraction through hydrogen bonding or molecular interactions. The biobased bicyclic diols isosorbide and isomannide (1,4:3,6-dianhydride of sorbitol and mannitol, respectively) can act as a hard segment due to their rigid structure (Kricheldorf 1997; Fenouillot et al. 2010). Thus, the rigidity of isosorbide improves resistance to heat, UV rays, and chemicals and provides excellent optical and mechanical properties to the materials produced.



Scheme 10 PUs based on arabinitol and with pendant allylic groups. Functionalization of the double bond using the thiol-ene click reaction



Scheme 11 Biodegradable PUs containing disulfide linkages and pendant amino groups

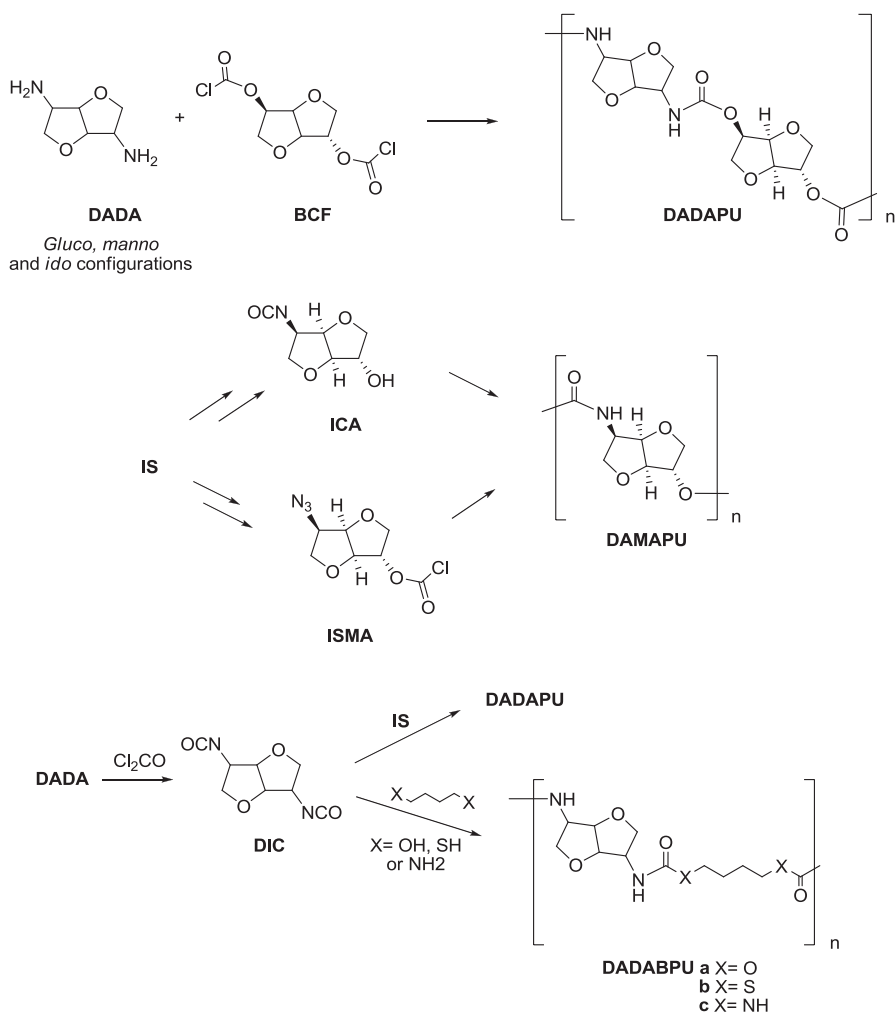


Scheme 12 PUs derived from D-isosorbide

Isosorbide (IS) has two hydroxyl groups, having either *endo* or *exo* orientation, attached to the two fused ether rings. The *exo*-oriented hydroxyl group is more accessible toward alkylation or acylation reactions. Conversely, the *endo*-OH group is involved in intramolecular H-bonding with the oxygen of the neighboring tetrahydrofuran ring. In spite of the steric hindrance, this intramolecular H-bonding makes the *endo* hydroxyl group a preferred reactive center in electronically driven reactions (Abenhaïm et al. 1994; Zhu et al. 2009).

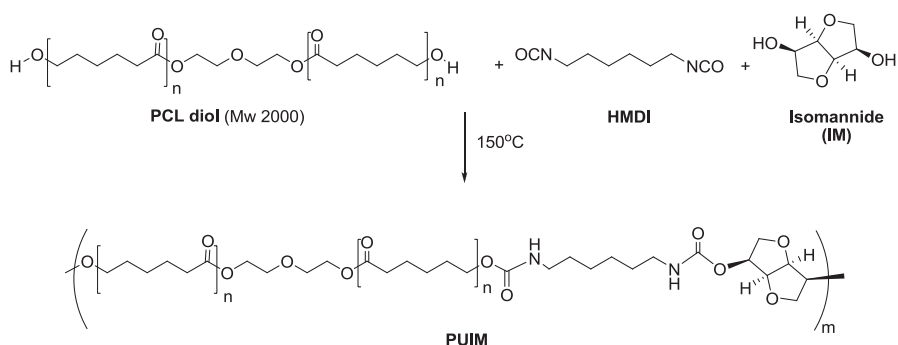
The synthesis of linear PUs using 1,4:3,6-dianhydroalditols as monomers was patented in 1984 (Dirlikov and Schneider 1984), and the first paper on this type of PUs appeared short later (Thiem and Lüders 1986) and then in the 1990s (Cognet-Georjon et al. 1995). In agreement with the originally patented procedure, the dianhydroalditols (alone or in combination with a second diol) were polymerized with a variety of diisocyanates using as catalysts dibutyltin laurate (Beldi et al. 2007; Marin et al. 2012) or *n*-butyltin oxide hydroxide hydrate (Lee et al. 2009) to afford PUs like **PUIS** (Scheme 12).

In the pioneering work by Thiem and Lüders (1986), the efficient conversion of 1,3:4,6-dianhydroalditols into the corresponding dianhydroalditol diamines (**DADA**)



Scheme 13 $[m,n]$ - or $[n]$ -type PUs based on 1,3:4,6-dianhydroditols and dianhydroditol diamines

was reported (Scheme 13). The interfacial polycondensation of **DADA** with the bis(chloroformate) (**BCF**) derived from isosorbide (**IS**) gave the PUs **DADAPU**, having M_n ca 3000. The diol **IS** was also employed as precursor of the isocyanate-alcohol **ICA** and the azide **ISMA**. The monomer **ICA**, which was obtained from **IS** in a five-step synthesis, was polymerized under catalysis with dibutyltin laurate to afford the $[n]$ -polyurethane **DAMAPU**. On the other hand, the amine released upon hydrogenolysis of the azide **ISMA** promoted the spontaneous polycondensation to **DAMAPU** (Bachmann et al. 1998). This was the first example of a $[n]$ -type PU (or [A, B]-polyurethane) derived from a carbohydrate.

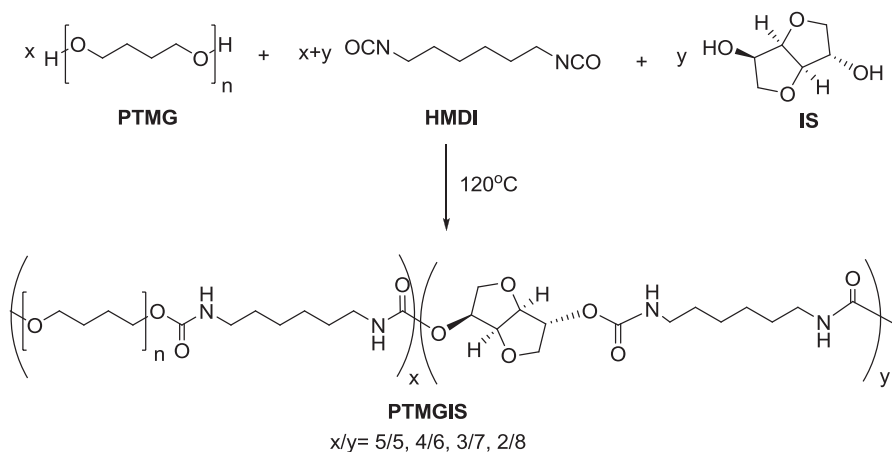


Scheme 14 PUs prepared from poly(ϵ -caprolactone) diol and isomannide as diol precursors

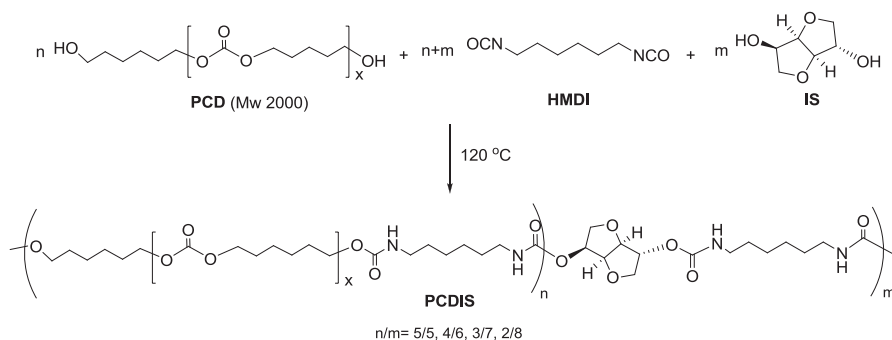
The diamines **DADA** reacted with phosgene to give the corresponding diisocyanates **DIC**, with *D-gluco*, *D-manno*, and *L-ido* configurations (a diisothiocyanate was also prepared) (Bachmann et al. 2001). Diisocyanates **DIC** were polymerized with diamines **DADA** to give polyureas and with dianhydroalditols (like **IS**) to afford PUs structurally related to **DADAPU**. Polymerizations of **DIC** were also conducted with 1,4-butanediol, 1,4-butanedithiol, 1,4-diaminobutane, or 1,3-diaminobenzene to afford a variety of polymers **DADABPU**, which were characterized using IR and NMR spectroscopy, viscosimetry, and DSC.

Several families of biocompatible and biodegradable PUs have been prepared from isosorbide (**IS**) or isomannide (**IM**) in one-step polymerizations and in the absence of catalysts, which has positive presumptions for toxicity. Polyurethanes **PUIM**, prepared with fixed HMDI level and varying ratios of **IM** and poly(ϵ -caprolactone) diol (**PCL diol**) (Scheme 14), gave T_g values between 25 and 30 °C. Degradation tests performed at 37 °C in phosphate buffer produced mass losses of 5–10% after 8 weeks (Lim et al. 2013). Similarly, PUs prepared from isosorbide, using the same approach, showed T_g s of 30–35 °C. The degradation tests showed a mass loss of around 5% after 12 weeks, except for the polymer with the highest isosorbide content which showed an initial rapid mass loss (Park et al. 2013).

Biobased, highly elastic polyurethanes were prepared from **HMDI** and various ratios of **IS** to poly(tetramethylene glycol) (**PTMG**) as a diol by a simple one-shot bulk polymerization without a catalyst (Scheme 15) (Kim et al. 2014). The resulting **PTMGIS** elastomer showed a very low T_g value (−47.8 °C) and exhibited not only excellent stress–strain properties but also superior resilience compared to the existing polyether-based polyurethane elastomers. The static and dynamic properties of the thermoplastic elastomer were suitable for dynamic applications, and in addition, the rigid diol imparted biocompatible and bioactive properties. Degradation tests performed at 37 °C in phosphate buffer solution showed a mass loss of 4–9% after 8 weeks, except for the polyurethane with the lowest isosorbide content, which showed an initial rapid weight loss. These polyurethanes offered significant promise



Scheme 15 PUs prepared from isosorbide and poly(tetramethylene glycol) as diol components



Scheme 16 PUs prepared from isosorbide and polycarbonate diol 2000 as diol components

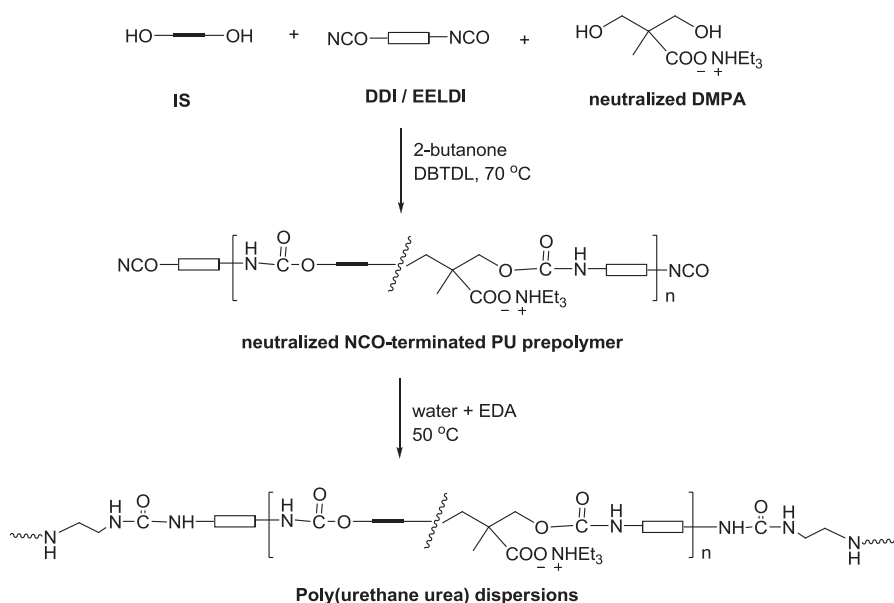
due to its soft, flexible, and biocompatible properties for soft tissue augmentation and regeneration.

A new family of highly elastic PUs partially based on renewable isosorbide was prepared by reaction of HMDI with varied ratios of **IS** and polycarbonate diol 2000 (**PCD**) via a one-step bulk condensation polymerization without catalyst (Scheme 16) (Oh et al. 2015). Variation of the ratio of **PCD** and **IS** led to a number of biocompatible **PCDIS** polyurethanes with different thermal and mechanical properties. They showed high M_n (number average molecular weights) ranging from 56,320 to 126,000 g mol^{-1} and tunable T_g values from $-34\text{ }^\circ\text{C}$ to $-38\text{ }^\circ\text{C}$. The **PCDIS** films were flexible, with breaking strains of 955–1,795% at 13.5–54.2 MPa tensile stress. In vitro degradation test, performed in phosphate buffer at $37\text{ }^\circ\text{C}$, showed that all the PUs had 0.9–2.8% weight lost over 4 weeks and continual slow weight loss of 1.1–3.6% within 8 weeks. Although the rate of proliferation of cells was slightly lower

than that of the tissue culture polystyrene as a control, the PU films were considered to be cytocompatible and nontoxic. These thermoplastic PUs were soft, flexible, and biocompatible polymers. These findings suggested that the elastic PUs have a high potential as a tissue engineering scaffold (for soft tissue augmentation and regeneration) and for other biomedical uses.

In polyurethane-coating applications, isosorbide is known to confer good thermal and mechanical properties to amorphous polymers, thanks to its rigid and asymmetric structure. Thus, new PUs based on MDI and isosorbide have been prepared (Cognet-Georjon et al. 1995). On the other hand, it was already mentioned that the asymmetric structure of the ethyl ester L-lysine diisocyanate (EELDI) may facilitate the formation of amorphous PUs. Therefore, the combination of IS with EELDI should give amorphous and rigid PUs with good UV stability.

Waterborne polyurethane dispersions (PUDs) are binary colloid systems in which PU particles containing stabilizing groups are dispersed in a continuous aqueous medium. Compared to solvent-borne coating systems, aqueous PUDs have reduced contents of volatile organic compounds, are non-flammable, show good adhesion to a variety of substrates, and have excellent resistance to chemicals and solvents. Symmetric and asymmetric building blocks were employed for the synthesis of NCO-terminated PU prepolymers and subsequent preparation of polyurethane dispersions (PUDs) with an overall renewable content of approximately 90% (Scheme 17). The reactivity and regioselectivity in reactions that involve EELDI and isosorbide were studied (Li et al. 2014a). The results obtained by performing



Scheme 17 Synthesis of poly(urethane urea) dispersions containing isosorbide

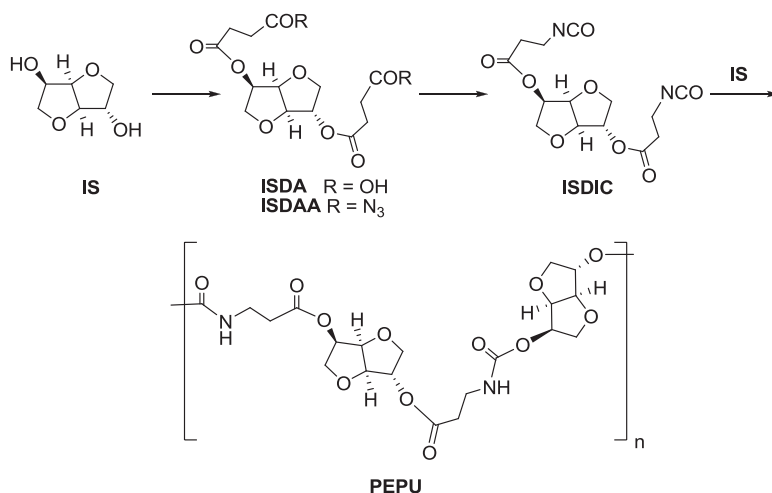
model reactions suggested slight reactivity differences between the α - and ε -NCO groups of EELDI and the *endo*- and *exo*-OH groups of **IS**, respectively. In addition, comparison of the condensation reaction rate between **IS** or dimethylolpropionic acid (**DMPA**) with **DDI** or **EELDI** revealed a rather low reactivity of **DMPA** compared to **IS**. Therefore, the PU prepolymers synthesized, based on these four components, might contain a relatively high content of **DMPA** near the prepolymer chain ends, which most probably facilitates their dispersion in water. Finally, the waterborne PU dispersions prepared from these four-component prepolymers showed good storage stability and a small particle size at low **DMPA** contents, especially at high **EELDI** and **IS** contents. According to these studies, renewable-based polyurea and PU dispersions might be constructed from **DDI**, **EELDI**, **IS**, and **DMPA**, in a more controlled way.

The preparation of PUD consists of two stages. The first stage is the synthesis of low molecular weight PU prepolymers containing isocyanate (NCO) end groups and an internal dispersing agent, e.g., dimethylolpropionic acid (**DMPA**), in a non-aqueous medium with a lower boiling point than water. The internal dispersing agent can be neutralized with, for instance, a tertiary amine either before or after the prepolymer synthesis. In the second stage, the aqueous PU dispersions are prepared by adding water to the prepolymer solution or vice versa, after which the low boiling organic solvent is removed (Dieterich 1981; Sardon et al. 2009).

The thermal and mechanical properties as well as the morphology of biobased poly(urethane urea) dispersion-cast films were correlated with the polymer composition (Li et al. 2014b). The dispersions showed a good electrostatic stability at pH values ranging from 4 to 12. The dispersion-cast films were thermally stable up to 245 °C (5% weight loss). An enhanced thermal stability was observed for films containing a relatively high dimer fatty acid-based diisocyanate (**DDI**) content, which was related to the reduced concentration of urethane and urea chains. Replacement of the flexible **DDI** with **EELDI**, as well as increasing the isosorbide contents in the monomer feed, led to a significant increment of the T_g from 18 to 58 °C (first heating cycle) and to above 70 °C (second cycle). The H-bond-induced micro-phase separation depends on the polymer composition. An improved phase mixing was related to the overall increased concentration of urethane/urea bonds, as a result of increasing **EELDI** contents. The coatings applied on aluminum panels have shown good resistance to acetone, moderate impact resistance at high **EELDI** and **IS** contents, and excellent adhesion to aluminum.

The use of the highly toxic phosgene in the production of polyurethanes is a serious disadvantage. Also the use of isocyanates constitutes a threat to both the environment and to the health of workers, due to the volatility and toxicity of the diisocyanates and their production through phosgenation of diamines. The replacement of these hazardous compounds constitutes an academic and industrial challenge at the present time. Several procedures for the synthesis of non-isocyanate polyurethanes have been reported (Rokicki et al. 2015; Datta and Włoch 2016).

Diisocyanates of isosorbide and isomannide have been prepared using a phosgene-free methodology which employs the Curtius rearrangement, as illustrated in Scheme 18 for **IS** (Zenner et al. 2013). The procedure involves the

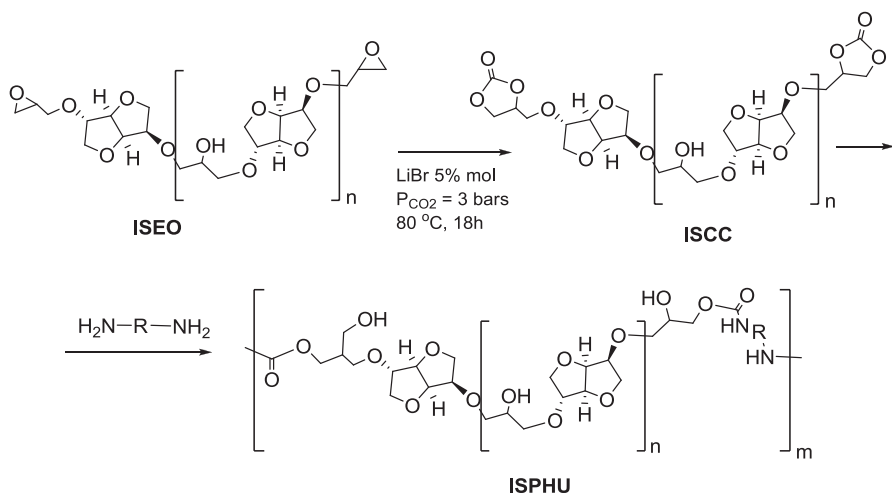


Scheme 18 Diisocyanates of isosorbide, obtained by Curtius rearrangement, and their polycondensation with isosorbide

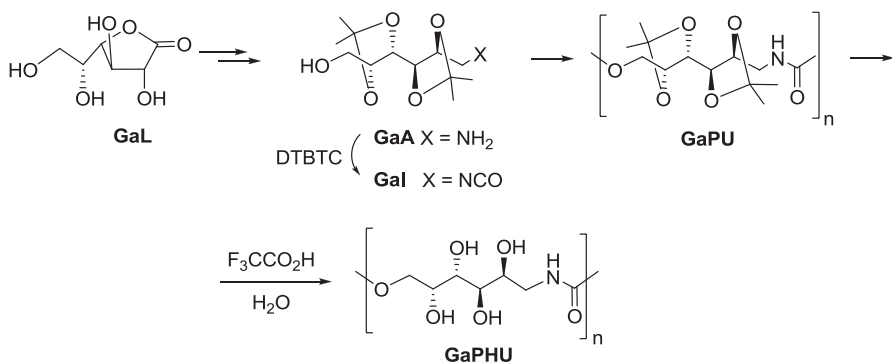
esterification of the hydroxyl groups of the anhydroalditols (i.e., **IS**) with succinic anhydride to give the diacids **ISDA**, which were converted into the diacyl chlorides, as precursors of the diacyl azides (**ISDAA**). Curtius rearrangement of the diacyl azides afforded the corresponding diisocyanates **ISDIC**, ready for the preparation of high-performance materials. Thus, a stereoregular polyester polyurethane (having the *D-manno* configuration in all the monomers) and a non-stereoregular one (*D-gluco* configuration, **PEPU**) have been obtained. Interestingly, the diacid **ISDA**, derived from **IS**, was so tacky that the same authors synthesized and characterized a group of thickeners with 100% biocontent (Zenner et al. 2015).

A cyclic carbonate intermediate was prepared, under rather drastic conditions, as precursor of **IS**-based PHUs of the type of **ISPHU** (Scheme 19) (Besse et al. 2013). Treatment of isosorbide with an excess of epichlorohydrin under alkaline conditions led to the epoxidized oligomers **ISEO**. The epoxides were converted into carbonates via a carbonation reaction with CO₂ in DMF and in the presence of LiBr (5% mol). The resulting cyclic carbonate **ISCC** was polycondensed with commercial diamines (e.g., 1,10-diaminodecane, diethylenetriamine, isophoronediamine), in the presence of catalyst to give the PHUs **ISPHU**. These materials showed low *T_g* (−8 to 59 °C), for which they are claimed to be suitable for coatings.

In the preparation of diisocyanates, less harmful substances have been employed to replace phosgene. For example, di-*tert*-butyltricarboxylate (DTBTC) has shown to be effective for the conversion of the amino group of an α,ω -amino alcohol into an α,ω -isocyanate alcohol. This monomer does not need isolation or manipulation and can be polycondensed to give a $[n]$ -polyurethane (Versteegen et al. 1999). We have employed this rather safe methodology for the synthesis of the linear $[n]$ -polyurethane **GaPU** (Scheme 20), from the intermediate amino alditol (**GaA**) and via the

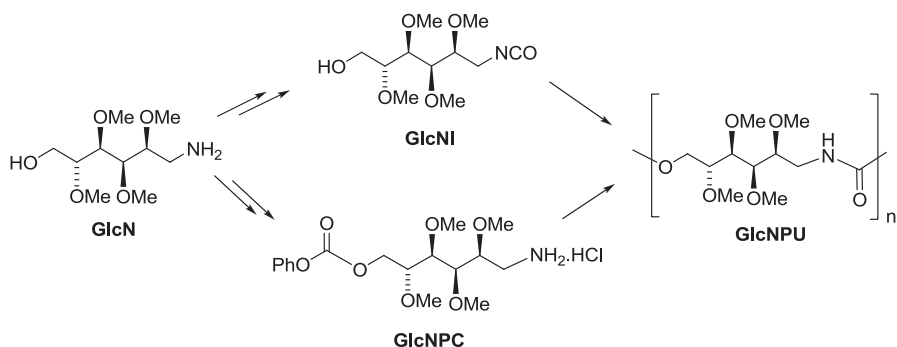


Scheme 19 Cyclic carbonate **ISCC** as precursor of isobutylene-based PHUs (**ISPHU**)

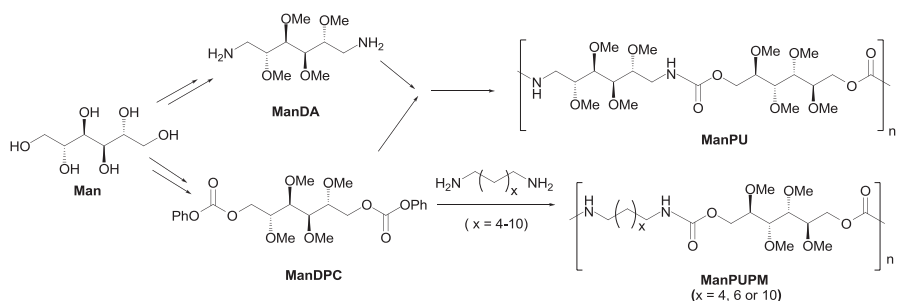


Scheme 20 Homopolymerization of the α,ω -isocyanate alcohol **GaI** to give the $[n]$ -polyurethane **GaPU**. Deprotection of **GaPU** to the PHU **GaPHU**

isocyanate (**GaI**) (Gomez and Varela 2009). Compound **GaA** was prepared from D-galactono-1,4-lactone (**GaL**) in a three-step synthetic route. Polymerization of α,ω -isocyanate alcohol **GaI** was conducted in THF and in the presence of $\text{Zr}(\text{acac})_4$ as catalyst. The resulting polyurethane **GaPU** was practically free of urea linkages. Removal of the acetal protecting groups by acid hydrolysis led to the polyhydroxyurethane **GaPHU**, having all the hydroxyl groups free. The polymers were fully characterized, and the analysis by SEM revealed surfaces with morphologies characteristic of crystalline polymers. This was the first synthesis reported for a $[n]$ -PHU derived from a carbohydrate monomer.



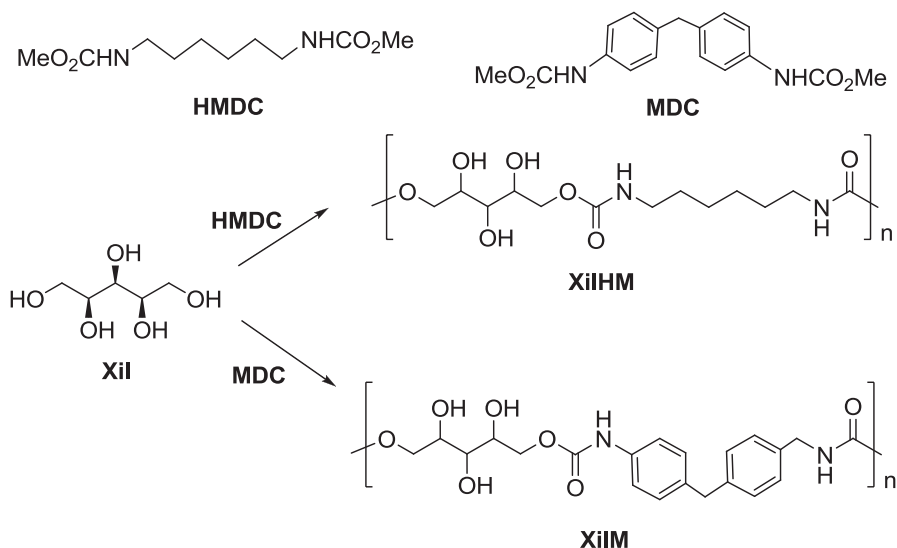
Scheme 21 Isocyanate-free synthesis of linear $[n]$ -polyurethanes from D-glucamine



Scheme 22 Isocyanate-free synthesis of $[n]$ -polyurethanes from D-mannitol

The DTBTC procedure for the synthesis of isocyanate alcohols, described in the previous paragraph, was also applied to D-glucamine (1-amino-1-deoxy-D-sorbitol, **GlcN**) (Kolender et al. 2011). The secondary hydroxyl groups of glucamine were protected as methyl ethers, and the amino was activated as isocyanate (**GlcNI**) with DTBCT (Scheme 21). Alternatively, a mild procedure, previously described in our laboratory (Arce et al. 2010), was employed for the activation of the primary hydroxyl group of **GlcN** as a phenyl carbonate (**GlcNPC**). Both monomers **GlcNI** and **GlcNPC** were polycondensed to give the linear $[n]$ -polyurethane **GlcNPU**.

We have also used the methodology of the diol activated as phenyl carbonate in the synthesis of $[m,n]$ -PUs derived from D-mannitol (**Man**), as a renewable and low-cost sugar alditol (Scheme 22) (Fidalgo et al. 2013). The key comonomer 1,6-di-O-phenylcarbonyl-2,3,4,6-tetra-O-methyl-D-mannitol (**ManDPC**) was polymerized with the diamine **ManDA**, also derived from mannitol, or with alkylenediamines, to give, respectively, the $[6,6]$ -polyurethane **ManPU**, entirely based on a carbohydrate, or $[m,n]$ -PUs (**ManPUPM**) having methyl ether units alternating with a polymethylene chain. The polymers were stereoregular due to the C_2 axis of symmetry



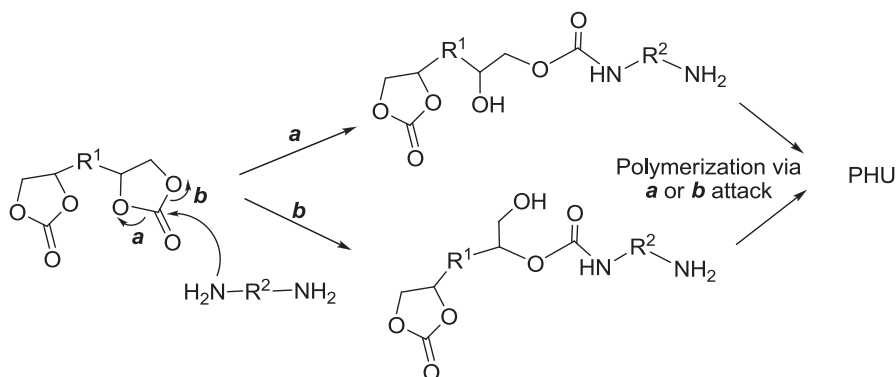
Scheme 23 Dicarbamates reacted with xylitol to afford hydrophilic $[m,n]$ -PUs

of **Man**, but they were amorphous materials. The T_g values depended on the structure and chain length of the diamine comonomers.

Dicarbamates have been employed as active monomers, instead of diisocyanates, in the preparation of hydrophilic $[m,n]$ -PUs and polyureas. Thus, derivatives of xylitol (**Xil**), with the hydroxyl groups free or partially protected, reacted with dimethyl hexamethylene dicarbamate (HMDC) or di-*tert*-butyl-4,4'-diphenylmethyl dicarbamate (MDC) (Scheme 23) (Begines et al. 2011). The polycondensation led to the PHUs **XilHM** or **XilM**, respectively. For comparison, polymerizations were also conducted using the analog diisocyanates HMDI or MDC. PHUs of the type of **XilHM** or **XilM** were, respectively, obtained; however, the higher reactivity of the diisocyanates with respect to the analogous carbamates led to some degree of cross-linking in these polymers. The PHUs were hydrolytically degradable under physiological conditions.

One of the most typical examples of the non-diisocyanate, non-phosgene routes to PUs may be the reaction of cyclic carbonates and amines to form a urethane linkage (Scheme 24). In this type of polymerization, one of the comonomers is a primary or secondary, aliphatic or aromatic diamine, and the other comonomer is a bicyclic carbonate. The product is usually a $[m,n]$ -PHU. In fact, structural isomers of PHUs with primary or secondary hydroxyl groups may be obtained since the carbonate ring has two ways of ring opening (**a** or **b**). The ratio of secondary (attack **a**) to primary (**b**) alcohol groups depends on the reaction conditions (especially on temperature).

The groups of Endo (Whelan et al. 1963; Kihara and Endo 1993; Kihara et al. 1996; Tomita et al. 2001; Rokicki and Piotrowska 2002) have contributed to the



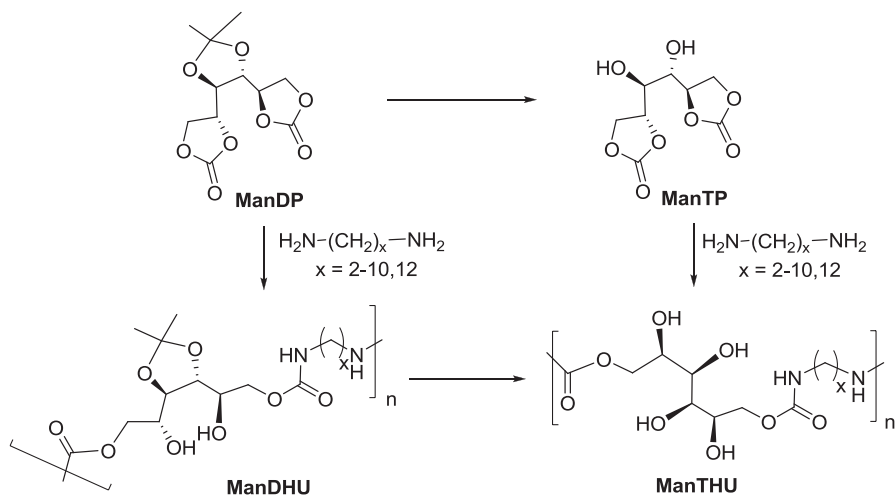
Scheme 24 Reaction of cyclic carbonates and amines to form a urethane linkage

synthesis of PHUs. They showed that the water absorption of these polymers is 15–35 times higher than that of commercial PU, but the thermal stability is comparable.

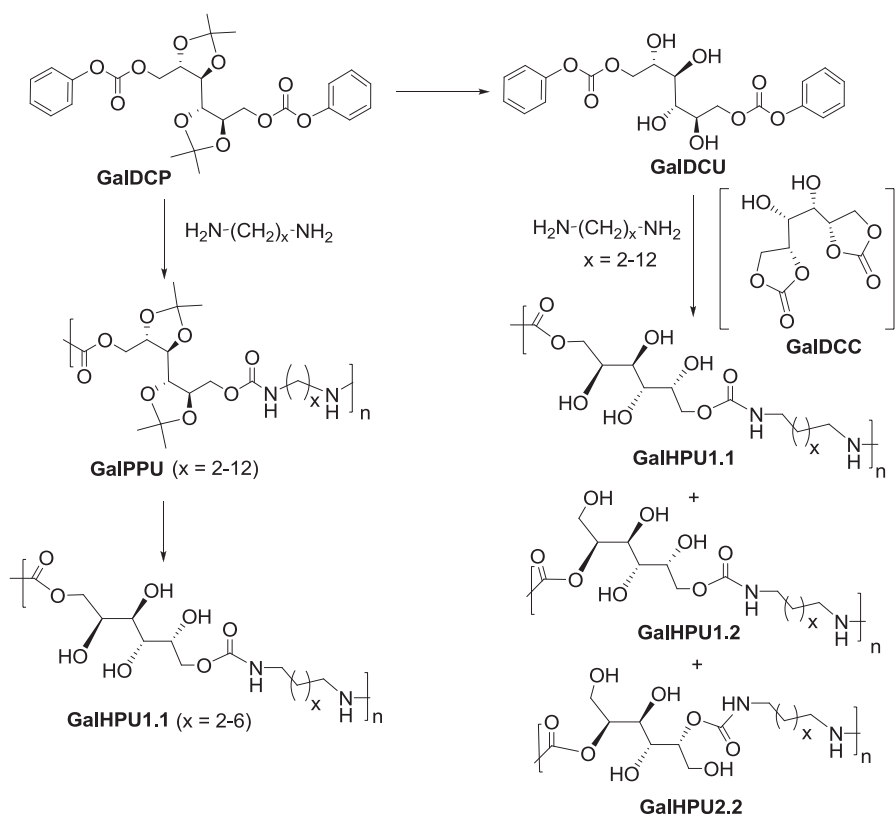
The production of PU from plant resources (in particular from vegetal oils) and the isocyanate-free preparation of PHUs from mono- and polycyclic carbonates have been recently reviewed (Nohra et al. 2013). The review covers also the varied methods for synthesizing five- and six-membered cyclic carbonates and their aminolysis by monoamines or polyamines. The numerous applications of PHUs and their synthesis from cyclic carbonates are also outlined. It is worth to mention that the technological barrier to obtain biobased cyclic carbonates could be overcome by using glycerol carbonates or epoxidized vegetal oils.

Bis(ethylene carbonate) monomers have been prepared from carbohydrates and polymerized with diamines. Thus, 1,2:5,6-dicarbonate derivatives of D-mannitol, fully (**ManFP**) or partially protected (**ManPP**), have been prepared and polymerized with diamines (Scheme 25) (Prömpers et al. 2005). The α,ω -polymethylene diamines of the type NH₂-(CH₂)_x-NH₂ (with $x = 2-10, 12$) were employed to afford PHUs with pendant hydroxyl groups. The polymer chains showed both primary and secondary hydroxyl groups in a ratio *ca* 15:85, as a consequence of the regioselectivity in the carbonate ring opening. The PHUs **ManDHU** were obtained from **ManDP** and hold in the repeating unit two free and two protected hydroxyl groups. PHUs **ManDHU** were semicrystalline materials. The polymers **ManTHU**, derived from **ManTP** and with four free hydroxyl groups in the repeating unit, were amorphous. The free hydroxyl groups of some PHUs were esterified using acyl chlorides (acetyl, lauryl, and stearyl) to afford the corresponding acylated PUs.

The same authors (Prömpers et al. 2006) prepared, from galactaric acid, the 1,6-bis-*O*-phenoxycarbonyl derivatives of galactitol fully protected (**GalDCP**) or unprotected (**GalDCU**) (Scheme 26). These AA-type monomers were polymerized with α,ω -polymethylene diamines ($x = 2-10, 12$). Due to the high reactivity and low selectivity of the diisocyanates and polyols, these polymers could not be obtained



Scheme 25 Bis(ethylene carbonate) monomers prepared from D-mannitol and their polymerizations with diamines



Scheme 26 Preparation of fully protected (**GalDCP**) or unprotected (**GalDCU**) diphenyl-carbonate derivatives of galactitol and their polymerizations with diamines

via classical routes using these monomers, because of cross-linking side reactions. The monomer **GalDCP** afforded PUs of the type of **GalPPU**, with all the secondary hydroxyl groups protected as acetals. However, under the same polycondensation conditions applied to **GalDCP**, the hydroxyl-unprotected monomer **GalDCU** led to formation of isomeric repeating units (**GalHPU1.1**, **GalHPU1.2**, and **GalHPU2.2**) as revealed by NMR. This result suggested the intramolecular cyclization of **GalDCU**, with elimination of phenol, to give the thermodynamically favored five-membered cyclic carbonate. This reaction may occur once or twice (to give the dicarbonate **GalDCC**). During the polyaddition, the carbonate ring opening results in the isomeric products. However, the **GalHPU1.1** could be obtained by acid hydrolysis of the acetal groups of **GalPPU**, without polymer degradation. The products showed thermal stability and good hydrophilic properties.

4 Combination of Polyurethanes with Oligo- or Polysaccharides

In order to enhance the mechanical performance of biopolymers and to overcome the poor biological properties of synthetic polymers, “bioartificial polymeric materials” have been designed and prepared (Cascone et al. 2001). For example, natural biopolymers are useful scaffolds for cell growth, since they are usually biocompatible. In contrast, synthetic polymers may contain toxic compounds or impurities that may not allow cell growth. On the other hand, synthetic polymers have better thermal and mechanical properties than the natural counterparts (Sionkowska 2013). Therefore, materials based on blends of two or more natural biomacromolecules as well as their combinations with synthetic polymers lead to bioartificial polymers with improved mechanical properties and biocompatibility (Giusti et al. 1994; Cascone 1997; Sionkowska 2013).

Since polysaccharides are the most abundant biopolymers found in nature, they may be employed for the preparation of bioartificial polymers. Particularly, polyurethanes have been used as synthetic polymers for the preparation of bioartificial materials based on polysaccharides. As conventional PUs are insoluble in water, hydrophilic groups (including ionic or nonionic agents) must be added to their backbones in order to disperse them in water (Liu et al. 2011). Additionally, incorporation of a natural component into a synthetic polymer structure can enhance degradation. For example, incorporation of so-called weak chain into the macromolecule became a well-established method to enhance the degradation, and in many cases, natural carbohydrates serve as the “weak chain” (Donnelly et al. 1991; Witt et al. 2001; Varma et al. 2004). The degradation is one of the most effective methods to overcome the pollution of the environment caused by accumulation of nondegradable polymers. These new materials are usually prepared in line with the principles of “green chemistry.”

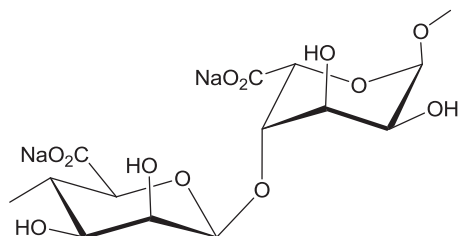
Degradable PU ionomers have been obtained by incorporating natural compounds such as mono-, di-, and polysaccharides into a PU (Travinskaya et al. 2014). Recently, new functional elastic PU foams, degradable under environmental abiotic and biotic conditions, which retain the properties inherent in the conventional foams, were synthesized using isocyanate precursors based on disaccharides: lactose, maltose, and sucrose (Savelyev et al. 2015). Model reactions of these disaccharides with phenyldiisocyanate showed that both the primary and secondary hydroxyl groups of the carbohydrate reacted to form urethane linkages. The main properties of disaccharide-based foams were similar to those of conventional PU foams prepared from common polyols. However, the new materials underwent enhanced acid/alkaline hydrolysis and degradation compared with PU foam matrix when incubated in soil. Mass losses of incubated polyurethane-disaccharide-based foams significantly exceeded the actual carbohydrate content (28.6%) and after 12 months reached 40–53%. In contrast, under the same conditions, common PU foam matrix lost only 2–2.5%, confirming that incorporation of natural compounds into the polymer chain impacted the degradation processes.

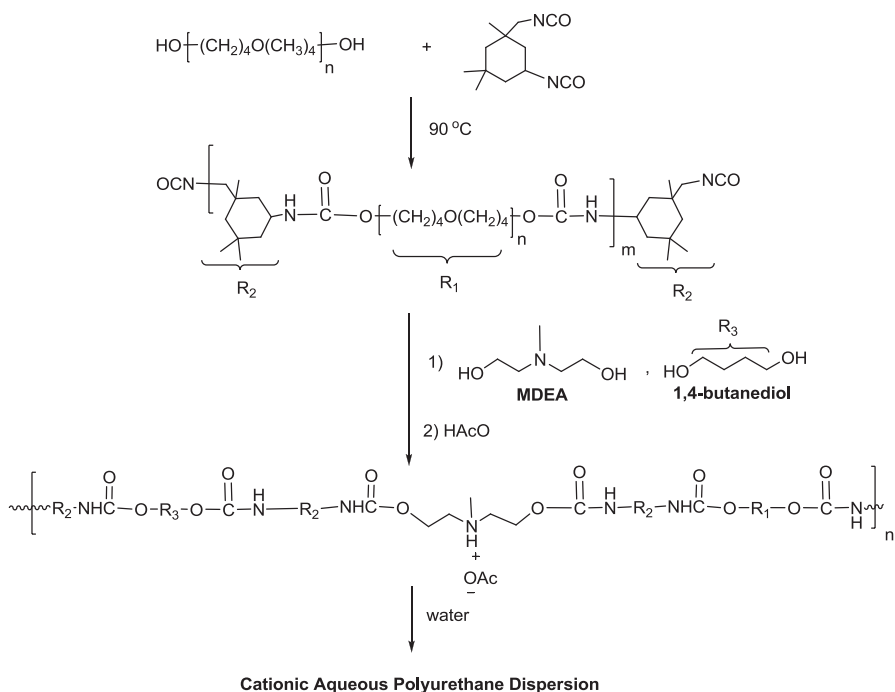
Alginate, starch, chitosan, and other naturally abundant polysaccharides, listed below, have been employed for the synthesis of bioartificial polymers with a wide range of applications.

4.1 Alginate

Among the polysaccharides, alginate is widely used in food and textile industries as thickener, stabilizer, and gel and film former, among other uses (Zia et al. 2015). Alginate, usually isolated from brown seaweeds, is a (1-4)-linked block copolymer of β -D-mannuronate and its C-5 epimer α -L-guluronate, with regions in which approximately the disaccharide repeating structure shown below prevails (Scheme 27) (Haug et al. 1966; Rees and Samuel 1967). Alginate displays nontoxicity and excellent biocompatibility and biodegradability (Mørch et al. 2007; Draget 2009) and can be readily modified as microspheres, microcapsules, fibers, sponges, elastomers, hydrogels, foams, etc. This versatility led to applications of alginate in such fields as tissue engineering and drug delivery (Venkatesan et al. 2015).

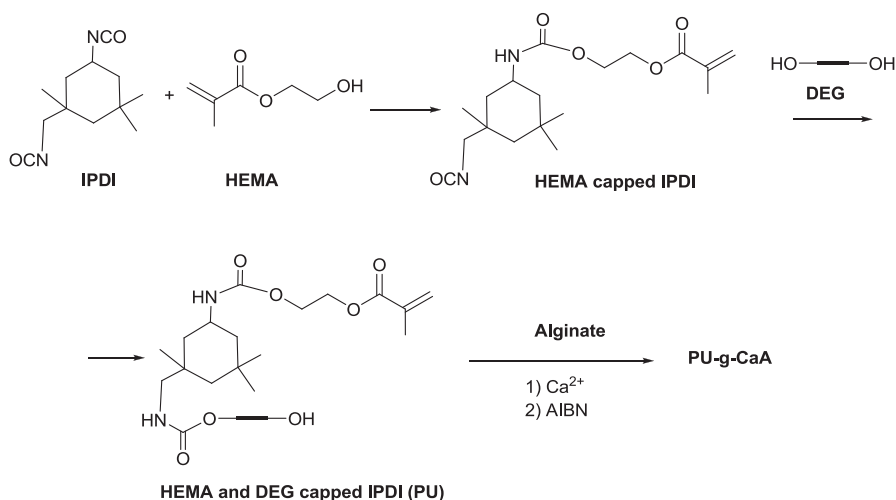
Scheme 27 Disaccharide repeating unit of alginate





Scheme 28 Preparation of cationic aqueous PU dispersions, which combined with sodium alginate nanoparticles afforded compatible elastomeric materials

Recently, Barikani and coworkers (Daemi et al. 2013) have prepared novel compatible elastomeric materials based on aqueous cationic PU dispersions – sodium alginate nanoparticles – and studied the physical, thermal, mechanical, and morphological properties (Scheme 28). Both polymers displayed intense coulombic forces between anionic and cationic groups, which corresponded, respectively, to the carboxylate groups of alginate and the quaternary ammonium functions included in the PU. The thermal stability of the materials increased with increasing of alginate content in the blends. This was due to the higher thermal stability of the uronic acid monomers in comparison with that of the PU. The elastomeric blend can be stretched to more than 11 times its original length without rupture. Thus, the elastomers that contain sodium alginate exhibited excellent mechanical properties and had higher mechanical strengths than the neat cationic PU. The higher strengths and lower elongations may be result of the brittle nature of the uronic residues and the hydrogen bonds between their functional groups and those of PU segments. In addition, the hydrophilicity of PU films rose significantly with addition of sodium alginate content because of the presence of hydrophilic carboxylate and hydroxyl groups of this polysaccharide. The composites showed two interesting nanobead and nanorod morphologies, depending on the molecular weights of the sodium alginate employed.



Scheme 29 Preparation of a PU and grafting polymerization in the presence of calcium alginate gel microspheres (CaA) to give PU-g-CaA

Alginate hydrogels are susceptible to biodegradation and swelling (Leonard et al. 2004), while PUs are endowed of high strength and anti-swelling properties because of its crystallinity (Strand et al. 2003). Wang et al. (2014) proposed the preparation of polyurethane-grafted calcium alginate gel microspheres (PU-g-ACa) with the aim of forming crystallizing areas in the polysaccharide matrix. The addition of physical cross-linking points in grafted PU was expected to provide better thermal and swelling stability. Thus, the PU synthesized by the reaction of isophorone diisocyanate (IPDI), 2-hydroxyethyl methacrylate (HEMA), and diethylene glycol (DEG) (Scheme 29) was polymerized in the presence of the calcium alginate gel microspheres (CaA). The grafting polymerization was carried out using azobisisobutyronitrile (AIBN) as an initiator. The morphology of the surface of starting and final materials was determined by SEM. Such studies revealed that calcium alginate hydrogel microspheres possessed coarse surface and big cavities, while the PU grafted with calcium alginate (PU-g-ACa) showed a dense and smooth surface. These results were attributed to the formation of crystalline regions by hydrophobic PU side chains, which intensified the intermolecular force.

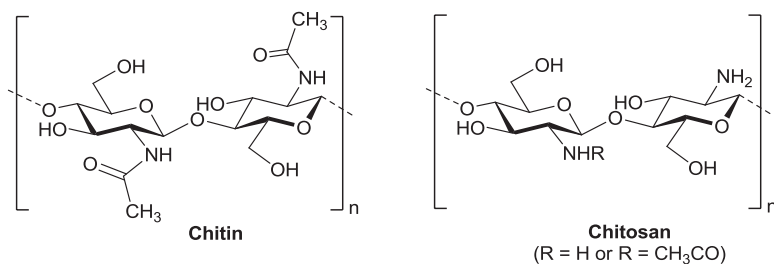
An increase in the grafting reaction temperature first decreased and then the swelling degree increased. This fact was mainly attributed to the formation of crystalline regions of PU side chains that enhance the intermolecular interaction and facilitate the loss of inner water. Meanwhile, the hydrophobic nature of the PU also prevented water diffusion toward the inner material. The minimum swelling degree of PU-g-ACa was decreased to 90% (w/w), lower than the swelling ratios obtained for calcium alginate grafted with polyvinyl acetate (300%) (Ying et al. 2013) and for calcium phosphate/alginate hybrid polymer microspheres (900%) (Zhao et al. 2008).

Alginate may be an interesting candidate for protein imprinting. Molecularly imprinted polymers (MIPs) are cross-linked polymeric networks designed to specifically recognize a target molecule and to be capable of mimicking natural systems (Fu et al. 2008). These materials have been successfully applied to the recognition of small molecules such as sugars, metal ions, and amino acids (Ge and Turner 2008; Wang et al. 2010; Flavin and Resmini 2009; Efe-Sanden and Toomey 2014). However, large size and fragile conformation of proteins bring challenges to MIPs designed for protein imprinting and recognition (Bayer et al. 2011; Verheyen et al. 2011). In this context, the use of alginate for protein imprinting is still challenged by limitations in material stability and recognition sites' precision. Considering these difficulties, some modifications of alginate have been developed, for example, alginate interpenetrating networks (Zhang et al. 2006), alginate blending (Zhao et al. 2008), and alginate-grafted polymer (Ying et al. 2013). However, most of the developments involved a radical reaction in the presence of protein, which led to the denaturation of protein and deterioration of the specific recognition of MIPs.

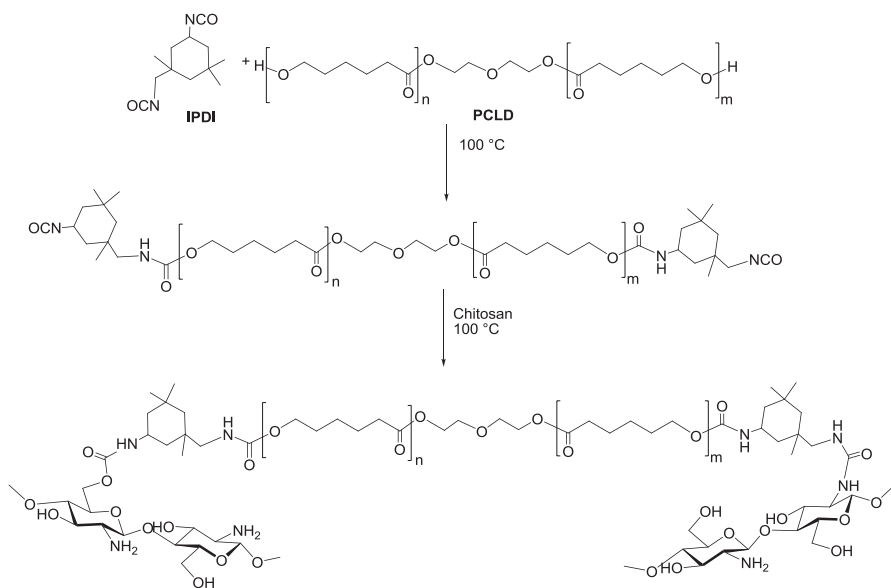
A protein-imprinted hydrogel based on polyurethane-grafted calcium alginate (PU-g-CaA) has been recently prepared (Li et al. 2015). The adsorption behavior, imprinting efficiency, and selectivity of the hydrogel were determined. The grafted PU side chains have been previously confirmed to construct physical cross-linking points and improve the mechanical and chemical stability of hydrogel (Wang et al. 2014). The introduction of PU side chains is useful for the specific recognition of protein, which is confirmed by the enhanced imprinting efficiency. Moreover, the protein is protected from initiator radical denaturation because the grafting modification was performed prior to adding protein templates. The grafting reaction was conducted in aqueous media, before gelating with Ca^{2+} . The PU was synthesized with IPDI, 2-hydroxyethyl methacrylate, and dimethylolpropionic acid. The imprinted polymers with lower grafting ratios were not efficient in maintaining the specific steric structure and the binding capacity was reduced. When the grafting degree increased, more accessible and stable imprinting sites were achieved in MIPs, which led to a higher specific recognition. Compared with calcium alginate, PU-g-CaA MIPs exhibited higher rebinding selectivity and were more capable of recognizing and separating target protein molecules, having nice potential applications for chemical sensing and bio-separation.

4.2 Chitin and Chitosan

Chitin is a high molecular weight polymer of an *N*-acetylglucosamine, which is found as component of the cell walls of fungi and the exoskeletons of arthropods (mainly crustaceans) and insects. Chitin forms crystalline nanofibrils or whiskers and is widely applied for varied medicinal, industrial, and biotechnological purposes. Deacetylation of chitin by alkali yields chitosan, composed of randomly distributed β -(1 \rightarrow 4)-linked *D*-glucosamine and *N*-acetyl-*D*-glucosamine



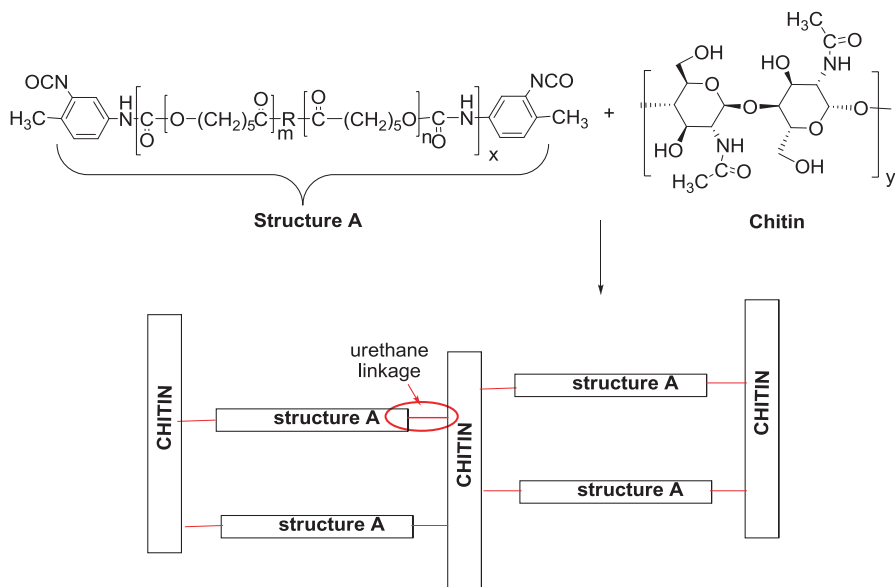
Scheme 30 The repeating units of chitin and chitosan



Scheme 31 Synthesized polycaprolactone (PCL) diisocyanate prepolymers and grafting to chitosan to give biodegradable elastomers

(Scheme 30). The degree of deacetylation in commercial chitosans ranges from 60% to about 100%.

With the aim of obtaining biodegradable PU elastomers with increased hydrophilicity and improved thermal stabilities, Barikani and coworkers synthesized polycaprolactone (PCL) diisocyanate prepolymers, which were grafted to polysaccharides such as starch (Barikani and Mohammadi 2007), chitin (Zia et al. 2008a, b), or chitosan (Barikani et al. 2009, 2010). The route shown in Scheme 31 illustrates the synthesis of chitosan-based biodegradable elastomers. The prepolymers were prepared by reaction of PCL diol (PCLD) with different diisocyanates (HMDI, MDI, or IPDI). It should be noted that the structure depicted in the original papers for the PCL diol was wrong. Therefore, the structures shown in the



Scheme 32 Bioartificial materials prepared by combining chitin and polyurethane diisocyanate prepolymers

following scheme have been corrected. Polysaccharide grafting was achieved by treatment of the prepolymer with different mass ratios of a polysaccharide and a diol (1,4-butanediol or dimethylolpropionic acid or (2,2-bis(hydroxymethyl)propionic acid)).

Bioartificial materials, with potential biomedical applications, have been prepared (Scheme 32) by combining chitin and polyurethane diisocyanate prepolymers (**Structure A**) (Matsui et al. 2012). These polymers were mixed to afford blends or tridimensional networks. Both systems presented high stability with low mass loss in media simulating living tissue. No toxic products were released and the adhesion to Vero cells was low. These preliminary results in vitro indicated that the materials are potentially biocompatible.

The synthesis of shape-memory bionanocomposites based on chitin nanocrystals (CHNCs) and segmented thermoplastic polyurethane (STPU) has been reported (Saralegi et al. 2013). Shape-memory polymers represent a set of materials that can memorize temporary shapes and revert to their permanent shape upon exposure to an external stimulus, such as heat (Liu et al. 2007), light (Lendlein et al. 2005), moisture (Huang et al. 2005; Mendez et al. 2011) or a magnetic field (Mohr et al. 2006). Their ability to change their shape under a predetermined stimulus makes them attractive for biomedical and industrial applications, such as adaptive medical devices (Lendlein and Langer 2002; Metcalfe et al. 2003) implants for minimally invasive surgery (Yakacki et al. 2007), sensors and actuators (Metzger et al. 2002; Small et al. 2005), etc. Due to the thermodynamic

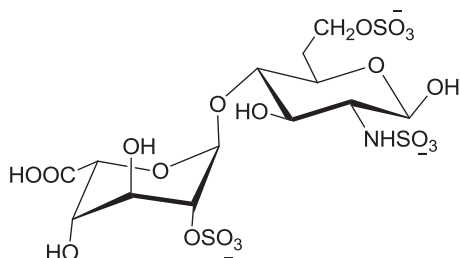
incompatibility between the soft and hard segments (SS and HS, respectively) of PUs, these phases separate and hence these materials are good candidates for shape-memory applications. The SS can act as the switching segment (responsible for shape fixity), which requires glass transition or melting transition in a suitable temperature range. On the other hand, HSs serve as net points and provide the rubber elasticity required for shape recovery.

The shape-memory bionanocomposites based on CHNCs were synthesized by in situ polymerization with variable amounts of nanocrystals (0.25–2 wt%), a semi-crystalline polyol derived from castor oil and propanediol, as corn sugar-based chain extender, in order to maximize the content of carbon from renewable resources. The reaction between hydroxyl groups from CHNC surface and isocyanate groups from polyurethane precursors, either HMDI or prepolymer, resulted in PU chains anchored to CHNCs, improving the dispersion of nanocrystals and increasing the surface roughness. In addition, CHNCs act as nucleation agents rather than chemical cross-linkers, obtaining thermoplastic bionanocomposites, even with 2% of CHNCs. The most important benefit of the addition of CHNCs was the substantial increase of the R_r (shape recovery) values in successive thermomechanical cycles. Neat PU presented poor shape-memory properties, while the addition of CHNCs increased physical cross-linking among hard domains, due to the nucleation effect of such nanoparticles on the hard phase. Thus, bionanocomposites with outstanding shape-memory properties were obtained by adding small amounts of CHNCs (R_r values close to 100% for the second thermomechanical cycle were achieved). Additionally, PU-CHNC bionanocomposites displayed nontoxic behavior; therefore, they are promising candidates for use in biomedical applications as smart materials.

4.3 Heparin

Heparin is a member of the [glycosaminoglycan](#) family, which also includes [heparan sulfate](#), and consists of a variably sulfated [disaccharide](#) as the repeating unit. The most common disaccharide moiety is composed of a 2-*O*-sulfated L-[iduronic acid](#) α -(1,4)-linked to 6-*O,N*-disulfated glucosamine (Scheme 33). This is the main component of heparins from beef lung and porcine intestinal mucosa.

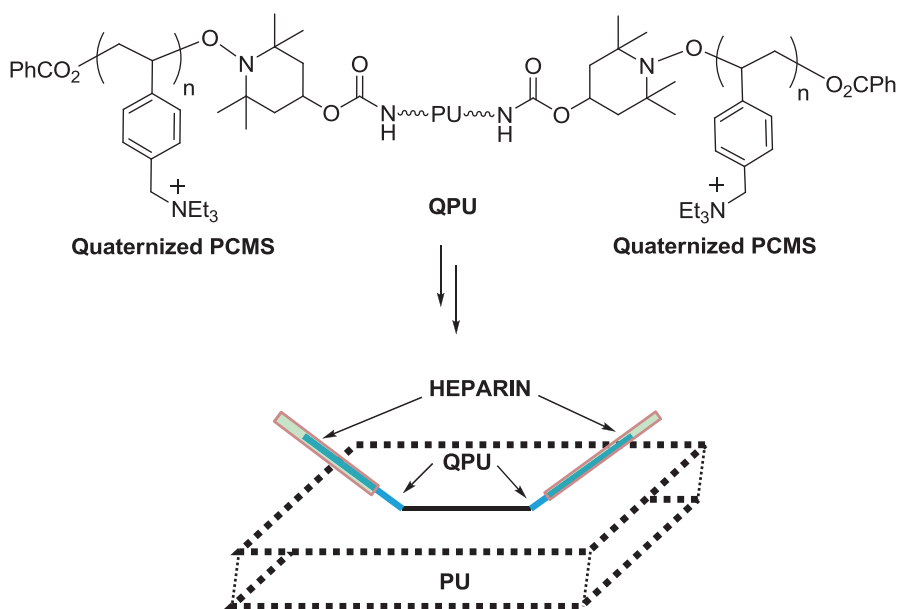
Scheme 33 A common disaccharide moiety of heparin



The functionalization of a PU scaffold surface with heparin beholds great potential for tissue engineering purposes. The porosity of the functionalized scaffold should be considered for each specific application. When used in a load-bearing environment, caution is necessary due to reduction in mechanical stiffness.

Polyurethane scaffolds have been functionalized with diamines and cross-linked to heparin (de Mulder et al. 2013). The PU was a copolymer of polylactic acid and polycaprolactone which reacted with HMDI to introduce urethane bonds. Then, controlled aminolysis of urethane linkages with 1,6-hexanediamine led to free amine groups on the surface of the PU. Subsequently, these scaffolds were cross-linked with heparin. Immunohistochemistry demonstrated that the biopolymer was homogeneously distributed throughout the 3D porous scaffold and over the entire film. Young's modulus decreased significantly till 50% of the native stiffness after aminolysis and did not change after heparin cross-linking. The decrease of contact angle on PU films indicated a more hydrophilic surface, which could potentially result in a faster ingrowth of cells and tissues when cultured or implanted. Furthermore, subcutaneously implanted heparin coated on polymer scaffolds increased neovascularization, which can enhance tissue regeneration.

Macromolecular surface modifiers with high affinity for host polymeric molecules could resist erosion and extraction by several common solvents such as water, ethanol, and acetone (Xu et al. 2010). A polyurethane-block-poly(chloromethyl styrene) (PU-b-PCMS) copolymer was synthesized by coupling hydroxyl-terminated poly(chloromethyl styrene) with a diisocyanate-terminated polyurethane and further quaternized with triethylamine (Scheme 34). The resulting QPU was used as a



Scheme 34 Surface modification of PU by blending

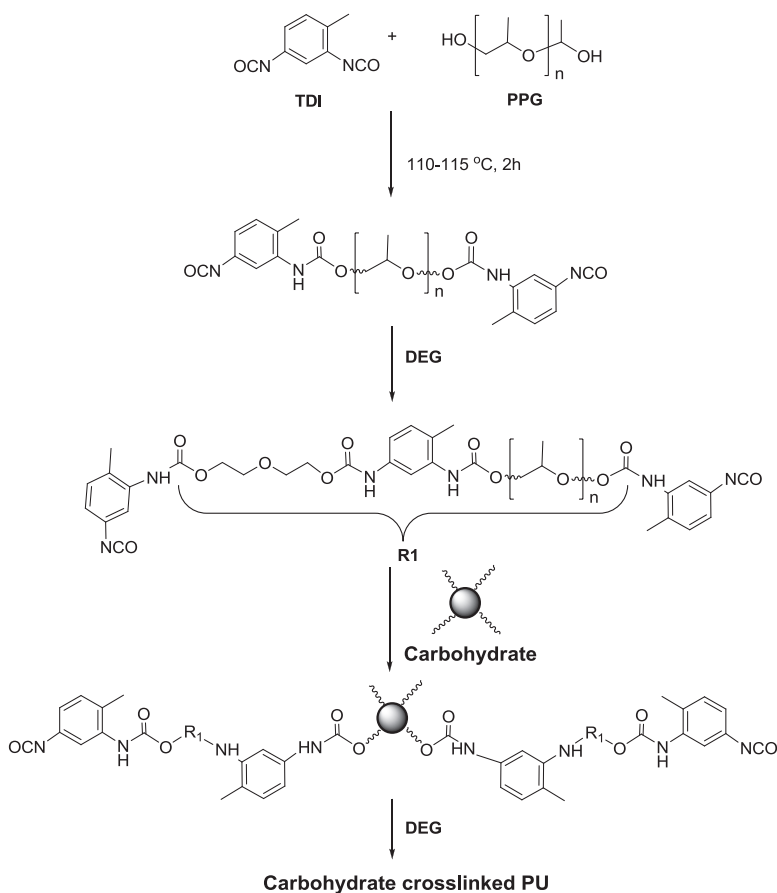
macromolecular biocompatible surface modifier of the PU, in order to achieve a cationic surface able to interact with anionic heparin (Zhang et al. 2015). The surface modifier was blended with polyurethane and heparin was absorbed on the cationic surface. This modification gave a heparin surface on the PU and effectively increased hydrophilicity and water absorption, in comparison with bare PU film. In addition, the product showed lower platelet adhesion, lower extent of hemolysis, and longer plasma recalcification times. The surface-modified films could maintain a better cell viability than the host material. All the results indicated that the blood and cell compatibilities of the heparinized PU films were improved significantly, demonstrating that this surface-modified PU was biocompatible and potentially useful as a biomaterial.

Polyurethane–heparin nanoparticles (PU-Hep-NPs) have been employed to prepare an electrochemical glucose biosensor that can be used directly for whole blood samples (Sun et al. 2013). The accurate measurement of glucose is extremely important in the diagnosis of diabetes and prediabetes. The amperometric glucose biosensor was found to keep excellent blood compatibility and did not induce coagulation when used to detect glucose in the whole blood directly. The anticoagulation properties of PU-Hep-NPs can efficiently suppress blood–cell adhesion and increase the microenvironment for glucose oxidase to undergo facile electron-transfer reactions. The sensor was applied to determine glucose in human blood samples of diabetic and healthy people. The samples were first analyzed in the hospital by traditional procedures and then with the proposed biosensor, giving very close values. These novel electrochemical biosensors can be conveniently applied to evaluate the level of blood glucose with the help of antibiofouling technology.

4.4 Starch and Cellulose

Starch and cellulose are well-known polysaccharides composed of glucose (glucanes) which are widely distributed in nature. Starch, which is found in large amounts in potatoes, wheat, corn, and rice, consists of two types of molecules, the linear amylose and the branched amylopectin. The main chain of both molecules is formed by glucose residues bonded by $\alpha(1\rightarrow4)$ linkages. Depending on the plant, starch generally contains 20–25% amylose and 75–80% amylopectin by weight. Cellulose is a linear chain polysaccharide consisting of several hundreds to many thousands of $\beta(1\rightarrow4)$ -linked D-glucose units.

Biocompatible and biodegradable PUs based on castor oil and polypropylene glycols were prepared using various carbohydrate cross-linkers (Scheme 35): monosaccharide (glucose), disaccharide (sucrose), and polysaccharides (starch and cellulose) (Solanki et al. 2014). The mechanical and thermal properties were investigated and interpreted on the basis of SEM analysis. The advantage of incorporating carbohydrates is to have tunable mechanical properties and biodegradability. The polyol type has a more pronounced effect than the cross-linker type on the glass transition temperature and sorption behavior. The study supports the suitability of



Scheme 35 Synthesis of a cross-linked carbohydrate-based PU

carbohydrates as important components of biocompatible PUs for development of biomedical devices. The combination of polyols and carbohydrates led to a wide spectrum of significant mechanical properties, which can be further tuned by varying the NCO/OH ratio and polyol/cross-linker ratio.

Furthermore, the PUs possessed reasonable thermal stability and interesting sorption properties, along with biodegradability and biocompatibility for potential applications as drug delivery systems. The drug loading and release kinetics were studied by using lamotrigine as a model drug. Lamotrigine is an antiepileptic agent employed for the treatment of seizures. The polymers were designed in such a way that the drug release was tailored by differences in the stoichiometry of polymers (Solanki et al. 2015). PU films were obtained via a prepolymer, prepared from polypropylene glycol (PPG) 2000 and 2,4-toluene diisocyanates (TDI), while glucose, starch, and cellulose were used as cross-linkers and diethylene glycol (DEG) as chain extender.

The carbohydrate cross-linker plays a major role for enhanced mechanical properties, such as an increased mechanical strength. Also, the incorporation of the carbohydrate into the PU network results in the formation of amorphous polymer–polymer microdomains, which resembles an integrated system formed due to the presence of covalent and hydrogen bonds between the components. The kinetics and release mechanisms were determined to be a function of the type of cross-linker (glucose, cellulose, or starch), polyol/cross-linker ratio, and polyol/chain extender ratio. All the PUs were observed to be non-cytotoxic in normal lung cell line L132 and exhibited good mechanical strength, tunable release rates, and biocompatibility. Due to these properties, they are potentially useful for biomedical applications like wound dressing, biomedical implants, and drug delivery carriers.

Several commercially available cellulose derivatives differing in the type of substituent and substitution degree (α -cellulose, methylcellulose, 2-hydroxyethylcellulose, methyl 2-hydroxyethylcellulose, and cellulose acetate/propionate) have been functionalized with HMDI and subsequently dispersed in castor oil to obtain chemical oleogels. These materials may be used in lubricating grease formulations completely based on renewable resources (Gallego et al. 2015). The oleogels showed a wide range of rheological properties and thermal stability. Cellulose derivatives used as thickeners exhibited a reduced thermal resistance after NCO functionalization due to the inclusion of the HMDI segments in the cellulose structure. However, the resulting oleogels presented suitable thermal resistance. The rheological responses obtained, from solid-like to weak gels, were found to be basically dependent on the balance of the molar ratio between nonpolar and polar substituents in the biopolymer and on the size of these substituents. The presence of nonpolar groups reduces cellulose polarity and, therefore, increases the affinity by the oil medium, while large substituents seem to hinder the development of the three-dimensional gel network. Thus, the rheological response of NCO-functionalized methyl 2-hydroxyethylcellulose- and methylcellulose-based oleogels corresponds to a solid-like gel behavior, characteristic of traditional lubricating greases. Consequently, these systems have been proposed as promising biobased alternatives to such products. On the other hand, NCO-functionalized α -cellulose, 2-hydroxyethylcellulose, and cellulose acetate/propionate provided weak gels in castor oil, as a consequence of high polarity and/or larger substituents.

5 Concluding Remarks

This overview about the recent advances in the development and applications of polyurethanes derived from carbohydrates, one of the most important renewable resources, highlighted the great diversity of biobased materials that can be obtained. In the field of sugar-based polyurethanes, monomers have been prepared entirely from common sugars, while others result from the combination of natural biopolymers with synthetic monomers or polymers. Also, PUs with carbohydrates as pendant groups or as constituents of the soft part of the polymer chain have been reported.

The properties can be tailored by selecting the proper building blocks, in order to get improved physical–mechanical behavior and features such as bio-identity, biocompatibility, and biodegradability. The carbohydrate-based polymers are witnessing a rapid ascent, pushing the limits of their potential applications in the areas of material sciences, biomedicine, and technology.

Acknowledgments Financial support by the National Research Council of Argentina (CONICET, Project PIP 11220110100370CO), the National Agency for Promotion of Science and Technology (ANPCyT, PICT 2012-0717), and the University of Buenos Aires (Project 20020130100571BA) is gratefully acknowledged. The authors are research members from CONICET.

References

- Abenhaïm D, Loupy A, Munnier L, Tamion R, Marsais F, Quéguiner G (1994) Selective alkylations of 1,4:3,6-dianhydro-D-glucitol (isosorbide). *Carbohydr Res* 261:255–266
- Abraham GA, Marcos-Fernández A, Román JS (2006) Bioresorbable poly(ester-ether urethane)s from L-lysine diisocyanate and triblock copolymers with different hydrophilic character. *J Biomed Mater Res* 76A:729–736
- Alves P, Ferreira P, Gil MH (2012) Biomedical polyurethanes-based materials. In: Cavaco LI, Almeida Melo J (eds) *Polyurethane: properties, structure and applications*, Polymer science and technology. Nova Science Publishers, New York, pp 25–50
- Arce SM, Kolender AA, Varela O (2010) Synthesis of ω -amino- α -phenylcarbonate alkanes and their polymerization to [n]-polyurethanes. *Polym Int* 59:1212–1220
- Bachmann F, Reimer J, Ruppenstein M, Thiem J (1998) Synthesis of a novel starch-derived AB-type polyurethane. *Macromol Rapid Commun* 19:21–26
- Bachmann F, Reimer J, Ruppenstein M, Thiem J (2001) Synthesis of novel polyurethanes and polyureas by polyaddition reactions of dianhydrohexitol configured diisocyanates. *Macromol Chem Phys* 202:3410–3419
- Barikani M, Mohammadi M (2007) Synthesis and characterization of starch-modified polyurethane. *Carbohydr Polym* 68:773–780
- Barikani M, Honarkar H, Barikani M (2009) Synthesis and characterization of polyurethane elastomers based on chitosan and poly(ϵ -caprolactone). *J Appl Polym Sci* 112:3157–3165
- Barikani M, Honarkar H, Barikani M (2010) Synthesis and characterization of chitosan-based polyurethane elastomer dispersions. *Monatsh Chem* 141:653–659
- Bayer CL, Pérez Herrero E, Peppas NA (2011) Alginate films as macromolecular imprinted matrices. *J Biomater Sci Polym Ed* 22:1523–1534
- Begines B, Zamora F, Roffé I, Mancera M, Galbis JA (2011) Sugar-based hydrophilic polyurethanes and polyureas. *J Polym Sci Part A: Polym Chem* 49:1953–1961
- Begines B, Zamora F, Benito E, García-Martín MDG, Galbis JA (2012) Conformationally restricted linear polyurethanes from acetalized sugar-based monomers. *J Polym Sci Part A: Polym Chem* 50:4638–4646
- Beldi M, Medimagh R, Chatti S, Marque S, Prim D, Loupy A, Delolme F (2007) Characterization of cyclic and non-cyclic poly-(ether-urethane)s bio-based sugar diols by a combination of MALDI-TOF and NMR. *Eur Polym J* 43:3415–3433
- Besse V, Auvergne R, Carlotti S, Boutevin G, Otazaghine B, Caillol S, Pascault JP, Boutevin B (2013) Synthesis of isosorbide based polyurethanes: an isocyanate free method. *React Funct Polym* 73:588–594
- Campañez MD, Aguilar-de-Leyva A, Ferris C, de Paz MV, Galbis JA, Caraballo I (2013) Study of the properties of the new biodegradable polyurethane PU (TEG-HMDI) as matrix forming excipient for controlled drug delivery. *Drug Dev Ind Pharm* 39:1758–1764

- Cascone MG (1997) Dynamic–mechanical properties of bioartificial polymeric materials. *Polym Int* 43:55–69
- Cascone MG, Barbani N, Cristallini C, Giusti P, Ciardelli G, Lazzeri L (2001) Bioartificial polymeric materials based on polysaccharides. *J Biomater Sci Polym Ed* 12:267–281
- Cherng JY, Hou TY, Shih MF, Talsma H, Hennink WE (2013) Polyurethane-based drug delivery systems. *Int J Pharm* 450:145–162
- Cognet-Georjon E, Mechin F, Pascault JP (1995) New polyurethanes based on diphenylmethane diisocyanate and 1,4:3,6-dianhydrosorbitol, 1. Model kinetic studies and characterization of the hard segment. *Makromol Chem* 196:3733–3751
- Daemi H, Barikani M, Barmar M (2013) Highly stretchable nanoalginate based polyurethane elastomers. *Carbohydr Polym* 95:630–636
- Datta J, Włoch M (2016) Progress in non-isocyanate polyurethanes synthesized from cyclic carbonate intermediates and di- or polyamines in the context of structure-properties relationship and from an environmental point of view. *Polym Bull* 73:1459–1496
- Delebecq E, Pascault J-P, Boutevin B, Ganachaud F (2013) On the versatility of urethane/urea bonds: reversibility, blocked isocyanate, and non-isocyanate polyurethane. *Chem Rev* 113:80–118
- Dieterich D (1981) Aqueous emulsions, dispersions and solutions of polyurethanes: synthesis and properties. *Prog Org Coat* 9:281–340
- Dirlikov SK, Schneider CJ (1984) Polyurethanes based on 1,4-3:6 dianhydrohexitols. US Patent 4,443,563
- Donnelly MJ, Still RH, Stanford JL (1991) The conversion of polysaccharides into polyurethanes: a review. *Carbohydr Polym* 14:221–240
- Donnelly MJ, Stanford JL, Still RH (1993) Polyurethanes from renewable resources –I: properties of polymers derived from glucose and xylose based polyols. *Polym Int* 32:197–203
- Draget KI (2009) Alginates. In: Phillips GO, Williams PA (eds) *Handbook of hydrocolloids*. Woodhead Publishing Limited, Elsevier, Cambridge, pp 807–828
- Drotleff S, Lungwitz U, Breunig M, Dennis A, Blunk T, Göpferich A (2004) Biomimetic polymers in pharmaceutical and biomedical sciences. *Eur J Pharm Biopharm* 58:385–407
- Efe-Sanden G, Toomey R (2014) Poly(N-isopropylacrylamide) networks conjugated with Gly–Gly–his via a Merrifield solid-phase peptide synthesis technique for metal-ion recognition. *Macromol Chem Phys* 215:1342–1349
- Fenouillot F, Rousseau A, Colomines G, Saint-Loup R, Pascault J-P (2010) Polymers from renewable 1,4:3,6-dianhydrohexitols (isosorbide, isomannide and isoidide): a review. *Prog Polym Sci* 35:578–622
- Fernández CE, Bermúdez M, Versteegen RM, Meijer EW, Vancso GJ, Muñoz-Guerra S (2010) An overview on 12-polyurethane: synthesis, structure and crystallization. *Eur Polym J* 46:2089–2098
- Ferris C, De Paz MV, Zamora F, Galbis JA (2010) Dithiothreitol-based polyurethanes. Synthesis and degradation studies. *Polym Degrad Stab* 95:1480–1487
- Ferris C, De Paz MV, Galbis JA (2011) L-arabinitol-based functional polyurethanes. *J Polym Sci Part A: Polym Chem* 49:1147–1154
- Ferris C, de Paz MV, Galbis JA (2012) Synthesis of functional sugar-based polyurethanes. *Macromol Chem Phys* 213:480–488
- Ferris C, de Paz MV, Aguilar-de-Leyva A, Caraballo I, Galbis JA (2014) Reduction-sensitive functionalized copolyurethanes for biomedical applications. *Polym Chem* 5:2370–2381
- Fidalgo DM, Kolender AA, Varela O (2013) Stereoregular poly-O-methyl [m, n]-polyurethanes derived from D-mannitol. *J Polym Sci Part A: Polym Chem* 51:463–470
- Flavin K, Resmini M (2009) Imprinted nanomaterials: a new class of synthetic receptors. *Anal Bioanal Chem* 393:437–444
- Fu G-Q, Yu H, Zhu J (2008) Rebinding and recognition properties of protein-macromolecularly imprinted calcium phosphate/alginate hybrid polymer microspheres. *Biomaterials* 29:2138–2142
- Furukawa M, Mitsui Y, Fukumaru T, Kojio K (2005) Microphase-separated structure and mechanical properties of novel polyurethane elastomers prepared with ether based diisocyanate. *Polymer* 46:10817–10822

- Galbis JA, García-Martín MG, de Paz MV, Galbis E (2016) Synthetic polymers from sugar-based monomers. *Chem Rev* 116:1600–1636
- Gallagher JJ, Hillmyer MA, Reineke TM (2014) Degradable thermosets from sugar-derived dilactones. *Macromolecules* 47:498–505
- Gallego R, Arteaga JF, Valencia C, Franco JM (2015) Thickening properties of several NCO-functionalized cellulose derivatives in castor oil. *Chem Eng Sci* 134:260–268
- Gandini A, Lacerda TM, Carvalho AJF, Trovatti E (2016) Progress of polymers from renewable resources: furans, vegetable oils, and polysaccharides. *Chem Rev* 116:1637–1669
- Garçon R, Clerk C, Gesson JP, Bordado J, Nunes T, Carço S, Gomes PT, Minas da Piedade ME, Rauter AP (2001) Synthesis of novel polyurethanes from sugars and 1,6-hexamethylene diisocyanate. *Carbohydr Polym* 45:123–127
- Ge Y, Turner APF (2008) Too large to fit? Recent developments in macromolecular imprinting. *Trends Biotechnol* 26:218–224
- Giusti P, Lazzeri L, Petris S, Palla M, Cascone MG (1994) Collagen-based new bioartificial polymeric materials. *Biomaterials* 15:1229–1233
- Gomez RV, Varela O (2009) Synthesis of polyhydroxy [n]-polyurethanes derived from a carbohydrate precursor. *Macromolecules* 42:8112–8117
- Hashimoto K, Okada M, Honjoh N (1990) Ring-opening polyaddition of D-glucaro-1,4:6,3-dilactone with p-xylylenediamine. *Makromol Chem Rapid Commun* 11:393–396
- Hashimoto K, Mori K, Okada M (1992) Anionic ring-opening polymerization of a novel optically active bicyclic lactam synthesized from an acidic saccharide. *Macromolecules* 25:2592–2598
- Hashimoto K, Wibullucksanakul S, Matsuera M, Okada M (1993a) Macromolecular synthesis from saccharic lactones. Ring-opening polyaddition of D-glucaro- and D-mannaro-1,4:6,3-dilactones with alkylenediamines. *Polym Sci Part A: Polym Chem* 31:3141–3149
- Hashimoto K, Wibullucksanakul S, Okada M (1993b) Polyaddition of saccharic dilactones with hexamethylene diisocyanate. *Chem Rapid Commun* 14:591–595
- Hashimoto K, Hashimoto N, Kamaya T, Yoshioka J, Okawa H (2011) Synthesis and properties of bio-based polyurethanes bearing hydroxy groups derived from alditols. *J Polym Sci Part A: Polym Chem* 49:976–985
- Haug A, Larsen B, Smidsrod O (1966) A study of the constitution of alginic acid by partial acid hydrolysis. *Acta Chem Scand* 20:183–190
- van Haveren J, Scott EL, Sanders J (2008) Bulk chemicals from biomass. *Biofuels Bioprod Biorefin* 2:41–57
- Hu S, Luo X, Li Y (2014) Polyols and polyurethanes from the liquefaction of lignocellulosic biomass. *ChemSusChem* 7:66–72
- Huang WM, Yang B, An L, Li C, Chan YS (2005) Water-driven programmable polyurethane shape memory polymer: demonstration and mechanism. *Appl Phys Lett* 86:114105
- Kihara N, Endo T (1993) Synthesis and properties of poly(hydroxyurethane)s. *J Polym Sci Part A: Polym Chem* 31:2765–2773
- Kihara N, Cusida Y, Endo T (1996) Optically active poly(hydroxyurethane)s derived from cyclic carbonate and L-lysine derivatives. *J Polym Sci Part A: Polym Chem* 34:2173–2179
- Kim H-J, Kang M-S, Knowles JC, Gong M-S (2014) Synthesis of highly elastic biocompatible polyurethanes based on bio-based isosorbide and poly(tetramethylene glycol) and their properties. *J Biomater Appl* 29:454–464
- Kloosterboer JG (1988) Network formation by chain crosslinking photopolymerization and its applications in electronics. *Adv Polym Sci* 84:1–61
- Kolender AA, Arce SM, Varela O (2011) Synthesis and characterization of poly-O-methyl-[n]-polyurethane from a D-glucamine-based monomer. *Carbohydr Res* 346:1398–1405
- Kricheldorf HR (1997) Sugar diols as building blocks of polycondensates. *J Macromol Sci Rev Macromol Chem Phys* 37:599–631
- Król P (2009) Polyurethanes – a review of 60 years of their syntheses and applications. *Polimery* 54:489–500
- Langer R, Cima LG, Tamada JA, Wintermantel E (1990) Future directions in biomaterials. *Biomaterials* 11:738–745

- Lee CH, Takagi H, Okamoto H, Kato M, Usuki A (2009) Synthesis, characterization, and properties of polyurethanes containing 1,4:3,6-dianhydro-D-sorbitol. *J Polym Sci A Polym Chem* 47:6025–6031
- Lendlein A, Langer R (2002) Biodegradable, elastic shape-memory polymers for potential biomedical applications. *Science* 296:1673–1676
- Lendlein A, Jiang H, Junger O, Langer R (2005) Light-induced shape-memory polymers. *Nature* 434:879–882
- Leonard M, Rastello de Boisseon M, Hubert P, Dellacherie E (2004) Production of microspheres based on hydrophobically associating alginate derivatives by dispersion/gelation in aqueous sodium chloride solutions. *J Biomed Mater Res* 68A:335–342
- Li Y, Noordover BAJ, van Benthem RATM, Koning CE (2014a) Reactivity and regio-selectivity of renewable building blocks for the synthesis of water-dispersible polyurethane prepolymers. *ACS Sustain Chem Eng* 2:788–797
- Li Y, Noordover BAJ, van Benthem RATM, Koning CE (2014b) Property profile of poly(urethane urea) dispersions containing dimer fatty acid-, sugar- and amino acid-based building blocks. *Eur Polym J* 59:8–18
- Li L, Ying X, Liu J, Li X, Zhang W (2015) Molecularly imprinted polyurethane grafted calcium alginate hydrogel with specific recognition for proteins. *Mater Lett* 143:248–251
- Lim D-I, Park H-S, Park J-H, Knowles JC, Gong M-S (2013) Application of high-strength biodegradable polyurethanes containing different ratios of biobased isomannide and poly(ϵ -caprolactone) diol. *J Bioact Compat Polym* 28:274–288
- Liu C, Qin H, Mather PT (2007) Review of progress in shape-memory polymers. *J Mater Chem* 17:1543–1558
- Liu X, Xu K, Liu H, Cai H, Su J, Fu Z, Guo Y, Chen M (2011) Preparation and properties of waterborne polyurethanes with natural dimer fatty acids based polyester polyol as soft segment. *Prog Org Coat* 72:612–620
- Marín R, Muñoz-Guerra S (2008) Linear polyurethanes made from threitol: acetalized and hydroxylated polymers. *J Polym Sci Part A: Polym Chem* 46:7996–8012
- Marín R, de Paz MV, Ittobane N, Galbis JA, Muñoz-Guerra S (2009) Hydroxylated linear polyurethanes derived from sugar alditols. *Macromol Chem Phys* 210:486–494
- Marín R, Alla A, Martínez de Ilarduya A, Muñoz-Guerra S (2012) Carbohydrate-based polyurethanes: a comparative study of polymers made from isosorbide and 1,4-butanediol. *J Appl Polym Sci* 123:986–994
- Matsui M, Ono L, Akcelrud L (2012) Chitin/polyurethane networks and blends: evaluation of biological application. *Polym Test* 31:191–196
- Mendez J, Annamalai PK, Eichhorn SJ, Rusli R, Rowan SJ, Foster EJ, Weder C (2011) Bioinspired mechanically adaptive polymer nanocomposites with water-activated shape-memory effect. *Macromolecules* 44:6827–6835
- Metcalfe A, Desfaits AC, Salazkin I, Yahia L, Sokolowski WM, Raymond J (2003) Cold hibernated elastic memory foams for endovascular interventions. *Biomaterials* 24:491–497
- Metzger MF, Wilson TS, Schumann D, Matthews DL, Maitland DJ (2002) Mechanical properties of mechanical actuator for treating ischemic stroke. *Biomed Microdevices* 4:89–96
- Mohr R, Kratz K, Weigel T, Lucka-Gabor M, Moneke M, Lendlein A (2006) Initiation of shape-memory effect by inductive heating of magnetic nanoparticles in thermoplastic polymers. *Proc Natl Acad Sci U S A* 103:3540–3545
- Mørch YA, Holtan S, Donati I, Strand BL, Skjåk-Braek G (2007) Effect of Ca^{2+} , Ba^{2+} , and Sr^{2+} on alginate microbeads. *Biomacromolecules* 7:1471–1480
- de Mulder ELW, Hannink G, Koens MJW, Löwik DWPM, Verdonschot N, Buma P (2013) Characterization of polyurethane scaffold surface functionalization with diamines and heparin. *J Biomed Mater Res Part A* 101A:919–922
- Nohra B, Candy L, Blanco JF, Guerin C, Raoul Y, Mouloungim Z (2013) From petrochemical polyurethanes to biobased polyhydroxyurethanes. *Macromolecules* 46:3771–3792
- Noreen A, Mahmood Zia K, Zuber M, Tabasum S, Fawad Zahoor A (2016) Bio-based polyurethane: an efficient and environment friendly coating systems. *Prog Org Coat* 91:25–32

- Oh S-Y, Kang M-S, Knowles JC, Gong M-S (2015) Synthesis of bio-based thermoplastic polyurethane elastomers containing isosorbide and polycarbonate diol and their biocompatible properties. *J Biomater Appl* 30:327–337
- Parisi M, Manzano VE, Flor S, Lissarrague MH, Ribba L, Lucangioli S, D'Accorso NB, Goyanes S (2015) Polymeric prosthetic systems for sitespecific drug administration: physical and chemical properties. In: Kumar Thakur V, Kumari Thakur M (eds) *Handbook of polymers for pharmaceutical technologies, structure and chemistry, Structure and chemistry, vol 1*. Scrivener Publishing/Wiley, Hoboken, pp 369–412
- Park H-S, Gong M-S, Knowles JC (2013) Catalyst-free synthesis of high elongation degradable polyurethanes containing varying ratios of isosorbide and polycaprolactone: physical properties and biocompatibility. *J Mater Sci Mater Med* 24:281–294
- de Paz MV, Marín R, Zamora F, Hakkou K, Alla A, Galbis JA, Muñoz-Guerra S (2007) Linear polyurethanes derived from alditols and diisocyanates. *J Polym Sci Part A: Polym Chem* 45:4109–4117
- de Paz MV, Zamora F, Begines B, Ferris C, Galbis JA (2010) Glutathione-mediated biodegradable polyurethanes derived from L-arabinitol. *Biomacromolecules* 11:269–276
- Prömpers G, Keul H, Höcker H (2005) Polyurethanes with pendant hydroxy groups: polycondensation of D-mannitol-1,2:5,6-dicarbonate with diamines. *Des Monomers Polym* 8:547–569
- Prömpers G, Keul H, Höcker H (2006) Polyurethanes with pendant hydroxy groups: polycondensation of 1,6-bis-O-phenoxy-carbonyl-2,3:4,5-di-O-isopropylidene-galactitol and 1,6-di-O-phenoxy-carbonyl-galactitol with diamines. *Green Chem* 8:467–478
- Rees DA, Samuel JWB (1967) The structure of alginic acid. Part VI Minor features and structural variations. *J Chem Soc C*:2295–2298
- Rokicki G, Piotrowska A (2002) A new route to polyurethanes from ethylene carbonate. *Polymer* 43:2927–2935
- Rokicki G, Parzuchowski, Mazurek M (2015) Non-isocyanate polyurethanes: synthesis, properties, and applications. *Polym Adv Technol* 26:707–761
- Sanda F, Takata T, Endo T (1995) Synthesis of a novel optically active nylon-1 polymer: anionic polymerization of L-leucine methylester isocyanate. *J Polym Sci A Polym Chem* 33:2353–2358
- Saralegi A, Fernandes SCM, Alonso-Varona A, Palomares T, Foster EJ, Weder C, Eceiza A, Corcuera MA (2013) Shape-memory bionanocomposites based on chitin nanocrystals and thermoplastic polyurethane with a highly crystalline soft segment. *Biomacromolecules* 14:4475–4482
- Sardon H, Irusta L, Fernández-Berridi MJ (2009) Synthesis of isophorone diisocyanate (IPDI) based waterborne polyurethanes: comparison between zirconium and tin catalysts in the polymerization process. *Prog Org Coat* 66:291–295
- Savelyev Y, Markovskaya L, Olga Savelyeva O, Akhranovich E, Parkhomenko N, Travinskaya T (2015) Degradable polyurethane foams based on disaccharides. *J Appl Polym Sci* 132:42131
- Sideridou ID, Achilias DS, Karava O (2006) Reactivity of benzoyl peroxide/amine system as an initiator for the free radical polymerization of dental and orthopaedic dimethacrylate monomers: effect of the amine and monomer chemical structure. *Macromolecules* 39:2072–2080
- Sionkowska A (2013) Natural polymers as components of blends for biomedical applications. In: Dumitriu S, Popa V (eds) *Polymeric biomaterials, Structure and Function, vol 1*. CRC Press, Boca Raton, pp 309–342
- Small W, Wilson TS, Bennett WJ, Loge J, Maitland D (2005) Laser-activated shape memory polymer intravascular thrombectomy device. *Opt Express* 13:8204–8213
- Solanki A, Mehta J, Thakore S (2014) Structure–property relationships and biocompatibility of carbohydrate crosslinked polyurethanes. *Carbohydr Polym* 110:338–344
- Solanki AR, Kamath BV, Thakore S (2015) Carbohydrate crosslinked biocompatible polyurethanes: synthesis, characterization, and drug delivery studies. *J Appl Polym Sci* 132:42223
- Strand BL, Mørch YA, Syvertsen KR, Espevik T, Skjåk-Braek G (2003) Visualization of alginate–poly-L-lysine–alginate microcapsules by confocal laser scanning microscopy. *Biotechnol Bioeng* 82:386–394
- Sun X, Gao H, Wu G, Wang Y, Fan Y, Ma J (2011) Biodegradable and temperature-responsive polyurethanes for adriamycin delivery. *Int J Pharm* 412:52–58

- Sun C, Niu Y, Tong F, Mao C, Huang X, Zhao B, Shen J (2013) Preparation of novel electrochemical glucose biosensors for whole blood based on antibiofouling polyurethane-heparin nanoparticles. *Electrochim Acta* 97:349–356
- Szycher M (2013) Waterborne polyurethanes. In: Szycher M (ed) *Szycher's handbook of polyurethanes*, 2nd edn. CRC Press, Boca Raton, pp 417–448
- Thiem J, Lüders H (1986) Synthesis and properties of polyurethanes derived from diaminodianhydroalditols. *Makromol Chem* 187:2775–2785
- Tomita H, Sand F, Endo T (2001) Structural analysis of polyhydroxyurethane obtained by polyaddition of bifunctional five-membered cyclic carbonate and diamine based on the model reaction. *J Polym Sci Part A: Polym Chem* 39:851–859
- Travinskaya T, Savelyev Y, Mishchuk E (2014) Waterborne polyurethane based starch containing materials: preparation, properties and study of degradability. *Polym Degrad Stab J* 101:102–108
- Varma AJ, Kennedy JF, Galgali P (2004) Synthetic polymers functionalized by carbohydrates: a review. *Carbohydr Polym* 56:429–445
- Velankar S, Cooper SL (1998) Microphase separation and rheological properties of polyurethane melts. 1. Effect of block length. *Macromolecules* 31:9181–9192
- Velankar S, Cooper SL (2000a) Microphase separation and rheological properties of polyurethane melts. 2. Effect of block incompatibility on the microstructure. *Macromolecules* 33:382–394
- Velankar S, Cooper SL (2000b) Microphase separation and rheological properties of polyurethane melts. 3. Effect of block incompatibility on the viscoelastic properties. *Macromolecules* 33:395–403
- Venkatesan J, Bhatnagar I, Manivasagan P, Kang K, Kim S (2015) Alginate composites for bone tissue engineering: a review. *Int J Biol Macromol* 72:269–281
- Verheyen E, Schillemans JP, van Wijk M, Demeniex M-A, Hennink WE, van Nostrum CF (2011) Challenges for the effective molecular imprinting of proteins. *Biomaterials* 32:3008–3020
- Versteegen RM, Sijbesma RP, Meijer EW (1999) [n]-polyurethanes: synthesis and characterization. *Angew Chem Int Ed* 38:2917–2919
- Vlakh EG, Tennikova TB (2009) Applications of polymethacrylate-based monoliths in high-performance liquid chromatography. *J Chromatogr A* 1216:2637–2650
- Wang Y, Zhang Z, Jain V, Yi J, Mueller S, Sokolov J, Liu Z, Levon K, Rigas B, Rafailovich MH (2010) Potentiometric sensors based on surface molecular imprinting: detection of cancer biomarkers and viruses. *Sensors Actuators B Chem* 146:381–387
- Wang J, Ying X, Li X, Zhang W (2014) Preparation, characterization and swelling behaviors of polyurethane-grafted calcium alginate hydrogels. *Mater Lett* 126:263–266
- Whelan Jr JM, Hill M, Cotter RJ (1963) Multiple cyclic carbonate polymers. US Patent 3072613
- Wibullucksanakul S, Hashimoto K, Okada M (1996a) Synthesis of polyurethanes from saccharide-derived diols and diisocyanates and their hydrolyzability. *Macromol Chem Phys* 197:135–146
- Wibullucksanakul S, Hashimoto K, Okada M (1996b) Swelling behavior and controlled release of new hydrolyzable poly(ether urethane) gels derived from saccharide and L-lysine derivatives and poly(ethylene glycol). *Macromol Chem Phys* 197:1865–1876
- Wibullucksanakul S, Hashimoto K, Okada M (1997) Hydrolysis and release behavior of hydrolyzable poly(etherurethane) gels derived from saccharide-, L-lysine-derivatives, and poly(propylene glycol). *Macromol Chem Phys* 198:305–319
- Witt U, Einig T, Yamamoto M, Kleeberg I, Deckwer WD, Muller RJ (2001) Biodegradation of aliphatic-aromatic copolyesters: evaluation of the final biodegradability and ecotoxicological impact of degradation intermediates. *Chemosphere* 44:289–299
- Xu M, Shi XH, Chen HJ, Xiao T (2010) Synthesis and enrichment of a macromolecular surface modifier PP-b-PVP for polypropylene. *Appl Surf Sci* 256:3240–3244
- Yakacki CM, Shandas R, Lanning C, Rech B, Eckstein A, Gall K (2007) Unconstrained recovery characterization of shape-memory polymer networks for cardiovascular applications. *Biomaterials* 28:2255–2263
- Yamanaka C, Hashimoto K (2002) Synthesis of new hydrolyzable polyurethanes from L-gulonic acid-derived diols and diisocyanates. *J Polym Sci Part A: Polym Chem* 40:4158–4166

- Ying X, Qi L, Li X, Zhang W, Cheng G (2013) Stimuli-responsive recognition of BSA-imprinted poly vinyl acetate grafted calcium alginate core-shell hydrogel microspheres. *J Appl Polym Sci* 127:3898–3909
- Zdrahala RJ, Zdrahala IJ (1999) Biomedical applications of polyurethanes: a review of past promises, present realities, and a vibrant future. *J Biomater Appl* 14:67–90
- Zenner MD, Xia Y, Chen JS, Kessler MR (2013) Polyurethanes from isosorbide-based diisocyanates. *ChemSusChem* 6:1182–1185
- Zenner MD, Madbouly SA, Chen JS, Kessler MR (2015) Unexpected tackifiers from isosorbide. *ChemSusChem* 8:448–451
- Zhang F, Cheng G, Ying X (2006) Emulsion and macromolecules templated alginate based polymer microspheres. *React Funct Polym* 66:712–719
- Zhang Q, Liao J-F, Shi X-H, Qiu Y-G, Chen H-J (2015) Surface biocompatible construction of polyurethane by heparinization. *J Polym Res* 22:68
- Zhao K, Cheng G, Huang J, Ying X (2008) Rebinding and recognition properties of protein-macromolecularly imprinted calcium phosphate/alginate hybrid polymer microspheres. *React Funct Polym* 68:732–741
- Zhu Y, Molinier V, Durand M, Lavergne A, Aubry JM (2009) Amphiphilic properties of hydrotropes derived from isosorbide: Endo/exo isomeric effects and temperature dependence. *Langmuir* 25:13419–13425
- Zia KM, Barikani M, Bhatti IA, Zuber M, Bhatti HN (2008a) Synthesis and characterization of novel, biodegradable, thermally stable chitin-based polyurethane elastomers. *J Appl Polym Sci* 110:769–776
- Zia KM, Bhatti IA, Barikani M, Zuber M, Sheikh MA (2008b) XRD studies of chitin-based polyurethane elastomers. *Int J Biol Macromol* 43:136–141
- Zia KM, Zia F, Zuber M, Rehman S, Ahmad MN (2015) Alginate based polyurethanes: a review of recent advances and perspective. *Int J Biol Macromol* 79:377–387

Part I
Medical Applications

Biodegradable Polymers for Bone Tissue Engineering

M. Susana Cortizo and M. Soledad Belluzo

1 Introduction

The destruction of bone tissue due to disease (osteonecrosis, tumors, osteoporosis) or inefficient healing posttraumatic injury is a problem affecting the world population. The repair of small defect may be mediated by the osteoblast and osteoclast activity which ensures a balanced control of bone resorption and formation, allowing the bone repair, renewal, and growth. However, when the defect reaches a crucial size, it is necessary to appeal to the promising field of tissue engineering in order to develop a new methodology of bone regeneration. Tissue engineering was defined as “an interdisciplinary field of research that applies the principles of engineering and the life sciences towards the development of biological substitutes that restore, maintain or improve tissue function” (Langer and Vacanti 1993). This strategy has been exponentially developed in the last years and currently constitutes an expansive field of research.

Tissue engineering is based on three fundamental pillars, as can be represented in Fig. 1. Porous 3D scaffolds, made of adequate biomaterial, act as a template for tissue formation and have the capacity to support cell adhesion and proliferation induced by growth factors, together promoting tissue regeneration.

Scaffolds used for tissue engineering not only provide a temporary three-dimensional support during tissue repair but also regulate the cell behavior, such as cell adhesion, proliferation, and differentiation (Guo et al. 2015). Thus, this three-dimensional matrix mimics the extracellular matrix, providing structural and mechanical integrity to tissue while communicating with the cellular components it supports to help facilitate and regulate daily cellular processes and wound healing.

M.S. Cortizo (✉) • M.S. Belluzo
Instituto de Investigaciones Físicoquímicas Teóricas y Aplicadas (INIFTA),
Facultad de Ciencias Exactas, Universidad Nacional de La Plata, CONICET,
CCT-La Plata, CC 16 Suc. 4, La Plata, Argentina
e-mail: gcortizo@inifta.unlp.edu.ar

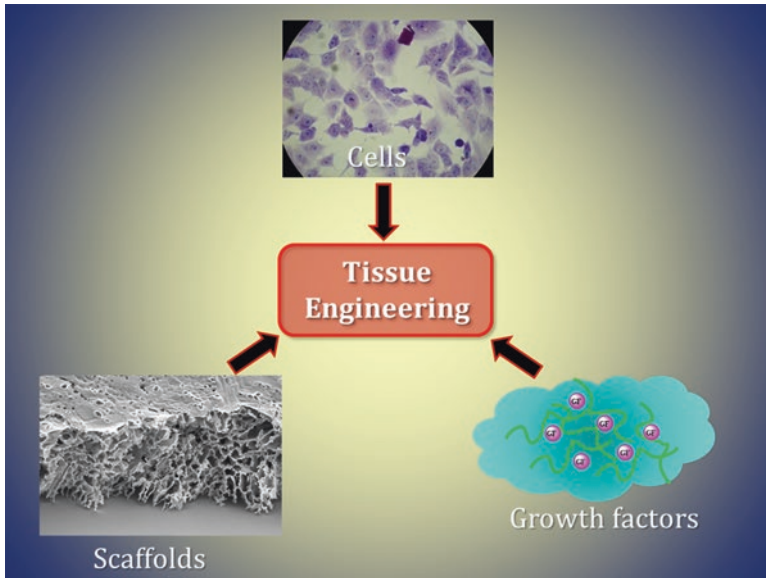


Fig. 1 Fundamental pillars of the tissue engineering: interrelationship between scaffold, cells, and growth factors

However, the appropriated design of scaffold strictly may meet a series of properties that make it suitable for tissue engineering applications. In particular, scaffolds which will be applied to bone tissue regeneration should be biocompatible (well integrated in the host's tissue without eliciting an immune response); possess a highly porous structure with interconnected pores of adequate size which allows cell penetration and nutrient and waste transportation; have good surface properties (chemical and topographic) which favor the cell adhesion and proliferation; be osteoinductive (be able to recruit immature cells and to stimulate these cells to develop into pre-osteoblasts), with sufficient mechanical strength to withstand the hydrostatic pressures and to maintain the space required for cell growth and matrix production; and finally exhibit a degradation rate in line with the growth rate of the neo-tissue, so that the time of the injury site is totally regenerated, the scaffold is totally degraded (Salgado et al. 2004). Based on these considerations and taking into account the important advances achieved along the years, it is clear that one of the most critical issues in tissue engineering is the design of the scaffold with the appropriated characteristics to efficiently regenerate the target tissue. Numerous materials have been used as scaffolds to satisfy the above requirements; among them are ceramics and natural or synthetic polymers, as well as blend and composite biomaterials (Mano et al. 2007; Tian et al. 2012; Goonoo et al. 2016).

This chapter presents the main developments in the area of biodegradable biomaterials, a brief description of the biodegradation mechanisms, and the biomaterial features and more relevant properties, currently developed for bone tissue engineering.

2 Biodegradation of Polymeric Materials

The polymer scaffold material has to be chosen that will degrade and resorb at a controlled rate at the same time as the specific tissue cells seeded into the 3D construct attach, spread, and increase in quantity as well as in quality (Hutmacher 2000). The degradation process consists of cleavage of chemical bond leading to polymer chain scission, decrease of polymer molecular weight, and ultimately producing the loss of mechanical stability of the biomaterial. The biodegradation is the degradation process which is carried out in biological environment which included body fluid, cellular activities, and enzymatic reactions. The mechanisms of biodegradation depend on the chemical nature of the material as well as the physical and morphological properties of polymers. For example, hydrophobic polymers limit water accessibility and typically have decreased hydrolytic degradation rates compared to their more hydrophilic counterparts (Gopferich 1996). Further, amorphous polymers or polymers with lower glass transition temperature (T_g) usually degrade faster than semicrystalline or with high T_g polymers. This degradation behavior is applied to both natural and synthetic polymers.

It has been recognized that the biological environment is surprisingly harsh and can lead to rapid or gradual breakdown of many materials (Coury et al. 2004). The mechanism involved in these processes may be considered through synergic pathways due to different factors that converge and contribute to the aforementioned biodegradation process, for example, superficial cracks, swelling, water uptake, plasticization, or alteration of local pH induced by the presence of degradation products, among others.

Two different mechanisms are accepted as responsible for the polymer biodegradation “in vivo”: hydrolytic and oxidative process.

2.1 Hydrolytic Biodegradation

The hydrolytic degradation is the scission of chemical bonds of functional group susceptible to reaction with water, which can be favored by different catalytic conditions (acids, bases, or enzymes). Between the polymers more vulnerable to hydrolytic degradation, polyanhydrides, polyesters, polycarbonates, polyamides, and acetals must be mentioned. In particular, the mechanism of degradation of polyglycolic acid (PGA) and polylactic acid (PLA), two of the most widely used polyesters in biomedical application, was extensively studied (Chu 1989). This mechanism takes place in two stages, the first being associated with the attack on amorphous regions, releasing some of glycolic acid. The second phase of degradation starts more slowly than the first because of the difficulty of hydrolyzing the crystalline regions, and at the end of this step, glycolic acid is released rapidly. Hydrolytic degradation mechanism of this kind of polymers can be represented as is shown in Fig. 2.

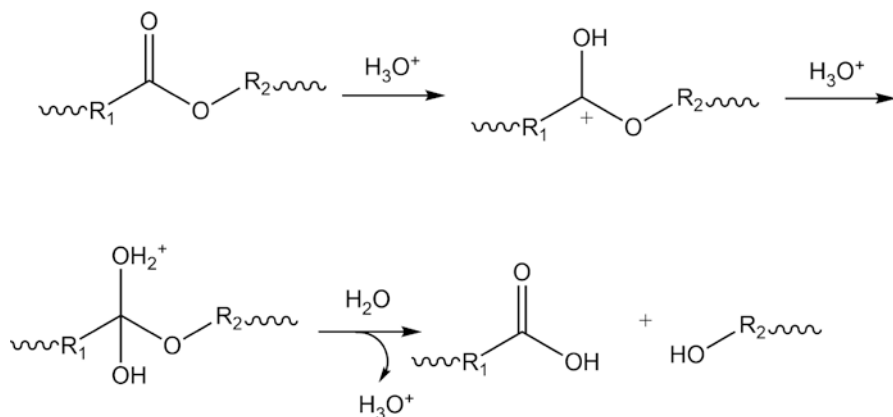


Fig. 2 Reaction mechanism of the polyester hydrolysis

The hydrolytic degradation of aromatic polyesters exhibited important differences; due to that, the water diffusivity is very low, as was demonstrated for polyethylene terephthalate (PET), the major aromatic polyester used medically, with extensive application in vascular prostheses (Williams 1989).

Polymer with other heteroatoms, such as amino group in chain polymer, i.e., nylon or polyamino acids, exhibited variable behavior of hydrolytic degradation, depending on their hydrophilicity. So, nylon 6 hydrolyzes faster than nylon 11, although the reaction mechanism followed a similar step (Zaikov 1985). Also the influence of enzymes on the rate of degradation was demonstrated; papain, trypsin, and chymotrypsin degrade nylon 66, while esterase had no effect (Smith et al. 1987). The biodegradability of polyamino acids and the role of enzymes, in particular, have been known for some years and have been discussed by Dickinson et al. (1981).

In biomedical applications, polyurethanes (PU) are usually classified as either poly(ester urethane)s or poly(ether urethane)s, based on the nature of the soft segments (ester or ether group included in this segment). The hydrolytic degradation of both kinds of PU is different and so do their biomedical applications. Hafeman et al. (2011) studied the degradation mechanism of poly(ester urethane) scaffolds prepared from lysine triisocyanate or a trimer of hexamethylene diisocyanate under hydrolytic, esterolytic, and oxidative conditions. They proposed that the primary mechanism of degradation was hydrolysis of ester bonds to yield α -hydroxy acids, together with other unidentified but water soluble products. Similar pathways for hydrolytic degradation were suggested for polyurethane copolymers which were prepared from 1,6-diisocyanatohexane (HDI), polycaprolactone diol (PCL), 2,2-bis(hydroxymethyl) propionic acid (DMPA), and ethylene glycol (EG). In the case of poly(ester urethane), the hydrolytic degradation rate of ester group is significantly faster than urethane, urea, or amide functional group. This results in relatively high percentage of oligomeric products due to the preferential degradation of

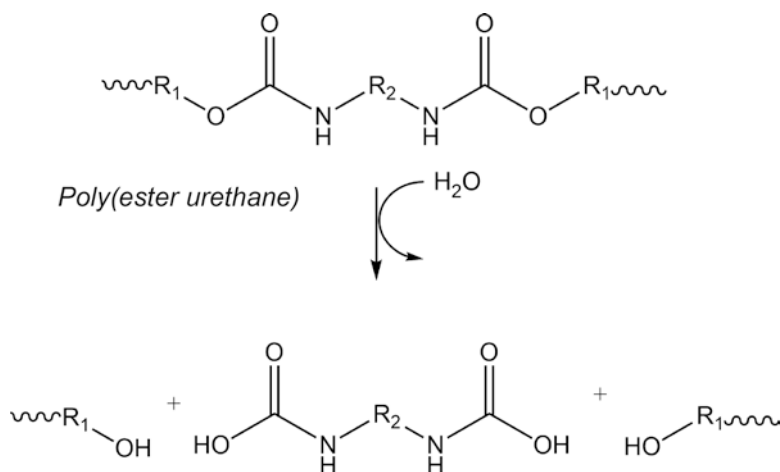


Fig. 3 Scheme of main pathways for hydrolytic degradation of poly(ester urethane)

ester group within the PU structure, particularly during the early stages of the degradation (Gunatillake and Adhikari 2011). Figure 3 shows the schematic pathways of PU degradation based on a generalized structure.

In the last years, new polyurethanes have been developed which included blended soft segments, in order to control the degradation rate and mechanical properties of scaffolds applied in tissue regeneration. For example, the partial replacement of the polyester units with polycarbonate (PC) or polycaprolactone (PCL) with polyethylene glycol (PEG) fragments in the soft segment has resulted in polymers with better modulated degradation kinetics of the materials (Zhang et al. 2016).

Due to the relatively faster hydrolysis of polyanhydrides in comparison with polyesters, they are a main class of polymers used in drug delivery (Murthy et al. 2012). Polyanhydrides can be formulated from a variety of monomer units, which allow engineers to design materials that can degrade and/or release therapeutics at a particular rate that is appropriate for the desired application. They are hydrolyzed predominantly by base- and water-catalyzed hydrolysis. The overall hydrolysis mechanism is similar to that of polyesters, as can be seen in Fig. 4. The first step is the addition of base to the carbonyl carbon, followed by generation of a tetrahedral intermediate. The tetrahedral intermediate formed during polyanhydride hydrolysis generally results in the leaving of the attached ester.

Numerous reports have demonstrated that the hydrolysis of polyanhydrides is proportional to the pH of the surrounding medium (Leong et al. 1985; Park et al. 1996; Santos et al. 1999). The results of these studies demonstrated that polyanhydrides degrade more rapidly at high pH which is in accordance with a base-catalyzed hydrolysis mechanism.

A class of synthetic polymers which can be considered biodegradable are poly(alkylcyanoacrylates) (Coury et al. 2004). These class of polymers were extensively studied as tissue adhesives for the closure of skin wounds, as surgical glue,

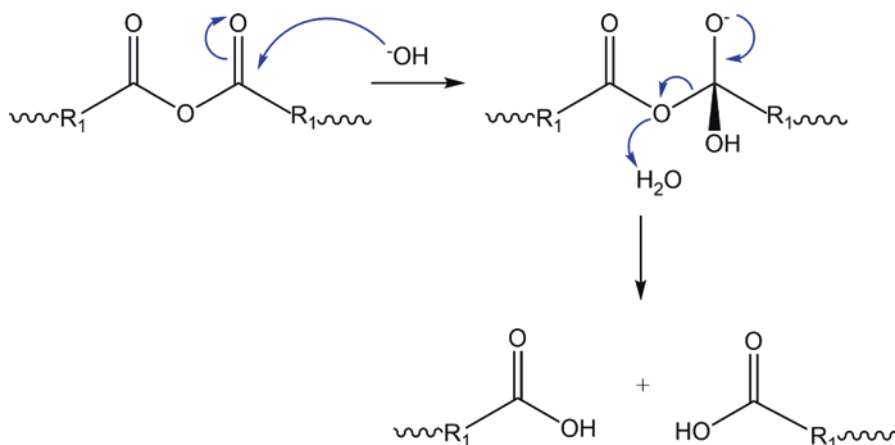


Fig. 4 Base-catalyzed anhydride hydrolysis (Adapted from Murthy et al. 2012)

and as embolitic material for endovascular surgery (Vauthier et al. 2003). Different hydrolysis mechanisms were proposed for these kinds of polymers that include C—C bonds in the main chain. One of them is through a “reverse Knoevenagel” reaction, as can be represented in Fig. 5 (Leonard et al. 1966). It was proposed that this reaction occurs because the methylene ($-\text{CH}_2-$) hydrogen in the polymer is highly activated inductively by electron-withdrawing neighboring groups. In vivo, the water associated with the tissue could be inducing the polymer hydrolysis, as well as basic or enzymatic process. Other degradation mechanisms described in the literature consist of the hydrolysis of the ester bond of the alkyl side chain of the polymer (Lenaerts et al. 1984). Degradation products consist of an alkyl alcohol and poly(cyanoacrylate), which are soluble in water and can be eliminated in vivo via kidney filtration. However, the first of the two mechanisms mentioned is too slow to compete with the other, much more rapid, mechanisms occurring in vivo catalyzed by enzymes (Vauthier et al. 2003).

2.2 Oxidative Biodegradation

The biodegradation of polymer “in vivo” is a process mediated by enzymes, which can be hydrolytic or oxidative. The hydrolytic mechanism involves enzyme that attacks on susceptible and specific chemical bond, as previously described. The oxidative biodegradation involves reactive molecules that are derived from activated phagocytic cells (neutrophils and monocytes) responding to the injury and the properties of the foreign body at the implant site (Coury et al. 2004). Sites favored for initial oxidative attack, consistent with a homolytic or heterolytic pathway, are those that allow abstraction of an atom or ion and provide resonance stabilization of the resultant radical or ion. Thus, different kinds of polymers could be susceptible to

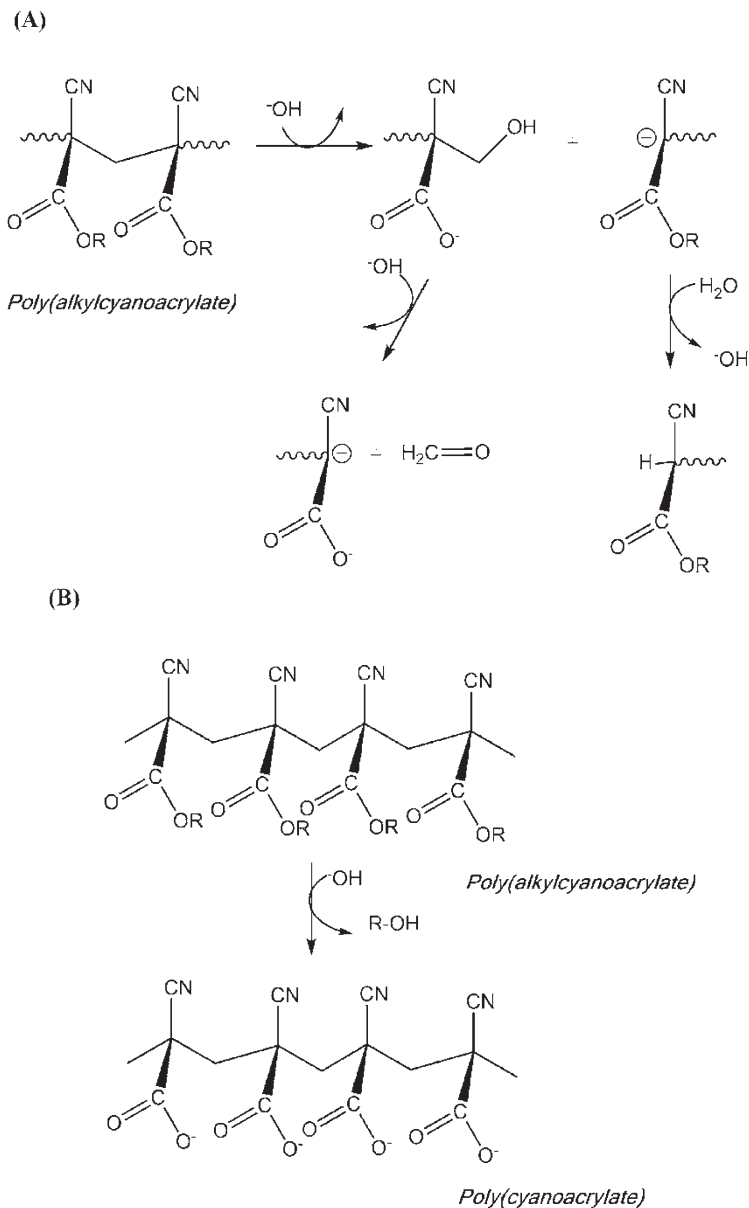


Fig. 5 Degradation pathways of poly(alkylcyanoacrylate): (a) “Reverse Knoevenagel” mechanism (Adapted from Leonard et al. 1966). (b) Basic hydrolysis mechanism (Adapted from Vauthier et al. 2003)

oxidative biodegradation, such as polyolefins, polymers including aromatic ring, polyethers, polyacrylic or polymethacrylic acids, and polyols, to mention a few. It is considered that neutrophils and macrophages metabolize oxygen to form a superoxide anion (O^{-2}). This intermediate can undergo transformation to more powerful oxidants and conceivably can initiate homolytic reactions on the polymer through a radical (R^{\cdot}) or heterolytic mechanism (Coury et al. 2004). The oxidation processes induced by phagocytes are the result of oxidants produced by general foreign-body responses. The macrophages are activated by the presence of released product of polymer degradation, such as monomer or oligomers. Figure 6 shows the proposed

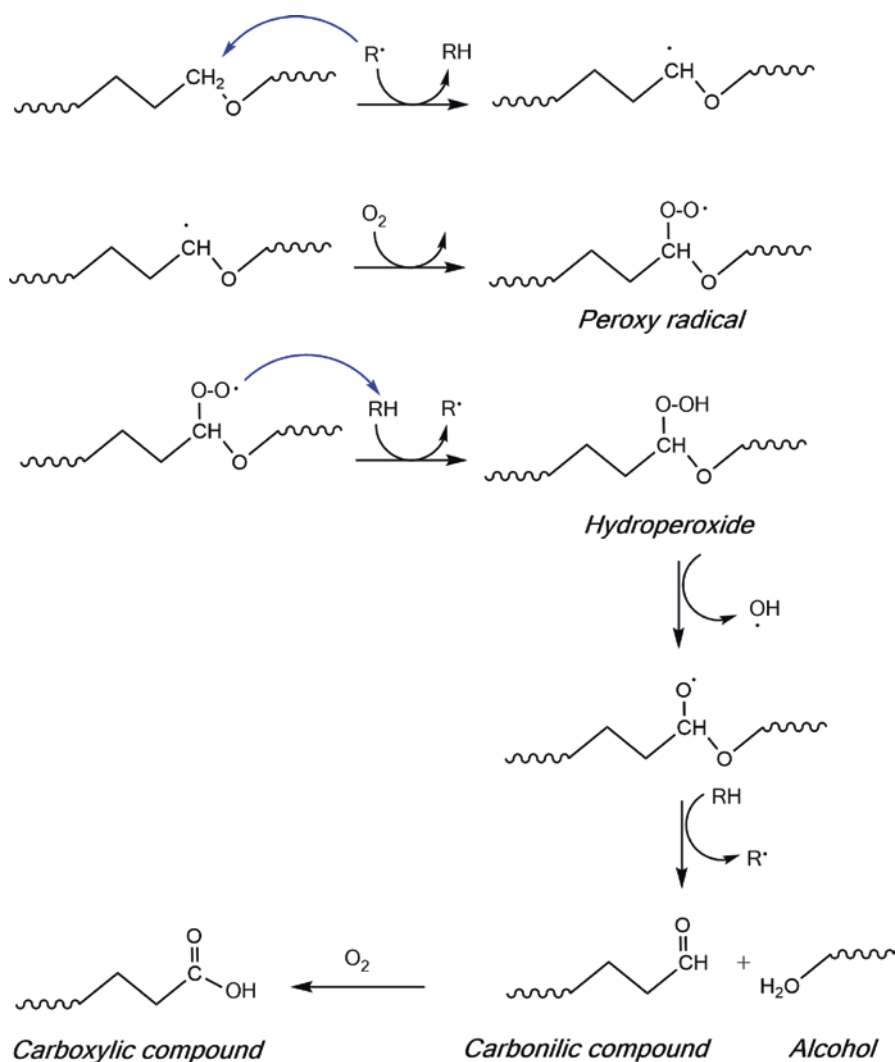


Fig. 6 Pathway for radical oxidative fragmentation of polyethers (Adapted from Coury et al. 2004)

pathways for oxidative fragmentation of polyethers mediated by radical species, as was suggested by Schubert et al. (1997) and Coury et al. (2004).

The consequence of this process is the formation of more polar molecular species with lower average molecular weight, which will be more soluble and therefore have greater speed of diffusion. This characteristic will facilitate the process of phagocytosis and then the biodegradation of the polymeric material “in vivo.”

3 Biodegradable Polymer Used as Biomaterials for Bone Tissue Engineering

Biodegradable polymers used as scaffold materials for bone tissue engineering can be divided, considering their origin, in two groups: synthetic and natural. The main advantage of the synthetic polymers is that they can be produced under controlled conditions and therefore exhibit in general predictable and reproducible mechanical and physical properties such as tensile strength and elastic modulus and degradation rate (Rezwan et al. 2006). On the other hand, the benefits of biomaterials based on natural polymers are their low immunogenic potential, the potential bioactive behavior, and the capability of interacting with the host’s tissue, chemical versatility, and in some cases their source, as in starch and chitosan, which is almost unlimited (Salgado et al. 2004).

3.1 Synthetic Polymer for TE

In addition to the previously mentioned advantages of synthetic polymers, it must be mentioned that they can be fabricated into various shapes with desired pore morphology and conductive features and designed with chemical functional groups that can induce tissue ingrowth (Gunatillake and Adhikari 2003).

3.1.1 Polyesters

Biodegradable synthetic aliphatic polyesters are the most extensively used polymers for bone tissue engineering, such as the poly(glycolic acid) (PGA), the stereoisomer forms of poly(lactic acid) (PLA), and their copolymer poly(lactic-co-glycolide) (PLGA). Their properties and application were exhaustively described in several papers and reviews (Guo et al. 2015; Gunatillake and Adhikari 2003). As was noted, with the exception of PGA, the polymers in this family are soluble in many common organic solvents, and thus it can be processed by a variety of thermal and solvent-based methods. However, the degradation products of these polyesters caused some drawbacks because it reduces the local pH value, which in turn may accelerate the polyesters’ degradation rates and induce an inflammatory reaction.

These inflammatory processes are often ascribed to acidosis caused (chemically unavoidable) by the release of acidic degradation products (monomeric or oligomeric hydroxycarboxylic acids) (Martin et al. 1996; Winet and Bao 1997).

Nanocomposites based on nano-sized hydroxyapatite (HA) and bioactive glass (BG) fillers in combination with biodegradable polyesters as biomaterials for applications in bone regeneration were described by Allo et al. (2012).

Poly(ϵ -caprolactone) (PCL) is another aliphatic polyester that has been intensively investigated as a biomaterial. This polymer exhibited low melting point (59–64 °C), high thermal stability, biocompatibility, and biodegradability although with slower degradation rate than the previously mentioned polyesters (Mondrinos et al. 2006). The addition of HA increased the compression modulus of composite toward bone fixation, but until some level, the failure mechanism of the composites changes from plastic to brittle (easily rupture), hence lowering the mechanical properties of PCL and other biodegradable polymers (Razak et al. 2012). In recent years, new nanocomposites based on PCL were designed by different techniques and studied as potential scaffolds for biomedical regeneration (Mkhabela and Ray 2014).

Polypropylene fumarate (PPF) is an unsaturated linear polyester whose degradation products (i.e., propylene glycol and fumaric acid) are biocompatible and readily removed from the body (Peter et al. 1997). This polymer can be cross-linked by reaction of the double bond using photochemical or thermal radical polymerization. The mechanical properties can be regulated by appropriate molecular weight control as well as cross-linking conditions and the incorporation of reinforcement (Lalwani et al. 2013; Horch et al. 2004).

Recently, there has been a growing interest in the development of bio-polyesters from renewable resources due to limited fossil fuel reserves, rise of petrochemical price, and emission of greenhouse gasses (Zia et al. 2016). Between them, novel materials such as poly(1,8-octanediol-co-citrate) (POC) combined with hydroxyapatite (HA), polyhydroxyalkanoates (PHA)/isosorbide copolyesters, and polyesters based on citric and tartaric acid, among others, are included (Qiu et al. 2006; Zhang et al. 2013; Jiang et al. 2012). Blends and composites of polyesters and hydrophilic natural polymers have been receiving significant attention, since they could lead to the development of novel biodegradable polyesters with properties suitable for extraordinary biomedical applications (Zia et al. 2016).

3.1.2 Polyanhydrides

Polyanhydrides have limited mechanical properties that restrict their use in load-bearing applications such as in orthopedics (Uhrich et al. 1995). To combine good mechanical properties of polyimides with surface-eroding characteristics of polyanhydrides, poly(anhydrides-co-imides) have been developed (Attawia et al. 1995; Uhrich et al. 1997). Anseth et al developed a new family of photopolymerizable, methacrylated anhydride monomers and oligomers that combine high strength, controlled degradation, and photoprocessibility (Anseth et al. 1999). They also demonstrate, by *in vivo* studies in rats, that these networks possess excellent osteocompatibility.

3.1.3 Polymers Including C—C Bond in Main Chain

Very few polymers with C—C structure in the main chain were proposed as biomaterial for bone tissue engineering, the majority of which are composite materials. Recently, a polymer scaffold with Ca^{2+} was synthesized by copolymerization of acrylamide (AM), 2-hydroxyethyl acrylate (HEA), and calcium methacrylate (CDMA) (Kang et al. 2017). This polymer was combined with calcium phosphate in order to increase the attachment of organic and inorganic interface and greatly enhance the mechanical properties of the composite scaffolds. The biocompatibility of the prepared materials was also improved by minerals coating at a certain degree, as evaluated by L929 cell viability.

Hybrid material scaffolds consisting of methacryloxypropyl trimethoxysilane, zirconium propoxide, and 2-(dimethylamino)ethyl methacrylate (DMAEMA) were obtained as composite scaffolds for bone repair (Chatzinikolaidou et al. 2015). The scaffolds' ring structure exhibited a complex 3D geometry which showed good cell adhesion and proliferation, similar to the polystyrene control.

Some research is being directed to the design of hybrid scaffolds that combine the properties of synthetic and natural polymers. One of them is proposed by Galperin et al., an integrated bilayered scaffold based on degradable poly(hydroxyethyl methacrylate) hydrogel layer coated with hydroxyapatite particles and a second layer that had 200 μm pores with surfaces decorated with hyaluronan (Galperin et al. 2013). The scaffold supported the simultaneous growth of chondrocytes and human mesenchymal stem cells (hMSCs) by providing a suitable environment for cell attachment, infiltration, proliferation, and differentiation of hMSCs to osteoblasts (for the designated bone layer) and retention of chondrocyte phenotype (for the designated cartilage layer).

However, in very few of these studies, the biodegradability of the scaffold was analyzed, which is a relevant property for the applications in tissue engineering.

Fernandez et al. prepared a biomimetic bone scaffold based on PCL and poly(diisopropyl fumarate) (PDIPF) blends obtained by sonication (Fernández et al. 2010). PDIPF was synthesized by microwave radical polymerization and presents a characteristic structure of C—C bond. The mechanical properties of this blend were comparable to those of the trabecular bone, while the biocompatibility studies show that osteoblasts plated on the compatibilized blend adhered to and proliferated more than on either homopolymer. Later, HAP–blend composite, with improved physical, mechanical, and osteoinductive properties, was developed and their non-cytotoxicity was demonstrated (Fernández et al. 2011, 2014). PCL is known to be biodegraded by hydrolytic mechanism, as was previously indicated. Previously, biodegradation studies of PDIPF were performed both in PBS buffer and using an in vitro macrophage degradation assay (Cortizo et al. 2008). The polymer was only degraded in the presence of RAW264.7 macrophages, as was demonstrated by the decrease of the average molecular weight (21 days), and the cells' morphological change was observed, from a rounded monocytic appearance to an activated phagocytic phenotype as can be seen in Fig. 7. These results indicated that the polymer can be degraded by a phagocytic process through an oxidative mechanism and thus could be a good candidate for applications in bone regeneration.

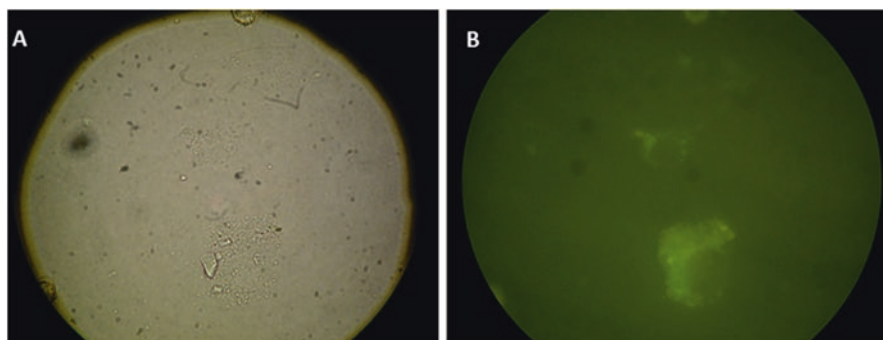


Fig. 7 RAW264.7 macrophages growing on PDIPF*. Cells were cultured on a fluorescent PDIPF matrix for 20 days. Light (a) and fluorescent (b) microscopy revealed the presence of fluorescent particles included in the cytoplasm of activated macrophages. Obj. 40 \times

3.2 Natural Polymer for TE

3.2.1 Polyhydroxyalkanoates

Natural polyesters from the group of polyhydroxyalkanoates (PHAs) have emerged as promising materials for various tissue engineering applications, due to their biocompatibility and biodegradability, as well as their broad range of mechanical properties (Freier 2006). Current methods for PHA production at the industrial scale are based on their synthesis from microbial isolates in either their wild form or by recombinant strains (Dias et al. 2006). The cost of PHA production is still too high for PHA to become a competitive commodity plastic material. The most significant factor in the production costs of PHA is the price of the substrate and the corresponding fermentation strategies. The use of renewable carbon sources based on agricultural or industrial wastes and the development of processes requiring lower investment can contribute to reducing the production costs. Besides it, PHA production processes based on mixed microbial cultures are being investigated as a possible technology to decrease production costs, since no sterilization is required and bacteria can adapt quite well to the complex substrates that may be present in waste material.

Poly(3-hydroxybutyrate), P3HB, is the simplest and most widely studied member of the group of PHAs. The high crystallinity of the isotactic P3HB leads to stiffness and brittleness, as well as slow hydrolysis *in vitro* and *in vivo*, while P4HB films are characterized by low stiffness and high elongation at break (Freier 2006). PHA with elastomeric properties can be obtained from P3HB copolymers containing more than 20% of 4-hydroxybutyrate or medium chain-length (C6–18) 3-hydroxyalkanoate units, as well as medium chain-length PHA homopolymers. This characteristic is very important in tissue engineering applications. Moreover, mechanical stimuli promote the formation of functional tissue, for example, in car-

diovascular or cartilage tissue engineering, and allow for gradual stress transfer from the degrading synthetic matrix to the newly formed tissue.

Scaffolds based on P3HB/HA or P3HB/tricalcium phosphate (TCP) composites were found that exhibited better mechanical properties and biocompatibility, which are important for bone tissue engineering (Hayati et al. 2011; Rasoga et al. 2017).

In vitro degradation studies on P3HB films in buffer solution (pH 7.4, 37 °C) showed no mass loss after 180 days but a decrease in molecular weight starting after an induction period of about 80 days, the hydrolysis process being described in two stages (Doi et al. 1989). In vivo studies demonstrated that P3HB is a completely resorbable polymer, with a degradation rate comparable to that of slowly degrading synthetic polyesters such as high molecular weight poly(L-lactide) (Gogolewski et al. 1993).

3.2.2 Collagen

Collagen is the most abundant structural protein in the body and is the principal component of extracellular matrix (ECM). There are 28 types of collagen decrypted (Mienaltowski and Birk 2014); collagen types I, II, and III have been commonly found in human tissues like the skin, blood vessel, tendon, cartilage, and bone. These types of collagen receive the name of fibril-forming collagen (O'Brien 2011; Pina et al. 2015; Dong and Lv 2016).

Collagen is a non-cytotoxic, biocompatible, and biodegradable protein, extensively used for a wide range of biomedical applications and considered a valid alternative to synthetic materials due to its inherent biocompatibility involving low antigenicity, inflammation, and cytotoxic responses (Gorgieva and Kokol 2011; Meghezi et al. 2015). This biopolymer has low elasticity and poor mechanical strength but relatively stable structure due to covalent cross-link formation among collagen fibrils (Dong and Lv 2016).

Collagen is easy to obtain from many animals and plant sources (Gómez-Guillén et al. 2011), especially from tissues rich in fibrous collagen such as the dermis, tendon, and bone. The isolation of this protein is mostly from rat, bovine, porcine, and sheep, but the extraction of collagen from fish skin and bones has recently been reported (Yamada et al. 2014). Another source of collagen is the production of recombinant human collagen from yeast, bacteria, or mammalian cells, among others (Yu et al. 2014). This approach is promising due to the possibility for mass production.

The interest in collagen-based scaffolds for bone tissue engineering lies on the ability of this protein in mimicking the ECM with the presence of functional groups that can enhance osteoblast adhesion and migration (Ma 2008; Gorgieva and Kokol 2011) and its excellent physicochemical properties. Collagen can be processed into fibers, films, membranes, sponges (Ferreira et al. 2012; Dong and Lv 2016; Rau 2016), blends (with other polymers), and composites.

Scaffold geometry affects cell adhesion, proliferation, and distribution by affecting cell ingrowths, vascularization, and access of nutrients and oxygen. Scaffolds'

pore size and interconnectivity seem to be able to modulate osteogenesis, due to cell osteogenic response to particular pore dimensions (Polo-Corrales et al. 2014). In this way, 3D micropattern porous collagen scaffolds with controlled pore structure were obtained by Chen et al. (2015). After culturing L6 myoblast in the micro-groove collagen scaffolds, it can be seen that myoblast was well aligned and had high expression of myosin heavy chain and synthesis of muscle extracellular matrix, demonstrating the potential use for implantation to restore disease tissue. In another study, a biomimetic scaffold for tissue engineering using bovine collagen with different topographic characteristics was developed, using matrices with random or parallel-arranged collagen fibers (Cortizo et al. 2012). Adhesion, proliferation, alkaline phosphatase activity, and mineralization were significantly improved when cells were grown on the ordered collagen matrix, and no significant increase in proinflammatory cytokine release was observed.

Although several cross-linking strategies for the enhancement of mechanical properties of collagen scaffold have been reported, these methods may have cytotoxic effects (Dong and Lv 2016). Therefore, the combination of different natural polymers can be used as a strategy for the preparation of polymeric scaffold with better properties. Arakawa et al. (2017) synthesized a photopolymerizable hydrogel consisting of photocross-linkable methacrylated glycol chitosan (MeGC) and semi-interpenetrating collagen (Col) with a riboflavin photoinitiator under blue light, with enhanced compressive modulus and slowed degradation rate. MeGC–Col composite hydrogels significantly enhanced cellular attachment, spreading, proliferation, and osteogenic differentiation of mouse bone marrow stromal cells (BMSCs) seeded on the hydrogels compared with pure MeGC hydrogels, as observed by alkaline phosphatase activity as well as increased mineralization. These findings demonstrate that MeGC–Col composite hydrogels may be useful in promoting bone regeneration. Other collagen natural polymer scaffolds for bone regeneration in combination with silk fibroin (Sun et al. 2015; Sangkert et al. 2016), hyaluronic acid (Zhang 2014; Bornes 2015), and alginate (Bendtsen and Wei 2015) had also been described.

Collagen-blending scaffolds made with synthetic polymers also make it possible to achieve both mechanical and biological optimal properties. Scaffolds composed of collagen and synthetic polymers, such as poly(ϵ -caprolactone) (PCL), polylactic acid (PLA), poly(ethylene glycol) (PEG), polyglycolide (PGA), poly(lactide-co-glycolide) (PLGA), and polyvinyl alcohol (PVA), have been widely used for tissue engineering (Dong and Lv 2016). A 3D macrochanneled poly- ϵ -caprolactone (PCL) scaffold, fabricated via the robotic dispensing technique, with the bioactive properties of collagen was prepared by Yu et al. (2012). Rat mesenchymal stem cells (MSCs) were loaded into collagen hydrogels, which were then combined with macrochanneled PCL scaffolds. The cells actively proliferated within the combined scaffold for up to 7 days. MSC-loaded collagen–PCL scaffolds were subsequently cultured under flow perfusion to promote proliferation and osteogenic differentiation. Cells are proliferated to levels significantly higher in flow perfusion culture than that under static conditions during 21 days. The activity of collagen/PCL scaffolds and alkaline phosphatase (ALP), an early osteogenic marker, was also significantly upregulated at 14 days, as well as the expression of the osteogenic genes OPN, OCN, and BSP.

As natural bone is mainly composed of collagen type I and Hap, it is understandable to think that, when aiming to emulate bone tissue regeneration, porous collagen scaffolds are often combined with calcium phosphates (Van Vlierbergh et al. 2011). Several inorganic materials such as hydroxyapatite (HA) and β -tricalcium phosphate (β -TCP) have been used in the field of bone regeneration (Ngiam et al. 2009; Mate Sanchez de Val et al. 2015; Sarikaya and Aydin 2015). These materials show increased mechanical strength as compared to pure collagen scaffolds due to a strong interaction between calcium-binding residues on the polymer macromolecules and the nanoparticle surface (Wahl and Czernuszka 2006). Ngiam et al. (2009) modified electrospun PLLA/collagen scaffolds with HA by an alternating soaking method. They found that HA improved the hydrophilicity of the scaffolds significantly and could enhance the cell capture efficiency of scaffolds to osteoblasts, which was beneficial to early cell capture of bone graft materials. In another study, in vitro osteogenic potential of an electrospun PLLA/collagen/HA scaffold was also studied by Raghavendran (Raghavendran et al. 2014). They indicated that the scaffold exhibited good cytocompatibility and superior osteoinductivity, an upregulated osteogenic lineage gene expression associated with human MSCs. This fact demonstrates that PLLA/collagen/HA scaffolds may be supportive for stem cell-based therapies for bone repair and reconstruction.

Another innovate type of collagen-based scaffolds is carbon nanotube-collagen scaffolds. Since CNT can interact with collagen at a molecular way, these combined scaffolds increased the stiffness due to its rigidity and enhanced the functionality of collagen for biomedical applications (Dong and Lv 2016). Several authors have developed composite and scaffold materials with CNTs (Venkatesan et al. 2014).

Gelatin is the denaturalized form of collagen. Despite the lack of structural characteristics of the collagen, it is biocompatible, bioresorbable, and non-immunogenic. For bone tissue engineering uses, it is often combined with ceramics like HA. Azami et al. (2010) designed a gelatin/HAp nanostructured scaffold with mechanical strength comparable to the spongy bone, with an excellent capacity of cell attachment, migration, and penetration into the pores of the nanocomposite. Recently, the same group tested a nano-hydroxyapatite/gelatin (HA/gel) nanocomposite scaffold in vitro using rat mesenchymal stem cells (Samadikuchaksaraei et al. 2016), and in vivo studies, the HA/gel/OC nanocomposite was implanted in the critical size bone defect created on rat calvarium as well.

3.3 *Silk Fibroin*

The uses of silk proteins have gain more interest in the last years due to its properties like elasticity, impressive mechanical strength, morphologic flexibility, biocompatibility, and biodegradability with controllable degradation rates.

Silk is composed of two major proteins, SF (fibrous protein) and sericin (globular protein), and SF can be isolated from several sources in the form of an aqueous protein solution (Melke et al. 2016). Studies have demonstrated that while native fibroin-sericin proteins can activate the adaptive response, purified fibroin does not

(Aramwit et al. 2009), so the isolation of purified SF is essential for biomedical applications and can be achieved by eliminating sericin via boiling in an alkaline solution (Pina et al. 2015).

Silk proteins are produced by an enormous variety of insect and spider species including ants, fleas, and crickets (Thurber et al. 2015). In spite of that, for biomedical applications, the main silk source is natural silk fibroin of the domesticated *Bombyx mori* (Hardy et al. 2016; Melke et al. 2016). Recently, other authors report the obtaining of recombinantly produced silk-inspired proteins, an interesting alternative because it is possible to produce large quantities of such silks with designed primary sequences (Fredriksson et al. 2009; Humenik et al. 2011; Teulé et al. 2012).

For biomedical applications, silk can be fabricated into a wide range of material formats with the possibility to achieve desirable mechanical and degradation properties. SF can be easily modified into different physical forms such as hydrogels, sponges, fibers, particles, microspheres, tubes, and electrospun fibers (Koh et al. 2015; Melke et al. 2016; Yao et al. 2016). Also, a few studies have been conducted using SF as a material for bioprinting processes.

Schacht et al. prepared a 3D printing scaffold without cross-linking with a recombinant spider silk protein eADF4(C16). The adhesion of different cell types which were seeded after the printing process was tested and revealed that osteoblasts showed a much better adhesion than fibroblasts, myoblasts, HeLa cells, or keratinocytes (Schacht et al. 2015).

Silk-based composite scaffolds in combination with components like collagen and CaPs (calcium phosphates) are also reported. He et al. (2016) prepared a silk fibroin/cellulose nanowhiskers–chitosan (SF/CNW–CS) composite scaffold by layer-by-layer assembly and tested in vitro using human MG-63 osteosarcoma cells. The results indicated that the composite scaffold supporting cell proliferation and promoting the levels of biomineralization is a promising candidate for bone generation and implantation. In another study, macro-/microporous silk/nano-sized calcium phosphate was developed, and the new bone formation ability in rat femur of the composite scaffold was evaluated in vivo. New bone growth was observed directly on the scaffolds' surface, demonstrating osteoconductive properties as they can promote de novo bone formation (Yan et al. 2013).

Other silk fibroin blend scaffolds were also prepared with natural polymers as cellulose, gelatin, chitosan, hyaluronan, alginate (Freddi et al. 1995; He et al. 2010; Das et al. 2015, Kapoor and Kundu 2016), and synthetic polymers like acrylic polymer, PVA, PEO (polyethylene oxide), PAA (polyacrylic acid), PU, and PEG (Sun et al. 1997; Hardy et al. 2016; Kapoor and Kundu 2016).

3.4 Chitosan

Chitosan is a deacetylated form of chitin, a polysaccharide present in marine crustacean exoskeleton like crab, shrimp, and lobster (Pina et al. 2015; Logith Kumar 2016). Chitosan is a linear polysaccharide composed of glucosamine and

N-acetylglucosamine units linked by β -(1,4)-glycosidic bonds, and different forms of pure chitosan differ by their degrees of deacetylation (DD) and molecular weights (Levengood and Zhang 2014). The degree of deacetylation represents the glucosamine to N-acetylglucosamine ratio and generally falls in the range of 50–95%. Chitosan solutions can easily be prepared by dilution of the polymer in dilute organic acids like acetic or formic acid.

This biopolymer is interesting for biomedical applications due to its low toxicity, non-immunogenicity, biodegradability, ability for cell ingrowth, and intrinsic antibacterial nature. Additionally, chitosan is the only positively charged biopolymer and is able to interact with negatively charged polymers and structural molecules present in the ECM.

Chitosan can support the attachment and proliferation of bone-forming osteoblast cells as well as formation of a mineralized bone matrix *in vitro* and *in vivo* neovascularization (Costa-Pinto et al. 2011; Saravanan et al. 2013). For bone regenerative applications, chitosan can be developed in different forms like sponges, fibers, films, foams, hydrogels, and particles (Croisier and Jérôme 2013; Niranjana et al. 2013; Pina et al. 2015; Logith Kumar et al. 2016) and can be processed by several methods from physical blends (to form polyelectrolyte complexes) to novel techniques as rapid prototyping and electrospinning (Levengood and Zhang 2014). The use of ultrasound to compatibilize chitosan-based scaffolds was also described (Belluzo et al. 2016). Several materials for bone tissue engineering using functionalized chitosan (such as quaternization, carboxyalkylation, hydroxylation, phosphorylation, sulfation, and copolymerization) also have been described (Logith Kumar et al. 2016).

To enhance the properties of the scaffolds for bone remediation, chitosan can be combined with other polymers and inorganic materials. For example, the blending of chitosan with alginate stabilized the system by their electrostatic interaction (Venkatesan et al. 2015). The inclusion of chicken feather keratin nanoparticles within chitosan significantly improved the protein adsorption and probed biocompatibility with human osteoblastic cells (Saravanan et al. 2013). Chitosan/gelatin scaffolds promoted osteoblast proliferation *in vivo*, showing a complete degradation in 8 weeks (Oryan et al. 2016).

Also, incorporation of ceramics can enhance mechanical properties and osteoconductive properties of chitosan composite materials. Kim et al. (2015) prepared a chitosan/alginate matrix with nanoHA and probed to enhance the mechanical property of the scaffold as well as stimulated the differentiation of mouse pre-osteoblastic cells (MC3T3-E1) to osteocytes. Chitosan/hyaluronic acid scaffolds with addition of calcium phosphate cement exhibited a significant increase in ALP activity with no significant change in the rate of osteoblastic cell proliferation (Hesarakı and Nezafati 2014). The addition of nHAp to chitosan/gelatin matrix not only increased the mechanical property of the scaffolds but also stimulated the proliferation and differentiation of induced pluripotent stem cells of gingival fibroblasts to osteocytes (Isikli et al. 2012). The incorporation of chondroitin sulfate into chitosan scaffolds increased apatite deposition which facilitated the spreading of bone marrow stromal cells and significantly enhanced the compressive modulus (Park et al. 2013).

Several materials combining chitosan with synthetic polymer also were used over the year to bone tissue engineering. Ku et al. (2009) designed PLLA/chitosan multilayered membrane composed of the outer layers of chitosan mesh for ease of cell adherence and the middle layer of nanoporous PLLA for sufficient mechanical strength. The membrane maintained its integrity for up to 8 weeks while allowing gradual degradation. Mohammadi et al. (2007) developed a 3D nanofibrous hybrid scaffolds consisting of poly(ϵ -caprolactone), poly(vinyl alcohol), and chitosan via an electrospinning method and assed the differentiation of mesenchymal stem cells into osteoblasts. The result revealed that cells were well attached, penetrated into the construct, and uniformly distributed. The expression of early and late phenotypic markers of osteoblastic differentiation was upregulated in the constructs cultured in the osteogenic medium. Other groups developed a borax cross-linked scaffold based on fumarate–vinyl acetate copolymer and chitosan for osteochondral tissue engineering. Biocompatibility studies demonstrate the versatility of this material since it allows BMPC osteogenic development and supports primary chondrocyte growth and extracellular matrix deposition, without evident signs of cytotoxicity in the in vitro system (Lastra et al. 2016).

3.5 Alginate

Alginate is a naturally occurring anionic polymer typically obtained from brown algae (Phaeophyceae) including *Laminaria hyperborea*, *Laminaria digitata*, *Laminaria japonica*, *Ascophyllum nodosum*, and *Macrocystis pyrifera* through treatment with aqueous alkali solutions (Venkatesan et al. 2015). Alginate is a block copolymer composed of two monomers, (1,4)-linked β -D-mannuronate (M) and α -L-guluronate (G), and the ratio of guluronate to mannuronate varies depending on the natural source influencing the properties of the alginate (Pina et al. 2015, Lee and Mooney 2012). This polymer has been extensively investigated and used for many biomedical applications, due to its outstanding properties in terms of biocompatibility, biodegradability, nonantigenicity, relatively low cost, abundant source, and chelating ability. The preparation of alginate scaffolds can be achieved by diverse cross-linkers that are calcium based due to the ability of mild gelation by addition of divalent cations such as Ca^{2+} . Alginate can be easily modified in any form such as hydrogels, microspheres, microcapsules, sponges, foams, and fibers, by several methods including lyophilization, electrospinning, and cross-linking (Lee and Mooney 2012; Sun and Tan 2013). Among these, alginate gels can be introduced into the body in a minimally invasive way, representing an advantage for bone repairing by filling irregularly shaped defects. The polymer composition, molecular weight, purity, and concentration used in the scaffolds play the biggest role in providing mechanical strength, biocompatibility, cell adhesion, proliferation, and osteogenic differentiation (Venkatesan et al. 2015). Specially, the molecular weight of alginate influences the degradation rate and mechanical properties of the scaffolds – the slower the degradation rate, the higher the molecular weight – because of the decreases in the number of reactive positions available for hydrolysis degradation.

Chemical modifications of alginate as, for example, oxidation or introduction of chemical moieties in the backbone of this polymer also have been used to enhance the scaffold properties (Lee and Mooney 2012).

Alginate-based blends with other natural polymers and ceramic component have interesting properties for bone repair. A nano-sized hydroxyapatite/alginate/chitosan composite scaffold was achieved by Kim et al. (2015), with high strength and controlled pore structures that helped a better differentiation and mineralization of the MC3T3-E1 cells. Bharatham et al. (2014) prepared a novel scaffold combining alginate with a naturally obtained biomineral (nano-cockle shell powder/nCP) and tested it in vitro using MG63 human osteoblast cells. Hydrogels based on methacrylated alginate and collagen were developed, and MC3T3-E1 cells that grow in the scaffolds exhibited a rapid proliferation and a facilitated osteogenic differentiation. This chemical modification of the alginate also provides the capacity to control the degradation rate, swelling, and mechanical properties of this material.

The addition of synthetic polymers onto alginate normally increases the mechanical strength of the composite material (Venkatesan et al. 2015). Chan et al. (2015) described the technique for synthesizing of biocompatible alginate/poly(γ -glutamic acid) base gel with potential application as injectable bone repair material. Evaluation of its mechanical properties, swelling behavior, and blood compatibility showed its nontoxicity and use for repairing bone defects.

3.6 Cellulose

Cellulose is a polysaccharide consisting of a linear chain of several hundred to over 10,000 β -(1-4)-linked D-glucose units. Cellulose is considered as one of the world's most abundant natural and renewable resource of raw material. Natural cellulose is present in a wide variety of living species, being mainly obtained from wood, hemp, cotton, and linen. Intra- and intermolecular hydrogen bonds and high molecular weight give cellulose important characteristics such as chemical stability, mechanical strength, biocompatibility, and biodegradability. Nevertheless, the chemical nature of cellulose makes dissolution in common solvents difficult and complicates tissue engineering use. To overcome this problem, several alternatives like using cellulose derivatives (as carboxymethyl cellulose) or bacterial cellulose have been used for scaffold preparation. Bacterial cellulose can be obtained by biosynthesis from bacteria, *Acetobacter xylinum* being the most efficient and investigated producer of this biopolymer (Gomes de Oliveira Barud et al. 2016). Bacterial cellulose is identical to plant cellulose in chemical structure, but it can be produced without contaminant molecules, such as lignin and hemicelluloses, and does not require intensive purification processes (Novotna 2013). Several studies with BC have been developed in this way, using BC with a mineral phase (i.e., hydroxyapatite [HA]) to emulate bone composition. A membrane composed of BC and hydroxyapatite (HA) was developed as biomaterial for potential bone regeneration, which delivered prone growth of osteoblast cells, high level of alkaline phosphatase activity, and greater bone nodule formation (Tazi et al. 2012). Saska et al. prepared BC-HA

nanocomposites and evaluated the biological properties and performance of the material with respect to bone regeneration in defects of rat tibia (Saska et al. 2011). The composite BC–HA membranes were effective for bone regeneration and accelerated new bone formation. In addition, reabsorption of the membranes was slow, suggesting that it takes longer to this composite to be completely reabsorbed. Pigossi et al. (2015) evaluated the potential of BC–HA composites associated with osteogenic growth peptide (OGP) or pentapeptide OGP (10–14) in bone regeneration in critical-sized calvarial defects in mice analyzed at 3, 7, 15, 30, 60, and 90 days. The researchers found that at 60 and 90 days, a high percentage of bone formation was observed by micro-computed tomography (CT) and a high expression of some bone biomarkers, such as ALP, was also observed. They concluded that the BC–HA membrane promoted a better bone formation in critical-sized mice calvarial defects.

Composite blend constructs with cellulose and different natural polymers also are probed to be interesting for BTE. Liuyun and col (Liuyun et al. 2009) reported the novel composite of nanoHA–chitosan–carboxymethyl cellulose, which was prepared by freeze-drying method. Nanocomposite scaffold with 30% wt. carboxymethyl cellulose had the most ideal porous structure and the highest compressive strength. Cell attachment and proliferation on the scaffold indicate that the nHA–chitosan–carboxymethyl cellulose is nontoxic and has good cytocompatibility. Lee and his group (2013) evaluated in vivo assays by implanting silk fibroin–BC membranes to successfully promote the complete healing of segmental defects of zygomatic arch of rats.

In another work, Aravamudhan reports the fabrication and characterization of cellulose and collagen-based micro-nanostructured scaffolds using human osteoblasts (Aravamudhan et al. 2013). These porous micro-nanostructured scaffolds exhibited mechanical properties in the midrange of human trabecular bone and supported great adhesion and phenotype maintenance of cultured osteoblast as reflected by higher levels of osteogenic enzyme alkaline phosphatase and mineral deposition.

Finally, some works using all-cellulose composites are described elsewhere. He et al. (He et al. 2014) fabricated uniaxially aligned cellulose nanofibers with well-oriented cellulose nanocrystals (CNCs) via electrospinning. The incorporation of CNCs into the spinning dope resulted in more uniform morphology of the electrospun cellulose/CNC nanocomposite nanofibers (ECCNN), and a remarkable enhancement of their physical properties was observed. Cell culture experiments demonstrated that cells could proliferate rapidly not only on the surface but also deep inside the composite material, and the aligned nanofibers exhibited a strong effect on directing cellular organization.

3.7 Hyaluronic Acid

Hyaluronic acid is an anionic, non-sulfated glycosaminoglycan, consisting of repeating D-glucuronic acid– β -1,3-N-acetyl-D-glucosamine– β -1,4 units. Hyaluronic acid can be found in extracellular matrix of all connective tissues in the body and

display several properties like excellent viscoelasticity, water solubility, biocompatibility, and non-immunogenicity (Pina et al. 2015). Another important feature is the capability of hyaluronic acid-based scaffolds to be degraded by enzymatic action. The rate of enzymatic degradation will depend both on the number of cleavage sites in the polymer and the amount of available enzymes in the scaffold biological environment and is catalyzed by hyaluronidase. Recently, Schante et al. have published work on improved enzymatic stability of hyaluronic acid by grafting with amino acids (Schante et al. 2012).

For bone tissue engineering, material with several forms as hydrogels (Bae et al. 2014), fibers (Fischer et al. 2012), meshes (Rhodes et al. 2011), and foams (Dehghani and Annabi 2011) has been created. Also, scaffold of hyaluronic acid derivatives or hyaluronic acid-based composites has been widely used for bone tissue engineering (Collins and Birkinshaw 2013; Sarkar and Lee 2015), aiming to improve mechanical strength, structural integrity, or toughness. For example, photocross-linked methacrylated HA hydrogel loaded with simvastatin or differentiation factor 5 to promote osteogenesis showed better mechanical properties (Bae et al. 2011, 2014). These materials evidence good biocompatibility and higher level of MC3T3-E1 cell proliferation and differentiation in vitro, and in vivo tests using male adult New Zealand white rabbits showed a significant improvement on osteogenesis.

Blending made of hyaluronic acid with natural polymers and bioceramic has also been used as a strategy for bone healing. Hyaluronic acid–gelatin hydrogel loaded into a biphasic calcium phosphate (BCP) ceramic scaffold, with unique micro- and macroporous orientation, was previously obtained (Nguyen and Lee 2014). Both in vitro and in vivo tests were conducted, showing a significant increase in cell proliferation at 3 and 7 days, high alkaline phosphatase activities at 14 and 21 days, and a rapid bone formation (confirmed by histological section) and collagen mineralization after 3 months of implantation. In another study, an injectable nano-hydroxyapatite/glycol chitosan/hyaluronic acid composite hydrogel has been obtained (Huang et al. 2016). In vitro cytocompatibility was evaluated by using MC-3T3-E1 cells to confirm that the developed composite hydrogels were cytocompatible and nontoxic, and cells were found to be attached and well spread out on the hydrogels after 7 days of co-incubation.

4 Conclusions

Tissue engineering is a multidisciplinary field of research oriented to the search of new materials whose biodegradation processes are dependent on their applications, focusing in the type of tissue to be regenerated and rate of cell growth. Currently, an ideal biomaterial that meets all the necessary requirements for its application in bone tissue regeneration does not exist. However, the increasing development of TE shows that current trends are focused on composite materials (including nanomaterials), mixing natural and/or synthetic polymers with nanofillers, especially bioceramics. This strategy combines suitable biodegradation and biocompatibility

properties with adequate mechanical strength for each class of tissue to be repaired, together with low cytotoxicity.

Despite advances in the field and the large amount of materials developed, very few of these materials have been tested in clinical trials until today. The study of the interaction between these materials and the tissue to be regenerated, the mechanical strength, the time of degradation optimum to allow the creation of new tissue, and the inclusion of factors that can promote the cellular growth and differentiation are crucial to achieve this goal.

References

- Allo BA, Costa DO, Dixon SJ, Mequanint K, Rizkalla AS (2012) Bioactive and biodegradable nanocomposites and hybrid biomaterials for bone regeneration. *J Funct Biomater* 3:432–463
- Anseth KS, Shastri VR, Langer R (1999) Photopolymerizable degradable poly(anhydrides) with osteocompatibility. *Nat Biotechnol* 17:156–159
- Arakawa C, Ng R, Tan S, Kim S, Wu B, Lee M (2017) Photopolymerizable chitosan-collagen hydrogels for bone tissue engineering. *J Tissue Eng Regen Med* 11:164–174
- Aramwit P, Kanokpanont S, De-Eknamkul W, Srichana T (2009) Monitoring of inflammatory mediators induced by silk sericin. *J Biosci Bioeng* 107:556–561
- Aravamudhan A1, Ramos DM, Nip J, Harmon MD, James R, Deng M, Laurencin CT, Yu X, Kumbar SG (2013) Cellulose and collagen derived micro-nano structured scaffolds for bone tissue engineering. *J Biomed Nanotechnol* 9:719–731
- Attawia MA, Uhrich KE, Botchwey E, Fan M, Langer R, Laurencin CT (1995) Cytotoxicity testing of poly(anhydride) for orthopaedic applications. *J Biomed Mater Res* 29:1233–1240
- Azami M, Samadikuchaksaraei A, Poursamar SA (2010) Synthesis and characterization of a laminated hydroxyapatite/gelatin nanocomposite scaffold with controlled pore structure for bone tissue engineering. *Int J Artif Organs* 33:86–95
- Bae MS, Yang DH, Lee JB, Heo DN, Kwon YD, Youn IC, Choi K, Hong JH, Kim GT, Choi YS, Hwang EH, Kwon IK (2011) Photo-cured hyaluronic acid-based hydrogels containing simvastatin as a bone tissue regeneration scaffold. *Biomaterials* 32:8161–8171
- Bae MS, Ohe JY, Lee JB, Heo DN, Byun W, Bae H, Kwon YD, Kwon IK (2014) Photocured hyaluronic acid-based hydrogels containing growth and differentiation factor 5 (GDF-5) for bone tissue regeneration. *Bone* 59:189–198
- Belluzo MS, Medina LF, Cortizo AM, Cortizo MS (2016) Ultrasonic compatibilization of polyelectrolyte complex based on polysaccharides for biomedical applications. *Ultrason Sonochem* 30:1–8
- Bendtsen ST, Wei M (2015) Synthesis and characterization of a novel injectable alginate–collagen–hydroxyapatite hydrogel for bone tissue regeneration. *J Mater Chem B* 3:3081–3090
- Bharatham BH, Abu Bakar MZ, Perimal EK, Yusof LM, Hamid M (2014) Development and characterization of novel porous 3D alginate-cockle shell powder nanobiocomposite bone scaffold. *Biomed Res Int* 2014:146723
- Bornes TD, Jomha NM, Mulet-Sierra A, Adesida AB (2015) Hypoxic culture of bone marrow-derived mesenchymal stromal stem cells differentially enhances in vitro chondrogenesis within cell-seeded collagen and hyaluronic acid porous scaffolds. *Stem Cell Res Ther* 6:84
- Chan WP, Kung FC, Kuo YL, Yang MC, Lai WF (2015) Alginate/Poly(γ -glutamic Acid) base biocompatible gel for bone tissue engineering. *Biomed Res Int* 2015:185841
- Chatzinikolaïdou M, Rekstyte S, Danilevicius P, Pontikoglou C, Papadaki H, Farsari M, Vamvakaki M (2015) Adhesion and growth of human bone marrow mesenchymal stem cells on precise-geometry 3D organic-inorganic composite scaffolds for bone repair. *Mater Sci Eng C Mater Biol Appl* 48:301–309

- Chen S, Nakamoto T, Kawazoe N, Chen G (2015) Engineering multi-layered skeletal muscle tissue by using 3D microgrooved collagen scaffolds. *Biomaterials* 73:23–31
- Chu CC (1989) In: Williams DF (ed) *Biocompatibility of degradable polymers*. CRC Press, Boca Raton
- Collins MN, Birkinshaw C (2013) Hyaluronic acid based scaffolds for tissue engineering—a review. *Carbohydr Polym* 92:1262–1279
- Cortizo MS, Molinuevo MS, Cortizo AM (2008) Biocompatibility and biodegradation of polyester and polyfumarate based-scaffolds for bone tissue engineering. *J Tissue Eng Regen Med* 2:33–42
- Cortizo AM, Ruderman G, Correa G, Mogilner IG, Tolosa EJ (2012) Effect of surface topography of collagen scaffolds on cytotoxicity and osteoblast differentiation. *J Biomater Tissue Eng* 2:125–132
- Costa-Pinto AR, Reis RL, Neves NM (2011) Scaffolds based bone tissue engineering: the role of chitosan. *Tissue Eng Part B Rev* 17:331–347
- Coury AJ, Levy RJ, Ratner BD, Shoen FJ, Williams DF, Williams RL (2004) Degradation of materials in the biological environment, chapter 6. In: Ratner, Hoffman, Shoen, Lemons (eds) *Biomaterials science*. Elsevier Ac. Press, San Diego, pp 411–453
- Croisier F, Jérôme C (2013) Chitosan-based biomaterials for tissue engineering. *Eur Polym J* 49:780–792
- Das S, Pati F, Choi YJ, Rijal G, Shim JH, Kim SW, Ray AR, Cho DW, Ghosh S (2015) Bioprintable, cell-laden silk fibroin–gelatin hydrogel supporting multilineage differentiation of stem cells for fabrication of three-dimensional tissue constructs. *Acta Biomater* 11:233–246
- Dehghani F, Annabi N (2011) Engineering porous scaffolds using gas-based techniques. *Curr Opin Biotechnol* 22:661–666
- Dias JM, Lemos PC, Serafim LS, Oliveira C, Eiroa M, Albuquerque MG, Ramos AM, Oliveira R, Reis MA (2006) Recent advances in polyhydroxyalkanoate production by mixed aerobic cultures: from the substrate to the final product. *Macromol Biosci* 6:885–906
- Dickinson HR, Hiltner A, Gibbons DF, Anderson JM (1981) Biodegradation of a poly(α -amino acid) hydrogel. I. In vivo. *J Biomed Mater Res* 15:577–589
- Doi Y, Kanesawa Y, Kawaguchi Y, Kunioka M (1989) Hydrolytic degradation of microbial poly(hydroxyalkanoates). *Makromol Chem Rapid Commun* 10:227–230
- Dong C, Lv Y (2016) Application of collagen scaffold in tissue engineering: recent advances and new perspectives. *Polymers* 8:42
- Fernández JM, Molinuevo MS, Cortizo AM, McCarthy AD, Cortizo MS (2010) Characterization of poly(ϵ -caprolactone)/Polyfumarate blends as scaffolds for bone tissue engineering. *J Biomater Sci Polym Ed* 21:1297–1312
- Fernández JM, Molinuevo MS, Cortizo MS, Cortizo AM (2011) Development of an osteoconductive PCL–PDIPF–hydroxyapatite composite scaffold for bone tissue engineering. *J Tissue Eng Regen Med* 5:e126–e135
- Fernández JM, Cortizo MS, Cortizo AM (2014) Fumarate/ceramic composite based scaffolds for tissue engineering: evaluation of hydrophobicity, degradability, toxicity and biocompatibility. *J Biomater Tissue Eng* 4:1–8
- Ferreira AM, Gentile P, Chiono V, Ciardelli G (2012) Collagen for bone tissue regeneration. *Acta Biomater* 8:3191–3200
- Fischer RL, McCoy MG, Grant SA (2012) Electrospinning collagen and hyaluronic acid nanofiber meshes. *J Mater Sci Mater Med* 23:1645–1654
- Freddi G, Romanò M, Massafra MR, Tsukada M (1995) Silk fibroin/cellulose blend films: preparation, structure, and physical properties. *J Appl Polym Sci* 56:1537–1545
- Fredriksson C, Hedhammar M, Feinstein R, Nordling K, Kratz G, Johansson J, Huss F, Rising A (2009) Tissue response to subcutaneously implanted recombinant spider silk: an in vivo study. *Materials* 2:1908–1922
- Freier T (2006) Biopolyesters in tissue engineering applications. *Adv Polym Sci* 203:1–61
- Galperin A, Oldinski RA, Florczyk SJ, Bryers JD, Zhang M, Ratner BD (2013) Integrated bi-layered scaffold for osteochondral tissue engineering. *Adv Healthc Mater* 2:872–883

- Gogolewski S, Jovanovic M, Perren SM, Dillon JG, Hughes MK (1993) You have full text access to this content tissue response and in vivo degradation of selected polyhydroxyacids: Polylactides (PLA), poly(3-hydroxybutyrate) (PHB), and poly(3-hydroxybutyrate-co-3-hydroxyvalerate) (PHB/VA). *J Biomed Mater Res* 27:1135–1148
- Gomez de Oliveira Barud H, da Silva RR, da Silva Barud H, Tercjak A, Gutierrez J, Lustrri WR, de Oliveira OB Jr, Ribeiro SJ (2016) A multipurpose natural and renewable polymer in medical applications: bacterial cellulose. *Carbohydr Polym* 153:406–420
- Gómez-Guillén MC, Giménez B, López-Caballero ME, Montero MP (2011) Functional and bio-active properties of collagen and gelatin from alternative sources: a review. *Food Hydrocoll* 25:1813–1827
- Goonoo N, Bhaw-Luximon A, Passanha P, Esteves SR, Jhurry D (2016) Third generation poly(hydroxyacid) composite scaffolds for tissue engineering. *J Biomed Mater Res B Appl Biomater*. doi:10.1002/jbm.b.33674
- Gopferich A (1996) Mechanisms of polymer degradation and erosion. *Biomaterials* 17:103–114
- Gorgieva S, Kokol V (2011) Collagen- vs. gelatine-based biomaterials and their biocompatibility: review and perspectives, Chapter 2. In: Pignatello R (ed) *Biomaterials applications for nanomedicine*. InTech, Rijeka, pp 17–52
- Gunatillake PA, Adhikari R (2003) Biodegradable synthetic polymers for tissue engineering. *European Cells and Materials* 5:1–16
- Gunatillake PA, Adhikari R (2011) Biodegradable polyurethanes: design, synthesis, properties and potential applications, Chapter 9. In: Felto GP (ed) *Biodegradable polymers: processing, degradation and applications*. Nova Science Publishers, Hauppauge, pp 431–470
- Guo B, Lei B, Li P, Ma PX (2015) Functionalized scaffolds to enhance tissue regeneration. *Regen Biomater* 2015:47–57
- Hafeman AE, Zienkiewicz KJ, Zachman AL, Sung HJ, Nanney LB, Davidson JM, Guelcher SA (2011) Characterization of the degradation mechanisms of lysine-derived aliphatic poly(ester urethane) scaffolds. *Biomaterials* 32:419–429
- Hardy JG, Torres-Rendon JG, Leal-Egaña A, Walther A, Schlaad H, Cölfen H, Scheibel TR (2016) Biomaterialization of engineered spider silk protein-based composite materials for bone tissue engineering. *Materials* 9:560
- Hayati AN, Rezaie HR, Hosseinalipour SM (2011) Preparation of poly(3-hydroxybutyrate)/nano-hydroxyapatite composite scaffolds for bone tissue engineering. *Mater Lett* 65:736–739
- He J, Wang Y, Cui S, Gao Y, Wang S (2010) Structure and properties of silk fibroin/carboxymethyl chitosan blend films. *Polym Bull* 65:395–409
- He X, Xiao Q, Lu C, Wang Y, Zhang X, Zhao J, Zhang W, Zhang X, Deng Y (2014) Uniaxially aligned electrospun all-cellulose nanocomposite nanofibers reinforced with cellulose nanocrystals: scaffold for tissue engineering. *Biomacromolecules* 15:618–627
- He J-X, Tan W-L, Han Q-M, Cui S-Z, Shao W, Sang F (2016) Fabrication of silk fibroin/cellulose whiskers–chitosan composite porous scaffolds by layer-by-layer assembly for application in bone tissue engineering. *J Mater Sci* 51:4399–4410
- Hesaraki S, Nezafati N (2014) In vitro biocompatibility of chitosan/hyaluronic acid-containing calcium phosphate bone cements. *Bioprocess Biosyst Eng* 37:1507–1516
- Horch RA, Shahid N, Mistry AS, Timmer MD, Mikos AG, Barron AR (2004) Nanoreinforcement of poly(propylene fumarate)-based networks with surface modified alumoxane nanoparticles for bone tissue engineering. *Biomacromolecules* 5:1990–1998
- Huang Y, Zhang X, Wua A, Xu H (2016) An injectable nano-hydroxyapatite (n-HA)/glycol chitosan (G-CS)/hyaluronic acid (HyA) composite hydrogel for bone tissue engineering. *RSC Adv* 6:33529–33536
- Humenik M, Smith AM, Scheibel T (2011) Recombinant spider silks-biopolymers with potential for future applications. *Polymers* 3:640–661
- Hutmacher DW (2000) Scaffolds in tissue engineering bone and cartilage. *Biomaterials* 21: 2529–2543
- Isikli C, Hasirci V, Hasirci N (2012) Development of porous chitosan-gelatin/hydroxyapatite composite scaffolds for hard tissue-engineering applications. *J Tissue Eng Regen Med* 6:135–143

- Jiang M, Liu Q, Zhang Q, Ye C, Zhou G (2012) You have full text access to this content A series of furan-aromatic polyesters synthesized via direct esterification method based on renewable resources. *J Polym Sci Part A: Polym Chem* 50:1026–1036
- Kang Z, Zhang X, Chen Y, Akram MY, Nie J, Zhu X (2017) Preparation of polymer/calcium phosphate porous composite as bone tissue scaffolds. *Mater Sci Eng C* 70:1125–1131
- Kapoor S, Kundu SC (2016) Silk protein-based hydrogels: promising advanced materials for biomedical applications. *Acta Biomater* 31:17–32
- Kim HL, Jung GY, Yoon JH, Han JS, Park YJ, Kim DG, Zhang M, Kim DJ (2015) Preparation and characterization of nano-sized hydroxyapatite/alginate/chitosan composite scaffolds for bone tissue engineering. *Mater Sci Eng C Mater Biol Appl* 54:20–25
- Koh L-D, Cheng Y, Teng Y-P, Khin Y-W, Loh X-J, Tee S-Y, Low M, Ye E, Yu H-D, Zhang Y-W, Han M-Y (2015) Structures, mechanical properties and applications of silk fibroin materials. *Prog Polym Sci* 46:86–110
- Ku Y, Shim IK, Lee JY, Park YJ, Rhee S-H, Nam SH, Park JB, Chung CP, Lee SJ (2009) Chitosan/poly(l-lactic acid) multilayered membrane for guided tissue regeneration. *J Biomed Mater Res A* 90:766–772
- Lalwani G, Henslee AM, Farshid B, Lin L, Kasper FK, Qin YX, Mikos AG, Sitharaman B (2013) Two-dimensional nanostructure-reinforced biodegradable polymeric nanocomposites for bone tissue engineering. *Biomacromolecules* 14:900–909
- Langer R, Vacanti JP (1993) Tissue engineering. *Science* 260:920–926
- Lastra ML, Molinuevo MS, Cortizo AM, Cortizo MS (2016) Fumarate copolymer–chitosan cross-linked scaffold directed to osteochondrogenic tissue engineering. *Macromol Biosci*. doi:10.1002/mabi.201600219
- Lee KY, Mooney DJ (2012) Alginate: properties and biomedical applications. *Prog Polym Sci* 37:106–126
- Lee JM, Kim JH, Lee OJ, Park CH (2013) The fixation effect of a silk fibroin-bacterial cellulose composite plate in segmental defects of the zygomatic arch: an experimental study. *JAMA Otolaryngol Head Neck Surg* 139:629–635
- Lenaerts V, Couvreur P, Christiaens-Leyh D, Joiris E, Roland M, Rollman B, Speiser P (1984) Degradation of poly(isobutylcyanoacrylate) nanoparticles. *Biomaterials* 5:65–68
- Leonard F, Kulkarni RK, Brandes G, Nelson J, Cameron JJ (1966) Synthesis and degradation of poly(alkyl α -cyanoacrylates). *J Polym Sci* 10:259–272
- Leong KW, Brott BC, Langer RJ (1985) Bioerodible polyanhydrides as drug-carrier matrices. I: characterization, degradation, and release characteristics. *Biomed Mater Res* 19:941–955
- Levengood SL, Zhang M (2014) Chitosan-based scaffolds for bone tissue engineering. *J Mater Chem B Mater Biol Med* 2:3161–3184
- Liuyun J, Yubao L, Chengdong X (2009) Preparation and biological properties of a novel composite scaffold of nano-hydroxyapatite/chitosan/carboxymethyl cellulose for bone tissue engineering. *J Biomed Sci* 16:65
- Logith Kumar R, Keshav Narayan A, Dhivya S, Chawla A, Saravanan S, Selvamurugan N (2016) A review of chitosan and its derivatives in bone tissue engineering. *Carbohydr Polym* 151:172–188
- Ma PX (2008) Biomimetic materials for tissue engineering. *Adv Drug Deliv Rev* 60:184–198
- Mano JF, Silva GA, Azevedo HS, Malafaya PB, Sousa RA, Silva SS, Boesel LF, Oliveira JM, Santos TC, Marques AP, Neves NM, Reis RL (2007) Natural origin biodegradable systems in tissue engineering and regenerative medicine: present status and some moving trends. *J R Soc Interface* 4:999–1030
- Martin C, Winet H, Bao JY (1996) Acidity near eroding polylactidepolyglycolide in vitro and in vivo in rabbit tibial bone chambers. *Biomaterials* 17:2373–2380
- Maté Sánchez de Val JE, Calvo Guirado JL, Ramírez Fernández MP, Delgado Ruiz RA, Mazón P, De Aza PN (2015) In vivo behavior of hydroxyapatite/ β -TCP/collagen scaffold in animal model. Histological, histomorphometrical, radiological, and SEM analysis at 15, 30, and 60 days. *Clin Oral Implants Res* 102:1037–1046

- Meghezi S, Seifu DG, Bono N, Unsworth L, Mequanint K, Mantovani D (2015) Engineering 3D cellularized collagen gels for vascular. Tissue regeneration. *J Vis Exp* 100:1–12
- Melke J, Midha S, Ghosh S, Ito K, Hofmann S (2016) Silk fibroin as biomaterial for bone tissue engineering. *Acta Biomater* 31:1–16
- Mienaltowski MJ, Birk D (2014) Structure, physiology, and biochemistry of collagens. *Adv Exp Med Biol* 802:5–29
- Mkhabela VJ, Ray SS (2014) Poly(ϵ -caprolactone) nanocomposite scaffolds for tissue engineering: a brief overview. *J Nanosci Nanotechnol* 14:535–545
- Mohammadi Y, Soleimani M, Fallahi-sichani M, Gazme A, Haddadiasl V, Arefian E, Kiani J, Moradi R, Atashi A, Ahmadbeigi N (2007) Nanofibrous poly(ϵ -caprolactone)/poly(vinyl alcohol)/chitosan hybrid scaffolds for bone tissue engineering using mesenchymal stem cells. *Int J Artif* 30:204–211
- Mondrinos MJ, Dembzyński R, Lu L, Byrapogu VKC, Wootton DM, Lelkes PI, Zhou J (2006) Porogen-based solid freeform fabrication of polycaprolactone-calcium phosphate scaffolds for tissue engineering. *Biomaterials* 27:4399–4408
- Murthy N, Wilson S, Sy JC (2012) Biodegradation of polymers. In: Matyjaszewski K, Möller M (eds) *Polymer science: a comprehensive reference*. Amsterdam, Elsevier, pp 547–560
- Ngiam M, Liao S, Patil AJ, Cheng Z, Yang F, Gubler MJ, Ramakrishna S, Chan CK (2009) Fabrication of mineralized polymeric nanofibrous composites for bone graft materials. *Tissue Eng Part A* 15:535–546
- Nguyen TB, Lee BT (2014) A combination of biphasic calcium phosphate scaffold with hyaluronic acid-gelatin hydrogel as a new tool for bone regeneration. *Tissue Eng Part A* 20:1993–2004
- Niranjan R, Koushik C, Saravanan S, Moorthi A, Vairamani M, Selvamurugan N (2013) A novel injectable temperature-sensitive zinc doped chitosan/ β -glycerophosphate hydrogel for bone tissue engineering. *Int J Biol Macromol* 54:24–29
- Novotna K, Havelka P, Sopuch T, Kolarova K, Vosmanska V, Lisa V, Svorcik V, Bacakova L (2013) Cellulose-based materials as scaffolds for tissue engineering. *Cellulose* 20:2263–2278
- O'Brien F (2011) Biomaterials and scaffolds for tissue engineering. *Mater Today* 14:88–95
- Oryan A, Alidadi S, Bigham-Sadegh A, Moshiri A (2016) Comparative study on the role of gelatin, chitosan and their combination as tissue engineered scaffolds on healing and regeneration of critical sized bone defects: an in vivo study. *J Mater Sci Mater Med* 27:155
- Park ES, Maniar M, Shah J (1996) Effects of model compounds with varying physicochemical properties on erosion of polyanhydride devices. *J Control Release* 40:111–121
- Park H, Choi B, Nguyen J, Fan J, Shafi S, Klokkevold P, Lee M (2013) Anionic carbohydrate-containing chitosan scaffolds for bone regeneration. *Carbohydr Polym* 97:587–596
- Peter SJ, Nolley JA, Widmer MS, Merwin JE, Yazemski MJ, Yasko AW, Engel PS, Mikos AG (1997) In vitro degradation of a poly(propylene fumarate)/ β -tricalciumphosphate composition orthopaedic scaffold. *Tissue Eng* 3:207–215
- Pigossi SC, de Oliveira GJ, Finoti LS, Nepomuceno R, Spolidorio LC, Rossa C Jr, Ribeiro SJ, Saska S, Scarel-Caminaga RM (2015) Bacterial cellulose-hydroxyapatite composites with osteogenic growth peptide (OGP) or pentapeptide OGP on bone regeneration in critical-size calvarial defect model. *J Biomed Mater Res A* 103:3397–3406
- Pina S, Oliveira JM, Reis RL (2015) Natural-based nanocomposites for bone tissue engineering and regenerative medicine: a review. *Adv Mater* 27:1143–1169
- Polo-Corrales L, Latorre-Esteves M, Ramirez-Vick JE (2014) Scaffold design for bone regeneration. *J Nanosci Nanotechnol* 14:15–56
- Qiu H, Yang J, Kodali P, Koh J, Ameer GA (2006) Citric acid-based hydroxyapatite composite for orthopedic implants. *Biomaterials* 27:5845–5854
- Raghavendran HRB, Puvaneswary S, Talebian S, Murali MR, Naveen SV, Krishnamurthy G, McKean R, Kamarul T (2014) A comparative study on in vitro osteogenic priming potential of electron spun scaffold PLLA/HA/Col, PLLA/HA, and PLLA/Col for tissue engineering application. *PLoS One* 9:e104389
- Rașoga O, Sima L, Chirițoiu M, Popescu-Pelin G, Fufă O, Grumezescu V, Socol M, Stănculescu A, Zgură I, Socol G (2017) Biocomposite coatings based on Poly(3-hydroxybutyrate-co-3-

- hydroxyvalerate)/calcium phosphates obtained by MAPLE for bone tissue engineering. *Appl Surf Sci* 417:204–212. doi:10.1016/j.apsusc.2017.01.205
- Rau JV, Antoniac I, Cama G, Komlev VS, Ravaglioli A (2016) Bioactive materials for bone tissue engineering. *Biomed Res Int* 2016:3741428; 1–3
- Razak SIA, Sharif NFA, Rahman WAWA (2012) Biodegradable polymers and their bone applications: a review. *Int J Basic Appl Sci* 12:31–49
- Rezwan K, Chen QZ, Blaker JJ, Boccaccini AR (2006) Biodegradable and bioactive porous polymer/inorganic composite scaffolds for bone tissue engineering. *Biomaterials* 27:3413–3431
- Rhodes NP, Hunt JA, Longinotti C, Pavesio A (2011) In vivo characterization of Hyalonect, a novel biodegradable surgical mesh. *J Surg Res* 168:31–38
- Salgado AJ, Coutinho OP, Reis RL (2004) Bone tissue engineering: state of the art and future trends. *Review. Macromol Biosci* 4:743–765
- Samadikuchaksaraei A, Gholipourmalekabadi M, Erfani Ezadyar E, Azami M, Mozafari M, Johari B, Kargozar S, Jameie SB, Korourian A, Seifalian AM (2016) Fabrication and in vivo evaluation of an osteoblast-conditioned nano-hydroxyapatite/gelatin composite scaffold for bone tissue regeneration. *J Biomed Mater Res A* 104:2001–2010
- Sangkert S, Meesane J, Kamonmattayakul S, Chai WL (2016) Modified silk fibroin scaffolds with collagen/decellularized pulp for bone tissue engineering in cleft palate: morphological structures and biofunctionalities. *Mater Sci Eng C* 58:1138–1149
- Santos CA, Freedman BD, Leach KJ, Press DL, Scarpulla M, Mathiowitz E (1999) Poly(fumaric-co-sebacic anhydride): a degradation study as evaluated by FTIR, DSC, GPC and X-ray diffraction. *J Control Release* 60:11–22
- Saravanan S, Sameera DK, Moorthi A, Selvamurugan N (2013) Chitosan scaffolds containing chicken feather keratin nanoparticles for bone tissue engineering. *Int J Biol Macromol* 62:481–486
- Sarikaya B, Aydin HM (2015) Collagen/beta-tricalcium phosphate based synthetic bone grafts via dehydrothermal processing. *Biomed Res Int* 2015:576532
- Sarkar SK, Lee BT (2015) Hard tissue regeneration using bone substitutes: an update on innovations in materials. *Korean J Intern Med* 30:279–293
- Saska S, Barud HS, Gaspar AM, Marchetto R, Ribeiro SJ, Messaddeq Y (2011) Bacterial cellulose-hydroxyapatite nanocomposites for bone regeneration. *Int J Biomater* 2011:175362
- Schacht K, Jüngst K, Schweinlin M, Ewald A, Groll J, Scheibel T (2015) Biofabrication of cell-loaded 3D spider silk constructs. *Angew Chem* 54:2816–2820
- Schante CE, Zuber G, Herlin C, Vandamme TF (2012) Improvement of hyaluronic acid enzymatic stability by the grafting of amino-acids. *Carbohydr Polym* 87:2211–2216
- Schubert MA, Wiggins MJ, Anderson JM, Hiltner A (1997) Role of oxygen in biodegradation of poly(etherurethaneurea) elastomers. *J Biomed Mater Res* 34:519–530
- Smith R, Oliver C, Williams DF (1987) The enzymatic degradation of polymers *in vitro*. *J Biomed Mater Res* 21:991–1003
- Sun J, Tan H (2013) Review alginate-based biomaterials for regenerative medicine applications. *Materials* 6:1285–1309
- Sun Y, Shao Z, Ma M, Hu P, Liu Y, Yu T (1997) Acrylic polymer-silk fibroin blend fibers. *J Appl Polym Sci* 65(5):959–966
- Sun K, Li H, Li R, Nian Z, Li D, Xu C (2015) Silk fibroin/collagen and silk fibroin/chitosan blended three-dimensional scaffolds for tissue engineering. *Eur J Orthop Surg Traumatol* 25:243–249
- Tazi N, Zhang Z, Messaddeq Y, Almeida-Lopes L, Zanardi LM, Levinson D, Rouabhia M (2012) Hydroxyapatite bioactivated bacterial cellulose promotes osteoblast growth and the formation of bone nodules. *AMB Express* 2:61
- Teulé F, Miao Y-G, Sohn B-H, Kim Y-S, Hull JJ, Fraser MJ (2012) Silkworms transformed with chimeric silkworm/spider silk genes spin composite silk fibers with improved mechanical properties. *Proc Natl Acad Sci* 109:923–928
- Thurber AE, Omenetto FG, Kaplan DL (2015) In vivo bioresponses to silk proteins. *Biomaterials* 71:155–157

- Tian H, Tang Z, Zhuang X, Chen X, Jing X (2012) Biodegradable synthetic polymers: preparation, functionalization and biomedical application. *Prog Polym Sci* 37:237–280
- Uhrich KE, Gupta A, Thomas TT, Laurencin C, Langer R (1995) Synthesis and characterization of degradable polyanhydrides. *Macromolecules* 28:2148–2193
- Uhrich KE, Thomas TT, Laurencin CT, Langer R (1997) In vitro degradation characteristics of poly(anhydride-imide) containing trimellitylimidoglycine. *J Appl Polym Sci* 63:1401–1411
- Van Vlierberghe S, Dubruel P, Schacht E (2011) Biopolymer-based hydrogels as scaffolds for tissue engineering applications: a review. *Biomacromolecules* 12:1387–1314
- Vauthier C, Dubernet C, Fattal E, Pinto-Alphandary H, Couvreur P (2003) Poly(alkylcyanoacrylates) as biodegradable materials for biomedical applications. *Adv Drug Deliv Rev* 55:519–548
- Venkatesan J, Pallela R, Kim S-K (2014) Applications of carbon nanomaterials in bone tissue engineering. *J Biomed Nanotechnol* 10:3105–3123
- Venkatesan J, Bhatnagar I, Manivasagan P, Kang KH, Kim SK (2015) Alginate composites for bone tissue engineering: a review. *Int J Biol Macromol* 72:269–281
- Wahl DA, Czernuszka JT (2006) Collagen-hydroxyapatite composites for hard tissue repair. *Eur Cell Mater* 28:43–56
- Williams DF (1989) Polymer degradation in biological environments, Chapter 5. In: Allen G, Aggarwal SL, Russo S (eds) *Comprehensive polymer science*, vol 6. Pergamon Press, Oxford, UK
- Winet H, Bao JY (1997) Comparative bone healing near eroding polylactide-polyglycolide implants of differing crystallinity in rabbit tibial bone chambers. *J Biomater Sci Polym Edn* 8:517–532
- Yamada S, Yamamoto K, Ikeda T, Yanagiguchi K, Hayashi Y (2014) Potency of fish collagen as a scaffold for regenerative medicine. *Biomed Res Int* 2014:302932
- Yan L-P, Salgado AJ, Oliveira JM, Oliveira AL, Reis RL (2013) De novo bone formation on macro/microporous silk and silk/nano-sized calcium phosphate scaffolds. *J Bioact Compat Polym* 28:439–452
- Yao D, Liu H, Fan Y (2016) Silk scaffolds for musculoskeletal tissue engineering. *Exp Biol Med* 241:238–245
- Yu H-S, Won J-E, Jin G-Z, Kim H-W (2012) Construction of mesenchymal stem cell-containing collagen gel with a macrochanneled polycaprolactone scaffold and the flow perfusion culturing for bone tissue engineering. *Biores Open Access* 1:124–136
- Yu Z, An B, Ramshaw JA, Brodsky B (2014) Bacterial collagen-like proteins that form triple-helical structures. *J Struct Biol* 186:451–461
- Zaikov GE (1985) Quantitative aspects of polymer degradation in the living body. *J Macromol Sci, Part C* 25:551–597
- Zhang N, Zeng C, Wang L, Ren J (2013) Preparation and properties of biodegradable poly(lactic acid)/poly(butylene adipate-co-terephthalate) blend with epoxy-functional styrene acrylic copolymer as reactive agent. *J Polym Environ* 21:286–292
- Zhang J, Ma X, Fan D, Zhu C, Deng J, Hui J, Ma P (2014) Synthesis and characterization of hyaluronic acid/human-like collagen hydrogels. *Mater Sci Eng C Mater Biol Appl* 43:547–554
- Zhang X, Battiston KG, McBane JE, Matheson LA, Labow RS, Santerre JP (2016) Design of biodegradable polyurethanes and the interactions of the polymers and their degradation by-products within in vitro and in vivo environments, Chapter 3. In: Cooper SL, Guan J (eds) *Advances in polyurethane biomaterials*. Woodhead Publishing, Duxford, pp 75–114
- Zia KM, Noreen A, Zuber M, Tabasum S, Mujahid M (2016) Recent developments and future prospects on bio-based polyesters derived from renewable resources: a review. *Int J Biol Macromol* 82:1028–1040

Seaweed Polysaccharides: Structure and Applications

Vanina A. Cosenza, Diego A. Navarro, Nora M.A. Ponce, and Carlos A. Stortz

1 Introduction

Seaweeds produce polysaccharides usually as storage products and as part of their cell walls (Graham and Wilcox 2000). Within the latter, these macromolecules are found both in the fibrillar wall and the intercellular matrix, generally together with other biopolymers. Polysaccharides of industrial and biomedical relevance have been isolated from red seaweeds or Rhodophyta (carrageenans, agarans, etc.), brown seaweeds or Phaeophyta (alginates, fucoidans, etc.), and some green seaweeds, within the Chlorophyta (ulvans, among others). Each of these polysaccharides has a defined chemical structure, which may vary between species, life stages, season of harvest, habitat, and even extraction procedures (Pomin 2011; Synytsya et al. 2015). Furthermore, they are generally available in large quantities from renewable sources, are nontoxic, and carry rheological and/or biological properties, which render them useful for a large variety of applications.

This chapter includes an updated presentation of the structure and properties of the polysaccharides from seaweeds, focusing on those with known or potential industrial and biomedical applications as well as biological activities.

V.A. Cosenza

Facultad de Ciencias Exactas y Naturales, Departamento de Química Orgánica, Universidad de Buenos Aires, Pabellón 2, Ciudad Universitaria, C1428EHA Buenos Aires, Argentina

D.A. Navarro • N.M.A. Ponce • C.A. Stortz (✉)

Facultad de Ciencias Exactas y Naturales, Departamento de Química Orgánica, Universidad de Buenos Aires, Pabellón 2, Ciudad Universitaria, C1428EHA Buenos Aires, Argentina

Consejo Nacional de Investigaciones Científicas y Técnicas (CONICET)-UBA, Centro de Investigación en Hidratos de Carbono (CIHIDECAR), Buenos Aires, Argentina

e-mail: stortz@qo.fcen.uba.ar

2 Polysaccharides from Red Seaweeds

2.1 Structure

Red seaweeds produce storage polysaccharides, such as the floridean starch or floridean glycogen ($[\alpha\text{-}(1\rightarrow4)\text{-D-Glcp}]$, branched at C-6), and cell wall polysaccharides (Usov 2011). The latter include fibrillar polysaccharides (cellulose, $\beta\text{-}(1\rightarrow4)$ mannans, $\beta\text{-}(1\rightarrow4)$ and $\beta\text{-}(1\rightarrow3)$ xylans) and the amorphous matrix gelling or thickening polysaccharides (sulfated galactans or mannans) (Craigie 1990). These last polysaccharides are the most abundant and have several applications. Sulfated galactans are found in most orders, whereas sulfated mannans are found mainly within the Nemaliales (Usov 2011).

Sulfated galactans are generally composed of repeating units of $[\rightarrow3)\text{-}\beta\text{-D-Galp-}(1\rightarrow4)\text{-}\alpha\text{-Galp-}(1\rightarrow)]$. The configuration of the α -linked unit defines the type of galactan: carrageenans, D-series; agarans, L-series; and DL-hybrids, both series (Stortz and Cerezo 2000). The basic backbone of each of these galactans undergoes small modifications and diverse substitutions that lead to a wide variety of polysaccharides. The most frequent natural modification is the cyclization of α -galactose 6-sulfate to yield 3,6-anhydrogalactose. This could also occur at the laboratory level with the so-called alkaline treatment reaction (Usov 2011). Substitution of the hydroxyls occurs mainly by sulfate groups, though methyl ethers and pyruvic acid ketals, as well as single stubs of xylose and 4-O-methylgalactose, were also found (Stortz and Cerezo 2000).

2.1.1 Carrageenans

Carrageenans are mostly biosynthesized by red seaweeds belonging to the order Gigartinales. As previously mentioned, their backbone is only composed by D-Galp, mainly substituted by sulfate groups, as other substituents are rarely found. Carrageenans are grouped in four families depending on the location of the sulfate groups in the β -galactose moiety and then classified according to the presence or absence of the 3,6-anhydro sugar, as well as to the location of the sulfate groups in the α -galactose moiety (Fig. 1). This classification is based on ideal structures, though “real” carrageenans may have mixtures of diads or slightly modified structures.

The κ -family comprises κ - and ι -carrageenans, their precursors μ -carrageenan and ν -carrageenan, and o-carrageenan. The latter is the rarest member of the family, only found in some species of the families Phyllophoraceae and Solieriaceae (Craigie 1990). The best known members of the family are κ - and ι -carrageenan, as they have commercial applications due to their gelling properties (Campos et al. 2009). They are usually found in nature together with their precursors in a substantial number of species of the order Gigartinales (Fig. 2, Usov 2011). The families Gigartinaceae and Phyllophoraceae produce these carrageenans only in the gametophytic stage of their reproductive cycle (Stortz and Cerezo 2000; Usov 2011).

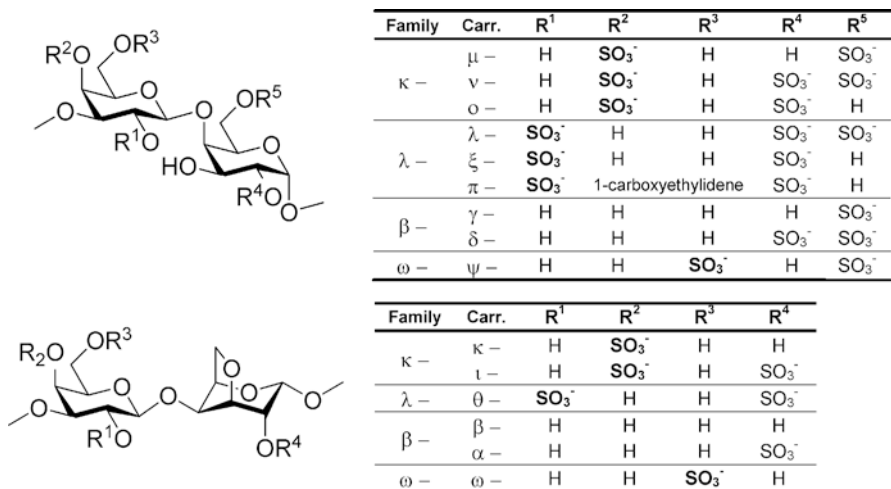


Fig. 1 Classification of the ideal repeating units of the carrageenans

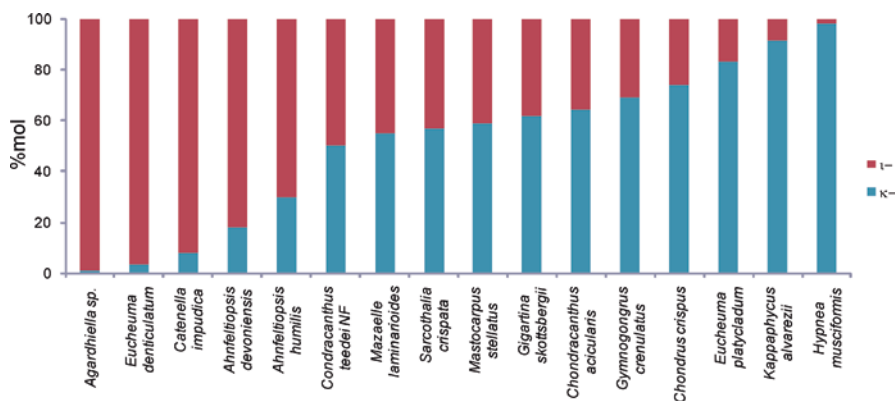


Fig. 2 κ- and ι-content in κ/ι-hybrid obtained from different species from order Gigartinales (Van de Velde et al. 2005; Pereira 2013; Soares et al. 2016)

Ideal carrageenans composed only of κ- or ι-diads are rarely found in nature. Generally, both diads are found together (κ/ι-hybrids). When these hybrids have 45–80% of κ-diads, they are known as kappa 2 (van de Velde et al. 2005). It is not known if these hybrids are inseparable mixtures of homopolymeric chains of κ- and ι-carrageenan or if they are heteropolymers with both diads coexisting, either in blocks or randomly (van de Velde et al. 2005).

The members of the λ-family are λ-, ξ-, π-, and θ-carrageenan. They are mainly produced by the tetrasporic plants of the families Phylloporaceae, Petrocelidaceae, and Gigartinaceae (Stortz and Cerezo 2000; Usov 2011). λ-Carrageenan is the most important member of this family as it is industrially used due to its thickening

properties (Campos et al. 2009). Actually, natural λ -carrageenans bearing the “ideal” diads (i.e., three sulfate groups per diad) are rarely found (Stortz et al. 1994; Guibet et al. 2006). ξ -Carrageenan is usually found in some tetrasporic plants of species belonging to the Gigartinales and Phylloporaceae, such as *Gigartina clavifera*, *G. alveata* (Usov 2011), and *Stenogramme interrupta* (Cáceres et al. 2000). π -Carrageenan is also found in *Petrocelis middendorffii*, *G. clavifera*, and *G. alveata* (Usov 2011). θ -Carrageenan is not commonly found in nature, though it has been isolated from *Callophyllis hombroniana* (Usov 2011).

Carrageenans belonging to the β -family include β - and α -carrageenan and their precursors γ - and δ -carrageenan. They are usually found together with the members of the κ -family. κ - β -Hybrids, sometimes called furcellarans, were isolated mainly from *Furcellaria lumbricalis* (Knutsen et al. 1990), while a κ - β - γ -hybrid was found in *Eucheuma gelatiniae* (Greer and Yaphe 1984). ι - α - δ -Hybrids were found in the cystocarpic plants of *Catenella nipae* (Falshaw et al. 1996) and *Stenogramme interrupta* (Cáceres et al. 2000). There are only two members of the ω -family: ω - and its precursor ψ -carrageenan. A κ - ω -hybrid was isolated from *Rissoella verruculosa* (Mollion et al. 1988). ψ -Carrageenan was found as the main component of the tetrasporic plants of *S. interrupta* from New Zealand (Miller 2001), although a sample of the same seaweed in Chile was reported to give a ξ -carrageenan (Cáceres et al. 2000), thus showing the relevance of the collection place for structural studies.

2.1.2 Agarans

The name “agaran” was used for the polysaccharides with a backbone of $[\rightarrow 3) \beta$ -D-Galp-(1 \rightarrow 4)-(3,6-An)- α -L-Galp] (Fig. 3). Unlike carrageenans, it is not possible to develop a sharp classification of agarans. Nonetheless, Miller (1997) proposed the following classification: (a) agarose $[\rightarrow 3) \beta$ -D-Galp-(1 \rightarrow 4)-3,6-An- α -L-Galp-(1 \rightarrow); (b) agar, similar to agarose but with some precursor units and few sulfates and

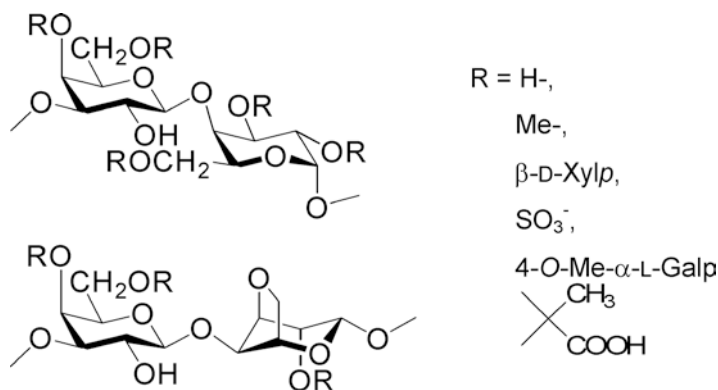


Fig. 3 Structures of different agarans (Adapted from Usov 2011)

pyruvic ketals; and (c) agaroids which are highly substituted by sulfate groups, methoxyl groups, xylose or 4-*O*-methylgalactose stubs, etc., and do not have gelling properties (unlike agar and agarose).

There are several red seaweed orders that produce agarans. Agarose and highly “pure” agar are mainly produced by the orders Gelidiales (genera *Gelidium*, *Gelidiella*, and *Pterocladia*) and Ahnfeltiales (genus *Ahnfeltia*) (Ciancia and Matulewicz 2015). These galactans may be substituted with methoxyl groups. Sulfated agar was isolated from the genus *Gracilaria* (order Gracilariales). Polysaccharides from this last genus may present, besides sulfate substitution, sugar branching and methyl and pyruvic acid substituents (Murano 1995).

The structure of non-gelling agaroids is much more complex. Porphyrans are galactans produced by the genus *Porphyra* whose backbone is made of (6-*O*-methyl)- β -D-galactose and 3,6-anhydro- α -L-galactose or α -L-galactose 6-sulfate (Usov 2011). These polysaccharides have gelling properties only after alkaline treatment which converts them into a partially methoxylated agarose.

Corallinans are agarans produced by the order Corallinales. These galactans are highly branched with xylose (generally on C-6 of the β -galactose), methylated and sulfated (at O-2 or O-3 of α -L-galactose) and do not carry 3,6-anhydrogalactose or galactose 6-sulfate (Usov 2011). The corallinans of *Jania rubens* are an exception, as they carry some anhydro sugar (Navarro and Stortz 2008). An interesting discovery is that the seaweeds of this order produce, besides the corallinans, alginic acid (Usov 2011), a polysaccharide found profusely in brown seaweeds.

Species from the order Ceramiales produce a wide variety of agaroids, though some similarities were found between families and genera (Miller 2003). Seaweeds belonging to the family Ceramiaceae produce an agarose-like polysaccharide with important amounts of precursors sulfated at different positions and β -galactose units methoxylated in C-6 (Usov 2011). The family Delesseriaceae produces highly sulfated agarans, with low amounts of 3,6-anhydrogalactose (Miller 2005). Agarans produced in the family Rhodomelaceae are diverse: Species belonging to genus *Polysiphonia* produce a polysaccharide with an agarose-like structure, but sulfated or branched with xylose stubs, in C-6 of the β -galactose (Miller 2003). Those from the genus *Laurencia* produce agarans with important amounts of 3,6-anhydrogalactose (Usov and Elashvili 1991), though it was reported that *L. thyrsoifera* presents lower levels of 3,6-anhydrogalactose (Miller et al. 1993). Substitution of the backbone is diverse, including sulfate, methoxyl, and pyruvic groups as well as xylose stubs, and they are usually highly substituted (Ciancia and Matulewicz 2015).

2.1.3 DL-Hybrids

Traditionally, it was assumed that red seaweeds produce either carrageenans or agarans as the main polysaccharides of the amorphous matrix, though some species, mainly those belonging to the old order Cryptonemiales, produce DL-hybrids (Stortz and Cerezo 2000). In the early 1990s, Craigie and Rivero-Carro (1992) observed the presence of these hybrids in carragenophytic species (i.e., seaweeds that produce

carrageenans). Since then, these galactans were found in many carrageenophyte and agarophyte species (Table 1).

The structure determined for different hybrids is diverse. They always show the typical backbone of red seaweed galactans, with different proportions of D- and L- α -galactose, going from agaran-rich hybrids, carrageenan-rich hybrids, and evenly distributed hybrids. Further fractionation of the DL-hybrids found in *I. undulosa* (Stortz et al. 1997), *K. alvarezii* (Estévez et al. 2004), and *H. musciformis* (Cosenza et al. 2017) showed that they were actually a mixture of galactans with different proportions of D- and L-galactose in each fraction. Moreover, as it happens with κ - λ -hybrids, it is still unclear whether these galactans are single polymeric backbones having α -galactose units belonging to both series or just an inseparable mixture of carrageenans and agarans.

Substitution among these hybrids is varied, including sulfate and methyl groups as well as single stubs of xylose and 4-*O*-methylgalactose (Stortz and Cerezo 2000; Usov 2011). A recent study of the DL-hybrid isolated from *H. musciformis* showed the presence of an unusual monosaccharide: 3-*C*-carboxy-D-erythrose or (2*R*,3*R*)-apiuronic acid. This sugar was found in its β -furanosic form as a side stub substituting the C-6 of the β -galactose of those fractions bearing both carrageenan and agaran diads (Cosenza et al. 2017). Furthermore, small amounts of this sugar were also found in the DL-hybrids of *I. undulosa* and *K. alvarezii*. The appearance of this novel monosaccharide raises the question about its biosynthetic role.

2.1.4 Sulfated Mannans and Xylomannans

Sulfated mannans and xylomannans have been mainly found in red seaweeds belonging to the order Nemaliales. These polysaccharides generally have a backbone composed of [\rightarrow 3) α -D-Manp (1 \rightarrow)], except for the mannans isolated from *Galaxaura rugosa*, which carry β -(1 \rightarrow 3) linkages, and can be substituted with sulfate groups or single stubs of xylose. The pattern of substitution depends on the seaweed. The first sulfated mannans encountered from *Nemalion vermiculare* were sulfated at O-4 and O-6 and branched at C-2 with a β -xylopyranoside residue (Usov 2011). Mannans isolated from *Liagora valida* (Usov and Dobkika 1991) and *N. helminthoides* (Pérez Recalde et al. 2009) were sulfated at O-4 and O-6 and, in some cases, substituted at C-2 with xylose. *Nothogenia fastigiata* produces a mannan sulfated at O-2 and O-6 and branched at C-2 (Kolender et al. 1997), while the mannan from *Scinaia hatei* was sulfated only at O-4, with single stubs of xylose found in all three possible positions (Mandal et al. 2008).

Sulfated mannans were also found in some species of other orders. *Sebdenia flabellata* (formerly *S. polydactyla*, Sebdeniales) produces a polysaccharide similar to that isolated from *Nothogenia fastigiata*, but the branching occurred at C-6 (Gosh et al. 2009). *Chondrophycus papillosus* and *C. flagelliferus* (Ceramiales), on the other hand, produced a mannan with a completely different backbone as the mannose units are β -(1 \rightarrow 4) linked, sulfated at O-2, and branched at C-6 with β -xylopyranose or β -mannopyranose 2-sulfate units (Cardoso et al. 2007).

Table 1 Red seaweeds producing DL-hybrids

Order	Family	Species	Galactans
Bonnemaisoniales	Bonnemaisoniaceae	<i>Asparagopsis armata</i>	DL-Hybrids
Ceramiales	Rhodomelaceae	<i>Digenea simplex</i>	Agar + DL-hybr.
		<i>Neorhodomela larix</i> ^a	Agar + DL-hybr.
Gigartinales	Cystocloniaceae	<i>Hypnea musciformis</i> ^{b1}	κ/ι-Carr. + DL-hybr.
		<i>Rhodophyllis divaricata</i>	λ-Carr. + DL-hybr.
	Dumontiaceae ^c	<i>Constantinea rosa-marina</i>	Agar + DL-hybr.
		<i>Constantinea subulifera</i>	DL-Hybrids
		<i>Cryptosiphonia woodii</i>	DL-Hybrids
		<i>Neodilsea borealis</i>	DL-Hybrids
		<i>Neodilsea natashae</i>	DL-Hybrids
		<i>Neodilsea yendoana</i>	DL-Hybrids
	Endocladiaaceae ^c	<i>Endocladia muricata</i>	κ-β-Carr. + DL-hybr.
		<i>Gloiopeltis furcata</i>	Agar + DL-hybr.
	Gigartinaceae	<i>Chondrus crispus</i>	κ-ι-Carr. + DL-hybr. ^d
		<i>Chondracanthus canaliculatus</i>	κ-ι-Carr. + DL-hybr. ^d
		<i>Gigartina skottsbergii</i>	κ-ι-Carr. + DL-hybr. ^d
		<i>Mazzaella leptorhynchus</i>	κ-ι-Carr. + DL-hybr. ^d
		<i>Iridaea undulosa</i>	λ-Carr. + DL-hybr. ^e
	Kallymeniaceae ^c	<i>Euthora cristata</i> ^f	DL-Hybrids
		<i>Cirrularia gmelini</i>	DL-Hybrids
	Phyllophoreaceae	<i>Gymnogongrus griffithsia</i> ^{b2}	κ-ι-Carr. + DL-hybr. ^d
		<i>Gymnogongrus tenuis</i> ^{b3}	κ-ι-Carr. + DL-hybr.
		<i>Gymnogongrus torulosus</i>	κ-ι-Carr. + DL-hybr. ^d
<i>Mastocarpus stellatus</i>		κ-ι-Carr. + DL-hybr. ^d	
Solieriaceae	<i>Kappaphycus alvarezii</i> ^{b4}	κ-ι-Carr. + DL-hybr.	
	<i>Meristotheca gelidium</i> ^{b5,g}	κ-ι-Carr. + DL-hybr.	
Halymeniales ^c	Halymeniaceae	<i>Aeodes nitidissima</i> ^{b6}	DL-Hybrids
		<i>Cryptonemia crenulata</i> ^{b2}	DL-Hybrids
		<i>Cryptonemia seminervis</i> ^{b7}	DL-Hybrids
		<i>Grateloupia indica</i>	DL-Hybrids
		<i>Grateloupia divaricata</i>	DL-Hybrids
		<i>Halymenia durvilleri</i> ^{b8}	DL-Hybrids
Nemastomatales	Schizymeniaceae	<i>Schizymenia binderi</i> ^{b9}	DL-Hybrids
		<i>Schizymenia dubyi</i>	λ-Carr. + DL-hybr
		<i>Schizymenia pacifica</i>	DL-Hybrids
Plocamiales	Plocamiaceae	<i>Plocamium cirrhosum</i> ^h	DL-Hybrids
	Sarcodiaceae	<i>Sarcodia montagneana</i>	λ-Carr. + DL-hybr.

(continued)

Table 1 (continued)

Order	Family	Species	Galactans
Rhodiales	Champiaceae	<i>Champia novae-zelandiae</i>	DL-Hybrids
	Lomentariaceae	<i>Fushitsunagia catenata</i> ⁱ	DL-Hybrids
	Hymenocladaceae	<i>Hymenocladia chondricola</i> ^j	DL-Hybrids

Adapted and renewed from Takano et al. (2003)

^aFormely known as *Rhodomela larix*

^bNew citations: 1- Cosenza et al. (2014, 2017) , 2- Talarico et al. (2004), 3- Pérez Recalde et al. (2016), 4- Estévez et al. (2004), 5- de SF-Tiescher et al. (2006), 6- Miller and Blunt (2005), 7- Mendes et al. (2014), 8- Fenoradosa et al. (2009), 9- Matsuhiro et al. (2005)

^cOrder or family belonging to the old Cryptonemiales order

^dDL-Hybrids only observed in cystocarpic phase

^eDL-Hybrids only observed in tetrasporic phase

^fFormely known as *Callophyllis cristata*

^gFormely known as *Meristiella gelidium*

^hFormely known as *Plocamium costatum*

ⁱFormely known as *Lomentaria catenata*

^jFormely known as *Hymenocladia sanguinea*

2.2 Industrial Applications

Red seaweed galactans are widely used at an industrial level due to their rheological behavior, i.e., thickening (λ -carrageenan) or gelling (agarose, κ - and ι -carrageenan) properties. Gelation of these galactans is a complex process not completely understood. It implies an initial coil-to-helix transition, followed by the aggregation of the helices and consequent network formation (Piculell 2006). This process depends on different factors such as temperature, structure, concentration, presence of cations, etc. Gelling galactans have high amounts of 3,6-anhydrogalactose in their backbone, as the ¹C₄ conformation of this sugar (Figs. 1 and 3) favors the helix formation. Alkaline treatment is usually performed when used for commercial purposes as it raises the proportion of the anhydro sugar. The rheological properties of commercial galactans allow them to be used in different applications (Table 2).

Carrageenans are industrially extracted from different Gigartinales seaweeds: *Kappaphycus alvarezii* (κ -carrageenan), *Eucheuma denticulatum* (ι -carrageenan), *Gigartina skottsbergii* (κ - ι -hybrids or λ -carrageenan), and *Chondrus crispus* (κ - ι -hybrids or λ -carrageenan). *Hypnea musciformis* (κ -carrageenan) and *Sarcothalia crispata* (κ - ι - or λ -carrageenan) are also used (Bixler and Porse 2011). These galactans have the highest sale volume and lower price among the different commercial seaweed polysaccharides. Depending on the extraction process, two types of commercial carrageenans are found: refined and semi-refined (simpler extraction, less pure carrageenan); both are reported to be suitable for human consumption (Bixler and Porse 2011).

Table 2 Properties of the different gels of the commercial galactans

	Agar/agarose	κ -Carrageenan	ι -Carrageenan	λ -Carrageenan
Rheological property	Firm, rigid gel	Strong, rigid gel in the presence of K^+	Elastic gel in the presence of Ca^{2+}	Viscous solution
Thermal hysteresis	Large	Medium	Low	–
Syneresis	Large	Medium	No	–

Adapted from García Tasende and Manríquez-Hernández (2016)

In the food industry, they are used in the dairy production as they interact with the positive charges present in milk (Mc Hugh 2003). In particular, κ -carrageenan is used to prevent whey separation and keep the cocoa in suspension in chocolate milk, while λ -carrageenan improves the stability and texture of the products. Interaction of carrageenans with proteins is also used for wine clarification (Cabello-Pacini et al. 2005). Gelling carrageenans are also used as gelatin or pectin substitutes for deserts and jellies, mainly for low-calorie, vegetarian, or vegan products (García Tasende and Manríquez-Hernández 2016). In the meat industry, they are used mainly for the precooked products, as they avoid water loss during the cooking process and in low-fat products as they improve texture and moisture, giving fat-like characteristics (Mc Hugh 2003). Due to the ability to absorb water, carrageenans are also used in bakery products, mainly in dough and pastes (Kohajdova and Karovčova 2009). Another interesting application of carrageenans in food industry is in edible coatings mainly of fresh-cut fruit (Campos et al. 2011).

Other industries also use carrageenans. ι -Carrageenan is used as toothpaste binder due to its thixotropic properties, whereas κ -carrageenan is used in air freshener gels and in pet foods (Mc Hugh 2003; Bixler and Porse 2011). Both carrageenans are also used in water-based paints due to their ability to prevent the settling of particles (García Tasende and Manríquez-Hernández 2016). In addition, carrageenans are also used in shampoos and hand lotions as they act as thickening and stabilizing agents as well as promoting soft skin and silky hair.

In the biotechnological area, carrageenans are used as microorganism-immobilizing agents for industrial treatment, as well as in the production of 6-aminopenicillanic acid, L-alanine, among others (Neccas and Bartosikova 2013).

Agar is obtained from species of the genera *Gelidium* and *Gracilaria* and less from *Ahnfeltia* and *Pterocladia* sp. (Mc Hugh 2003). *Gelidium* and *Pterocladia* spp. produce higher-quality agar (i.e., stronger gels) than *Gracilaria* sp. Agar isolated from species of this last genus requires alkaline treatment to be commercially used. Agarose is generally obtained from the *Gelidium* agar (Bixler and Porse 2011). Agar has the lowest sale volume of commercial seaweed polysaccharides and the highest average price. Both agar and agarose gels have higher stiffness and thermal hysteresis than carrageenan gels (Stanley 2006). Substitution of the backbone alters these properties, e.g., natural methylation increases the gelling temperature while sulfation lowers syneresis.

Due to its price, agar is less used in food industry than carrageenan. The high melting and gelification temperature of agar gels make it useful for pastry fillings and glazes (Bixler and Porse 2011) as well as for generating gelled meat and fish (Mc Hugh 2003). In bakery products, the water-binding properties of agar improve the viscoelastic characteristics as well as the texture and moisture of dough and pastes (Venugalpa Menon 2011). Agar is also used in confectionery, to improve stability and texture of sherbets and ice creams as well as in cheese and fermented milk products (Stanley 2006).

Agar and agarose are also used in microbiology and molecular biology. The large thermal hysteresis of the gel makes it suited for culture media for bacteriological use (Stanley 2006). Furthermore it can be used as an encapsulating agent for microorganisms and cells (Rinaudo 2008; Zajkoska et al. 2013). Agarose is mostly used in gel electrophoresis analyses (Bixler and Porse 2011) and also for cell encapsulation (Rinaudo 2008). Moreover, modified beaded agarose is used as matrix in affinity, size-exclusion, and ion-exchange chromatography (Zucca et al. 2016).

2.3 *Biological Activities*

Red seaweed polysaccharides, as most sulfated polysaccharides from seaweeds, have many biological properties, including anticoagulant, antithrombotic, anti-inflammatory, antitumor, and antiviral, among others. These properties derive from their negative charge and their resemblance to the glycosaminoglycans (GAGs) present in the cell membranes of mammals (Pujol et al. 2007). The antiviral activity is attributed to the capacity of the sulfated polysaccharides to prevent the adhesion and/or penetration of the virus to the cell as they interfere in the interaction between the virus and the GAGs (Spillmann 2001). The antitumor activity of these polysaccharides could be related to the destabilization of the interaction of the GAGs of the tumor cell and the proteins of the extracellular matrix (Haijin et al. 2003). The anticoagulant activity could be attributed to the similarity of the sulfated polysaccharides to heparin (Mestechkina and Shcherbukhin 2010).

It is worth mentioning that chemical modifications, mainly sulfation and depolymerization, may alter the biological activities of sulfated polysaccharides of red seaweeds (Damonte et al. 2004; Synytsya et al. 2015; Cosenza et al. 2016).

2.3.1 **Antiviral Activity**

Red seaweed polysaccharides have shown inhibitory capacity *in vitro* against different enveloped viruses, mainly herpes simplex virus types 1 and 2 (HSV-1 and HSV-2) and human immunodeficiency virus (HIV) but also others such as human cytomegalovirus (HCMV), dengue virus (DENV-1 to DENV-4), Influenza A virus, etc. (Pujol et al. 2007). Carrageenans have also shown activity against human papillomavirus (HPV), a non-enveloped virus (Buck et al. 2006).

Table 3 Spectrum of antiviral activity of different polysaccharides isolated from red seaweeds

	Species	Polysaccharide	Virus
Carrageenans	<i>Hypnea musciformis</i> ^{a1}	κ -Carr.	HSV
	<i>Gigartina skottsbergii</i>	κ -/ ι -, μ -/ ν -, λ -Carr.	HSV
	<i>Gymnogongrus griffithsiae</i> ^{a2}	κ -/ ι -Carr.	HSV
	<i>Meristotheca gelidium</i> ^{a3,b}	κ -/ ι -Carr.	DENV, HSV
	<i>Schizymenia pacifica</i>	λ -Family	HIV
	<i>Sphaerococcus coronopifolius</i> ^{a4}	λ -Family	HIV, HSV
	<i>Stenogramme interrupta</i>	ι -/ α -, ξ -/ λ -Carr.	HSV
Agarans	<i>Agardhiella tenera</i>	Sulfated agaran	HSV, HIV, HCMV
	<i>Boergesenella thuyoides</i> ^{a4}	Sulfated agaran	HIV, HSV
	<i>Bostrychia montagnei</i>	Sulfated agaran	HSV
	<i>Cryptopleura ramosa</i>	Sulfated agaran	HSV
	<i>Gracilaria corticata</i>	Sulfated agaran	HSV
	<i>Pterocladia capillacea</i>	Sulfated agaran	HCMV, HSV
DL-Hybrids	<i>Asparagopsis armata</i>	DL-Hybrid	HIV
	<i>Cryptonemia crenulata</i> ^{a2}	DL-Hybrid	HSV
	<i>Cryptonemia seminervis</i> ^{a5}	DL-Hybrid	HMPV
	<i>Digenea simplex</i>	Agar + DL-hybr.	HIV
	<i>Gymnogongrus griffithsiae</i> ^{a2}	DL-Hybrid	HSV
	<i>Gymnogongrus torulosus</i>	DL-Hybrid	DENV, HSV
	<i>Schizymenia binderi</i> ^{a6}	DL-Hybrid	HSV
Sulfated mannans	<i>Nemalion helminthoides</i> ^{a7}	Sulf. xylomannan	DENV, HSV
	<i>Nothogenia fastigiata</i>	Sulf. xylomannan	HIV, HSV
	<i>Scinaia hatei</i> ^{a8}	Sulf. xylomannan	HSV
	<i>Sebdenia flabellata</i> ^{a9,c}	Sulf. xylomannan	HSV

Adapted and renewed from Damonte et al. (2004)

^aNew citations: 1- Cosenza et al. (2015), 2- Talarico et al. (2004), 3- de SF-Tiescher et al. (2006), 4- Bouhlal et al. (2011), 5- Mendes et al. (2014), 6- Matsuhiro et al. (2005), 7- Perez Recalde et al. (2012), 8- Mandal et al. (2008), 9-Ghosh et al. (2009)

^bFormely known as *Meristiella gelidium*

^cFormely known as *Sebdenia polydactyla*

Different sulfated polysaccharides extracted from red seaweeds have been studied for their antiviral activity against different viruses (Table 3). Generally these compounds are capable of inhibiting the virus in concentrations of the order of 1 μ g/ml, or even lower, and exhibit high selectivity indices (i.e., relationship between the cytotoxic dose and the effective antiviral dose).

Among carrageenans, λ - and μ -/ ν -carrageenans are the most active against HSV-1 and HSV-2, followed by ι -carrageenan and finally κ -carrageenan (Damonte et al. 2004), i.e., in decreasing order of sulfation. θ -Carrageenan has similar antiviral properties as λ -carrageenan.

Agarans usually have lower sulfate contents and molecular weights, thus affecting adversely the antiviral activity (Damonte et al. 2004). Nonetheless, there are

examples of agarans presenting such activities, mainly against HSV (Table 3). The galactan from *Cryptopleura ramosa* is active against HSV-1 and HSV-2, despite its low molecular weight (2.8 kDa), due to its high sulfation levels ($\approx 30\%$) (Carlucci et al. 1997a).

The antiviral activity of DL-hybrids could be justified considering these polysaccharides as mixtures or block copolymers of carrageenans and agarans (Sect. 2.1.3). For example, the carrageenan-rich DL-hybrids extracted from *Gymnogongrus torulosus* are as active against HSV-2 as κ -carrageenans (Pujol et al. 2002). The DL-hybrid from *Schizymenia binderi*, also rich in carrageenan structures, has a higher inhibitory activity against HSV-1 and HSV-2 than many of the reported sulfated galactans (Matsuhira et al. 2005).

Sulfated mannans and xylomannans are also active against different enveloped virus. For example, the sulfated mannan extracted from *Nothogenia fastigiata* has a high inhibitory activity against herpes virus (Damonte et al. 1994).

Although highly promising in vitro, sulfated polysaccharides have some drawbacks for their utilization in vivo: low bioavailability, high degradation, low penetration in infected cells, and anticoagulant properties (Pujol et al. 2007). Some of these drawbacks can be solved by performing appropriate chemical modifications, but the main applications of these polysaccharides as antivirals are for topical use. Two formulations containing carrageenans have reached clinical trials. The first one is Carraguard®, a microbicidal gel made of κ - and λ -carrageenan against HIV, HSV, and HPV (The Carraguard Phase II South Africa Study Team 2010). Although it has not been possible to demonstrate its effectiveness against HIV, some reduction in the HPV infection was observed (Marais et al. 2011; Friedland et al. 2016). The other formulation is a nasal spray against common cold (human rhinovirus, human enterovirus, influenza virus, etc.) containing ι -carrageenan. This product is in phase IV of the clinical trial with promising results (Eccles et al. 2015).

2.3.2 Anticoagulant Activity

Anticoagulant activity has been described for carrageenans (Carlucci et al. 1997b; Farias et al. 2000; Sokolova et al. 2014), agarans (Zhang et al. 2010; Liang et al. 2014), DL-hybrids (Sen et al. 2002), and sulfated mannans (Perez Recalde et al. 2012).

Anticoagulant activity is modulated by sulfation. λ -Carrageenan resulted most potent than less sulfated κ - and κ - β -carrageenan (Sokolova et al. 2014). However, when comparing κ - ι -carrageenan and λ -carrageenan (one to two and three sulfate groups per disaccharidic unit, respectively), the latter resulted less active in APTT (activated partial thromboplastin time) assay, suggesting that other factors may also affect the activity (Yermak et al. 2012).

In porphyrans and agarose (agarans), anticoagulant activity was only observed when they were oversulfated, showing again the importance of the proportion of sulfate groups in this property (Zhang et al. 2010; Liang et al. 2014).

2.3.3 Antitumor Activity and Related Activities

Red seaweed galactans may also exhibit antitumor activity, though this biological property has been studied more deeply in polysaccharides from brown seaweeds (Pomin 2011). Nonetheless, these sulfated galactans are beginning to gain importance as anticancer agents. Sulfated polysaccharides extracted from *Champia feldmannii* (Lins et al. 2009), *Chondrus ocellatus* (Zhou et al. 2004), *Gracilaria lemaneiformis* (Fan et al. 2012), and *Grateloupia longifolia* (Zhang et al. 2006) presented antitumor activity in vivo and/or cytotoxic activity in vitro. Interestingly, the polysaccharide isolated from *C. feldmannii* was only active in vivo, probably related to the immunomodulating activity of the galactan. Depolymerization of carrageenans favors their antitumor activity (Haijin et al. 2003; Zhou et al. 2004; Bondu et al. 2010; Wang and Zhang 2014).

The anticancer activity in these polysaccharides is generally related to their immunomodulatory and/or antioxidant activity (Haijin et al. 2003; Lins et al. 2009; Bondu et al. 2010; Wang and Zhang 2014). The immunomodulating activity is mainly based on macrophage modulations, and it was studied in carrageenans (Abdala-Díaz et al. 2011), agarans (Yoshisawa et al. 1995), and sulfated mannans (Pérez-Recalde et al. 2014). λ -Carrageenan presents the highest activity of the macrophage-phosphatase, in the formation of reactive oxygen species and production of calcium on the cytoplasm, probably due to its high sulfate content (Yermak et al. 2012). The antioxidant activity of carrageenans is associated with the sulfation degree and pattern; λ -carrageenan resulted more active than κ - and ι -carrageenan when performing in vitro studies (Rocha de Sousa et al. 2007).

2.3.4 Other Biological Activities

Red seaweed galactans also present antihypertensive (Ren et al. 1994) and antilipidemic activity (Ren et al. 1994; Panlasiguin et al. 2003; Inoue et al. 2009) as well as blood cholesterol-lowering effects (Panlasiguin et al. 2003). The suppression of lipid synthesis by porphyrans reduces the secretion of apolipoprotein B100, a component in very low-density lipoprotein (Inoue et al. 2009). In addition, a study performed with humans showed that carrageenan reduces triglycerides and total cholesterol in serum but increases the high-density lipoprotein (HDL, Panlasiguin et al. 2003).

2.3.5 Toxicity of Carrageenans

There is a controversy regarding the toxicity of carrageenans for human intake. Although they have low cytotoxicity when tested for the different activities previously mentioned, several studies have demonstrated that *low molecular weight* carrageenans may induce and promote ulceration and intestinal neoplasms (Tobacman et al. 2001). However, most of the literature reports do not consider undegraded

carrageenans as toxic. As most formulations are made up of native carrageenans, no risk seems to be involved as there is no real evidence of the generation of depolymerized galactans in the gastrointestinal track (Nekas and Bartosikova 2013).

Considering the possible toxic effect of carrageenans, different organizations have evaluated their use in humans. The International Agency for Research on Cancer has designated *degraded* carrageenans as Group 2B (possibly carcinogenic to humans) and undegraded carrageenan in Group 3 (not classifiable as carcinogenic to humans) (IARC 1983). Furthermore, since 2002, the World Health Organization and the Food and Agriculture Organization decided to allocate carrageenans in the ADI “not specific” which includes food substances with very low toxicity consumed in low levels (JECFA 2002).

2.4 Biomedical Applications

Taking into account the biocompatibility of red seaweed galactans, they have been used for different medical applications such as improvement of drug formulations, delays in drug release, delivery systems, and tissue engineering, among others. Furthermore, chemical modifications and blends or cross-linking with other polysaccharides and polymers have been applied to these galactans to obtain novel biomaterials for biomedical applications (Rinaudo 2008; Synytsya et al. 2015; Cosenza et al. 2016; Zucca et al. 2016).

Carrageenans can be used as matrix excipients, mainly with the purpose of modifying their release behavior in tablets. In contact with water, the carrageenans in these tablets swell and/or erode releasing the drug (Pavil et al. 2010). The three commercial carrageenans were tested with different drugs and in some cases mixed with other excipients (Miyasaki et al. 2011; Nanaki et al. 2010). In addition, κ -carrageenan has replaced microcrystalline cellulose (MCC) as an extrusion aid for pharmaceutical pellets (Bornhöff et al. 2005). These pellets showed better quality than those obtained with MCC and were evaluated with different fillers and drugs (Thommes and Kleinebudde 2006).

The generation of particles for delivery systems has taken advantage of the gelling properties of red seaweed galactans. κ -Carrageenan/ K^+ system has been used for both drug (Sipahigil and Dortunc 2001) and enzyme (Sankalia et al. 2006a, b) encapsulation. ι -Carrageenan gels were used for encapsulation, whereas controlled release of trypsin using ι -carrageenan/spermine system was efficiently achieved (Patil and Speaker 1998). When comparing κ - and ι -carrageenan microspheres for encapsulation of allopurinol and local anesthetic agents, the release was prolonged in the former (Tomoda et al. 2009). Agarose beads and nanoparticles have been used for controlled drug delivery (El-Raheem and El-Said 1988) as well as for stabilization of gold and copper nanoparticles (Kattumuri et al. 2006; Datta et al. 2008). Gold nanoparticles encapsulated in porphyrans were used as carriers for drug delivery (Venkatpurwar et al. 2011).

In addition, gelling galactans were used for tissue engineering applications, especially agarose (Popa et al. 2015). A modified agarose (with lower melting point) was used so that the cell viability is not affected (Raghunath et al. 2007). Cell encapsulation for cartilage regeneration was studied, both *in vitro* and *in vivo*, using chondrocyte and mesenchymal stem cells (Guaccio et al. 2008; Bian et al. 2010; Ng et al. 2010; Vinardell et al. 2012). Agarose beads have also been used for encapsulation of islet (pancreatic endocrine tissue that releases insulin) as a treatment for type 1 diabetes (Teramura and Iwata 2010). Several studies have been done both *in vitro* and *in vivo* (Bloch et al. 2005; Luan and Iwata 2012; Holdcraft et al. 2014). This galactan has also been suggested as a candidate for nervous system tissue regeneration (Stokols and Tuszynski 2006; Gao et al. 2013).

In addition, the κ -carrageenan/ K^+ system successfully encapsulated three different types of cells: human adipose-derived stem cells, human nasal chondrocytes, and chondrocytic cells of line ATDC5 suggesting a potential application in cartilage regeneration (Popa et al. 2012). This system has also efficiently encapsulated and delivered platelet-derived growth factors with possible applications in bone tissue engineering (Santos et al. 2009).

3 Polysaccharides from Brown Seaweeds

3.1 Structure

Brown seaweeds produce laminarans [$\rightarrow 3$) β -Galp (1 \rightarrow)] as storage products, while a complex system of polysaccharides constitutes the cell wall. The fibrillar wall is built up of cellulose, whereas the mucilaginous matrix contains two charged polysaccharides: alginates and fucoidans (Davis et al. 2003). Alginates have a structural function, giving both strength and flexibility to the tissue, whereas fucoidans are believed to play a key role as a connection between the cellulose and the alginates (Kloareg et al. 1986; Davis et al. 2003).

3.1.1 Alginates

Alginates were first described in 1881 (Draget et al. 2006a) and comprise almost 40% of the dry weight of brown seaweeds. They are a linear, non-branched copolymer made up of β -(1 \rightarrow 4) D-mannuronic acid (M) and α -(1 \rightarrow 4) L-guluronic acid (G) blocks. Within the seaweed, they are found as gels containing different cations as Na, K, Mg, Ba, and Sr (Haug and Smisdrød 1967). Although these polysaccharides are mainly isolated from brown seaweeds, they can also be found in the Corallinales order of red algae (see Sect. 2.1.2).

Alginates are actually biosynthesized in the cells as a homomannuronan, and then, some units are partially converted to G by a C-5 epimerase (Synytsya et al.

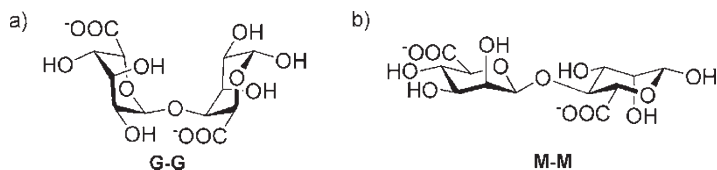


Fig. 4 (a) α -(1 \rightarrow 4) L-guluronic acid dimer, (b) β -(1 \rightarrow 4) D-mannuronic acid dimer

2015). In this way, three types of blocks can be found in alginate: M blocks (polymannuronan), G blocks (polyguluronan), and MG blocks (alternating both units) as shown in Fig. 4.

The ratio between mannuronic acid and guluronic acid, or M:G ratio, varies in alginates extracted from different seaweeds, ranging between 4.0 in *Durvillaea antarctica* and 0.19 in *Sargassum fluitans* (Synytsya et al. 2015). This relationship is actually a way to characterize the different alginates (high M, high G, or intermediate), as the M:G ratio affects their rheological properties (see Sect. 3.2). The M:G ratio together with the distribution of the different units along the chain depends not only on the seaweed source but also on the location and season of collection, the age of the plant, and the extraction methodology (Synytsya et al. 2015). Actually, it was observed that the proportion of G usually increases in older tissues (Haug et al. 1974). This is important, as G-rich alginates have larger affinity for Ca^{2+} cations, leading to stronger gels (see Sect. 3.2).

3.1.2 Fucoidans

Fucoidans are polysaccharides that contain mainly fucose and sulfate groups but also minor-to-moderate amounts of other sugars, including neutral sugars, amino sugars, uronic acids, as well as acetate groups (Nishino et al. 1994; Duarte et al. 2001; Ponce et al. 2003; Bilan et al. 2010, 2002). Fucoidan structure cannot be systematized as easily as that of red seaweed galactans, as they present a large variability in linkage, branching, sulfate position, and sugar composition. Nonetheless, at least three different types of polysaccharides were found within fucoidan samples: one containing mostly fucose and sulfate, with (in some cases) scarce amounts of other sugars (the “fucan”); another with high proportion of fucose, galactose, and sulfate groups (the “galactofucan” or “fucogalactan”); and the last one containing different monosaccharide moieties, less sulfate, and important proportions of uronic acid (the “uronofucoidan”) (Duarte et al. 2001; Ponce et al. 2003). This last component was later subdivided into “fucoglucuronans” and “fucoglucuronomannans” (Bilan et al. 2010; Croci et al. 2011).

Fucans may also be divided into two main types: one carrying 3- and 4-linked L-Fucp units and another one carrying only 3-linked L-Fucp units. The fucoidan from *Fucus vesiculosus* was one of the first whose structure was studied in detail. At first, it was proposed that the polysaccharide had a backbone of 2-linked α -Fucp

with sulfate at O-4 and branched with sulfated fucose single stubs every five units (Conchie and Percival 1950). Later a new model was proposed (Patankar et al. 1993), consisting of a core of 3-linked α -Fucp with sulfate at O-4, branched with fucose single stubs at C-2. Other species from the order Fucales, such as *Sargassum binderi* (Lim et al. 2016) and *S. fusiformis* (Jin et al. 2014), also produce a fucoidan with a backbone of 3-linked fucose but sulfated at O-2.

Some seaweeds from the order Laminariales also produce 3-linked fucans. The fucoidan from *Ecklonia kurome* was highly branched with fucose (both furanose and pyranose) and sulfated in different positions (Nishino et al. 1991). *Laminaria cichorioides* produced a polysaccharide whose core was mainly composed of 3-linked fucose, though some 4-linked fucose was also found, and it was sulfated at O-2 and/or O-4 (Zvyagintseva et al. 2003). The 3-linked fucan from *Saccharina latissima* was sulfated at O-4 and/or O-2 and branched with L-fucose at C-2 (Bilan et al. 2010). A similar fucoidan was found in *Chorda filum*, though this polysaccharide was also substituted at O-2 with sulfate or acetyl groups (Chizhov et al. 1999).

The fucoidan of *Fucus evanescens*, on the contrary, has a backbone of repeating units of $[\rightarrow 3)\text{-}\alpha\text{-L-Fucp}(2\text{SO}_3^-)\text{-(1}\rightarrow 4)\text{-}\alpha\text{-L-Fucp}(2\text{SO}_3^-)\text{-(1}\rightarrow]$ with sulfate groups also at O-4 of the 3-linked moieties and acetate groups in some of the remaining hydroxyl groups (Bilan et al. 2002). This structure was revised confirming the structure of the backbone, though minor amounts of sulfated galactose and xylose as well as uronic acid were also present, mainly as side chains (Anastyuk et al. 2009). The fucoidans from *F. distichus* (Bilan et al. 2004) and *F. serratus* (Bilan et al. 2006a) have a structure similar to that found in *F. evanescens*. The polysaccharide of *F. serratus*, in particular, was also substituted at C-4 of the 3-linked units with side chains of $[\alpha\text{-L-Fucp}\text{-(1}\rightarrow 4)\text{-}\alpha\text{-L-Fucp}\text{-(1}\rightarrow 3)\text{-}\alpha\text{-L-Fucp}\text{-(1}\rightarrow]$ and with xylose and galactose single stubs. *Coccophora langsdorfii* (Imbs et al. 2016) and *Laminaria brasiliensis* (Pereira et al. 1999) also produce a 3- and 4-linked fucoidan, both sulfated at O-2. The former is branched at C-4 with side chains of 3-linked fucose, while the latter is sulfated in O-3.

Fucoidans from *Ascophyllum nodosum* were also studied in detail. Chevolut et al. (1999, 2001) proposed a structure with a predominant repeating unit of $[\rightarrow 3)\text{-}\alpha\text{-L-Fucp}(2\text{SO}_3^-)\text{-(1}\rightarrow 4)\text{-}\alpha\text{-L-Fucp}(2,3\text{SO}_3^-)\text{-(1}\rightarrow]$. Marais and Joseleau (2001), on the other hand, suggested a core mainly composed of 3-linked α -Fucp and only few 4-linked α -Fucp, branched at C-2 with side chains of $[\rightarrow 3)\text{-}\alpha\text{-L-Fucp}\text{-(1}\rightarrow]$ of different lengths and with a more complex sulfation pattern.

Among the fucose containing heteropolysaccharides, fucose moieties could be found either as part of the backbone and/or as side chains. *Saccharina latissima*, for instance, produces, besides the fucan previously described, three other sulfated fucoidans: a sulfate-rich fucogalactan with a core of D-Galp branched with fucose and galactose, a fucoglucuronan with a backbone of D-glucuronic acid branched with partially sulfated fucose, and a fucoglucuronomannan with a backbone made of D-glucuronic acid and mannose (half sulfated at O-6) branched with partially sulfated fucose (Fig. 5; Bilan et al. 2010). These last two fucoidans were together and could only be separated after desulfation, raising the question of whether they

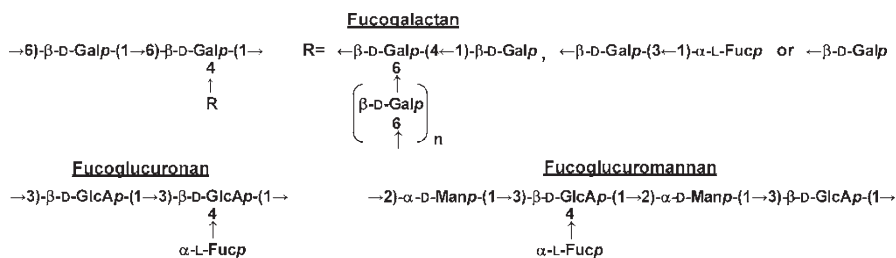


Fig. 5 Structural fragments of the desulfated heteropolysaccharides isolated from *Saccharina latissima* (Adapted from Bilan et al. 2010)

are two independent polysaccharides or just one partially hydrolyzed during desulfation.

Other fucoidans with large amounts of fucose and galactose have been found in other brown seaweeds. *Sargassum crassifolium* and *Padina australis* produce polysaccharides with a backbone of $[\rightarrow 4]\text{-}\alpha\text{-L-Fucp}\text{-}(1\rightarrow 3)\text{-}\alpha\text{-L-Fucp}\text{-}(1\rightarrow]$, and galactose is present in the side chains, in the first seaweed as a 4-linked oligogalactan, while in *P. australis* as a single stub or as a fucose–galactose disaccharide (Yuguchi et al. 2016). Two fucogalactans have been isolated from *S. fusiforme*: one with a core of 6-linked 2-sulfated D-galactose units branched at C-4 with sulfated fucose and another one whose backbone has galactose and 2-sulfated fucose, either in an alternating fashion or in blocks (Jin et al. 2014). A fucogalactan isolated from *S. polycystum* has a main chain of 3-linked 4-sulfated $\alpha\text{-D-galactose}$ alternating with rather short sequences of 2,4-disulfated $\alpha\text{-D-galactose}$ (Bilan et al. 2013). *Undaria pinnatifida* produces a galactofucan with alternating blocks of 3-linked fucose sulfated at O-2 and O-4 and 3-linked sulfated galactose (Hemmingson et al. 2006; Skriptsova et al. 2010). The fucogalactan of *Adenocystis utricularis* has a “fucan part” with 3-linked 4-sulfated $\alpha\text{-L-fucose}$ units branched at C-2 with fucopyranoside and fucofuranoside single stubs and a “galactan part” made of 3- and 6-linked 4-sulfated $\alpha\text{-}$ and $\beta\text{-D-galactopyranose}$ (Ponce et al. 2003). The distribution of these “parts” along the polysaccharide was not determined.

Sargassum stenophyllum produces a sulfated fucoidan with a backbone of 6-linked D- β -galactose and 2-linked $\beta\text{-D-mannose}$ (Duarte et al. 2001). Branching occurred with side chains of 3- and 4-linked $\alpha\text{-L-fucose}$ and minor amounts of 4-linked $\alpha\text{-D-glucuronic acid}$ and $\alpha\text{-D-glucose}$ or terminal $\beta\text{-D-xylose}$.

Xylofucans have been isolated from *Punctaria plantaginea* (Bilan et al. 2014) and *Padina tetrastromatica* (Karmakar et al. 2009). The former has a backbone of $[\rightarrow 3]\text{-}\alpha\text{-L-Fucp}(2\text{SO}_3^-)\text{-}(1\rightarrow 3)\text{-}\alpha\text{-L-Fucp}(2\text{SO}_3^-)\text{-}(1\rightarrow 3)\text{-}\alpha\text{-L-Fucp}\text{-}(1\rightarrow]$ with xylose single stubs in four positions. *P. tetrastromatica* produces a sulfated fucoidan with a backbone of 2- and 3-linked $\alpha\text{-L-fucose}$. Branching of both xylose and fucose single stubs has been found.

Fucoglucuronans from *Spatoglossum schröderi* (Leite et al. 1998) have the same backbone as those found for *Saccharina latissima* but branched at C-4 with 3-linked 2-sulfated fucose oligosaccharides which, at the same time, could be

branched at C-4 with partially sulfated xylose units. *Cladosiphon okamuranus*, on the other hand, produces a fucoidan with a backbone of 3-linked α -L-fucose sulfated at O-4 and partially acetylated and branched at C-2 with α -glucuronic acid (Nagaoka et al. 1999).

Kjellmaniella crassifolia (Sakai et al. 2003), *Hizikia fusiforme* (Li et al. 2006), and *Sargassum fusiforme* (Cong et al. 2016) produce fucoglucuronomannans similar to those reported for *S. latissima*. The formers were sulfated at O-6 of the mannose and at O-3 or O-2 and O-4 of single stubs of fucose. The product from *H. fusiforme* also presented minor amounts of 4-linked galactose in the backbone and was branched with side chains of variable lengths of fucose, galactose, and xylose. The fucoidan from *S. fusiforme* was branched with 3-linked sulfated fucose, fucogalactan or fucoglucuronan, and single stubs of partially sulfated xylose.

The fucoidan from *Padina pavonica* has an internal core of 4-linked D-mannose, D-glucuronic acid, and D-glucose and partially sulfated heteropolymeric side chains of D-galactose, D-glucose, L-fucose, and D-xylose, all with β -configuration, except for the fucose (Hussein et al. 1980). Other uronofucoidans were found in *Sargassum stenophyllum* (Duarte et al. 2001) and in *Adenocystis utricularis* (Ponce et al. 2003). Both are scarcely sulfated with important amounts of uronic acid and fucose; the former also has galactose while the latter has mannose.

3.1.3 Industrial Applications

Alginates are, by far, the polysaccharides from brown seaweeds mostly used for industrial applications (in food, textile, and pharmaceutical industries, among others). Three different rheological properties of these phycocolloids are employed: thickening, gelling, and film forming (Mc Hugh 2003). The thickening ability of alginates, i.e., capability to increase the viscosity of a solution, is related to the molecular weight of the polysaccharide and the ionic strength of the solution (Smidsrød 1970). Gelation can occur either by cross-linking with divalent cations (Ca^{2+}) or by hydrogen bond interaction at low pH. The first one generates individual boxes of Ca^{2+} complexed with four guluronic acid units. A sequence of these individual boxes generates an egg-box-like scheme (Fig. 6), cross-linking two or more chains and favoring the gelation of alginates (Grant et al. 1973). In contrast to carrageenan and agar gels, gelation of alginates with Ca^{2+} is not temperature dependent (Mc Hugh 2003). Gels produced in acid medium are more turbid and have a brittle texture compared to the ionotropic gels (Draget et al. 2006b). Furthermore, in the gelation of alginic acid, both G and M blocks take part in the formation of the junction boxes, though the latter in lower extent. Film formation can be achieved with both the calcium and the sodium salt of alginates, while fibers can only be made from the calcium salt (Mc Hugh 2003).

Alginates are extracted from different brown seaweed species from the genera *Laminaria* and *Lessonia*, which produce medium to high G alginates, and are the most exploited nowadays given the industrial need for strong and rigid gels (Bixler and Porse 2011). *Macrocystis pyrifera* and *Ascophyllum nodosum* (high M) are also

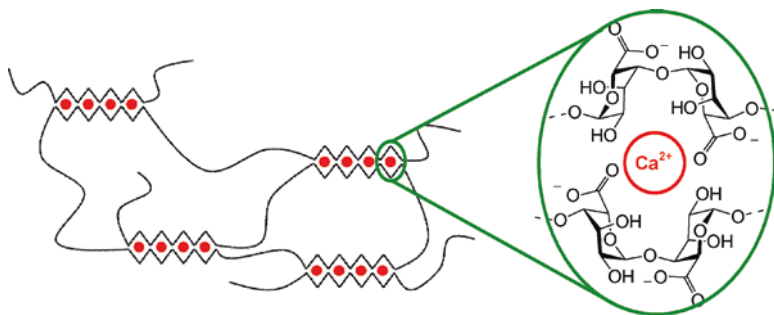


Fig. 6 Gelation of alginate with Ca^{2+} : egg-box model

used. Furthermore, *Sargassum* sp. is used to obtain low-viscosity alginates, whereas *M. pyrifera*, depending on the extraction procedure, can give medium- or high-viscosity alginates (Mc Hugh 2003). Alginates have an intermediate volume sale and retail price when compared to agar and carrageenans (Bixler and Porse 2011).

There are several industrial uses for alginates. Thickening behavior of alginates is applied for sauces, syrups, and ice-cream toppings (Mc Hugh 2003). They are also used to avoid separation in mayonnaise and to prevent sedimentation in juices and in chocolate milk. For acid solutions, polypropylene glycol alginate is used as a thickening agent, as alginic acid forms gels (Draget et al. 2006a). This derivative is added to beer to favor foam formation and to yogurt for milk protein stabilization.

Gelling properties of alginates are used in jellies and desserts, especially for instant formation products, as a gel can easily be made by mixing calcium alginate powder and water (Mc Hugh 2003). In addition, mixtures of alginates and pectins develop synergistic thermoreversible gels in condition where neither of them gelled, applicable to low calories jellies (Toft et al. 1986). Furthermore, artificial cherries and fruit substitutes can be made by doping fruit pulp and alginates in a calcium solution (Mc Hugh 2003). Alginate gels are also applied in restructured food due to their interaction with proteins (Venugalpa Menon 2011). In meat restructured products such as nuggets, meat loaf, and even steaks, the different meat pieces are bound together with a mixture of sodium alginate, calcium carbonate, lactic acid, and calcium lactate (Mc Hugh 2003). Vegetable restructured products include onion rings and olive fillings.

These phycocolloids could also be used as edible coatings due to their film-forming properties, though they give strong and brittle films with poor water resistance (Campos et al. 2011). Calcium alginate jelly applied to frozen fish is used to protect the product from air and oxidation (Mc Hugh 2003).

In addition to the above-mentioned applications, alginates share some uses with carrageenans, as in wine clarification (Cabello-Pacini et al. 2005), fat replacement in precooked beef patties (Venugalpa Menon 2011), and in other slimming diet products where they function as indigestible dietary fibers which swell in the stomach giving the feeling of satiety.

Alginates have also important applications in other industries. In textile printing, alginates can replace starch as thickener for the dye preparations (Mc Hugh 2003). Although they are more expensive than starch, they lead to better quality products. In the paper industry, alginates, generally mixed with starch, can be used for coating (Mc Hugh 2003). They are also used for molds in dentistry (Rinaudo 2008). In welds, alginate coatings can be applied to welding rods or electrodes as it improves extrusion and flux (Mc Hugh 2003).

Cell and enzyme encapsulation using alginate gels is used for different applications in biotechnology. This technique is used for encapsulation of *Saccharomyces cerevisiae* (beer yeast) for the production of ethanol (Bekatorou et al. 2016) and of probiotic bacteria in food as it improves the survival of probiotics through the gastrointestinal track (Vodnar et al. 2016). Other industrial applications of alginate beads include generation of penicillin derivatives and production of amino acids, among others (Mc Hugh 2003). In addition, these beads are used to immobilize bacteria for water waste treatment (Sergio and Bustos 2009).

Fucoidans, on the other hand, do not have as many industrial applications as alginates. Their main use is in the nutraceutical and cosmetic industries, given their large amount of biological properties (Vo and Kim 2013; Cunha and Grenha 2016).

3.2 *Biological Activities*

As previously mentioned in Sect. 2.3, sulfated polysaccharides are those with most interesting biological activities. For this reason, this section is devoted to discuss the biological properties of fucoidans.

3.2.1 *Antiviral Activity*

Fucoidans, as other sulfated polysaccharides, have shown antiviral activity against different enveloped viruses both in vivo and in vitro and possess low cytotoxicity (Pujol et al. 2007). As it can be seen in Table 4, fucoidans from different brown seaweeds have presented promising antiviral properties, in some cases with an $IC_{50} < 1 \mu\text{g/ml}$.

Given the complexity of these polysaccharides, in some cases, the antiviral activity was performed in non-completely characterized polysaccharides. Nonetheless, some correlation between structure and antiviral activity was found. As it happens with the sulfated polysaccharides from red seaweeds, this property is dependent of the sulfate content and molecular weight. Comparison of the antiviral activity of fucoidans from the same (Ponce et al. 2003) or different species, but with structural similarities (Prokofjeva et al. 2013), showed that high molecular weight polysaccharides are generally the most effective inhibitors. In addition, it was observed that oversulfation of an active fucoidan enhances its antiviral activity (Sinha et al. 2010).

Table 4 List of some fucoidan fractions and/or extracts with antiviral activity

Order	Species	Virus	Results
Dictyotales	<i>Dictyota dichotoma</i> ^{a1}	HSV-1	IC ₅₀ = 7.5–375 µg/ml
		CVB3	IC ₅₀ = 12.5–>100 µg/ml
	<i>Dictyota mertensii</i> ^{a2}	HIV	85.5–99.1% ^{b,c}
	<i>Padina australis</i>	HSV-1	EC ₅₀ = 58.9 µg/ml
	<i>Padina tetrastromatica</i> ^{a3}	HSV-1	IC ₅₀ = 0.74–1.05 µg/ml
		HSV-2	IC ₅₀ = 0.30–0.39 µg/ml
	<i>Spatoglossum schröderi</i> ^{a2}	HIV	84.0–98.1% ^{b,c}
<i>Stoechospermum marginatum</i>	HSV-1	EC ₅₀ = 3.6 µg/ml ⁻¹	
Ectocarpales	<i>Adenocystis utricularis</i> ^{a4}	HSV-1	IC ₅₀ = 0.28–7.94 µg/ml
		HSV-2	IC ₅₀ = 0.52–0.84 µg/ml
		HIV	IC ₅₀ = 0.6–70 µg/ml
	<i>Colpomenia sinuosa</i>	HSV-1	EC ₅₀ = 22.1 µg/ml
	<i>Hydroclathrus clathratus</i>	HSV-1	EC ₅₀ = 1.6–6.5 µg/ml
	<i>Leathesia difformis</i> ^{a5}	HSV-1	IC ₅₀ = 0.7–3.1 µg/ml
		HSV-2	IC ₅₀ = 0.5–2.5 µg/ml
HCMV		IC ₅₀ = 1.9–7.5 µg/ml	
Fucales ^c	<i>Cystoseira indica</i>	HSV-1	EC ₅₀ = 2.8 µg/ml
	<i>Fucus evanescens</i> ^{a6}	HSV-1	IC ₅₀ = 0.01 µg/ml ^d
	<i>Fucus vesiculosus</i> ^{a2}	HIV	84.0–98.1% ^{b,c}
	<i>Sargassum horneri</i>	HSV-1	EC ₅₀ = 19.1 µg/ml
	<i>Sargassum naozhouense</i>	HSV-1	EC ₅₀ = 8.92 µg/ml
	<i>Sargassum patens</i>	HSV-1	EC ₅₀ = 5.5 µg/ml
	<i>Sargassum swartzii</i> ^{a7}	HIV	78.9% ^b
	<i>Sargassum tenerrimum</i> ^{a8}	HSV-1	IC ₅₀ = 1.4 µg/ml
Laminariales	<i>Saccharina cichoroides</i> ^{a6}	HSV-1	IC ₅₀ = 0.005 µg/ml ^d
	<i>Saccharina gurjanovae</i> ^{a6}	HSV-1	IC ₅₀ = 0.045 µg/ml ^d
	<i>Saccharina japonica</i> ^{a6}	HSV-1	IC ₅₀ = 0.001 µg/ml ^d
	<i>Undaria pinnatifida</i> ^{a9}	HSV-1	IC ₅₀ = 2.5 µg/ml
		HSV-2	IC ₅₀ = 2.6 µg/ml
	Influenza A	IC ₅₀ = 15 µg/ml	

Adapted and renewed from De Souza Barros et al. (2015)

^aNew citation: 1- Rabanal et al. (2014), 2- Queiroz et al. (2008), 3- Karmakar et al. (2010), 4- Ponce et al. (2003) and Trincherro et al. (2009), 5- Feldman et al. (1999), 6- Prokofjeva et al. (2013), 7- Dinesh et al. (2016), 8- Sinha et al. (2010), 9- Lee et al. (2004)

^bReverse transcriptase inhibition (%)

^cTwo different template primers were used

^dUsing a model system based on lentiviral vectors

Furthermore, it was observed that the presence of sulfate at O-4 of 3-linked fucose units plays a crucial role for the antiherpetic activity (Li et al. 2008). As expected, desulfation significantly attenuates the inhibitory activity of these polysaccharides. Interestingly, the polysaccharide from *Leathesia difformis* was active against HSV-1, HSV-2, and HCMV despite its low sulfate content (Feldman et al. 1999).

Besides sulfate content and molecular weight, sugar composition also plays an important role in the antiviral activity of these polysaccharides. Fucose-rich

fucoidans are usually more active (Feldman et al. 1999; Damonte et al. 2004). Actually, Damonte et al. (2004) proposed that this could be due to the hydrophobic character of the C-6 methyl group in the sugar that could interact with the hydrophobic pocket of the viral proteins. Furthermore, the authors suggested that not only the presence of fucose is important but also its spatial distribution.

In addition, it should be pointed out that, unlike sulfated galactans, fucoidans also have two anionic groups: sulfates and carboxylates from the uronic acids. The presence of the latter also affects the antiviral properties. In *Adenocystis utricularis*, only the fucogalactan showed antiherpetic activity suggesting that the low sulfated uronofucoidans are not good inhibitors (Ponce et al. 2003). However, in *Dictyota dichotoma*, some fractions carrying larger amounts of xylose, mannose, and uronic acids seem to have moderate activity against HSV-1 (though not against CVB3) (Rabanal et al. 2014). The xylofucoglucuronans of *Spatoglossum schröderi* inhibit the reverse transcriptase (Queiroz et al. 2008), but this activity is lost after carboxy-reduction, suggesting that the loss of negative charges rules out a conformation recognizable by the enzyme.

3.2.2 Anticoagulant Activity

Sulfated polysaccharides from several brown seaweeds, such as sulfated fucans from *Fucus vesiculosus* (Pereira et al. 1999), *F. serratus* (Cumashi et al. 2007), *F. distichus* (Cumashi et al. 2007), *Laminaria brasiliensis* (Pereira et al. 1999), *Ecklonia kurome* (Nishino et al. 1989), *Ascophyllum nodosum* (Pereira et al. 1999), and *Saccharina latissima* (Crocchi et al. 2011) and the fucogalactomannan from *Sargassum stenophyllum* (Duarte et al. 2001), among others, have shown anticoagulant activity.

It is believed that the mechanism is related with both the antithrombin and the heparin cofactor II-mediated activities (Ale et al. 2011). Furthermore, the structure of the fucoidans (i.e., composition, degree and pattern of sulfation, molecular weight, etc.) plays an important role in the anticoagulant activity, although no complete correlation has been found yet, given the structural complexity of fucoidans. Nonetheless, some attempts have been made. It has been observed that disulfated fucan chains enhance this activity (Duarte et al. 2001). In particular, sulfation at O-2 and/or O-3 favors the anticoagulant properties. In addition, the fact that the uronofucans from *Cladosiphon okamuranus* (Cumashi et al. 2007) and *Saccharina latissima* (Crocchi et al. 2011) were not active suggests that both high sulfate and fucose contents are essential for exhibiting anticoagulant properties.

3.2.3 Antitumor Activity and Related Activities

Antitumor activity of sulfated fucoidans has been widely studied, though their mechanism still continues to be investigated. Their antitumor effect is associated with the following effects: inhibition of tumor cell proliferation, stimulation of the

apoptosis of cancer cells, blocking of cancer cell metastasis, inhibition of blood vessel formation (antiangiogenic properties), and enhancement of various immune responses (immunomodulatory properties) (Synytsya et al. 2015).

Different fucoidans, including fucans from *Fucus vesiculosus* (Kim et al. 2010), *F. evanescens* (Alekseyenko et al. 2007), *Saccharina latissima* (Crocì et al. 2011), and *Sargassum horneri* (Ermakova et al. 2011) and sulfated galactofucans from *Undaria pinnatifida* (Vishchuk et al. 2011), *Saccharina japonica* (Vishchuk et al. 2011), and *Costaria costata* (Ermakova et al. 2011), among others, showed antitumor activity in in vivo and/or in vitro studies.

It was demonstrated for the fucoidans of *S. latissima* that only the fraction with the sulfated fucans and fucogalactans was active, whereas the low sulfated, uronic acid-containing fraction was inactive, as occurred with the antiviral and anticoagulant activity (Crocì et al. 2011). Furthermore, it was found that besides the sulfate content (Teruya et al. 2007), the reduction of the molecular weight (Yang et al. 2008; Zhang et al. 2013) favors this activity.

Fucoidans reduce the blood vessel formation, thus reducing the active supply of blood to the tumor (Vo and Kim 2013). Antiangiogenic activity was observed in the fucans from *Saccharina latissima* (Crocì et al. 2011), *Fucus serratus* (Cumashi et al. 2007), and *F. evanescens* (Cumashi et al. 2007), as well as in the fucoglucuronomannan from *Sargassum fusiforme* (Cong et al. 2016). It should be noted that in *S. latissima*, the fucoglucuronomannan did not result active (Crocì et al. 2011). In addition, inhibition of the tumor growth and metastatic process is favored by the ability of fucoidans to enhance the immune response (Vo and Kim 2013). Several fucoidans have shown immunomodulatory activity (Ale et al. 2011; Vo and Kim 2013).

Antioxidant activity may also be related to the antitumor activity of the polysaccharides. Fucoidans from different seaweeds have been suggested as antioxidants due to their scavenging effect on biologically harmful oxidants (Vo and Kim 2013; Synytsya et al. 2015).

3.2.4 Other Biological Activities

Fucoidans present other biological activities. Antiobesity activity of these polysaccharides is associated with the increase in the expression of the hormone-sensitive lipase, both phosphorylated and not, and the decrease of the glucose uptake into adipocytes which leads to the stimulation of lipolysis (Vo and Kim 2013). Furthermore, fucoidans from *Laminaria japonica* have shown antilipidemic and cholesterol-lowering properties both in animals and in serum of patients with hyperlipidemia (Li et al. 2008). In addition, fucoidans have presented hepato- and gastro-protective, antihypertensive, antiallergenic, and antibacterial properties (Li et al. 2008; Synytsya et al. 2015).

3.3 *Biomedical Applications*

As occurs with carrageenans and agarose, alginates have several biomedical applications, mainly in drug delivery and tissue engineering. Furthermore, in many cases, chemical modifications such as blend with other polymers have been used to improve the properties of these polysaccharides and their biomedical applications (Wong 2011; Lee and Mooney 2012; Synytsya et al. 2015).

Probably the most well-known commercial application is in wound dressing (Koltostat®, Sorbsan®, among others) and in treatment of gastrointestinal reflux (Gaviscon®) (Rinaudo 2008). In the first case, calcium alginate fibers form a non-woven dressing that in contact with the wound begins to absorb the fluids and swell, with easy removal (Thomas 2000). The other commercial application is based in the ability of alginates to form gels in acid medium generating a physical barrier for reflux (Hampson et al. 2010).

Alginates can also be used in controlled release systems. In tablet matrices, the release of the drug was modulated by the chemical characteristics of the alginates, the pH, the Ca^{2+} concentration, the particle size, etc. (Liew et al. 2006; Pongjanyakul and Puttipipatkachorn 2007). Like carrageenans, calcium alginate can also be used as an extrusion aid for pharmaceutical pellets (Sriamornsak et al. 2008). In addition, beads and nanoparticles made of ionically cross-linked alginates have been used for the encapsulation and delivery of drugs (Ahmad et al. 2006; Han et al. 2007). Encapsulation with alginates has also been studied for enzymes and other proteins (Well and Sheardown 2007). This method has the advantage of working under mild conditions, thus avoiding denaturation of proteins (Lee and Mooney 2012).

Given the ability of alginates to gel and encapsulate cells (see Sect. 3.2), these polysaccharides were used for tissue engineering applications. Cells do not adhere to alginates due to their negative charge, so if cell interaction with the polysaccharides is necessary, small binding peptides and sugars should be attached to the alginates (Rinaudo 2008; Lee and Mooney 2012). Encapsulation with alginates has been used for regeneration of the bone (Kolambkar et al. 2011), cartilage (Sanchez et al. 2002), nerves (Prang et al. 2006), blood vessels (Ruvinov et al. 2011), and pancreas (Calafiore 2003), among others.

Fucoidans have also been used for biomedical applications, though less than alginate. This is mainly attributed to the difficulties in finding well-characterized fractions and the lack of thickening or gelling properties of these polysaccharides (Chollet et al. 2016; Cunha and Grenha 2016). For these reasons, fucoidans have been used for delivery of drugs and proteins as well as regenerative medicine, either blended with other polysaccharides and/or other biocompatible polymers or chemically modified (Chollet et al. 2016; Cunha and Grenha 2016).

4 Green Seaweed Polysaccharides

Green seaweeds are widely distributed in the world (Graham and Wilcox 2000). They are classified into two phyla: Chlorophyta and Streptophyta. This section will just focus on the polysaccharides found in species belonging to the class Ulvophyceae (Chlorophyta) as they are the most studied and have shown several potential applications.

4.1 Structure

Cell wall polysaccharides from Ulvophyceae include both neutral and sulfated polysaccharides. The first are usually fibrillar polysaccharides, including cellulose, 4-linked β -mannans, and 3-linked β -xylans (Domozych et al. 2012). The presence of each of these polysaccharides depends on the species and, in some cases, of the life cycle. Sulfated polysaccharides, on the other hand, possess a wide variety of structures (Percival 1979; Lahaye and Robic 2007; Fernández et al. 2014; Cho and You 2015). According to Percival (1979), these sulfated polysaccharides could be classified according to their sugar composition: those with important amounts of uronic acids, including glucuronoxylorhamnans and glucuronoxylorhamnogalactans, and those without, or scarcely charged sugars, as the xyloarabinogalactans. Nonetheless, this classification is oversimplified given the large variability of structures found (Lahaye and Robic 2007; Cho and You 2015).

Seaweeds belonging to the order Ulvales (mainly *Ulva* sp. and, in a lesser amount, *Enteromorpha* sp.) produce uronate-rich sulfated polysaccharides, known as ulvans. First studies have shown that they produce xylose-, rhamnose-, and glucuronic acid-containing polysaccharides (Brading et al. 1954; McKinnel and Percival 1962). More recently, iduronic acid was also found in sulfated polysaccharides from *Ulva* sp. (Quemener et al. 1997; Lahaye et al. 1999). A more detailed compositional study performed on different species (*U. rigida*, *U. rotundata*, *U. olivascens*, *U. scandinavica*, among others) collected in different places and seasons showed that ulvans were composed of rhamnose (42.2–54.8 mol%), xylose (5.4–23.8 mol%), glucuronic acid (11.6–30.4 mol%), and iduronic acid (6.0–7.0 mol%) (Lahaye et al. 1999).

Structural studies performed on oligosaccharides from *U. rigida* showed the presence of two main disaccharidic units (Fig. 7a): ulvanobiouronic acid 3-sulfate type A or A_{3S} and type B or B_{3S} (Lahaye and Ray 1996; Quemener et al. 1997). Furthermore, two other disaccharidic sequences were found in the seaweed (Fig. 7b): ulvanobiose 3-sulfate or U_{3S} and 2',3-disulfate or $U_{2,3S}$ (Lahaye 1998).

Bryopsidales (mostly *Codium* and, in lesser amount, *Bryopsis* and *Caulerpa*) produce polysaccharides mostly devoid of uronic acids (Domozych et al. 2012; Fernández et al. 2014). First studies performed on the sulfated polysaccharides from *Codium fragile* indicated the presence of D-galactose and L-arabinose (Love and

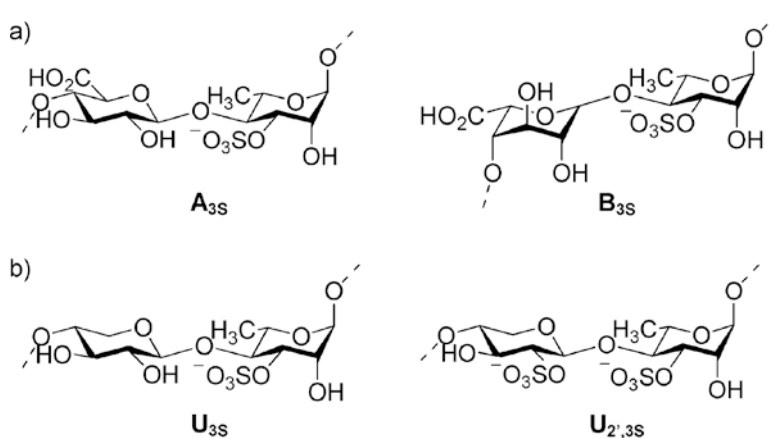


Fig. 7 Disaccharidic repeating units found in *Ulva rigida*: (a) ulvanobiouronic acids **A_{3S}** and **B_{3S}** and (b) ulvanobiose **U_{3S}** and **U_{2,3S}**

Percival 1964). Further investigations on species of this genus determined that the polysaccharide backbone was a 3-linked β -galactan. In particular, the galactans from *C. yezoensis* were sulfated at O-4 and, in fewer cases, at O-6 (Bilan et al. 2006b, 2007). In addition, pyruvic acid was found forming a ketal with O-3 and O-4, generating a five-member ring with *S* configuration. In lesser amounts, a six-member ring ketal of pyruvic acid at O-4 and O-6 (*R* configuration) was also found. This galactan was highly branched (nearly 40%) at C-6 with single stubs or small oligosaccharides of galactose. Polysaccharides from other species of this genus, such as *C. fragile* (Ciancia et al. 2007; Estevez et al. 2009; Ohta et al. 2009), *C. isthmocladum* (Farias et al. 2008), *C. vermilara* (Ciancia et al. 2007), *C. decorticutum* (Fernandez 2015), and *C. divaricatum* (Li et al. 2015, 2016), were studied in more detail. It was observed that they all have the same galactose backbone substituted with variable amounts of pyruvic acid, sulfate groups, and side chains of variable length. *Bryopsis plumosa* also produces a galactan with common structural features with those found in the genus *Codium* (Ciancia et al. 2012). *Caulerpa* sp. produces complex sulfated heterogalactans whose structures have not been completely clarified (Wang et al. 2014).

Besides galactans, some species from *Codium* also produce sulfated arabinans and mannans. *C. vermilara* (Fernández et al. 2013) and *C. decorticutum* (Fernández et al. 2015) produce a 3-linked β -arabinan sulfated at O-2 and/or O-4 and branched at C-2 with single stubs of arabinose. In addition, *C. vermilara* also produces a 4-linked β -mannan sulfated at O-2 and branched at C-6 with single stubs of xylose or arabinose (Fernández et al. 2012).

The genus *Monostroma* (Ulotrichales) produces 2-, 3-, and 4-linked rhamnans sulfated at O-2, O-3, and O-4 (Mao et al. 2008, 2009; Zhang et al. 2008; Li et al. 2017).

4.2 Biological Activities

4.2.1 Antiviral Activity

Sulfated polysaccharides from green seaweeds have been studied for their potential antiviral activity, mainly against enveloped virus. Furthermore, in many cases, they have shown inhibitory activities lower than 1 $\mu\text{g/ml}$, similar to those found for some polysaccharides from red and brown seaweeds (Wang et al. 2014).

Sulfated arabinans or arabinogalactans of three *Codium* species have shown to be active against HSV-1 (Fernández et al. 2014). Though no detailed structural study was performed, a relationship between the antiviral activity and the sulfate content was observed. The sulfated galactan from *C. fragile* inhibits, in vitro, the replication of HSV-2 (Ohta et al. 2009). Sulfated rhamnans from *Monostroma lattissima* resulted potent inhibitors of HSV-1, HCMV, and HIV-1 (Lee et al. 1999). In addition, the sulfated heterogalactans from the different *Caulerpa* spp. have antiviral activity against HSV-1, HSV-2, and DENV-2 (Pujol et al. 2012; Wang et al. 2014).

4.2.2 Anticoagulant Activity

Sulfated polysaccharides of green seaweeds also exhibit anticoagulant activity. Furthermore, a relationship between the anticoagulant activity and the molecular weight, the degree and position of sulfates, and sugar composition was also observed. Sulfated polysaccharides from different *Codium* species, namely, *C. fragile*, *C. vermilara*, *C. isthmocladum*, *C. divaricatum*, *C. adhaerens*, *C. latum*, *C. dwarkense*, *C. cylindricum*, *C. pugniformis*, and *C. tomentosum*, have been studied for their anticoagulant properties (Fernández et al. 2014; Wang et al. 2014; Alves 2015; Li et al. 2015). The sulfated arabinans isolated from these species resulted active, though with a different mechanism than heparin, while the sulfated galactans do not have important anticoagulant activity (Fernández et al. 2014).

Sulfated rhamnans from the genus *Monostroma* have also shown anticoagulant properties (Mao et al. 2008, 2009; Cho and You 2015; Li et al. 2017). In addition, though there are few examples in the literature, ulvans, in particular the sulfate-rich ulvans from *U. conglobata*, show anticoagulant activity (Mao et al. 2006).

4.2.3 Antitumor Activity and Related Activities

Sulfated polysaccharides from green seaweeds have also shown antitumor activity. The sulfated glucorhamnans from *Monostroma nitidum* (Karnajanapratum and You 2011) and the ulvans from *U. lactuca* (Thanh et al. 2016) were cytotoxic against different cancer cell lines, while the sulfated rhamnase-rich polysaccharide from *Enteromorpha intestinalis* (Jiao et al. 2009) only showed in vivo antitumor activity. Given that this polysaccharide has shown immunomodulatory properties, it was

deduced that its antitumor activity was related to this last property. The ulvan extracted from *U. rigida* also presented immunomodulatory properties (Leiro et al. 2007). The sulfated galactan from *Codium cylindricum*, on the other hand, showed antiangiogenic activity (Matsubara et al. 2003).

Antioxidant activity was also observed in polysaccharides from green seaweeds. A study performed on the polysaccharides from *Ulva fasciata* demonstrated that the antioxidant activity was a function of different factors (molecular weight, sugar composition, etc.), though it was observed that scarcely sulfated polysaccharides resulted more active (Shao et al. 2013). In addition, depolymerization of ulvans from *U. pertusa* showed that the antioxidant properties of the oligosaccharides increase with the reduction of the molecular weight (Qi et al. 2005).

4.2.4 Other Biological Activities

Ulvans isolated from different *Ulva* spp. were reported to have antihyperlipidemic activity (Pengzan et al. 2003; Sathivel et al. 2008). In addition, the water extract from *Ulva reticulata* showed antihepatotoxic activity (Rao et al. 2004).

4.3 Biomedical Applications

Green seaweed polysaccharides have been less explored for biomedical applications despite their chemical and biological diversity. Nonetheless, some studies have been reported, both on drug delivery and tissue engineering, mainly of blends of ulvans with other polysaccharides or polymers (Cunha and Grenha 2016).

5 Conclusions

Seaweeds are a versatile, abundant, and valuable resource. In particular, their polysaccharides have been widely used for decades as non-expensive hydrocolloids for many industries which require them in bulk amounts. Carrageenans, agars, and alginates are the main exponents of this category. However, a review of the work carried out in the two last decades shows that other applications, with a higher added value, appear for these and other abundant seaweed polysaccharides, like fucoidans, DL-hybrids, and green seaweed polysaccharides. They include several biological activities like antiviral, anticoagulant, antitumor, and antioxidant and several functions in drug release and other biomedical applications. It is expected that the near future will bring lower costs of current applications of some of these seaweed polysaccharides, as well as improvements in the needs of our societies. Furthermore, new, fresh ideas or applications may appear for further purposes.

Acknowledgments This work was supported by grants from UBA (Q-203), CONICET (PIP 298/14), and ANPCyT (PICT 2013-2088).

References

- Abdala Díaz RT, Chabrilón M, Cabello-Pasini A, Gómez-Pinchetti JL, Figueroa FL (2011) Characterization of polysaccharides from *Hypnea spinella* (Gigartinales) and *Halopithys incurva* (Ceramilales) and their effect on RAW 264.7 macrophage activity. *J Appl Phycol* 23:523–528
- Ahmad Z, Pandey R, Sharma S, Khuller GK (2006) Pharmacokinetic and pharmacodynamic behaviour of antitubercular drugs encapsulated in alginate nanoparticles at two doses. *Int J Antimicrob Agents* 27:409–416
- Ale MT, Mikkelsen JD, Meyer AS (2011) Important determinants for fucoidan bioactivity: a critical review of structure-function relations and extraction methods for fucose-containing sulfated polysaccharides from brown seaweeds. *Mar Drugs* 9:2106–2130
- Alekseyenko TV, Zhanayeva SY, Venediktova AA, Zvyagintseva TN, Kuznetsova TA, Besdnova NN, Korolenko TA (2007) Antitumor and antimetastatic activity of fucoidan, a sulfated polysaccharide isolated from the Okhotsk Sea *Fucus evanescens* brown alga. *Bull Exp Biol Med* 143:730–732
- Alves A (2015) Sulfated polysaccharides from green seaweeds. In: Gama M, Nader HB, de Oliveira Rocha HA (eds) Sulfated polysaccharides. Nova Science Publishers, New York, pp 135–153
- Anastyuk SD, Shevchenko NM, Nazarenko EL, Dmitrenok PS, Zvyagintseva TN (2009) Structural analysis of a fucoidan from the brown alga *Fucus evanescens* by MALDI-TOF and tandem ESI mass spectrometry. *Carbohydr Res* 344:779–787
- Bekatorou A, Plessas S, Mallouchos A (2016) Cell immobilization technologies for applications in alcoholic beverages. In: Mishra M (ed) Handbook of encapsulation and controlled release. CRC Press Taylor & Francis Group, Boca Raton, pp 933–956
- Bian L, Fong JV, Lima EG, Stoker AM, Ateshian GA, Cook JL, Hung CT (2010) Dynamic mechanical loading enhances functional properties of tissue-engineered cartilage using mature canine chondrocytes. *Tissue Eng Part A* 16:1781–1790
- Bilan MI, Grachev AA, Ustuzhanina NE, Shashkov AS, Nifantiev NE, Usov AI (2002) Structure of a fucoidan from the brown seaweed *Fucus evanescens* C.Ag. *Carbohydr Res* 337:719–730
- Bilan MI, Grachev AA, Ustuzhanina NE, Shashkov AS, Nifantiev NE, Usov AI (2004) A highly regular fraction of a fucoidan from the brown seaweed *Fucus distichus* L. *Carbohydr Res* 339:511–517
- Bilan MI, Grachev AA, Shashkov AS, Nifantiev NE, Usov AI (2006a) Structure of a fucoidan from the brown seaweed *Fucus serratus* L. *Carbohydr Res* 341:238–245
- Bilan MI, Vinogradova EV, Shashkov AS, Usov AI (2006b) Isolation and preliminary characterization of a high pyruvylated galactan sulfate from *Codium yezoense* (Bryopsidales, Chlorophyta). *Bot Mar* 49:259–262
- Bilan MI, Vinogradova EV, Shashkov AS, Usov AI (2007) Structure of a high pyruvylated galactan sulfate from the Pacific green alga *Codium yezoense* (Bryopsidales, Chlorophyta). *Carbohydr Res* 342:586–596
- Bilan MI, Grachev AA, Shashkov AS, Kelly M, Sanderson CJ, Nifantiev NE, Usov AI (2010) Further studies on the composition and structure of a fucoidan preparation from the brown alga *Saccharina latissima*. *Carbohydr Res* 345:2038–2047
- Bilan MI, Grachev AA, Shashkov AS, Thuy TTT, Van TTT, Ly BM, Nifantiev NE, Usov AI (2013) Preliminary investigation of a highly sulfated galactofucan fraction isolated from the brown alga *Sargassum polycystum*. *Carbohydr Res* 377:48–57

- Bilan MI, Shashkov AS, Usov AI (2014) Structure of a sulfated xylofucan from the brown alga *Punctaria plantaginea*. *Carbohydr Res* 393:1–8
- Bixler HJ, Porse H (2011) A decade of change in the seaweed hydrocolloids industry. *J Appl Phycol* 23:321–335
- Bloch K, Lozinsky VI, Galaev IY, Yavriyantz K, Vorobeychik M, Azarov D, Damshkaln LG, Mattiasson B, Vardi P (2005) Functional activity of insulinoma cells (INS-1E) and pancreatic islets cultured in agarose cryogel sponges. *J Biomed Mater Res* 75A:802–809
- Bondu S, Deslandes E, Fabre MS, Berthou C, Guangli Y (2010) Carrageenan from *Solieria chordalis* (Gigartinales): structural analysis and immunological activities of the low molecular weight fractions. *Carbohydr Polym* 81:448–460
- Bornhöft M, Thommes M, Kleinebudde P (2005) Preliminary assessment of carrageenan as excipient for extrusion/spheronisation. *Eur J Pharm Biopharm* 59:127–131
- Bouhlal R, Haslin C, Chermann JC, Collic-Jouault S, Sinquin C, Somin G, Cerantola S, Riadi H, Bourgougnon N (2011) Antiviral activities of sulfated polysaccharides isolated from *Sphaerococcus coronopifolius* (Rhodophyta, Gigartinales) and *Boergeseniella thuyoides* (Rhodophyta, Ceramiales). *Mar Drugs* 9:1187–1209
- Brading JWE, Georg-Plant MMT, Hardy DM (1954) The polysaccharide from the alga *Ulva lactuca*. Purification, hydrolysis, and methylation of the polysaccharide. *J Chem Soc* 319–324
- Buck CB, Thompson CD, Roberts JN, Müller M, Lowy DR, Schiller JT (2006) Carrageenan is a potent inhibitor of papillomavirus infection. *PLoS Pathog* 2:671–680
- Cabello-Pacini A, Victoria-Cota N, Macias-Carranza V, Hernandez-Garibay E, Muñoz-Salazar R (2005) Clarification of wines using polysaccharides extracted from seaweed. *Am J Enol Vitic* 56:52–56
- Cáceres PJ, Carlucci MJ, Damonte EB, Matsuhira B, Zúñiga EA (2000) Carrageenans from Chilean samples of *Stenogramme interrupta* (Phyllophoraceae): structural analysis and biological activity. *Phytochemistry* 53:81–86
- Calafiore R (2003) Alginate microcapsules for pancreatic islet cell graft immunoprotection: struggle and progress towards the final cure for type 1 diabetes mellitus. *Exp Opin Biol Ther* 3:201–205
- Campos CA, Gerschenson LN, Flores SK (2011) Development of edible films and coatings with antimicrobial activity. *Food Bioprocess Technol* 4:849–875
- Campos VL, Kawano DF, da Silva DB, Carvalho I (2009) Carrageenans: biological properties, chemical modifications and structural analysis – a review. *Carbohydr Polym* 77:167–180
- Cardoso MA, Noseda MD, Fujii MT, Zibetti RGM, Duarte MER (2007) Sulfated xylomannans isolated from red seaweeds *Chondrophycus papillosus* and *C. flagelliferus* (Ceramiales) from Brazil. *Carbohydr Res* 342:2766–2775
- Carlucci MJ, Scolaro LA, Errea MI, Matulewicz MC, Damonte EB (1997a) Antiviral activity of natural sulphated galactans on herpes virus multiplication in cell culture. *Planta Med* 63:429–432
- Carlucci MJ, Pujol CA, Ciancia M, Noseda MD, Matulewicz MC, Damonte EB, Cerezo AS (1997b) Antiherpetic and anticoagulant properties of carrageenans from the red seaweed *Gigartina skottsbergii* and their cyclized derivatives: correlation between structure and biological activity. *Int J Biol Macromol* 20:97–105
- Chevolot L, Foucault A, Chaubet F, Kervarec N, Sinquin C, Fisher A-M, Boisson-Vidal C (1999) Further data on the structure of brown seaweed fucans: relationships with anticoagulant activity. *Carbohydr Res* 319:154–165
- Chevolot L, Mulloy B, Ratiskol J, Foucault A, Collic-Jouault S (2001) A disaccharide repeat unit is the major structure in fucoidans from two species of brown algae. *Carbohydr Res* 330:529–535
- Chizhov AO, Dell A, Morris HR, Haslam SM, McDowell RA, Shashkov AS, Nifant'ev NE, Khatuntseva EA, Usov AI (1999) A study of fucoidan from the brown seaweed *Chorda filum*. *Carbohydr Res* 320:108–119

- Cho M, You S (2015) Sulfated polysaccharides from green seaweeds. In: Kim S-K (ed) Springer handbook of marine biotechnology. Springer, Berlin, pp 941–953
- Chollet L, Saboural P, Chauvierre C, Villemin J-N, Letourneur D, Chaubet F (2016) Fucoidans in nanomedicine. *Mar Drugs* 14:145
- Ciancia M, Alberghina J, Arata PX, Benavides H, Leliaert F, Verbruggen H, Estevez JM (2012) Characterization of cell wall polysaccharides of the coencocytic green seaweed *Bryopsis plumosa* (Bryopsidaceae, Chlorophyta) from Argentine coast. *J Phycol* 48:326–335
- Ciancia M, Quintana I, Vizcargüénaga MI, Kasulin L, de Dios A, Estevez JM, Cerezo AS (2007) Polysaccharides from the green seaweeds *Codium fragile* and *C. vermilara* with controversial effects on hemostasis. *Carbohydr Polym* 41:641–649
- Ciancia M, Matulewicz MC (2015) Agarans: sulfated precursors and derivatives from agarose, and related sulfated galactans. In: Gama M, Nader HB, de Oliveira Rocha HA (eds) Sulfated polysaccharides. Nova Science Publishers, New York, pp 199–216
- Conchie J, Percival EGV (1950) Fucoidan. Part II. The hydrolysis of a methylated fucoidan prepared from *Fucus vesiculosus*. *J Chem Soc* 827–832
- Cong Q, Chen H, Liao W, Xiao F, Wang P, Qin Y, Dong Q, Ding K (2016) Structural characterization and effect on anti-angiogenic activity of a fucoidan from *Sargassum fusiforme*. *Carbohydr Polym* 136:899–907
- Cosenza VA, Navarro DA, Fissore EN, Rojas AM, Stortz CA (2014) Chemical and rheological characterization of the carrageenans from *Hypnea musciformis* (Wulfen) Lamoroux. *Carbohydr Polym* 102:780–789
- Cosenza VA, Navarro DA, Pujol CA, Damonte EB, Stortz CA (2015) Partial and total C-6 oxidation of gelling carrageenans. Modulation of the antiviral activity with the anionic character. *Carbohydr Polym* 128:199–206
- Cosenza VA, Navarro DA, Stortz CA (2016) Chemical modification of carrageenans and application of the modified product. In: Pereira L (ed) Carrageenans: sources and extraction methods, molecular structure, bioactive properties and health effects. Nova Science Publishers, New York, pp 189–227
- Cosenza VA, Navarro DA, Stortz CA (2017) Minor polysaccharidic constituents from the red seaweed *Hypnea musciformis*. Appearance of a novel branched uronic acid. *Carbohydr Polym* 157:156–166
- Craigie JS (1990) Cell wall. In: Cole KM, Sheath RG (eds) Biology of red algae. Cambridge University Press, New York, pp 221–258
- Craigie JS, Rivero-Carro H (1992) Agarocolloids from carrageenophytes. *Proceed Int Seaweed Symp* 14:71
- Croci DO, Cumashi A, Ushakova NA, Preobrazhenskaya ME, Piccoli A, Totani L, Ustyuzhanina NE, Bilan MI, Usov AI, Grachev AA, Morozevich GE, Berman AE, Sanderson CJ, Kelly M, Di Gregorio P, Rossi C, Tinari N, Iacobelli S, Rabinovich GA, Nifantiev NE (2011) Fucans, but not fucomannoglucuronans, determine the biological activities of sulfated polysaccharides from *Laminaria saccharina* brown seaweed. *PLoS One* 6:e17283
- Cumashi A, Ushakova NA, Preobrazhenskaya ME, D’Incecco A, Piccoli A, Totani L, Tinari N, Morozevich GE, Berman AE, Bilan MI, Usov AI, Ustyuzhanina NE, Grachev AA, Sanderson CJ, Kelly M, Rabinovich GA, Iacobelli S, Nifantiev NE (2007) A comparative study of the anti-inflammatory, anticoagulant, antiangiogenic, and antiadhesive activities of nine different fucoidans from brown seaweeds. *Glycobiology* 17:541–552
- Cunha L, Grenha A (2016) Sulfated seaweed polysaccharides as multifunctional materials in drug delivery applications. *Mar Drugs* 14:42
- Damonte E, Neyts J, Pujol CA, Snoeck R, Andrei G, Ikeda S, Witvrouw M, Reymen D, Haines H, Matulewicz MC, Cerezo A, Coto CE, De Clerco E (1994) Antiviral activity of a sulphated polysaccharide from the red seaweed *Nothogenia fastigiata*. *Biochem Pharmacol* 47:2187–2192
- Damonte EB, Matulewicz MC, Cerezo AS (2004) Sulfated seaweed polysaccharides as antiviral agents. *Curr Med Chem* 11:2399–2419

- Datta KKR, Srinivasan B, Balaram H, Eswaramoorthy M (2008) Synthesis of agarose-metal/semi-conductor nanoparticles having superior bacteriocidal activity and their simple conversion to metal-carbon composites. *J Chem Sci* 120:579–586
- Davis TA, Volesky B, Mucci A (2003) A review of the biochemistry of heavy metal biosorption by brown algae. *Water Res* 37:4311–4330
- De S.F-Tischer PC, Talarico LB, Nosedo ND, Guimarães SMPB, Damonte EB, Duarte MER (2006) Chemical structure and antiviral activity of carrageenans from *Meristiella gelidium* against herpes simplex and dengue virus. *Carbohydr Polym* 63:459–465
- De Souza Barros C, Laneuville Teixeira V, Paixão ICNP (2015) Seaweeds with anti-herpes simplex virus type 1 activity. *J Appl Phycol* 27:1623–1637
- Dinesh S, Menon T, Hanna LE, Suresh V, Sathuvan M, Manikannan M (2016) In vitro anti-HIV-1 activity of fucoidan from *Sargassum swartzii*. *Int J Biol Macromol* 82:83–88
- Domozych DS, Ciancia M, Fangel JU, Mikkelsen MD, Ulvskov P, Willats WGT (2012) The cell walls of green algae: a journey through evolution and diversity. *Front Plant Sci* 3:82
- Draget KI, Moe ST, Skjåk-Bræk G, Smidsrød O (2006a) Alginate. In: Stephen AM, Phillips GO, Williams PA (eds) *Food polysaccharides and their applications*, 2nd edn. CRC Press Taylor and Francis Group, Boca Raton, pp 289–334
- Draget KI, Skjåk-Bræk G, Stokke BT (2006b) Similarities and differences between alginic acid gels and ionically crosslinked alginate gels. *Food Hydrocol* 20:170–175
- Duarte MER, Cardoso MA, Nosedo MD, Cerezo AS (2001) Structural studies on fucoidans from the brown seaweed *Sargassum stenophyllum*. *Carbohydr Res* 333:281–293
- Eccles R, Winther B, Johnston SL, Robinson P, Trampisch M, Koelsch S (2015) Efficacy and safety of iota-carrageenan nasal spray versus placebo in early treatment of the common cold in adults: the ICICC trial. *Respir Res* 16:121
- El-Raheem El-Helw A, El-Said Y (1988) Preparation and characterization of agar beads containing phenobarbitone sodium. *J Microencapsul* 5:159–163
- Ermakova S, Sokolova R, Kim S-M, Um B-H, Isakov V, Zvyagintseva T (2011) Fucoidans from brown seaweeds *Sargassum horneri*, *Ecklonia cava*, *Costaria costata*: structural characteristics and anticancer activity. *Appl Biochem Biotechnol* 164:841–850
- Estevez JM, Ciancia M, Cerezo AS (2004) The system of galactans of the red seaweed *Kappaphycus alvarezii*, with emphasis on its minor constituents. *Carbohydr Res* 339:2575–2592
- Estevez JM, Fernández PV, Kasulin L, Dupree P, Ciancia M (2009) Chemical and in situ characterization of macromolecular components of the cell walls from the green seaweed *Codium fragile*. *Glycobiology* 19:212–228
- Falshaw R, Furneaux RH, Wong H, Liao M-L, Bacic A, Chandkrachang S (1996) Structural analysis of carrageenans from Burmese and Thai samples of *Catenella nipae* Zanardini. *Carbohydr Res* 285:81–98
- Fan Y, Wang W, Song W, Chen H, Teng A, Liu A (2012) Partial characterization and anti-tumor activity of an acidic polysaccharide from *Gracilaria lemaneiformis*. *Carbohydr Polym* 88:1313–1318
- Farias EHC, Pomin VH, Valente A-P, Nader HB, Rocha HAO, Mourão PAS (2008) A preponderantly 4-sulfated, 3-linked galactan from the green alga *Codium isthmocladum*. *Glycobiology* 18:250–259
- Farias WRL, Valente A-P, Pereira MS, Mourão PAS (2000) Structure and anticoagulant activity of sulfated galactans. Isolation of a unique sulfated galactan from the red algae *Botryocladia occidentalis* and comparison of its anticoagulant action with that of sulfated galactans from invertebrates. *J Biol Chem* 275:29299–29307
- Feldman SC, Reynaldi S, Stortz CA, Cerezo AS, Damonte EB (1999) Antiviral properties of fucoidan fractions from *Leathesia difformis*. *Phytomedicine* 6:335–340
- Fenoradosa TA, Delattre C, Laroche C, Wadouachi A, Dulong V, Picton L, Andriamadio P, Michaud P (2009) Highly sulphated galactan from *Halymenia durvillei* (Halymeniales, Rhodophyta), a red seaweed of Madagascar marine coasts. *Int J Biol Macromol* 45:140–145

- Fernández PV, Estevez JM, Cerezo AS, Ciancia M (2012) Sulphated β -D-mannan from green seaweed *Codium vermilara*. *Carbohydr Polym* 87:916–919
- Fernández PV, Quintana I, Cerezo AS, Caramelo JJ, Pol-Fachin L, Verli H, Estevez JM, Ciancia M (2013) Anticoagulant activity of a unique sulfated pyranosic (1 \rightarrow 3)- β -L-arabinan through direct interaction with thrombin. *J Biol Chem* 288:223–233
- Fernández PV, Arata PX, Ciancia M (2014) Chapter 9- polysaccharides from *Codium* species: chemical structure and biological activity. Their role as components of cell wall. *Adv Bot Res* 71:253–278
- Fernández PV, Raffo MP, Alberghina J, Ciancia M (2015) Polysaccharide from the green seaweed *Codium decortcatum*. Structure and cell wall distribution. *Carbohydr Polym* 117:836–844
- Friedland BA, Stoner M, Chau MM, Plagianos MG, Govender S, Morar N, Altini L, Skoler-Karpoff S, Ahmed K, Ramjee G, Monedi C, Maguire R, Lähteenmäki P (2016) Baseline predictors of high adherence to a coitally dependent microbicide gel based on an objective marker of use: findings from the Carraguard phase 3 trial. *AIDS Behav* 20:2565–2577
- Gao M, Lu P, Bednark B, Lynam D, Conner JM, Sakamoto J, Tuszynski MH (2013) Templated agarose scaffolds for the support of motor axon regeneration into sites of complete spinal cord transection. *Biomaterials* 34:1529–1536
- García Tasende M, Manríquez-Hernández JA (2016) Carrageenan properties and applications: a review. In: Pereira L (ed) Carrageenans: sources and extraction methods, molecular structure, bioactive properties and health effects. Nova Science Publishers, New York, pp 17–50
- Ghosh T, Pujol CA, Damonte EB, Sinha S, Ray B (2009) Sulphated xylomannans from the red seaweed *Sebdenia polydactyla*: structural features, chemical modification and antiviral activity. *Antivir Chem Chemother* 19:235–242
- Graham LE, Wilcox LW (2000) *Algae*. Prentice-Hall, New Jersey
- Grant GT, Morris ER, Rees DA, Smith PJC, Thom D (1973) Biological interactions between polysaccharides and divalent cations: the egg-box model. *FEBS Lett* 32:195–198
- Greer CW, Yaphe W (1984) Characterization of hybrid (beta-kappa-gamma) carrageenan from *Eucheuma gelatinosa* J. Agardh (Rhodophyta, Solieriaceae) using carrageenase, infrared and ^{13}C - nuclear magnetic resonance spectroscopy. *Bot Mar* 27:473–478
- Guaccio A, Borselli C, Oliviero O, Netti PA (2008) Oxygen consumption of chondrocytes in agarose and collagen gels: a comparative analysis. *Biomaterials* 29:1484–1493
- Guibet M, Kervarec N, Génicot S, Chevotot Y, Helbert W (2006) Complete assignment of ^1H and ^{13}C NMR spectra of *Gigartina skottsbergii* λ -carrageenan using carrabiose oligosaccharides prepared by enzymatic hydrolysis. *Carbohydr Res* 341:1859–1869
- Haijin M, Xiaolu J, Huashi G (2003) A κ -carrageenan derived oligosaccharide prepared by enzymatic degradation containing anti-tumor activity. *J Appl Phycol* 15:297–303
- Hampson FC, Jolliffe IG, Bakhtyari A, Taylor G, Sykes J, Johnstone LM, Dettmar PW (2010) Alginate–antacid combinations: raft formation and gastric retention studies. Alginate raft formation and gastric retention. *Drug Dev Ind Pharm* 36:614–623
- Han MR, Kwon MC, Lee HY, Kim JC, Kim JD, Yoo SK, Sin IS, Kim SM (2007) pH-dependent release property of alginate beads containing calcium carbonate particles. *J Microencapsul* 24:787–796
- Haug A, Larsen B, Smidsrød O (1974) Uronic acid sequence in alginate from different sources. *Carbohydr Res* 32:217–225
- Haug A, Smidsrød O (1967) Strontium-calcium selectivity of alginates. *Nature* 215:757
- Hemmingson JA, Falshaw R, Furneaux RH, Thompson K (2006) Structure and antiviral activity of the galactofucan sulfates extracted from *Undaria pinnatifida* (Phaeophyta). *J Appl Phycol* 18:185–193
- Holdcraft RW, Gazda LS, Circle L, Adkins H, Harbeck SG, Meyer ED, Bautista MA, Martis PC, Laramore MA, Vinerean HV, Hall RD, Smith BH (2014) Enhancement of in vitro and in vivo function of agarose-encapsulated porcine islets by changes in the islet microenvironment. *Cell Transplant* 23:929–944

- Hussein MM-D, Abdel-Aziz A, Salem HM (1980) Some structural features of a new sulphated heteropolysaccharide from *Padina pavonica*. *Phytochemistry* 19:2133–2135
- IARC (1983) Carrageenans. IARC monographs on the evaluation of carcinogenic risks to humans 3: 79–94. Available on line: <https://monographs.iarc.fr/ENG/Monographs/vol1-42/mono31.pdf>
- Imbs TI, Ermakova SP, Malyarenko (Vishchuk) OS, Isakov VV, Zvyagintseva TN (2016) Structural elucidation of polysaccharide fractions from the brown alga *Coccophora langsdorffii* and in vitro investigation of their anticancer activity. *Carbohydr Polym* 135:162–168
- Inoue N, Yamano N, Sakata K, Nagao K, Hama Y, Yanagita T (2009) The sulfated polysaccharide porphyrin reduces apolipoprotein B100 secretion and lipid synthesis in HepG2 cells. *Biosci Biotechnol Biochem* 73:447–449
- JECFA (2002) Thickening agent: carrageenan and processed *Eucheuma* seaweed (addendum). Safety evaluation of certain food additives and contaminants. WHO Food Additives Series 48. pp 91–101. Available on line: <http://apps.who.int/iris/handle/10665/42501>
- Jiao L, Li X, Li T, Jiang P, Zhang L, Wu M, Zhang L (2009) Characterization and anti-tumor activity of alkali-extracted polysaccharide from *Enteromorpha intestinalis*. *Int Immunopharmacol* 9:324–329
- Jin W, Zhang W, Wang J, Ren S, Song N, Duan D, Zhang Q (2014) Characterization of laminaran and a highly sulfated polysaccharide from *Sargassum fusiforme*. *Carbohydr Res* 385:58–64
- Karmakar P, Ghosh T, Sinha S, Saha S, Mandal P, Ghosal PK, Ray B (2009) Polysaccharides from the brown seaweed *Padina tetrastrum*: characterization of a sulfated fucan. *Carbohydr Polym* 78:416–421
- Karmakar P, Pujol CA, Damonte EB, Ghosh T, Ray B (2010) Polysaccharides from *Padina tetrastrum*: structural features, chemical modification and antiviral activity. *Carbohydr Polym* 80:513–520
- Karjanapratum S, You S (2011) Molecular characteristics of sulfated polysaccharide from *Monostroma nitidum* and their in vitro anticancer and immunomodulatory activities. *Int J Biol Macromol* 48:311–318
- Kattumuri V, Chandrasekhar M, Guha S, Raghuraman K, Katti KV, Ghosh K, Patel RJ (2006) Agarose-stabilized gold nanoparticles for surface-enhanced Raman spectroscopic detection of DNA nucleosides. *Appl Phys Lett* 88:153114
- Kim EJ, Park SY, Lee J-Y, Park JHY (2010) Fucoidan present in brown algae induces apoptosis of human colon cancer cells. *BMC Gastroenterol* 10:96
- Kloareg B, Demarty M, Mabeau S (1986) Polyanionic characteristics of purified sulphated homofucans from brown algae. *Int J Biol Macromol* 8:380–386
- Knutsen SH, Myslabodski DE, Grasdalen H (1990) Characterization of carrageenan fractions from Norwegian *Furcellaria lumbricalis* (Huds.) Lamour by ¹H-n.m.r. spectroscopy. *Carbohydr Res* 206:367–372
- Kohajdova Z, Karovcova J (2009) Application of hydrocolloids as baking improvers. *Chem Pap* 63:26–38
- Kolender AA, Pujol CA, Damonte EB, Matulewicz MC, Cerezo AS (1997) The system of sulfated α -(1→3)-linked D-mannans from the red seaweed *Nothogenia fastigiata*: structures, antiherpetic and anticoagulant properties. *Carbohydr Res* 304:53–60
- Kolambkar YM, Dupont KM, Boerckel JD, Huebsch N, Mooney DJ, Huttmacher DW, Gulberg RE (2011) An alginate-based hybrid system for growth factor delivery in the functional repair of large bone defects. *Biomaterials* 32:65–74
- Lahaye M (1998) NMR spectroscopic characterisation of oligosaccharides from two *Ulva rigida* ulvan sample (Ulvales, Chlorophyta) degraded by a lyase. *Carbohydr Res* 314:1–12
- Lahaye M, Ray B (1996) Cell-wall polysaccharides from marine green alga *Ulva* “rigida” (Ulvales, Chlorophyta)- NMR analysis of ulvan oligosaccharides. *Carbohydr Res* 283:161–173
- Lahaye M, Robic A (2007) Structure and functional properties of ulvan, a polysaccharide from green seaweed. *Biomacromolecules* 8:1765–1774

- Lahaye M, Alvarez-Cabal Cimadevilla E, Kuhlenkamp R, Quemener B, Lognoné V, Dion P (1999) Chemical composition and ^{13}C NMR spectroscopic characterization of ulvans from *Ulva* (Ulvales, Chlorophyta). *J Appl Phycol* 11:1–7
- Lee J-B, Hayashi K, Hayashi T, Sankawa U, Maeda M (1999) Antiviral activities against HSV-1, HCMV, and HIV-1 of rhamnan sulfate from *Monostroma lasissimum*. *Planta Med* 65:439–441
- Lee J-B, Hayashi K, Hashimoto M, Nakano T, Hayashi T (2004) Novel antiviral fucoidan from sporophyll of *Undaria pinnatifida* (Mekabu). *Chem Pharm Bull* 52:1091–1094
- Lee KY, Mooney DJ (2012) Alginate: properties and biomedical applications. *Prog Polym Sci* 37:106–126
- Leiro JM, Castro R, Arranz JA, Lamas J (2007) Immunomodulation activities of acidic sulphated polysaccharides obtained from the seaweed *Ulva rigida* C. Agardh. *Int Immunopharmacol* 7:879–888
- Leite EL, Medeiros MGL, Rocha HAO, Farias GGM, da Silva LF, Chavante SF, de Abreu LD, Dietrich CP, Nader HB (1998) Structure and pharmacological activities of a sulfated xylofucoglucuronan from the alga *Spatoglossum schröderi*. *Plant Sci* 132:215–228
- Li B, Wei X-J, Sun J-L, Xu S-Y (2006) Structural investigation of a fucoidan containing a fucose-free core from the brown seaweed, *Hizikia fusiforme*. *Carbohydr Res* 341:1135–1146
- Li B, Lu F, Wei X, Zhao R (2008) Fucoidan: structure and bioactivity. *Molecules* 13:1671–1695
- Li N, Mao W, Yan M, Liu X, Xia Z, Wang S, Xiao B, Chen C, Zhang L, Cao S (2015) Structural characterization and anticoagulant activity of a sulfated polysaccharide from the green alga *Codium divaricatum*. *Carbohydr Polym* 121:175–182
- Li N, Mao W, Liu X, Wang S, Xia Z, Cao S, Li L, Zhang Q, Liu S (2016) Sequence analysis of the pyruvylated galactan sulfate-derived oligosaccharide by negative-ion electrospray tandem mass spectrometry. *Carbohydr Res* 433:80–88
- Li N, Liu X, He X, Wang S, Cao S, Xia Z, Xian H, Qin L, Mao W (2017) Structure and anticoagulant property of a sulfated polysaccharide isolated from the green seaweed *Monostroma angicava*. *Carbohydr Polym* 159:195–206
- Liang W, Mao X, Peng X, Tang S (2014) Effects of sulfate group in red seaweed polysaccharides on anticoagulant activity and cytotoxicity. *Carbohydr Polym* 101:776–785
- Liew CV, Chan LW, Ching AL, Heng PWS (2006) Evaluation of sodium alginate as drug release modified in matrix tablets. *Int J Pharm* 309:25–37
- Lim SJ, Wan Aida WA, Maskat MY, Latip J, Badri KH, Hassan O, Yamin BM (2016) Characterisation of fucoidan extracted from Malaysian *Sargassum binderi*. *Food Chem* 209:267–273
- Lins KOAL, Bezerra DP, Alves APNN, Alencar NMN, Lima MW, Torres VM, Farias WRL, Pessoa C, de Moraes MO, Costa-Lotuf LV (2009) Antitumor properties of a sulfated polysaccharide from the red seaweed *Champia feldmannii* (Diaz-Pifferer). *J Appl Toxicol* 29:20–26
- Love J, Percival E (1964) The polysaccharide of the green seaweed *Codium fragile*. Part II. The water-soluble sulphated polysaccharide. *J Chem Soc* 3338–3345
- Luan NM, Iwata H (2012) Xenotransplantation of islets enclosed in agarose microcapsule carrying soluble complement receptor 1. *Biomaterials* 33:8075–8081
- Mao W, Zang X, Li Y, Zhang H (2006) Sulfated polysaccharides from marine green algae *Ulva conglobata* and their anticoagulant activity. *J Appl Phycol* 18:9–14
- Mao W-J, Fang F, Li H-Y, Qi X-H, Sun H-H, Chen Y, Guo S-D (2008) Heparinoid-active two sulfated isolated from marine green algae *Monostroma nitidum*. *Carbohydr Polym* 74:834–839
- Mao W, Li H, Zhang H, Qi X, Sun H, Chen Y, Guo S (2009) Chemical characteristic and anticoagulant activity of the sulfated polysaccharide isolated from *Monostroma latissimum* (Chlorophyta). *Int J Biol Macromol* 44:70–74
- Mandal P, Pujol CA, Carlucci MJ, Chattopadhyay K, Damonte EB, Ray B (2008) Anti-herpetic activity of a sulfated xylomannan from *Scinaia hatei*. *Phytochemistry* 69:2193–2199
- Marais D, Gawarecki D, Allan B, Ahmed K, Altini L, Cassim N, Gopolang F, Hoffman M, Ramjee G, Williamson AL (2011) The effectiveness of Carraguard, a vaginal microbicide, in protecting women against high-risk human papillomavirus infection. *Antivir Ther* 16:1219–1226

- Marais M-F, Joseleau J-P (2001) A fucoidan fraction from *Ascophyllum nodosum*. Carbohydr Res 336:155–159
- Matsubara K, Mori M, Matsumoto H, Hori K, Miyazawa K (2003) Antiangiogenic properties of a sulfated galactan isolated from a marine green alga, *Codium cylindricum*. J Appl Phycol 15:87–90
- Matsuhiro B, Conte AF, Damonte EB, Kolender AA, Matulewicz MC, Mejias EG, Pujol CA, Zuñiga EA (2005) Structural analysis and antiviral activity of a sulphated galactan from the red seaweed *Schizymenia binderi* (Gigartinales, Rhodophyta). Carbohydr Res 340:2392–2402
- McHugh DJ (2003) A guide to the seaweed industry. FAO Fish Tech Pap 441:1–105
- McKinnel JP, Percival E (1962) Structural investigations on the water-soluble polysaccharide of the green seaweed *Enteromorpha compressa*. J Chem Soc 3141–3148
- Mendes GS, Duarte MER, Colodi FG, Noseda MD, Ferreira LG, Berté SD, Cavalcanti JF, Santos N, Romanos MTV (2014) Structure and anti-metapneumovirus activity of sulfated galactans from the red seaweed *Cryptonemia seminervis*. Carbohydr Polym 101:313–323
- Mestechkina NM, Shcherbukhin VD (2010) Sulfated polysaccharides and their anticoagulant activity: a review. Appl Biochem Microbiol 46:267–273
- Miller IJ (1997) The chemotaxonomic significance of the water-soluble red algal polysaccharides. Recent Res Dev Phytochem 1:531–565
- Miller IJ (2001) The structure of the carrageenan extracted from the tetrasporophytic form of *Stenogramme interrupta* as determined by ^{13}C NMR spectroscopy. Bot Mar 44:583–587
- Miller IJ (2003) Evaluation of the structures of polysaccharides from two New Zealand members of the Rhodomelaceae by ^{13}C NMR spectroscopy. Bot Mar 46:386–391
- Miller IJ (2005) Evaluation of the structures of polysaccharides from three taxa in the genus *Hymenena* and from *Acrosorium decumbens* (Rhodophyta, Delesseriaceae). Bot Mar 48:148–156
- Miller IJ, Blunt JW (2005) The structure of the galactan from *Aeodes nitidissima* (Halymeniales, Rhodophyta). Bot Mar 48:137–142
- Miller IJ, Falshaw R, Furneaux RH (1993) The chemical structures of polysaccharides from New Zealand members of Rhodomelaceae. Bot Mar 36:203–208
- Miyazaki S, Ishitani M, Takahashi A, Shimoyama T, Itho K, Attwood D (2011) Carrageenan gels for oral sustained delivery of acetaminophen to dysphagic patients. Biol Pharm Bull 34:164–166
- Mollion J, Morvan H, Bellanger F, Moreau S (1988) ^{13}C -NMR study of heterogeneity in the carrageenan system from *Rissoella verruculosa*. Phytochemistry 27:2023–2026
- Murano E (1995) Chemical structure and quality of agars from *Gracilaria*. J Appl Phycol 7:245–254
- Nagaoka M, Shibata H, Kimura-Takagi I, Hashimoto S, Kimura K, Makino T, Aiyama R, Ueyama S, Yokokura T (1999) Structural study of fucoidan from *Cladosiphon okamuranus tokida*. Glycoconj J 16:19–26
- Nanaki S, Karavas E, Kalantzi L, Bikiaris D (2010) Miscibility study of carrageenan blends and evaluation of their effectiveness as sustained release carriers. Carbohydr Polym 79:1157–1167
- Navarro DA, Stortz CA (2008) The system of xylogalactans from the red seaweed *Jania rubens* (Corallinales, Rhodophyta). Carbohydr Res 343:2613–2622
- Necas J, Bartosikova L (2013) Carrageenan: a review. Vet Med 58:187–205
- Ng KW, Lima EG, Bian L, O'Conor CJ, Jayabalan PS, Stoker AM, Kuroki K, Cook CR, Ateshian GA, Cook JL, Hung CT (2010) Passaged adult chondrocytes can form engineered cartilage with functional mechanical properties: a canine model. Tissue Eng Part A 16:1041–1051
- Nishino T, Yokoyama G, Dobashi K, Fujihara M, Nagumo T (1989) Isolation, purification, and characterization of fucose-containing sulfated polysaccharides from brown seaweed *Ecklonia kurome* and their blood-anticoagulant activities. Carbohydr Res 186:119–129
- Nishino T, Kiyohara H, Yamada H, Nagumo T (1991) An anticoagulant fucoidan from the brown seaweed *Ecklonia kurome*. Phytochemistry 30:535–539

- Nishino T, Nishioka C, Ura H, Nagumo T (1994) Isolation and partial characterization of a novel aminosugar-containing fucan sulphate from commercial *Fucus vesiculosus* fucoidan. *Carbohydr Res* 255:213–224
- Ohta Y, Lee J-B, Hayashi K, Hayashi T (2009) Isolation of sulfated galactan from *Codium fragile* and its antiviral effect. *Biol Pharm Bull* 32:892–898
- Panlasigui LN, Baello OQ, Dimatungal JM, Dumelod BD (2003) Blood cholesterol and lipid-lowering effects of carrageenan on human volunteers. *Asia Pac J Clin Nutr* 12:209–214
- Patankar MS, Oehninger S, Barnett T, Williams RL, Clark GF (1993) A revised structure for fucoidan may explain some of its biological activities. *J Biol Chem* 268:21770–21776
- Patil RT, Speaker TJ (1998) Carrageenan as an anionic polymer for aqueous microencapsulation. *Drug Deliv* 5:179–182
- Pavli M, Vrečer F, Baumgartner S (2010) Matrix tablets based on carrageenans with dual controlled release of doxazosin mesylate. *Int J Pharm* 400:15–23
- Pengzhan Y, Quanbin Z, Ning L, Zuhong X, Yanmei W, Zhi'en L (2003) Polysaccharides from *Ulva pertusa* (Chlorophyta) and preliminary studies on their antihyperlipidemia activity. *J Appl Phycol* 15:21–27
- Percival E (1979) The polysaccharides of green, red and brown seaweeds: their basic structure, biosynthesis and function. *Br Phycol J* 14:103–117
- Pereira L (2013) Population studies and carrageenan properties in eight Gigartinales (rhodophyta) from western coast of Portugal. *Sci World J* 2013:939830
- Pereira MS, Mulloy B, Mourão PAS (1999) Structure and anticoagulant activity of sulfated fucans. Comparison between the regular, repetitive and linear fucans from echinoderms with the more heterogeneous and branched polymers from brown algae. *J Biol Chem* 274:7656–7667
- Pérez Recalde M, Nosedá MD, Pujol CA, Carlucci MJ, Matulewicz MC (2009) Sulfated mannans from the red seaweed *Nemalion helminthoides* of the South Atlantic. *Phytochemistry* 70:1062–1068
- Pérez Recalde M, Carlucci MJ, Nosedá MD, Matulewicz MC (2012) Chemical modifications of algal mannans and xylomannans: effects on antiviral activity. *Phytochemistry* 73:57–64
- Pérez-Recalde M, Matulewicz MC, Pujol CA, Carlucci MJ (2014) In vitro and in vivo immunomodulatory activity of sulfated polysaccharides from red seaweed *Nemalion helminthoides*. *Int J Biol Macromol* 63:38–42
- Pérez Recalde M, Canelón DJ, Compagnone RS, Matulewicz MC, Cerezo AS, Ciancia M (2016) Carrageenan and agaran structures from the red seaweed *Gymnogongrus tenuis*. *Carbohydr Polym* 136:1370–1378
- Piculell L (2006) Gelling carrageenans. In: Stephen AM, Phillips GO, Williams PA (eds) *Food polysaccharides and their applications*, 2nd edn. CRC Press Taylor and Francis Group, Boca Raton, pp 239–288
- Pomin VH (2011) Structure and use of algal sulfated fucans and galactans. In: Kim S-K (ed) *Handbook of marine macroalgae: biotechnology and applied phycology*. Wiley, Chichester, pp 229–261
- Ponce NMA, Pujol CA, Damonte EB, Flores ML, Stortz CA (2003) Fucoidans from the brown seaweed *Adenocystis utricularis*: extraction methods, antiviral activity and structural studies. *Carbohydr Res* 338:153–165
- Pongjanyakul T, Puttipipatkachorn S (2007) Modulating drug release and matrix erosion of alginate matrix capsules by microenvironmental interaction with calcium ion. *Eur J Pharm Biopharm* 67:187–195
- Popa E, Reis R, Gomes M (2012) Chondrogenic phenotype of different cells encapsulated in κ -carrageenan hydrogels for cartilage regeneration strategies. *Biotechnol Appl Biochem* 59:132–141
- Popa EG, Reis RL, Gomes ME (2015) Seaweed polysaccharide-based hydrogels used for the regeneration of articular cartilage. *Crit Rev Biotechnol* 35:410–424

- Prang P, Müller R, Eljaouhari A, Heckmann K, Kunz W, Weber T, Faber C, Vroemen M, Bogdahn U, Weidner N (2006) The promotion of oriented axonal regrowth in the injured spinal cord by alginate-based anisotropic capillary hydrogels. *Biomaterials* 27:3560–3569
- Prokofjeva MM, Imbs TI, Shevchenko NM, Spirin PV, Horn S, Fehse B, Zvyagintseva TN, Prassolov VS (2013) Fucoidans as potential inhibitors of HIV-1. *Mar Drugs* 11:3000–3014
- Pujol CA, Estévez JM, Carlucci MJ, Ciancia M, Cerezo AS, Damonte EB (2002) Novel DL-galactan hybrids from the red seaweed *Gymnogongrus torulosus* are potent inhibitors of herpes simplex virus and dengue virus. *Antivir Chem Chemother* 13:83–89
- Pujol CA, Carlucci MJ, Matulewicz MC, Damonte EB (2007) Natural sulfated polysaccharides for the prevention and control of viral infections. *Top Heterocycl Chem* 11:259–281
- Pujol CA, Ray S, Ray B, Damonte EB (2012) Antiviral activity against dengue virus of diverse classes of algal sulfated polysaccharides. *Int J Biol Macromol* 51:412–416
- Qi H, Zhao T, Zhang Q, Li Z, Zhao Z, Xing R (2005) Antioxidant activity of different molecular weight sulfated polysaccharides from *Ulva pertusa* Kjellm (Chlorophyta). *J Appl Phycol* 17:527–534
- Queiroz KCS, Medeiros VP, Queiroz LS, Abreu LRD, Rocha HAO, Ferreira CV, Jucá MB, Aoyama H, Leite EL (2008) Inhibition of reverse transcriptase activity of HIV by polysaccharides of brown algae. *Biomed Pharmacother* 62:303–307
- Quemener B, Lahaye M, Bobin-Dubigeon C (1997) Sugar determination in ulvans by a chemical-enzymatic method coupled to high performance anion exchange chromatography. *J Appl Phycol* 9:179–188
- Rabanal M, Ponce NMA, Navarro DA, Gómez RM, Stortz CA (2014) The system of fucoidans from the brown seaweed *Dictyota dichotoma*: chemical analysis and antiviral activity. *Carbohydr Polym* 101:804–811
- Raghunath J, Rollo J, Sales KM, Butler PE, Seifalian AM (2007) Biomaterials and scaffold design: key to tissue-engineering cartilage. *Biotechnol Appl Biochem* 46:73–84
- Rao HBR, Sathivel A, Devaki T (2004) Antihepatotoxic nature of *Ulva reticulata* (Chlorophyceae) on acetaminophen-induced hepatotoxicity in experimental rats. *J Med Food* 7:495–497
- Ren D, Noda H, Amano H, Nishino T, Nishizawa K (1994) Study on antihypertensive and antihyperlipidemic effects of marine algae. *Fish Sci* 60:83–88
- Rinaudo M (2008) Main properties and current applications of some polysaccharides as biomaterials. *Polym Int* 57:397–430
- Rocha de Souza MC, Marques CT, Guerra Dore CM, Ferreira da Silva FR, Oliveria Rocha HA, Leite EL (2007) Antioxidant activities of sulfated polysaccharides from brown and red seaweeds. *J Appl Phycol* 19:153–160
- Ruvinov E, Leor J, Cohen S (2011) The promotion of myocardial repair by the sequential delivery of IGF-1 and HGF from an injectable alginate biomaterial in a model of acute myocardial infarction. *Biomaterials* 32:565–578
- Sakai T, Kimura H, Kojima K, Shimanaka K, Ikai K, Kato I (2003) Marine bacterial sulfated fucoglucuronomannan (SFGM) lyase digests brown algal SFGM into trisaccharides. *Mar Biotechnol* 5:70–78
- Sanchez C, Mateus MM, Defresne M-P, Crielaard J-MR, Reginster J-YL, Henrotin YE (2002) Metabolism of human articular chondrocytes cultured in alginate beads. Longterm effects of interleukin 1beta and nonsteroidal antiinflammatory drugs. *J Rheumatol* 29:772–782
- Sankalia MG, Mashru RC, Sankalia JM, Sutariya VB (2006a) Physico-chemical characterization of papain entrapped in ionotropically cross-linked kappa-carrageenan gel beads for stability improvement using Doehlert shell design. *J Pharm Sci* 95:1994–2013
- Sankalia MG, Mashru RC, Sankalia JM, Sutariya VB (2006b) Stability improvement of alpha-amylase entrapped in kappa-carrageenan beads: physicochemical characterization and optimization using composite index. *Int J Pharm* 312:1–14
- Santo VE, Frias AM, Carida M, Cancedda R, Gomes ME, Mano JF, Reis RL (2009) Carrageenan-based hydrogels for the controlled delivery of PDGF-BB in bone tissue engineering applications. *Biomacromolecules* 10:1392–1401

- Sathivel A, Raghavendran HRB, Srinivasan P, Devaki T (2008) Anti-peroxidative and anti-hyperlipidemic nature of *Ulva lactuca* crude polysaccharide on D-galactosamine induced hepatitis in rats. *Food Chem Toxicol* 46:3262–3267
- Sen AK Sr, Das AK, Sarkar KK, Siddhanta AK, Takano R, Kamei K, Hara S (2002) An agaroid-carrageenan hybrid type backbone structure for the antithrombotic sulfated polysaccharide from *Grateloupia indica* Boergensen (Halymeniales, Rhodophyta). *Bot Mar* 45:331–338
- Sergio AMD, Bustos TY (2009) Biodegradation of wastewater pollutants by activated sludge encapsulated inside calcium-alginate beads in a tubular packed bed reactor. *Biodegradation* 20:709–715
- Shao P, Chen M, Pei Y, Sun P (2013) In vitro antioxidant activities of different sulfated polysaccharides from chlorophycean seaweeds *Ulva fasciata*. *Int J Biol Macromol* 59:295–300
- Sinha S, Astani A, Ghosh T, Schnitzler P, Ray B (2010) Polysaccharides from *Sargassum tenerrimum*: structural features, chemical modification and anti-viral activity. *Phytochemistry* 71:235–242
- Sipahigil O, Dortunc B (2001) Preparation and in vitro evaluation of verapamil HCl and ibuprofen containing carrageenan beads. *Int J Pharm* 228:119–128
- Skriptsova AV, Shevchenko NM, Zvyagintseva TN, Imbs TI (2010) Monthly changes in the content and monosaccharide composition of fucoidan from *Undaria pinnatifida* (Laminariales, Phaeophyta). *J Appl Phycol* 22:79–86
- Smidsrød O (1970) Solution properties of alginate. *Carbohydr Res* 13:359–372
- Soares F, Chopin T, Pereira L (2016) Review of the chemotaxonomic significance of some phycolloids present in economically important algae (Gigartinales, Rhodophyta). In: Pereira L (ed) *Carrageenans: sources and extraction methods, molecular structure, bioactive properties and health effects*. Nova Science Publishers, Inc., New York, pp 161–188
- Sokolova EV, Byankina AO, Kalitnik AA, Kim YH, Bogdanovich LN, Solov'eva TF, Yermak IM (2014) Influence of red algal sulfated polysaccharides on blood coagulation and platelets activation in vitro. *J Biomed Mater Res Part A* 102:1431–1438
- Spillmann D (2001) Heparan sulfate: anchor for the viral intruders? *Biochimie* 83:811–817
- Sriamornsak P, Nunthanid J, Luangtana-anan M, Weerapol Y, Puttipipatkachorn S (2008) Alginate-based pellets prepared by extrusion/spheronization: effect of the amount and type of sodium alginate and calcium salts. *Eur J Pharm Biopharm* 69:274–284
- Stanley NF (2006) Agars. In: Stephen AM, Phillips GO, Williams PA (eds) *Food polysaccharides and their applications*, 2nd edn. CRC Press Taylor and Francis Group, Boca Raton, pp 217–238
- Stokols S, Tuszynski MH (2006) Freeze-dried agarose scaffolds with uniaxial channels stimulate and guide linear axonal growth following spinal cord injury. *Biomaterials* 27:443–451
- Stortz CA, Bacon BE, Cherniak R, Cerezo AS (1994) High-field NMR spectroscopy of cystocarpic and tetrasporic carrageenans from *Iridaea undulosa*. *Carbohydr Res* 261:317–326
- Stortz CA, Cases MR, Cerezo AS (1997) The system of agaroids and carrageenans from the soluble fraction of the tetrasporic stage of the red seaweed *Iridaea undulosa*. *Carbohydr Polym* 34:61–65
- Stortz CA, Cerezo AS (2000) Novel findings in carrageenans, agaroids and “hybrid” red seaweed galactans. *Curr Top Phytochem* 4:121–134
- Synysya A, Čopíková J, Kim WJ, Park YI (2015) Cell wall polysaccharides of marine algae. In: Kim S-K (ed) *Springer handbook of marine biotechnology*. Springer, Berlin, pp 543–590
- Takano R, Shiomoto K, Kamei K, Hara S, Hirase S (2003) Occurrence of carrageenan structure in agar from the red seaweed *Digenea simplex* (Wulfen) C. Agardh (Rhodomelaceae, Ceramiales) with short review of carrageenan-agarocolloid hybrid in the Florideophycidae. *Bot Mar* 46:142–150
- Talarico LB, Zibetti RGM, Faria PCS, Scolaro LA, Duarte MER, Noseda MD, Pujol CA, Damonte EB (2004) Anti-herpes simplex virus activity of sulfated galactans from the red seaweeds *Gymnogongrus griffithsiae* and *Cryptonemia crenulata*. *Int J Biol Macromol* 34:63–71
- Teramura Y, Iwata H (2010) Bioartificial pancreas: microencapsulation and conformal coating of islet of Langerhans. *Adv Drug Deliv Rev* 62:827–840

- Teruya T, Konishi T, Uechi S, Tamaki H, Tako M (2007) Anti-proliferative activity of oversulfated fucoidan from commercially cultured *Cladosiphon okamuranus* Tokida in U937 cells. *Int J Biol Macromol* 41:221–226
- Thanh TTT, Quach TMT, Nguyen TN, Luong DV, Bui ML, Tran TTV (2016) Structure and cytotoxic activity of ulvan extracted from green seaweed *Ulva lactuca*. *Int J Biol Macromol* 93:695–702
- The Carraguard Phase II South Africa Study Team (2010) Expanded safety and acceptability of the candidate vaginal microbicide Carraguard® in South Africa. *Contraception* 82:563–571
- Thomas S (2000) Alginate dressings in surgery and wound management – part 1. *J Wound Care* 9:56–60
- Thommes M, Kleinebudde P (2006) Use of κ -carrageenan as alternative pelletisation aid to microcrystalline cellulose in extrusion/spheronisation. II. Influence of drug and filler type. *Eur J Pharm Biopharm* 63:68–75
- Tobacman JK (2001) Review of harmful gastrointestinal effects of carrageenan in animal experiments. *Environ Health Perspect* 109:983–994
- Toft K, Grasdalen H, Smidsrød O (1986) Synergistic gelation of alginates and pectins. *ACS Symp Ser* 310:117–132
- Tomoda K, Asahiyama M, Ohtsuki E, Nakajima T, Terada H, Kanebako M, Inagi T, Makino K (2009) Preparation and properties of carrageenan microspheres containing allopurinol and local anesthetic agents for the treatment of oral mucositis. *Coll Surf B* 71:27–35
- Trincherro J, Ponce NMA, Córdoba OL, Flores ML, Pampuro S, Stortz CA, Salomón H, Turk G (2009) Antiretroviral activity of fucoidans extracted from the brown seaweed *Adenocystis utricularis*. *Phytother Res* 23:707–712
- Usov AI (2011) Polysaccharides of the red algae. *Adv Carbohydr Chem Biochem* 65:115–217
- Usov AI, Dobkina IM (1991) Polysaccharides of algae. 43. Neutral xylan and sulfated xylomannan from the red seaweed *Liagora valida*. *Bioorg Khim* 17:1051–1058
- Usov AI, Elashvili MY (1991) Polysaccharides of algae. 44. Investigation of sulfated galactan from *Laurencia nipponica* Yamada (Rhodophyta, Rhodomelaceae) using partial reductive hydrolysis. *Bot Mar* 34:553–560
- van de Velde F, Antipova AS, Rollema HS, Burova TV, Grinberg NV, Pereira L, Gilseman PM, Tromp RH, Rudolf B, Grinberg VY (2005) The structure of κ/ι -hybrid carrageenans II. Coil–helix transition as a function of chain composition. *Carbohydr Res* 340:1113–1129
- Venkatapurwar V, Shiras A, Pokharkar V (2011) Porphyran capped gold nanoparticles as a novel carrier for delivery of anticancer drug: in vitro cytotoxicity study. *Int J Pharm* 409:314–320
- Venugalpa Menon V (2011) Seaweed polysaccharides – food applications. In: Kim S-K (ed) *Handbook of marine macroalgae: biotechnology and applied phycology*. Wiley, Chichester, pp 541–556
- Vinardell T, Sheehy EJ, Buckley CT, Kelly DJ (2012) A comparison of the functionality and in vivo phenotypic stability of cartilaginous tissues engineered from different stem cell sources. *Tissue Eng Part A* 18:1161–1170
- Vishchuk OS, Ermakova SP, Zvyagintseva TN (2011) Sulfated polysaccharides from brown seaweeds *Saccharina japonica* and *Undaria pinnatifida*: isolation, structural characteristics, and antitumor activity. *Carbohydr Res* 346:2769–2776
- Vo T-S, Kim S-K (2013) Fucoidans as a natural bioactive ingredient for functional foods. *J Funct Foods* 5:16–27
- Vodnar DC, Pop OL, Socaciu C (2016) Microencapsulation: probiotics. In: Mishra M (ed) *Handbook of encapsulation and controlled release*. CRC Press, Taylor & Francis Group, Boca Raton, pp 685–696
- Wang L, Wang X, Wu H, Liu R (2014) Overview on biological activities and molecular characteristics of sulfated polysaccharides from marine green algae in recent years. *Mar Drugs* 12:4984–5020
- Wang X, Zhang Z (2014) The antitumor activity of a red alga polysaccharide complexes carrying 5-fluorouracil. *Int J Biol Macromol* 69:542–545

- Wells LA, Sheardown H (2007) Extended release of high pI proteins from alginate microspheres via a novel encapsulation technique. *Eur J Pharm Biopharm* 65:329–335
- Wong TW (2011) Alginate graft copolymers and alginate–co-excipient physical mixture in oral drug delivery. *J Pharm Pharmacol* 63:1497–1512
- Yang C, Chung D, Shin I-S, Lee H, Kim J, Lee Y, You S (2008) Effects of molecular weight and hydrolysis conditions on anticancer activity of fucoidans from sporophyll of *Undaria pinnatifida*. *Int J Biol Macromol* 43:433–437
- Yermak IM, Barabanova AO, Aminin DL, Davydova VN, Sokolova EV, Solov'eva TF, Kim YH, Shin KS (2012) Effects of structural peculiarities of carrageenans on their immunomodulatory and anticoagulant activities. *Carbohydr Polym* 87:713–720
- Yoshizawa Y, Ametani A, Tsunehiro J, Nomura K, Itoh M, Fukui F, Kaminogawa S (1995) Macrophage stimulation activity of the polysaccharide fraction from a marine alga (*Porphyra yezoensis*): structure–function relationships and improved solubility. *Biosci Biotechnol Biochem* 59:1933–1937
- Yuguchi Y, Tran VTT, Bui LM, Takebe S, Suzuki S, Nakajima N, Kitamura S, Thanh TTT (2016) Primary structure, conformation in aqueous solution, and intestinal immunomodulating activity of fucoidan from two brown seaweed species *Sargassum crassifolium* and *Padina australis*. *Carbohydr Polym* 147:69–78
- Zajkoska P, Rebroš M, Rosenberg M (2013) Biocatalysis with immobilized *Escherichia coli*. *Appl Microbiol Biotechnol* 97:1441–1455
- Zhang C, Yang F, Zhang X-W, Wang S-C, Li M-H, Lin L-P, Ding J (2006) Grateloupia longifolia polysaccharide inhibits angiogenesis by downregulating tissue factor expression in HMEC-1 endothelial cells. *Br J Pharmacol* 148:741–751
- Zhang H-J, Mao W-J, Fang F, Li H-Y, Sun H-H, Chen Y, Qi X-H (2008) Chemical characteristics and anticoagulant activities of a sulfated polysaccharide and its fragments from *Monostroma latissimum*. *Carbohydr Polym* 71:428–434
- Zhang Z, Zhang Q, Wang J, Song H, Zhang H, Niu X (2010) Regioselective syntheses of sulfated porphyrans from *Porphyra haitanensis* and their antioxidant and anticoagulant activities in vitro. *Carbohydr Polym* 79:1124–1129
- Zhang Z, Teruya K, Eto H, Shirahata S (2013) Induction of apoptosis by low-molecular-weight fucoidan through calcium- and caspase-dependent mitochondrial pathways in mda-mb-231 breast cancer cells. *Biosci Biotechnol Biochem* 77:235–242
- Zhou G, Sun Y, Xin H, Zhang Y, Li Z, Xu Z (2004) In vivo antitumor and immunomodulation activities of different molecular weight lambda-carrageenans from *Chondrus ocellatus*. *Pharmacol Res* 50:47–53
- Zucca P, Fernandez-Lafuente R, Sanjust E (2016) Agarose and its derivatives as supports for enzyme immobilization. *Molecules* 21:1577
- Zvyagintseva TN, Shevchenko NM, Chizhov AO, Krupnova TN, Sundukova EV, Isakov VV (2003) Water-soluble polysaccharides of some far-eastern brown seaweeds. Distribution, structure, and their dependence on the developmental conditions. *J Exp Mar Biol Ecol* 294:1–13

Innovative Systems from Clickable Biopolymer-Based Hydrogels for Drug Delivery

C. García-Astrain, L. Martin, M.A. Corcuera, A. Eceiza, and N. Gabilondo

1 Introduction

One of the major challenges faced by the pharmaceutical industry nowadays is the development of advanced drug delivery systems (DDS) intended to deliver drugs in a controlled manner and at a specific site. Novel therapies are no longer based in conventional pharmaceutical formulations but in more sophisticated DDS (Peppas et al. 2000). DDS should release the drug at some specific rate which could be tuned by external stimuli to reach the target site. Controlled-release formulations can also be used to reduce the amount of drug necessary to cause the same therapeutic effect in patients while preventing side effects, waste of drug, or frequent dosing (Huang and Brazel 2001; Simões et al. 2012). Moreover, DDS can be used to protect bioactive compounds with a very short half-time and can solve drug stability problems.

Hydrogels have attracted huge attention in the field of drug delivery due to their unique properties and are being extensively used for the development of smart drug carriers. Hydrogels are three-dimensional hydrophilic polymeric networks which can absorb huge amounts of water (up to thousands of times their dry weight) while

C. García-Astrain
BioTeam/ICPEES-ECPM, UMR CNRS 7515, Université de Strasbourg,
25 rue Becquerel, 67087 Strasbourg, Cedex 2, France

L. Martin
Macrobehavior-Mesostructure-Nanotechnology General Research Service (SGIker),
Faculty of Engineering of Gipuzkoa, University of the Basque Country,
Donostia-San Sebastián, Spain

M.A. Corcuera • A. Eceiza • N. Gabilondo (✉)
'Materials + Technologies' Group, Department of Chemical and Environmental Engineering,
Faculty of Engineering of Gipuzkoa, University of the Basque Country,
Donostia-San Sebastián, Spain
e-mail: nagore.gabilondo@ehu.eus

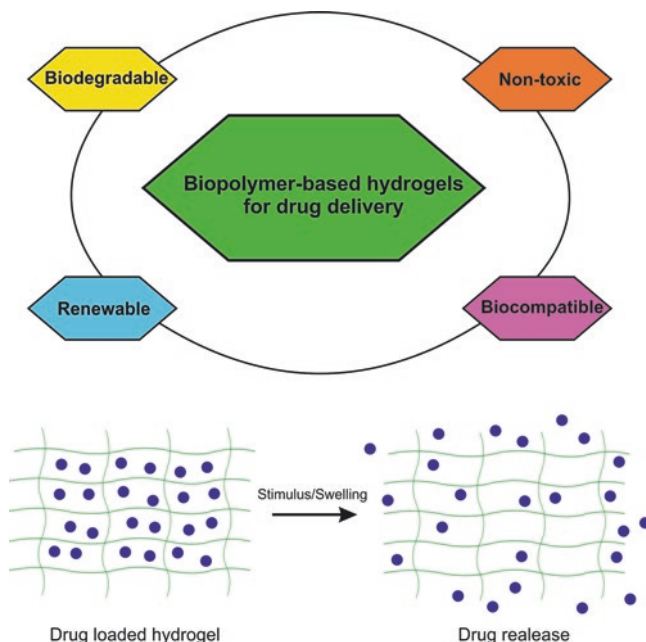


Fig. 1 Benefits of biopolymers for the design of drug delivery systems and schematic representation of drug release from hydrogels

maintaining their structure (Simões et al. 2012). Due to their high water content, hydrogels are generally compatible with biological systems (Calo and Khutoryanskiy 2015). Moreover, they can be also designed to exhibit significant changes in their physical or chemical behavior in response to environmental factors such as pH, ionic strength, temperature, and electric or magnetic field, resulting in the release of entrapped drug in a controlled manner (Kwon et al. 2015; Feng et al. 2012; Ruel-Gariépy and Leroux 2004; Navaei et al. 2016; Zamora-Mora et al. 2015).

In particular, biopolymer-based hydrogels appear as excellent candidates for the design of DDS (Fig. 1). Biopolymers offer excellent biocompatibility and are generally biodegradable since they are susceptible to human enzymes (Liu et al. 2012). Comparing to synthetic polymers, biopolymers possess more functional groups opening the way to diverse and highly selective coupling chemistries (Balakrishnan and Banerjee 2011). However, the poor mechanical strength and fast degradation profile of biopolymer-based hydrogels limit their extensive usage (Ulery et al. 2011). For that reason, chemical cross-linking, biopolymer modification, or preparation of hybrid hydrogels by combination with synthetic polymers is being developed in order to explore the beneficial aspects of these new systems in terms of biocompatibility, controlled degradation, and mechanical strength (Balakrishnan and Banerjee 2011).

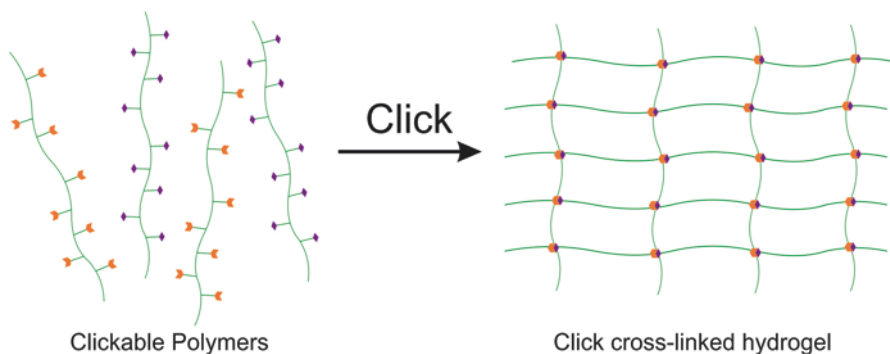


Fig. 2 Mechanism of hydrogel network formation using click chemistry

2 Hydrogels and Click Chemistry

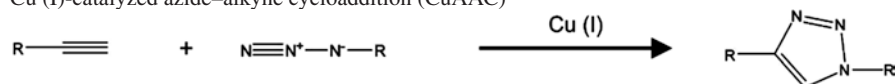
Generally, hydrogels are water swollen polymeric structures containing either physical or chemical cross-links (Peppas et al. 2000). Physical hydrogels result from hydrogen bonds or strong Van der Waals interactions between chains and can be formed through changes in environmental conditions (i.e., pH or temperature). However, as mentioned before, this type of hydrogels shows low mechanical properties as well as poor long-term stability. *By contrast*, chemical cross-links result from covalent bonds between polymer chains. Chemically cross-linked hydrogels have been obtained by radical polymerization, chemical reactions, irradiation, or enzymatic cross-linking (Zhang and Eastal 2008; Chiou et al. 2006; Zhang et al. 2014; Bode et al. 2011). Nevertheless, even if generally chemically cross-linked hydrogels display higher mechanical properties compared to their physical counterparts, the residual chemical cross-linkers, organic solvents, catalysts, or initiators may cause cytotoxicity problems (Annabi et al. 2014).

Recently, “click” chemistry has emerged as the most promising strategy to prepare hydrogels with varying properties due to its high reactivity, excellent selectivity, and mild reaction conditions (Fig. 2) (Jiang et al. 2014). The most common click reactions are listed in Table 1. The term “click” chemistry was introduced by Sharpless and coworkers to describe reactions that are orthogonal and regioselective, with high yields, and which generate no harmful by-products (Kolb et al. 2001). Moreover, click reactions must require only simple reaction conditions, using benign solvents and mild temperatures. For all these reasons, “click” reactions are really compelling for biomaterials design as they are highly compatible with living systems. In particular, the use of copper-free “click” chemistry such as strain-promoted azide–alkyne cycloaddition, radical-mediated thiol–ene chemistry, Diels–Alder reaction (DA), or the Michael reaction allows the formation of hydrogels without using potentially toxic catalysts (Jiang et al. 2014).

Table 1 Schemes of the click chemistry reactions

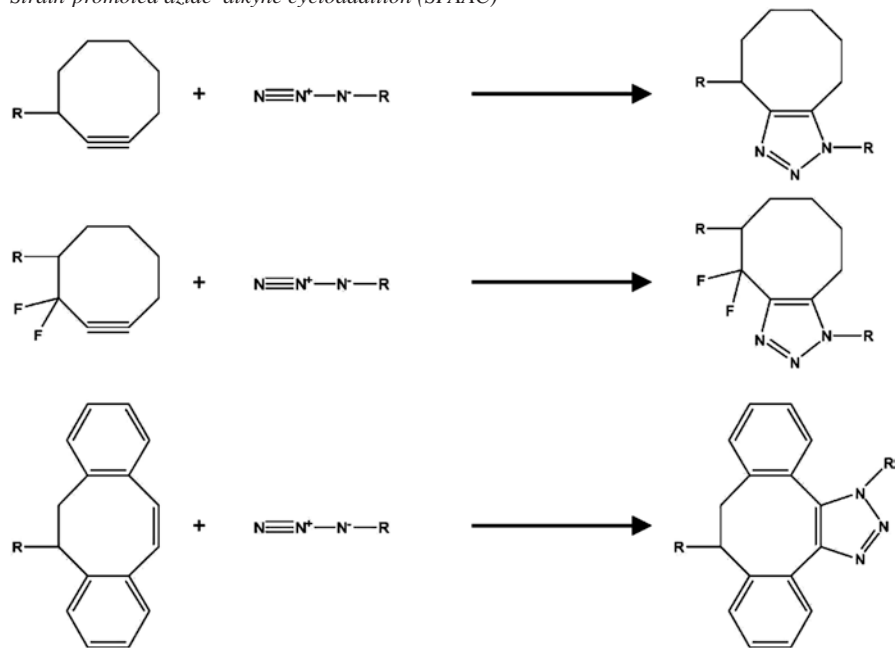
Click chemistry reactions

Cu (I)-catalyzed azide–alkyne cycloaddition (CuAAC)

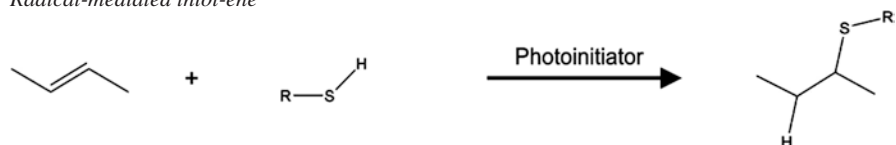


Copper-free click chemistry

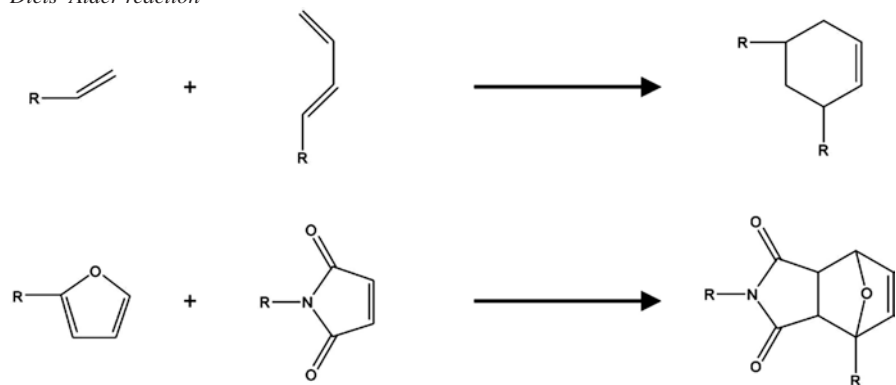
Strain-promoted azide–alkyne cycloaddition (SPAAC)



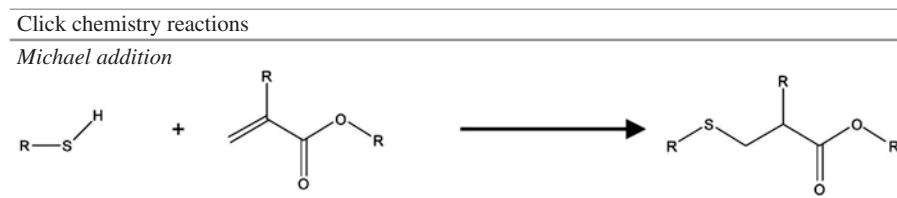
Radical-mediated thiol-ene



Diels–Alder reaction



(continued)

Table 1 (continued)

3 Copper-Catalyzed Azide–Alkyne (CuAAC) Reaction

The copper(I)-catalyzed azide–alkyne cycloaddition (CuAAC) is one of the most common examples of click chemistry. This reaction was first reported by Sharpless and Meldal in 2002 who introduced the Cu (I) catalyst to the classic Huisgen cycloaddition (Rostovtsev et al. 2002; Tornøe et al. 2002). This reaction proceeds between an alkyne and an azide to form a triazole ring. After the addition of Cu (I), the reaction can proceed at low temperatures with high rates, regioselectivity, and bio-orthogonality. This reaction is of particular advantage for biomedical applications since the azides and alkynes are stable within biological systems. Moreover, alkynes and azides cannot be found in nature, thus limiting side reactions and rendering this reaction compatible with proteins and cells (Jiang et al. 2014).

The Huisgen cycloaddition is a good candidate for hydrogel synthesis because it can be performed in aqueous solution under mild reaction conditions. This reaction has been applied to a wide variety of biopolymers in order to obtain clickable hydrogel systems. Cellulose has been modified with both alkyne and azide groups for hydrogel formation where the degree of substitution of cellulose proved to have an impact on the gelation time (Fig. 3) (Koschella et al. 2011). These materials showed interesting porous microstructure for their application as DDS. This “click” reaction proved to be also very useful for the cross-linking of hyaluronic acid-based systems. Hyaluronic acid (HA) was functionalized with azide groups after the reaction with 11-azido-3,6,9-trioxaundecan-1-amine and cross-linked with dialkyne reagents of different length (Testa et al. 2009). In view of the potential application of these systems in postsurgical oncology treatments, the release of doxorubicin, a potent anti-cancer agent, from the network was studied. It was observed that by varying the polymer or drug concentration in the hydrogel, the drug release could be modulated in order to achieve a more targeted delivery. Complementary azide and alkyne hyaluronic acid-based precursors were also prepared for hydrogel cross-linking (Crescenzi et al. 2007). In this case, the release of doxorubicin was also studied and hydrogels displayed a controlled drug release profile. Hyaluronic acid has also been used in combination with other biopolymers such as gelatin or chondroitin sulfate for hydrogel formation (Hu et al. 2011). HA and chondroitin sulfate were modified with 11-azido-3,6,9-trioxaundecan-1-amine, and gelatin was in turn modified with propionic acid. Hydrogels were obtained after short time periods by means of copper-catalyzed 1,3-dipolar cycloaddition. Other polysaccharides such as chitosan,

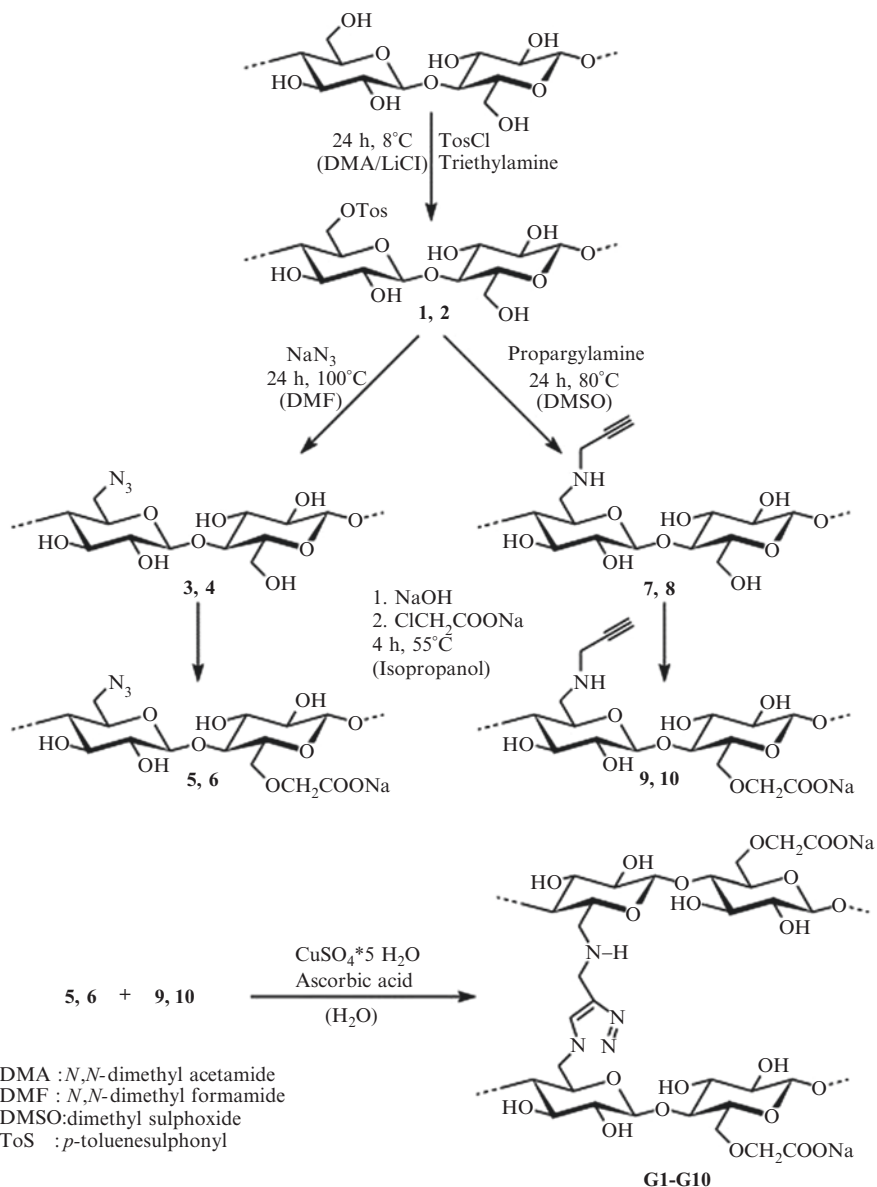


Fig. 3 Cellulose-based hydrogels cross-linked by copper-catalyzed 1,3-dipolar cycloaddition (Reprinted from Koschella et al. (2011), Copyright (2017), with permission from Elsevier)

alginate, amylose, or guar were also used as precursors for hydrogel formation via Huisgen reaction. Alkyne-functionalized guar were cross-linked with α,β -diazidopoly[(ethylene glycol)-co-(propylene glycol)] (Tizzotti et al. 2010). The authors studied the release of doxorubicin from these networks and demonstrated

the potential of these systems as temperature-dependent drug release devices. Moreover, the release ability of these hydrogels could be adjustable by changing the cross-linker concentration and, thus, influencing their thermo-dependent microstructure. Chitosan was decorated with azide functionalities via mesylation of hydroxyl groups and cross-linked with bifunctional dialkyne polyethylene oxide (Tirino et al. 2014). The resulting “click” hydrogel showed promising swelling properties in view of controlled-release applications compared with other chitosan hydrogels reported in literature. Furthermore, these properties could be tuned by varying the substitution degree of chitosan and the amount of cross-linker employed in each formulation. The CuAAC reaction has been also applied to alginate hydrogels aiming at preparing materials with improved properties compared to conventional alginate hydrogels (Breger et al. 2015). These systems showed superior stability and higher permeability to small size molecules than conventional calcium-cross-linked alginate hydrogels. Finally, azide-functionalized amylose was conjugated via click chemistry with alkyne-modified poly (L-lysine) dendrons for gene delivery applications (Pang et al. 2015). This system showed lower cytotoxicity and better gene delivery capability than commonly used gene vectors.

Protein-based hydrogels have been also cross-linked using CuAAC “click” chemistry. Biodegradable peptide-based hydrogels were prepared via “click” chemistry after the reaction of alkyne-functionalized polyethylene glycol (PEG) with a bis-azido peptide (N α -(azido)-D-alanyl-phenylalanyl-lysyl-(2-azidoethyl)-amide) (van Dijk et al. 2010). In this way, enzymatically degradable hydrogels with variable properties as a function of polyethylene glycol molecular weight and architecture or azide/alkyne molar ratio were prepared.

4 Copper-Free Click Chemistry

4.1 Strain-Promoted Azide–Alkyne Cycloaddition (SPAAC)

One of the main limitations of CuAAC for hydrogel design is the potential cytotoxicity of copper ions (Jiang et al. 2014). As an alternative of the use of copper as catalyst, SPAAC reaction between cyclooctyne and azides represents a more benign cycloaddition that takes place under mild reaction conditions. SPAAC reactions rely on the use of strained cyclooctynes with a remarkably lower activation energy than terminal alkynes, and, thus, they do not require the use of catalysts. Injectable hydrogels were prepared from azide- and cyclooctyne-modified hyaluronic acid (Takahashi et al. 2013). In vitro studies revealed that the material was completely degraded by hyaluronidase in 9 days whereas in vivo experiments proved that the rate of degradation was dependent on the administration route. Photodegradable gelatin-based hydrogels were also prepared using the SPAAC reaction (Fig. 4) (Truong et al. 2015). In this case, gelatin containing either azide or cyclooctyne moieties was cross-linked with four-arm PEG functionalized with the complementary clickable groups. Cyclooctyne groups were

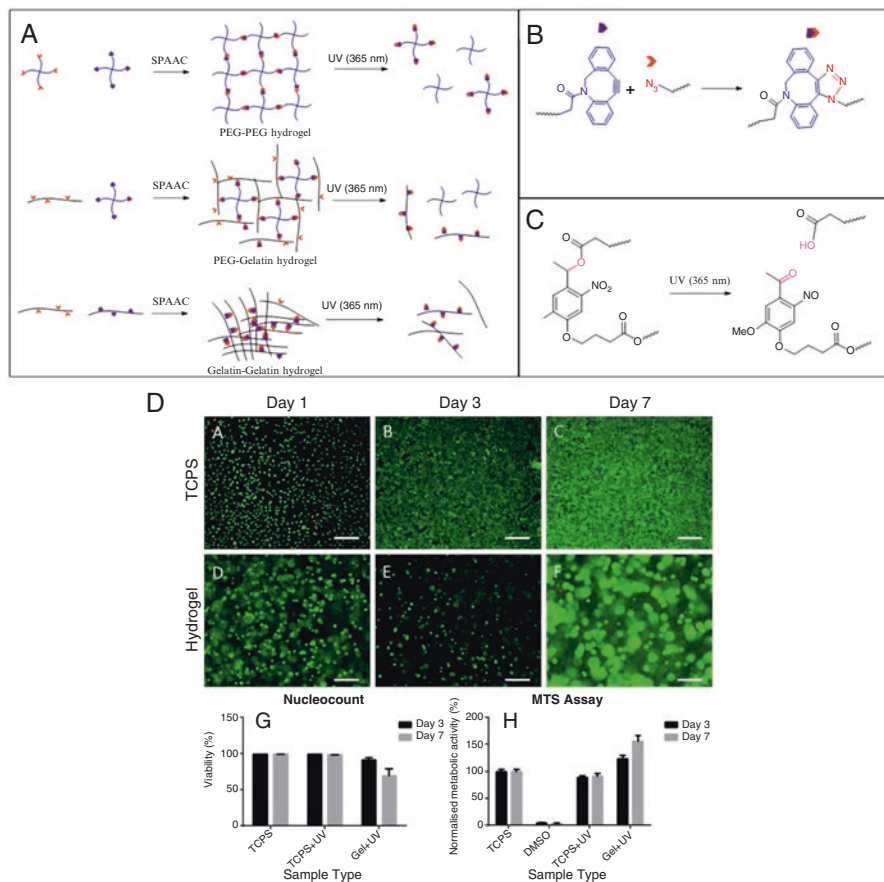


Fig. 4 (a) Scheme for the formation and photodegradation of PEG–PEG, PEG–gelatin, and gelatin–gelatin hydrogels. (b) Scheme for SPAAC chemistry. (c) Photocleavage of nitrobenzyl moiety and (d) viability assessment of L929 fibroblasts in situ with live/dead assay cultured on polystyrene (a–c) or PEG–gelatin hydrogels (d–f) at days 1, 3, and 7 (Adapted with permission from Truong et al. (2015). Copyright (2017) American Chemical Society)

introduced by dibenzylcyclooctyne-C4-acid whereas 4-(4-(1-((4-azidobutanoyl)oxyethyl)-2-methoxyphenoxy)-butanoic acid was used as the photosensitive acid. The introduction of nitrobenzyl moieties in the network structure allows for a spatiotemporal control of the network properties and open new avenues for the controlled delivery of biomolecules from the matrix.

Thermoresponsive biopolymer-based hydrogels have been also prepared via SPAAC “click” chemistry. Hemati et al. designed a tragacanth gum-based hydrogel after the functionalization of the carbohydrate with azide groups and subsequent cross-linking with amphiphilic alkyne terminated terpolymers consisting of methylated PEG, polycaprolactone, and poly(dimethylaminoethylmethacrylate) (Hemmati

and Ghaemy 2016). The developed hydrogels were intended for oral administration of hydrophobic drug and the release of quercetin from the system resulted to be pH dependent.

4.2 Radical-Mediated Thiol-ene Chemistry

The thiol-ene reaction is another example of “click” chemistry which can be used in hydrogel design. This reaction involves a radical-mediated addition between a thiol and an alkene to form an alkyl sulfide. Typically, the initiator generates radicals that initiate the reaction between thiol and alkene (Kharkar et al. 2016). Radicals can be achieved using thermal, oxidation–reduction, or photochemical processes. Although first reported in 1905, it was not until 2003 when this reaction was used for the first time for hydrogel formation (Qui et al. 2003). This reaction is of particular interest for hydrogel design since thiol-ene reactions often proceed under mild conditions compatible with biological systems, in high yields, and with nontoxic by-products. Moreover, radical-mediated processes allow for spatial and temporal control of the cross-linking procedure by controlling the radical source (Aimetti et al. 2009).

Aimetti et al. (2009) employed the thiol-ene photopolymerization to prepare degradable hydrogels by cross-linking a peptide to PEG. This hydrogel was sensitive to human neutrophil elastase and allowed for selective release of therapeutics upon exposure to the enzyme. In this way, thiol-ene reaction was used for the incorporation of an enzyme-cleavable peptide to the hydrogel backbone. Enzyme-responsive protein vehicles were prepared to selectively release proteins at inflammation sites.

Gramlich et al. used the thiol-ene reaction as a photopatterning approach to prepare hyaluronic acid-based hydrogels (Gramlich et al. 2013). The polymer was functionalized with norbornene groups and reacted with dithiols to create cross-linked hydrogels with great potential for cell encapsulation. The mechanical properties of this material can be tuned by changing the amount of cross-linker. Furthermore, the extent of cross-linking was controlled to allow remaining pendant norbornene groups that can react with thiol-containing biomolecules.

Other polysaccharides such as carboxymethylcellulose (CMC) were also cross-linked using thiol-norbornene photo-“click” reaction for the preparation of pH-sensitive hydrogels (Fig. 5) (Lee et al. 2016). Norbornene functionalized tetra-arm PEG was reacted with thiol-containing CMC. It was observed that the presence of CMC favored the release of bovine serum albumin from the matrix and was responsible for the pH sensitivity of the hydrogel. In this way, the physical properties of the hydrogels can be controlled by varying the content of CMC. The control over the “click” reaction allowed for a modulation of the network density and, thus, influenced the drug release.

Li et al. (2016) employed the thiol-ene “click” chemistry for starch cross-linking (Fig. 6). In their work, starch was functionalized both with thiol and allyl group.

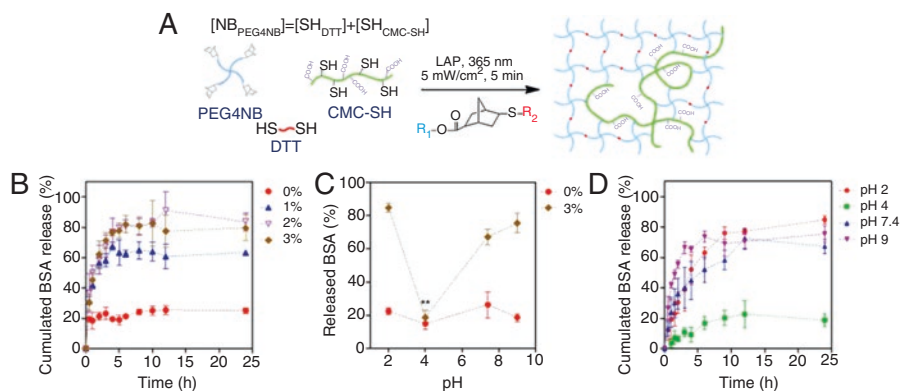


Fig. 5 (a) Schematic representation of thiol-ene reaction for the formation of PEG-CMC hydrogel using lithium arylophosphinate as photoinitiator. (b) Bovine serum albumin (BSA) profiles of PEG-CMC hydrogels for gels formed with different CMC-SH contents. (c) Total amounts of released BSA from the as-prepared hydrogels at various pH and (d) BSA release profiles of 3% CMC-SH contained PEG-CMC hydrogels at various pH (Reprinted from Publication Lee et al. (2016), Copyright (2017), with permission from Elsevier)

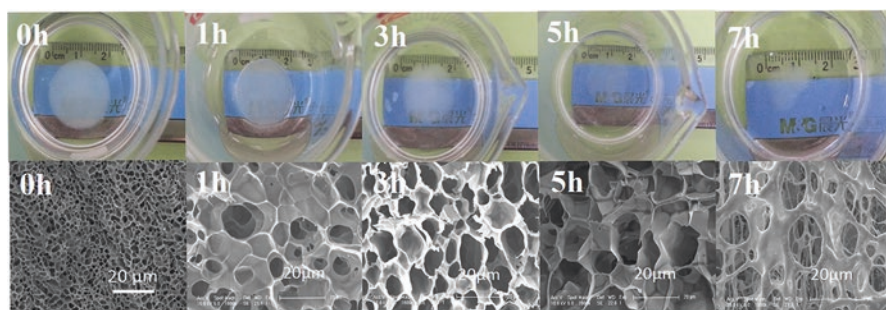


Fig. 6 Pictures of hydrogel degradation at different times and morphology observed by SEM (Reprinted from Li et al. (2016), Copyright (2017), with permission from Elsevier)

The network properties could also be modulated by tuning the thiol-ene molar ratio. Due to their good swelling properties and their biodegradability, these systems are promising for drug delivery applications.

4.3 Diels–Alder Reaction

The Diels–Alder reaction (DA) is the oldest known “click” reaction, first reported by Otto Diels and Kurt Alder in 1928 (Diels and Alder 1928). The DA reaction is a highly selective [4 + 2] cycloaddition between a diene and a dienophile to form an adduct. This reaction is free from by-products or catalysts, and it is greatly

accelerated when using water as solvent due to increased hydrophobic effects (Jiang et al. 2014). The DA reaction is also characterized by its thermal reversibility which takes place at different temperature ranges depending on the diene/dienophile combination (Gandini 2013). Adduct formation is predominant near 65 °C with reasonable reaction rates, whereas the reverse reaction (retro-DA) leading to initial precursors takes place around 110 °C (Gandini et al. 2010).

In the last years, the DA reaction has been used for the design of different types of biopolymer-based hydrogel systems. One of the most attractive couples for the DA reaction is the furan/maleimide one, since furan derivatives descend from renewable resources, an important aspect regarding sustainable (green) chemistry and materials science. Furthermore, furans possess a pronounced dienic character which favor the reaction in terms of yield and kinetics (Gheneim et al. 2002). On the other hand, maleimides are the most commonly employed dienophiles because of their high reactivity and the broad range of structural possibilities which can be offered by the substituent at the nitrogen atom (Mantovani et al. 2005). Hyaluronic acid, chitosan, or gelatin has been functionalized with furan or maleimide groups to produce hydrogel with varying properties.

Tan et al. used complementary hydrogel precursors for Diels–Alder cross-linking under physiological conditions after the functionalization of hyaluronic acid with both furan and maleimide groups (Tan et al. 2011). The release kinetics of these biodegradable hydrogels varied as a function of the charge of the loaded molecule, which could be taken as an adjustable factor of release profiles. Fan et al. studied the release of dexamethasone from Diels–Alder cross-linking hyaluronic acid hydrogels using also complementary furan and maleimide-functionalized hyaluronic acid (Fan et al. 2015). In this case, dexamethasone, an adipogenic factor, was immobilized within hyaluronic acid chains using also “click” chemistry. Aqueous Diels–Alder reaction results to be extremely selective and proceeds with high efficiency both for hydrogel cross-linking and covalent immobilization of molecules. Moreover, the ratio of clickable precursors used for hydrogel formation seemed to play a role in the most relevant properties of the matrix such as microstructure, swelling kinetics, mechanical properties, and drug release behavior. The Diels–Alder reaction proved to be also appropriate for chitosan cross-linking. Montiel-Herrera et al. worked on the cross-linking of furan-modified chitosan with bifunctional bismaleimides for the preparation of both macroscale hydrogels and microspheres (Montiel-Herrera et al. 2015). These materials exhibited interesting controlled-release properties for the design of DDS. The Diels–Alder cross-linking strategy was also used for the covalent cross-linking of maleimide-functionalized gold nanoparticles into furan-modified chitosan chains (García-Astrain et al. 2016a). The presence of gold nanoparticles within these pH-responsive materials is beneficial in terms of controlled drug delivery which could be triggered by the use of UV-light.

Gelatin was also susceptible to Diels–Alder cross-linking, and different hydrogel systems have been prepared using furan-functionalized gelatin and different maleimide-containing cross-linkers. Furan-functionalized gelatin was cross-linked with different amounts of polyetheramine-based bismaleimides resulting in

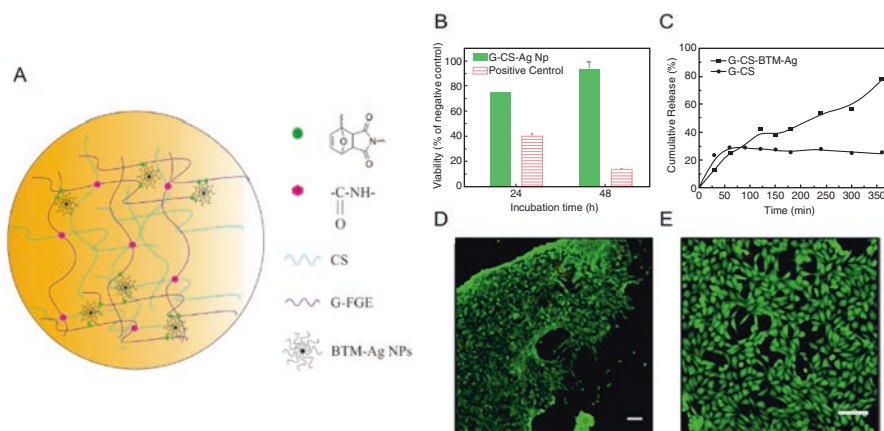


Fig. 7 (a) Schematic representation of silver nanoparticle-cross-linked chondroitin sulfate/gelatin hydrogel. (b) Cell viability of L-929 murine fibroblast from polyvinyl chloride (positive control), high-density polyethylene (negative control), and the bionanocomposite hydrogel. (c) Drug release profile of chloramphenicol for control and bionanocomposite hydrogels. (d, e) Live/dead assay for bionanocomposite hydrogel (Adapted with permission from García-Astrain et al. (2015a). Copyright (2017) American Chemical Society)

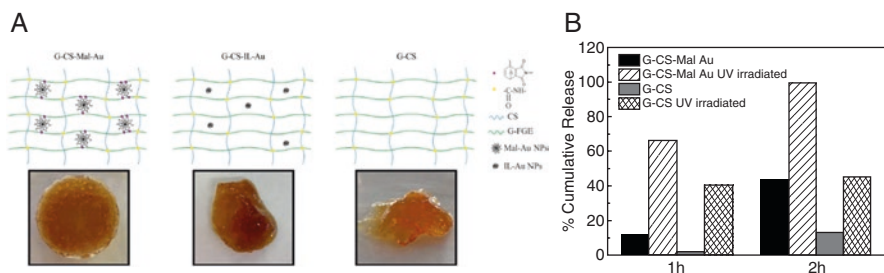


Fig. 8 (a) Scheme of the network structure of gold nanoparticle-cross-linked chondroitin sulfate/gelatin hydrogels and (b) drug release efficiency of the bionanocomposite hydrogels after UV irradiation (Adapted from García-Astrain et al. (2015b) with the permission from The Royal Society of Chemistry)

hydrogels with interesting properties (García-Astrain et al. 2014, 2016b). The mechanism governing the drug release from these systems resulted to be dependent on porosity and the amount of cross-linker used and could be modulated by adjusting the degree of cross-linking. Different types of nanoentities have also been employed for the cross-linking of furan-functionalized gelatin in the presence of chondroitin sulfate (Figs. 7 and 8). Maleimide-containing gold, silver, and titanium dioxide nanoparticles were used for the preparation of “click” cross-linked bionanocomposite hydrogels which could be used as drug delivery vehicles (García-Astrain et al. 2015a, b, 2016c). Furthermore, cellulose nanocrystals were

also functionalized with maleimide groups in order to prepare completely renewable hydrogel composites (García-Astrain et al. 2016d).

Apart from the furan/maleimide couple, biopolymer-based hydrogels have been also cross-linked using Diels–Alder chemistry between fulvene-modified dextran and dichloromaleic-acid-modified PEG (Wei et al. 2013). The resulting material displayed self-healing properties under physiological conditions opening new avenues for the design of DDS with improved efficiency.

4.4 Michael Addition

During the last decade, the Michael addition has been used for the development of tailored polymeric architectures including hydrogels. It refers to the addition of a nucleophile (i.e., enolates, thiols, amines) to an α - β -unsaturated carbonyl containing molecule to form the Michael adduct (Mather et al. 2006). The base-catalyzed addition takes place under mild conditions, with high conversions and desirable reaction rates and at room temperature.

The Michael-type addition reaction for the synthesis of new hydrogels has been usually carried out with synthetic polymers, mostly PEG-type functionalized derivatives in combination with other hydrophilic polymers and, more recently, with natural macromolecules such as proteins or polysaccharides. In that way, several investigations had been reported using heparin as biopolymer. Tae et al. used a thiol-functionalized low molecular weight heparin (LMWH) and diacrylate-terminated PEG for the synthesis of hydrogels with promising properties as an *in vitro* cell encapsulating matrix or an injectable *in vivo* cell delivery system (Tae et al. 2007). As they concluded, by controlling the degree of thiolation of heparin, the mechanical properties, gelation kinetics, and swelling ratios of the hydrogels could be modulated. In a symmetrical approach, Baldwin and Kiick (2013) reported the synthetic strategy of hydrogels with labile succinimide–thioether cross-linked by the Michael reaction between maleimide-functionalized LMWH and thiolated four-arm star PEGs at room temperature. The hydrogels were proposed as good candidates for targeted release of chemotherapeutic drugs as they were highly sensitive to the glutathione-mediated reduction.

Apart from heparin, other polysaccharides had been properly functionalized and then reacted with a variety of PEG derivatives, such as hyaluronic acid (Censi et al. 2013), starch (Dong et al. 2016), or dextran (Hiemstra et al. 2007). All biopolymer-based hydrogels have been also prepared by applying the Michael-type addition reaction. Zhao et al. designed the hydrogel for antibiotic delivery system by complementary functionalization of both dextran and chitosan with maleic acid and thiol end modifier, respectively (Zhao et al. 2014). They obtained a highly macroporous spongelike structure, with decreasing pore size as the cross-linking density was higher depending on the molar ratio thiol group to maleic group. The *in situ* forming polysaccharide-based hydrogel presented sustained drug release profiles that could be adjustable by the relative amount of the two functionalized biopolymers (Fig. 9).

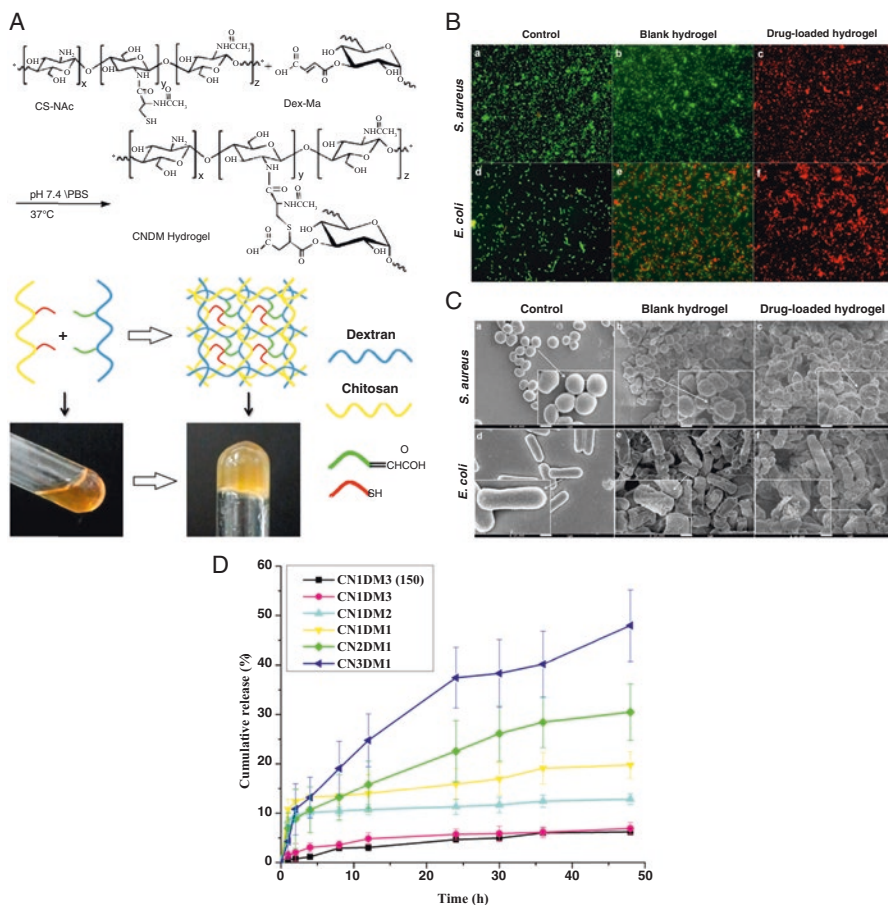


Fig. 9 (a) Scheme of chitosan/dextran hydrogel formation using Michael addition. (b) Fluorescent micrograph of *E. coli* and *S. aureus* after being treated with the as-prepared hydrogels. (c) SEM images of *E. coli* and *S. aureus* after the treatment and nontreatment of the as-prepared hydrogels and (d) cumulative release of vancomycin from the as-prepared hydrogels (Adapted from Zhao et al. (2014), Copyright (2017), with the permission from Elsevier)

5 Conclusions (Future Prospects)

The need of advanced drug delivery systems has resulted in the preparation of polymeric materials with reduced toxicity, increased absorption, and improved drug release profiles. Hydrogels have the ability to encapsulate drugs and cells and show great potential for drug delivery applications. In recent years, “click” reactions have emerged as versatile strategies for the design of novel functional hydrogels for drug release. Moreover, the high efficiency, specificity, and orthogonality of “click” reactions make them highly compatible with biological processes. The variety of

hydrogel systems reported in this chapter have demonstrated the utility and versatility of “click” chemistry in creating novel hydrogels with controlled-release properties. Moreover, the incorporation of biopolymers to the “click” chemistry toolbox broadens the application of clicked materials in the biomedical field. A wide range of biopolymers, including polysaccharides and proteins, proved to be versatile for the design of “click” hydrogels, displaying in most cases temperature- or pH-dependent properties. Furthermore, these biopolymers have the ability to mimic the extracellular matrix in terms of structural characteristics and mechanical properties, thus emerging as promising candidates for the fabrication of biomimetic materials. The development of “click” hydrogels from renewable polymers is a growing research field, and promising findings are expected in the next years, including new synthetic pathways to tailor the network properties on demand in order to have a precise control of the release process and efficiency.

References

- Aimetti AA, Machen AJ, Anseth KS (2009) Poly(ethylene glycol) hydrogels formed by thiol-ene photopolymerization for enzyme-responsive protein delivery. *Biomaterials* 30:6048–6054
- Annabi N, Tamayol A, Uquillas JA et al (2014) Rational design and applications of hydrogels in regenerative medicine. *Adv Mater* 26:85–124
- Balakrishnan B, Banerjee R (2011) Biopolymer-based hydrogels for cartilage tissue engineering. *Chem Rev* 111:4453–4474
- Baldwin AD, Kiick KL (2013) Reversible maleimide–thiol adducts yield glutathione-sensitive poly(ethylene glycol)–heparin hydrogels. *Polym Chem* 4:133–143
- Bode F, Alves da Silva M, Drake AF et al (2011) Enzymatically cross-linked tilapia gelatin hydrogels: physical, chemical, and hybrid networks. *Biomacromolecules* 12:3741–3752
- Breger JC, Fisher B, Samy R et al (2015) Synthesis of “click” alginate hydrogel capsules and comparison of their stability, water swelling, and diffusion properties with that of Ca²⁺ crosslinked alginate capsules. *J Biomed Mater Res B Appl Biomater* 103:1120–1132
- Calo E, Khutoryanskiy VV (2015) Biomedical applications of hydrogels: a review of patents and commercial products. *Eur Polym J* 65:252–267
- Censi R, Fiertens PJ, di Martino P et al (2013) In situ forming hydrogels by tandem thermal gelling and Michael addition reaction between thermosensitive triblock copolymers and thiolated hyaluronan. *Macromolecules* 43:5771–5778
- Chiou BS, Avena-Bustillos RJ, Shey J et al (2006) Rheological and mechanical properties of cross-linked fish gelatins. *Polymer* 47:6379–6386
- Crescenzi V, Cornelio L, Di Meo C et al (2007) Novel hydrogels via click chemistry: synthesis and potential biomedical applications. *Biomacromolecules* 8:1844–1850
- Diels O, Alder K (1928) Synthesen in der hydroaromatischen reihe. *Eur J Org Chem* 460:98–122
- Dong D, Li J, Cui M et al (2016) In situ “clickable” zwitterionic starch-based hydrogel for 3D cell encapsulation. *ACS Appl Mater Interfaces* 8:4442–4455
- Fan M, Ma Y, Zhang Z et al (2015) Biodegradable hyaluronic acid hydrogels to control release of dexamethasone through aqueous Diels–Alder chemistry for adipose tissue engineering. *Mater Sci Eng* 56:311–317
- Feng Y, Taraban M, Yu YB (2012) The effect of ionic strength on the mechanical, structural and transport properties of peptide hydrogels. *Soft Matter* 8:11723–11731
- Gandini A (2013) The furan/maleimide Diels–Alder reaction: a versatile click-unclick tool in macromolecular synthesis. *Prog Polym Sci* 38:1–29

- Gandini A, Silvestre AJD, Coelho D (2010) Reversible click chemistry at the service of macromolecular materials. 2. Thermoreversible polymers based on the Diels-Alder reaction of an A-B furan/maleimide monomer. *J Polym Sci A1* 48:2053–2056
- García-Astrain C, Gandini A, Peña C et al (2014) Diels-Alder “click” chemistry for the cross-linking of furfuryl-gelatin-polyetheramine hydrogels. *RSC Adv* 4:35578–35587
- García-Astrain C, Chen C, Burón M et al (2015a) Biocompatible hydrogel nanocomposite with covalently embedded silver nanoparticles. *Biomacromolecules* 16:1301–1310
- García-Astrain C, Ahmed I, Kendziora D et al (2015b) Effect of maleimide-functionalized gold nanoparticles on hybrid biohydrogels properties. *RSC Adv* 5:50268–50277
- García-Astrain C, Hernández R, Guaresti O et al (2016a) Click cross-linked chitosan/gold nanocomposite hydrogels. *Macromol Mater Eng* 301:1295–1300
- García-Astrain C, Guaresti O, González K et al (2016b) Click gelatin hydrogels: characterization and drug release behaviour. *Mater Lett* 182:134–137
- García-Astrain C, Miljevic M, Ahmed I et al (2016c) Designing hydrogel nanocomposites using TiO₂ as clickable cross-linkers. *J. Mater Sci* 51:5073–5081
- García-Astrain C, González K, Gurra T et al (2016d) Maleimide-grafted cellulose nanocrystals as cross-linkers for bionanocomposite hydrogels. *Carbohydr Polym* 49:94–101
- Gheneim R, Perez-Berumen C, Gandini A (2002) Diels-Alder reaction with novel polymeric dienes and dienophiles: synthesis of reversibly cross-linked elastomers. *Macromolecules* 35:7246–7253
- Gramlich WM, Kim IL, Burdick JA (2013) Synthesis and orthogonal photopatterning of hyaluronic acid hydrogels with thiol-norbornene chemistry. *Biomaterials* 34:9803–9811
- Hemmati K, Ghaemy M (2016) Synthesis of new thermos/pH sensitive drug delivery systems based on tragacanth gum polysaccharide. *Int J Biol Macromol* 87:415–425
- Hiemstra C, van der Aa LJ, Zhong Z et al (2007) Rapidly in situ-forming degradable hydrogels from dextran thiols through Michael addition. *Biomacromolecules* 8:1548–1556
- Hu X, Li D, Zhou F et al (2011) Biological hydrogel synthesized from hyaluronic acid, gelatin and chondroitin sulfate by click chemistry. *Acta Biomater* 7:1618–1626
- Huang X, Brazel CS (2001) On the importance and mechanisms of burst release in matrix-controlled drug delivery systems. *J Control Release* 73:121–136
- Jiang Y, Chen J, Deng C et al (2014) Click hydrogels, microgels and nanogels: emerging platforms for drug delivery and tissue engineering. *Biomaterials* 35:4969–4985
- Kharkar PM, Rehmman MS, Skeens KM et al (2016) Thiol-ene click hydrogels for therapeutic delivery. *ACS Biomater Sci Eng* 2:165–179
- Kolb HC, Finn MG, Sharples KB (2001) Click chemistry: diverse chemical function from a few good reactions. *Angew Chem Int Ed* 40:2004–2021
- Koschella A, Hartlieb M, Heinze T (2011) A “click-chemistry” approach to cellulose-based hydrogels. *Carbohydr Polym* 86:154–161
- Kwon SS, Kong BJ, Park SN (2015) Physicochemical properties of pH-sensitive hydrogels based on hydroxyethyl cellulose-hyaluronic acid and for applications as transdermal delivery systems for skin lesions. *Eur J Pharm Biopharm* 92:146–154
- Lee S, Park YH, Ki CS (2016) Fabrication of PEG-carboxymethylcellulose hydrogel by thiol-norbornene photo-click chemistry. *Int J Biol Macromol* 83:1–8
- Li Y, Tan Y, Xu K et al (2016) A biodegradable starch hydrogel synthesized via thiol-ene click chemistry. *Polym Degrad Stab*. doi:[10.1016/j.polymdegradstab.2016.07.015](https://doi.org/10.1016/j.polymdegradstab.2016.07.015)
- Liu LS, Kost J, Yan F et al (2012) Hydrogels from biopolymer hybrid for biomedical, food, and functional food applications. *Polymer* 4:997–1011
- Mantovani G, Lecolley F, Tao L et al (2005) Design and synthesis of n-maleimido-functionalised hydrophilic polymers via copper-mediated living radical polymerization: a suitable alternative to pegylation chemistry. *J Am Chem Soc* 127:2966–2973
- Mather BD, Viswanathan K, Miller KM et al (2006) Michael addition reactions in macromolecular design for emerging technologies. *Prog Polym Sci* 31:487–531
- Montiel-Herrera M, Gandini A, Goycoolea FM et al (2015) N-(furfural) chitosan hydrogels based on Diels-Alder cycloadditions and application as microspheres for controlled drug release. *Carbohydr Polym* 128:220–227

- Navaei A, Moore N, Sullivan RT et al (2016) Electrically conductive hydrogel-based microtopographies for the development of organized cardiac tissues. *RSC Adv.* doi:[10.1039/C6RA26279A](https://doi.org/10.1039/C6RA26279A)
- Pang JD, Zhuang BX, Mai K et al (2015) Click modification of helical amylose by poly(L-lysine) dendrons for non-viral gene delivery. *Mater Sci Eng* 49:485–492
- Peppas NA, Bures P, Leobandung W et al (2000) Hydrogels in pharmaceutical formulations. *Eur J Pharm Biopharm* 50:27–46
- Qui B, Stefanos S, Ma J et al (2003) A hydrogel prepared by in situ crosslinking of a thiol-containing poly(ethylene glycol)-based copolymer: a new biomaterial for protein drug delivery. *Biomaterials* 24:11–18
- Rostovtsev VV, Green LG, Fokin VV et al (2002) A stepwise Huisgen cycloaddition process: copper (I)-catalyzed regioselective “ligation” of azides and terminal alkynes. *Angew Chem Int Ed* 41:2596–2599
- Ruel-Gariépy E, Leroux JC (2004) In situ-forming hydrogels-review of temperature-sensitive systems. *Eur J Pharm Biopharm* 58:409–426
- Simões S, Figueiras A, Veiga F (2012) Modular hydrogels for drug delivery. *J Biomater Nanobiotechnol* 3:185–199
- Tae G, Kim Y-J, Choi W-I et al (2007) Formation of a novel heparin-based hydrogel in the presence of heparin-binding biomolecules. *Biomacromolecules* 8:1979–1986
- Takahashi A, Suzuki Y, Suhara T et al (2013) In situ cross-linkable hydrogel of hyaluronan produced via copper-free click chemistry. *Biomacromolecules* 14:3581–3588
- Tan H, Rubin JP, Marra KG (2011) Direct synthesis of biodegradable polysaccharide derivative hydrogels through aqueous Diels–Alder chemistry. *Macromol Rapid Commun* 32:905–911
- Testa G, Di Meo C, Nardecchia S et al (2009) Influence of dialkyne structure on the properties of new click-gels based on hyaluronic acid. *Int J Pharm* 378:86–92
- Tirino P, Laurino R, Maglio G et al (2014) Synthesis of chitosan-PEO hydrogels via mesylation and regioselective Cu(I)-catalyzed cycloaddition. *Carbohydr Polym* 112:736–745
- Tizzotti M, Labeau MP, Hamaide T et al (2010) Synthesis of thermosensitive guar-based hydrogels with tunable physico-chemical properties by click chemistry. *J Polym Sci Part A* 48:2733–2742
- Tomøe CW, Christensen C, Meldal M (2002) Peptidotriazoles on solid phase: [1,2,3]-triazoles by regioselective copper (I) catalyzed 1,3-dipolar cycloadditions of terminal alkynes to azides. *J Organomet Chem* 67:3057–3064
- Truong VX, Tsang KM, Simon GP et al (2015) Photodegradable gelatin-based hydrogels prepared by biorthogonal click chemistry for cell encapsulation and release. *Biomacromolecules* 16:2246–2253
- Ulery BD, Nair LS, Laurencin CT (2011) Biomedical applications of biodegradable polymers. *J Polym Sci B Polym Phys* 49:832–864
- van Dijk M, van Nostrum CF, Hennink WE et al (2010) Synthesis and characterization of enzymatically biodegradable PEG and peptide-based hydrogels prepared by click chemistry. *Biomacromolecules* 11:1608–1614
- Wei Z, Yang JH, Du XJ et al (2013) Dextran-based self-healing hydrogels formed by reversible Diels–Alder reaction under physiological conditions. *Macromol Rapid Commun* 34:1464–1470
- Zamora-Mora V, Soares PIP, Echeverria C et al (2015) Composite chitosan/agarose ferrogels for potential applications in magnetic hyperthermia. *Gels* 1:69–80
- Zhang C, Easteal AJ (2008) Rheological properties of poly(ethylene glycol)/ poly(*n*-isopropylacrylamide-co-2-acrylamido-2-methylpropanesulphonic acid) semi-interpenetrating networks. *J Appl Polym Sci* 109:3578–3589
- Zhang M, Cheng Z, Zhao T et al (2014) Synthesis, characterization, and swelling behaviors of salt-sensitive maize bran–poly(acrylic acid) superabsorbent hydrogel. *J Agric Food Chem* 62:8867–8874
- Zhao C, van der Aa LJ, Zhong Z et al (2014) In situ cross-linked polysaccharide hydrogel as extracellular matrix mimics for antibiotics delivery. *Carbohydr Polym* 105:63–69

Applications of Glycosaminoglycans in the Medical, Veterinary, Pharmaceutical, and Cosmetic Fields

José Kovensky, Eric Grand, and María Laura Uhrig

1 Introduction

Most of the cells in multicellular organisms are surrounded by a complex mixture of nonliving materials that make up the extracellular matrix (ECM). It is composed of a variety of secreted molecules pseudo-organized as an amorphous mixture of proteoglycans (PGs) and proteins (Kim et al. 2011). PGs are heavily glycosylated proteins (Schaefer and Schaefer 2010) whose polysaccharide chains are called glycosaminoglycans (GAGs). GAGs are the most abundant heteropolysaccharides present in humans, expressed in all tissues. Thus, the consistency of the ECM is the result of the complex arrangement of glycoproteins, collagens, and other fibrous proteins, with PGs and GAG chains, which define the volume, shape, and strength of the living tissues as bones and cartilage, giving support and functionality to the cells (Schnabelrauch et al. 2013).

Among the proteins that interact with GAGs to form this cross-linked material, we can mention laminin, elastin, fibronectin, and collagens (Kirn-Safran et al. 2008). Another role of GAGs is the participation in the binding process of certain growing factors by controlling the diffusion of these factors through the extracellular space. Therefore, they play a role as protector barriers of the cells (Yip et al. 2006).

J. Kovensky • E. Grand

Laboratoire de Glycochimie, des Antimicrobiens et des Agroressources (LG2A) CNRS UMR 7378, Institut de Chimie de Picardie CNRS FR 3085, Université de Picardie Jules Verne, 33 rue Saint Leu, 80039 Amiens Cedex, France
e-mail: jose.kovensky@u-picardie.fr; eric.grand@u-picardie.fr

M.L. Uhrig (✉)

Facultad de Ciencias Exactas y Naturales, Departamento de Química Orgánica, Universidad de Buenos Aires, Pabellón 2, Ciudad Universitaria, C1428EHA Buenos Aires, Argentina

Consejo Nacional de Investigaciones Científicas y Técnicas (CONICET)-UBA, Centro de Investigación en Hidratos de Carbono (CIHIDECAR), Buenos Aires, Argentina
e-mail: mluhrig@qo.fcen.uba.ar

From the structural point of view, GAGs are high molecular weight, unbranched polysaccharides, composed of repeating disaccharide units of alternating uronic acids (or galactose for KS) and hexosamines (Table 1). Post-translational modifications, such as epimerization and sulfation, result in structural diversity and formation of specific binding motifs for many ligands. All of them, as a result of their strong negative charge, attract cations (Na^+) and water molecules (Zhao et al. 2012). Connective tissues such as the skin, bone, cartilage, and the intervertebral discs are particularly rich in GAGs, which can be found inside and outside the cells. As mentioned before, their ubiquity and singular structural features, together with their ability to interact with a number of proteins, make them participate in the control of a high number of physiological and pathological events, including cell–cell communication process: they are receptors of growing factors, act as inhibitors of enzymes, and have a role on the regulation of the cellular proliferation and inflammatory and wound repair processes (Aquino and Park 2010). Neurodegenerative disorders such as Alzheimer's disease (AD) have been ascribed to the biochemistry of GAGs (Papy-García et al. 2011; Kwok et al. 2012).

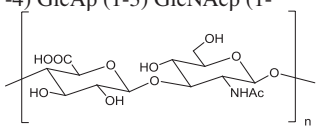
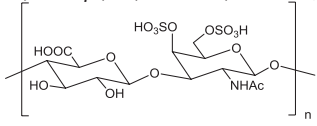
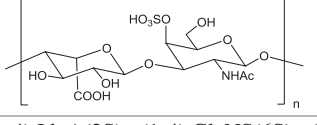
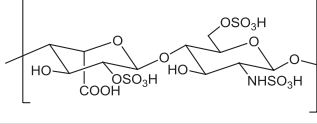
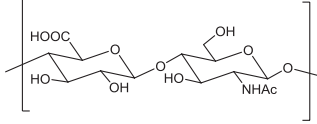
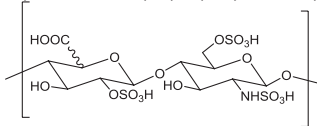
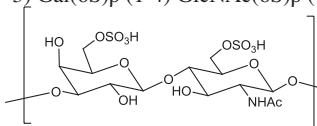
Among the most abundant GAGs, we found hyaluronic acid (HA), heparin (HP), heparan sulfate (HS), chondroitin sulfate (CS), dermatan sulfate (DS), and keratan sulfate (KS). Their relative distribution depends on the tissue, environmental factors, age, and general health conditions. Beyond the structural features they share, the different species of the GAG family show distinct characteristics, summarized as follows.

Hyaluronic acid (HA) is characterized by the lack of sulfate groups, is located on the surface of the cells, and is not covalently linked to a protein. It is highly hygroscopic and has interesting viscoelastic properties, due to its high capacity to retain water molecules. As a result, HA and derivatives are seen as promising molecules in the cosmetic industry for hydration therapies and wrinkle prevention (Volpi et al. 2009; Beasley et al. 2009).

Chondroitin sulfate (CS) is the most abundant GAG in the body. CS is found in the cartilage, tendon, ligament, and aorta and binds to proteins (like collagen) to form aggregates. It has been implicated in diverse physiological events such as cytokinesis, morphogenesis, and neuronal plasticity (Mikami and Kitagawa 2013). CS helps repair the articular surface in osteoarthritis (Bottegoni et al. 2014). During polymerization, CS is sulfated at various positions, thus resulting in polymer chains with variable sulfation patterns. CS-A, CS-C, CS-D, and CS-E are the most common sulfation patterns, differentiated by the number of sulfates per disaccharide, their position, and, consequently, the interactions they can establish (Bedini and Parrilli 2012).

Dermatan sulfate (DS) is a component of the skin, blood vessels, and heart valves. One particularly well-studied DS-binding interaction occurs with HP cofactor II. This serpin homolog of antithrombin III acts by inhibiting the procoagulative effect of thrombin. DS proteoglycans bind a diverse range of molecules including (but not limited to) growth factors, protease inhibitors, cytokines, chemokines, and pathogen virulence factors (Liaw et al. 2001).

Table 1 Structures of the major disaccharides present in GAGs

GAG	Major disaccharide	Comments
Hyaluronic acid or hyaluronan (HA)	-4) GlcA β (1-3) GlcNAc β (1- 	HA is not sulfated
Chondroitin sulfate (CS)	-4) GlcA β (1-3) GalNAc(4S/6S/4S,6S) β (1- 	CS is the most abundant GAG CS lacks IdoA
Dermatan sulfate (DS)	-4) IdoA α (1-3) GalNAc(4S) β (1- 	IdoA is the major uronic acid in DS
Heparin (HP)	-4) IdoA(2S) α (1-4) GlcNS(6S) α (1- 	HP displays a higher degree of sulfation and iduronic acid content compared to HS
Heparan sulfate (HS)	-4) GlcA β (1-4) GlcNAc α (1- 	HS is very similar to HP with alternate domains of sulfated and non-sulfated residues
	-4) IdoA/GlcA(2S) α (1-4) GlcNS(6S) α (1- 	
Keratan sulfate (KS)	-3) Gal(6S) β (1-4) GlcNAc(6S) β (1- 	Gal residues instead of uronic acid residues

The ability of HP to bind to proteins is widely known (Conrad 1998; Capila and Linhardt 2002; Barrowcliffe 2012; Zhao et al. 2012). Growth factors, cytokines, metabolic enzymes, and structural proteins rich in basic amino acids (arginine and lysine) are able to bind HP, which is highly negatively charged due to the presence of carboxylate groups from uronic acid residues and sulfate groups. The well-known

anticoagulant activity of HP is the result of the formation of a complex HP–anti-thrombin–thrombin that inhibits the active form of several coagulation factors (Barrowcliffe 2012). Recently, the expression “heparin interactome” has been proposed to characterize the big family of proteins able to form a cross-linked network interconnected by interaction with HP (Pomin 2015a, b). Even though the use of HP as an anticoagulant is probably the most emblematic example of applications of any GAG in medicine, this review will not focus on this topic, as there is abundant literature on this subject nowadays (Gray et al. 2012; Pomin and Mulloy 2015).

Heparan sulfate (HS) is considered the major constituent of the ECM. Its structure, closely related to that of HP, consists of an average chain containing 50–200 repetitive disaccharide units, linked through a tetrasaccharide (Xyl, Gal, GlcA), to a protein core. HS participates in the binding process of growth factors, controlling their diffusion through the extracellular space and acting as a protector barrier of the cells (Yip et al. 2006). HS is a regulator of several biological processes such as cell proliferation, differentiation, and migration, and its properties are largely related to the sulfation pattern of their sugar chains (Conrad 1998; Capila and Linhardt 2002; Coombe and Kett 2005). The saccharide–protein interactions are at the basis of a number of HS fundamental biological roles (Nugent 2000).

Corneal keratan sulfate (KS) is the most extensively characterized GAG. It is composed of sulfated galactose and glucosamine residues, lacking uronic residues. The amount of KS in the cornea is more than tenfold that in the cartilage and is two to four orders of magnitude greater than KS found in other tissues. The high abundance of KS appears to be related to maintenance of a level of tissue hydration critical for corneal transparency. KS would also be an active participant in the cellular biology of the tissues in which it is located (Funderburgh 2000).

2 Recent Advances in the Production of GAGS

Traditionally, standard protocols for the efficient extraction of PGs and GAGs require the use of chaotropic salts, such as guanidine, and detergents in an appropriate buffer. Anion-exchange chromatography or ethanol precipitation, before or after treatment with proteases and DNAases, are among the classic steps used to obtain purified materials. GAGs are in general released from their core proteins by β -elimination in the presence of NaBH_4 to avoid the “peeling” reaction (Esko 2001; Nakano et al. 2010; Staples and Zaia 2011). Since the GAG structures are not strictly regular, the evolution of the chromatographic technologies had a great impact in the characterization and elucidation of the structural features responsible for the many biological activities.

As stated above, as a three-dimensional macromolecular network, the ECM provides a physical scaffold to the cells and also constitutes the environment where many cellular processes such as differentiation, migration, homeostasis, growth, etc., occur. The ECM is highly heterogenic and dynamic, suffering a constant remodeling process as cells secrete, assemble, and constantly modify its composition, which is

highly dependent on the specific tissue (Theocharis et al. 2016). ECM from various origins have been used as source of GAGs. There are many methodologies to obtain decellularized ECM materials in order to recover its components, which include sonication, mechanical pressure, or freeze-thawing procedures, in combination with washing steps and processing with ionic solutions and various detergents (Gilbert et al. 2006). The optimal method is highly dependent on the type of tissue (Keane et al. 2015), and it is desirable that the composition and the structure of the decellularized ECM should be similar to the original ECM (Hoshiba et al. 2016). The decellularized ECM presents a 3D fibrous and porous topography, with properties similar to the native materials. Decellularized tissues and organs have been brought to market to be used as natural scaffolds for the reparation of injured tissue. In this respect, a number of clinical successes have been reported (as discussed below for the case of Alloderm®).

In the human body, HA occurs in the salt hyaluronate form and is found in high concentrations in the skin, umbilical cord, and vitreous humor. HA is also present in the capsules of certain microbial strains (e.g., strains of streptococci). Traditionally HA was extracted from rooster combs, and now it is mainly produced via microbial fermentation with lower production costs and less environmental pollution. HA has been successfully produced on an industrial scale by biotechnology, with *Streptococcus* sp. as the main producer. Nevertheless, the production of HA from *Streptococcus* sp. is facing a growing concern due to the fact that streptococci are pathogenic. Recently, the production of HA via recombinant systems has received increasing interest due to the avoidance of potential toxins. In their review, Liu et al. (2011) summarized the research history and current commercial market of HA, and then deeply analyzed the current state of microbial production of HA by *Streptococcus zoepidemicus* and recombinant systems, and finally discussed the challenges facing microbial HA production and proposed several research outlines to meet the challenges.

Boeriu et al. (2013) then reviewed the chronological production of HA, from the traditional extraction from animal waste until biotechnological synthesis. Genetic/metabolic engineering has been applied in the area of tailor-made HA synthesis. The advantages and drawbacks of the different technologies have been discussed. The extraction from animal materials is a well-established technology and leads to a natural product of very high molecular weight (M_w) up to 20 MDa but presents a risk of contamination (proteins, nucleic acids, viruses) and needs extensive purification. Bacterial production affords a HA of high M_w (1–4 MDa) in high yield; however, the risk of contamination is always present. Finally, enzymatic synthesis allows the control of M_w (0.55–2.5 MDa) without contamination risks, although the economic viability has still to be demonstrated.

DeAngelis et al. (2013) reviewed recent advances in the chemoenzymatic synthesis of GAGs, using enzymes and precursors as uridine 5'-diphosphosphate-sugar donors, sulfate donors, acceptors, and oxazoline precursors, including the use of microfluidic technology. They claimed that even at an early stage of technology development, nearly monodisperse GAGs can be made with either natural or artificial structures.

Recently, a review by Fu et al. (2016) focused on the complex biology of HPs and HS in human health and disease. They discussed and compared the advantages and drawbacks of the synthesis, the extraction from animal tissues, the chemical and enzymatic depolymerization, and focused on the use of recombinant technology in the chemoenzymatic synthesis and metabolic engineering of HP and HS.

3 Alzheimer's Disease

Aberrant brain ECM structure is associated with brain neurodegenerative disorders as Alzheimer's disease (AD) (Manveen et al. 2017). AD is biologically characterized by a loss of neurons, accumulation of β -amyloid peptides, and aggregation of Tau protein. Proteins and GAGs are involved in the process via multiple interactions. Sulfated GAGs are of importance in the development and the prevention of AD, through the binding of anionic oligo- or polysaccharides to various biological molecules such as proteins, growth factors, or cytokines (Wang and Ding 2014; Papy-García et al. 2011).

In patients suffering of AD, 3-*O*-sulfated HS binds to Tau protein and modifies its conformation leading to abnormal phosphorylation and aggregation. Various oligo-/polysaccharides can bind Tau protein in place of 3-*O*-sulfated HS and prevent its abnormal phosphorylation. In particular, dextran with various degrees of polymerization and substitution (sulfation, carboxymethylation) can be used as a protection against AD (Papy-García et al. 2013). Dextran sulfate can also inhibit the interaction of β -amyloid oligomers with the cellular prion protein responsible for synaptic dysfunction and showed protective effects (Aimi et al. 2015).

HS interacts with β -amyloid peptides promoting their aggregation (Zhang et al. 2016; Liu et al. 2016). These peptides aggregate into plaques in the brains of AD patients and have interactions with cell surface receptors (Da Costa Dias et al. 2011). HS mimetics can trigger the β -secretase (BACE-1), responsible for the production of toxic β -amyloid peptides. Inhibition of the beta-secretase 1 (BACE-1), by HS mimetics, should prevent the formation of plaques and damage to neural cells (Zhou and Jin 2016). Multimeric 6-*O*-sulfate-*N*-acetylglucosamine (mono-, di-, and trimers) inhibited β -sheeted β -amyloid aggregation (Fukuda et al. 2015). The strongest inhibition observed for the dimer was probably due to its proper sulfate density allowing a conformational change of β -amyloid peptides. Dendritic tetravalent HS mimetics have been synthesized with sulfated mono-, di-, or tetrasaccharides (Tyler et al. 2015). Their inhibition activities toward BACE-1 were evaluated. Inhibition of BACE-1 was also observed by the use of polyacrylamides substituted by various sulfated glucosamines, in particular with 3,4,6-tri-*O*-sulfo-GlcNAc polyacrylamide (Nishimura et al. 2013). Inhibition of BACE-1 can be also observed by the use of oligosaccharides obtained from HP and HS. Their inhibitory activities were correlated to the degree of sulfation and size of the oligosaccharides (Zhang et al. 2016). HS hexa- to dodecasaccharides have been synthesized and their potency to inhibit BACE-1 was evaluated (Schwoerer et al. 2013). A small octasaccharide showed an

interesting activity as it should cross the blood–brain barrier. Low Mw CS possessed neuroprotective properties against toxic effects induced by β -amyloid peptides. This low Mw CS is capable of passing the blood–brain barrier and can be useful in prevention or treatment of AD (Zhang et al. 2015). In the same way, treatment by chondroitinase ABC allows treating injuries to the neural system and disorders like AD by degradation of CS (Kwok et al. 2012; Khaderi 2014). CS mimetic oligomers with controlled size and sulfation can interact with growth factors and be active in neuronal protection and protection against neurodegenerative diseases as AD. Linear alkyl polymers (polymeric degree from 1 to 100) carrying sulfated di- or tetrasaccharides have been synthesized by ring opening metathesis polymerization to make CS mimetics (Rawat and Hsieh-Wilson 2014). Histones are intracellular proteins, but they also appear with aberrant level in extracellular space in AD. As histones are known to bind GAG, a structure activity relationship study allowed identifying small sulfated oligosaccharides able to modulate histone H1 activity among a large library of oligosaccharides with various structures and sizes (Campion et al. 2012). The receptor for advanced glycation end products (RAGE) is implicated in inflammatory diseases and AD. Advanced glycation end products (AGE) represent a class of covalently modified proteins and lipids generated by oxidative and non-oxidative pathways, involving sugars or their degradation products. They are generated by the nonenzymatic reaction of reactive carbonyl species produced by lipid peroxidation and lipid metabolism, with the nucleophilic residues of macromolecules. They exert a biological damaging activity through different mechanisms, and they are considered factors in aging and in the development or worsening of many degenerative diseases, such as AD (Vistoli et al. 2013).

RAGE can bind the β -amyloid peptide and the β -sheets of amyloid proteins. These interactions mediate Alzheimer's dementia. Partially or fully sulfated HS can inhibit RAGE (Prestwich et al. 2011, 2013). A computational study allowed a better understanding of the interaction between sulfated oligosaccharides and β -amyloid peptides. Three sulfated disaccharides derived from HP have been identified for inhibition of β -amyloid peptide aggregation (Paul et al. 2016). An experimental approach using nuclear magnetic resonance gave useful information about the domains of a low Mw HP involved in the interaction with amyloid fibrils (Stewart et al. 2016).

Various sulfated disaccharides produced a reduction of reactive oxygen species and had neuroprotective activity. They have been envisaged as potential therapeutics for the prevention or treatment of AD (Verges Milano et al. 2011).

4 Antimicrobials and Antivirals

Microbial pathogens interact with host GAGs in various stages of progression and development. In the early stages of infection, GAGs are involved in the invasion mechanisms of pathogens and also participate in the migration steps and in many protection mechanisms to evade the immune system. As GAGs are contact

molecules of numerous receptors leading to biological events, they are a major key in the regulation of the infection from various pathogens, i.e., bacteria, virus, and others (Ströh and Stehle 2014; García et al. 2016; Aquino and Park 2016). In this aspect, the activity of GAGs in native form or as drug carriers has been studied as inhibitors of pathogens. Some of the latest reports are discussed below.

Bacteria The perturbation of the adhesion of *Lactobacillus salivarius* Lv72 (from human vaginal exudates) to HeLa cells by several GAGs has been studied. HP, HS, and CS-A and CS-C inhibited partially the adhesion at the same level, while DS (with iduronic acid) improved it. The bacterial adhesin OppA was identified as the protein responsible for the attachment (Martin et al. 2013).

Recurrent bacterial cystitis has been treated by intravesical instillations of a mixture of HA and CS. CS was employed to regenerate GAGs, while HA reduced inflammatory cytokines and reduced cell adherence of *Escherichia coli*, the pathogen responsible for most of the cystitis (De Vita and Giordano 2012). It has been observed that breast-fed infants were protected from infection by the presence of anti-adhesive GAGs in the human milk (Coppa et al. 2016).

The effects of GM-0111, a sulfated HA on the inhibition of *Porphyromonas gingivalis* and *Aggregatibacter actinomycetemcomitans*, pathogenic bacteria associated with periodontitis, were studied. The antibacterial effects of GM-0111 were stronger than HA and were the consequence of inhibition of multiple molecular events involved in periodontitis (Savage et al. 2016).

A patent on the use of GAGs (such as HA, HP, or CS) substituted by hydroxymethyl groups, for treatment and prevention of infectious disorders, was reported (Reinmueller and Dirting 2012).

In a comparative study, the properties of 6-diamino and 6-tetraamino derivatives of 6-desoxy cellulose sulfate to inhibit *E. coli* (Gram negative bacteria), *Staphylococcus aureus* (Gram positive bacteria), and *Candida glabrata* (fungus) were evaluated and compared to CS at pH 5.0 and 6.8. Inhibition by CS was not sufficient at any pH for all pathogens. The cellulosic derivatives were active against *S. aureus* and *C. glabrata*, and the activity was pH dependent. At pH 5.0, the antimicrobial activity was better due to the cationic ammonium groups. Inhibition of *E. coli* was low because of the differences in the membrane. There was no inhibition of the adhesion, as sulfate groups are hidden by positive charges (Genco et al. 2012). Zwitterionic polymers were synthesized by substitution of various polymers or polysaccharides like HA or HP by carboxybetaine derivatives. The resulting zwitterionic polymers can form hydrogels with antimicrobial or antifouling properties. The antifouling properties prevent cell or protein adhesion to a surface of an implanted device (Cheng and Cao 2015).

Liquid crystals can be formed by mixing the anionic HP with the cationic polypeptide antibiotic colistin. This new gel formulation was able to release slowly colistin over time. The gel inhibited *Pseudomonas aeruginosa* without loss of colistin antibacterial activity (Tangso et al. 2016). Multilayer implants for antimicrobial drug delivery need the development of biocompatible polymers or materials. Biocompatible ionically bound multilayers such as polycationic poly-L-lysine and

sulfated GAGs, CS, and HP can be used to deliver growth factors or antibiotics (Grohman et al. 2014). Polymeric implants composed of two layers, both containing GAGs such as HA, HP, CS, DS, and KS or chitosan with different degrees of acetylation and derivatives, were prepared. Modulation of the degree of acetylation had an impact on the in vivo persistence of the implant and drug delivery (Ladet 2013). Depolymerized GAGs such as CS or HA were used to make metal (gold or silver) salts with antimicrobial properties. The material showed greater stability than the native CS metal salts (Flores Salgado et al. 2013). Multiple layers pellets can be used to treat enteric diseases. A microcrystalline cellulose core was covered by an antimicrobial drug layer, then a layer of HA or other GAGs, and an enteric polymer. The pellets had to go through the digestive system to join colon for drug delivery. The GAG could carry the drug to the triggered cells by intermolecular interactions and deliver the drug in the cell environment (Chang 2014).

Viruses The inhibition activity of four CS fractions (CS-A, CS-C, CS-D, and CS-E) toward human T-cell leukemia virus type 1 (HTLV-1) was studied. CS-E exhibited anti-HTLV-1 activity by interaction with envelope proteins (Jinno-Oue et al. 2013).

Inhibition of the infectivity of respiratory syncytial virus (RSV) by various sulfated K5 *Escherichia coli* polysaccharide derivatives (as mimetics of the HP/HS precursor) was studied. The effect of the degree of sulfation and disposition of the sulfate groups (*N*-sulfation/*O*-sulfation/*N,O*-disulfation) was evaluated. The best inhibition results were obtained for the K5 *O*-sulfated or *N,O*-disulfated with a high degree of sulfation (Cagno et al. 2014).

Various GAGs (HS, CS, DS) were evaluated as inhibitors of the attachment of the hepatitis C virus (HCV) to the host cells. HS from the liver strongly bound to the HCV proteins responsible for the attachment, probably due to its high sulfate contents. This binding was better than the one of highly sulfated HP for the same proteins. Sulfation at 6-*O*- or *N*- positions seemed to be important for the activity (Kobayashi et al. 2012).

Soluble CS-E was evaluated to inhibit Japanese encephalitis virus infection on different cell types. CS-E inhibited virus attachment, and thus inhibition of viral infection, excepted in on cell type where the infection was enhanced probably due to increased viral RNA replication (Kim et al. 2011).

Infection of epithelial cells by human papillomavirus (HPV) showed differences depending on the virus type. Inhibition by HP, CS-A/C, or ι-carrageenan was effective with some types and ineffective with other types, showing different mechanisms (GAG dependent or not) to bind and enter into the cell (Cruz and Meyers 2013).

The inhibition of human immunodeficiency virus 1 (HIV-1) by a FGAG and its chemically modified analogs was studied. This FGAG possesses a CS-like backbone and sulfated fucose branches. The native FGAG showed the best inhibition and the higher binding affinity for the factors CD4i of gp120 probably due to the fucose branches (Lian et al. 2013).

Infection of cells by chikungunya virus (CHIKV) and its prevention by the use of GAGs have been evaluated. The results showed that inhibition is virus strain

dependent. DS and HS were more potent inhibitors than HP or CS-A when used in preincubation protocols. When GAGs were used by incubation with the virus, HP gave the best inhibiting properties (Silva et al. 2014). Arthritogenic alphaviruses, CHIKV and Ross River virus, can generate inflammation and cartilage damage. Treatment with pentosan polysulfate, a GAG mimetic, reduced the proinflammatory cytokines and the concomitant damages (Herrero et al. 2015).

Ebola virus (EBOV) and Marburg virus (MARV) are filoviruses which can infect humans and other animals, causing hemorrhagic fever with a high mortality. These viruses enter into the cells by the participation of a single filoviral glycoprotein (GP). The ability of HS, HP, CS-A, and CS-B to block GP-mediated viral entry of EBOV and MARV was evaluated. The four GAGs inhibited infection by interaction with GP (O'Hearn et al. 2015).

Henipavirus Nipah virus (NIV) and Hendra virus (HEV) are emerging and highly pathogenic, zoonotic paramyxoviruses. The binding of NIV and HEV to cells was inhibited by HP, while CS-A, CS-C, and DS were inactive. The inhibition occurs as HP binds henipavirus G-protein as well as ephrin receptors and may thus displace the virus from the cell surface and prevent it from reaching its entry receptors (Mathieu et al. 2015).

In another example, it was reported that murine leukemia virus was inhibited by HP by interaction with the envelope viral glycoprotein. The *O*-sulfate groups were of importance in the inhibition activity (Seki et al. 2012).

Concerning dengue virus (DENV), Hidari et al. reviewed in 2013 the carbohydrate and noncarbohydrate compounds with similar inhibitory mechanisms against DENV entry. Disruption of syndecan – DENV interaction can inhibit virus uptake and infection. Syndecans are transmembrane proteoglycans with attachment sites for HS and CS. Thus, the use of HP or HS to control the infection is a promising tool (Arevalo et al. 2011).

Formulations Liposomes covalently substituted by an HS octasaccharide showed inhibiting properties toward few viruses: RSV, herpes simplex virus (HSV), and human parainfluenza virus 3 (HPIV3). The liposomes were more efficient than the HS octasaccharide itself or HP (Hendricks et al. 2015).

CS has been modified by transformation of carboxylates by long-chain amino groups. This gave hydrophobic properties to the CS. The inhibition of CS and hydrophobic CS with or without presence of α -cyclodextrin toward HSV-2 was evaluated. Native CS did not present any anti-HSV-2 activity, while HP was active, the density of sulfate being the cause. Hydrophobic CS showed inhibitory activity, and cyclodextrin enhanced it because of the well-structured new nanoassemblies (Galus et al. 2016).

Formulations which contain GAGs (purified GAGs or extracts) can be used to treat or prevent influenza virus infection or symptoms after infection. Anionic polysaccharides containing fucose or rhamnose could be used and also CS and HS (Fitton and Gardiner 2011).

Silica nanoparticles have been covered by benzenesulfonates to make a GAG mimetic in terms of anionic charges. The silica GAG mimetic inhibited the HSV-1 and HSV-2 attachment and penetration into cells (Lee et al. 2016).

Despite the fact that some anionic GAGs are known to inhibit virus invasion (as described above), their used as vaginal microbiocides failed. This is probably due to the reversibility of the interaction that can let the virion free or complexed to the GAG. PG545 (a cholesterol conjugated to a persulfated maltotetraose) was the best oligosaccharide to disrupt the lipid envelope of HSV particles compared to other substituted oligosaccharides. PG545 played the role of carrier of cholesterol which destabilized the virion envelope (Lundin et al. 2012; Said et al. 2016).

A polymer or a protein cross-linked to a GAG as HP, CS-A, or DS could be a material able to release a loaded chemokine RANTES. This chemokine binds to the receptor CCR5 which is also a receptor for HIV cellular entry. The competition would prevent HIV binding and infection. Sustained release can be obtained as RANTES has affinity for GAGs, allowing the device to be long-term HIV preventive (Von Recum and Hijaz 2014).

Non-anticoagulant GAGs such as DS or HA can be used in the formulation of nanoparticle carriers containing a combination of an antiviral agent, a protease inhibitor, and a polymerase inhibitor to treat HCV which limit the emergence of resistance (Mousa 2016).

5 Cancer

Cancer development involves a number of cellular events such as cell adhesion, cell migration, invasiveness, cell growing, angiogenesis, etc. Most of these events depend on the interaction between oligo- or polysaccharides and protein receptors. In this sense, the role of GAGs is crucial. The potential use of GAGs for cancer therapies defines nowadays a complex field, taking into consideration that they are ubiquitous in mammalian tissues as components of the ECM. As mentioned before (Table 1), GAGs show differences in their structures (monosaccharides, oligosaccharide sequences), in their charges (sulfates, carboxylates), in their density of charges (number of anionic charge per monosaccharide or per fine oligosaccharide portion), and in their localization on the tissue. As all GAGs play important roles in the “communication” of the cell with proteins, growth factors, cytokines, and cell surface receptors, it is not difficult to deduce that they can be associated to many of the mechanisms involved in cancer development, including the associated inflammatory processes (Nikitovic et al. 2012; Memi et al. 2012; Afratis et al. 2012; Basappa et al. 2014).

Most of the patents and studies are focused on a small number of cancer-related targets which are summarized below:

- *RAGE*: The RAGEs are known to play a role in several diseases like arthritis, AD, or even cancer by binding to various ligands (CS, HS, etc.) with high affinity and

are involved in cancer metastasis (Mizumoto et al. 2012). CS is related to invasion, adhesion, migration of tumoral cells and angiogenesis. CS was identified as functional RAGE ligand in tumors (Mizumoto and Sugahara 2013).

- *P-selectin*: P-selectin is a vascular cell adhesion molecule that lines the inner surface of blood vessels and activated platelets (thrombocytes). P-selectin mediates tumor cell interactions with platelets, leukocytes, and the vascular endothelial cells. P-selectin is necessary for the binding of tumor cells to platelets facilitating endothelial attachment and extravasation of tumor cells from blood vessels to organs. P-selectin and other selectins can bind to various GAGs (Martinez et al. 2013). Holothurian GAG (a fucosylated CS) behaved as a ligand-competitive inhibitor of P-selectin allowing the inhibition of the entire events P-selectin dependent (Yue et al. 2015).
- *Heparanase*: Heparanase is an endoglycosidase that degrades HS expressed on the surface of cells and then facilitates tumor cell invasion (Fux et al. 2009; Pisano et al. 2014). Heparanase promotes cell proliferation, metastasis, and angiogenesis by releasing growth factors such as the fibroblast growth factor-2 (FGF2) and the vascular endothelial growth factor (VEGF) from HS. The role of HP (and its formulation) in cancer treatment has been reviewed (Ahmad and Ansari 2011; Kozlowski and Pavao 2011; Afratis et al. 2016). HP inhibits heparanase activity and P-selectin and growth factors (FGF, VEGF) binding. Nevertheless, the well-known anticoagulant activity of HP, together with its relative unspecific mode of targeting, is a drawback for a generally used anticancer agent. Still, HP has been evaluated in clinical trials for cancer treatment (Belting 2014). HS modulates signal transduction into tumor cells by interacting with various growth factors such as FGF2. HS plays a major role in tumor metastasis. HS has been defined as a modulator in breast cancer (Gomes et al. 2013).
- *CD44* (“cluster of differentiation 44”): CD44 is a transmembrane glycoprotein which has been described as the HA receptor. It is expressed at low levels on various cell types. CD44 is implicated in cell migration, apoptosis, and other phenomena (Misra et al. 2015; Lompardía et al. 2016). Activated CD44 is overexpressed in solid tumors. HA is considered as a key player in cancer progression (Wu et al. 2017; Mirsa et al. 2015). HA interacts with CD44 receptor and increases viscosity, preventing tumoral cells migration but also limiting the accessibility for the drug. Hyaluronidase and other enzymes cleave HA facilitating cell migration and making CD44 accessible for tumoral cells adhesion. HA fragments can generate disappearance of CD44. The minimal size of HA able to bind CD44 is a hexasaccharide. These HA oligosaccharides have also shown to modulate growth and cell survival and sensitize breast cancer cells to cytotoxic drugs (vincristine). Thus, they are considered promising leads for cancer treatment (Cordo Russo et al. 2008).

Synthetic Analogs and Modified GAGs Synthetic analogs or modified GAGs may overcome to the unwanted side effects of natural GAGs and be complementary (Pomin 2015a). Low Mw HP but also DS, sulfated alginate, pentosan polysulfate, and fucoidan have the property to inhibit cell growth and proliferation, interfering

the interaction between the tumor cell surface and platelets (Fabricius 2015). Inhibition is dependent on the polysaccharide structure and on its degree of sulfation (between 1 and 1.4 sulfates per monosaccharide unit). A higher size and a higher sulfate/carboxylate ratio of HP are preferable for the release of tissue factor pathway inhibitor. HA, HP, DS, and depolymerized GAGs with Mw lower than 10 kDa interact with cell surface and cytokine and modulate their activity (Eklund et al. 2013). Sulfated HA is an inhibitor of hyaluronidase and has an anticancer activity by interfering the formation of complexes between HA and its receptors (Benitez et al. 2011). Sulfated HA is an inhibitor of prostate cancer. HA could be chemically modified by introduction of an alkyl or fluoro alkyl or sulfate group on various positions. The resulting compounds showed anticancer activities by inhibition of P-selectin, L-selectin, and RAGE and have low coagulant properties (Prestwich and Kennedy 2011).

SST0001 is a chemically modified HP 100% *N*-acetylated and 25% of the uronic acid residues cleaved at the C₂–C₃ bond. This modified HP inhibits growth of myeloma tumors, and one of the mechanisms is the inhibition of heparanase (Ritchie et al. 2011). M402 is a low molecular weight HP derivative obtained by nitrous acid depolymerization and then cleavage of the C₂–C₃ bond of uronic acid residues; M402 inhibits angiogenesis (Zhou et al. 2011). CS disaccharides sulfated in various positions have been synthesized and their capacity to inhibit breast cancer was evaluated, showing the importance of the sulfate positions on the disaccharides (Zhong et al. 2015). The cytotoxic activity of hydroxynaphthylxyloside-primed GAGs has been studied. Primed CS or DS showed to be cytotoxic depending on their disaccharide composition. The cytotoxic activity was due to induction of apoptosis by the GAG part of the hydroxynaphthylxyloside-primed GAG (Persson et al. 2016). Synthetic C–C linked dimers of sulfated tri-mannose (GAG mimetic) showed both inhibitions of heparanase and P-selectin and an anticoagulant activity (Borsig et al. 2011).

GAGs in Nanocarriers Carriers can be used in cancer treatment to transport a drug. This formulation is adapted to hydrophobic drugs to enhance their solubility, bioavailability, and stability. The carrier can serve to trigger cancer cells using GAG interactions. Moreover, the carrier can deliver the drug inside the tumoral cell. The GAG can be part of the core or of the shell of a nanostructure; it allows the carrier to target specifically tumoral cells. The carried drug can be incorporated to the nanostructure or covalently linked to the GAG. An anticancer agent (lenalidomide or gemcitabine) can be chemically bound to HA to be carried in the environment of tumor cells (Lin 2015). Anticancer agents can be encapsulated in GAGomers (nanoparticles covered by HA) as carrier. The carrier can trigger tumor cells CD44v+ to make the delivery of the anticancer agent efficiently toward cancer metastasis (Cayre and Allouche 2017). The anticancer agent mitomycin C has been entrapped in GAGomers coated with HA (Bachar et al. 2011). The carrier is able to target tumoral cells with highly expressed CD44 receptors. The anticancer drug docetaxel has been encapsulated into micelles of amphiphilic hexadecyl-HA conjugates. The micelles were coated with a polyethylene glycol (PEG) diamine to be stabilized. The hexadecyl-HA micelles demonstrated excellent tumor targeting and cellular

uptake ability by interacting with CD44 receptor (Zheng et al. 2016). The use of HA-based nanoparticles in hydrogel formulations has been recently reviewed (Rankin and Frankel 2016). HP-based nanocarriers have been designed; they show anticoagulant activity, growth factor binding, and antiangiogenic and apoptotic effects (Liang and Kiick 2014; Sakiyama-Elbert 2014). A recent review exposes all the possibilities to employ HP-based nanocarriers for cancer treatments (Yang et al. 2015). HP can be ionically or covalently bound to the shell of nanoparticles containing a chemotherapeutic agent (Mousa 2015). Nanoparticles of iron oxide coated by chitosan and then covered by HP gave a magnetic resonance imaging agent able to target tumors in vivo. The interactions between fibrinogen-derived product in the solid tumor and the HP-coating nanoparticles should be responsible for the concentration of nanoparticles at the tumor (Yuk et al. 2011). Heparosan, a precursor of HP and HS, has been used to make prodrugs complexes of an anticancer agent like cisplatin (DeAngelis and Lane 2016). The prodrug increased the efficacy and reduced the side effects of the parental drug. Microspheres were formed with mixtures of Nucant (a multivalent peptide anticancer agent) and a GAG (HP, CS A, B, or C). The microspheres can be used in cancer treatment (Zimmer and Courty 2012). Hybrids of mesoporous silica and CS have been synthesized; CS was covalently bound to silica by an amide function. This new material can serve as carrier for curcumin. When phagocytized, the nanoparticles were exposed to hyaluronidase for degradation and drug delivery (Radhakrishnan et al. 2015). Liposomes containing a nucleic acid to treat cancer were coated with various GAG, HA, CS, DS, KS, HP, and HS. The GAG was bind to the surface of liposomes by amide linkages (Peer 2015).

Heterogeneous GAGs Extracts GAG extracts can be used in treatments of cancers or cancer metastasis. Extracts from whelk or cockle species that contain HS, CS, and DS showed a strong anticancer activity, while commercial HS or CS did not (Pye and Ogundipe 2016). Extracts from the skins of gray triggerfish and smooth hound that contain CS and DS showed antiproliferative properties (Krichen et al. 2017). Extracts from the Norway lobster shell that contain HS and DS showed antiproliferative but also anticoagulant activities (Sayari et al. 2016). Extracts from sea cucumber *Holothuria leucospilota* showed good efficacy toward tumor metastasis (Qian et al. 2015). Two DS isolated from ascidian species showed to inhibit P-selectin and thus present anti-metastatic activities (Kozlowski et al. 2011). HS isolated from bivalve mollusk *N. nodosus* extracts showed inhibition of P-selectin adhesion, but also of heparanase (Gomes et al. 2015).

GAGs in Tumor Cells Imaging A fluoresceinamine-labeled HA has been synthesized. The carboxylates of HA can form a complex with a cationic conjugated polymer which emits fluorescence. In the presence of CD44, the complex is broken as HA can bind CD44, and the emission of fluorescence stopped (Huang et al. 2014). This labeling can be used to detect cells with overexpression of CD44. Superparamagnetic iron oxide nanoparticles have been modified by linkage of HA. The new nanoparticles were efficient probes for targeted magnetic resonance imaging of liver carcinoma (Yang et al. 2014).

6 Inflammation and Immunity

An inflammation process is triggered in the body by a harmful determinant, for example, the presence of a pathogen or an irritating substance. Damaged and cancer cells can also be the cause of inflammation. The objective of this process is the elimination of the adverse agent to restore the normal functionality of the affected tissues, which usually takes a short period of time and then disappears when the pathogen is gone and the repair process has started. So, the inflammatory process is a fundamental manifestation of a healthy innate immune system. However, if it is not properly regulated, it can result in serious damage and lead to a pathological state (Lee-Sayer et al. 2015; Kavasi et al. 2017). The symptoms involve the participation of several nonprotein molecules (such as leukotrienes) and a variety of proteins present in the surface of the cells produced by the immune system (leukocytes) which act together with the circulatory system. As a characteristic feature, an edema and a concomitant swelling appear in the affected area, as a result of the excretion (exudation) of plasma proteins from the blood vessels.

Among the proteins involved, several members of the complex group of polypeptides that compose the cytokines (with MW up to 20 kDa), such as chemokines, interferons, interleukins, lymphokines, and tumor necrosis factors, as well as the family of selectins (also known as the cell adhesion molecules [CAM]), participate in cell signaling events through the many phases of the acute inflammation. On the other hand, there is a variety of diseases, characterized by chronic inflammation conditions, for example, atherosclerosis, some allergies, and cardiopathies, which have been described as inflammatory-based illnesses. In cancer tissues, inflammation plays also an important role contributing to the metastatic proliferation of the abnormal cells.

There are many reports that involve GAGs in inflammation processes. Cytokines (TNF, IL-1, and others), L- and P-selectins, and chemokines bind to therapeutic HP and purified HS. Furthermore, HP blocks L- and P-selectin *in vivo* in mice (Ley et al. 1991). Computational methods revealed a variety of potential nonclassic ligands for HS, most of them expressed intracellularly (Davis and Parish 2013). In fact, the administration of exogenous sulfated glycans that could mimic the structures and functions of GAGs reduces inflammation. Sulfated glycans of various sources such as HP, HS, CS, and DS have proved to be anti-inflammatory (Pomin 2015b).

The anti-inflammatory activity of CS has been reported in 1998 (Ronca et al. 1998). Since then, CS was shown to reduce pain and other symptoms associated with osteoarthritis, a chronic disease characterized by the irreversible and progressive damage of joint cartilage, consequence of a misbalance of GAGs, and progressive degradation of the matrix components. The major symptoms are pain and rigidity and, thus, loss of ability and reduced quality of life. The oral administration of CS contributes to the restitution of the natural properties of the cartilage, by favoring the biosynthesis of HA and collagen and, at the same time, inhibiting a number of proteases (Monfort et al. 2008). It was estimated that after oral administration, the absorption of the polymerized CS occurs at approximately 10%, while

the remaining 90% of the product is incorporated as oligosaccharides of low Mw. In general, a wide range of doses are used and an optimal effect is attained after 3–6 months of treatment and persists after suspension of the therapy. There are several products in the market based on CS recommended for osteoarthritis treatment; many of them include free glucosamine. They are considered safe, with no adverse events, and they are recommended by the Osteoarthritis Research Society International (OARSI), the European League Against Rheumatism (EULAR), and other societies (Bottegoni et al. 2014). CS is also used in pet and veterinary products, such as Artroglycan®, and is frequently administered as a nutritional supplement to horses to preserve joint health.

With respect to the role of HS, it has been shown that HS provides adhesion sites for several pathogens, facilitating the invasion, but, on the other hand, HS can modulate the recruitment of neutrophils (the most abundant leukocytes in charge of the phagocytosis of the microbes) to sites of infection or injury (Xu et al. 2015). A large number of studies on the role and activity of the various sulfotransferases involved in the biosynthesis of HS revealed the complex dependence of the sulfation pattern with the immune response, as an accelerated recruitment of neutrophils does not always mean a beneficial immune response.

In general, when the sulfation or the uronic acid content is reduced or inhibited in HS, the binding and/or activity of most ligands decreases, presumably because of the loss of negatively charged groups precludes the favorable electrostatic interactions with positively charged residues in the ligands. Nevertheless, it has been also shown that the inactivation of a HS biosynthetic enzyme (2-*O*-sulfotransferase) results in enhanced binding of three HP-binding proteins, L-selectin, IL-8, and MIP-2 (Axelsson et al. 2012), as a result of enhanced *N*- and 6-*O*-sulfation.

HA has an important role in the regulation of the immune response, as it also participates in inflammatory mechanisms (Dicker et al. 2014). Even though HA was first considered a space filling substance with a high capacity to associate with water molecules to maintain a hydrated structure, the accumulation of HA has been associated to several inflammatory conditions such as rheumatoid arthritis and inflammatory liver disease (Petrey and de la Motte 2014). Moreover, HA turnover is perturbed during inflammation, and HA fragments produced by the action of hyaluronidases accumulate extracellularly. These fragments are associated with propagating the inflammatory response, as they are involved in a number of signaling events including cellular proliferation, migration, differentiation, angiogenesis, and leukocyte trafficking (Dicker et al. 2014). On the contrary, full-length high Mw HA is associated with the resolution of inflammation. Cartilages are rich in HA, and its degradation produces its vulnerability. While all immune cells express the main HA receptor, CD44, not many bind HA under homeostatic conditions. However, this changes when immune cells become activated.

One procedure for osteoarthritis involves the intra-articular injection of HA. This practice contributes to the restoration of joints by improving the lubrication and the rheological properties of synovial fluid. Materials obtained by chemical modification of HS are expected to be more stable, and many strategies have been developed to provide finely tuned materials (Jia and Kiick 2009). The mechanic and chemical

properties and stability of the scaffolds have been improved by chemical modification by a variety of covalently linked residues, for example, adipic acid hydrazide, tyramide, benzyl esters, glycidyl methacrylate, thiopropionyl hydrazide, or bromoacetate, either at the carboxylic acid of the glucuronic residue or at the C-6 hydroxyl group of the *N*-acetylglucosamine (Bonafe et al. 2014). Modification of the HS chain by hexadecyl (C-16) side chains through amide bonds at 1–3 mol% degree of substitution of repeating units, led to hydrogels, which are stable at very low concentrations (0.3% w/v) (Finelli et al. 2009). Materials derived from HS that have hydrogels properties are particularly interesting for their physical properties and biocompatibility. In another approach, HA has been also covalently linked to the glucocorticoid dexamethasone (DEX), which is usually used to treat rheumatic problems. The release of the drug is gradual, and it was shown in culturing macrophages that this gel diminishes the production of inflammatory cytokines, possibly through the synergistic actions of HA and the released DEX (Xiao et al. 2013). This material has promising properties for the treatment of osteoarthritis. Still, the use of these modified materials is controversial, considering the complexity of the varied roles of HA in pathologies such as inflammatory process and cancer.

One of the most effective clinical uses of GAGs is their use in patients having interstitial cystitis, a chronic bladder disease originated by the disruption of the urothelium GAG layer associated to alterations in the bladder wall permeability. The weekly topic administration of Mw HA (Cystistat™), low Mw HA (Hyacyst™), and CS (Gepan™) improves the patient's functional capacity, as the urothelium is repaired by replacing lost proteoglycans (Kallestrup et al. 2005; Nickel et al. 2010).

7 Skin and Cosmetics

HA is the predominant GAG in the skin. Thanks to its remarkable property to retain water molecules, it is responsible to maintain a correct level of hydration of the skin and its characteristic elastic tone (Kroma et al. 2012). HA turnover is highly dynamic, being its half-life of less than a day in the skin (Papakonstantinou et al. 2012), while in the circulation it is 3–5 min. Among the many proteins that bind to HA (Li et al. 2013), collagen is the most important related to the appearance of the skin. On the other hand, the HA receptor CD44 is constitutively expressed on cells in the skin and seems to be essential to HA retention in the skin (Rilla et al. 2008). External harmful factors, in addition to the normal aging processes (which are mainly governed by hormonal changes), cause the loss of moisture of the skin, as a result of HA break (Vuillermoz et al. 2005). Thus, a progressive deterioration of its functional properties arises, a process which is traduced in coarsening of the skin and wrinkles. On the other hand, HA plays an important role in wound healing (Salbach et al. 2012), as elevated levels are found in the initial stages of reparation process (Weigel et al. 1986; Stern and Maibach 2008). By exposure to the UV light from the sun, the HA levels are strongly affected (Bernstein et al. 1996), and the reaction of the skin to repeated expositions is similar to a typical wound healing response.

To restore the moisture content of the skin, the levels of HA chains should be raised as well as the time it remains in the skin. It would be desirable also to preserve all the HA-binding proteins at appropriate levels, as they contribute to the skin properties. In the cosmetic field several approaches have been attained for this objective, as part of “rejuvenation” techniques (Beasley et al. 2009). This approach has been used since the 1990s when many patents on the cosmetic use of HA and derivatives appeared. In fact, nowadays, there is a huge variety of skin moisturizing facial creams containing HA in the market, many of them in gel presentations for topic uses. High molecular weight HS components are expected to be more biocompatible as mimetics of natural HS present in the skin. Nevertheless, HA fragments can penetrate easier than polymeric HA and also seem to have positive effects, even though they are not retained in the extracellular compartments of skin.

On the other hand, the application of tissue fillers as HA or collagen injections, used alone or in combination with other active principles, is nowadays a procedure currently available under a minimum medical survey. There are many injectable products in the market based on HA to correct wrinkles, especially for nasolabial folds.

As the effect is temporary (usually less than 12 months in the case of the tissue fillers), many formulations have been proposed in an attempt to obtain products with increased residence times, either for topical cosmetic creams or tissue fillers. They include the preparation of partially depolymerized GAGs gold or silver salts (Flores Salgado et al. 2013), the combination of HS with liposomes to facilitate the passage through the skin (Scott 1988), the modification by esterification of HS to increase biodisponibility (Della Valle and Romeo 1989), the preparation of HS covalently attached to phospholipids (Turley 2010), etc.

8 Tissue Engineering: Cross-Linked GAGs for Biomedical Applications

Cross-linked products obtained from GAGs are promising materials for biomedical applications, given their consistencies, their tendency to form hydrogels, and their biocompatibility. We summarize here some of the more recent reports on this approach.

A hydrogel biomaterial combining elastin/collagen and GAGs has been developed against the degeneration of the intervertebral discs, a process that leads to pain and temporary or permanent disability. The material has been obtained by cross-linking of both molecules. Carboxyl groups from HA or CS were activated by a water-soluble carbodiimide and conjugated to primary amines. A cross-linking agent as a succinimide derivative was used. A second cross-linking was performed using phenolic compounds to afford the final product (Simionescu and Mercuri 2016).

In another approach, a hydrogel was prepared by lyophilization of a collagen–GAG suspension in order to obtain a homogeneous porous scaffold to facilitate osteoblast differentiation and matrix mineralization (Murphy et al. 2016; Ren et al.

2016). Largest pore sizes (325 μm) improved cell infiltration; however, the authors suggested that optimal scaffold pore size for successful bone tissue engineering can be cell-type specific. In addition, the combination of these hydrogels and the growth factor BMP-9 stimulates chondrocytic and steogenic differentiation of primary human mesenchymal stem cells. By a similar procedure, fibrin has been incorporated to collagen–GAG hydrogels, enhancing the mechanical stability of the biomaterial (Brougham et al. 2015).

Radical polymerization has been used for the construction of CS cross-linked hydrogels. Methacrylated CS (prepared by reaction of carboxylic groups with glycidyl methacrylate) was photocopolymerized with oligoethylenglycol diacrylates. Copolymerization with a low MW comonomer improved the cross-linking effectiveness, reducing the swelling without impacting on the fracture strain (Khanlari et al. 2013, 2015a, b). The strategy has been extended to HA hydrogels (Khanlari et al. 2015c). These materials would be useful for biomedical applications.

Recently, hydrogels were obtained by coupling photo-cross-linkable methacrylated HA with selected cartilaginous molecules of the extracellular matrix including CS and type I collagen. The effect of this material in the regulation of initial chondrogenesis, subsequent hypertrophy, and tissue mineralization was studied in human mesenchymal stem cells. The results would help on the application of these hybrid hydrogels in the repair of different musculoskeletal defects (Zhu et al. 2016). Photo-cross-linked hyaluronan hydrogels were also investigated for use in a layered, synthetic, tissue-engineered heart valve (Puperi et al. 2016).

Biohybrid hydrogels were prepared by reacting the carbodiimide/*N*-hydroxysulfosuccinimide -activated carboxylic acid group of desulfated HP with amine-functionalized four-armed (star-shaped) poly(ethylene glycol) and applied for sustainable administration of various therapeutically relevant growth factors. The formation of network structures is related to the degree of sulfation (Zieris et al. 2014). Indeed, this Star-PEG HP showed that HP desulfation modulates VEGF release and angiogenesis in diabetic wounds (Freudenberget al. 2015).

A mixture of sulfated GAGs and HA was obtained by extraction from the extracellular matrix of Wharton's jelly and its biocompatibility was confirmed, as they do not cause cytotoxicity, hemolysis, or an inflammatory response. The material was cross-linked using divinylsulfone or 1,4-butanediol diglycidyl ether to give hydrogels. These scaffolds were combined with adipose mesenchymal stem cells or fibroblasts for application to chondral or dermal defects, respectively. The results showed that these scaffolds are promising candidates for use in regenerative medicine (Herrero-Mendez et al. 2015).

9 Other Applications

The isolation and use of ECM from several sources have been patented for their use in several medical conditions. Some of the them include small intestine mucosa (Badylak et al. 1994), urinary bladder submucosa (Badylak et al. 1995), stomach

submucosa (Badylak et al. 1997), and liver basement membrane (Badylak 1997). Decellularized extracellular matrix materials have been shown to be effective for treating and preventing cardiac arrhythmia after heart surgery or myocardial infarction (Matheny 2015). The ECM can be produced *in vitro* using mammalian cells of extracted from mammalian tissues. This treatment inhibits scar formation, promotes the regeneration of damaged tissue, and reduces inflammation. There are several products in the market, for example, CorMatrix ECM™, which is described as “a naturally occurring bioscaffold that remodels over time into organized, healthy tissue.” It is indicated as an intracardiac repair device for tissue repair or reconstruction of peripheral vasculature including the carotid, renal, iliac, femoral, and tibial blood vessels. AlloDerm® is also an acellular tissue matrix isolated from the skin. Since its introduction to dentistry in 1997, AlloDerm Regenerative Tissue Matrix has been a widely accepted acellular dermal matrix for soft tissue applications. AlloDerm supports tissue regeneration by allowing rapid revascularization, white cell migration, and cell population – ultimately being transformed into host tissue for a strong, natural repair.

The administration of GAGs for the treatment of focal segmental glomerulosclerosis, a kidney disorder involving formation of scar tissue in some of the glomeruli, has also been reported (Spero et al. 2005).

Sulodexide is marketed in Europe under the trademark Vessel Due F® and is prescribed for the treatment of vascular pathologies with thrombotic risk such as peripheral occlusive arterial disease, healing of venous leg ulcers, and intermittent claudication. Sulodexide is a mixture of low molecular weight HP (80%) and DS (20%) (Harenberg 1998; Crepaldi et al. 1990). Marchi and Tamagnone (1994) patented a method of treatment of diabetic nephropathy by the administration of sulodexide.

10 Conclusions

Due to their widely biochemical interactions, GAGs have been found to have multiple applications in the medical, veterinary, pharmaceutical, and cosmetic fields as hydrating agents, anticancer and anti-inflammatory agents, antibacterial and antiviral drugs, and constituents of nanocarriers and a variety of biocompatible materials. A variety of GAG-derived products are nowadays in the market for the treatment of inflammatory conditions and as constituents of cosmetic products, among others. Their ability to bind a diversity of extracellular proteins and receptors is also a drawback to target very specific interactions. Some progress has been made by the incorporation of GAGs in adequate formulations or by modification of natural polysaccharide chains. The use of synthetic or semisynthetic analogs can also be useful to reduce or even eliminate undesirable effects. For these reasons, the study of GAGs and their biochemical properties is still a fascinating open field requiring further research for the development of finely tuned natural-based chemotherapeutic products.

References

- Afratis NA, Gialeli C, Nikitovic D, Tsegenidis T, Karousou E, Theocharis AD, Pavao MS, Tzanakakis GN, Karamanos NK (2012) Glycosaminoglycans: key players in cancer cell biology and treatment. *FEBS J* 279:1177–1197
- Afratis NA, Karamanos NK, Piperigkou Z, Vynios DH, Theocharis AD (2016) The role of heparins and nano-heparins as therapeutic tool in breast cancer. *Glycoconj J*. 2016. doi:[10.1007/s10719-016-9742-7](https://doi.org/10.1007/s10719-016-9742-7)
- Ahmad S, Ansari AA (2011) Therapeutic roles of heparin anticoagulants in cancer and related disorders. *Med Chem* 7:504–517
- Aimi T, Suzuki K, Hoshino T, Mizushima T (2015) Dextran sulfate sodium inhibits amyloid- β oligomer binding to cellular prion protein. *J Neurochem* 134:611–617
- Aquino SA, Park PW (2010) Diverse functions of glycosaminoglycans in infectious diseases. *Prog Mol Biol Transl Sci* 93:373–394
- Aquino SA, Park PW (2016) Glycosaminoglycans and infection. *Front Biosci (Landmark Ed)* 21:1260–1277
- Arevalo MT, Simpson-Haidaris PJ, Jin X, Chen H, Quinn MH (2011) Compositions and methods for inhibition of or treatment of dengue virus infection. *PCT Int Appl WO* 2011153458
- Axelsson J, Xu D, Kang BN, Nussbacher JK, Handel TM, Ley K, Sriramarao P, Esko JD (2012) Inactivation of heparan sulfate 2-O-sulfotransferase accentuates neutrophil infiltration during acute inflammation in mice. *Blood* 120:1742–1751
- Bachar G, Cohen K, Hod R, Feinmesser R, Mizrachi A, Shpitzer T, Katz O, Peer D (2011) Hyaluronan-grafted particle clusters loaded with mitomycin C as selective nanovectors for primary head and neck cancers. *Biomaterials* 32:4840–4848
- Badylak SF (1997) Biomaterial derived from vertebrate liver tissue. US Patent 6,379,710
- Badylak SF, Demeter RJ, Hiles M, Voytik SL, Knapp PM Jr (1994) Fluidized intestinal submucosa and its use as an injectable tissue graft. US Patent 5,275,826 A
- Badylak SF, Voytik SL, Brightman A, Waninger M (1995) Urinary bladder submucosa derived tissue graft. US Patent 5,554,389
- Badylak SF, Voytik-Harbin SL, Brightman AO, Tullius RS (1997) Stomach submucosa derived tissue graft. US Patent 6,099,567
- Barrowcliffe TJ (2012) History of heparin. *Handb Exp Pharmacol* 207:3–22
- Basappa, Rangappa KS, Sugahara K (2014) Roles of glycosaminoglycans and glycanmimetics in tumor progression and metastasis. *Glycoconj J* 31:461–467
- Beasley KL, Weiss M, Weiss RA (2009) Hyaluronic acid fillers: a comprehensive review. *Facial Plast Surg* 25:86–94
- Bedini E, Parrilli M (2012) Synthetic and semi-synthetic chondroitin sulfate oligosaccharides, polysaccharides, and glycomimetics. *Carbohydr Res* 356:75–85
- Belting M (2014) Glycosaminoglycans in cancer treatment. *Thromb Res* 133:S95–S101
- Benitez A, Yates TJ, Lopez LE, Cerwinka WH, Bakkar A, Lokeshwar VB (2011) Targeting hyaluronidase for cancer therapy: antitumor activity of sulfated hyaluronic acid in prostate cancer cells. *Cancer Res* 71:4085–4095
- Bernstein EF, Underhill CB, Hahn PJ, Brown DB, Uitto J (1996) Chronic sun exposure alters both the content and distribution of dermal glycosaminoglycans. *Br J Dermatol* 135:255–262
- Boeriu CG, Springer J, Kooy FK, van den Broek LAM, Eggink G (2013) Production methods for hyaluronan. *Int J Carbohydr Chem*. Article ID 624967 2013:14
- Bonafe F, Govoni M, Giordano E, Caldara C, Guarnieri C, Muscari C (2014) Hyaluronan and cardiac regeneration. *J Biomed Sci* 21:100. 13 pp
- Borsig L, Vlodavsky I, Ishai-Michaeli R, Torri G, Vismara E (2011) Sulfated hexasaccharides attenuate metastasis by inhibition of P-selectin and heparanase. *Neoplasia* 13:445–452
- Bottegoni C, Muzzarelli RAA, Giovannini F, Busilacchi A, Gigante A (2014) Oral chondroprotection with nutraceuticals made of chondroitin sulphate plus glucosamine sulphate in osteoarthritis. *Carbohydr Polym* 109:126–138

- Brougham CM, Levingstone TJ, Jockenhoevel S, Flanagan TC, O'Brien FJ (2015) Incorporation of fibrin into a collagen–glycosaminoglycan matrix results in a scaffold with improved mechanical properties and enhanced capacity to resist cell-mediated contraction. *Acta Biomater* 26:205–214
- Cagno V, Donalisio M, Civra A, Volante M, Veccelli E, Oreste P, Rusnati M, Lembo D (2014) Highly sulfated K5 *Escherichia coli* polysaccharide derivatives inhibit respiratory syncytial virus infectivity in cell lines and human tracheal-bronchial histocultures. *Antimicrob Agents Chemother* 58:4782–4794
- Campion C, Pini APJ, Gogoi RN, Gilthorpe J (2012) Sulfated oligosaccharides for use in treatment of neurodegenerative diseases. PCT Int Appl WO 2012/160337
- Capila I, Linhardt RJ (2002) Heparin-protein interactions. *Angew Chem Int Ed Eng* 41:390–412
- Cayre Y, Allouche R (2017) Produit pour lutter contre la prolifération des cellules cancéreuse. Fr Demande FR 3039065
- Chang P-h (2014) Pharmaceutical formulation containing glycosaminoglycan. PCT Int Appl WO 2014142938, PCT Int Appl WO 2014143085
- Cheng G, Cao B (2015) Zwitterionic polysaccharide polymers having antifouling, antimicrobial and optical transparency properties. PCT Int Appl WO 2015057645 A1
- Conrad HE (ed) (1998) Heparin-binding proteins. Academic, San Diego
- Coombe DR, Kett WC (2005) Heparan sulfate-protein interactions: therapeutic potential through structure-function insights. *Cell Mol Life Sci* 62:410–424
- Coppa GV, Facinelli B, Magi G, Marini E, Zampini L, Mantovani V, Galeazzi T, Padella L, Marchesiello RL, Santoro L, Coscia A, Peila C, Volpi N, Gabrielli O (2016) Human milk glycosaminoglycans inhibit in vitro the adhesion of *Escherichia coli* and *Salmonella typhi* to human intestinal cells. *Pediatr Res* 79:603–607
- Cordo Russo RI, García MG, Alaniz L, Blanco G, Alvarez E, Hajos SE (2008) Hyaluronan oligosaccharides sensitize lymphoma resistant cell lines to vincristine by modulating P-glycoprotein activity and PI3K/Akt pathway. *Int J Cancer* 122:1012–1018
- Crepaldi G, Fellin R, Calabrò A, Rossi A, Ventura A, Mannarino E, Senin U, Ciuffetti G, Descovich GC, Gaddi A, Rimondi S, Pozza G, Vicari A, Carandente O, Mancini M, Rubba P, Postiglione A, Strano A, Avellone G, Davì G, Novo S, Pinto A, Capurso A, Resta F, Mogavero AM, Bucci A, Antonini R, Lalloni L (1990) Double-blind multicenter trial on a new medium molecular weight glycosaminoglycan current therapeutic effects and perspectives for clinical use. *Atherosclerosis* 81:233–243
- Cruz L, Meyers C (2013) Differential dependence on host cell glycosaminoglycans for infection of epithelial cells by high-risk HPV types. *PLoS One* 8:e68379
- Da Costa Dias B, Jovanovic K, Gonsalves D, Weiss SFT (2011) Structural and mechanistic commonalities of amyloid- β and the prion protein. *Prion* 5:126–137
- Davis DAS, Parish CR (2013) Heparan sulfate: a ubiquitous glycosaminoglycan with multiple roles in immunity. *Front Immunol* 4:470. 7 pp
- De Vita D, Giordano S (2012) Effectiveness of intravesical hyaluronic acid/chondroitin sulfate in recurrent bacterial cystitis: a randomized study. *Int Urogynecol J* 23:1707–1713
- DeAngelis PL, Lane RS (2016) Heparosan/therapeutic prodrug complexes and methods of making and using same. WO 2016/065309
- DeAngelis PL, Liu J, Linhardt RJ (2013) Chemoenzymatic synthesis of glycosaminoglycans: re-creating, re-modeling and re-designing nature's longest or most complex carbohydrate chains. *Glycobiology* 23:764–777
- Della Valle F, Romeo A (1989) Esters of hyaluronic acid. US Patent 4,851,521
- Dicker KT, Gurski LA, Pradhan-Bhatt S, Witt RL, Farach-Carson MC, Jia X (2014) Hyaluronan: a simple polysaccharide with diverse biological functions. *Acta Biomater* 10:1558–1570
- Eklund E, Ekman-Ordeberg G, Malmstrom A (2013) Treatment of cytokine mediated conditions. Can Pat Appl CA 2779838
- Esko JD (2001) Special considerations for proteoglycans and glycosaminoglycans and their purification. *Curr Protoc Mol Biol* 17:17.2.1–17.2.9

- Fabricius H-A (2015) Sulfated polysaccharides for use in the treatment of cancer. PCT Int Appl WO 2015/059177
- Finelli I, Chiessi E, Galesso D, Renier D, Paradossi G (2009) Gel-like structure of a hexadecyl derivative of hyaluronic acid for the treatment of osteoarthritis. *Macromol Biosci* 9:646–653
- Fitton H, Gardiner V (2011) Anti-viral formulations. PCT Int Appl WO 2011/100805
- Flores Salgado F, Benítez Jimenez AF, Costa Rierola M, Flores Costa R, Flores Costa L (2013) Partially depolymerized glycosaminoglycan silver and gold salts. PCT Int Appl WO 2013/121001
- Freundenberg U, Zieris A, Chwalek K, Tsurkan MV, Maitz MF, Atallah P, Levental KR, Eming SA, Werner C (2015) Heparin desulfation modulates VEGF release and angiogenesis in diabetic wounds. *J Control Release* 220(Part A):79–88
- Fu L, Suflita M, Linhardt RJ (2016) Bioengineered heparins and heparan sulfates. *Adv Drug Deliv Rev* 97:237–249
- Fukuda T, Matsumoto E, Miura Y (2015) Interaction between multimeric sulfated saccharides and Alzheimer amyloid β (1–42). *Chem Lett* 44:1482–1484
- Funderburgh JL (2000) Keratan sulfate: structure, biosynthesis, and function. *Glycobiology* 10:951–958
- Fux L, Ilan N, Sanderson RD, Vlodaysky I (2009) Heparanase: busy at the cell surface. *Trends Biochem Sci* 34:511–519
- Galus A, Mallet J-M, Lembo D, Cagno V, Djabourov M, Lortat-Jacob H, Bouchemal K (2016) Hexagonal-shaped chondroitin sulfate self-assemblies have exalted anti-HSV-2 activity. *Carbohydr Polym* 136:113–120
- García B, Merayo-Llodes J, Martín C, Alcalde I, Quirós LM, Vazquez F (2016) Surface proteoglycans as mediators in bacterial pathogens infections. *Front Microbiol* 7:220. 11 pp
- Genco T, Zemljič LF, Bračić M, Stana-Kleinschek K, Heinze T (2012) Physicochemical properties and bioactivity of a novel class of cellulose: 6-deoxy-6-amino cellulose sulfate. *Macromol Chem Phys* 213:539–548
- Gilbert TW, Sellaro TL, Badylak SF (2006) Decellularization of tissues and organs. *Biomaterials* 27:3675–3683
- Gomes AM, Stelling MP, Pavão MSG (2013, 2013) Heparan sulfate and heparanase as modulators of breast cancer progression. *BioMed Res Int*:852093. 11 pp
- Gomes AM, Kozłowski EO, Borsig L, Teixeira FCOB, Vlodaysky I, Pavão MSG (2015) Antitumor properties of a new non-anticoagulant heparin analog from the mollusk *Nodidipeten nodosus*: effect on P-selectin, heparanase, metastasis and cellular recruitment. *Glycobiology* 25:386–393
- Gray E, Hogwood J, Mulloy B (2012) The anticoagulant and antithrombotic mechanisms of heparin. *Handb Exp Pharmacol* 207:43–61
- Grohmann S, Hildebrand G, Liefeth K (2014) Active substance-loaded biocompatible polyelectrolyte multilayers based on sulfated glycosaminoglycans, methods for producing the multilayers, and use of the multilayers. PCT Int Appl WO 2014/147080; Ger Offen DE 102013204742
- Harenberg J (1998) Review of pharmacodynamics, pharmacokinetics, and therapeutic properties of sulodexide. *Med Res Rev* 18:1–20
- Hendricks GL, Velazquez L, Pham S, Qaisar N, Delaney JC, Viswanathan K, Albers L, Comolli JC, Shriver Z, Knipe DM, Kurt-Jones EA, Fyngson DK, Trevejo JM, Wang JP, Finberg RW (2015) Heparin octasaccharide decoy liposomes inhibit replication of multiple viruses. *Antivir Res* 116:34–44
- Herrero LJ, Foo S-S, Sheng K-C, Chen W, Forwood MR, Bucala R, Mahalingam S (2015) Pentosan polysulfate: a novel glycosaminoglycan-like molecule for the effective treatment of alphavirus-induced cartilage destruction and inflammatory disease. *J Virol* 89:8063–8076
- Herrero-Mendez A, Palomares T, Castro B, Herrero J, Granado MH, Bejar JM, Alonso-Varona A (2015) HR007: a family of biomaterials based on glycosaminoglycans for tissue repair. *J Tissue Eng Regen Med*. doi:[10.1002/term.1998](https://doi.org/10.1002/term.1998)
- Hidari KI, Abe T, Suzuki T (2013) Carbohydrate-related inhibitors of dengue virus entry. *Viruses* 5:605–618

- Hoshiba T, Chen G, Endo C, Maruyama H, Wakui M, Nemoto E, Kawazoe N, Tanaka M (2016) Decellularized extracellular matrix as an in vitro model to study the comprehensive roles of the ECM in stem cell differentiation. *Stem Cells Int*. Article ID 6397820, 10 pp
- Huang Y, Yao X, Zhang R, Ouyang L, Jiang R, Liu X, Song C, Zhang G, Fan Q, Wang L, Huang W (2014) Cationic conjugated polymer/fluoresceinamine-hyaluronan complex for sensitive fluorescence detection of CD44 and tumor-targeted cell imaging. *ACS Appl Mater Interfaces* 6:19144–19153
- Jia X, Kiick KL (2009) Hybrid multicomponent hydrogels for tissue engineering. *Macromol Biosci* 9:140–156
- Jinno-Oue A, Tanaka A, Shimizu N, Mori T, Sugiura N, Kimata K, Isomura H, Hoshino H (2013) Inhibitory effect of chondroitin sulfate type E on the binding step of human T-cell leukemia virus type 1. *AIDS Res Hum Retrovir* 29:621–629
- Kallestrup E, Jørgensen S, Nordling J, Hald T (2005) Treatment of interstitial cystitis with Cystistat®, a hyaluronic acid product. *Scand J Urol Nephrol* 39:143–147
- Kavasi RM, Berdiaki A, Spyridaki I, Corsini E, Tsatsakis A, Tzanakakis G, Nikitovic D (2017) HA metabolism in skin homeostasis and inflammatory disease. *Food Chem Toxicol* 101:128–138
- Keane TJ, Swinehart IT, Badylak SF (2015) Methods of tissue decellularization used for preparation of biologic scaffolds and in vivo relevance. *Methods* 84:25–34
- Khaderi K (2014) Compositions and methods for treating injuries to the visual system of a human. US Patent 0,212,404 A1
- Khanlari A, Detamore MS, Gehrke SH (2013) Increasing cross-linking efficiency of methacrylated chondroitin sulfate hydrogels by copolymerization with oligo(ethylene glycol) diacrylates. *Macromolecules* 46:9609–9617
- Khanlari A, Suekama TC, Gehrke SH (2015a) Structurally versatile glycosaminoglycan hydrogels for biomedical applications. *Macromol Symp* 358:67–77
- Khanlari A, Suekama TC, Detamore MS, Gehrke SH (2015b) Structurally diverse and readily tunable photocrosslinked chondroitin sulfate based copolymers. *J Polym Sci Part B Polym Phys* 53:1070–1079
- Khanlari A, Schulteis JE, Suekama TC, Detamore MS, Gehrke SH (2015c) Designing crosslinked hyaluronic acid hydrogels with tunable mechanical properties for biomedical applications. *J Appl Polym Sci* 132. doi:[10.1002/APP.42009](https://doi.org/10.1002/APP.42009)
- Kim E, Okumura M, Sawa H, Miyazaki T, Fujikura D, Yamada S, Sugahara K, Sasaki M, Kimura T (2011) Paradoxical effects of chondroitin sulfate-E on Japanese encephalitis viral infection. *Biochem Biophys Res Commun* 409:717–722
- Kim S-H, Turnbull J, Guimond SJ (2011) Extracellular matrix and cell signalling: the dynamic cooperation of integrin, proteoglycan and growth factor receptor. *Endocrinology* 209:139–151
- Kirn-Safran CB, D'Souza SS, Carson DD (2008) Heparan sulfate proteoglycans and their binding proteins in embryo implantation and placentation. *Semin Cell Dev Biol* 19:187–193
- Kobayashi F, Yamada S, Taguwa S, Kataoka C, Naito S, Hama Y, Tani H, Matsuura Y, Sugahara K (2012) Specific interaction of the envelope glycoproteins E1 and E2 with liver heparan sulfate involved in the tissue tropism infection by hepatitis C virus. *Glycoconj J* 29:211–220
- Kozlowski EO, Pavao MSG (2011) Effect of sulfated glycosaminoglycans on tumor invasion and metastasis. *Front Biosci Sch Ed* S3:1541–1551
- Kozlowski EO, Pavao MSG, Borsig L (2011) Ascidian dermatan sulfates attenuate metastasis, inflammation and thrombosis by inhibition of P-selectin. *J Thromb Haemost* 9:1807–1815
- Krichen F, Volpi N, Sila A, Maccari F, Mantovani V, Galeotti F, Ellouz-Chaabouni S, Bougateg A (2017) Purification, structural characterization and antiproliferative properties of chondroitin sulfate/dermatan sulfate from tunisian fish skins. *Int J Biol Macromol* 95:32–39
- Kroma A, Feliczak-Guzik A, Nowak I (2012) The use of glycosaminoglycans in cosmetic products. *Chemik* 66:136–139
- Kwok JCF, Warren P, Fawcett JW (2012) Chondroitin sulfate: a key molecule in the brain matrix. *Int J Biochem Cell Biol* 44:582–586
- Ladet S (2013) Multilayer implants for delivery of therapeutic agents. PCT Int Appl WO 2013046057

- Lee EC, Davis-Poynter N, Nguyen CTH, Peters AA, Monteith GR, Strounina E, Popat A, Ross BP (2016) GAG mimetic functionalised solid and mesoporous silica nanoparticles as viral entry inhibitors of herpes simplex type 1 and type 2 viruses. *Nanoscale* 8:16192–16196
- Lee-Sayer SSM, Dong Y, Arif AA, Olsson M, Brown KL, Johnson P (2015) The where, when, how, and why of hyaluronan binding by immune cells. *Front Immunol* 6:150
- Ley K, Cerrito M, Arfors KE (1991) Sulfated polysaccharides inhibit leukocyte rolling in rabbit mesentery venules. *Am J Phys* 260:1667–1673
- Li Y, Liu Y, Xia W, Lei D, Voorhees JJ, Fisher GJ (2013) Age-dependent alterations of decorin glycosaminoglycans in human skin. *Sci Rep* 3:2422. 8 pp
- Lian W, Wu M, Huang N, Gao N, Xiao C, Li Z, Zhang Z, Zheng Y, Peng W, Zhao J (2013) Anti-HIV-1 activity and structure-activity-relationship study of a fucosylated glycosaminoglycan from an echinoderm by targeting the conserved CD4 induced epitope. *Biochim Biophys Acta* 1830:4681–4691
- Liang Y, Kiick KL (2014) Heparin-functionalized polymeric biomaterials in tissue engineering and drug delivery applications. *Acta Biomater* 10:1588–1600
- Liaw PC, Becker DL, Stafford AR, Fredenburgh JC, Weitz JI (2001) Molecular basis for the susceptibility of fibrin-bound thrombin to inactivation by heparin cofactor II in the presence of dermatan sulfate but not heparin. *J Biol Chem* 276:20959–20965
- Lin H-Y (2015) Compound of glycosaminoglycan, preparation method and use thereof. PCT Int Appl WO 2015/028172 A1; US Patent Appl Publ US 20150065446
- Liu L, Liu Y, Li J, Du G, Chen J (2011) Microbial production of hyaluronic acid: current state, challenges, and perspectives. *Microb Cell Factories* 10:99–108
- Liu C-C, Zhao N, Kanekiyo T, Yamaguchi Y, Cirrito JR, Holtzman DM, Bu G (2016) Neuronal heparan sulfates promote amyloid pathology by modulating brain amyloid- β clearance and aggregation in Alzheimer's disease. *Sci Transl Med* 8:332ra44
- Lomparđía SL, Díaz M, Papademetrio DL, Mascaró M, Pibuel M, Álvarez E, Hajos SE (2016) Hyaluronan oligomers sensitize chronic myeloid leukemia cell lines to the effect of Imatinib. *Glycobiology* 26:343–352
- Lundin A, Bergström T, Andrighetti-Fröhner CR, Bendrioua L, Ferro V, Trybala E (2012) Potent anti-respiratory syncytial virus activity of a cholesterol-sulfated tetrasaccharide conjugate. *Antivir Res* 93:101–109
- Manveen K, Sethi MK, Zaia J (2017) Extracellular matrix proteomics in schizophrenia and Alzheimer's disease. *Anal Bioanal Chem* 409:379–394
- Marchi E, Tamagnone G (1994) Method of treatment of diabetic nephropathy by means of sulfoxide of medicines containing it. US Patent 5,496,807
- Martín R, Martín C, Escobedo S, Suárez JE, Quirós LM (2013) Surface glycosaminoglycans mediate adherence between HeLa cells and lactobacillus salivarius Lv72. *BMC Microbiol* 13:210. 11 pp
- Martinez P, Vergoten G, Colomb F, Bobowski M, Steenackers A, Carpentier M, Allain F, Delannoy P, Julien S (2013) Over-sulfated glycosaminoglycans are alternative selectin ligands: insights into molecular interactions and possible role in breast cancer metastasis. *Clin Exp Metastasis* 30:919–931
- Matheny RG (2015) Compositions and methods for preventing cardiac arrhythmia. US Patent 2015/0164959 A1
- Mathieu C, Dhondt KP, Chalons M, Mely S, Raoul H, Negre D, Cosset F-L, Gerlier D, Vives RR, Horvat B (2015) Heparan sulfate-dependent enhancement of henipavirus infection. *MBio* 6:1–10
- Memi E, Karakiulakis G, Goma F, Papakonstantinou E (2012) The functional role of glycosaminoglycans in the pathophysiology of the thyroid gland and their putative role as prognostic, diagnostic and therapeutic agents in thyroid pathologies. *Rev Clin Pharmacol Pharmacokinet Int Ed* 26:61–86
- Mikami T, Kitagawa H (2013) Biosynthesis and function of chondroitin sulfate. *Biochim Biophys Acta Gen Subj* 1830:4719–4733
- Misra S, Hascall VC, Markwald RR, Ghatak S (2015) Interactions between hyaluronan and its receptors (CD44, RHAMM) regulate the activities of inflammation and cancer. *Front Immunol* 6:201. 31 pp

- Mizumoto S, Sugahara (2013) Glycosaminoglycans are functional ligands for receptor for advanced glycation end-products in tumors. *FEBS J* 280:2462–2470
- Mizumoto S, Takahashi J, Sugahara K (2012) Receptor for advanced glycation end products (RAGE) functions as receptor for specific sulfated glycosaminoglycans, and anti-RAGE antibody or sulfated glycosaminoglycans delivered in vivo inhibit pulmonary metastasis of tumor cells. *J Biol Chem* 287:18985–18994
- Monfort J, Pelletier J-P, Garcia-Giralto N, Martel-Pelletier J (2008) Biochemical basis of the effect of chondroitin sulphate on osteoarthritis articular tissues. *Ann Rheum Dis* 67:735–740
- Mousa SA (2015) Composition and method for sulfated non-anticoagulant low molecular weight heparins in cancer and tumor metastasis. US Patent Appl Publ US 20150132399
- Mousa SA (2016) Composition and method of use for combinations of anti-viral protease, polymerase inhibitors and natural bioactive compounds in the treatment of hepatitis C infection. US Patent Appl Publ US20160346308 A1
- Murphy CM, Duffy GP, Schindeler A, O'Brien FJ (2016) Effect of collagen-glycosaminoglycan scaffold pore size on matrix mineralization and cellular behavior in different cell types. *J Biomed Mater Res Part A* 104:291–304
- Nakano T, Betti M, Pietrasik Z (2010) Extraction, isolation and analysis of chondroitin sulfate glycosaminoglycans. *Recent Pat Food Nutr Agric* 2:61–74
- Nickel JC, Egerdie RB, Steinhoff G, Palmer B, Hanno P (2010) A multicenter, randomized, double-blind, parallel group pilot evaluation of the efficacy and safety of intravesical sodium chondroitin sulfate versus vehicle control in patients with interstitial cystitis/painful bladder syndrome. *Urology* 76:804–809
- Nikitovic D, Chatzinikolaou G, Tsiaoussis J, Tsatsakis A, Karamanos NK, Tzanakakis GN (2012) Insights into targeting colon cancer cell fate at the level of proteoglycans/glycosaminoglycans. *Curr Med Chem* 19:4247–4258
- Nishimura Y, Shudo H, Seto H, Hoshino Y, Miura Y (2013) Syntheses of sulfated glycopolymers and analyses of their BACE-1 inhibitory activity. *Bioorg Med Chem Lett* 23:6390–6395
- Nugent MA (2000) Heparin sequencing brings structure to the function of complex oligosaccharides. *Proc Natl Acad Sci U S A* 97:10301–10303
- O'Hearn A, Wang M, Cheng H, Lear-Rooney CM, Koning K, Rumschlag-Booms E, Varhegyi E, Olinger G, Rong L (2015) Role of EXT1 and glycosaminoglycans in the early stage of filovirus entry. *J Virol* 89:5441–5449
- Papakonstantinou E, Roth M, Karakioulakis G (2012) Hyaluronic acid: a key molecule in skin aging. *Dermato-Endocrinol* 4:253–258
- Papy-Garcia D, Christophe M, Huynh MB, Sineriz F, Sissoeff L, Sepulveda-Diaz JE, Raisman-Vozari R (2011) Glycosaminoglycans, protein aggregation and neurodegeneration. *Curr Protein Pept Sci* 12:258–268
- Papy-Garcia D, Huynh MB, Soussi-Yanicostas N, Vozari R, Sineriz F, Yanicostas C (2013) Method of diagnosis, prognosis, or treatment of neurodegenerative diseases. PCT Int Appl WO 2013/053954.
- Paul TJ, Kelly H, Zuchniarz J, Ahmed T, Prabhakar R (2016) Design of heparin oligosaccharide based molecules for inhibition of Alzheimer amyloid beta (A β 40) aggregation. *Can J Chem* 94:1090–1098
- Peer D (2015) Liposomal formulations for delivery of nucleic acids. *Int Appl WO* 2015/198326
- Persson A, Tykesson E, Westergren-Thorsson G, Malmström A, Ellervik U, Mani K (2016) Xyloside-primed chondroitin sulfate/dermatan sulfate from breast carcinoma cells with a defined disaccharide composition has cytotoxic effects in vitro. *J Biol Chem* 291:14871–14882
- Petry AC, de la Motte CA (2014) Hyaluronan, a crucial regulator of inflammation. *Front Immunol* 5:101
- Pisano C, Vlodavsky I, Ilan N, Zunino F (2014) The potential of heparanase as a therapeutic target in cancer. *Biochem Pharmacol* 89:12–19
- Pomin VH (2015a) A dilemma in the glycosaminoglycan-based therapy: synthetic or naturally unique molecules? *Med Res Rev* 35:1195–1219

- Pomin VH (2015b) Sulfated glycans in inflammation. *Eur J Med Chem* 92:353–369
- Pomin VH, Mulloy B (2015) Current structural biology of the heparin interactome. *Curr Opin Struct Biol* 34:17–25
- Prestwich GD, Kennedy TP (2011) Methods for treating or preventing the spread of cancer using semi-synthetic glycosaminoglycosan ethers. *PCT Int Appl WO* 2011/094149
- Prestwich GD, Oottamasathien S, Kennedy T (2011) Applications of partially and fully sulfated hyaluronan. *PCT Int Appl WO* 2011/156445
- Prestwich GD, Oottamasathien S, Kennedy TP (2013) Applications of partially and fully sulfated hyaluronan. *US Patent Appl* 0,209,531
- Puperi DS, O'Connell RW, Punske ZE, Wu Y, West JL, Grande-Allen KJ (2016) Hyaluronan hydrogels for a biomimetic spongiosa layer of tissue engineered heart valve scaffolds. *Biomacromolecules* 17:1766–1775
- Pye DA, Ogundipe OD (2016) Pharmaceutical extracts and uses thereof. *PCT Int Appl WO* 2016/067008
- Qian W, Tao L, Wang Y, Zhang F, Li M, Huang S, Wang A, Chen W, Yue Z, Chen L, Liu Y, Huang C, Zhang L, Li Y, Lu Y (2015) Downregulation of integrins in cancer cells and anti-platelet properties are involved in holothurian glycosaminoglycan-mediated disruption of the interaction of cancer cells and platelets in hematogenous metastasis. *J Vasc Res* 52:197–209
- Radhakrishnan K, Tripathy J, Datey A, Chakravorty D, Raichur AM (2015) Mesoporous silica-chondroitin sulphate hybrid nanoparticles for targeted and bio-responsive drug delivery. *New J Chem* 39:1754–1760
- Rankin KS, Frankel D (2016) Hyaluronan in cancer – from the naked mole rat to nanoparticle therapy. *Soft Matter* 12:3841–3848
- Rawat M, Hsieh-Wilson L (2014) Glycosaminoglycan mimetics. *US Patent* 8,912,149 B1
- Reinmueller J, Dirting K (2012) Antiinfective composition. *PCT Int Appl WO* 2012/168462; *Ger Offen DE* 102011077393
- Ren X, Weisgerber DW, Bischoff D, Lewis MS, Reid RR, He T-C, Yamaguchi DT, Miller TA, Harley BAC, Lee JC (2016) Nanoparticulate mineralized collagen scaffolds and BMP-9 induce a long-term bone cartilage construct in human mesenchymal stem cells. *Adv Healthc Mater* 5:1821–1830
- Rilla K, Tiihonen R, Kultti A, Tammi M, Tammi R (2008) Pericellular hyaluronan coat visualized in live cells with a fluorescent probe is scaffolded by plasma membrane protrusions. *J Histochem Cytochem* 56:901–910
- Ritchie JP, Ramani VC, Ren Y, Naggi A, Torri G, Casu B, Penco S, Pisano C, Carminati P, Tortoreto M, Zunino F, Vlodaysky I, Sanderson RD, Yang Y (2011) SST0001, a chemically modified heparin, inhibits myeloma growth and angiogenesis via disruption of the heparanase/syndecan-1 axis. *Clin Cancer Res* 17:1382–1393
- Ronca F, Palmieri L, Panicucci P, Ronca G (1998) Anti-inflammatory activity of chondroitin sulfate. *Osteoarthritis Cartil* 6(Suppl A):14–21
- Said JS, Trybala E, Görander S, Ekblad M, Liljeqvist J-A, Jennische E, Lange S, Bergström T (2016) The cholesterol-conjugated sulfated oligosaccharide PG545 disrupts the lipid envelope of herpes simplex virus particles. *Antimicrob Agents Chemother* 60:1049–1057
- Sakiyama-Elbert SE (2014) Incorporation of heparin into biomaterials. *Acta Biomater* 10:1581–1587
- Salbach J, Rachner TD, Rauner M, Hempel U, Anderegg U, Franz S, Simon J-C, Hofbauer LC (2012) Regenerative potential of glycosaminoglycans for skin and bone. *J Mol Med* 90:625–635
- Savage JR, Pulsipher A, Rao NV, Kennedy TP, Prestwich GD, Ryan ME, Lee WY (2016) A modified glycosaminoglycan, GM-0111, inhibits molecular signaling involved in periodontitis. *PLoS One* 11:e0157310/1
- Sayari N, Balti R, Ben Mansour M, Ben Amor I, Graiet I, Gargouri J, Bougatef A (2016) Anticoagulant properties and cytotoxic effect against HCT116 human colon cell line of sulfated glycosaminoglycans isolated from the Norway lobster (*Nephrops norvegicus*) shell. *Biomed Pharmacother* 80:322–330

- Schaefer L, Schaefer RM (2010) Proteoglycans: from structural compounds to signaling molecules. *Cell Tissue Res* 339:237–246
- Schnabelrauch M, Scharnweber D, Schiller J (2013) Sulfated glycosaminoglycans as promising artificial extracellular matrix components to improve the regeneration of tissues. *J Curr Med Chem* 20:2501–2523
- Schwoerer R, Zubkova OV, Turnbull JE, Tyler PC (2013) Synthesis of a targeted library of heparan sulfate hexa- to dodecasaccharides as inhibitors of β -secretase: potential therapeutics for Alzheimer's disease. *Chem Eur J* 19:6817–6823
- Scott IR (1988) Skin treatment composition. EP 0295092 B1
- Seki Y, Mizukura M, Ichimiya T, Suda Y, Nishihara S, Masuda M, Takase-Yoden S (2012) O-sulfate groups of heparin are critical for inhibition of ecotropic murine leukemia virus infection by heparin. *Virology* 424:56–66
- Silva LA, Khomandiak S, Ashbrook AW, Weller R, Heise MT, Morrison TE, Dermody TS (2014) A single-amino-acid polymorphism in chikungunya virus E2 glycoprotein influences glycosaminoglycan utilization. *J Virol* 88:2385–2397
- Simionescu D, Mercuri JJ (2016). Shape-memory sponge hydrogel biomaterial. US Patent 9,283,301
- Spero M, Weiss MS, Kopp JB (2005) Methods using glycosaminoglycans for the treatment of kidney disease. PCT Int Appl WO 2006039709 A1
- Staples GO, Zaia J (2011) Mass spectrometry in carbohydrate sequencing and binding analysis. In: Wang B, Boons G-J (eds) *Carbohydrate recognition: biological problems, methods, and applications*. Wiley, Hoboken, pp 257–300
- Stern R, Maibach HI (2008) Hyaluronan in skin: aspects of aging and its pharmacologic modulation. *Clin Dermatol* 26:106–122
- Stewart KL, Hughes E, Yates EA, Akien GR, Huang T-Y, Lima MA, Rudd TR, Guerrini M, Hung S-C, Radford SE, Middleton DA (2016) Atomic details of the interactions of glycosaminoglycans with amyloid β fibrils. *J Am Chem Soc* 138:8328–8331
- Ströh LJ, Stehle T (2014) Glycan engagement by viruses: receptor switches and specificity. *Ann Rev Virol* 1:285–306
- Tangso KJ, da Cunha PHCD, Spicer P, Li J, Boyd BJ (2016) Antimicrobial activity from colistin-heparin lamellar-phase complexes for the coating of biomedical devices. *ACS Appl Mater Interfaces* 8:31321–31329
- Theocharis AD, Skandalis SS, Gialeli C, Karamanos NK (2016) Extracellular matrix structure. *Adv Drug Deliv Rev* 97:4–27
- Turley E (2010) Topically administered, skin-penetrating glycosaminoglycan formulations suitable for use in cosmetic and pharmaceutical applications. CA 2703532 A1; PCT Int Appl WO 2011/140630 A1
- Tyler PC, Guimond SE, Turnbull JE, Zubkova OV (2015) Single-entity heparan sulfate glycomimetic clusters for therapeutic applications. *Angew Chem Int Ed* 54:2718–2723
- Verges Milano J, Garcia Garcia A, Ruhi Roura R, Montell Bonaventura E, Garcia Lopez M, Alaez Verson CR, Escaich Ferrer J, Egea Maiquez J, Lorrio Gonzalez S, Negrodo Madrigal P (2011) Sulphated disaccharides for the treatment of neurodegenerative and/or neurovascular diseases. PCT Int. Appl. WO 2011/080203
- Vistoli G, De Maddis D, Cipak A, Zarkovic N, Carini M, Aldini G (2013) Advanced glycoxidation and lipoxidation end products (AGEs and ALEs): an overview of their mechanisms of formation. *Free Radic Res* 47:3–27
- Volpi N, Schiller J, Stern R, Soltes L (2009) Role, metabolism, chemical modifications and applications of hyaluronan. *Curr Med Chem* 16:1718–1745
- Von Recum HA, Hijaz A (2014) Glycosaminoglycans for chemokine drug delivery. U.S. Pat. Appl. Publ. US 20140364360
- Vuillermoz B, Wegrowski Y, Contet-Audonneau J-L, Danoux L, Pauly G, Maquart F-X (2005) Influence of aging on glycosaminoglycans and small leucine-rich proteoglycans production by skin fibroblasts. *Mol Cell Biochem* 277:63–72

- Wang P, Ding K (2014) Proteoglycans and glycosaminoglycans in misfolded proteins formation in Alzheimer's disease. *Protein Pept Lett* 21:1048–1056
- Weigel PH, Fuller GM, LeBoeuf RD (1986) A model for the role of hyaluronic acid and fibrin in the early events during the inflammatory response and wound healing. *J Theor Biol* 119:219–234
- Wu RL, Huang L, Zhao H-C, Geng X-P (2017) Hyaluronic acid in digestive cancers. *J Cancer Res Clin Oncol* 143:1–16
- Xiao L, Tong Z, Chen Y, Pochan DJ, Sabanayagam CR, Jia X (2013) Hyaluronic acid-based hydrogels containing covalently integrated drug depots: implication for controlling inflammation in mechanically stressed tissues. *Biomacromolecules* 14:3808–3819
- Xu D, Olson J, Cole JN, van Wijk XM, Brinkmann V, Zychlinsky A, Nizet V, Esko JD, Chang Y-C (2015) Heparan sulfate modulates neutrophil and endothelial function in antibacterial innate immunity. *Infect Immun* 83:3648–3656
- Yang R-M, Fu C-P, Li N-N, Wang L, Xu X-D, Yang D-Y, Fang J-Z, Jiang X-Q, Zhang L-M (2014) Glycosaminoglycan-targeted iron oxide nanoparticles for magnetic resonance imaging of liver carcinoma. *Mater Sci Eng C Mater Biol Appl* 45:556–563
- Yang X, Du H, Liu J, Zhai G (2015) Advanced nanocarriers based on heparin and its derivatives for cancer management. *Biomacromolecules* 16:423–436
- Yip GW, Smollich M, Götte M (2006) Therapeutic value of glycosaminoglycans in cancer. *Mol Cancer Ther* 5:2139–2148
- Yue Z, Wang A, Zhu Z, Tao L, Li Y, Zhou L, Chen W, Lu Y (2015) Holothurian glycosaminoglycan inhibits metastasis via inhibition of P-selectin in B16F10 melanoma cells. *Mol Cell Biochem* 410:143–154
- Yuk SH, Oh KS, Cho SH, Lee BS, Kim SY, Kwak BK, Kim K, Kwon IC (2011) Glycol chitosan/heparin immobilized iron oxide nanoparticles with a tumor-targeting characteristic for magnetic resonance imaging. *Biomacromolecules* 12:2335–2343
- Zhang Q, Li J, Liu C, Song C, Li P, Yin F, Xiao Y, Jiang W, Zong A, Zhang X, Wang F (2015) Protective effects of low molecular weight chondroitin sulfate on amyloid beta (A β)-induced damage in vitro and in vivo. *Neuroscience* 305:169–182
- Zhang RR, Strebe JK, Kuo JS (2016) Heparan sulfates promote amyloid pathology in Alzheimer disease. *Neurosurgery* 79:N12–N13
- Zhang X, Zhao X, Lang Y, Li Q, Liu X, Cai C, Hao J, Li G, Yu G (2016) Low anticoagulant heparin oligosaccharides as inhibitors of BACE-1, the Alzheimer's β -secretase. *Carbohydr Polym* 151:51–59
- Zhao W, McCallum SA, Xiao Z, Zhang F, Linhardt RJ (2012) Binding affinities of vascular endothelial growth factor (VEGF) for heparin-derived oligosaccharides. *Biosci Rep* 32:71–81
- Zheng S, Jin Z, Han J, Cho S, Nguyen VD, Young Ko S, Park J-O, Park S (2016) Preparation of HIFU-triggered tumor-targeted hyaluronic acid micelles for controlled drug release and enhanced cellular uptake. *Colloids Surf B: Biointerfaces* 143:27–36
- Zhong WP, Chin HG, Lee EJ, Guo S, Yip GW, Lam Y (2015) Divergent synthesis of chondroitin sulfate disaccharides and identification of sulfate motifs that inhibit triple negative breast cancer. *Sci Rep* 5:14355. 8 pp
- Zhou X, Jin L (2016) The structure-activity relationship of glycosaminoglycans and their analogues with β -amyloid peptide. *Protein Pept Lett* 23:358–364
- Zhou H, Roy S, Cochran E, Zouaoui R, Chu CL, Duffner J, Zhao G, Smith S, Galcheva-Gargova Z, Karlgren J, Dussault N, Kwan RY, Moy E, Barnes M, Long A, Honan C, Qi YW, Shriver Z, Ganguly T, Schultes B, Venkataraman G, Kishimoto TK (2011) M402, a novel heparan sulfate mimetic, targets multiple pathways implicated in tumor progression and metastasis. *PLoS One* 6:e21106
- Zhu M, Feng Q, Sun Y, Li G, Bian L (2016) Effect of cartilaginous matrix components on the chondrogenesis and hypertrophy of mesenchymal stem cells in hyaluronic acid hydrogels. *J Biomed Mater Res Part B Appl Biomater*. doi:10.1002/jbm.b.33760

- Zieris A, Dockhorn R, Röhrich A, Zimmermann R, Müller M, Welzel PB, Tsurkan MV, Sommer J-U, Freudenberg U, Werner C (2014) Biohybrid networks of selectively desulfated glycosaminoglycans for tunable growth factor delivery. *Biomacromolecules* 55:4439–4446
- Zimmer R, Courty J (2012) Compositions comprising multivalent synthetic ligands of surface nucleolin and glycosaminoglycans. *PCT Int Appl WO 2012/045750*

Bacterial Cellulose Nanoribbons: A New Bioengineering Additive for Biomedical and Food Applications

M. Osorio, C. Castro, J. Velásquez-Cock, L. Vélez-Acosta, L. Cáracamo, S. Sierra, R. Klaiss, D. Avendaño, C. Correa, C. Gómez, R. Zuluaga, D. Builes, and P. Gañán

1 Introduction

The *Gluconacetobacter* genera are classified into the *Acetobacteraceae* family with nine more: *Acetobacter*, *Gluconobacter*, *Acidomonas*, *Asaia*, *Kozakia*, *Saccharibacter*, *Swaminathania*, *Neoasaia*, and *Granulibacter* (Trček 2005; Yukphan et al. 2005; Greenberg et al. 2006). The clear majority of the highest cellulose-producing species belongs to these genera.

In recent years, there have been isolated and characterized new species of *Gluconacetobacter* from different resources such as fruits, flowers, wines, and vinegars (Dellaglio et al. 2005). However, with the latest techniques to characterize,

M. Osorio • J. Velásquez-Cock • L. Cáracamo • S. Sierra • P. Gañán (✉)
Facultad de Ingeniería Química, Universidad Pontificia Bolivariana,
Circular 1°, No 70-01, Medellín, Colombia
e-mail: piedad.ganan@upb.edu.co

C. Castro
Facultad de Ingeniería Textil, Universidad Pontificia Bolivariana,
Circular 1°, No 70-01, Medellín, Colombia

L. Vélez-Acosta • C. Gómez • R. Zuluaga
Facultad de Ingeniería Agroindustrial, Universidad Pontificia Bolivariana,
Circular 1°, No 70-01, Medellín, Colombia

R. Klaiss • D. Avendaño
Facultad de Ingeniería Mecánica, Universidad Pontificia Bolivariana,
Circular 1°, No 70-01, Medellín, Colombia

C. Correa
Grupo de Nuevos Materiales, Universidad Pontificia Bolivariana,
Circular 1°, No 70-01, Medellín, Colombia

D. Builes
I&D Síntesis, Mezclas y Procesos, Andercol, Autopista, Norte 95-84, Medellín, Colombia

many have been reclassified or declared as new species such as the case of *Gluconacetobacter medellinensis* (Castro et al. 2013).

Gluconacetobacter medellinensis were isolated from homemade vinegar obtained from a commercially available homemade vinegar culture (Castro et al. 2012). A sample of vinegar was acquired at the central market in Medellin, Colombia. The membrane on the surface was observed, and the strain was examined under light microscopy and put into Hestrin–Schramm medium (HS) culture media containing 0.01% w/v antifungal to inhibit yeast growth. This process was repeated until the yeast was removed from the culture. The pure strain was incubated in Hestrin–Schramm medium (HS) solid for 3 days at 28 °C to observe the colonies, which were analyzed phenotypically and genotypically.

Phenotypic and genotypic analysis concluded that this strain is a new species of the genus *Gluconacetobacter*, for which the name *Gluconacetobacter medellinensis* was proposed (Castro et al. 2012). The strain proved 100% 16S rRNA similarity with a strain that was previously misclassified by K. Kondo as *Acetobacter xylinum* subsp. *sucrofermentans*. On the other hand, high level of DNA–DNA relatedness (>70%) between those ensures that they belong to the same species, and low level of DNA–DNA relatedness (<70%) between *K. medellinensis* and a *Gluconacetobacter xylinus* subsp. *sucrofermentans* (*Gluconacetobacter sucrofermentans* strain) concludes that they do not belong to *Gluconacetobacter xylinus* species group (Castro et al. 2013).

Recent studies of Yamada (2014) reclassified *Gluconacetobacter medellinensis* along with *Gluconacetobacter kakiaceti* and *Gluconacetobacter maltaceti* as a new genus because they were phylogenetically independent from *Gluconacetobacter* and should therefore be reclassified as novel combinations in the genus *Komagataeibacter* (Yamada 2014); thus, *Gluconacetobacter medellinensis* was named as *Komagataeibacter medellinensis*.

Komagataeibacter medellinensis produces nanocellulose using Hestrin–Schramm medium (HS) containing 2 w/v% D (+) glucose, 0.5 w/v% peptone, and 0.5 w/v% yeast extract 0.27 w/v% Na₂HPO₄. HS medium is acidified using citric acid to pH c.a. 3.6; the culture conditions are static to allow the formation of a thick membrane on the liquid–air interface after 8 days at 28 °C. *K. medellinensis* has the peculiarity of producing bacterial nanocellulose at low pH of 3.5 corresponding to the highest BNC yield, which is an advantage in increasing the production by recycling the culture media. In addition, it is also capable of producing cellulose from unconventional substrates like agro-industrial wastes (unsuitable for human consumption); For instance, using pineapple wastes, the BNC yield was 6.2 g/L, which represents a yield enhancement of more than 55% compared to Hestrin–Schramm medium (commercial culture medium for these bacteria); also there were similar results using sugar cane media; therefore, the production of BNC using *K. medellinensis* is relatively high with similar properties to that produced in HS medium. These results suggest that it is possible to produce BNC from low-cost resources in order to increase its production to a larger scale (Castro et al. 2011).

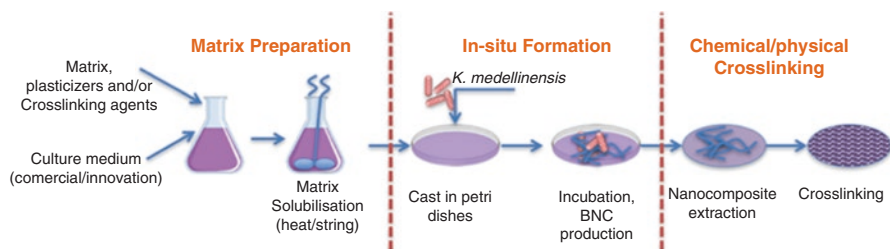


Fig. 1 In situ processing of nanocomposites

2 Bacterial Nanocellulose In Situ Nanocomposites

BNC exhibits remarkable mechanical properties due to its uniform ultrafine fiber network structure, consisting in ribbons of width c.a. 50–70 nm, high planar ribbons orientation when compressed into sheets, good chemical stability, and high water binding capacity (Castro et al. 2013; Grande et al. 2009). *K. medellinensis* culture media can be modified by several compounds, such as polyvinyl alcohol (PVA), thermoplastic starch (TPS), among others, without losing the BNC production capacity of the bacterium (Osorio et al. 2014a, b); the above properties make *K. medellinensis* suitable to produce BNC nanocomposites by in situ fermentation.

In situ fermentation enables the nanocomposite development during the production of the BNC by *K. medellinensis*; the main advantage of this technique is that the reinforcement (BNC) is homogeneously distributed into the matrix (percolation) and BNC is composed of an interconnected 3D network of ribbons, rather than single fibers, which allows an excellent stress transfer in the nanocomposite (Torres et al. 2012; Wan et al. 2006). The in situ fermentation process is described in Fig. 1.

Culture medium for *K. medellinensis* from commercial sources, commonly Hestrin and Schramm culture medium (HS) (Schramm and Hestrin 1954), or innovative culture media from agro-industrial wastes as explained above is modified by the polymer matrix of the nanocomposite, this matrix should be non-toxic for the bacterium and water soluble in order to promote homogenization in the culture medium (Huang et al. 2010; Osorio et al. 2014a, b, c). After the fermentation, it is necessary to generate cross-linking in order to improve its water stability and to consolidate the nanocomposite (Castro et al. 2014; Reddy and Yang 2010).

Polyvinyl alcohol (PVA) and thermoplastic starch (TPS) are nontoxic and water-soluble polymers; they are investigated for biomedical and packaging applications, respectively (Castro et al. 2014; Grande et al. 2009, 2008; Hassan and Peppas 2000; Montoya et al. 2012; Osorio et al. 2014a, b, c; Wang et al. 2010). Nonetheless, in order to improve its water stability and mechanical and thermal properties, they have been reinforced via in situ fermentation with BNC produced by *K. medellinensis* (Castro et al. 2014; Osorio et al. 2014a, b, c).

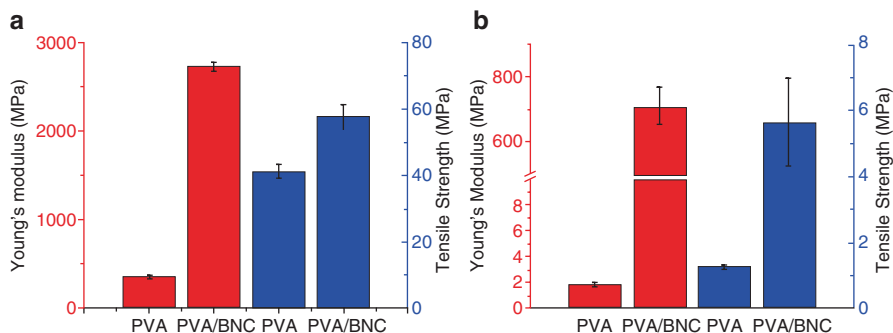


Fig. 2 Young's modulus and tensile strength of nanocomposites by in situ fermentation. (a) PVA/BNC nanocomposites and (b) TPS/BNC nanocomposites

Table 1 Onset temperature of nanocomposite by in situ fermentation

Material	Onset temperature (°C)
PVA	245
PVA/BNC	255
TPS	282
TPS/BNC	301

PVA/BNC nanocomposite (14 wt.% of BNC) improved both Young's modulus and tensile strength, enhancements of 682 and 40% were obtained when compared with the respective BNC-free systems (See Fig. 2a).

Thermogravimetric analysis (see Table 1) also indicates that the nanocomposites had a higher thermal stability compared to the respective matrices. This further supports the evidence of high entanglement between the components produced as a three-dimensional network of nanoscale BNC after biosynthesis by the microorganisms. Overall, the BNC network is postulated to afford percolation within the matrix accompanied by an improved bonding between the reinforcing BNC and PVA (hydrogen bonds and crosslinking). This can explain the exceptional mechanical performance of the nanocomposites (Castro et al. 2014).

TPS/BNC system performs similar behavior to PVA/BNC; the in situ BNC reinforcement of TPS (18 wt.%) and chemical cross-linking allowed high thermal (see Table 1) and water stability and improved the mechanical behavior compared to TPS (tensile strength of 5.7 ± 1.4 MPa and Young's modulus of 715.8 ± 56.8 MPa; see Fig. 2b), because of the addition of in situ nanoribbon network and the formation of covalent bonds (Osorio et al. 2014a, b, c).

BNC of *K. medellinensis* also has been used to develop nanocomposites ex situ; nanocomposites of TPS/BNC and chitosan (Chit)/BNC have been successfully developed. TPS/BNC nanocomposites via ex situ showed a similar behavior to that via in situ, the mechanical and thermal properties of TPS were improved with the addition of BNC nanoribbons in aqueous suspension, and Young's modulus improved from 31.0 ± 4.3 to 412.9 ± 10.6 MPa and the tensile strength from 3.3 ± 0.3 to 9.4 ± 1.2 MPa. Thermal properties of TPS/BNC likewise showed an

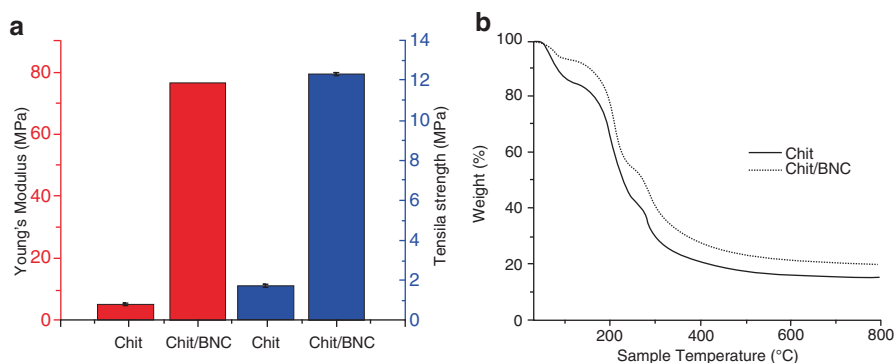


Fig. 3 Mechanical and thermal properties of chitosan/BNC nanocomposites via ex situ. (a) Young's modulus and tensile strength; (b) TGA Chit/BNC of the nanocomposites

improvement, shifting from 227.6 °C (decomposition of 25 wt.%) for TPS to 265.8 °C for TPS/BNC (Montoya et al. 2012).

Incorporation of 5 wt.% of BNC in chitosan (dissolved in acetic acid) improves significantly its mechanical and thermal properties (see Fig. 3). BNC showed a reinforcement effect on chitosan, increasing Young's modulus by 1500% and tensile strength by 673% (Velásquez-Cock et al. 2014), the onset temperature of the chitosan (see Fig. 3b) improves slightly with the addition of BNC, and its degradation temperature improves in 5 °C, because chitosan has a similar thermal stability to BNC (Fernandes et al. 2009).

BNC obtained by *K. medellinensis*, as explained previously, is suitable for reinforcing applications of polymer matrices that enhance its mechanical and thermal properties, and overall BNC has the advantage of allowing both in situ and ex situ processing methods in the development of nanocomposites. Nanocomposites reinforced with BNC are used for packaging and biomedical applications, due to the biodegradability and the biocompatibility of BNC (Iguchi et al. 2000; Kaushik et al. 2010).

3 Biomedical Applications of Bacterial Nanocellulose

BNC have several applications in the biomedical field; recently a good number of papers have described the biocompatibility of BNC with different kinds of human cells such as fibroblast, osteoblast, and keratinocytes, among others (Cai and Kim 2009; Sanchavanakit et al. 2006; Zaborowska et al. 2010); moreover, animal and clinical trials have proved in vivo biocompatibility of BNC. Due to the outstanding in vitro and in vivo BNC properties, some researchers have jumped to the development of biomedical devices like wound dressings, vascular grafts, dura mater, and artificial skin, among others (Fu et al. 2013).

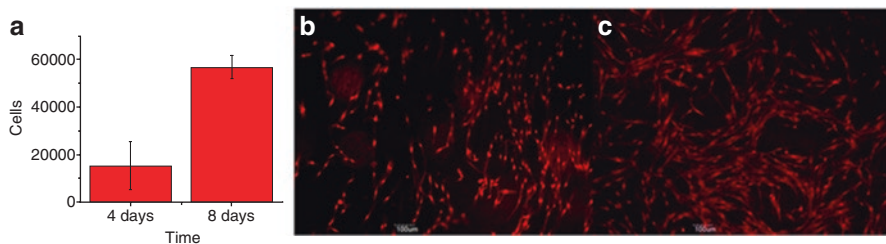


Fig. 4 Fibroblast proliferation on BNC (a) cell number, (b) fluorescent image at 4 incubation days, (c) fluorescent image at 8 incubation days

Biomedical applications of BNC have been possible due to its physical and mechanical properties such as liquid loading capacity, chemical purity, collagen biomimetic, non-allergenic and non-toxic reaction, and, as explained above, in vitro and in vivo biocompatibility (Czaja et al. 2007a, b; Fu et al. 2013; Gao et al. 2010; Klemm et al. 2009).

Most untransformed mammalian cells fail to proliferate when they are prevented from attaching to a solid substrate, a phenomenon known as anchorage dependence of growth (Fang et al. 1996; Lee et al. 1995). Anchorage dependence has been attributed to the arrest cell cycle life progression, resulting from a lack of substrate adhesion (Fang et al. 1996). Nowadays several researchers are looking for the development of scaffolds that can mimic the environment of mammalian cells in order to promote their anchorage and proliferation; polymers as spider silk, chitosan, and BNC have been reported suitable for this applications (Fu et al. 2013; Leal-Egaña and Scheibel 2010; Lina et al. 2009; Rouse and Van Dyke 2010). BNC of *K. medellinensis* have been proved to promote cell anchorage and proliferation in studies with human fibroblast from primary culture. Figure 4 shows a proliferation test of fibroblast on BNC.

Figure 4b, c shows fibroblasts proliferating with fusiform and confluent morphology, which is reported as a healthy cell morphology for fibroblast (Hakkinen et al. 2011). BNC has a collagen-like morphology with a dimension under 100 nm (Bäckdahl et al. 2006; Fink et al. 2007); furthermore it has three hydroxyl groups per monomer, which interact with their counterparts in the polar sites of the cell through hydrogen bonds, and its high hydrophilicity, facilitate nutrient migration to the biomaterial from the cell to the culture medium (Osorio et al. 2014a, b). The above properties of BNC allow the anchorage and cell proliferation on BNC. According to Fig. 4a, at 8 incubation days, cells have fourfold the number of cells and it is similar to a cell culture on polystyrene well of 3 cm of diameter (c.a. 60,000 cells per well).

On BNC, the fibroblast anchorage occurs on monolayer on the biomaterial surface (see Fig. 5a), because of the nanoporosity of BNC does not allow the migration of fibroblasts within the material.

BNC, obtained from *K. medellinensis*, can be shaped in situ in several shapes, i.e., gloves (see Fig. 5b), along with the properties of BNC as skin cells scaffolds,

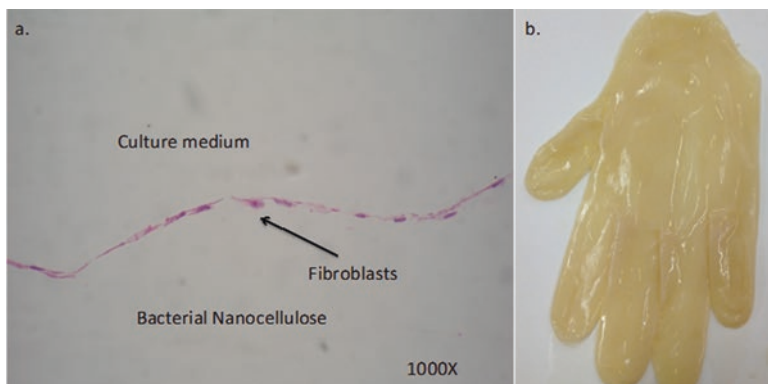


Fig. 5 Proliferation of fibroblast on BNC. (a) Monolayer growth of fibroblast on BNC (Image taken at 100 \times), (b) Glove shaped BNC pellicle

membranes of BNC shaped as gloves, mask, limbs, and so on, are suitable for applications in wound dressings. Czaja et al. (2007a, b) used the BNC in clinical studies and found that the BNC reduces scar formation, furthermore, the wounds were isolated from the environment, because of the membrane can cover the wound replicating the wound surface at nanoscale and creating an optimal moist condition, which accelerate wound healing and skin regeneration (Czaja et al. 2007a, b).

BNC wound dressings can be modified with bioactive agents in order to improve the healing effects, for instance, nanosilver-coatings for antimicrobial wound dressings (Wan and Guhadós 2013), or the incorporation of collagen, chitosan, hyaluronic acid, or proteins in order to accelerate the healing processes (Dong and Snyder 2013).

BNC obtained from *K. medellinensis* is being modified by the incorporation of bioactive agents derived from plant extracts to promote growth and maturation of fibroblast. To the date of this chapter, these bioactive wound dressings are still under development.

4 Bacterial Nanocellulose in Food

BNC as well as other kinds of celluloses are well established as dietary fiber. Dietary fiber offers a range of health benefits, for instance it can reduce the risk of diabetes, obesity, cardiovascular disease, among others (Anderson et al. 2009). BNC is classified as “generally recognized as safe” (GRAS) by the US Food and Drug Administration (Shi et al. 2014). Shi et al. (2014) pointed out some advantages of BNC for food formulations:

- BNC is a highly pure form of cellulose that does not require harsh chemical treatments to isolate and purify it, as it is necessary for cellulose derived from plant sources.

- Bacteria can utilize a culture medium such as fruit syrup to grow, reproduce, and secrete in situ flavor and color from the media. The BNC cultured in these media can acquire the natural flavor and pigment of fruits.
- BNC can produce a range of shapes and textures, such as films, multishaped pulps, filaments, spheres, particles, whiskers, among others.
- BNC is within the nanoscale with a fine three-dimensional network structure, which enables BNC to be used in novel food manufacturing processes (Shi et al. 2014).

Recent applications of BNC in food can be summarized in two categories, raw material for food and multifunctional food ingredient (Shi et al. 2014); in the first category, BNC is used straight away in the formulation, i.e., nata de coco, nata de pina, and nata from blueberry juice (Castro et al. 2013; Iguchi et al. 2000; Parant Rodewald 2005; Shi et al. 2014). The second category groups the uses of BNC for two or more purposes, for example, BNC is suitable as thickening, gelling, stabilizing, emulsifying, and water-binding agent (Okiyama et al. 1993; Shi et al. 2014) and thermal protector of vitamins (Osorio et al. 2014a, b, c).

BNC of *K. medellinensis* is being researched as a thermal protection agent of water-soluble vitamins. In nanocomposite applications, as explained previously, BNC is able to enhance the thermal stability of polymer matrices; this property can be used to protect thermally sensitive vitamins, which are heat sensitive and lose easily their biological activity after being exposed to high temperatures (Osorio et al. 2014a, b, c). A first approach of this method was made with vitamin B3.

Vitamin B3, nicotinic acid or niacin (N), is a water-soluble vitamin that is a precursor of more than 450 gene redox reactions; a low intake of it can cause pellagra, cancer, among others diseases (Kirkland 2012); to prevent them, a continuous supply of vitamin B3 is necessary; nonetheless, due to its heat sensitivity, it degrades during the cooking of the foods (Moreschi et al. 2009). BNC can adsorb the vitamin from an aqueous solution and can protect until 11.67% (vitamin B3/nanocellulose relation) via adsorption in its surface (Osorio et al. 2014a, b, c) (see Fig. 6).

Bacterial nanocellulose also was successfully added in a cookie formulation (Osorio et al. 2014a, b, c), see Fig. 7.

Figure 7 shows that cookies with BNC are brighter and have less color tone than the cookies without BNC, which is related to the slowing of Maillard and caramelization reactions (Badui Dergal et al. 2006), because of the water-binding properties of BNC (Shi et al. 2014). Finally, in the same figure, the result of the insoluble dietary fiber is presented; BNC provides all its weight in insoluble dietary fiber (Osorio et al. 2014a, b, c).

5 Concluding Remarks

Komagataeibacter medellinensis is a promising new species of nanocellulose-producing bacteria, derived from Colombian homemade vinegar. This bacterium can produce nanoribbons of BNC using commercial cultures and innovative ones

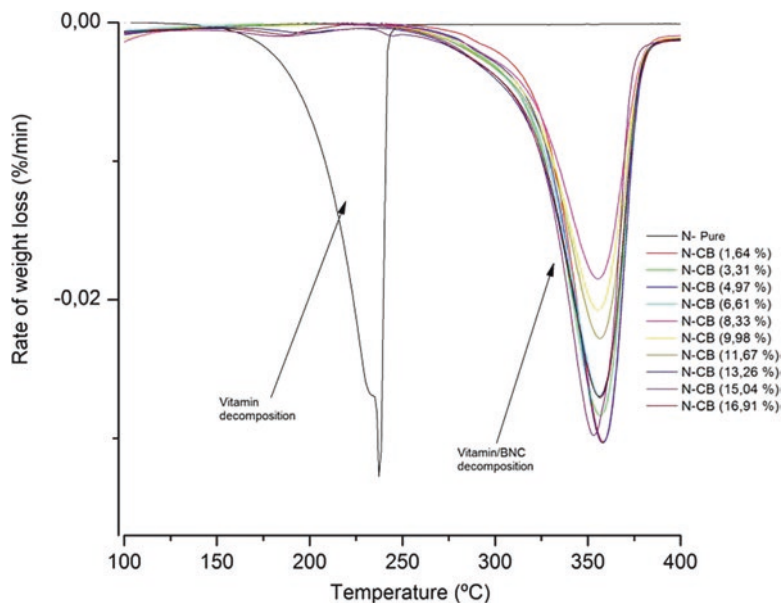
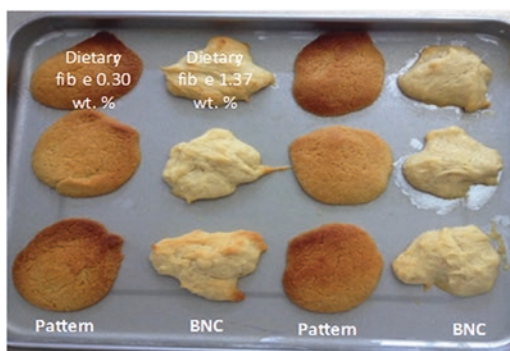


Fig. 6 Vitamin B3 thermal protection with BNC

Fig. 7 Incorporation of 0.77 wt.% of bacterial nanocellulose in a cookie formulation



derived from agro-industrial wastes. *K. medellinensis* has the advantage of producing nanocellulose at lower pH (c.a. 3.6), which is an advantage for reuse culture media and development of agro-industrial culture media. BNC derived from *K. medellinensis* is a promising nanomaterial for a wide range of applications such as packaging and medical devices, thanks to its morphological, chemical, mechanical, thermal, physical, and biological properties. BNC improves the mechanical properties of PVA, TPS, and chitosan matrices, while it does not reduce their biodegradability or biological properties. Because of its water-holding capability and collagen-like microstructure, it can be used as wound dressing and in the development of medical devices. BNC thermal stability is advantageous for thermal protection of vitamins,

while it can be used as dietary fiber for food formulations. To conclude, BNC is a high-performance nanomaterial from a humble origin, in which its potential had not been explored until the emerging of nanotechnology. BNC may be ideal for cutting-edge applications due to it is an environmentally friendly material.

References

- Anderson J, Baird P, Davis R et al (2009) Health benefits of dietary fiber. *Nutr Rev* 67:188–205
- Bäckdahl H, Helenius G, Bodin A et al (2006) Mechanical properties of bacterial cellulose and interactions with smooth muscle cells. *Biomaterials* 27:2141–2149
- Badui Dergal S, Sara D, Valdés E et al (2006) *Química de los alimentos*, Cuarta edición edn. Pearson Educación, México, p 703
- Cai Z, Kim J (2009) Bacterial cellulose/poly(ethylene glycol) composite: characterization and first evaluation of biocompatibility. *Cellulose* 17:83–91
- Castro C, Zuluaga R, Putaux J-L et al (2011) Structural characterization of bacterial cellulose produced by *Gluconacetobacter swingsii* sp. from Colombian agroindustrial wastes. *Carbohydr Polym* 84:96–102
- Castro C, Cleenwerck I, Trcek J et al (2013) *Gluconacetobacter medellinensis* sp. nov., cellulose- and non-cellulose-producing acetic acid bacteria isolated from vinegar. *Int J Syst Evol Microbiol* 63:1119–1125
- Castro C, Vesterinen A, Zuluaga R et al (2014) In situ production of nanocomposites of poly(vinyl alcohol) and cellulose nanofibrils from *Gluconacetobacter* bacteria: effect of chemical cross-linking. *Cellulose* 21:1–10
- Czaja W, Kawecki M, Wróblewski P et al (2007a) Biomedical applications of microbial cellulose in burn wound recovery. In: Brown RMJ, Saxena IM (eds) *Cellulose: molecular and structural biology*. Springer, Dordrecht, pp 307–321
- Czaja W, Young D, Kawecki M et al (2007b) The future prospects of microbial cellulose in biomedical applications. *Biomacromolecules* 8:1–12
- Dellaglio F, Cleenwerck I, Felis G et al (2005) Description of *Gluconacetobacter swingsii* sp. nov. and *Gluconacetobacter rhaeticus* sp. nov., isolated from Italian apple fruit. *Int J Syst Evol Microbiol* 55:2365–2370
- Dong H, Snyder J (2013) Nanocellulose foam containing active ingredients. US Patent No. US 20130330417 A1
- Fang F, Orend G, Watanabe N et al (1996) Dependence of cyclin E-CDK2 kinase activity on cell anchorage. *Science* 271:499–502
- Fernandes S, Oliveira L, Freire C et al (2009) Novel transparent nanocomposite films based on chitosan and bacterial cellulose. *Green Chem* 11:2023–2029
- Fink H, Gustafsson L, Bodin A et al (2007) Influence of cultivation conditions on mechanical and morphological properties of bacterial cellulose tubes. *Biotechnol Bioeng* 97:425–434
- Fu L, Zhang J, Yang G (2013) Present status and applications of bacterial cellulose-based materials for skin tissue repair. *Carbohydr Polym* 92:1432–1442
- Gao C, Wan Y, Yang C et al (2010) Preparation and characterization of bacterial cellulose sponge with hierarchical pore structure as tissue engineering scaffold. *J Porous Mater* 18:139–145
- Grande C, Torres F, Gomez C et al (2008) Morphological characterisation of bacterial cellulose-starch nanocomposites. *Polym Polym Compos* 16:181–185
- Grande C, Torres F, Gomez C et al (2009) Development of self-assembled bacterial cellulose-starch nanocomposites. *Mater Sci Eng C* 29:1098–1104
- Hakkinen K, Harunaga J, Doyle A et al (2011) Direct comparisons of the morphology, migration, cell adhesions, and actin cytoskeleton of fibroblasts in four different three-dimensional extracellular matrices. *Tissue Eng Part A* 17:713–724

- Hassan C, Peppas N (2000) Structure and morphology of freeze/thawed PVA hydrogels. *Macromolecules* 33:2472–2479
- Huang H, Chen L-C, Lin S-B et al (2010) In situ modification of bacterial cellulose network structure by adding interfering substances during fermentation. *Bioresour Technol* 101:6084–6091
- Iguchi M, Yamanaka S, Budhiono A (2000) Bacterial cellulose — a masterpiece of nature's arts. *J Mater Sci* 35:261–270
- Kaushik A, Singh M, Verma G (2010) Green nanocomposites based on thermoplastic starch and steam exploded cellulose nanofibrils from wheat straw. *Carbohydr Polym* 82:337–345
- Kirkland J (2012) Niacin requirements for genomic stability. *Mutat Res* 733:14–20
- Klemm D, Schumann D, Kramer F et al (2009) Nanocellulose materials – different cellulose, different functionality. *Macromol Symp* 280:60–71
- Leal-Egaña A, Scheibel T (2010) Silk-based materials for biomedical applications. *Biotechnol Appl Biochem* 55:155–167
- Lee Y, Kouvroutoglou S, McIntire L et al (1995) A cellular automaton model for the proliferation of migrating contact-inhibited cells. *Biophys J* 69:1284–1298
- Lina F, Yue Z, Jin Z et al (2009) Bacterial cellulose for skin repair materials. In: Fazel-Rezai R (ed) *Biomedical engineering – frontiers and challenges*. Rijeka, Intech, pp 249–274
- Montoya Ú, Zuluaga R, Castro C et al (2012) Development of composite films based on thermoplastic starch and cellulose microfibrils from colombian agroindustrial wastes. *J Thermoplast Compos Mater* 27:413–426
- Moreschi E, Matos J, Almeida-Muradian L (2009) Thermal analysis of vitamin PP Niacin and niacinamide. *J Therm Anal Calorim* 98:161–164
- Okiyama A, Motoki M, Yamanaka S (1993) Bacterial cellulose IV. Application to processed foods. *Food Hydrocoll* 6:503–511
- Osorio M, Ortiz I, Caro G, Restrepo L et al (2014a) Matrices nanocompuestas de alcohol de polivinilo (PVA)/celulosa bacteriana (CB) para el crecimiento celular y la ingeniería de tejidos. *Rev Colomb Mater* 1:338–346
- Osorio M, Restrepo D, Zuluaga R et al (2014b) Synthesis of thermoplastic starch-bacterial cellulose nanocomposites via in situ fermentation. *J Braz Chem Soc* 25:1607–1613
- Osorio M, Zuluaga R, Gañán P et al (2014c) Protección térmica de vitamina B3 con celulosa bacteriana y su aporte de fibra dietaria. *Rev Fac Nac Agron* 67:634–637
- Parant N (2005) Elaboración de Gel Celulósico (nata) Producido por *Acetobacter xylinum* Sobre Jugo de Arándano (*Vaccinium corymbosum*). Univ. Austral Chile. Universidad Austral de Chile, Valdivia, p 47
- Reddy N, Yang Y (2010) Citric acid cross-linking of starch films. *Food Chem* 118:702–711
- Rouse J, van Dyke M (2010) A review of keratin-based biomaterials for biomedical applications. *Materials (Basel)* 3:999–1014
- Sanchavanakit N, Sangrungraugroj W, Kaomongkolgit R et al (2006) Growth of human keratinocytes and fibroblasts on bacterial cellulose film. *Biotechnol Prog* 22:1194–1199
- Schramm M, Hestrin S (1954) Factors affecting production of cellulose at the air/liquid interface of a culture of *Acetobacter xylinum*. *J Gen Microbiol* 11:123–129
- Shi Z, Zhang Y, Phillips G et al (2014) Utilization of bacterial cellulose in food. *Food Hydrocoll* 35:539–545
- Torres F, Commeaux S, Troncoso O (2012) Biocompatibility of bacterial cellulose based biomaterials. *J Funct Biomater* 3:864–878
- Velásquez-Cock J, Ramírez E, Betancourt S et al (2014) Influence of the acid type in the production of chitosan films reinforced with bacterial nanocellulose. *Int J Biol Macromol* 69:208–213
- Wan W, Guhados G (2013) Nanosilver coated bacterial cellulose. Patent: US 20130211308 A1
- Wan W, Hutter J, Millon L et al (2006) Bacterial cellulose and its nanocomposites for biomedical applications. In: Oksman K (ed) *Cellulose nanocomposites*. American Chemical Society, Washington, DC, pp 221–241
- Wang J, Gao C, Zhang Y et al (2010) Preparation and in vitro characterization of BC/PVA hydrogel composite for its potential use as artificial cornea biomaterial. *Mater Sci Eng C* 30:214–218

- Yamada Y (2014) Transfer of *Gluconacetobacter kakaiceti*, *Gluconacetobacter medellinensis* and *Gluconacetobacter maltaceti* to the genus *Komagataeibacter* as *Komagataeibacter kakaiceti* *comb. nov.*, *Komagataeibacter medellinensis* *comb. nov.* and *Komagataeibacter maltaceti* *comb. nov.* Int J Syst Evol Microbiol 64:1670–1672
- Zaborowska M, Bodin A, Bäckdahl H et al (2010) Microporous bacterial cellulose as a potential scaffold for bone regeneration. Acta Biomater 6:2540–2547

Part II

Oil Industry

Biobased Additives in Oilwell Cement

A. Vázquez and T.M. Pique

1 Introduction

Oil and gas are usually extracted from the earth through very deep holes known as wellbores. Wellbores are drilled into a subterranean formation that is an oil or gas reservoir. Typically, a wellbore must be drilled 100/3000 m. The greater the depth of the formation is, the higher the temperature and pressure on the well. After the hole is drilled, a steel pipe, also known as casing, is placed inside the wellbore. The casing provides structural integrity to the borehole (the wall of the wellbore).

Between the borehole and steel casing, cement slurry is placed for sealing the annular space, annulus. After it sets, the cement slurry forms an annular sheath of hardened and impermeable cement. It provides zonal isolation, isolates porous formations, supports vertical and radial loads to the casing, protects the casing from corrosion, and bonds its exterior surface to the walls of the wellbore (Rincon-Torres and Hall 2013; Fink 2015). Figure 1 represents the casing, the borehole, the cement slurry, and the formation. It schemes the placing of the cement slurry between the casing and the different formations.

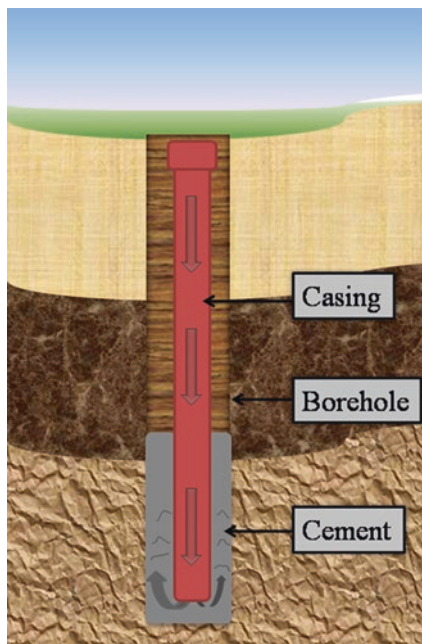
The cement slurry, also known as cement paste, is a mix of Portland cement, water, and additives. Portland cement was patented in 1824 as artificial cement produced by burning a blend of limestone and clay. It is often referred to as hydraulic cement because it hydrates when mixed with water. It is first a thick slurry. Subsequently, as a result of chemical reactions between water and chemical compounds present in the cement, it sets and hardens. This hydration reaction is responsible for the impermeable, resistant, solid, hardened cement paste. The final product is a synthetic rock insoluble in water under normal conditions, with low permeability

A. Vázquez • T.M. Pique (✉)

Instituto de Tecnología en Polímeros y Nanotecnología (ITPN), Universidad de Buenos Aires (UBA) – CONICET, Buenos Aires, Argentina

e-mail: tpique@fi.uba.ar

Fig. 1 Scheme of the placing of the cement slurry between the casing and the different formations



and extraordinary compressive strength (Robertson et al. 1989). In most of the world, oilwell cement is manufactured according to the chemical and physical standards given by the American Petroleum Institute (API): API Standards 10A “Specifications for Oilwell Cements and Cement Additives” (American Petroleum Institute 1979).

The water to cement ratio (w/c) is a very important parameter of the cement slurry, since it governs the mechanical properties of the hardened material. The lower the w/c is, the higher the final compressive strength. It also controls the flow behavior of cement before it sets, if no additives are added. It provides workability and the ability of the cement paste to be mixed, transported, placed, compacted, and finished before the initial setting time begins. In the oilwell cement industry, the usual w/c is between 0.38 and 0.46 (Fink 2015). Many desirable properties can be obtained by selecting the adequate w/c , although, to extend the offered properties of the cement paste, additives and admixtures are used (Vorderbruggen et al. 2016).

Finally, there are the additives. Oilwell cement must sometimes be pumped into 2000/3000 m deep wellbores where the temperature goes up to 200 °C and pressures to 140 MPa. Pumping might take more than 6 h and setting immediately after pumping is crucial to avoid gas migrations. Some boreholes are so weak that they cannot support the hydrostatic pressure of the fluid column exerted by the cement slurries with densities higher than 1.00 kg m^{-3} . There are also circumstances where high-density slurries are needed. Each formation and borehole condition needs tailored oilwell cement slurry. Its particular requirement is achieved by the use of additives.

Additives, in the oil and gas industry, are all additions to cement and cement slurries. Unlike in the construction industry, in the oil and gas industry, there is no differentiation between additives (larger additions) and admixtures (less than 5 % by weight of cement additions, usually chemical admixtures) (Bensted 1996).

Additives would be defined, then, as non-cementitious materials added to the cement slurry to optimize some specific property. The term is so broad that it includes slag, silica fumes, hollow glass, quartz, different chemicals, foams, and many different types of polymers. They can act on the cement hydration, accelerating or decelerating it, making the cement paste fluid with a low w/c, making it more viscous or more cohesive, and even shear thinning, depending on the material added and its interaction with the cement slurry. In the hardened state of the cement paste, these can be added to reduce the cement content, reduce the hardened material density, make it resistant to supercritical CO₂, and increase its mechanical properties (Ramachandran 1996).

Additives can control, for example, the thickening time for a projected temperature and pressure condition; hence, the slurry remains pumpable throughout the time required to place the cement. Thickening time is the open time, the time needed to manipulate the slurry after mixing the cement with water. As soon as cement contacts the water, viscosity starts increasing with time because of the hydration reaction. When viscosity is too great, the slurry is no longer pumpable. Thus, it is necessary to place the cement within a certain period of time after mixing. The viscosity can be regulated with the proper additive added in an amount fixed for that special cement slurry design for the particular conditions of the wellbore. The thickening time is influenced by temperature and pressure; consequently, it is important to know the conditions in the wellbore. If the cementing remains incomplete, expensive hard work must be done to fix it (Fink 2015).

Many factors must be considered for designing cement slurries, for example, the desired compressive strength of the hardened cement paste. This must be higher than the axial forces or crush loadings that are expected to be exerted against it. As it was established before, the rheology of the slurry should be such that the viscosity is not too high so it can be pumped, but it is enough to maintain the slurry as a uniform suspension. The slurry should not be dehydrated, losing water to the permeable formations, so that the cement slurry retains the cement filtrate (water and the dissolved ions from dissolution of the aqueous phase of cement). This particular dehydration is known as fluid loss, and there are many additives, known as fluid loss agents, designed to prevent it. The most used are cellulose ethers. Furthermore, the consistency of the slurry should reduce the free fluid, minimizing the volume of fluid that separates from it and collects at the vertical surface on the top of a slurry column. This effect is also known as bleeding.

Wellbore cementing is an example of a material design that consists in 6–12 different, single-action components: cement, water, and additives. The diverse variety of additives include accelerators, dispersants, fluid loss agents, gas migration additives, latexes, retarders, and weighting agents, among others. It is wise to notice that additives might interact with each other when mixed together. This interaction must be studied before implementation.

Some of these additives, the chemical admixtures in particular, are biobased and come from renewable biomass products. Not only due to environmental regulations but also due to the recent increase in environmental consciousness, these products are more consumed nowadays, also because many of them have some unique properties that make them irreplaceable (Vorderbruggen et al. 2016). In this chapter, additives used in the oilwell industry for tailoring the cement slurries are described, and some of the most important biobased ones will be particularly addressed.

2 Additives

2.1 Retarders

Setting is the period during which the cement reaction with water generates sufficient hydration products so that these percolate. There is an initial setting time, also referred to as a thickening time, before which the slurry should be placed, and a final setting time, after which the slurry is already a hardened artificial rock.

Retarders are additives that delay the initial setting time; hence, there is more time to place the slurry. These are needed in the oilwell drilling when wellbores are to be cemented in 1000/3000 m or more in depth with high temperatures and pressures, when the cementing operation might require a long period of time. It is well known that the setting time shortens with high temperatures (Fig. 2). Successful placement of the slurry requires that it remains fluid and pumpable at high temperatures for the sufficient amount of hours to fill the annulus; thereafter, the initial setting time of the cement slurry must be adjusted to each cementing operation. Additionally, after the slurry has been pumped into place, it is required that it sets at a normal rate. Then the time of initial set and the thickening time should be retarded; thus, the slurry remains pumpable for the necessary time, and yet the period of time between initial and final setting time should not be modified. The passage of the slurry from a liquid to a solid state should occur rapidly to guarantee complete seal and prevent any unwanted fluid or gas flow. This can be achieved by adding the accurate dosage of specific retarders to the cement slurry.

2.2 Fluid Loss Control

Fluid loss refers to the unwanted leakage of the fluid phase of the cement slurry into formations across the surface of the borehole. When the slurry dehydrates, w/c is altered, changing the whole slurry design and affecting the quality of the hardened cement. It can cause failure due to premature setting, immobilizing the slurry before it reaches the desired position. It can also be detrimental to water sensitive shale sections of the wellbores that may weaken and break down due to

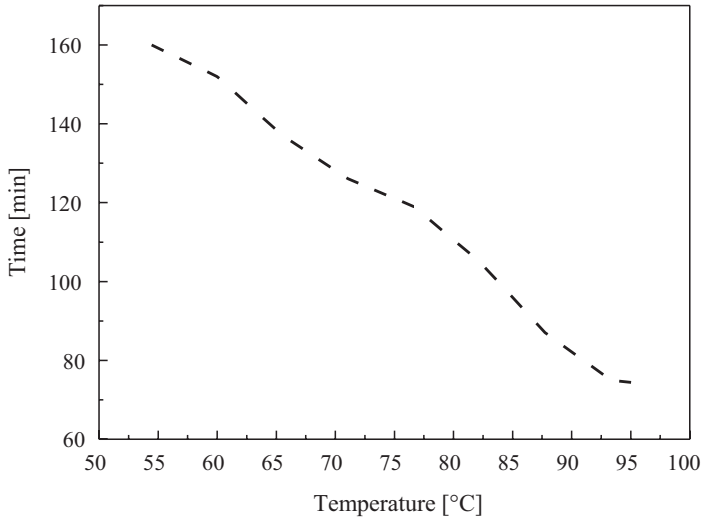


Fig. 2 Effect of temperature on time of initial setting of neat Portland cement with a w/c 0.6 (Adapted from Craft et al. 1934)

the filtration of liquids into clays that can swell causing partial or complete blocking of the wellbore.

Fluid loss control refers to treatments designed to reduce the undesirable leakage, and it has been achieved by two basic mechanisms (Rincon-Torres and Hall 2013). The first one is based on increasing the viscosity and the suspension stability of the cement slurry using high polymer concentrations. The second one is by developing a filter cake in the borehole surface using fluid loss additives to plug the pore throats of the formation. Fluid loss additives retain the key characteristics of the cement slurries, including viscosity, thickening time, density, and compressive strength development, all of which are affected by the amount of water on the cement slurry (Navarrete et al. 2000).

2.3 Free Water Control

Another mechanism, which is detrimental to the w/c ratio, is the sedimentation of cement particles down to the bottom of the pumped slurry and supernatant water on the surface of the cemented borehole due to the different densities. These can also affect the w/c and the stability of the cement suspension. One of the objectives of a slurry design is to keep the annular column with a homogeneous cement suspension until it sets; thus, a proper cement placement and, therefore, hydraulic annulus seal are obtained.

The separation of the different specific gravity particles can be prevented if the viscosity of the slurry increases. An additive that increases the viscosity can enhance

the ability of the fluid to suspend and carry particles without sedimentation. There are several kinds of viscosity increasing additives. These can be referred to as viscosifying agent, viscosifier, thickener, gelling agent, or suspending agent.

2.4 *Dispersants*

Cement slurry is a non-Newtonian fluid. It actually behaves as a Bingham's fluid. It presents an initial high shear stress that has to be overcome with pumping energy during the placing in the annulus. Sometimes, due to different additions or wellbore conditions, this initial shear stress is too high. To lower it down, dispersants are added to the slurry. Dispersants, also known as water reducers, are additives that increase the slurry's fluidity without adding additional water or reduce the water content and, hence, the water to cement ratio for a given fluidity in order to increase the hardened slurry's strength.

Dispersants interact with cement particles leading to its adsorption on the cement particle surfaces. The electrical charge repulsion of adsorbed dispersant molecules can prevent flocculation of cement particles, promoting their homogeneous dispersion in fresh cement slurries. Figure 3 is a schematic representation of the electrostatic repulsion.

Dispersants have a thinning effect that can ease the mixing and placing of the slurry. These can lower the friction and the pressure during pumping. They can also be used to reduce the pressure exerted on the borehole protecting depleted or weak formations and preventing circulation lost.

2.5 *Lost Circulation Materials*

Lost circulation is another serious problem cement slurries have to overcome. It is the reduction or total loss of the slurry during cementing operation. It occurs in high permeability formation, with vugs or naturally fractured formation and unconsolidated zones. It can also happen when the hydrostatic pressure of the cement slurry exerted over the borehole exceeds the fracture gradient of the formation. In each of these cases, slurry can flow and circulate outside the annulus failing to seal the space between the formation and the casing. Figure 4 represents a wellbore where the slurry can be lost during the cementing operation.

There are different ways to avoid the loss of circulation of the slurry. Lightening the slurry's density is one way. With low-density slurries the pressure drops by friction during the slurry placement, allowing to mitigate the circulation loss since, by reducing this pressure, the pressure exerted by the cement slurry on the formation is also reduced. Another alternative is the use of thixotropic cement slurries, sensitive to shear stress, which gels when the shear ceases. These slurries develop high gel strength as soon as they flow into a formation by plugging the area. Another option is to use fast-setting cement. Moreover, some materials and fibers have been successfully used to avoid circulation loss because they

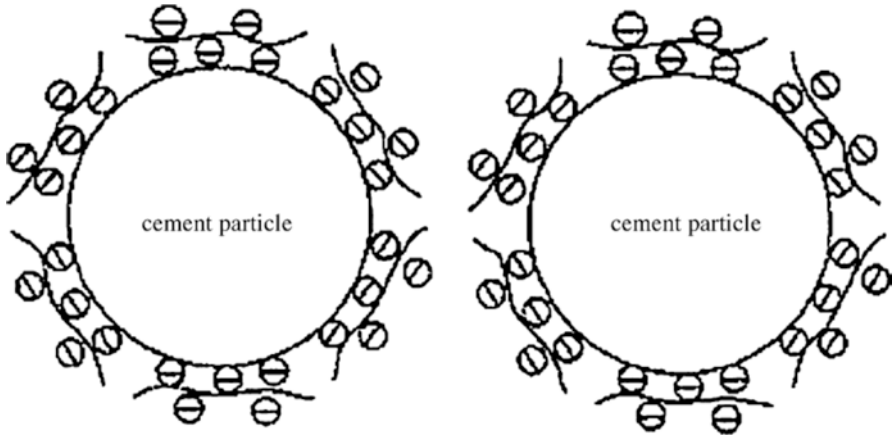


Fig. 3 Electrostatic repulsion: a schematic representative of two cement particles adsorbed with dispersants or water reducer molecules (Ouyang et al. 2006)

act as bridging agents tamponing some borehole voids, avoiding that the slurry circulates outside the annulus (Abbas et al. 2004).

2.6 *Lightweight Additives*

As mentioned before, some weak formation require low-density cement slurries; thus, the hydrostatic pressure of the fluid column is low enough for the formation to resist. These slurries avoid or minimize circulation loss. The lightweight slurries require also less energy to transport and pump. To lower the slurries' densities, these can be foamed by injecting gas, usually nitrogen, into the slurry. The density drastically falls but also the slurry's mechanical strength. Adding additional water to the cement slurry is a common mean of reducing its density. The cement slurry will thus require water-extending additives. These help maintaining the slurry stability and compensate the low compressive strength due to the high w/c. Some of these extenders are lightweight aggregates such as hollow glass microspheres and fibers, which also can contribute to reduction of the cement slurry density.

3 **Biobased Additives**

3.1 *Cellulose*

In the construction chemical industry, cellulose products are very important. Cellulose is mostly used in the form of ether derivatives, specially carboxymethyl cellulose and methyl cellulose. Other than ethers, very small quantities of cellulose products are used, such as micro and nanocellulose fibers (Plank 2005).

Fig. 4 Scheme of a wellbore with permeable formations with vugs and natural fractures, where the slurry can lose during the cementing operation (Abbas et al. 2004)



3.1.1 Cellulose Derivatives

Cellulose ethers have been used in the oilwell cement industry for decades. A patent from 1953 claims the use of alkyl hydroxylalkyl cellulose mixed ethers, where the alkyl group contained 1–4 carbon atoms and the hydroxylalkyl group contained 2–4 carbon atoms, as set retarding agent using it within 0.5–5 % by weight of cement (bwoc) (Kaveler 1953). Another patent in 1957 claimed the use of sulfoalkyl cellulose ethers and their salts as cement set retarders but also as thickening time extending and fluid loss control agents (Kaveler 1957). Not only sulfoalkyl cellulose ethers were reported as fluid loss control and thickening time extending agents and set retarders, carboxymethyl hydroxyethyl cellulose (CMHEC) was reported as well, and nowadays it is still used for this purpose (Rust and Wood 1959; Vázquez and Pique 2016).

Cellulose ethers (CE) are available in the construction industry as methyl cellulose (MC), methyl hydroxyethyl cellulose (MHEC), methyl hydroxypropyl cellulose (MHPC), hydroxyethyl cellulose (HEC), hydroxypropyl cellulose (HPC), Na-carboxymethyl cellulose (CMC), Na-carboxymethyl hydroxyethyl cellulose (CMHEC), ethyl cellulose (EC), and ethyl hydroxyethyl cellulose (EHEC). Cellulose ethers are obtained by the substitution of the hydroxyl groups of cellulose that can be replaced with, for example, methyl, hydroxypropyl, hydroxyethyl, and carboxymethyl groups. The etherificated cellulose becomes a water-soluble polymer. Figure 5 represents the structure of some water-soluble cellulose ethers used in the construction industry.

The most used in the oilwell cement industry are HEC and CMHEC. HEC is a very good fluid loss control agent and can perform under diverse salinity conditions up to

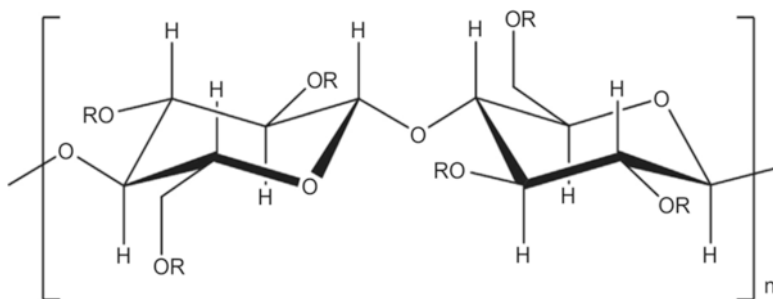


Fig. 5 Structure of water-soluble cellulose derivatives (R = H for cellulose and R = H, ($-\text{CH}_3$), ($-\text{CH}_2-\text{CH}_2\text{OH}$), ($-\text{CH}_2-\text{CHOHCH}_3$), or ($-\text{CH}_2-\text{COOH}$) for methyl cellulose, hydroxyethylmethyl cellulose, hydroxypropylmethyl cellulose, or carboxymethyl hydroxyethyl cellulose, respectively) (Vázquez and Pique 2016)

150 °C. Nevertheless, when using HEC, dispersants have to be added to the cement slurry to control its thickening effect. HEC can enhance the viscosity of the cement slurry, which is not always desirable for pumpable slurries. Typical HEC products used in well cementing have a degree of substitution (DS) of 1.5–2.5. When using CMHEC, the carboxylic group introduces a set retarding effect on the cement slurry among its fluid loss control capacity. Typical commercial products used in well cementing exhibit a degree of substitution (DS carboxymethyl) of 0.3–0.4 and a molar degree of substitution (MS hydroxyethyl) of 0.3–2.0 (Plank 2005).

Figure 6 represents some of the results of a research conducted by Bülischen and Plank. It shows the measurement of the fluid loss of CMHEC according to the American Petroleum Institute (API) specifications. Fluid loss decreases from 1163 ml at 0.1 % bwoc CMHEC, to 42 mL at 0.5 % bwoc CMHEC. The concentration of CMHEC needed to achieve an API fluid loss of below 100 ml/30 min at 27 °C was found to be 0.4 % bwoc. The columns in Fig. 6 represent the amount of polymer retained from the filtrated volumes of cement slurries containing CMHEC at 27 °C (Bülischen and Plank 2012). The same research was done for HEC. For this biopolymer fluid loss decreases from 318 ml at 0.4 % bwoc HEC to 36 mL at 1.0 % bwoc HEC. The concentration of HEC needed to achieve an API fluid loss of below 100 ml/30 min at 27 °C was found to be 0.7 % bwoc (Bülischen and Plank 2011).

Recently a new derivatized-cellulosic polymer has been tested in field cases. Cellulose was modified, so the additive fulfills many of the cementing slurries' desired properties such as fluid loss control, dispersability, free water control, and lightweight, for use in wells up to 120 °C. This was achieved by modifying cellulosic material after an in-depth structure activity study of the polymer. The molecular substitution and degree of substitution of the ether side chains structures were tuned along with its molecular weight. The size of the particles was also optimized to control the hydrolysis rate of the polymer (Vorderbruggen et al. 2016). This means that the cellulose-based additives are still an actual research topic; it is still being tuned and optimized to reach the perfect additive.

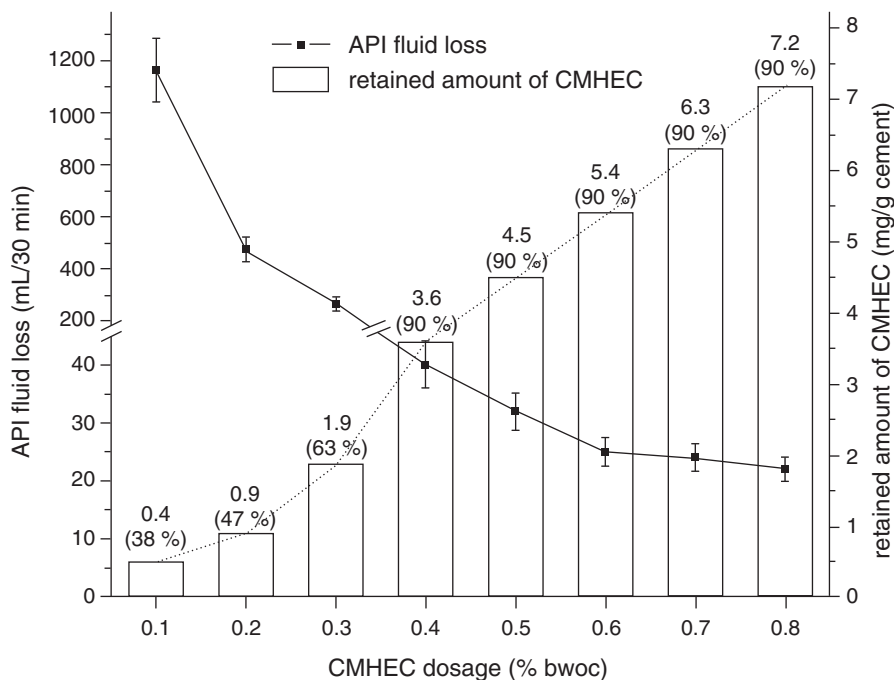


Fig. 6 Fluid loss measured according to API specification and the retained amount of CMHEC as a function of polymer dosage (Bilichen and Plank 2012)

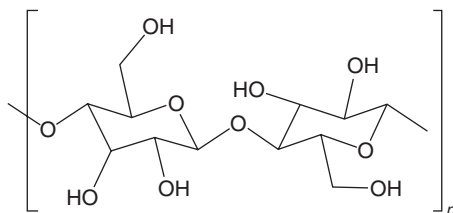
3.1.2 Micro- and Nanocellulose Fibers

Cellulose fibers and their derivatives constitute one of the most abundant renewable polymer resources available on earth. The use of cellulosic fibers to reinforce cement-based materials has been widely applied. Many types of natural fibers are commonly used to reinforce construction materials (Gómez Hoyos and Vázquez 2014). Bensted stated that the most common lost circulation controllers employed in the North Sea in 1996 were, among mica and calcium carbonate, walnut shells, while in Asia, coconut shells and sugar cane were also frequently utilized (Bensted 1996). Sugar cane fiber, for example, can reduce the density of the cement slurry, the free water, and the fluid loss content and prevent the lost circulation problem acting as a bridging agent (Samsuri and Phuong 2002).

Microcrystalline cellulose was found to increase the amount of hydration products when added to a cement-based material, thus increasing its impermeability, since hydration products grow to fulfill the cement porous structure. It was also found that the initial shear stress of the cement paste grew 260 % when 3.0 % of microcrystalline cellulose was added (Gómez Hoyos et al. 2013).

With the advances of nanotechnology, the use of fibers in oilwell cementing has reached to the use of nanofibers, especially of nanocellulose (NC). Nanocellulose materials have repetitive molecular structure composed of a linear backbone of $\beta(1\rightarrow4)$ -linked d-glucose units. Its chemical structure is plotted in Fig. 7.

Fig. 7 Chemical structure of nanocellulose materials (Lafitte et al. 2013)



Nanocellulose is a rather interesting material since it has a large surface-to-volume ratio, high strength and stiffness, very low thermal expansion coefficient, low weight, low density, high aspect ratio and is biodegradable. It can be obtained from every cellulose source, specially from lignocellulosic fibers, including a family of sea animals called tunicates, some algae and bacteria, such as bacteria from the *Acetobacter* species (Charreau et al. 2013).

Extraction of nanocellulose from lignocellulosic fibers is one of the most studied topics in the literature today since this particular nanocellulose is renewable and abundant, and the cost of the raw material is low. Nanocellulose from wood and natural fibers has traditionally been extracted mainly by acid hydrolysis and via mechanical treatment. When extracted by acid hydrolysis, the so-called nanocrystalline cellulose (NCC) or cellulose nanowhiskers (CNW) are obtained. These are rodlike particles with diameters in the range of 2–20 nm and 100–600 nm in length. Cellulose nanowhiskers are characterized by high crystallinity, and their aqueous suspensions display a colloidal behavior (Vázquez et al. 2015).

Cellulose nanowhiskers are of high strength, low density, and thermally stable above 180 °C, which is highly important for oilwell materials. Then, it can be used as a cement reinforcement and to prevent circulation loss of the cement slurry. Furthermore, because the product is insoluble in aqueous solution and its ability to enhance viscosity is via hydrogen-bonding interactions, the cellulose nanowhiskers can be used in cement slurries for thixotropy and to improve its static suspension ability (Rincon-Torres and Hall 2013). Figure 8 shows the effect of different percentages of cellulose nanofibrils on the cement slurry's viscosity. Being τ_0 the initial shear stress of the cement paste, it is established how the shear stress of the slurry increases almost exponentially with the addition of small amounts of cellulose nanofibrils (Gomez Hoyos 2013).

Additionally, Gómez Hoyos studied the cement paste modified with 0–0.4 % bwoc of cellulose nanofibrils by means of dynamic mechanical analysis between a temperature range of 25 °C and 200 °C (Gómez Hoyos et al. 2017). It was demonstrated that the storage modulus of the modified cement paste was relatively constant until 100 °C, the same as the unmodified cement paste. After the analysis, FE-SEM images were taken from the tested samples and smaller cracks were found for modified cement paste. Furthermore, cement paste modified with 0.4 % bwoc of cellulose nanofibrils showed the smallest amount of microcracks. This sample had the highest storage modulus and lost only a 10 % of it at 200 °C.

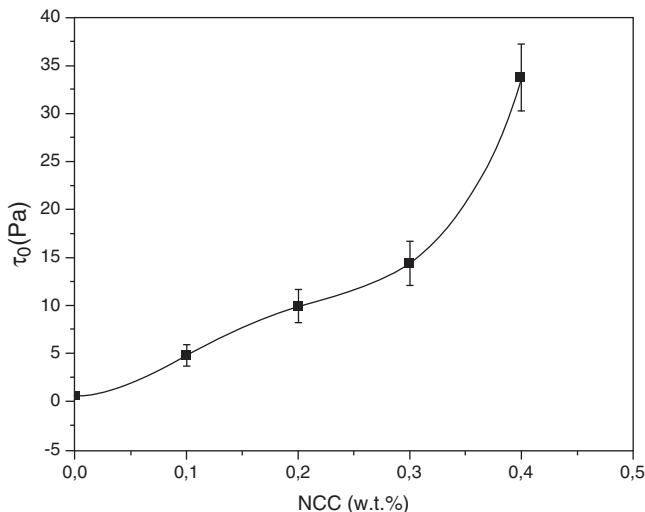


Fig. 8 Effect of different percentages of cellulose nanofibrils on cement slurry in its initial shear stress (Gomez Hoyos 2013)

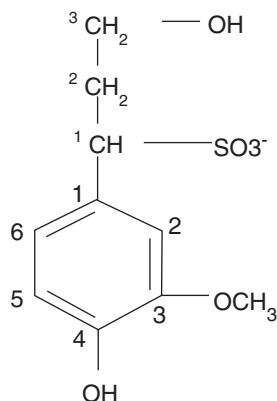
Surface modification of nanocellulose may be employed to increase or attenuate one or more enhancing properties of the abovementioned uses. Some cement slurries can even be additivated with more than one NCC with different surface modifications. Nanocellulose is usually used at concentrations between 0.01 % bwoc (Lafitte et al. 2013).

3.2 Lignin

Lignosulfonates are produced from lignin, a biopolymer contained at 20–30 wt% in wood. Pure lignin is a water-insoluble anionic surfactant obtained during wood pulping. Its surface activity may promote surface adsorption, foaming, and further particle dispersion. Lignosulfonate is the main component in the liquid waste from chemical pulp mills. It contains both hydrophilic groups (sulfonic, phenylic hydroxyl, and alcoholic hydroxyl) and hydrophobic groups (carbon chain) as it is represented in Fig. 9.

Lignosulfonate-based admixtures are the largest admixtures used, by volume, in the construction industry, typically used in dosages between 0.1% and 0.3% bwoc in concrete. They have been used as dispersants for more than 70 years (Aitcin 2000). They are low cost and can reduce up to 15% of the water content of a cement mixture, which means, decrease the w/c, increasing the mechanical properties of the hardened material, without affecting the workability during the cementing operation. These admixtures influence both the dispersion of the cement in the presence of water and the hydration rate of the cement, becoming the most used water-reducing/water-retarding admixture in the concrete industry (Vázquez and Pique 2016).

Fig. 9 Typical structural unit of lignosulfonate (Ouyang et al. 2006)



Due to their natural product source, they have to be processed because they can vary in performance from batch to batch (Vorderbruggen et al. 2016). Sulfomethylation with sodium sulfite and formaldehyde is the most common process to obtain an optimized water-soluble lignosulfonate. It yields Na-lignosulfonates (NL) or Ca-lignosulfonates (CL) with a degree of sulfonation between 0.5 and 0.6. Lignosulfonates in solution have a wide range of molecular weights. The highest the molecular weight is, the highest the water-reducing capacity in the cement paste (Ouyang et al. 2006).

It is well known that surface activity and foaming capability of the water reducers have a positive effect on the solid particles dispersing into liquid. In order to improve the water-reducing ratio of lignosulfonate, Ouyang et al. proposed to modify the lignosulfonate molecules by increasing the amount of sulfonic group, thereby altering its surface and foaming activities (Ouyang et al. 2006).

The retarding mechanism of NL is explained since lignosulfonates form complexes with calcium ions available in the cement matrix, which precipitate onto the surface of cement. Thus, the access of water to these sites is blocked and further growth of the cement hydration products is inhibited. The higher the amount of polymer precipitated on the surface, the greater the retardation (Recalde Lummer and Plank 2012).

3.3 Microbial Polysaccharides

Microbial polysaccharides are additives economically competitive with natural gums, produced from marine algae and other plants, in the oilwell industry. Plant- and seaweed-derived gums used traditionally are affected by environmental factors; there are exceptions, of course, such as carrageenan, a high molecular weight polysaccharide derived from seaweed (Fink 2015). Microorganisms, on the contrary, can be grown under controlled conditions and offer a wide range of polymers with unique structural properties. Xanthan from *Xanthomonas campestris*, sphingans

(gellan, welan, diutan, rhamsan) from *Sphingomonas* sp., and cellulose from *Acetobacter xylinum* are some of the microbial polysaccharides extensively studied due to their commercial importance (Kaur et al. 2014).

Biopolymers made by fermentation usually have a shear-thinning type of viscosity; this is what makes them so important in the oilwell industry. This means that most of the microbial biopolymers increase the yield point and show a low plastic viscosity. This is particularly useful in oilwell slurries because low viscosity when being pumped is desirable, since it decreases the pumping energy and prevents the circulation loss, and high viscosity is desirable when the pumping is over, because it favors the gel strength and the stability of the slurry (Plank 2004).

3.3.1 Xanthan Gum

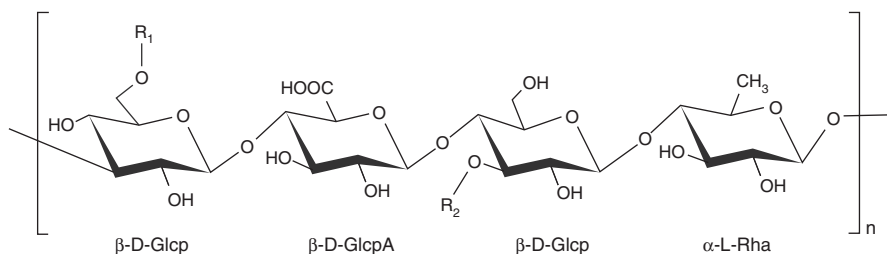
Xanthan gum was the first microbial biopolymer to be used in the construction industry and the most used nowadays. It is an exocellular biopolymer secreted by *Xanthomonas campestris*. The molecular weight of the gum is reported to be of approximately 2×10^6 Da, and it has a double helix molecular arrangement (Caenn et al. 2017). It was also stated that solutions of xanthan gum exhibits thickening properties with a pseudoplastic behavior. Xanthan gum has been used extensively in the oil industry as a viscosifier for different applications due to this unique rheological property. It is also very popular because of its suspension capabilities to water-based drilling fluids. The rheological behavior of xanthan-based fluids can be used, in addition, to control fluid loss.

Xanthan gum performs well in high viscosity systems but cross-links in the presence of calcium ions and high pH, both found in the cement slurry. It also presents some limitations; it is sensitive to high temperatures and has low tolerance to field contaminants (Gallino et al. 1996; Navarrete et al. 2000).

3.3.2 Welan Gum

Welan gum is one of the different variations of sphingans. Sphingans are structurally similar exopolysaccharides that have a comparable backbone structure except for the location of side chains as it is shown in Fig. 10. This gives the biopolymers different physical properties (Kaur et al. 2014).

It is an industrial grade of a bacterial polysaccharide gum produced by the growth of the *Sphingomonas* sp. It contains principally the neutral sugars l-mannose (L-Manp), l-rhamnose (L-Rha), d-glucose (D-Glcp), and d-glucuronic acid (D-GlcpA) in the molar ratios 1.0:4.5:3.1:2.3 (Dial et al. 2001). The welan molecule is rather stiff, whereby it becomes relatively insensitive to temperature and pH variation. This, together with its tolerance of high calcium ion concentrations, makes it ideal for applications in cement systems. It acts as a thickening, suspending, binding, and emulsifying agent, stabilizer, and viscosifier. It is used in oilwell cementing because it retains its stability and viscosity at elevated temperatures.



Name of sphingan	R ₁	R ₂
Gellan	H	H
Welan	H	←-1)-α-L-Rha or ←-1)-α-L-Manp
Rhamsan	←-1)-α-D-Glcp-(6←-1)-β-D-Glcp	H
Diutan	H	←-1)-α-L-Rha-(4←-1)-α-L-Rha

Fig. 10 Scheme of the structure of sphingan biopolymer showing different side chain and their linkage positions for gellan, welan, rhamsan, and diutan. *Glcp* is glucose, *GlcpA* is glucuronic acid, *Rha* is rhamnose, and *Manp* is mannose (Kaur et al. 2014)

Of all microbial biopolymers, welan gum was found to be the best to stabilize cement slurries and to prevent surface fluid loss at concentrations in the range of 0.01–0.9% bwoc (Kaur et al. 2014). Allen et al. claim that welan gum controls the water loss from cement slurries and remains stable until temperatures in the range of 93–127 °C (Allen et al. 1990). Üzer and Plank found that the stabilizing effect of welan gum only derives from its strong viscosifying effect on the aqueous phase of the cement slurry (Üzer and Plank 2016).

Welan gum can also stabilize a dispersant's suspension. Rapidly hydrating welan gum acts as a liquefied viscosity agent with the dispersant. Welan gum particles swell in the dispersant, resulting in a stable suspension without much viscosity increase; it is then used usually in cement slurry already containing dispersants. Nevertheless, due to its adsorption effect, it induces a retarding behavior in the cement setting (Allen et al. 1990; Kaur et al. 2014; Üzer and Plank 2016).

The use of low viscosity welan gum in cement slurries can also reduce the fluid loss. It can be obtained in a wide range of viscosities and still exhibit good fluid loss control. In some applications, the cement slurry is viscous enough; thus, additional viscosity induced by the additive would be undesirable. For these applications, a lower viscosity welan gum can be prepared which retains fluid loss control (Allen et al. 1990).

3.3.3 Diutan Gum

Diutan gum was isolated from the *Sphingomonas* genus in the 2000 decade (Navarrete et al. 2001). The chemical structure of the monomer is shown in Fig. 10. Diutan gum has an average molecular weight of 5×10^6 Da, which is much higher

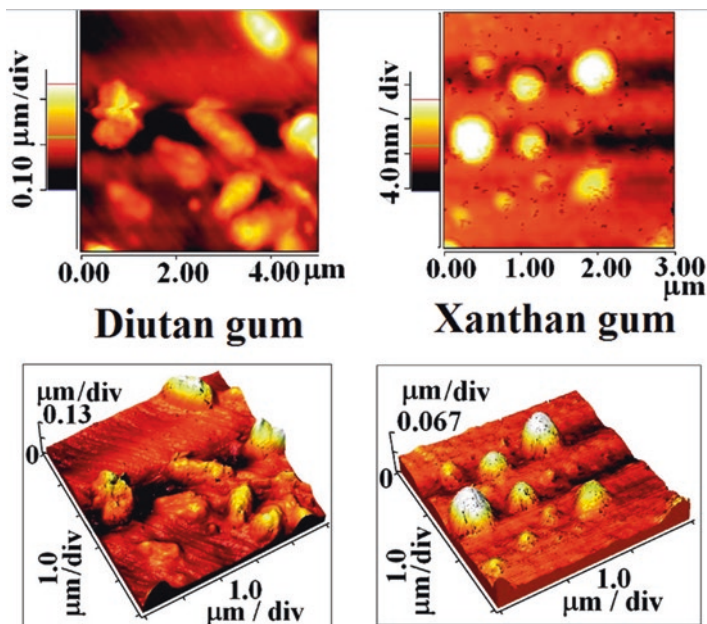


Fig. 11 Topological 2D (*top*) and 3D (*bottom*) images of diutan and xanthan gum (Adapted with permission from Mukherjee et al. (2010). Copyright 2010 American Chemical Society)

than those of welan and xanthan gum. Topological images of diutan gum, 2D and 3D, are shown in Fig. 11 and are compared with xanthan gum.

Diutan is a more efficient viscosifier than xanthan and welan gums at ambient temperature in low concentration, even in salt systems, usually present in wellbores, and at temperatures between 90 and 150 °C. The thermal stability of diutan can be improved to at least 160 °C by the presence of NaCl. Diutan is more elastic than xanthan gum and is more shear thinning than xanthan and welan, resulting in lower friction pressure losses at comparable concentrations (Navarrete et al. 2001).

Figure 12 shows the viscosity of different concentrations of xanthan, welan, and diutan gums in synthetic seawater at 24 °C. Viscosity increases with the concentration. The more viscous one is diutan, followed by xanthan and welan gums.

3.3.4 Bacterial Nanocellulose

As it was mentioned before, cellulose nanofibers can be obtained through lignocellulosic fibers or through microorganisms. Specific bacteria synthesize cellulose microfibrils as a primary metabolite. These overlap and intertwist to form a non-woven mat with very high water content (Vázquez et al. 2013). Figure 13 shows a FE-SEM image of the freeze-dried bacterial nanocellulose mat.

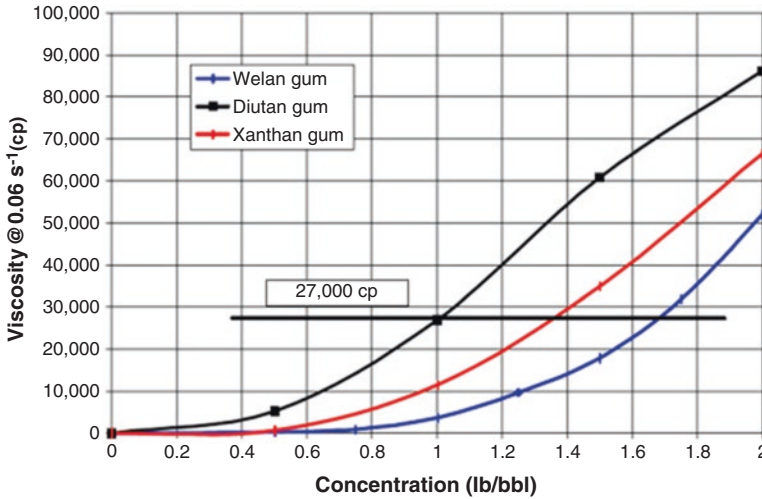
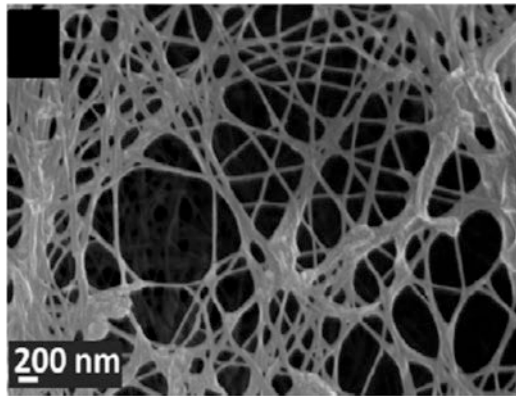


Fig. 12 Viscosity of different concentrations of xanthan, welan and diutan gums in synthetic seawater at 24 °C (Caenn et al. 2017)

Fig. 13 FE-SEM images of freeze-dried bacterial nanocellulose (Menchacanal et al. 2016)



No recent patent or papers were found that use bacterial nanocellulose in oilwell cement, but research is being done. In a recent conference, Martin et al. evaluate the modification of an oilwell cement slurry with 0.1% and 0.2% bwoc of bacterial nanocellulose. To introduce it to the slurry, the mat was mechanically mixed with the slurry’s water. As a result, the shear stress increases dramatically, the free water diminishes, and the compressive strength was enhanced (Martin et al. 2016). Many more studies should be done, but the first results show promising.

4 Conclusions (Outlook and Future Trends)

The oilwell cement industry is very demanding on chemical admixtures. Biopolymers have fulfilled these demands and are widely used in this industry, competing hand to hand with the synthetic ones. The most used are cellulose and lignin based, as well as in the general construction industry. Furthermore, the oilwell cementing industry has included the microbial biopolymers. The oilwell industry has always been ahead in technology due to its technical complexities. Therefore, there is to expect that microbial biopolymers will soon be accepted in the construction industry as well.

Biopolymers have an extra advantage over synthetic polymers. Lately, environmentally friendly products are more appreciated in many companies. An effort is being made to produce or use nontoxic, low emission, and leaching products that would be recyclable if needed and show no effects on the environment where they are fabricated and used. This applies to the construction chemicals used as additives in the oilwell cement industry.

Acknowledgments The authors acknowledge the Universidad de Buenos Aires/Facultad de Ingeniería (UBACyT 20020160100055BA), the Agencia Nacional de Promoción Científica y Tecnológica del Ministerio de Ciencia y Tecnología de la República Argentina (PICT-2016-4543) and the Consejo Nacional de Investigaciones Científicas y Técnicas (CONICET).

References

- Abbas R, Jarouj H, Dole S et al (2004) Una red de seguridad para controlar la pérdidas de circulación. *Oilfield Rev*: 20–29
- Aitcin P (2000) Cements of yesterday and today, concrete of tomorrow. *Cem Concr Res* 30:1349–1359
- Allen F, Best G, Lindroth T (1990) Welan gum in cement compositions. US5004506 A
- American Petroleum Institute (1979) Specification for Oil-well Cements and Cement Additives
- Bensted J (1996) Admixtures for oilwell cements. In: Ramachandran V (ed) *Concrete admixtures handbook*, 2nd edn. William Andrew Publishing, William Andrew Publishing, Park Ridge, pp 1077–1111
- Büllichen D, Plank J (2011) Formation of colloidal polymer associates from hydroxyethyl cellulose (HEC) and their role to achieve fluid loss control in oil well cement. In: *Proceedings of the SPE International Symposium on Oilfield Chemistry held in Texas, USA, 11–13 Apr 2011*
- Büllichen D, Plank J (2012) Mechanistic study on carboxymethyl hydroxyethyl cellulose as fluid loss control additive in oil well cement. *J Appl Polym Sci* 124:2340–2347
- Caenn R, Darley HCH, Gray G (2017) Water-dispersible polymers. In: *Composition and properties of drilling and completion fluids*, 7th edn. Gulf Professional Publishing, Boston, pp 135–150
- Charreau H, Foresti ML, Vázquez A (2013) Nanocellulose patents trends: a comprehensive review on patents on cellulose nanocrystals, microfibrillated and bacterial cellulose. *Recent Pat Nanotech* 7:56–80
- Craft B, Johnson T, Kirkpatrick H (1934) Effects of temperature, pressure and water-cement ratio on the setting time and strength of cement. In: *Proceedings of the Tulsa Meeting, Tulsa, USA, October 1934*
- Dial HD, Skaggs CB, Rakitsky WG (2001) Stable suspension of hydrocolloids. US 6221152:B1

- Fink J (2015) Cement additives. In: Fink J (ed) *Petroleum engineer's guide to oilfield chemicals and fluids*, 2nd edn. Gulf Professional Publishing, Boston, pp 317–367
- Gallino G, Guarneri A, Poli G et al (1996) Scleroglucan biopolymer enhances wbm performances. In: *Proceedings of the SPE Annual Technical Conference and Exhibition, Colorado, USA*, 6–9 Oct 1996
- Gómez Hoyos C (2013) *Utilización de las fibras naturales en la construcción*. PhD Thesis, Universidad de Buenos Aires, Buenos Aires
- Gómez Hoyos C, Vázquez A (2014) Cellulose composites for construction applications. In: Thakur VK (ed) *Applications of cellulose/polymer composites lignocellulosic polymer composites, processing, characterization, and properties*. Wiley, Hoboken, pp 435–452
- Gómez Hoyos C, Cristia E, Vázquez A (2013) Effect of cellulose microcrystalline particles on properties of cement based composites. *Mater Design* 51:810–818
- Gómez Hoyos C, Zuluaga R, Gañan P et al (2017) Use of cellulose nanofibrils as microcrack inhibitor in the cement paste. *Constr Build Mater*, submitted
- Kaur V, Bera M, Panesar P et al (2014) Welan gum: microbial production, characterization, and applications. *Int J Biol Macromol* 65:454–461
- Kaveler H (1953) Retarded set cement and slurries thereof. US2629667
- Kaveler H (1957) Sulfoalkyl cellulose ethers and their salts as hydraulic natural cement set retarders. US2795508 A
- Lafitte V, Lee JS, Ali SA et al (2013) Fluids and methods including nanocellulose. US20130274149 A1
- Martín CM, Vázquez A, Pique TM (2016) Modificación de lechadas de cemento petrolero con micro y nanoreforzados. In: *Proceedings of the VII Congreso Internacional y 21ª Reunión Técnica de la Asociación Argentina de Tecnología del Hormigón, Salta, Argentina*, 28–30 Sept 2016
- Menchaca-Nal S, Londoño-Calderón CL, Cerrutti P et al (2016) Facile synthesis of cobalt ferrite nanotubes using bacterial nanocellulose as template. *Carbohydr Polym* 137:726–731
- Mukherjee I, Sarkar D, Moulik S (2010) Interaction of gums (Guar, Carboxymethylhydroxypropyl guar, Diutan, and xanthan) with surfactants (DTAB, CTAB, and TX-100) in aqueous medium. *Langmuir* 23:17906–17912
- Navarrete R, Himes R, Seheult J (2000) Applications of xanthan gum in fluid-loss control and related formation damage. In: *Proceedings of the SPE Permian Basin Oil and Gas Recovery Conference, Texas, USA* 21–23 Mar 2000
- Navarrete R, Seheult J, Coffey M (2001) New biopolymers for drilling, drill-in, completions, spacer, and coil-tubing fluids, Part II. In: *Proceeding of SPE International Symposium on Oilfield Chemistry Texas, USA*, 13–16 Feb 2001
- Ouyang X, Qiu X, Chen P (2006) Physicochemical characterization of calcium lignosulfonate – a potentially useful water reducer. *Colloid Surf A* 282–283:489–497
- Plank J (2004) Applications of biopolymers and other biotechnological products in building materials. *Appl Microb Biotechnol* 66:1–9
- Plank J (2005) Applications of biopolymers in construction engineering. *Biopolymers Online*, 10
- Ramachandran V (1996) *Concrete admixtures handbook*, 2nd edn. William Andrew Publishing, Park Ridge
- Recalde Lummer N, Plank J (2012) Combination of lignosulfonate and AMPS®-co-NNDMA water retention agent – an example for dual synergistic interaction between admixtures in cement. *Cem Concr Res* 42:728–735
- Rincon-Torres M, Hall L (2013) Cellulose nanowhiskers in well services. US20130196883 A1
- Robertson JO, Chilingarian GV, Kumar S (1989) The manufacture, chemistry and classification of oilwell cements and additives. In Chilingarian G, Robertson J, Kumar S (ed) *Developments in petroleum Science Elsevier*, Vol 19, Part B, pp 61–100. ISSN 0376-7361, [http://dx.doi.org/10.1016/S0376-7361\(08\)70502-8](http://dx.doi.org/10.1016/S0376-7361(08)70502-8)

- Rust C, Wood W (1959) Laboratory evaluations and field testing of silica-CMHEC-cement mixtures. *J Pet Sci Eng* 12(10):1–5
- Samsuri A, Phuong B (2002) Cheaper cement formulation for lost circulation control. In: Proceedings of IADC/SPE Asia Pacific Drilling Technology, Jakarta, Indonesia, 8–11 Sept 2002
- Üzer E, Plank J (2016) Impact of welan gum stabilizer on the dispersing performance of polycarboxylate superplasticizers. *Cem Concr Res* 82:100–106
- Vázquez A, Pique TM (2016) Biotech admixtures for enhancing portland cement hydration. In Pacheco-Torgal F, Ivanov V, Karak N, Jonkers H (ed) *Biopolymers and Biotech Admixtures for Eco-Efficient Construction Materials* Woodhead Publishing, pp 81–98
- Vázquez A, Foresti ML, Cerruti P et al (2013) Bacterial cellulose from different low cost cultivation production media by *Gluconacetobacter xylinus*. *J Polym Environ* 21:545–554
- Vázquez A, Foresti ML, Morán J et al (2015) Handbook of polymer nanocomposites: processing, performance and applications. In: Pandey J, Takagi H, Nakagaito A, Kim H-J (eds) *Extraction and production of cellulose nanofibers*. Springer-Verlag GmbH, Berlin, pp 81–118
- Vorderbruggen M, Bryant S, Bottiglieri A (2016) Reducing cementing blend complexity: a single biopolymer capable of replacing multiple cement additives. In: Proceedings of the SPE Annual Technical Conference and Exhibition, Dubai, UAE, 26–28 Sept 2016

Polymers from Biomass Widely Spread in the Oil Industry

Isabel Natalia Vega and María Isabel Hernández

1 Introduction

Polysaccharides are natural polymers that come from renewable sources such as terrestrial and marine plants. For industrial purposes, these biopolymers usually present high molecular weight and are water-soluble or dispersible hydrocolloids. Recently, important improvements in bacterial biosynthesis of these polysaccharides have been carried out.

Among the gums coming from terrestrial plants that found many applications in the food industry, guar, arabic, and pectin can be mentioned. Their main features are their capacity to suspend solids and to increase viscosity, dispersibility, and emulsion stabilization (Whistler 2012).

Sometimes these carbohydrates coming from terrestrial sources behave as energy storage materials, and good examples are the seeds of locust bean gum and guar gum. The usefulness of this kind of biopolymers relies on the wide range of functional properties. As it was mentioned before, these polymers are also capable of thickening, chelating, emulsifying, suspending, and forming gels. The variety of structural conditions observed is much wider than that for synthetic polymers (Lapasin and Pricl 1995).

Guar was first introduced in the petroleum industry as drilling fluid additive in the early 1960s due to its rheological and friction-reducing properties. Later, due to the performance and cost, guar and its derivatives became the main component of the water-based fracturing fluids.

Regarding microbial polysaccharides, xanthan gum and dextran are the most popular. The use of xanthan gum is widely spread in the oil industry. It serves as viscosifying agent in drilling muds and fracturing operations, additive for filtration control in cementing as well as mobility control agent in enhanced oil recovery

I.N. Vega (✉) • M.I. Hernández

YPF Tecnología (YTEC), Av. Petróleo S/N Berisso (1923), Buenos Aires, Argentina
e-mail: isabel.n.vega@ypftecnologia.com; m.isabel.hernandez@ypftecnologia.com

(EOR) at high salinity. Other biopolymers from microbial source are scleroglucan and schizophyllan. They have potential use for EOR at high-temperature and salinity conditions.

This chapter will focus on the oil and gas applications of some of the carbohydrates mentioned above especially guar and xanthan gums. It intends to give insight into the chemistry and physicochemical properties of these water-soluble biopolymers.

2 Guar Gum and Its Derivatives

2.1 History

The guar, also called guaran, is a bean whose endosperm is basically a galactomannan (carbohydrate) known as guar gum. This annual legume has been source of food and soil crop improver for centuries. The origin of guar is unknown, but its farming is traced back in India and Pakistan. Nowadays, the growing is also spread in the United States, Australia, and Africa (Wistler and Hymowitz 1979).

Guar has many industrial applications such as food, textile, oil and gas, paper, and mineral processing, among others. As food additive, it binds water, prevents ice crystal in frozen products, and moisturizes, thickens, and suspends many liquid–solid systems. In textile, guar gum thickens dye solution enhancing printed patterns. In mineral processing, the guar gum works as flocculation agent. It enhances the separation of the mineral solids from the ore, resulting in a cleaner floated concentrate. This chapter will focus mainly on the uses of guar and its derivatives for the oil field industry.

The hydrocarbons are retained in the rock pores and its drainage to the near well-bore might be difficult. In order to stimulate the formation and make the production easier, the hydraulic fracturing allows connecting the rock pore throats and generates a pathway where the oil and gas can preferentially flow. This operation is also known as stimulation. The rock fracture is achieved by the injection of a fracturing fluid at very high pressure. This fluid is accompanied by proppant whose function is keeping the fracture open after the pumping is stopped. The most common proppant is sand, but depending on the rock hardness and depth, other solid particles like ceramics or resin-coated sands are also used.

The first fracturing treatments were performed with crude or refined oil as fracturing fluid. In 1953, water-based fluids were introduced in which starch was added to provide viscosity. Guar came into use because of its viscosifying and friction-reducing properties in addition to its safety in handling. The first fracturing treatment using cross-linked guar was performed in 1969 (Howard and Fast 1970).

Guar and its derivatives are the most extensively used polymers in fracturing fluids. The first commercial hydroxypropyl guar (HPG) was made in the early 1960s. The first commercial sale of HPG for use as fracturing fluid was in the late 1960s.

In relation to guar derivatization, to obtain hydroxypropyl guar (HPG), a reaction of guar with propylene oxide in basic media is carried out. The quantity of hydroxypropyls (HP) bonded to the polysaccharide is expressed as molar substitution. This term provides information of the total number of HP attached to the polymer.

The degree of substitution gives the average number of hydroxyls substituted per unit of sugar. If a subunit is defined as two mannoses and one galactose, nine hydroxyl units will be available for derivatization. Thus, the maximum degree of substitution turns out to be 3.

2.3 Hydraulic Fracturing Applications

Hydraulic fracture involves the use of fluids injected at high pressure to crack open hydrocarbon bearing zones. Guar is used to thicken the fracturing fluid so it can suspend and carry sand into the fractured rock. It is also known as primary gelling agent; hydrates in a pH range from 5 to 7 maintaining its water solubility without degradation. Guar derivatives such as hydroxypropyl guar (HPG) and carboxymethylhydroxypropyl guar (CMHPG) are also used as gelling agents. Other nonguar-based gelling agents could be hydroxyethyl cellulose (HEC), carboxymethyl cellulose (CMC), and xanthan. All of these gelling agents are water-soluble polymers that increase the viscosity of water. Increasing viscosity of water lowers friction pressure, increases proppant transport, lowers fluid loss, and increases fracture width. In the oil industry, the solution containing the hydrated gelling agent is called “linear gel” or “base gel.” Typical linear gel viscosity range is from 10 to 30 cP. These linear gels find application in stimulation with foams and in unconventional fractures.

In the case of the foams, the base gel is mixed together with a surfactant and a gas, usually nitrogen, to form the foam. Due to the fluid density affecting the surface injection pressure and the ability of the fluid to flow back after the treatment, these systems are especially applied in low-pressure reservoirs where low-density fluids are needed to improve the cleanup after fracturing.

Gelling agents are usually dry powders or hydrocarbon-based slurries. It is known that the stability of the biopolymer solutions is affected by temperatures higher than 50 °C, presence of bacteria, transition metals, and strong acids.

In order to enhance the fracturing fluids' rheological properties and their capacity for transporting proppant, guar gum or its derivatives are gelled. The most extended cross-linkers for this application are the borates. According to the oil industry best practices and with the objective of maintaining the proppant suspended in the fluid, the viscosity of a fracturing fluid should be at least 100 cp (API RP 39 1998).

Historically, the evolution of guar gum gels cross-linked with borates was full of obstacles and technical problems due to their high sensitivity to water quality, high-pressure pumping mechanical degradation, temperature limitations, and presence of bacteria and iron and sulfates that affect the gel quality.

In consequence, many developments have been carried out to obtain fracturing fluids resistant to high temperatures but conserving their rheological properties.

The cross-linkers that showed the best results for these harsh conditions were titanates and zirconates. They form stable covalent bonds with the polysaccharide, whereas the borate–guar bonds are reversible. The gels formed with organometallic cross-linkers provide reliable performance, and their breakage times can be adjusted according to the operative requirements.

However, the bonds of these systems were irreversible so they were easily and irreversibly degraded under applied shear stress. Due to this shear degradation, the proppant placement turned out to be a very difficult operation. That is why the efforts were concentrated in optimizing these systems. The strategy of delaying the cross-linking would prevent the mechanical degradation while pumping (Conway and Hsu 1981; La Groe et al. 1984). This effect was achieved by the addition of a ligand that chelated the metallic ion. At high temperatures, these chelates break and the metal ion is again available for bonding to guar.

In some cases when certain transport properties are required from the beginning of the pumping, the chelates are pumped together with a borate-type cross-linker that bonds to the polymer at low temperatures, where the organometallic cross-linker is inactive.

The fracturing fluid final viscosity is controlled by the polymer concentration. The fracture width is increased with the viscosity raise. The fluids that present high viscosities have been developed to obtain wider fractures better conductivity and capacity of transporting higher proppant concentrations. This kind of fluids is specially designed for in deep hydraulic stimulation where the pumping rate is low, so high viscosity and thermal stability are required. Figure 3 shows typical viscosity profiles for high-temperature fracturing gel. It can be observed that at higher temperatures, the gel stability is diminished.

These tests are galactose generally performed at three different shear rates, 170 s^{-1} , 100 s^{-1} , and 40 s^{-1} , to check the quality of the products to be injected and make any final adjustment to the formulation before each fracturing operation. The first rate (170 s^{-1}) simulates the fluid entering into the reservoir passing through

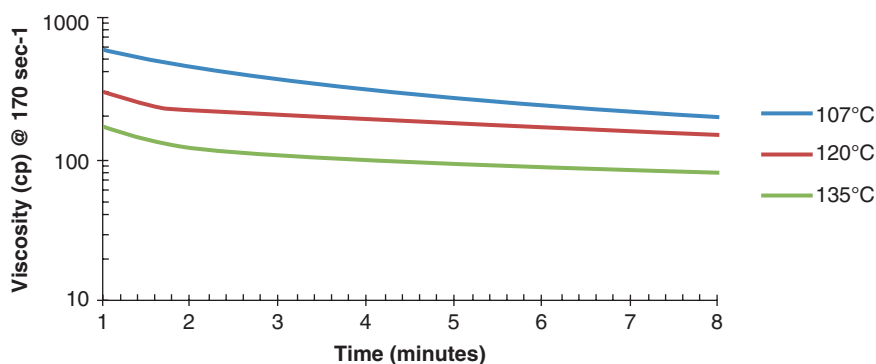
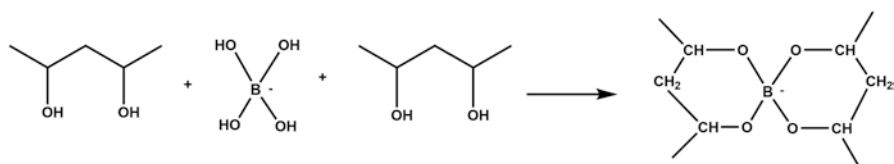


Fig. 3 Viscosity profiles: aqueous gel for high temperatures (Reprint from Seright et al. (2011). Copyright (2011) with permission from Seright)

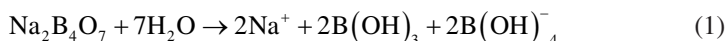


Scheme 1 Cross-linking of borates with the hydroxyl groups

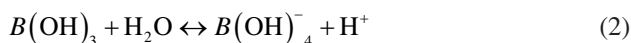
the shots, 100 s^{-1} is an average flow velocity, and 40 s^{-1} tests the proppant transportation capacity at low rates (the fluid flowing into the pipes).

When resistance to high temperature, shear stability, and viscosity capacity is required, guar should be replaced by more robust derivatives. CMHPG fulfills these requirements as well as low residue content.

With regard to guar–borax gels, the cross-linking effectiveness is a function of pH. The sodium tetraborate dissociates in water to form monoborate according to Eq. 1:



If the pH is raised by alkali addition, the equilibrium is displaced to the monoborate ions production (Eq. 2):



At room temperature and a pH of 8.5, the monoborate concentration is enough to start the cross-linking through the polysaccharide hydroxyl groups. These bonds are weak and labile (Zasadzinski et al. 1986; Kesavan and Prud'Homme 1992; Power et al. 1998) (Scheme 1).

The exact cross-linking mechanism is not well established due to the physical nature of these gels. The cross-linking points are weaker than covalent bonds and potentially reversible (London forces and hydrogen bonds). These points should act together to assure the gel stability. In physical gels, the forces by which the polymer chains are stuck together make it hard to establish the exact quantity of bonds because they are temporary. The number of bonds and their position fluctuate within time and temperature. Because of the reversibility of these unions with temperature, the physical gels are also known as thermoreversible gels (1989).

2.4 Drilling Applications

In the oil industry, the process by which a deep hole is open into the earth is known as drilling operation. The tool used to achieve this is a long bit attached to a string. This bit is lubricated with a special mud that circulates in and out of the hole. Moreover, the rock cuttings that are being generated during drilling are suspended

and transported by this mud. Once in the surface, the mud together with the cuttings passes through a sieve to remove the solids. The clean mud is then reinjected.

Viscosification of a drilling mud confers the property of suspending solids in it as the frac fluids support the proppant. The ability of guar and its derivatives of developing viscosity in freshwater as well as in brine makes them also useful for drilling applications. Synthetic polymers such as polyvinyl alcohol and polyacrylamide are also applied in mud viscosification.

2.5 Guar Properties

2.5.1 Hydration

One of the most important properties of guar gum for fracturing and drilling applications is the hydration capacity. Once the polymer is dispersed, the ability of absorbing water will dictate the hydration rate. When the guar particles contact the aqueous phase, they incorporate water and swell. If the particles do not disperse easily, the external particles will absorb water preventing further hydration. As a result, gel particles also called “fish eyes” appear and the theoretical viscosity target is not achieved. By the addition of some additives together with the adjustment of the particle size, the desired dispersibility can be enhanced.

The hydration will depend upon the pH, applied shear, polymer concentration, original mixing phases, salt type, and concentration. For charged polymers, the viscosity development is reduced by the increment of salt content, especially salts containing divalent ions. As long as guar and HPG are an uncharged polysaccharide, this is the reason why its viscosity is barely affected by the presence of monovalent salts. Nevertheless, the presence of multivalent ions at high concentrations could precipitate these biopolymers. In the case of the anionic CMHPG, even the monovalent cations affect the viscosity development. This behavior is due to the polymer chains’ contraction through the electrostatic repulsion of the anionic groups.

The hydration rate of guar and its derivatives is optimum at mild acidic pH (5–6). At extreme pHs, the guar gum is destroyed. Strong acids cause the hydrolysis of the polysaccharides. Once hydrated, guar and its derivatives remain in solution and are quite stable at room temperature. As biopolymers, these polysaccharides are susceptible to bacterial attack especially above 45 °C.

2.5.2 Rheology

Dynamic oscillatory measurements at small deformations provide powerful microstructural information. This technique is commonly used for determining gel microstructure and their gelling time. This last property is dependent on the polymer and cross-linker concentrations as well as the temperature and solution salinity.

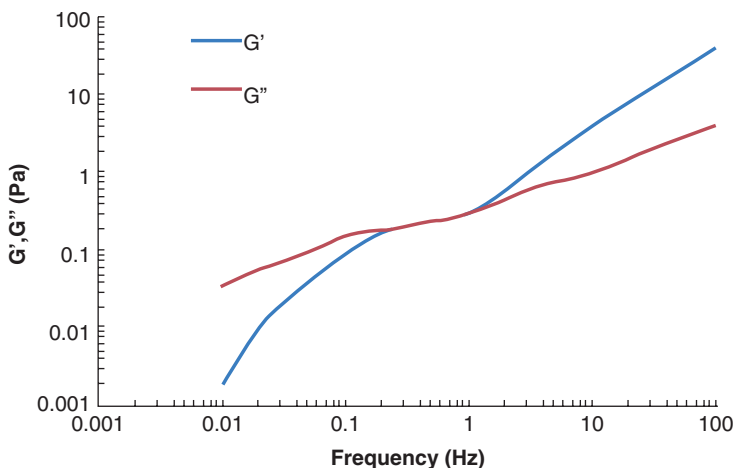


Fig. 4 Loss modulus (—) and storage modulus (—) as function of frequency of the guar gum solution

Some materials present intermediate properties between solids and liquids, known as viscoelastic materials. A tridimensional network such as the guar–borax gel is an example of a viscoelastic material. In rheology, the viscoelastic behavior can be described by two quantities, G' and G'' . The G' , known as the storage modulus, represents the elastic contribution of the gel and G'' is the loss modulus that is related to the viscous contribution of the system.

Below a critical frequency around 0.3 Hz, the liquid system behaves as a high molecular weight melted polymer where transient networks are formed due to the temporary chain entanglements. The viscous modulus is higher than G' . The dependence of the storage modulus with the frequency is directly proportional; meanwhile the loss modulus is proportional to the square of the frequency. At frequencies higher than 0.3 Hz, the system exhibits a solid-like behavior in which the G' is dominant (Fig. 4) (Vega et al. 2008).

The linear gel exhibits transient interactions between chains; that is why some changes in the rheological properties could be detected; but only in a tridimensional network, such as a gel, can a net transition from liquid to solid be observed. The guar–borax gel has a predominant solid-like behavior because G' turned out to be higher than G'' in all the studied range. The moduli were independent of the applied stress up to 5 Pa, being the limit of the linear viscoelastic range (Fig. 5).

2.5.3 Thermal Stability

Regarding guar–borax gel thermal stability, the storage modulus presents a pseudo-equilibrium plateau at lower temperatures, being G' rather independent of temperature. This pseudo-equilibrium is probably associated to the interactions between guar

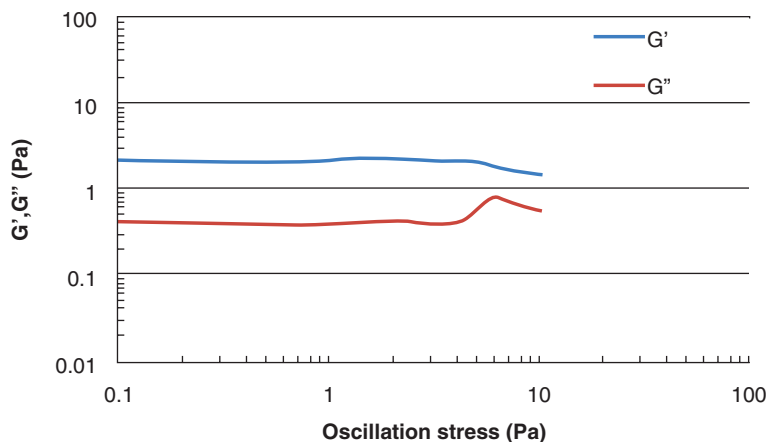


Fig. 5 Loss modulus (—) and storage modulus (—) as function of oscillation stress and 1 Hz at 25 °C for guar gum hydrogel

particles, through borax bridges, responsible for the hydrogel formation. As the temperature increases, the borax–guar interaction weakens and the elastic modulus decreases with temperature up to a complete disappearance of the interactions. Where G' crosses over the G'' , the melting process of the hydrogel is taking place (Fig. 6).

Although the gel breakage temperature is in some measure determined by the polymer and cross-linker concentrations, the guar–borax system should be recommended for moderate temperatures.

2.5.4 Chemical Stability

The guar chemical stability and its derivatives are affected by the presence of strong acids and transition metals.

On the one hand, the glycosidic linkage hydrolysis can be produced by the attack of strong acids, resulting in the polysaccharide chain scission. This leads to the solution viscosity loss due to the molecular weight reduction.

On the other hand, the oxidative/reductive reactions can also degrade the polysaccharides. This kind of reactions involves the biopolymer oxidation in the presence of oxygen via free radicals. Iron (II) and iron (III), among other transition metals ions, can promote this process. These ions help to produce very reactive species, such as oxygen and hydroxyl radical anions, hydroperoxides as well as hydrogen peroxide that degrade the polysaccharide. This oxidative process is also known as Fenton reactions (Ramsden and McKay 1986a, b). The metallic ions catalyze the hydroperoxides' and hydrogen peroxides' decomposition to give additional radicals. These radicals provoke further carbohydrate oxidation due to their power of abstracting hydrogen.

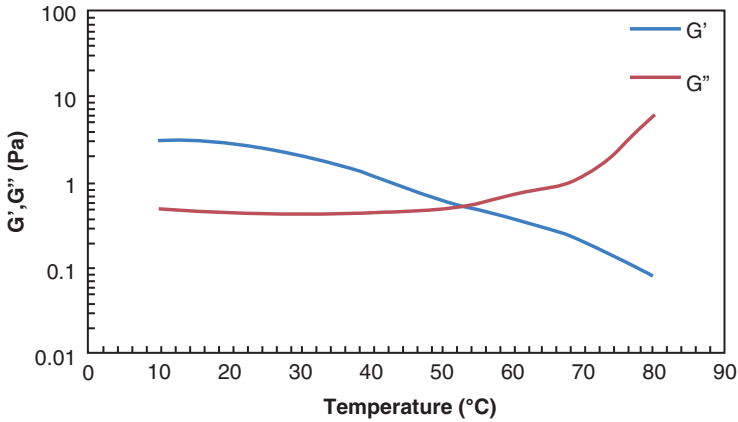


Fig. 6 Temperature sweep for the guar gum–borax hydrogel. Viscosity profiles: aqueous gel for high temperatures (Reprint from Seright et al. (2011). Copyright (2011) with permission from Seright)

The addition of oxygen scavengers such as methanol, thiourea, and sodium thiosulfate improves the carbohydrate solutions' stability especially at high temperatures.

Maintaining pH around 8–8.5 promotes the viscosity retention preventing the polysaccharide from acidic hydrolysis.

In solution, guar and its derivatives are easily degraded by aerobic and sulfate-reducing bacteria. The addition of biocides is a common practice to protect them from the attack. Aldehydes like glutaraldehyde, quaternary amines, and amides are incorporated as biocides.

Once the hydraulic fracture is completed and the proppant is placed into the formation, the fracturing fluid is brought back to surface in a broken form, and the fracture conductivity should be restored. This flow-back fluid must exhibit low viscosity to assure an easy cleanup after the treatment. If gel residues or invaded polymer remain in the proppant pack or in the naturally occurring fracture networks, they will cause severe damage and the oil production will be hindered. Thus, optimizing the breaker schedule is vital to the frac treatment success. Moreover, the mechanisms by which each breaker degrades should be taken into account for the treatment design.

The nature of the breakers can be enzymatic or chemical, and their aim is to produce a controlled and predictable viscosity loss. The rate of this degradation process is controlled by the type of breaker, concentration, and temperature.

One of the most commonly used breakers for fracturing fluid is the enzyme hemicellulase, whose effectiveness is optimum below 50 °C, losing its activity at higher temperatures. In those cases where enzymes cannot be applied, they could be replaced by oxidants such as ammonium or sodium persulfate.

3 Xanthan Gum in Enhanced Oil Recovery

Historically, the stages that describe the oil production from a reservoir are primary, secondary, and tertiary. Primary recovery results from the displacement energy naturally existing in a reservoir. Traditionally, secondary recovery process has been water flooding, and tertiary recovery or EOR (enhanced oil recovery) process uses some type of fluids (e.g., gas, steam, polymers, surfactants) that supplement the natural energy present in the reservoir or displace oil to a producing well. However, in many cases like heavy oil reservoir, EOR process is implemented from the beginning of the production; so far the oil viscosity is too high to be produced with their natural energy at economic rate. In other reservoir cases with combination of heterogeneity and high viscous oil, the secondary recovery become uneconomical and EOR process can be implemented as secondary recovery. It could be a great opportunity for the use of the polymer flood process.

Water flooding became the standard practice in many reservoirs. However, it has weaknesses, in particular, the inefficiency in oil displacement as a result of either an unfavorable mobility ratio (M) or large heterogeneity.

The mobility ratio and the polymer recovery mechanism are the key to understand how the water flooding may be remedied using polymer.

Mobility ratio (M) is defined as

$$M = \frac{\lambda_o / \mu_o}{\lambda_w / \mu_w} \quad (3)$$

where λ , μ , and K are mobility, viscosity, and effective permeability, respectively, and the subscripts o and w refer to oil and water. During water flooding, oil is left behind because it is in some way bypassed. Unfavorable mobility ratio is one of the most important aspects that contribute with this phenomenon, and a high oil viscosity and the reservoir heterogeneities are involved. When $M > 1$, the mobility ratio is unfavorable because the water moves faster. Increasing the water viscosity by using water-soluble polymers has been an extended technology. In many cases, it may be necessary to reduce the mobility ratio to less than 1, especially when larger-scale heterogeneities occur (vertical stratification or areal channel sands), which could need a high water viscosity and require a more efficient polymer (Sorbie 1991; Green and Willhite 1998).

Figure 7 (a and b) illustrates the improvement of the polymer flooding process as compared with water flooding.

During the polymer flood process, the mobility control agent should be able to transport through the reservoir during 2 or more years maintaining their integrity. It has been a big challenge for polymer molecules because they have to support the reservoir conditions such as temperature, salinity, and hardness and also be stable to the attack of some contaminants like redox par and bacteria. Other important required properties are mechanical stability, good injectivity, and low rock retention.

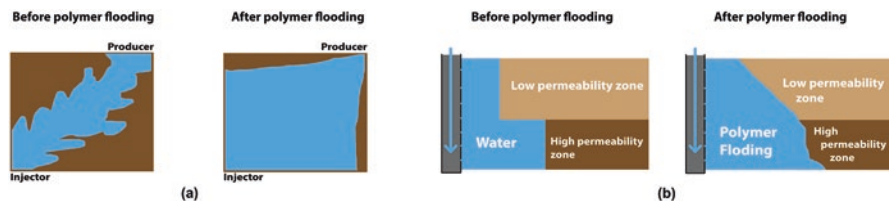


Fig. 7 A real sweep efficiency (a) and vertical sweep efficiency (b) using polymer

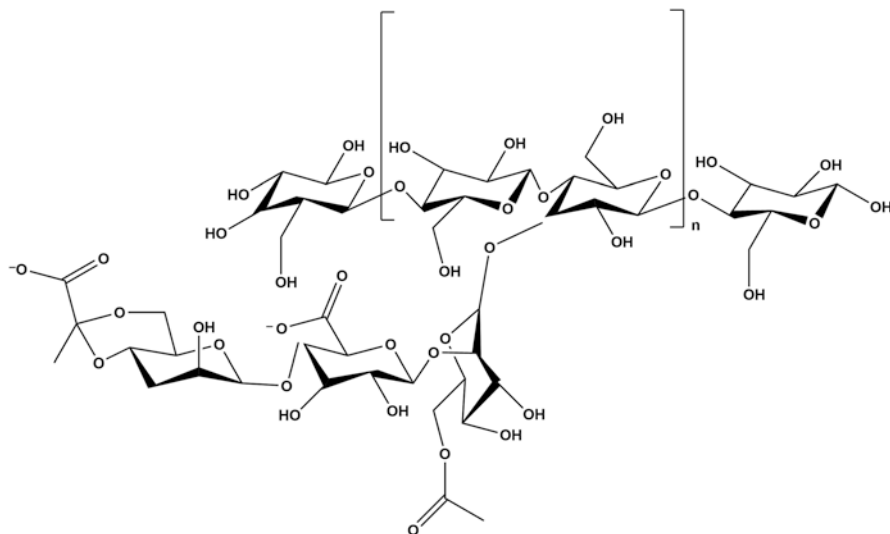


Fig. 8 Xanthan structure

3.1 Xanthan Gum Origin, Production, and Properties

Xanthan gum is an exopolysaccharide produced by a bacteria of the genus *Xanthomonas*. It was discovered at the Northern Regional Research Laboratory (NRRL) of the US Department of Agriculture while they were looking for substitutes of the gums of vegetable origin. This polysaccharide was reported for the first time in 1961 as a fermentation product of *Xanthomonas campestris* NRRL B-1459 and was called xanthan. Later, it was established that it consisted of a cellulosic backbone substituted on alternate D-glucose units by a side chain of D-mannose and D-glucuronic acid trisaccharides in a 2:1 molar ratio (Fig. 8). The β -linked or external mannose unit is substituted at positions 4 and 6 by the pyruvic acid acetal residues. On the other hand, the internal or α -linked mannose is O-acetylated at position 6. The molecular weight of xanthan ranges from 1.25 to 10 million g/mol (Azuaje and Sánchez 1999).

3.2 Industrial Production

The most important parameters involved in the xanthan gum production process are the source of carbon, nitrogen, and phosphorus, air flow, fermentation time, pH, temperature, and stirring rate. Lab tests indicate that the best xanthan production conditions to obtain a 24.01 g/l biomass concentration and a xanthan concentration of 15.21 g/l are using sucrose as the source of carbon, using peptone as the source of nitrogen, and a fermentation time of 96 h at 35 °C and a pH of 6.5 (Chavaran and Baig 2016). In general, a yield of 50–60% is very reasonable, considering the presence of cells, organic materials, and inorganic salts which are co-precipitated during the purification process. Sucrose is considered to be a better substrate than glucose and other sugars (Garcia-Ochoa et al. 2000).

The main objective of the purification process is to obtain microbiologically stable xanthan gum in solid form, which is easy to handle, store, and transport. In this process, it is also important reducing the level of non-polymeric solids to improve the functional performance. The inactivation of undesirable enzymes, such as cellulase, pectinase, etc., is sought to preserve the chemical properties of the polymer for special applications. The cell removal operation is a key requirement for food-grade xanthan gum. In order to remove the cells by conventional procedures such as centrifugation, filtration, and flocculation, it is necessary to conduct several dilutions of the broth until the appropriate viscosity is obtained. As an alternate method, cells may be removed by treating the stock with lytic and proteolytic enzymes in order to cleave the cells into low molecular weight molecules (Garcia-Ochoa et al. 2000). As can be deduced from the above, the purification procedures of xanthan gum determine the degree of purity, the content of non-polymeric solids, and its solution behavior; therefore, this will depend on the processes each manufacturing company uses.

3.3 Solution Properties

The molecular conformation of xanthan gum in aqueous solution may suffer a transition from an ordered helix-like structure into a disordered flexible coil depending on the temperature, the ionic strength, and pH value, as well as on the content of acetate and pyruvate present in the molecule (Gulrez et al. 2012; Milas and Rinaudo 1984). These conformational changes modify the solution properties and the stability. The temperature at which it occurs is named transition temperature (T_m) or melting temperature.

Figure 9 shows the conformational and structural changes of xanthan gum with temperature. It shows the native rigid double helical conformation. When heated to a temperature above the transition temperature (T_m), the polymer changes into a flexible coil conformation, where the hydrodynamic volume diminishes and accordingly so does the viscosity (Gulrez et al. 2012; Milas and Rinaudo 1984). T_m is very sensible to the water salinity and hardness. In very low-salinity water, T_m is near

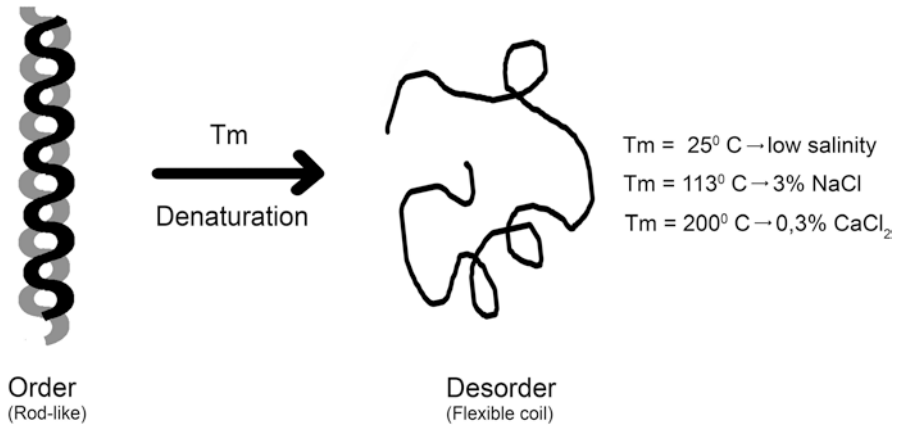


Fig. 9 Conformational changes and transition temperature (TM) (Reprint from Manichand and Seright (2014). Copyright (2014) with permission from Seright)

room temperature, and it is near 100°C in 3% of sodium chloride and near 200°C in 0.3% of calcium chloride (Seright and Henrici 1990).

Xanthan gum production conditions may also lead to compositional differences, such as changes in the ratio of acetate and pyruvate groups. They may change depending on the operational conditions, the growth conditions, and the strain of *Xanthomonas* used. This change in the composition translates into changes in its rheological behavior of the polymer (Sandford et al. 1977; Abbaszadeh et al. 2015). It has been established that the pyruvate concentration may range from 0% to 100% depending on the strain of *Xanthomonas* sp. used (Seright and Henrici 1990).

Xanthan polymers with a high acetate and/or pyruvate content produce higher viscosity aqueous solutions because intramolecular associations are favored. Likewise, the transition temperature (T_m) depends on the pyruvate and acetate content, as well as on the salt and polymer concentration and pH. High and low levels of acetate and pyruvate promote low transition temperatures and, therefore, destabilize the xanthan helix.

The destabilizing effect of pyruvate can be explained by an increase in the internal repulsion of the ionic side chains.

Acetate groups contain methyl groups, which are closer to the center of the helix and, therefore, less available for intermolecular interactions. Acetyl groups may form hydrogen bonds and, consequently, can act as stabilizers for xanthan (Abbaszadeh et al. 2015).

Operational xanthan gum manufacturing conditions also affect the average molecular weight of the polymer. Variables that have been studied so far emphasize the role of the pyruvate content as a quality indicator of the gum.

The modification of the nutrients used in the fermentation, for instance, the source of nitrogen or phosphorus affects the xanthan gum the composition of its monomeric units. The use of a source of organic nitrogen increases the pyruvate content in the xanthan molecule. However, other studies report that the best source

of nitrogen to obtain a high degree of pyruvates is acid ammonium phosphate (Casas et al. 2000).

Fermentation time is another important variable that affects the molecular structure of xanthan. Both acetate and pyruvate contents, and average molecular weight, increase with fermentation time under any operational condition.

Fermentation temperature is another variable to be taken into consideration. Temperatures above 34 °C produce a polymer with a low acetate and pyruvate content, as well as with a low average molecular weight and, therefore, low-viscosity solutions. The opposite happens at 25 °C, where xanthan with a high content of acetate and a high molecular weight is obtained, which generates high-viscosity solutions (Casas et al. 2000).

One of the most important properties of xanthan when used in enhanced oil recovery is the ability to produce high viscosities at low polymer concentrations in high-salinity and high-hardness water, where actually used partially hydrolyzed polyacrylamides (HPAM) suffer dramatic viscosity decrease and precipitation according to the divalent ions' concentration and temperature (Moradi-Araghi and Doe 1987). Polyelectrolytes, such as HPAM, show viscosity decreases in the presence of salts. The coil contracts leading to a decrease of the hydrodynamic volume. Xanthan gum, on the contrary, despite the fact of being a polyelectrolyte, suffers a cooperative transition from a disordered to an ordered and more rigid conformation. This allows the polymer to keep its viscosity properties even in high-salinity environments. In the Fig. 10, the HPAM viscosity behavior with salinity increment versus

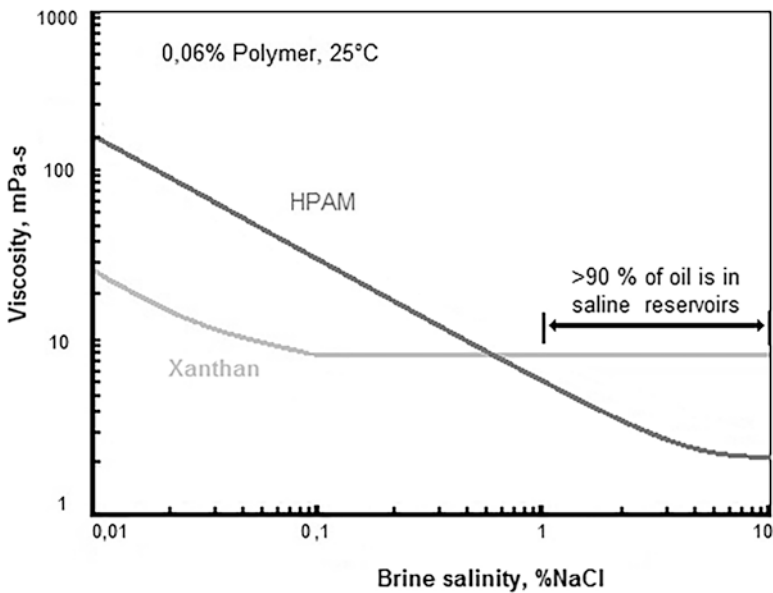


Fig. 10 Viscosity behavior of xanthan a HPAM in salinity water

xanthan is represented. The xanthan maintains the viscosity in a sodium chloride range of 0.1% to 1% that corresponds to the salinity range of the 90% of the reservoirs. The HPAM viscosity decreases dramatically.

The rheological behavior of xanthan shows that the viscosity decreases with shear rate over a wide range of shear rates. To very low rates, it shows a Newtonian plateau, which fits the Carreau model (Eq. 4).

$$\mu_{(\dot{\gamma})} = \mu_{\text{inf}} + (\mu_0 - \mu_{\text{inf}}) \left[1 + (\lambda \dot{\gamma})^2 \right]^{(n-1)/2} \quad (4)$$

where:

μ_0 = viscosity at zero shear rate (Pa.s)

μ_{inf} = viscosity at infinite shear rate (Pa.s)

λ = relaxation time (s)

n = power index

3.4 Stability of Xanthan Gum Under Operational Conditions

3.4.1 Thermal and Chemical Stability

The stability of xanthan is very associated with the T_m . Below this parameter, the structure is maintained rigid rodlike conformation and the macromolecule is more stabilized. In low-salinity aqueous solutions, the conformational transition of xanthan from rigid rodlike to flexible coil occurs at a temperature close to room temperature. The transition temperature (T_m) increases in direct proportion to the logarithm of the salt concentration. T_m is more sensitive to divalent cations than to monovalent ones and is also affected by the acetate and pyruvate content molecule. Therefore, high values of T_m are expected in high-salinity solutions such as formation brines. Therefore, thermal stability of xanthan gum is expected to be higher in brines than in de-ionized water. In saline solutions, xanthan gum molecules are protected against chain scission thanks to their helical conformation. In low-salinity solutions, xanthan gum is in a disordered coil conformation, which is susceptible to chemical attack (Seright and Henrici 1990).

Another relevant aspect is the degradation of xanthan gum by redox mechanisms involving free radicals. This phenomenon is the same as that described for guar gum (Ramsden and McKay 1986 a, b). Molecular oxygen may form hydroxyl and peroxide radicals during the oxidation of certain agents such as iron (II) and sulfides, which are commonly found in oil production water. These radicals play an important role in the degradation of both xanthan gum and polyacrylamides. The use of free-radical transfer agents (thiourea), sacrificial agents (oxidizable alcohol), and oxygen scavengers has been proposed to minimize these degradations.

However, nowadays the best way to control these kind of reactions is guaranteeing that the polymer is mixed under an inert atmosphere, keeping the whole

injection/flooding process completely sealed, and ensuring that pipelines have no corrosion cracks.

Another xanthan degradation mechanism is polymer hydrolysis. Some of the xanthan bonds are susceptible to hydrolytic degradation. Acetate groups are susceptible to base-catalyzed hydrolysis. Half-life of acetyl groups is expected to be 130 days at 60 °C at pH 6 and it decreases sharply with pH; therefore, when xanthan is injected in enhanced recovery operations and the polymer is submitted to temperatures above 60 °C, the polymer is expected to be completely free of acetate over the years, and this would reduce the solution viscosity of xanthan.

The other labile groups present in the xanthan molecule are the pyruvate-ketal groups, which may be hydrolyzed by acid catalysis. Also the glycosidic bonds are susceptible to hydrolysis. It is conceivable that hydrolysis is a degradation mechanism of xanthan given when the polymer remains in the reservoir for long periods of time (Seright and Henrici 1990).

3.4.2 Microbiological Stability

Xanthan gum is a polysaccharide with a high resistance to biological degradation by most of microorganisms. However, it has been reported that some microorganisms produce enzymes that are capable of degrading this polymer. The biological degradation process is mediated by the enzyme secretion to the media, and not all microorganisms are able to produce all the enzymatic machinery necessary to completely degrade or depolymerize the molecule of xanthan. The main enzyme reported in literature is xanthanase (endo- β -d-glucanase), which hydrolyzes the cellulosic backbone of xanthan. Another enzyme is xanthan lyase, which hydrolyzes the manose ends of the biopolymer side chains (Hovland 2015).

From an operational point of view, these facts indicate that, despite of xanthan molecule degradation resistance, there are bacteria, which are able to break it down, and therefore, it is essential to add biocides to the formulations. It is also important to know that some of the enzymes that degrade xanthan can resist sodium chloride concentrations of 4% and temperatures from 48 to 65 °C and show an optimal activity at a pH of 6 (Ahlgren 1991; Ruijsenaars et al. 1999). This would allow to infer that at reservoir temperatures above those values, at which xanthan is not resistant, these enzymes would be denatured and, therefore, unable to degrade it.

3.4.3 Mechanical Stability

When injected in the field, the solution may be submitted to high shear rates during the polymer mixing, and pumping processes, as well as due to the choke valves, and thus the polymer may be degraded. Polyacrylamides are very susceptible to this kind of degradations, while xanthan gum is practically inert. Additionally, during well injection, high shear and extensional stresses are created when the solution

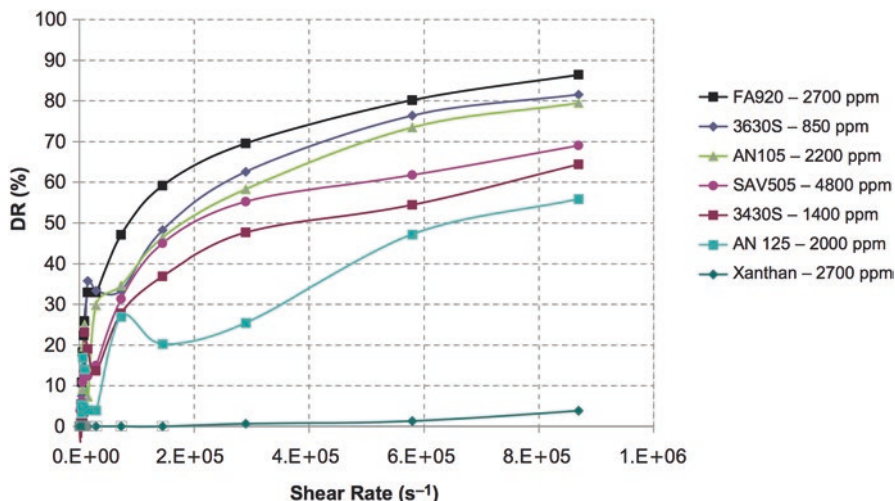


Fig. 11 Mechanical degradation of xanthan compared with several polyacrylamides

comes from a pipe flow and is forced into a porous media; molecules in flexible coil conformation, such as polyacrylamides, are degraded, while semirigid molecules, such as those of xanthan, which are rodlike, are easily aligned and pass through the pores without breaking down. Figure 11 shows a comparison of the degradation of a group of modified polyacrylamides and a xanthan gum when solutions are passed through a capillary tube. It can be observed that xanthan gum does not break down even when submitted to shear rates in the order of $870,000 \text{ s}^{-1}$. During the test, the strain regime applied was elongational flow at the entrance, followed by shear flow in the capillary tube and later relaxation at the exit. Coiled molecules are forced to stretch at the entrance of the capillary tube and this stretching causes the bonds breakage. On the contrary, xanthan gum, with its semirigid rodlike structure, does not stretch under shear and elongational stress. Furthermore, the length of the rod does not change ($0.8 \mu\text{m}$) and this value is considerably smaller than the one of a stretched polyacrylamide ($10 \mu\text{m}$), and therefore, friction forces on the carbon-carbon bonds are smaller (Zaitoun et al. 2012).

4 Behavior During Injection and Flow into the Reservoir

The development of a successful polymer injection process is important to understand and control some factors that can have negative impact on the economy of the project, such as polymer retention in the porous media, which would lead to significant polymer losses and a decrease in injectivity, with a consequent delay in the production of the hydrocarbon.

4.1 Retention

The polymer retention in the porous media creates a delay in the flow advance of the polymer solution in the reservoir, while enormous quantities of product are lost when retained. The retained quantity is expressed as polymer mass by rock mass unit (μg of polymer/g of rock) and can be estimated through experimental flow studies in reservoir rock, when comparing the polymer flow behavior with a small molecule named tracer (API RP 063 1990). However, today it is more convenient to quantify the retention during a pilot test as the result could be significantly higher than expected. It can impact the project economy (Manichand and Seright 2014).

There are three phenomena that contribute to the retention: adsorption, mechanical entrapment, and hydrodynamic entrapment. Polymer adsorption is the adhesion of the macromolecule onto the rock surface. When an aqueous polymer solution flows through natural porous media, there may occur a number of interactions between the polymer macromolecules and the rock surface, such as electrostatic attractions, Van der Waals forces, or hydrogen bonds, thus producing adsorption to a greater or lesser extent.

On the other hand, as the reservoir rock is constituted by a network of interconnected pores with a wide pore size distribution, which may have a lot of very thin throats, the transport of the macromolecules into the porous media may be affected by the of molecular entrapment effects. Since 70 decades, several mechanisms have been reported for these phenomena (Sorbie 1991; Zitha and Botermans 1998). The hydrodynamic entrapment is caused by the increase of hydrodynamic forces acting upon polymer molecule. It has been identified as strongly flow rate dependent and reversible (Zhang and Seright 2015).

Huh indicated that approximately half of xanthan retention was attributed to adsorption and half was because of mechanical entrapment (Huh et al. 1990).

Many studies have shown that the adsorption in reservoir rock is ruled by the presence and quantity of clays, as they have a positive charge on their faces, that interact electrostatically with the negative charges of the xanthan and the partially hydrolyzed polyacrylamide molecules. Additionally, clays have a great surface area, which increases the adsorbed amount to the same extent (Zaitoun and Kohler 1988; Chiappa et al. 1999).

More recently, it has been found that iron content also has an important role, together with aerobic or anaerobic conditions. In static experiments, siderite contents do not depend on whether the dissolved oxygen is present. For a broad range of pyrite contents, the adsorption is significantly lower in the absence of dissolved oxygen, than under aerobic conditions. It is related to the iron solubility (Wan and Seright 2016). This leads to the need to study rock mineralogy in detail and to evaluate the extent of the influence of these parameters when choosing a reservoir for a polymer flooding project.

Recently, a review about the factors affecting the retention of xanthan and polyacrylamides has been published. They analyze several parameters. In Table 1, a general summary from their results is shown (Manichand and Seright 2014).

Table 1 General conclusions from Manichand and Seright (2014)

Parameter	Conclusions
Mineralogy	Clay and Iron are very important
Polymer type	Xanthan had shown less retention than HPAM
Polymer concentration	Depends on concentration (diluted or semi-diluted)
Salinity	NaCl content not so important. Calcium content may be important
Permeability	Very important below 100 mD. Less important above 200 mD
Oil saturation	Minor effect

Modified with author authorization

The lower retention observed for xanthan compared to HPAM may be explained by the unavailability of functional groups in xanthan gum to interact physicochemically with the rock, on the one hand, and, on the other, by its rodlike conformation, which allows this polymer to align with the flow, thus reducing the possibility of entrapment.

Inaccessible pore volume (IAPV), which is opposed to retention, is another flow behavior that may be observed. It originates from the fact that macromolecules travel faster than the tracer due to a size exclusion effect. Nowadays, today this phenomenon is considered to be negligible and barely relevant at low permeabilities.

It is important to measure the extent of retention. In the past, the retention value was determined by flow experiments into natural rock using only one slug of polymer plus tracer (API RP 063 1990). Today it is recommended to inject, consecutively, two slugs of polymer with tracer. Between each slug, several water pore volumes (>50) have to be injected to displace them. Normalized concentration profiles for polymer and tracer allow to obtain the retention by using the difference in the area between polymer profile and tracer profile during the first slug injection. The IAPV can be obtained by the advance of polymer solution compared to tracer, during the second slug injection. This avoids the use of the washing part concentration profile, which is unstable (Lotsch et al. 1985; Manichand and Seright 2014).

It is good practice also to use field pilot tests to measure in situ adsorption, as it has been recently shown that real field values may be significantly higher, and this may impact on the economics of the expansion projects (Manichand and Seright 2014). J. Juri, using numerical simulations, reported the use of polymer injectivity test with flow-back analysis to obtain an estimate of polymer retention (Juri et al. 2015).

4.2 *Injectivity and Rheology in Porous Media*

When a viscous polymer solution is injected, the injectivity of the well may decrease significantly when compared to water flooding. The loss of injectivity resulting exclusively due to the viscous nature of the injected solution has been estimated approximately one-fifth of the one of water (Seright et al. 2009). An injectivity

reduction implies a slow displacement and delay in the production of hydrocarbons and severely impacts the economy. Other factors that may affect injectivity are plugging of the formation due to the presence of debris or microgels and the rheological behavior of the polymer solution at the entrance of the reservoir.

The presence of debris or microgels has shown to reduce injectivity and could cause plugging at the formation face. However, in most of the cases today, these species do not plug; they propagate slowly and generally will not penetrate deep into the formation. Their filtration does not affect the viscosity of the displacement front. Some of these undesirable fractions of xanthan may be eliminated by a proper hydration, while others can be attributed to high molecular weight species or cellular debris.

At low shear rate, it has been identified in core flow experiments that the presence of these species show high resistance factors (effective viscosity) with shear-thinning effects, while in the rheometer measurements, a Newtonian plateau is observed. Figure 12a illustrates the behavior of xanthan during flow through a long core (122 cm, 57 mD). The resistance factor (or effective viscosity) at the last section of the core shows the expected Newtonian plateau like in the rheometer measurements. Similar to xanthan, HPAM have presented effective viscosity higher than expected associated with high molecular weight species. In core experiments they are degraded due to the high pressure drop (high flow rates) (Seright et al. 2011).

At high shear rates, xanthan has better rheological properties at the entrance of the formation, as its effective viscosity decreases (or resistance factor), as can be seen in the rheometer. HPAM show a shear-thickening (or dilatant) behavior, the opposite of what is seen when tested with the rheometer, and then they are degraded. Figure 12b shows the flow behavior for a polyacrylamide after degradation of high molecular weight species (Seright et al. 2009, 2011).

Nowadays, it is essential to test the polymer injectivity in the field and how it affects the economy of projects in order to make the right decision on injecting at pressures above fracture pressure and to work on controlling the extent of the fracture.

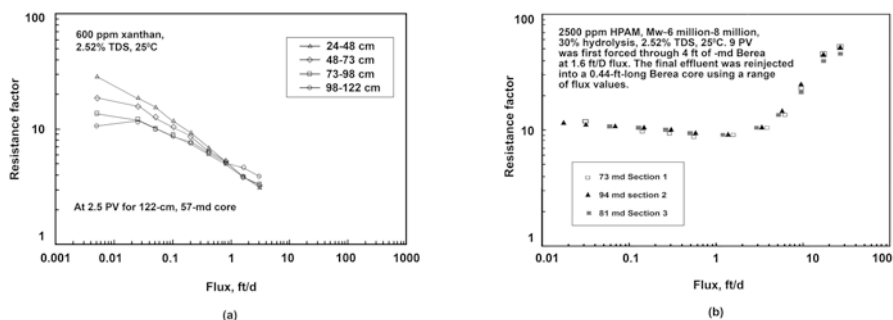


Fig. 12 Flow behavior in porous media: (a) xanthan gum, (b) HPAM (Reprint from Seright et al. (2009). Copyright (2009) with permission from Seright)

5 Xanthan vs. HPAM

In current EOR operations, polyacrylamides are still the most used. However, in this chapter, the potential of xanthan gum has been shown, because several properties demonstrate its superior behavior such as higher viscosity in salinity waters, which are common in the production of mature fields and the stability of mechanical degradation. A general summary of the significant properties in EOR for both polymers is shown in Table 2.

Greater expectations regarding the extended use of xanthan gum require that field applications increase in order to identify other operational and performance weaknesses and strengths. Efforts oriented to better understand and control hydrolytic and bacterial degradation would allow to increase the range of applications to higher temperatures at reasonable costs.

6 Other Biopolymers for Enhanced Recovery: Scleroglucan and Schizophyllan

Scleroglucan is a polysaccharide produced by a *Sclerotium* sp. fungus. Its chemical structure consists of a linear β -(1-3) D-glucose chain with a β -(1-6) D-glucose branch on every three glucose molecules of the backbone, as can be seen in Fig. 13.

The molecule shows a shear-thinning behavior in solution and is not susceptible to mechanical degradation. It also has a good chemical stability and is compatible with different types of brines, which is of great interest for its use in polymer flooding for enhanced recovery (Huang et al. 1993; Kalpakci et al. 1990).

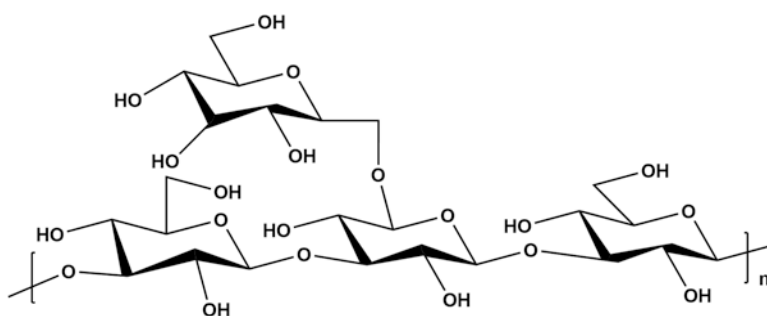
One of the drawbacks of this type of polysaccharide is its tendency to form clusters, for that reason only high-quality polymers must be used. This allows a good filterability. The permeability tests made in Berea cores have shown that it has a high viscosifying power regardless of salinity and that it is stable at high temperatures (90–100 °C) (in the absence of oxygen) for at least 3 months. Therefore, this biopolymer is a good candidate for mobility control at high temperatures at salinities of about 150 g/l TDS (Rivenq et al. 1991).

Recently, a biopolymer named schizophyllan, generated by the most widespread fungi (*Schizophyllum commune*) in Germany, has been produced at industrial scale to EOR application. Schizophyllan has the same repetitive molecular units as scleroglucan. Although very similar in structure, there might be some slight structural differences between two polysaccharides. This molecular structure has a rigid triple helical conformation, and therefore, it shows a high solution viscosity over a wide range of temperatures, pH, and ionic strength (Kosaric and Sukan 1993; Fang et al. 2004).

Recently the biopolymer schizophyllan has been used into a first field trial in a mature oil field located in Northern Germany. The preliminary results for more than 1 year of the polymer injection have shown a positive response in additional oil production (Leonhardt et al. 2014).

Table 2 General comparison of xanthan and HPAM properties

Property	Xanthan	Polyacrylamides (HPAM)
Viscosity vs. salinity	Higher when salinity is higher	Lower when salinity is higher
Rheology measured in a rheometer	Carreau model	Carreau model
Thermal stability	Defined by Tm. At higher salinity, the threshold increases. 70 °C is the accepted value	70 °C is the accepted value. Influenced by the degree of hydrolysis and hardness
Chemical stability	Susceptible to free-radical redox degradation and hydrolysis	Susceptible to redox reactions. The increment of hydrolysis degree with temperature causes precipitation in presence of divalent ions
Microbiological stability	Susceptible	Practically inert
Mechanical stability	Practically inert	Susceptible
Rheology in porous media	Keeps Carreau model. If there are debris or microgels, instead of the Newtonian plateau at lower rates, a shear-thinning behavior is observed	At higher rates, they are shear thickening and degrade. At lower rates, they may show the same behavior as xanthan if there are high MW species or microgels
Injectivity	Mainly influenced by the value of viscosity, low permeability, and the presence of debris	Mainly influenced by the value of viscosity, low permeability, microgels, shear-thickening rheology, and subsequent degradation

**Fig. 13** Molecular structure of scleroglucan

7 Conclusions

Regarding guar gum and its derivatives applied to the oil industry, the main uses are as gelling agents in fracturing fluids or viscosifying agents in drilling muds.

Guar and its derivatives have the capacity to cross-link with several additives to form robust gels capable of suspending and transporting the proppant to the fracture. The most extended cross-linker for this application is the borate. With respect to guar–borax gels, the cross-linking effectiveness is a function of pH. At room

temperature and a pH of 8.5, the monoborate concentration is enough to start the cross-linking through the polysaccharide hydroxyl groups. These gels are considered physical due to the transient unions. Because of the bonds' reversibility with temperature, these physical gels are thermoreversible.

The guar–borax gels are easily degraded while pumping. Other limitations are high temperatures, presence of bacteria, and transition metal ions. These factors seriously affect the quality of the gels. Cross-linkers such as titanates and zirconates are recommended for harsh conditions. When resistance to high temperatures, viscosity capacity, and stability to acids and alkali are required, titanate and zirconate complexes of guar are the best options. The disadvantage lies in their shear sensitivity because the gels once broken are not regenerated.

With regard to drilling operations, xanthan, guar, and its derivatives could be used as viscosifying agents, and similar to frac fluids, they confer the property of suspending solids in it.

Hydraulic fracturing technology is widely used to facilitate and enhance oil and gas production from conventional and unconventional reservoirs; otherwise they cannot be economically produced. As an example, all reservoirs containing conventional resources have very high percentage of unconventional resources that are now being produced or need to be produced in the near future (Rahim et al. 2012). For all that was explained above, the consumption prospect of guar and its derivatives should grow enormously.

In conventional fracturing operations, special efforts are being carried out in the development of delayed cross-linking boron–guar systems to be applied in deep formations (Agarwal 2016).

With regard to xanthan and scleroglucan in EOR application, their consumption should be in expansion, in particular for those fields that present high temperature and salinity conditions.

In addition, their chemical structure allows them to develop good viscosity even in high divalent and monovalent ions content in water. Another important aspect is the application in EOR using production water to avoid the use of high volumes of freshwater (usually taken from lake and rivers). This will help to preserve the environment.

Due to the rigid rodlike conformation of these microbial biopolymers that prevent mechanical degradation, it makes them powerful polysaccharides to be exploited in the future for mobility control applications.

Acknowledgments We acknowledge R. S. Seright for his suggestions over the xanthan in EOR topic. We also thank A. W. Chitty who contributed with technical discussions during the elaboration of this chapter.

References

- Abbaszadeh A, Lad M, Janin M, Morris G, MacNaughtan W, Sworn G, Foster T (2015) A novel approach to the determination of the pyruvate and acetate distribution in xanthan. *Food Hydrocoll* 44:162–171
- Agarwal S Delayed crosslinking composition or reaction product thereof for treatment of a subterranean formation. Paper presented at the Asia Pacific Drilling Conference, Singapore, Aug 22–24, 2016
- Ahlgren J (1991) Purification and characterization of a pyruvated-mannose-specific xanthan lyase from heat-stable, Salt-Tolerant Bacteria. *Appl Environ Microbiol*:2523–2528
- American Petroleum Institute (API) RP 39 (1998) Recommended practices on measuring the viscous properties of a cross-linked water-based fracturing fluid
- API RP-063 (1990) Recommended practices for evaluation of polymers used in enhanced oil recovery operations, First edn. American Petroleum Institute, Washington, DC
- Azuaje R, Sánchez J (1999) Producción de Xantanopor *Xanthomonas campestris* en un medio de cultivo no convencional. *Acta Cient Venez* 50:201–209
- Chavaran S, Baig M (2016) Relationship of biomass and xanthan gum production by *Xanthomonas campestris*: optimization of parameters. *British Biotechnology Journal* 11(1):1–8
- Chiappa L, Mennella A, Lookhart TP, Burrafato G (1999) Polymer adsorption at the brine/rock interface: the role of electrostatic interactions and wettability. *J Pet Sci Eng* 24:113–122
- Conway M, Hsu C. Fracturing fluids for deep hot formations. SPE 9707 Paper presented at the Oil and Gas Recovery Conference, Midland, TX, Mar 12–13, 1981
- Fang Y, Takahashi R, Nishinari K (2004) Rheological characterization of schizophyllan aqueous solutions after denaturation–renaturation treatment. *Biopolymers* 74:302–315
- García-Ochoa F, Santos V, Casas J, Gómez E (2000) Xanthan gum: production, recovery, and properties. *Biotechnol Adv* 18:549–579
- Grasdalen H, Painter T (1980) NMR studies of composition and sequence in legume-seed galactomannans. *Carbohydr Res* 81:59–66
- Green D W, Wilhite G P (1998). Enhanced oil recovery. SPE textbook series, vol 6. Richardson, pp 1–6
- Gulrez S, Al-Assaf S, Fang Y, Phillips G, Gunning A (2012) Revisiting the conformation of xanthan and the effect of industrially relevant treatments. *Carbohydr Polym* 90:1235–1243
- Hovland B (2015) Assessment of the biodegradability of xanthan in offshore injection water, Master Thesis in Microbiology University of Bergen
- Howard G, Fast C (1970) Hydraulic fracturing. SPE, 2
- Huang Y, Sorbie K, Watt H (1993) Scleroglucan behavior in flow through porous media: comparison of adsorption and in-situ rheology with xanthan. Paper SPE 25173 presented at SPE International Symposium on Oilfield Chemistry, 2–5 March, New Orleans, Louisiana
- Huh C, Lange E A, Cannella W J (1990) Polymer retention in porous media. Paper SPE 20235 presented at SPE/DOE Enhanced Oil Recovery Symposium, 22–25 April, Tulsa, Oklahoma
- Juri J E, Ruiz A M, Hernandez M I, Kaminszczik S (2015) Estimation of polymer retention from Extended Injectivity Test. Paper SPE 174627 presented at SPE Asia Pacific Enhanced Oil Recovery Conference, 11–13 August, Kuala Lumpur, Malaysia
- Kalpaki B, Jeans V, Magri N, Padolewski J (1990) BP research, thermal stability of scleroglucan at realistic reservoir conditions. Paper SPE/DOE 20237 presented at SPE/DOE Enhanced Oil Recovery Symposium, 22–25 April, Tulsa, Oklahoma
- Kesavan S, Prud'homme R (1992) Rheology of guar and hydroxypropylguar crosslinked by borate. *Macromolecules* 25:2026–2032

- Kosaric N, Suka FV (1993) *Biosurfactants: production-properties-applications*. Marcel Dekker, New York
- LaGroe C et al. Chemical evolution of high temperature fracturing fluid. SPE11794 Paper presented at the Oilfield and Geothermal Chemistry Symposium, Denver, June 1–3, 1984
- Lapasin R, Prici S (1995) *Rheology of industrial polysaccharides. Theory and applications*. Springer, Berlin
- Leonhardt B, Ernst B, Reimann S, Steigerwald A, Lehr F (2014) Field testing the polysaccharide schizophyllan: results of the first year. Paper SPE 169032 presented at SPE Improved Oil Recovery Symposium, 12–16 April, Tulsa, Oklahoma, USA
- Lotsch T, Muller T, Pusch G (1985) The effect of inaccessible pore volume on polymer core-flood experiments. Paper SPE 13590 presented at SPE Oilfield and Geothermal Chemistry Symposium, 9–11 March, Phoenix, Arizona
- Manichand RN, Seright RS (2014) Field vs laboratory polymer-retention values for a polymer flood in the Tambaredjo field. SPE Reserv Eval Eng 03:314–325
- Mc Cleary B (1979) Enzymatic hydrolysis, fine structure and gelling interaction of legume-seed D-galacto-D-mannans. *Carbohydr Res* 71:205–230
- Mc Cleary B, Clark A, Dea I, Rees D (1985) The fine structures of carob and guar galactomannans. *Carbohydr Res* 139:237–260
- Milas M, Rinaudo M (1984) On the existence of two different secondary structures for the xanthan in aqueous solutions. *Polym Bull* 12:507–514
- Moradi-Araghi A, Doe P (1987) Hydrolysis and precipitation of polyacrylamides in hard brines at elevated temperatures. *SPE Reserv Eng* 2:189–198
- Power D, Larson I, Hartley P, Dunstan D, Boger D (1998) Atomic force microscopy studies on hydroxypropylguar gels formed under shear. *Macromolecules* 31:8744–8748
- Rahim Z, Al-Anazi H, Al-Kanaan A, Habbtar A, Al-Omar A, Senturk N, Kalinin D 2012 Productivity increase using hydraulic fracturing in conventional and tight gas reservoirs. Expectations versus reality. *SOC Petrol Eng J* 153221. Paper presented at the Middle East Unconventional Gas Conference and Exhibition, Abu Dhabi, UAE, January 23–25
- Ramsden D, McKay K (1986a) Degradation of polyacrylamide in aqueous solution induced by chemically generated hydroxyl radicals part I-Fenton's reagent. *Polym Degrad Stab* 14:217–229
- Ramsden D, McKay K (1986b) Degradation of polyacrylamide in aqueous solution induced by chemically generated hydroxyl radicals part II-autoxidation of Fe²⁺. *Polym Degrad Stab* 15:15–31
- Rivenq RC, Donche A, Nolk C (1991) Improved scleroglucan for polymer flooding under harsh reservoir conditions. *SPE Reserv Eng* 7:15–20
- Ruijsenaars H, De Bont J, Hartmans S (1999) A Pyruvated mannose-specific xanthan Lyase involved in xanthan degradation by *Paenibacillus alginolyticus* XL-1. *Appl Environ Microbiol* 65:2446–2452
- Sandford P, Pittsley J, Knutson C, Watson P, Cadmus M, Jeanes A (1977) Variation in *Xanthomonas campestris* NRRL B-1459: characterization of xanthan products of differing pyruvic acid Content. *Extracellular microbial polysaccharides*. *ACS Symp Ser* 45(15):192–210
- Seright RS, Fan T, Wavrik K, Carvalho Balaban R (2011) New insights into polymer rheology in porous media. *SPE J* 16:35–42
- Seright R, Henrici B (1990) Xanthan stability at elevated temperatures. *SPE Reserv Eng* 5:52–60
- Seright RS, Seheult M, Talashek T (2009) Injectivity characteristics of EOR polymers. *SPE Reserv Eval Eng* 12:783–792
- Sorbie KS (1991). *Polymer-improved oil recovery*. Blackie Glasgow & Son, Ltd. Published in the USA and Canada by CRC Press, Inc. 2000 Corporate Blvd. NW; Boca Raton, FL 33431
- Vega I, Fernández E, Mijangos C, D'Accorso N, Lopez D (2008) Potential applications of poly(vinyl alcohol)-Congo red aqueous solutions and hydrogels as liquids for hydraulic fracturing. *J Appl Polym Sci* 110:695–700
- Wan H, Seright R S (2016) Is polymer retention different under anaerobic vs. aerobic conditions? *SPE J*, Aug 1–7

- Whistler R (2012) *Industrial gums: polysaccharides and their derivatives*. Elsevier, Amsterdam
- Whistler R, Hymowitz T (1979) *Guar: agronomy, production. Industrial use and nutrition*, Purdue Univ Press. West Lafayette Monograph. Wiley & sons inc, New Jersey
- Zaitoun A, Kohler N (1988) Two-phase flow through porous media: effect of an adsorbed polymer layer. Paper SPE 18085 presented at SPE Annual Technical Conference and Exhibition, 2–5 Oct, Houston
- Zaitoun A, Makakou P, Blin N, Al-Maamari RS, Al-Hashmi AR, Abdel-Goad M (2012) Shear stability of EOR polymers. *Soc Petrol Eng J*:335–339
- Zasadzinski J, Chu A, Prud Homme R (1986) Transmission electron microscopy of gel network morphology: relating microstructure to mechanical properties. *Macromolecules* 19:2960–2964
- Zhang G, Seright R S (2015) Hydrodynamic retention and rheology of EOR polymers in porous media. Paper SPE 173728 presented at SPE International Symposium on Oilfield Chemistry, 13–15 Apr, The Woodlands
- Zitha PLJ, Botermans CW (1998) Bridging adsorption of flexible polymers in low-permeability porous media. *SPE Production & Facilities* 13:15–20

Modified Starches Used as Additives in Enhanced Oil Recovery (EOR)

Olivia V. López, Luciana A. Castillo, Mario D. Ninago, Andrés E. Ciolino, and Marcelo A. Villar

1 Introduction

Nowadays, conventional oil recovery involves mainly three phases named primary, secondary, and tertiary, respectively. In the primary phase, the natural pressure of the reservoir is employed to push crude oil to the surface, allowing a yield up to 10%. In the secondary one, pressurized gas and water are injected to recover part of the remnant oil (~30%). Secondary extraction, which involves mainly the injection of water into oil wells, is the most used methodology due to its low complexity and cost, recovering less than 50% of the original oil. However, several difficulties are found along its application related to the water cut (or water channeling) phenomena and the consequently low oil recovery yield, making this process noneconomically attractive. Within this context, even if the oil recovery is improved in 1%, this increment represents hundreds of millions of tons without any exploration and development investment (Shi et al. 2015). However, heterogeneous nature of the reservoirs hinders the complete oil phase extraction by water flooding.

The non-homogeneity within reservoir structure is due to variations in permeability and porosity and to the existence of different fracture orientations (Van den

O.V. López

Planta Piloto de Ingeniería Química, PLAPIQUI (UNS-CONICET), Bahía Blanca, Argentina

L.A. Castillo • A.E. Ciolino • M.A. Villar (✉)

Planta Piloto de Ingeniería Química, PLAPIQUI (UNS-CONICET), Bahía Blanca, Argentina

Departamento de Ingeniería Química, Universidad Nacional del Sur (UNS),

Bahía Blanca, Argentina

e-mail: mvillar@plapiqui.edu.ar

M.D. Ninago

Planta Piloto de Ingeniería Química, PLAPIQUI (UNS-CONICET), Bahía Blanca, Argentina

Facultad de Ciencias Aplicadas a la Industria, Universidad Nacional de Cuyo,

San Rafael, Mendoza, Argentina

Hoek 2004). As a solution of these drawbacks, a tertiary phase has emerged, known as enhanced oil recovery (EOR). EOR is considered a multidisciplinary area, which involves not only scientific but also technological concepts for developing new methodologies to enhance crude oil extraction and to extend the production life of oil fields. EOR implementation arises as a supplementary technology to conventional ones, optimizing the not-easily recoverable oil phase. To have an idea, the estimation of the crude oil remnant in reservoirs after primary and secondary recoveries approaches to seven billion of barrels. This number is a good reason for searching alternative methodologies in order to maximize crude oil recovery. Within this context, one of the strategies proposed for EOR implies the use of sophisticated displacing fluids, which are pumped into the reservoir forcing the oil to flow toward the production wells. For such a purpose, fluids must be more viscous than water, like the well-known solutions based on water-soluble polymers. The use of water-soluble additives for EOR has been discussed during the last years, considering certain limitations associated with rheological properties of their suspensions. It is important to note that fluid flow behavior is directly related to the chemical structure of the used polymers, as well as the influence of external parameters, such as salts and surfactant concentrations, and temperature, among others (Wever et al. 2011; Gao 2015). Polymer flooding is the common name used for the injection of a polymer solution into petroleum reservoirs and has been successfully applied in several countries (Sorbie 2000; Silva et al. 2007; Morel et al. 2010; Nezhad and Cheraghian 2015). The most crucial criteria to select the appropriate polymer are its ability to generate a viscous solution at the minimum concentration (Shi et al. 2015). Besides, since this method relies on polymer adsorption on pores located at the rock walls, it is therefore important to consider this capacity in the selection of the polymer employed for injection purposes (Leslie et al. 2005). Among the polymers studied, one of the most water-soluble polymers used is partially hydrolyzed polyacrylamides (HPAM) because it increases significantly the fluid displacement viscosity, allowing a higher sweep of the oil phase. Nevertheless, since the interaction between polymers and salts present into reservoirs produces changes in the rheological behavior of the solution, this issue is also relevant for the proper selection of the additive. The experience has shown that large periods of successive flooding lead to a more marked heterogeneous reservoir by increasing the number of big-sized pores and the wellbore permeability. Consequently, the injected polymer suffers from the channeling phenomena in high permeability areas (Daripa and Pasa 2004; Bao et al. 2009).

Considering the water-soluble character of starch, this biopolymer can be used as an additive in EOR technologies. During the last six decades, starch has been modified by different physical and chemical methods obtaining derivatives for oil field applications. Nowadays, some of these modified starches are commercially available. Within this context, the low cost, worldwide availability, and high eco-friendly character make starch as a good candidate for developing additives to be used in the oil industry, an activity that consumes millions of pounds of starch and their derivatives per year (Qiao and Zhu 2010). At this point, it is important to note that additives obtained from natural polymers compete with those derived from synthetic ones.

Thus, the selection of additives to be used in EOR technologies must be based not only on its functional properties but also on its price and availability. Particularly, in the case of the modified starches, their price is mainly associated to their production costs. In this sense, reaction selectivity (fraction of reagent which reacts with starch) and starch reactivity (amount of modified starch that can be produced in certain reaction conditions) mostly determine the commercial cost of these derivatives.

Oil field applications of starch and their derivatives include filtrate-loss control, mud-rheology modification, shale stabilization, drag reduction, water shutoff, and EOR. For such a purpose, some characteristics of starch such as molar mass, chemical structure, and solubility, as well as reservoirs' salinity and temperature, influence the oil recovery efficiency (Zhang 2001). In this chapter, we will discuss the state of the art related to the use of different starch derivatives in EOR. Besides, diverse methodologies developed to synthesize modified starches are also presented, by analyzing the optimal conditions of each reaction. The degree of modification and the physicochemical properties of the derivatives are also included and discussed along the chapter, hoping that this interchange of ideas and methodologies will contribute to a better understanding of the use of modified starches for EOR.

2 Modified Starch for Oil Field Applications

Native starch has a granular morphology with special functional properties. In this sense, starch is slightly soluble in cold water and forms colloidal suspensions under heating. Besides, due to the high viscosity of starch pastes, this polysaccharide is usually used as adhesive, for thickening purposes, and as a texturing agent (Jaspreet et al. 2007). Tailor-made starches have been synthesized for specific applications in order to widen its application fields. These modifications involve changes in the granular structure, by modifying its gelatinization behavior, swelling degree, and solubility capacity (Barrios et al. 2012). Thus, it is possible to synthesize modified starches with different hydrophilic/hydrophobic characters, depending on the nature of the reactive agent as well as the medium and the reaction conditions (Heinz and Koschell 2005; Jaspreet et al. 2007). Among these derivatives, pre-gelatinized, etherified, grafted copolymers and cross-linked and blended starches can be mentioned. Considering their abundance, stability, and the inherent eco-friendly character, Leslie et al. (2005) reported the importance of using modified cationic polysaccharides and branched polymers based on cyclodextrins in EOR technologies. Within this context, it is relevant to evaluate the adsorption of these additives on core samples extracted from hydrocarbon reservoir rocks, considering charge density and molar mass of the polysaccharides. These authors found that polymer absorption is strongly dominated by a combination of electrostatic interactions between polymer and rock surfaces, as well as the size of the polymer.

Table 1 summarizes different modified starches used in the petroleum industry, especially in EOR.

Table 1 Modified starches used in the oil industry

Modified starch	Chemical structure	Functional characteristics	Reference
2-Hydroxy-3-(trimethylammonium)-propyl starch (HTPS, cationic)	$\text{Starch-CH}_2\text{CH(OH)CH}_2\text{N}^+(\text{CH}_3)_3\text{Cl}^-$	Good inhibition to water-sensitive clay and shale in oil fields	Zhang (2001), Pal et al. (2005), Qiao et al. (2012), Prado and Matulewicz (2014), and Chen et al. (2015)
Sodium carboxymethyl starch (CMS-Na, anionic)	$\text{Starch-CH}_2\text{COO}^-\text{Na}^+$	Reduction of fluid loss. Increment of viscosity	Zhang (2001), Stojanovic et al. (2005), Barros et al. (2012), Chen et al. (2015), and Fink (2015)
Potassium carboxymethyl starch (CMS-K-, anionic)	$\text{Starch-CH}_2\text{COO}^-\text{K}^+$	Reduction of fluid loss Increase of viscosity Inhibition of clay and shale hydration	Zhang (2001) and Chen et al. (2015)
2-Hydroxy-3-sulfopropyl starch (HSPS, anionic)	$\text{Starch-CH}_2\text{CH(OH)-CH}_2\text{SO}_3\text{H}$	Reduction of fluid loss Increase of viscosity	Zhang (2001) and Chen et al. (2015)
Hydroxyethyl starch (HES, nonionic)	$\text{Starch-CH}_2\text{CH}_2\text{CH}_2\text{OH}$	Reduction of fluid loss Increase of viscosity	Zhang (2001) and Chen et al. (2015)
Hydroxypropyl starch (HPS, nonionic)	$\text{Starch-CH}_2\text{CH}_2\text{CH}_2\text{CH}_2\text{OH}$	Reduction of fluid loss Increase of viscosity	Zhang (2001) and Chen et al. (2015)
Carboxymethyl starch and hydroxyethyl starch (CHES, anionic)	$\text{Starch-CH}_2\text{COOH}$ and $\text{starch-CH}_2\text{CH}_2\text{OH}$	Reduction of fluid loss Increase of viscosity	Zhang (2001) and Chen et al. (2015)
Starch- <i>graft</i> -poly(acrylamide- <i>co</i> -2-acrylamido-2-methylpropanesulfoacid)	$\text{Starch-g-p(AM-co-AMPS)}$	High resistance to temperature and shear rate High intrinsic viscosity	Song et al. (2007), Wever et al. (2011), and Chen et al. (2015)

3 Cationic Starches

Within starch derivatives, cationic-modified polymers have been used as functional additives in the petroleum industry (Fu et al. 2013). The modification is based on the substitution of starch hydroxyl groups by functional groups with positive charges, by employing different chemical reagents. In this sense, it is possible to introduce sulfonium, ammonium, amino, imino, or phosphonium groups (Bertolini 2009; Kuo and Lai 2009). These derivatives present a wide range of degree of substitution (DS), and they are usually synthesized by using starches from different botanical sources as substrates and several modifying agents. Concerning the methods employed, they are divided into batch and continuous processes. Regarding the first ones, they can be carried out via granular slurry, semidry, or solubilized paste; on the other hand, in the continuous processes, reactive extrusion is generally employed (Bertolini 2009).

Cationic starch moieties can be synthesized by employing a quaternary ammonium reactive (Pal et al. 2005), but in the last years, the chemical group most currently incorporated is 2-hydroxy-3-(trimethylammonium)propyl by etherification with 2,3-epoxypropyltrimethylammonium chloride (glycidyltrimethylammonium chloride, EPTAC) (Prado and Matulewicz 2014). EPTAC can be acquired commercially, but it is toxic and has a low chemical stability and a high cost. An alternative to overcome these limitations, especially at industrial scale, is the synthesis of this reagent in situ by using 3-chloro-2-hydroxypropyltrimethylammonium chloride (CHPTAC), which is also a commercially available reagent. A simple procedure for the synthesis of EPTAC is shown in Fig. 1.

Concerning the functionalization process, Prado and Matulewicz (2014) reported a two-step mechanism. In the first step, an alkoxide is formed, in an alkaline medium, from a starch hydroxyl group as it is shown in Fig. 2. Then, this alkoxide reacts with the EPTAC by a nucleophilic attack, by opening the epoxide group.

Considering batch processes employed to obtain these starch derivatives, the semidry and wet methods are the most used. Regarding the semidry technique, the reactive agents are spread over starch and submitted to an optimized time–temperature routine (Zhang et al. 2007). Meanwhile, the wet method can be performed in homogeneous as well as in heterogeneous conditions (Haack et al. 2002; Heinze et al. 2004; Sableviciene et al. 2005). In the homogeneous wet option, dimethyl sulfoxide (DMSO) is used as the reaction medium. On the other hand, in the heterogeneous wet process, suspensions, mainly based on water or alcohols under basic medium, are usually employed. Concerning continuous processes, reactive extrusion



Fig. 1 Synthesis of EPTAC

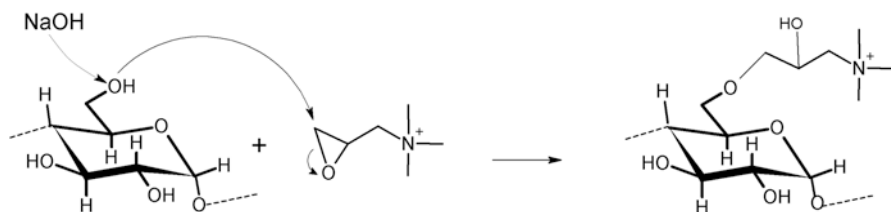


Fig. 2 Synthesis of 2-hydroxy-3-(trimethylammonium) propyl starch

is one of the most used methods at industrial scale. It is important to highlight that this process allows obtaining not only a functionalized starch but also a thermoplastic derivative. This material results from the reactive conditions (high shear stress and temperature) and the incorporation of a plasticizer during the extrusion process, improving starch processability (Ayoub and Bliard 2003; Ayoub et al. 2004; Tara et al. 2004). The most important advantage associated to both, semidry and extrusion techniques, is their easy procedure (the lack of additional steps which could lead to a partial loss of the synthesized derivative is their characteristic). However, the presence of some chemical products such as salts, reactive agents, and by-products influences reaction yield, as well as the quality of modified starches (Radosta et al. 2004).

The method that guarantees the production of derivatives with a high purity is the wet one, because reaction conditions preserve the integrity of the starch granules. Consequently, these functionalized starches play an important role as adsorbents and flocculants (Sableviciene et al. 2005; Klimaviciute et al. 2007). Despite these advantages, the problems associated to heterogeneous method are related to the incorporation of inorganic salts which are used for reducing the phenomenon of the swelling of the granules (Huber and BeMiller 2001; Butrim et al. 2008).

Scientific literature reports several works regarding the synthesis of cationic starches by wet process under homogeneous and heterogeneous conditions (Kuo and Lai 2007, 2009; Kavaliauskaite et al. 2008; Pi-xin et al. 2009; Hebeish et al. 2010; Wang and Xie 2010). By analyzing the open literature, it can be noticed that reaction efficiency, degree of substitution, and granule preservation, as well as functional properties of starch derivatives, depend on diverse factors, such as chemical reagents, molar ratio of reactive agents, and medium conditions, among others.

Regarding the synthesis of hydrosoluble derivatives based on starch, Heinze et al. (2004) studied three methods to obtain 2-hydroxy-3-(trimethylammonium) propyl starch (HTPS). These authors assayed different media and reaction conditions and the same reagent (2,3-epoxypropyltrimethylammonium chloride, EPTAC) for functionalization purposes. They employed several native starches from diverse botanical sources and variable amylose content. Particularly, the methods proposed for synthesizing modified starches involved heterogeneous, homogeneous, and pseudo-heterogeneous cationization. Figure 3 shows the reaction pathways used by Heinze et al. (2004) to obtain HTPS. In this sense, the effect of different variables, such as reaction medium, synthesis conditions, and properties of native starch over the DS of the obtained derivative was evaluated. From the analysis of the results

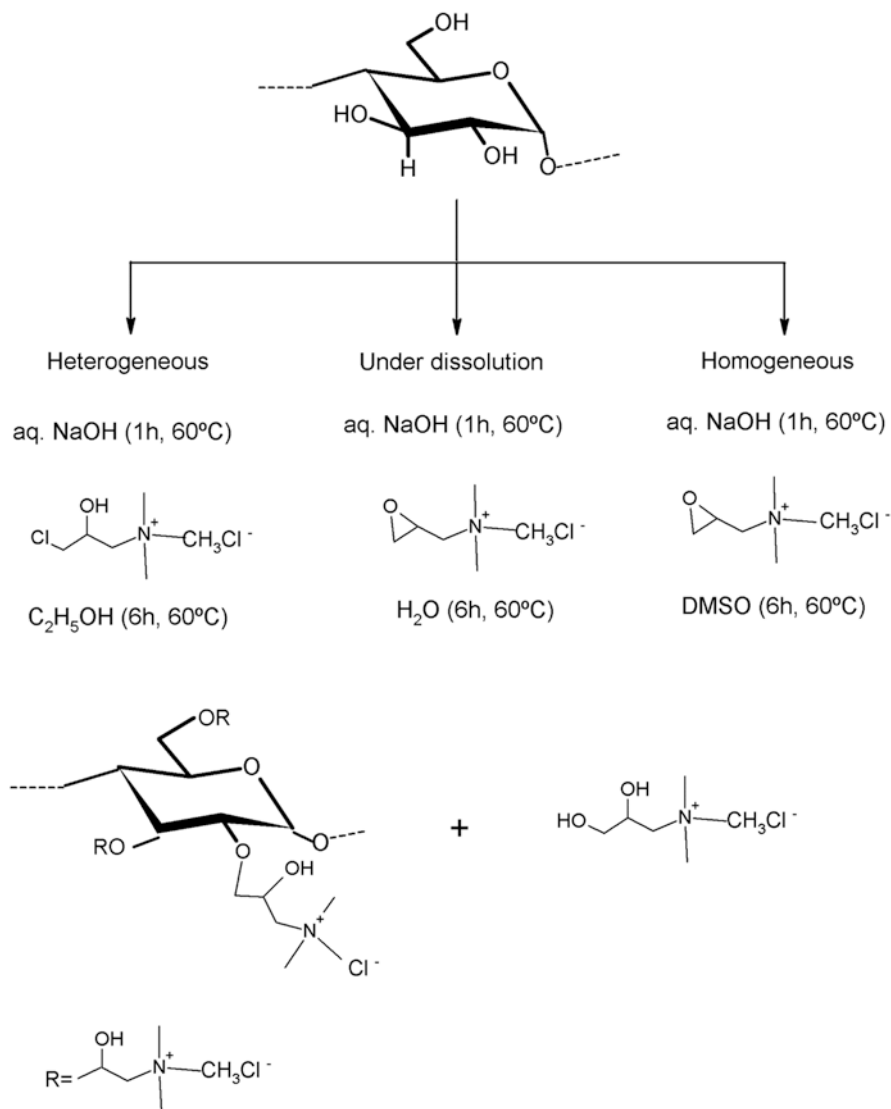


Fig. 3 Scheme of reaction used to synthesize 2-hydroxy-3-(trimethylammonium) propyl starch (HTPS) under different media and conditions (Taken from Heinze et al. 2004)

derived from this study, it is possible to infer that, generally, the DS does not depend on the botanical source or the amylose content of the native starch. However, a significant effect on the DS was observed for those starches containing a low amylose proportion, which were submitted to heterogeneous cationization.

It was demonstrated that modified derivatives with high DS values (up to 1) could be obtained by one-step homogeneous method using a molar ratio equal to 2 between the cationization agent and the anhydroglucose unit. According to the comparison

made between homogenous and heterogeneous methods, the first one resulted in being more efficient. In the heterogeneous method, the impeded diffusion of the reagent by the presence of positive groups located on the surfaces of starch granules obstructs the cationization reaction. On the other hand, homogeneous methods offer a less hindered surface thanks to the solubilization of the starch granules by enhancing the diffusion of the cationization agent. Despite homogeneous reaction is the most efficient method for synthesizing cationic starches, it is important to mention that employs more liquid than the heterogeneous technique. In order to reach a DS between 1.0 and 1.5, Heinze et al. (2004) proposed the use of an additional cationization stage. In that work, it is reported a complete structural characterization of the synthesized cationic starches from the aforementioned method, revealing that these derivatives resulted soluble in cold water. Taking into account that cationic starches could be used as additives in EOR technologies, solubility data are a relevant issue to be considered.

According to Siau et al. (2004), the cationization process increases the disruption of starch crystalline structure, by enhancing significantly the water uptake of the polymer and its thermal properties. The feasibility of using starch derivative solutions as oil displacement fluids is based on different aspects such as their high salt tolerance, their capacity to reduce the water cut phenomenon, and their adsorption properties on sand particles of oil reservoirs (Fu et al. 2013). It is possible to tailor the structural characteristics and functional properties of cationic starches by selecting the proper method of synthesis and by adjusting the optimal reaction conditions. In this regard, Bendoraitiene et al. (2012) stressed that derivatives with high sorption properties can be obtained with the aid of organic bases in the reaction system. On the other hand, it has been established that exposition to microwave radiation during the cationization reaction favors the production of starch derivatives with specific characteristics (Wei et al. 2008; Singh et al. 2013).

As it was aforementioned, even though HPAM flooding is one of the most used techniques in EOR processes, some disadvantages have been found (Daripa and Pasa 2004; Hou et al. 2009). Concerning advantages of the HPAM flooding, it can be mentioned a higher oil yield and a reduction of the water cut phenomenon. Reservoir flooding during long periods increased the stratum heterogeneity and the presence of big pores, conforming a more permeable region. Consequently, HPAM channeling takes place in this high permeability zone and a premature polymer loss from the wellbore occurred, affecting the oil phase displacement. Qiao and Zhou (2010) and Qiao et al. (2012) proposed an alternative to enhance the sweep efficiency, through sealing the big pores using the HPAM retained in the reservoir. These authors proposed the use of 2-hydroxy-3-(trimethylammonium)propyl starch (HTPS) in EOR technology, obtained from native corn starch and EPTAC as reagent. Thus, the injection of HTPS solutions after HPAM flooding allows reacting with the remnant polymer located in the high permeability regions, producing an in situ gelling system by electrostatic forces (Al-Muntasheri et al. 2007). This process offers a more economical option in order to replace other conventional additives such as metallic or organic cross-linking agents (Wang et al. 2003; Jeon et al. 2008; Chang et al. 2010). These gel-type structures act like profile modification agents since they

reduce the reservoir permeability, blocking and plugging the big pores. Along a cross-linking reaction, the HPAM–HTPS liquid phase is transformed into a viscoelastic solid, increasing the system strength. Firstly, the low strength of this cross-linked gel is responsible to reach deeper breakthrough into reservoir channels. However, when this reaction takes place, three-dimensional molecules are formed, increasing the viscosity and strengthening of gel system. The physical properties of this final cross-linked material lead to an obstruction and sealing of the channels and pores, reducing the reservoir permeability. The result of alternating injections of HPAM and HTPS solutions before water flooding improves oil production since water can displace the oil phase present in mid-low permeability regions (Sabhapondit et al. 2003; Wang et al. 2003).

In order to evaluate the viscoelastic behavior of HPAM–HTPS cross-linked gels, Qiao and Zhu (2010) and Qiao et al. (2012) performed rheological studies working on systems obtained from reactions of cationic starches and HPAM solutions with different concentrations. Rheological curves obtained from steady shear tests carried out at 25 °C for HPAM solution (1,500 mg/L) and a HPAM–HTPS gel system (prepared by mixing in equal volumetric proportion of 1,500 mg/L HPAM and 5,000 mg/L HTPS) are shown in Fig. 4. A pseudoplastic behavior for both HPAM solutions and gel systems at high shear rate values was evidenced. As it can be observed, the viscosity of HPAM and HPAM–HTPS gels decreased with an increase in shear rate. This tendency is associated to the shear thinning phenomenon and to cross-linking points shearing off. Thus, the flow resistance and, consequently, the viscosity are reduced. It is important to highlight that viscosity values of HPAM–HTPS gels were found to be higher than those corresponding to HPAM solutions over the shear rate range studied.

Qiao and Zhu (2010) and Qiao et al. (2012) also prepared formulations from HTPS and HPAM solutions with different concentration in order to evaluate the gel strength. As it can be observed in Fig. 5, as concentrations of the two fluids decrease, this viscoelastic property of the resulting gel is diminished.

It is well known that the efficiency of oil displacement is strongly influenced by the wettability of reservoir soils. In this sense, to analyze the capacity of cationic starch solutions for improving the oil phase recovery in EOR technologies, the wettability of a model soil is usually determined (Karabakal and Bagci 2004). Within this context, Qiao et al. (2012) studied the effect of using HTPS as EOR additive on the wettability of a montmorillonite-based reservoir (Mt). This property of the surface was evaluated comparatively between Mt-HTPS and Mt-HPAM systems, through measurements of contact angle values. The preparation of both systems was carried out by adding Mt to HTPS or HPAM solutions, and samples so obtained were submitted to several experimental steps (filtration, washing, drying, grinding, and sifting). The resulting wetting curves of Mt-HTPS and Mt-HPAM systems, as well as for the neat Mt in water are shown in Fig. 6.

For Mt-HTPS and Mt-HPAM, an opposite behavior was observed. The presence of HTPS on Mt increases the hydrophilic character of this substrate and, consequently, the soil wettability in water. On the other hand, the addition of HPAM slightly increases the hydrophobic nature of the Mt particles. Taking into account

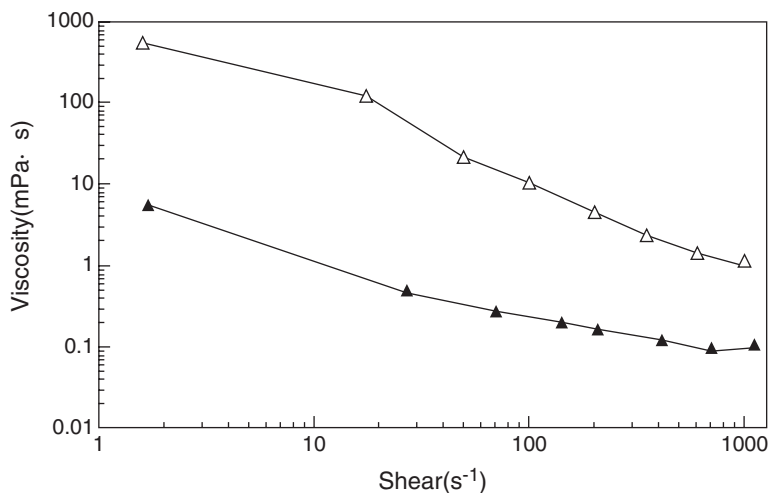


Fig. 4 Rheological curves of HPAM solution (1500 mg/L) and HPAM-HTPS gel system (1,500 mg/L HPAM and 5,000 mg/L HTPS). Symbols: (\blacktriangle) HPAM solution and (\triangle) HPAM-HTPS gel system (Taken from Qiao et al. 2012)

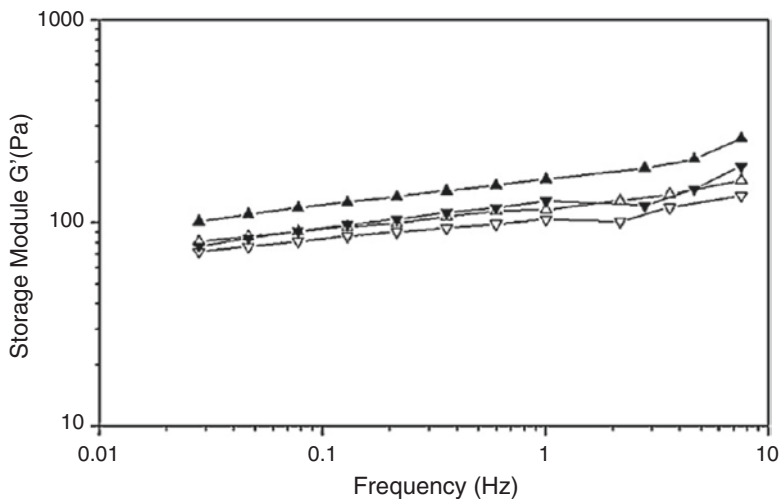


Fig. 5 Effect of solution concentration on storage moduli (G') of HPAM-HTPS gel systems. Symbols: (\blacktriangle) 5,000 mg/L HTPS +1,500 mg/L HPAM, (\triangle) 5,000 mg/L HTPS +1000 mg/L HPAM, (\blacktriangledown) 3,000 mg/L HTPS +1,500 mg/L HPAM, and (\triangledown) 3000 mg/L HTPS +1000 mg/L HPAM (Taken from Qiao et al. 2012)

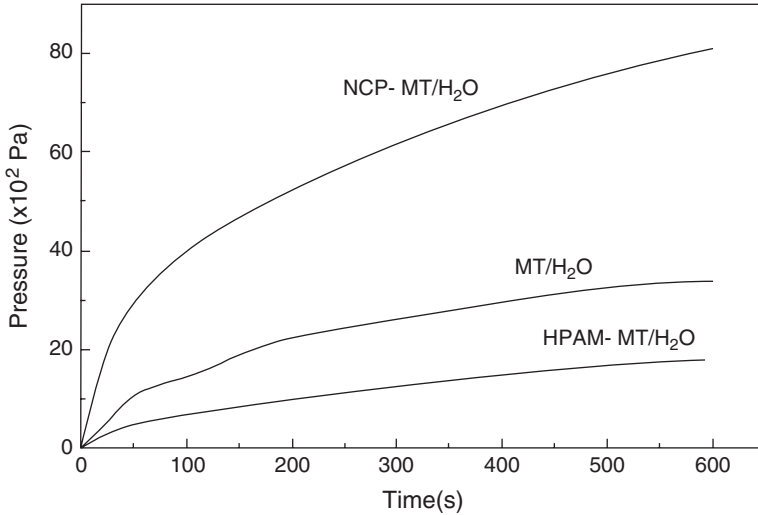


Fig. 6 Wetting curves of HTPS-Mt, HPAM-Mt, and raw Mt in water (Taken from Qiao et al. 2012)

these results, it is expected that the use of solutions based on HTPS would enhance oil displacement, by modifying soil wettability. The fact that the reservoir surface turned to a more marked hydrophilic character would facilitate taking off the oil layer adhered to the rock and would increase the flow resistance of ulterior water injections. As a consequence, water channeling would be reduced, improving the efficiency of the oil displacement.

Qiao and Zhu (2010) also carried out several simulations in order to evaluate if HPAM–HTPS gel systems were able to plug high permeable pores. In this sense, sand-pack core-flood assays were performed determining the influence of gel presence on water permeability of the reservoir. From the results derived from those tests, it was evidenced that an intermediate injection of the HTPS solution between two HPAM flooding reduced the polymer fingering, as well as its loss. Besides, Qiao and Zhu (2010) claimed that the use of HTPS solutions reduced significantly water cut phenomenon, by enhancing oil recovery.

4 Anionic Starches

Another alternative for EOR technologies are additives based on anionic modified starches. These derivatives are obtained through the incorporation of functional groups with negative charge, such as carboxymethyl and sulfonic groups (Chen et al. 2015). Modification provides anionic starches with enhanced functional properties such as solubility, hydrophilicity, and flocculation. The most studied derivative is the carboxymethyl starch (CMS), which is an attractive modification not only for academic but also for industrial fields (Kittipongpatana et al. 2006; Lawal et al. 2007;

Zhou et al. 2010). Among CMS derivatives, the sodium carboxymethyl starch (CMS-Na, anionic) can be mentioned.

Carboxymethylation process allows the synthesis of modified starches with useful functional properties for a wide variety of industries, including those related to oil recovery (Zhang 2001; Lazik et al. 2002; Jie et al. 2004; Volkert et al. 2004; Kittipongpatana et al. 2006; Moorthy et al. 2006; Zhou et al. 2007). Figure 7 shows the reaction scheme employed for carboxymethylation of starch molecules, based on Williamson's ether synthesis (Tijssen et al. 2001). As it can be observed, the anionization process involves the incorporation of carboxymethyl moieties to anhydroglucose units of starch molecules, obtaining more hydrophilic derivatives. This modification improves some functional properties of the resulting starch, such as stability in aqueous solutions and retrogradation at low temperatures (Barrios et al. 2012).

The mechanism involves two consecutive reactions. In the first stage, NaOH reacts with starch hydroxyl groups located at C2, C3, or C6. Then, the substitution reaction is carried out by the presence of the reactive agent, monochloroacetic acid (MCAA) or sodium monochloroacetate (SMCA).

Barrios et al. (2012) studied the carboxymethylation process as a way of synthesizing anionic starches using diverse reaction media as well as different reagents. In this sense, these authors proposed the use of isopropanol (IP), dimethyl sulfoxide (DMSO), and water as reaction solvents. Concerning modifying agents, the above-mentioned MCAA and SMCA were employed. Besides, the carboxymethylation process was optimized by adjusting the reaction conditions, such as starch/reagent

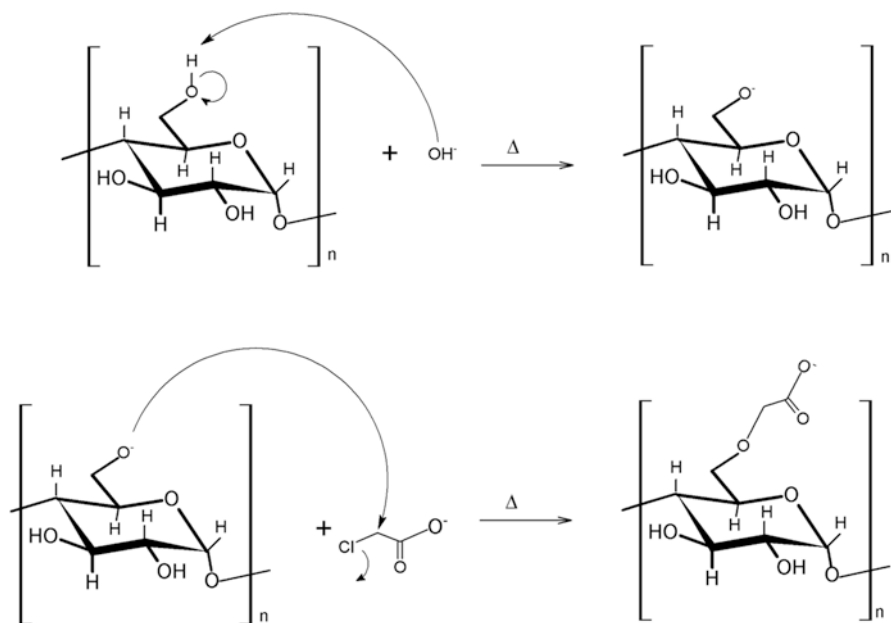


Fig. 7 Reaction scheme to synthesize sodium carboxymethyl starch (CMS-Na, anionic) (Taken from Barrios et al. 2012)

molar ratio, temperature, and time in order to obtain derivatives with high DS values. Additionally, one of the aims of the research was the synthesis of modified starches with high zero-shear viscosity in aqueous suspensions. At this point it is important to mention that the best reaction condition for producing starch derivatives with high DS usually favors the degradation of starch and, consequently, the decrease of solution viscosity (Jie et al. 2004; Sangseethong et al. 2005). Thus, Barrios et al. (2012) proposed an alternative strategy in order to optimize the anionization method that involved three steps: (i) the selection of the solvent by using the reaction conditions already employed by several authors (Heinz and Koschell 2005; Flores 2006; Mollega et al. 2011); (ii) the selection of the reagent among the most reported in the specific literature, taking into account the solvent previously chosen (Jie et al. 2004; Heinz and Koschell 2005; Sangseethong et al. 2005; Stojanovic et al. 2005; Mollega et al. 2011; Flores 2006); and (iii) the selection of the optimal anhydroglucose unit/reagent molar ratio, reaction temperature, and time for the anionization process.

Concerning the reaction medium, authors concluded that starch derivatives obtained by using DMSO or water resulted soluble in water. Meanwhile, those synthesized in IP were insoluble because a heterogeneous anionization process took place, since the modification process was observed only at the surface of starch granules. In order to select the best reactive agent, carboxymethylation process was carried out in a homogeneous medium, employing water as solvent, at 75 °C and 4 h. Obtained derivatives were tested through rheological assays in order to determine the zero-shear rate viscosity. In this sense, the use of SMCA led to derivatives with higher viscosity than those obtained by employing MCAA under the same reaction conditions (Sangseethong et al. 2005). The viscosity increment could be related to the electrostatic repulsion among carboxymethyl groups that would favor the expansion of the molecular structure of the starch. Consequently, a more hindered movement of starch chains is expected. From this result, it could be inferred that sodium carboxymethyl starches synthesized by using SMCA present a high DS value.

Regarding the optimal reaction conditions, Barrios et al. (2012) observed that higher values of DS and solution viscosity were obtained by employing water as solvent and by carrying out the reaction at 60 °C during 6 h, with the addition of an excess of SMCA. Besides, under the same conditions, modified starches obtained by using DMSO as solvent led to solutions with lower viscosity. This result could be associated to the degradation process of starch during the carboxymethylation reaction in DMSO. Finally, it should be mentioned that the use of CMS-Na presents limitations associated with troublesome shales in certain reservoirs with specific soil properties. Zhang (2001) proposed an alternative to overcome this drawback by employing sodium-free derivatives as drilling fluids, such as potassium-based starches (CMS-K).

5 Nonionic Starches

Alkyl ether starch derivatives were also investigated as additives for oil field applications, mainly because they can reduce the fluid loss and increase the viscosity of the fluid displacement. These derivatives are synthesized by incorporating nonionic

functionalities such as hydroxyethyl and hydroxypropyl groups. The industrial relevance of this kind of chemical modification relies on the stabilization of starch aqueous solutions, widening their applications in petroleum industry. According to Datta et al. (2014), hydroxyethyl starches (HES) have been one of the cornerstones in fluid management for over four decades. These modified starches are considered semisynthetic polymers that form polydisperse colloidal solutions conformed by polymerized amylopectin molecules with a high degree of ethylation. Figure 8 shows the chemical structure of HES derivative.

Modified starches are commercially available with different average molecular weights (MW). Derivatives with MW ranging from low (70–130 kg/mol), middle (~00 kg/mol) to high (>450 kg/mol) values are commercially available. Table 2 presents the main trade names of commercial HES, showing their DS and MW.

The industrial production of these derivatives is frequently carried out by an aqueous slurry phase process, by employing starches from different botanical sources. Besides, a two-phase gas–solid method can also be employed. Regarding slurry technology, HES are prepared by the reaction of starch with ethylene oxide in alkaline media through a batchwise process. An advantage of the slurry method is the relatively easy separation of starch granules in the downstream processing. The starting material may be native starch in its granular form or gelatinized in aqueous solutions. Modification of granular starch can be performed using three different reaction media: (i) water, (ii) organic solvents, and (iii) gaseous ethylene oxide. Regardless the media, this modification method involves the use of catalysts such as hydroxides or basic salts. DS and solubility properties are dependent on reaction conditions. Generally, the application of those methods which involve reactions using starch in granular form and in the absence of organic solvents is preferred. In this way, additional reaction

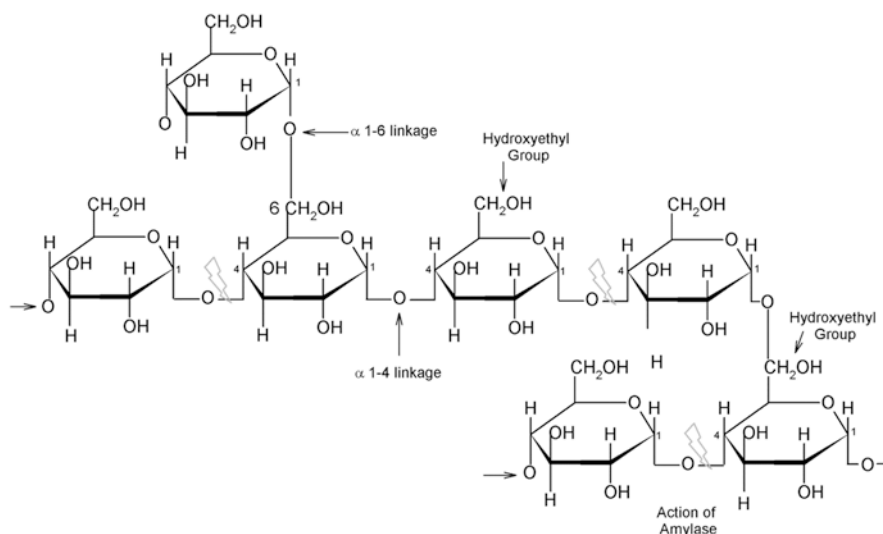


Fig. 8 Chemical structure of HES derivative (Taken from Datta et al. 2014)

stages such as purification after starch modification are avoided, reducing the cost of production of the derivatives. Figure 9 shows the reaction mechanism involved for HES synthesis. However, undesired side reactions like those involving the hydrolysis of ethylene oxide to ethylene glycol can also take place (Fig. 10).

Whether starch modifications are catalyzed or not, the glycol-forming reaction is always carried out. The low selectivity of the slurry process is mainly due to the occurring of this undesired side reaction, which is favored by the large amount of water. Another disadvantage of the suspension process is the long time required to perform the hydroxyethylation of starch. In order to prevent the gelatinization process, starch can be cross-linked before or during the modification. Due to the low starch reactivity, it is necessary to use a reaction temperature that favors the gelatinization of the polysaccharide. Meanwhile, sodium sulfate and sodium chloride are usually added to the reaction media in order to avoid the swelling of starch granules. Then, part of the ethylene oxide becomes ineffective because it reacts with the anion coming from the salt dissolution, as it is shown in Fig. 11.

Table 2 Commercial HES derivatives

Trade name	DS	Classification	MW
Hespan, Plasmasteril, Hextend (balanced)	0.7	Heptastarch	High
Elohes	0.6	Hexastarch	High-medium
HAES-steril, Pentaspan, Gemohes	0.5	Pentastarch	Medium
Voluven, Venofundin, Tetraspan (balanced), Volulyte (balanced), plasma volume Readybag (balanced)	0.4	Tetrasarch	Low

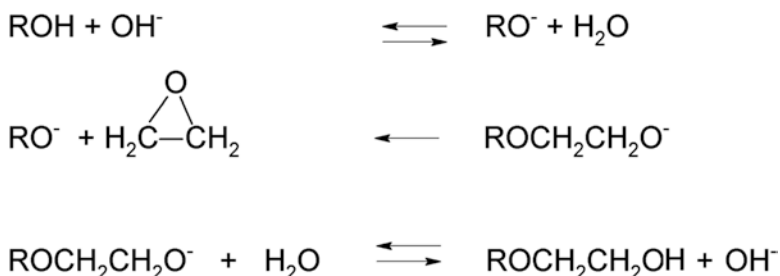


Fig. 9 Reaction mechanism of starch hydroxyethylation

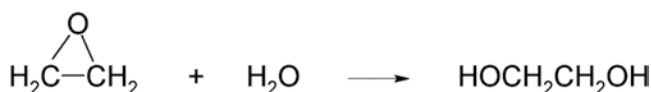


Fig. 10 Hydrolysis of ethylene oxide

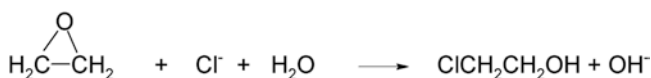


Fig. 11 Ethylene oxide reaction with chloride coming from sodium chloride

Usually, this abovementioned reaction is not desired in the slurry process. In fact, it is an expensive way to create hydroxyl ions to act as basic catalyst in the slurry media. Regarding the use of sodium sulfate or sodium chloride inhibitors for the swelling process of the granules, the second one is the most appropriate since the hydrolysis of ethylene oxide scarcely occurs.

An alternative to reduce the aforementioned drawbacks is the so called “dry, gas–solid” process. Even though the use of gaseous ethylene oxide plus the low moisture in the medium favors the hydrolysis of the reagent, starch reactivity can be enhanced by using higher reaction temperatures. Since starch derivatives can be used in petroleum industry, it is relevant to evaluate not only their efficiency as EOR additives but also their cost of production. In this sense, the selection of a hydroxyethylation method between the two aforementioned processes (slurry versus “dry, gas–solid” processes, by taking into account the optimized conditions and derivative properties) should be focused on the cost reduction associated to the synthetic pathway.

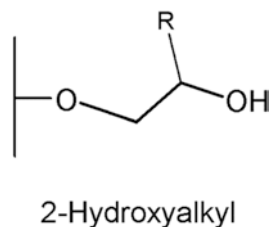
Similarly to hydroxyethyl starches, hydroxypropyl ones can be obtained by the alkaline addition of propylene oxide (Gonera 2004). Figure 12 shows the chemical structure of this starch derivative usually employed in EOR technologies.

According to Mark (2013), this derivative is one of the more produced, among starch hydroxyalkyl ethers, at industrial scale. Aqueous as well as alkaline slurry processes allow obtaining hydroxypropyl starches with low degree of modification (<0.1). On the other hand, starch etherification with propylene oxide in alcohol slurry and alkaline conditions represents the most suitable media reaction to synthesize derivatives with a high degree of modification. It is important to note that functional properties of these derivatives (such as solubility, pasting temperature, and viscosity stability) mainly depend on the degree of modification (Mark 2013).

6 Grafted Starches

Starch grafting is another strategy that produces derivatives with potential application in the petroleum industry (Kalia and Sabaa 2013). Thus, the use of this kind of modified starches as components of drilling fluids is mainly based on their capacity to control the filtrate loss and to act as thickener agents, as well as for stabilizing the soil of oil reservoirs. In this sense, it was demonstrated that these starch derivatives

Fig. 12 Chemical structure of hydroxypropyl starch. R: $-\text{CH}_2-\text{CH}_2-\text{CH}_3$ (Taken from Gonera 2004)



resulted in being more efficient than anionic or nonionic starches for inhibiting clay and shale hydration process. Furthermore, these derivatives can modify the fluid viscosity and reduce the oil field drag, being suitable as additives in EOR technologies. Kalia and Sabaa (2013) stressed that grafted starches presented a better thermal stability and shear rate than HPAM, the hydrosoluble polymer usually employed as additive in EOR technologies. For these reasons, grafted starches have received special attention not only at academic research but also at industrial level. Table 3 includes some grafted starches usually employed in the petroleum industry.

Among vinyl monomers, acrylamide and vinyl alcohol are the most extensively employed for grafting onto starch molecules, which allow obtaining nonionic products for drilling fluids. Starch-g-poly(acrylamide) derivatives are composed of

Table 3 Summary of grafted starches used in the petroleum industry. Taken from Zhang (2001) and Kalia and Sabaa (2013)

Starch	Grafted monomer	Function
Native starch	Acrylamide (AM)	To control the filtrate loss and to increase the viscosity of drilling muds
		To modify the viscosity of displacement fluids
Oxidized starch	AM	To modify the viscosity of displacement fluids
Soluble starch	AM	To modify the viscosity of displacement fluids
Native starch	Sulfomethylated AM	To control the filtrate loss and to increase the viscosity of drilling muds
Pre-gelatinized starch	Acrylonitrile (AN)	To reduce the filtrate loss of drilling muds
Native starch	2-Acrylamido-2-methyl-1-propanesulfonic acid (AMPS)	To control the filtrate loss of drilling muds
Native starch	Cationic allyl monomers	To inhibit the hydration of clay and shale
Native starch	AM and vinyl alcohol (VA)	To control the filtrate loss and to increase the viscosity of drilling muds
Native starch	AM and AMPS	To control the filtrate loss and to increase the viscosity of drilling muds
Native starch	AM and dimethyldiallylammonium chloride	To inhibit the hydration of clay and shale
Native starch	Potassium acrylate (AA) and 2-hydroxy-3-methyl-acrylamidopropyltrimethylammonium chloride (HMOPTA)	To control the filtrate loss and to increase the viscosity of drilling muds
		To inhibit the hydration of clay and shale

acrylamide or acrylamide–acrylic acid branches from a starch main chain. Their use as additives in EOR processes is mainly associated to the capacity of these derivatives to form highly viscous aqueous suspensions. Singh et al. (2006) reported the synthesis of this derivative by using microwave irradiation. The synthesis of grafted starches by this non-conventional method presents some advantages: heating is direct and highly selective, avoiding thermal inertia and heat exchange within the medium (Wiesbrock et al. 2004). In addition, the use of microwave radiation could be performed either in absence or with very low concentration of initiator (Singh et al. 2004, 2006). Figure 13 shows the starch grafting reaction with acrylamide, as well as the reaction conditions. Singh et al. (2006) demonstrated that this monomer was successfully grafted onto potato starch employing a little amount of potassium persulfate as initiator.

Grafting of acrylamide monomers onto starch molecules was corroborated by infrared spectroscopy (IR). In this sense, the detection of bands associated to N-H and C=O functional groups in the grafted starch was a clear evidence of the grafting process. Besides, microwave irradiation favored the reduction of the degree of crystallinity of potato starch, which is an indicative of an effective grafting. Singh et al. (2006) reported a high-yield reaction by carrying out the grafting process under the following conditions: 0.10 M acrylamide, 0.0025 M potassium persulfate, 0.1 g/25 mL potato starch, 720 W microwave power, 60 s exposure, and 25 mL of total reaction volume. In addition, it was demonstrated that an inert atmosphere was not a conditioning factor to perform the starch grafting by microwave irradiation.

On the other hand, Song et al. (2007) synthesized a starch derivative by a graft copolymerization with acrylamide (AM) and 2-acrylamido-2-methylpropane-sulfonic acid (AMPS). These authors reported the use of a complex initiation system of ceric sulfate (CS) and ammonium persulfate (APS) to favor the grafting reaction. Besides, they studied the influence of reaction conditions on yield and final properties of obtained derivatives, proposing these modified starches as a flooding additive for EOR technologies. When 0.2% of grafted starch [Starch-*g-p*(AM-*co*-AMPS)] was used as flooding agent, a higher enhanced oil recovery rate was obtained compared to HPAM. Results showed that the novel graft polymer exhibited a much better resistance to temperature and shear rate than HPAM, having potential application in EOR processes.

Eutamene et al. (2009) also studied starch-grafted polyacrylamide copolymers and evaluated their rheological properties, either in water or in water-based muds. Several grafted starches were synthesized by free-radical grafting of acrylamide

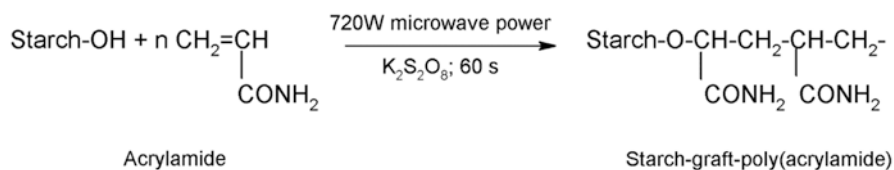


Fig. 13 Acrylamide grafting onto potato starch under microwave irradiation (Taken from Singh et al. 2006)

onto starch, employing ceric ammonium sulfate (CAS) as initiator. These authors stressed that intrinsic viscosity and molar mass of starch derivatives are mainly conditioned by the concentration of both CAS and monomer. Additionally, the behavior of obtained grafted starches under different oil field conditions was predicted, by evaluating the properties of their aqueous solutions. In this sense, water solubility, viscosity, and shear rate as function of temperature, salt concentration and type, and aging time were studied. It is important to highlight that the understanding of these properties is relevant for using grafted starches in drilling muds. Comparing grafted starches with acrylamide to the unmodified starch substrate, the first ones behaved as shear thinning and salt resistant; and their rheological properties were more stable with time.

7 Concluding Remarks

Along the previous sections, the synthetic pathways developed for producing modified starches susceptible to be employed as EOR agents were discussed. Then, an outlook of the research works provided by the scientific literature was provided. The synthesis of cationic, anionic, nonionic, and grafted starch derivatives was presented, with the inherent particularities regarding each kind of modification. Each type of synthesis depends on many reaction parameters (such as temperature, medium, or the presence of coagents as additives) as well as the technical methodology employed (homogeneous or heterogeneous slurry, microwave assisted, among others). In addition, the resulting product must present several particularities for its use in EOR technologies. For example, the interaction between modified starches and soil and the viscosity of the resulting starch solutions are critical parameters to take into account in order to achieve the objectives planned for the recovery. In such a sense, the research regarding this subject will increase in the next years for two main reasons: the availability of raw starch (as a commodity easily obtained from the biomass) and the increasing interest in novel technologies for oil recovery purposes. We hope that, in the near future, the data presented in the present work will be largely exceeded.

Acknowledgments Authors wish to thank the Consejo Nacional de Investigaciones Científicas y Técnicas de la República Argentina (CONICET) for the financial support given to this research.

References

- Al-Muntasheri G, Nasr-El-Din H, Hussein I (2007) A rheological investigation of a high temperature organic gel used for water shut-off treatments. *J Pet Sci Eng* 59(1–2):73–83
- Ayoub A, Bliard C (2003) Cationisation of glycerol plasticised wheat starch under microhydraulic molten conditions. *Starch/Stärke* 55:297–303
- Ayoub A, Berzin F, Tighzert L et al (2004) Study of the thermoplastic wheat starch cationisation reaction under molten condition. *Starch/Stärke* 56:513–519

- Bao M, Kong X, Jiang G et al (2009) Laboratory study on activating indigenous microorganisms to enhance oil recovery in Shengli oilfield. *J Pet Sci Eng* 66:42–46
- Barrios S, Contreras J, López-Carrasquero F et al (2012) Chemical modification of cassava starch by carboxymethylation reactions using sodium monochloro acetate as modifying agent. *Revista de la Facultad de Ingeniería UCV* 27(2):97–105
- Bendoraitiene J, Klimaviciute R, Zemaitaitis A (2012) Preparation of high substituted cationic starch in presence of organic bases. *Starch/Stärke* 64:696–703
- Bertolini A (2009) Trends in starch applications. In: Bertolini A (ed) *Starches: characterization, properties, and applications*. CRC Press, Boca Raton, pp 1–19
- Butrim S, Butrim N, Bil'dyukevich T et al (2008) Synthesis and physicochemical properties of low-substituted cationic ethers of starch. *Russ J Appl Chem* 81:2026–2032
- Chang Y, Eom J, Kim J et al (2010) Preparation and characterization of shape memory polymer networks based on carboxylated telechelic poly(ϵ -caprolactone)/epoxidized natural rubber blends. *J Ind Eng Chem* 16:256–260
- Chen Q, Yu H, Wang L et al (2015) Recent progress in chemical modification of starch and its applications. *RSC Adv* 5:67459–67474
- Daripa P, Pasa G (2004) An optimal viscosity profile in enhanced oil recovery by polymer flooding. *Int J Eng Sci* 42:2029–2039
- Datta R, Nair R, Pandey A et al (2014) Hydroxyethyl starch: controversies revisited. *J Anaesthesiol Clin Pharmacol* 30:472–480
- Eutamene M, Benbakhti A, Khodja M et al (2009) Preparation and aqueous properties of starch-grafted polyacrylamide copolymers. *Starch/Stärke* 61(2):81–91
- Fink J (2015) *Petroleum engineer's guide to oil field chemicals and fluids*, 2nd edn. Elsevier, Oxford
- Flores R (2006) Desarrollo de almidones funcionalizados y evaluación de las propiedades reológicas para su aplicación en la industria petrolera. Undergraduate Thesis, Simón Bolívar University, Caracas
- Fu J, Qiao R, Zhu L et al (2013) Application of a novel cationic starch in enhanced oil recovery and its adsorption properties. *Korean J Chem Eng* 30(1):82–86
- Gao C (2015) Application of a novel biopolymer to enhance oil recovery. *J Pet Explor Prod Technol* 6(4):749–753
- Gonera A (2004) *Aminofunctional starch derivatives: synthesis, analysis, and application*. Cuvillier Verlag, Göttingen
- Haack V, Heinze T, Oelmeyer G et al (2002) Starch derivatives of high degree of functionalization, 8. Synthesis and flocculation behavior of cationic starch polyelectrolytes. *Macromol Mater Eng* 287:495–502
- Hebeish A, Higazy A, El-Shafei A et al (2010) Synthesis of carboxymethyl cellulose (CMC) and starch-based hybrids and their applications in flocculation and sizing. *Carbohydr Polym* 79:60–69
- Heinz T, Koschell A (2005) Carboxymethyl ethers of cellulose and starch – a review. *Macromol Symp* 223:13–39
- Heinze T, Haak V, Rensing S (2004) Starch derivatives of high degree of functionalization. 7. Preparation of cationic 2-hydroxypropyltrimethylammonium chloride starches. *Starch/Stärke* 56:288–296
- Hou J, Li Z, Cao X et al (2009) Integrating genetic algorithm and support vector machine for polymer flooding production performance prediction. *J Pet Sci Eng* 68:29–39
- Huber K, BeMiller J (2001) Location of sites of reaction within starch granules. *Cereal Chem* 78:173–118
- Jaspreet S, Lovedeep K, Mccarthy O (2007) Factors influencing the physico-chemical, morphological, thermal and rheological properties of some chemically modified starches for food applications – a review. *Food Hydrocoll* 21:1–22
- Jeon Y, Lei J, Kim J (2008) Dye adsorption characteristics of alginate/polyaspartate hydrogels. *J Ind Eng Chem* 14:726–731
- Jie Y, Wem-Ren C, Manurung R et al (2004) Exploratory studies on the carboxymethylation of cassava starch in water-miscible organic media. *Starch/Stärke* 56:100–107
- Kalia S, Sabaa M (eds) (2013) *Polysaccharide based graft copolymers*. Springer, Berlin Heidelberg

- Karabakal U, Bagci S (2004) Determination of wettability and its effect on waterflood performance in limestone medium. *Energy Fuel* 18:438–449
- Kavaliauskaite R, Klimaviciute R, Zemaitaitis A (2008) Factors influencing production of cationic starches. *Carbohydr Polym* 73:665–675
- Kittipongpatana O, Sirithunyalug J, Laenger R (2006) Preparation and physicochemical properties of sodium carboxymethyl mungbean starches. *Carbohydr Polym* 63:105–112
- Klimaviciute R, Riauka A, Zemaitaitis A (2007) The binding of anionic dyes by cross-linked cationic starches. *J Polym Res* 14:67–73
- Kuo W, Lai H (2007) Changes of property and morphology of cationic corn starches. *Carbohydr Polym* 69:544–553
- Kuo W, Lai H (2009) Effects of reaction conditions on the physicochemical properties of cationic starch studied by RSM. *Carbohydr Polym* 75:627–635
- Lawal O, Lechner M, Hartmann B et al (2007) Carboxymethyl cocoyam starch: synthesis, characterisation and influence of reaction parameters. *Starch/Stärke* 59:224–233
- Lazik W, Heinz T, Pfeiffer K et al (2002) Starch derivatives of a high degree of functionalization. VI multistep carboxymethylation. *J Appl Polym Sci* 86:743–752
- Leslie T, Xiao H, Dong M (2005) Tailor-modified starch/cyclodextrin-based polymers for use in tertiary oil recovery. *J Pet Sci Eng* 46:225–232
- Mark H (2013) *Encyclopedia of polymer science and technology, concise*, 3rd edn. Wiley, New Jersey
- Mollega S, Barrios S, Freijoo J et al (2011) Modificación química de almidón de juca nativo mediante la reacción de carboximetilación en medio acuoso. *Revista de la Facultad de Ingeniería de la Universidad Central de Venezuela* 26(1):117–128
- Moorthy S, Andersson L, Eliasson A et al (2006) Determination of amylose content in different starches using modulated differential scanning calorimetry. *Starch/Stärke* 58:209–214
- Morel D, Vert M, Bouger Y (2010) First polymer injection in deep offshore field Angola. In: *Abstracts of the Annual Technical Conference and Exhibition, Florence, Italy, 19–22 Sept 2010*
- Nezhad S, Cheraghian G (2015) Mechanisms behind injecting the combination of nano-clay particles and polymer solution for enhanced oil recovery. *Appl Nanosci* 6(6):923–931
- Pal S, Mal D, Singh R (2005) Cationic starch: an effective flocculating agent. *Carbohydr Polym* 59:417–423
- Pi-xin W, Xiu-li W, Xue D et al (2009) Preparation and characterization of cationic corn starch with a high degree of substitution in dioxane–THF–water media. *Carbohydr Res* 344:851–855
- Prado H, Matulewicz M (2014) Cationization of polysaccharides: a path to greener derivatives with many industrial applications. *Eur Polym J* 52:53–75
- Qiao R, Zhu W (2010) Evaluation of modified cationic starch for impeding polymer channeling and in-depth profile control after polymer flooding. *J Ind Eng Chem* 16:278–282
- Qiao R, Zhang R, Zhu W et al (2012) Lab simulation of profile modification and enhanced oil recovery with a quaternary ammonium cationic polymer. *J Ind Eng Chem* 18:111–115
- Radosta S, Vorwerk W, Ebert A et al (2004) Properties of low-substituted cationic starch derivatives prepared by different derivatisation processes. *Starch/Stärke* 56:277–287
- Sabhapondit A, Borthakur A, Haque I (2003) Water soluble acrylamidomethyl propane sulfonate (AMPS) copolymer as an enhanced oil recovery. *Energy Fuel* 17:683–688
- Sableviciene D, Klimaviciute R, Bendoraitiene J et al (2005) Flocculation properties of high-substituted cationic starches. *Colloids Surf A Physicochem Eng Asp* 259:23–30
- Sangseethong K, Ketsilp S, Srirath K (2005) The role of reaction parameters on the preparation and properties of carboxymethyl cassava starch. *Starch/Stärke* 57:84–93
- Shi L, Zhu S, Zhang J et al (2015) Research into polymer injection timing for Bohai heavy oil reservoirs. *Pet Sci* 12:129–134
- Siau C, Karim A, Norziah M et al (2004) Effects of cationization on DSC thermal profiles, pasting and emulsifying properties of sago starch. *J Sci Food Agric* 84:1722–1730
- Silva I, De Melo M, Luvizotto J (2007) Polymer flooding: a sustainable enhanced oil recovery in the current scenario. In: *Abstracts of the Latin American Caribbean petroleum engineering conference, Buenos Aires, 15–18 Apr 2007*
- Singh V, Tiwari A, Tripathi D et al (2004) Microwave assisted synthesis of guar-g-polyacrylamide. *Carbohydr Polym* 51:1–6

- Singh V, Tiwari A, Pandey S et al (2006) Microwave-accelerated synthesis and characterization of potato starch-g-poly(acrylamide). *Starch/Stärke* 58:536–543
- Singh R, Pal S, Rana V et al (2013) Amphoteric amylopectine: a novel polymeric flocculant. *Carbohydr Polym* 91:294–299
- Song H, Zhang S, Ma X et al (2007) Synthesis and application of starch-graft-poly(AM-co-AMPS) by using a complex initiation system of CS-APS. *Carbohydr Polym* 69(1):189–195
- Sorbie K (2000) Polymer-improved oil recovery. CRC Press, Boca Raton
- Stojanovic Z, Jeremic K, Jovanovic S et al (2005) A comparison of some methods for the determination of the degree of substitution of carboxymethyl starch. *Starch/Stärke* 57:79–83
- Tara A, Berzin F, Tighzert L et al (2004) Preparation of cationic wheat starch by twin-screw reactive extrusion. *J Appl Polym Sci* 93:201–208
- Tijssen C, Kolk H, Stamhuis E et al (2001) An experimental study on the carboxymethylation of granular potato starch in non-aqueous media. *Carbohydr Polym* 45:219–226
- Van den Hoek P (2004) Impact of induced fractures on sweep and reservoir management in pattern floods. In: Abstracts of the SPE annual technical conference and exhibition, Texas, 24–29 Sept 2004
- Volkert B, Loth F, Lazik W et al (2004) Highly substituted carboxymethyl starch. *Starch/Stärke* 56:307–314
- Wang Y, Xie W (2010) Synthesis of cationic starch with a high degree of substitution in an ionic liquid. *Carbohydr Polym* 80:1172–1177
- Wang W, Liu Y, Gu Y (2003) Application of a novel polymer system in chemical enhanced oil recovery (EOR). *Colloid Polym Sci* 281:1046–1054
- Wei Y, Cheng F, Zheng H (2008) Synthesis and flocculating properties of cationic starch derivatives. *Carbohydr Polym* 74:673–679
- Wever D, Picchioni F, Broekhuis A (2011) Polymers for enhanced oil recovery: a paradigm for structure–property relationship in aqueous solution. *Prog Polym Sci* 36:1558–1628
- Wiesbrock F, Hoogenboom R, Schubert U (2004) Microwave assisted polymer synthesis: state-of-the-art and future perspectives. *Macromol Rapid Commun* 25:1739–1764
- Zhang L (2001) A review of starches and their derivatives for oil applications in China. *Starch/Stärke* 53:401–407
- Zhang M, Ju B-Z, Zhang S et al (2007) Synthesis of cationic hydrolyzed starch with high DS by dry process and use in salt-free dyeing. *Carbohydr Polym* 69:123–129
- Zhou X, Yang J, Qu G (2007) Study on synthesis and properties of modified starch binder foundry. *J Mater Process Technol* 183:407–411
- Zhou X, Yang J, Qian F et al (2010) Synthesis and application of modified starch as a shell-core main adhesive in a foundry. *J Appl Polym Sci* 116:2893–2900

Part III
Other Applications Related to
Environmental Care

Chitosan: From Organic Pollutants to High-Value Polymeric Materials

María I. Errea, Ezequiel Rossi, Silvia Nair Goyanes,
and Norma Beatriz D'Accorso

1 Introduction

Chitosan is a well-known biopolymer chemically obtained by partial deacetylation of the naturally occurring chitin ((1 → 4)-2-acetamido-2-deoxy-β-D-glucan) (Fig. 1).

After cellulose, chitin is the second most abundant natural polymer in the world. Despite the widespread occurrence of this polysaccharide, the main commercial natural sources of chitin have been crab and shrimp shells which are currently waste materials of the food processing industries.

Silvia Nair Goyanes and Norma Beatriz D'Accorso contributed equally to this work.

M.I. Errea

Departamento de Ingeniería Química, Instituto Tecnológico de Buenos Aires (ITBA),
Avda. Eduardo Madero 399, 1106 Ciudad Autónoma de Buenos Aires, Argentina

E. Rossi

Departamento de Ingeniería Química, Instituto Tecnológico de Buenos Aires (ITBA),
CONICET, Avda. Eduardo Madero 399, 1106 Ciudad Autónoma de Buenos Aires, Argentina

S.N. Goyanes (✉)

Facultad de Ciencias Exactas y Naturales, Departamento de Física, Laboratorio de Polímeros
y Materiales Compuestos (LP&MC), Universidad de Buenos Aires, Buenos Aires, Argentina

Consejo Nacional de Investigaciones Científicas y Técnicas (CONICET)-UBA, Instituto de
Física de Buenos Aires (IFIBA), Buenos Aires, Argentina

e-mail: goyanes@df.uba.ar

N.B. D'Accorso (✉)

Facultad de Ciencias Exactas y Naturales, Departamento de Química Orgánica, Universidad
de Buenos Aires, Buenos Aires, Argentina

Consejo Nacional de Investigaciones Científicas y Técnicas (CONICET)-UBA, Centro de
Investigación en Hidratos de Carbono (CIHIDECAR), Buenos Aires, Argentina

e-mail: norma@qo.fcen.uba.ar

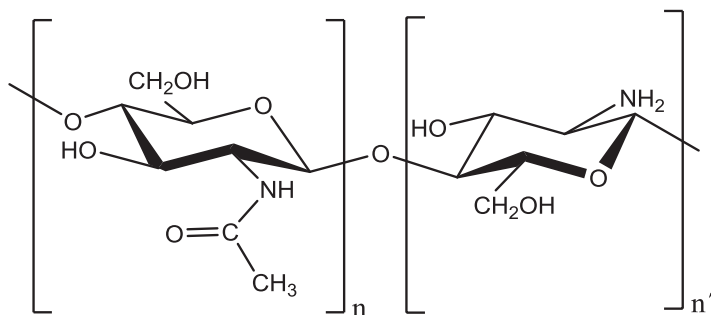


Fig. 1 Structure of partially acetylated chitosan

Because of chitosan polydispersity with respect to molecular weight, producers mainly refer to sample viscosity rather than molecular mass (Croisier and Jérôme 2013).

Besides, due to its poor water solubility, physical characterization of chitosan is not easy to perform. Different methods including pH-potentiometric titration, IR-spectroscopy, $^1\text{H-NMR}$ spectroscopy, UV-spectroscopy, colloidal titration, and enzymatic degradation are reported in the literature for the determination of chitosan deacetylation degree (Balázs and Sipos 2007), while its molecular mass is typically deduced from viscosimetry or determined by size exclusion chromatography (Croisier and Jérôme 2013).

Chitosan is the only positively charged, naturally occurring polysaccharide (Pavinatto et al. 2010). In fact, the amino groups of the D-glucosamine residues (Fig. 1) have a pK_a value of 6.5 (Nilsen-Nygaard et al. 2015), meaning that the amino groups are predominantly positively charged at pH values below 6.5. At those pH values, chitosan becomes a polycation that can subsequently form ionic complexes with a wide variety of natural or synthetic anionic species such as lipids, proteins, and DNA (Croisier and Jérôme 2013; Madihally and Matthew 1999). Many of the chitosan biomedical or industrial applications are based on the ability of these polysaccharides to form this type of complexes.

For example, it binds negatively charged red blood cells thereby promoting clotting, and this hemostatic property has made it an important component in wound dressings. Similar to other cationic polymers, chitosan possesses antimicrobial properties. Although the mechanisms behind its antimicrobial nature are not completely understood, it is thought that because chitosan is cationic, it likely disrupts anions in bacterial cell walls leading to suppression of biosynthesis and disruption of mass transport across the cell walls (Levengood and Zhang 2014).

Feasibility studies of use of chitosan-based materials for water treatment are also undergoing (Rinaudo 2006). Besides, the complexing ability of chitosan is further exploited for beverages clarification.

On the other hand, glucosamine residues may be specifically reacted with aldehyde functions under mild conditions through reductive amination (Rinaudo 2006). Various functionalizations can be introduced along chitosan backbone by this technique to further extend chitosan field of applications (Croisier and Jérôme 2013).

Besides, the amino group, as well as the primary hydroxyl group, of the chitosan chains can be easily involved in substitution reactions. Grafting of monomers onto chitosan by nucleophilic displacement is described elsewhere.

As was discussed before, it is clear the versatility of chitosan as raw material to be modified in search for the physical and/or chemical properties required for numerous and diverse applications.

2 Chitosan-Based Materials for Biomedical Application

Since long time ago, the scientific community has focused its attention on chitosan as a potential material for biomedical applications. This is because this polymer meets three essential properties that must have a material to be applied in the field of medicine: biocompatibility, biodegradability, and nontoxicity.

Since specific properties required for biomedical materials depend on the area of their application, the most common applications of chitosan-based material in the biomedical field are discussed separately.

2.1 Wound Dressing

Today, various forms of wound dressing materials based on chitin and chitosan derivatives are commercially available (e.g., HemCon® (HemCon Medical Technologies, Inc., Portland, OR), QuikClot® (Z-Medica Corporation, Wallingford, CT), and CELOX™ (SAM Medical, Tualatin, OR)) (Wedmore et al. 2006; Brown et al. 2009; Devlin et al. 2011). They have been developed mainly as external hemostatic agents in the control of hemorrhage and, at the same time, to achieve hemostasis when conventional methods fail.

Besides, there are studies which show that chitin-based dressings can accelerate repair of different tissues, facilitate contraction of wounds, and regulate secretion of the inflammatory mediators such as interleukin 8, prostaglandin E, interleukin 1 β , and others (Jayakumar et al. 2011).

2.2 Tissue Engineering

Although bones have the ability to regenerate when damaged, when bone defects are large enough or critical-sized, they cannot regenerate via normal physiological processes and require intervention in the form of bone grafts. The clinical standards for bone grafting are autograft, harvested from a secondary site in the patient, and allografts, harvested from cadavers and sterilized prior to use (Croisier and Jérôme 2013).

Bone tissue engineering, through the use of synthetic grafts to guide tissue regeneration, offers an alternative to autografts and allografts. A synthetic bone scaffold should be (1) osteoconductive to facilitate bone formation on its surface and (2) highly porous to allow for nutrient and waste transport, neovascularization/angiogenesis, and bone ingrowth. In addition a scaffold should have adequate mechanical strength, and it should degrade over time in concert with bone regeneration (Levengood and Zhang 2014).

Chitosan appears among the most promising biomaterials utilized for bone tissue engineering. The hydrophilic surface of the chitosan promotes cell adhesion and proliferation and evokes minimal foreign-body response. Besides, chitosan can be processed in multiple ways to produce a variety of three-dimensional scaffolds with different pore structures. In addition, hybrid materials with improve mechanical properties are also developed.

2.3 Drug Delivery

As was discussed above, the glucosamine primary amino groups are responsible for most of the biological properties of the chitosan, such as controlled drug release.

Several methods are described for controlling drug release, such as simple drug dissolution process, diffusion, erosion, membrane control, or osmotic systems. But, often, all these methods failed and ionic interactions are the only choice. A controlled release can be achieved for cationic drugs by using anionic polymeric excipients, for example, polyacrylates, sodium carboxymethyl cellulose, or alginate. In the case of anionic drugs, however, chitosan is the only choice (Bernkop-Schnürch and Dünnhaupt 2012).

Bhise et al. (2008), for instance, designed sustained release systems for the anionic drug naproxen using chitosan as drug carrier matrix. Using polyanionic drugs, the interactions between chitosan and the therapeutic agent are more pronounced, and stable complexes are formed from which the drug can be released over a prolonged time period. Sun et al. (2010), for example, designed enoxaparin/chitosan nanoparticulate delivery systems, providing very stable complexes that led to a significantly improved drug uptake.

Besides, chitosan can be homogenized with anionic polymeric excipients, such as polyacrylates, hyaluronic acid, alginate, or carrageenan, resulting in comparatively stable complexes of high density. From such complex, drugs are slowly released through diffusion and erosion processes.

On the contrary, mucoadhesive properties of the chitosan were weak to be useful in the development of peptide and protein delivery systems (Jintapattanakit et al. 2009). However, because of the great versatility of the chitosan to be chemically transformed, it is feasible that a polymer with the mucoadhesion required for this application can be achieved.

On the other hand, there are many reports of *in situ* gelling formulation of chitosans. For instance, Gupta et al. (Gupta and Vyas 2010) developed an *in situ* gelling

delivery system by the combination of polyacrylic acid and chitosan. The resulting formulation was in liquid state at pH 6.0 and underwent rapid transition into a viscous gel phase at physiological pH of 7.4 (Bernkop-Schnürch and Dünnhaupt 2012). The formulation was evaluated as an ophthalmic delivery system of an anti-glaucoma drug, timolol maleate. The results demonstrated that developed formulation was therapeutically efficacious and showed a fickian (diffusion-controlled)-type release behavior over 24 h periods. The developed system is thus a viable alternative to conventional eye drops and can also prevent the rapid drainage as in case of liposomes.

3 Chitosan-Based Materials in Food Industries

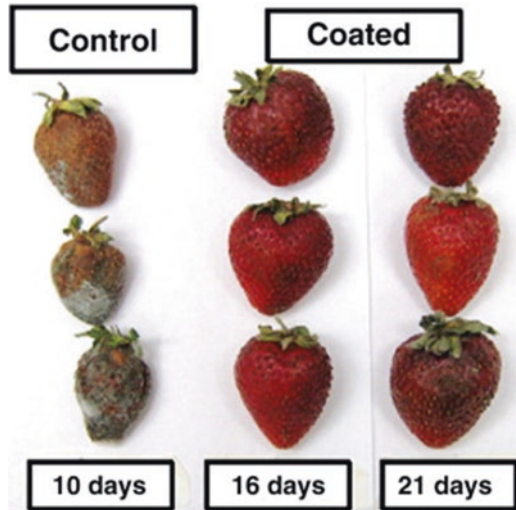
One of the major challenges that food industry is facing nowadays is related to packaging; particularly, packaging of food with a short shelf life period. Traditionally, the materials selected to this function were plastics and their derivatives due to their effectiveness for food preservation. However, the use of plastics creates serious environmental problems (Aider 2010).

Unlike plastics, chitosan-based edible films can be consumed along with the foods which makes its use environmentally safe. They form transparent films with good mechanical properties (Hamed et al. 2016), act as barrier to gases, reduce moisture transfer, restrict oxygen uptake, control respiration rate, retard ethylene production, and prevent the loss of volatiles (Aider 2010). In addition to all the chitosan properties mentioned before, chitosan-based edible coatings are a source of dietary fiber, which allows them to be prebiotic stimulating beneficial bacteria in the gastrointestinal tract (Hamed et al. 2016). Also, they can carry additional functional ingredients (such as antioxidants and antimicrobial agents), enhancing safety and nutritional quality (Kerch 2015; Elsabee and Abdou 2013).

The impact of chitosan-based edible coatings on shelf life, microbiological quality, and biochemical processes during postharvest storage of fruits and vegetables has been described in a number of recent publications. Some examples that can be highlighted are tomato (Elsabee et al. 2008), Chinese water chestnut (Pen and Jiang 2003), carrot (Li and Barth 1998; Barry-Ryan et al. 2000), mango (Chien et al. 2007), strawberry (Hernandez-Munoz et al. 2008; Vu et al. 2011), blueberry (Duan et al. 2011), banana (Maqbool et al. 2010), lotus root (Xing et al. 2010), apple (Qi et al. 2011), and broccoli (Ansorena et al. 2011), among others. In addition, some other food products that were widely studied are ricotta cheese (Di Pierro et al. 2011), pink salmon (Sathivel et al. 2007), and silver carp (Fan et al. 2009).

For example, Vu et al. (2011) developed edible bioactive coating based on modified chitosan for increasing the shelf life of strawberries during storage. Figure 2 shows that uncoated strawberries are dehydrated and are largely contaminated by molds at day 10, whereas coated strawberries kept a good hydrated, red-colored appearance even at day 21.

Fig. 2 Appearance of strawberries coated with modified chitosan-based formulation (Reprinted from Vu et al. 2011. Copyright (2011) with permission from Elsevier)



Another important aspect to be considered is the final cost of the product. Taking into account that the contribution of the packaging to the product total cost is highly significant, the cost of the raw material is one of the main factors to be analyzed. Besides the properties described above, from an economical point of view, chitosan also appears as an attractive raw material for food industries (Aider 2010).

4 Chitosan-Based Materials for Water Treatment

Water is an indispensable element for the viability and development of every civilization. This unquestionable fact challenges to take actions aimed at minimizing the deterioration that this vital resource has suffered in recent decades, due to the industrial, domestic, and agricultural wastes generated by human activities. These activities generate wastewater which contains both inorganic and organic pollutants. Some of the common pollutants are phenols, dyes, detergents, insecticides, pesticides, and heavy metals (Bhatnagar and Sillanpää 2009).

A number of methods such as coagulation, membrane process, adsorption, dialysis, photocatalytic degradation, ion-exchange resins, and biological methods have generally been used for the removal of toxic pollutants from water and wastewater (Bhatnagar and Sillanpää 2009). Although the type of the process to be employed may depend on nature of pollutant, adsorption process is one of the most popular. The increasing demand for new and economic processes for water treatment has led many research groups to investigate the possibility of using waste biomaterials for metal uptake (Bailey et al. 1999; Guibal 2004).

In this context, there are many reports of the potential of chitin and chitosan as adsorbent for dyes or metal removal from contaminated water. Beside, some international companies purchase industrial grade chitosan for wastewater treatment (Kyzas and Bikiaris 2015).

Some of the advances in this field are summarized below.

4.1 Critical Analysis of Feasibility of Use of Chitosan-Based Materials for Metal Removal

Chromium is one of the major trace heavy metal pollutants in the environment (Volesky 2001). It is well known that while Cr (III) is an essential nutrient required for sugar and fat metabolism, Cr (VI) is an extremely carcinogenic agent (Costa 1997). Therefore, it is essential to accurately define the individual quantity of Cr (VI) (Rossi et al. 2017).

Taking into account that in acidic aqueous medium, at low concentration, Cr (VI) exists as anion (HCrO_4^-), while at the same conditions Cr (III) exists as a positive ion, the use of an anion exchanger as solid sorbent is a good alternative for chromium speciation.

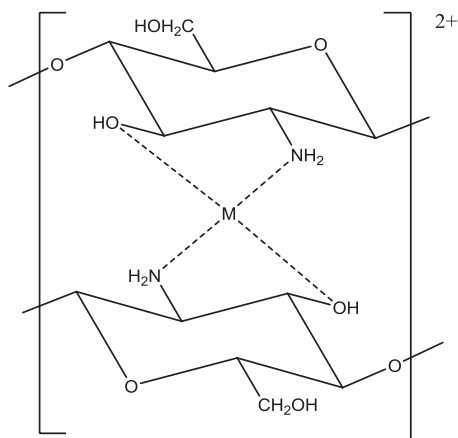
Considering that the pKa value of chitosan is 6.50, at pH below 5, more than 90% of the amino groups are in their protonated form ($-\text{NH}_3^+$) (Rojas et al. 2005), and chitosan derivatives have been proposed as an anionic exchanger. There are many articles published regarding the use of chitosan-based materials as adsorbents for chromium (VI) removal (Bhatt et al. 2015; Qin et al. 2003; Malarvizhi et al. 2010; Lee et al. 2005; Li et al. 2009; Whitacre 2014; Sharma et al. 2017; Rojas et al. 2005).

On the other hand, the contamination of natural waters by arsenic as arsenites As (III) and arsenates As (V) is also a serious problem in several countries. In addition to arsenic contamination from industry (Chatterjee et al. 1993), the high concentrations of arsenic found in groundwater and surface waters have raised concerns in many parts of the world, including Bangladesh (Nickson et al. 1998), Taiwan (Liao et al. 2005), India (Mazumder et al. 2010), Chile, Vietnam (Mazumder et al. 2010), the United States (Welch et al. 2000), and Argentina (Sabbatini et al. 2010).

Since arsenic in aqueous systems is in anionic form, like the Cr (VI), the use of protonated chitosan derivatives for the removal of arsenic from water was also a strategy evaluated by several research groups (Kwok et al. 2014; Boddu et al. 2008; Rahim and Mas Haris 2015).

However, taking into account the acidic lability of the glycosidic bonds, the stability of the chitosan and their derivatives at the pH values required for the amino groups remain mainly protonated is doubtful. This limitation makes unlikely the success of the industrial implementation of chitosan derivatives for the removal of metallic anions.

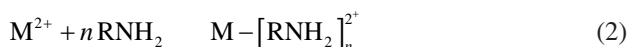
Fig. 3 Chitosan–metal ion complex



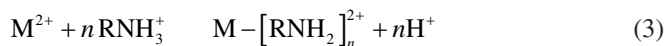
In the case of cations, such as lead, mercury, copper, cobalt, and cadmium, among others, the main mechanism involved in the metal retention is chelation rather than ion exchanger (Varma et al. 2004).

This could be attributed to the major role of the amino groups of chitosan chain, which served as coordination site for metal binding. In addition, the formation of a chitosan–metal ion complex may involve some hydroxyl groups (Fig. 3) (Gerente et al. 2007).

In acidic conditions, the amino groups of chitosan are protonated after reacting with H^+ ions as follows:



where M and RNH_2 represent metal and the amino group of chitosan, respectively, while n is the number of the unprotonated chitosan bound to the metal. Combination of Eqs. 1 and 2 gives the overall reaction as follows (Barakat 2011):



Equation 3 shows that an increase in pH enhances the formation of metal–chitosan complexes. Low pH favors the protonation of the amino sites diminishing the metal-chelating ability of chitosan, and this suggests that at a neutral pH, more metal ions will be adsorbed, depending on their concentrations. On the other hand, with further increase in the solution pH, the formation of metal hydroxide decreases the concentration of free metal cations which leads to the reduction in their removal. The optimum pH for the maximum removal depends on the nature of the cation but is always above 5.0 (Anitha et al. 2015).

Higher values of pH imply less degradation of the polysaccharide, which makes, from this point of view, the implementation of this material much more likely for wastewater treatments. In this context, the capacity of chitosan and their derivate for removing cations is well established (Bassi et al. 2000; Liu et al. 2016; Esmaeili and Khoshnevisan 2016; Zhang et al. 2016; Igberase and Osifo 2015).

Since the economic feasibility of the usage of the absorbent on industrial scale is related to its reusability, many studies looking for the number of cycles of regeneration were carried out.

Unfortunately, the acidic media usually used in this process lead to a fast degradation of the polysaccharide. In this condition, after five cycles of adsorption-desorption, a significant degradation was observed (Liu et al. 2016; Igberase and Osifo 2015).

Ethylenediaminetetraacetic acid (EDTA) could be a good alternative to remove metallic cations from the adsorbent without using an acidic medium. There are reports of high-efficiency metal recovery using this chelate agent, but further studies should be carried out (Chui et al. 1996; Igberase and Osifo 2015).

4.2 *Chitosan-Based Materials as Adsorbent for Dye Removal*

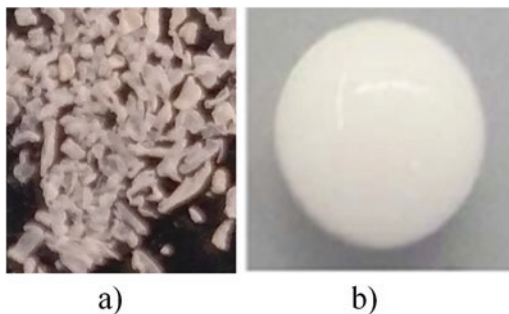
The main industrial wastewater sources are textile, paper, printing, leather, food, and plastic industries. Among them, one of the most worrying pollutants on wastewater is dyes because it not only can aesthetically cause issues but also it is harmful to biological organisms and ecology.

The most obvious impact of dye discharge is the persisting nature of the color. Low concentration of dye in water is easily visible and can reduce photosynthetic activities in aquatic environments by preventing the penetration of light. In addition, dyes have direct and indirect toxic effects on humans as they are associated with cancer, jaundice, tumors, skin irritation, allergies, heart defects, and mutations (Vakili et al. 2014; Sakkayawong et al. 2005).

Given their synthetic origin and complex aromatic structures, dyes are non-biodegradable substances that remain stable under different conditions. Due to their inert properties and the normally low concentration of dye molecules, their removal from wastewater is a complex challenge. Moreover, the high cost to remove trace amounts of impurities causes the conventional methods of removing dyes become unfavorable to be applied at a large scale (Vakili et al. 2014).

Adsorption with activated carbon appears to be the best prospect of eliminating dyes. However, this adsorbent is expensive and difficult to regenerate after use (Sakkayawong et al. 2005). In search for alternatives to activated carbon, adsorption techniques using chitosan composites have been developed to adsorb dyes as an alternative to conventional wastewater treatment processes (Vakili et al. 2014; Annadurai 2000; Cestari et al. 2008; Rosa et al. 2008; Crini 2006; Wong et al. 2004; Prado et al. 2004; Chatterjee et al. 2007; Gupta and Suhas 2009).

Fig. 4 Digital photos of (a) chitosan flakes. (b) Chitosan hydrogel bead (Reprinted from Luo et al. 2013. Copyright (2013) with permission from Elsevier)



Recently, hybrid materials based on chitosan have been developed and favorable synergistic effects were observed. For example, chitosan–zinc oxide nanoparticle composites exhibit remarkably improved mechanical properties, such as tensile strength (Mujeeb Rahman et al. 2016). Since its sorption capacity was not affected, this material has the potential to act as alternative industrial low-cost adsorbents (Abul et al. 2015).

On the other hand, Chang and Juang (2004) studied the chitosan/activated clay composites. They found that the adsorption capacity of the composite was comparable to chitosan bed, but the addition of activated clay enhances the capability of chitosan to agglomerate and round gel beads and improves the hardness of the beads. This is especially important for practical applications.

It is critical to keep in mind that chitosan can be molded in different shapes, such as flake, bead, fiber, or film, being flakes the easiest to obtain. Considering that dyes are removed by an adsorption process (a surface phenomenon), the efficacy of the treatment is related to the superficial area of the adsorbent. The adsorption capacity from bead-type chitosan (Fig. 4) is much greater than flake-type chitosan (Fig. 4) which is in agreement with the fact that the beads have a greater surface area than the flakes (Wan Ngah et al. 2002). Beads are prepared by casting an acidic chitosan solution into alkaline solution.

5 Conclusion

As can be seen from reading this chapter, chitosan has proved to be versatile for so many industrial applications and its versatility is the main value of this polymer.

However, the lability at acidic pH of chitosan is a limiting factor that affects mainly its industrial implementation for the removal of metallic anions from water.

In addition, the physical and mechanical properties may vary between two manufacturing batches due to the characteristic polydispersity of chitosan with respect to molecular weight and degree of acetylation. This variation could affect the industrial process and in some cases, when strict specifications are requested (e.g., drug delivery), increase the final cost of the product because a purification step prior to use is required.

Briefly, despite of the disadvantages mentioned before, due to its great versatility, its nontoxicity, its biodegradability, and the fact that it has a renewable resource, the industrial interest in chitosan and its application has been increasing remarkably in the last years.

Acknowledgment The authors acknowledge Instituto Tecnológico de Buenos Aires (ITBA) for financial support. Ezequiel Rossi has a fellowship from CONICET.

References

- Abul A, Samad S, Huq D, Moniruzzaman M, Masum M (2015) Textile dye removal from wastewater effluents using Chitosan-Zno nanocomposite. *J Textile Sci Eng* 5(200):2
- Aider M (2010) Chitosan application for active bio-based films production and potential in the food industry: review. *Food Sci Technol* 43(6):837–842
- Anitha T, Kumar PS, Kumar KS, Ramkumar B, Ramalingam S (2015) Adsorptive removal of Pb(II) ions from polluted water by newly synthesized chitosan–polyacrylonitrile blend: equilibrium, kinetic, mechanism and thermodynamic approach. *Process Saf Environ Prot* 98:187–197
- Annadurai G (2000) Design of optimum response surface experiments for adsorption of direct dye on chitosan. *Bioprocess Eng* 23(5):451–455
- Ansorena MR, Marcovich NE, Roura SI (2011) Impact of edible coatings and mild heat shocks on quality of minimally processed broccoli (*Brassica oleracea* L.) during refrigerated storage. *Postharvest Biol Technol* 59(1):53–63
- Bailey SE, Olin TJ, Bricka RM, Adrian DD (1999) A review of potentially low-cost sorbents for heavy metals. *Water Res* 33(11):2469–2479
- Balázs N, Sipos P (2007) Limitations of pH-potentiometric titration for the determination of the degree of deacetylation of chitosan. *Carbohydr Res* 342(1):124–130
- Barakat MA (2011) New trends in removing heavy metals from industrial wastewater. *Arab J Chem* 4(4):361–377
- Barry-Ryan C, Pacussi JM, O'Beirne D (2000) Quality of shredded carrots as affected by packaging film and storage temperature. *J Food Sci* 65(4):726–730
- Bassi R, Prasher SO, Simpson BK (2000) Removal of selected metal ions from aqueous solutions using chitosan flakes. *Sep Sci Technol* 35(4):547–560
- Bernkop-Schnürch A, Dünnhaupt S (2012) Chitosan-based drug delivery systems. *Eur J Pharm Biopharm* 81(3):463–469
- Bhatnagar A, Sillanpää M (2009) Applications of chitin- and chitosan-derivatives for the detoxification of water and wastewater – a short review. *Adv Colloid Interf Sci* 152(1–2):26–38
- Bhatt R, Sreedhar B, Padmaja P (2015) Adsorption of chromium from aqueous solutions using crosslinked chitosan–diethylenetriaminepentaacetic acid. *Int J Biol Macromol* 74:458–466
- Bhise KS, Dhupal RS, Paradkar AR, Kadam SS (2008) Effect of drying methods on swelling, erosion and drug release from chitosan–naproxen sodium complexes. *AAPS Pharm Sci Tech* 9(1):1–12
- Boddu VM, Abburi K, Talbott JL, Smith ED, Haasch R (2008) Removal of arsenic (III) and arsenic (V) from aqueous medium using chitosan-coated biosorbent. *Water Res* 42(3):633–642
- Brown MA, Daya MR, Worley JA (2009) Experience with chitosan dressings in a civilian EMS system. *J Emerg Med* 37(1):1–7
- Cestari AR, Vieira EFS, Tavares AMG, Bruns RE (2008) The removal of the indigo carmine dye from aqueous solutions using cross-linked chitosan – evaluation of adsorption thermodynamics using a full factorial design. *J Hazard Mater* 153(1–2):566–574
- Chang M-Y, Juang R-S (2004) Adsorption of tannic acid, humic acid, and dyes from water using the composite of chitosan and activated clay. *J Colloid Interface Sci* 278(1):18–25

- Chatterjee S, Chatterjee S, Chatterjee BP, Guha AK (2007) Adsorptive removal of congo red, a carcinogenic textile dye by chitosan hydrobeads: binding mechanism, equilibrium and kinetics. *Colloids Surf A Physicochem Eng Asp* 299(1–3):146–152
- Chatterjee A, Das D, Chakraborti D (1993) A study of ground water contamination by arsenic in the residential area of behala, calcutta due to industrial pollution. *Environ Pollut* 80(1):57–65
- Chien P-J, Sheu F, Yang F-H (2007) Effects of edible chitosan coating on quality and shelf life of sliced mango fruit. *J Food Eng* 78(1):225–229
- Chui VWD, Mok KW, Ng CY, Luong BP, Ma KK (1996) Removal and recovery of copper(II), chromium(III), and nickel(II) from solutions using crude shrimp chitin packed in small columns. *Environ Int* 22(4):463–468
- Costa M (1997) Toxicity and carcinogenicity of Cr(VI) in animal models and humans. *Crit Rev Toxicol* 27(5):431–442
- Crini G (2006) Non-conventional low-cost adsorbents for dye removal: a review. *Bioresour Technol* 97(9):1061–1085
- Croisier F, Jérôme C (2013) Chitosan-based biomaterials for tissue engineering. *Eur Polym J* 49(4):780–792
- Devlin JJ, Kircher S, Kozen BG, Littlejohn LF, Johnson AS (2011) Comparison of ChitoFlex®, CELOX™, and QuikClot® in control of hemorrhage. *J Emerg Med* 41(3):237–245
- Di Pierro P, Sorrentino A, Mariniello L, Giosafatto CVL, Porta R (2011) Chitosan/whey protein film as active coating to extend ricotta cheese shelf-life. *Food Sci Technol* 44(10):2324–2327
- Duan J, Wu R, Strik BC, Zhao Y (2011) Effect of edible coatings on the quality of fresh blueberries (Duke and Elliott) under commercial storage conditions. *Postharvest Biol Technol* 59(1):71–79
- Elsabee MZ, Abdou ES (2013) Chitosan based edible films and coatings: a review. *Mater Sci Eng C Mater Biol Appl* 33(4):1819–1841
- Elsabee MZ, Abdou ES, Nagy KSA, Eweis M (2008) Surface modification of polypropylene films by chitosan and chitosan/pectin multilayer. *Carbohydr Polym* 71(2):187–195
- Esmaili A, Khoshnevisan N (2016) Optimization of process parameters for removal of heavy metals by biomass of Cu and Co-doped alginate-coated chitosan nanoparticles. *Bioresour Technol* 218:650–658
- Fan W, Sun J, Chen Y, Qiu J, Zhang Y, Chi Y (2009) Effects of chitosan coating on quality and shelf life of silver carp during frozen storage. *Food Chem* 115(1):66–70
- Gerente C, Lee VKC, Cloirec PL, McKay G (2007) Application of chitosan for the removal of metals from wastewaters by adsorption—mechanisms and models review. *Crit Rev Environ Sci Technol* 37(1):41–127
- Guibal E (2004) Interactions of metal ions with chitosan-based sorbents: a review. *Sep Purif Technol* 38(1):43–74
- Gupta VK, Suhas (2009) Application of low-cost adsorbents for dye removal – a review. *J Environ Econ Manag* 90(8):2313–2342
- Gupta S, Vyas SP (2010) Carboxypol/chitosan based pH triggered in situ gelling system for ocular delivery of timolol maleate. *Sci Pharm* 78(4):959–976
- Hamed I, Özogul F, Regenstein JM (2016) Industrial applications of crustacean by-products (chitin, chitosan, and chitoooligosaccharides): a review. *Trends Food Sci Technol* 48:40–50
- Hernandez-Munoz P, Almenar E, Valle VD, Velez D, Gavara R (2008) Effect of chitosan coating combined with postharvest calcium treatment on strawberry (*Fragaria x ananassa*) quality during refrigerated storage. *Food Chem* 110(2):428–435
- Igberase E, Osifo P (2015) Equilibrium, kinetic, thermodynamic and desorption studies of cadmium and lead by polyaniline grafted cross-linked chitosan beads from aqueous solution. *J Ind Eng Chem* 26:340–347
- Jayakumar R, Prabakaran M, Sudheesh Kumar PT, Nair SV, Tamura H (2011) Biomaterials based on chitin and chitosan in wound dressing applications. *Biotechnol Adv* 29(3):322–337
- Jintapattanakit A, Junyaprasert VB, Kissel T (2009) The role of mucoadhesion of trimethyl chitosan and PEGylated trimethyl chitosan nanocomplexes in insulin uptake. *J Pharm Sci* 98(12):4818–4830

- Kerch G (2015) Chitosan films and coatings prevent losses of fresh fruit nutritional quality: a review. *Trends Food Sci Technol* 46(2):159–166
- Kwok KCM, Koong LF, Chen G, McKay G (2014) Mechanism of arsenic removal using chitosan and nanochitosan. *J Colloid Interface Sci* 416:1–10
- Kyzas G, Bikiaris D (2015) Recent modifications of chitosan for adsorption applications: a critical and systematic review. *Mar Drugs* 13(1):312
- Lee M-Y, Hong K-J, Shin-Ya Y, Kajiuchi T (2005) Adsorption of hexavalent chromium by chitosan-based polymeric surfactants. *J Appl Polym Sci* 96(1):44–50
- Levengood SKL, Zhang M (2014) Chitosan-based scaffolds for bone tissue engineering. *J Mater Chem B* 2(21):3161–3184
- Li P, Barth MM (1998) Impact of edible coatings on nutritional and physiological changes in lightly-processed carrots. *Postharvest Biol Technol* 14(1):51–60
- Li T, Geng B, Zhang N, Jin Z, Qi X (2009) Hexavalent chromium removal from water using chitosan-Fe₀ nanoparticles. *J Phys Conf Ser* 188(1):012057
- Liao C-M, Liang H-M, Chen B-C, Singh S, Tsai J-W, Chou Y-H, Lin W-T (2005) Dynamical coupling of PBPK/PD and AUC-based toxicity models for arsenic in tilapia *Oreochromis mossambicus* from blackfoot disease area in Taiwan. *Environ Pollut* 135(2):221–233
- Liu B, Chen W, Peng X, Cao Q, Wang Q, Wang D, Meng X, Yu G (2016) Biosorption of lead from aqueous solutions by ion-imprinted tetraethylenepentamine modified chitosan beads. *Int J Biol Macromol* 86:562–569
- Luo Y, Teng Z, Wang X, Wang Q (2013) Development of carboxymethyl chitosan hydrogel beads in alcohol-aqueous binary solvent for nutrient delivery applications. *Food Hydrocoll* 31(2):332–339
- Madhally SV, Matthew HWT (1999) Porous chitosan scaffolds for tissue engineering. *Biomaterials* 20(12):1133–1142
- Malarvizhi R, Venkateswarlu Y, Ravi babu V, Syghana Begum S (2010) Studies on removal of chromium (VI) from water using chitosan coated *Cyperus pangorei*. *Water Sci Technol* 62(10):2435–2441
- Maqbool M, Ali A, Ramachandran S, Smith DR, Alderson PG (2010) Control of postharvest anthracnose of banana using a new edible composite coating. *Crop Prot* 29(10):1136–1141
- Mazumder DNG, Ghosh A, Majumdar KK, Ghosh N, Saha C, Mazumder RNG (2010) Arsenic contamination of ground water and its health impact on population of district of Nadia, West Bengal, India. *Indian J Community Med* 35(2):331–338
- Mujeeb Rahman P, Abdul Mujeeb VM, Muraleedharan K, Thomas SK (2016) Chitosan/nano ZnO composite films: enhanced mechanical, antimicrobial and dielectric properties. *Arabian J Chem*. In press
- Nickson R, McArthur J, Burgess W, Ahmed KM, Ravenscroft P, Rahmann M (1998) Arsenic poisoning of Bangladesh groundwater. *Nature* 395(6700):338–338
- Nilsen-Nygaard J, Strand S, Vårum K, Draget K, Nordgård C (2015) Chitosan: gels and interfacial properties. *Polymers* 7(3):552
- Pavinatto FJ, Caseli L, Oliveira ON (2010) Chitosan in nanostructured thin films. *Biomacromolecules* 11(8):1897–1908
- Pen LT, Jiang YM (2003) Effects of chitosan coating on shelf life and quality of fresh-cut Chinese water chestnut. *Food Sci Technol* 36(3):359–364
- Prado AGS, Torres JD, Faria EA, Dias SCL (2004) Comparative adsorption studies of indigo carmine dye on chitin and chitosan. *J Colloid Interface Sci* 277(1):43–47
- Qi H, Hu W, Jiang A, Tian M, Li Y (2011) Extending shelf-life of fresh-cut ‘Fuji’ apples with chitosan-coatings. *Innov Food Sci Emerg Technol* 12(1):62–66
- Qin C, Du Y, Zhang Z, Liu Y, Xiao L, Shi X (2003) Adsorption of chromium (VI) on a novel quarternized chitosan resin. *J Appl Polym Sci* 90(2):505–510
- Rahim M, Mas Haris MRH (2015) Application of biopolymer composites in arsenic removal from aqueous medium: a review. *J Radiat Res Appl Sci* 8(2):255–263
- Rinaudo M (2006) Chitin and chitosan: properties and applications. *Prog Polym Sci* 31(7):603–632

- Rojas G, Silva J, Flores JA, Rodriguez A, Ly M, Maldonado H (2005) Adsorption of chromium onto cross-linked chitosan. *Sep Purif Technol* 44(1):31–36
- Rosa S, Laranjeira MCM, Riela HG, Fávère VT (2008) Cross-linked quaternary chitosan as an adsorbent for the removal of the reactive dye from aqueous solutions. *J Hazard Mater* 155(1–2):253–260
- Rossi E, Errea MI, de Cortalezzi MMF, Stripeikis J (2017) Selective determination of Cr (VI) by on-line solid phase extraction FI-SPE-FAAS using an ion exchanger resin as sorbent: an improvement treatment of the analytical signal. *Microchem J* 130:88–92
- Sabbatini P, Yrazu F, Rossi F, Thern G, Marajofsky A, Fidalgo de Cortalezzi MM (2010) Fabrication and characterization of iron oxide ceramic membranes for arsenic removal. *Water Res* 44(19):5702–5712
- Sakkayawong N, Thiravetyan P, Nakbanpote W (2005) Adsorption mechanism of synthetic reactive dye wastewater by chitosan. *J Colloid Interface Sci* 286(1):36–42
- Sathivel S, Liu Q, Huang J, Prinyawiwatkul W (2007) The influence of chitosan glazing on the quality of skinless pink salmon (*Oncorhynchus gorbuscha*) fillets during frozen storage. *J Food Eng* 83(3):366–373
- Sharma G, Naushad M, Al-Muhtaseb AH, Kumar A, Khan MR, Kalia S, Shweta BM, Sharma A (2017) Fabrication and characterization of chitosan-crosslinked-poly(alginate) nanohydrogel for adsorptive removal of Cr(VI) metal ion from aqueous medium. *Int J Biol Macromol* 95:484–493
- Sun W, Mao S, Wang Y, Junyaprasert VB, Zhang T, Na L, Wang J (2010) Bioadhesion and oral absorption of enoxaparin nanocomplexes. *Int J Pharm* 386(1–2):275–281
- Vakili M, Rafatullah M, Salamatinia B, Abdullah AZ, Ibrahim MH, Tan KB, Gholami Z, Amouzgar P (2014) Application of chitosan and its derivatives as adsorbents for dye removal from water and wastewater: a review. *Carbohydr Polym* 113:115–130
- Varma AJ, Deshpande SV, Kennedy JF (2004) Metal complexation by chitosan and its derivatives: a review. *Carbohydr Polym* 55(1):77–93
- Volesky B (2001) Detoxification of metal-bearing effluents: biosorption for the next century. *Hydrometallurgy* 59(2–3):203–216
- Vu KD, Hollingsworth RG, Leroux E, Salmieri S, Lacroix M (2011) Development of edible bioactive coating based on modified chitosan for increasing the shelf life of strawberries. *Food Res Int* 44(1):198–203
- Wan Ngah WS, Ab Ghani S, Hoon LL (2002) Comparative adsorption of lead(II) on flake and bead-types of chitosan. *J Chin Chem Soc* 49(4):625–628
- Wedmore I, McManus JG, Pusateri AE, Holcomb JB (2006) A special report on the chitosan-based hemostatic dressing: experience in current combat operations. *J Trauma Acute Care Surg* 60(3):655–658
- Welch AH, Westjohn DB, Helsel DR, Wanty RB (2000) Arsenic in ground water of the United States: occurrence and geochemistry. *Ground Water* 38(4):589–604
- Whitacre DM (2014) Reviews of environmental contamination and toxicology. vol 233. Springer International Publishing, Switzerland
- Wong YC, Szeto YS, Cheung WH, McKay G (2004) Adsorption of acid dyes on chitosan – equilibrium isotherm analyses. *Process Biochem* 39(6):695–704
- Xing Y, Li X, Xu Q, Jiang Y, Yun J, Li W (2010) Effects of chitosan-based coating and modified atmosphere packaging (MAP) on browning and shelf life of fresh-cut lotus root (*Nelumbo nucifera* Gaerth). *Innovative Food Sci Emerg Technol* 11(4):684–689
- Zhang L, Zeng Y, Cheng Z (2016) Removal of heavy metal ions using chitosan and modified chitosan: a review. *J Mol Liq* 214:175–191

PLA-Based Nanocomposites Reinforced with CNC for Food Packaging Applications: From Synthesis to Biodegradation

M.P. Arrieta, M.A. Peltzer, J. López, and L. Peponi

1 Introduction

The world plastic production, thermoplastics and poly(urethanes), has reached over 250 million tons the last years (Fig. 1a) (Plastic Europe 2015). High amount of these plastics are demanded by the packaging sector (Fig. 1b), which are generally short-term applications (Plastic Europe 2015).

Moreover, high amount of plastic packaging wastes go to landfills every year (Fig. 2) (European Commission 2013) creating an enormous amount of waste without energy or material recovery, mainly those generated from the food packaging sector. The most demanded plastics for food packaging applications are low-density poly(ethylene) (LDPE) (i.e., films), high-density poly(ethylene) (HDPE) (i.e., milk bottles), poly(styrene) (PS) (i.e., yogurt pots), poly(propylene) (PP) (i.e., packaging hinged caps), and polyethylene terephthalate (PET) (water bottles) (Plastic Europe 2015).

M. P. Arrieta and L. Peponi contributed equally to this work.

M.P. Arrieta (✉) • L. Peponi (✉)

Institute of Polymer Science and Technology (ICTP-CSIC),

Juan de la Cierva 3, 28006 Madrid, Spain

e-mail: marrieta@ictp.csic.es; lpeponi@ictp.csic.es

M.A. Peltzer

Department of Science and Technology, University of Quilmes,

Roque Sáenz Peña 352, B1876BXD Buenos Aires, Argentina

National Scientific and Technical Research Council (CONICET), Buenos Aires, Argentina

J. López

Instituto de Tecnología de Materiales, Universitat Politècnica de Valencia,

03801 Alcoy-Alicante, Spain

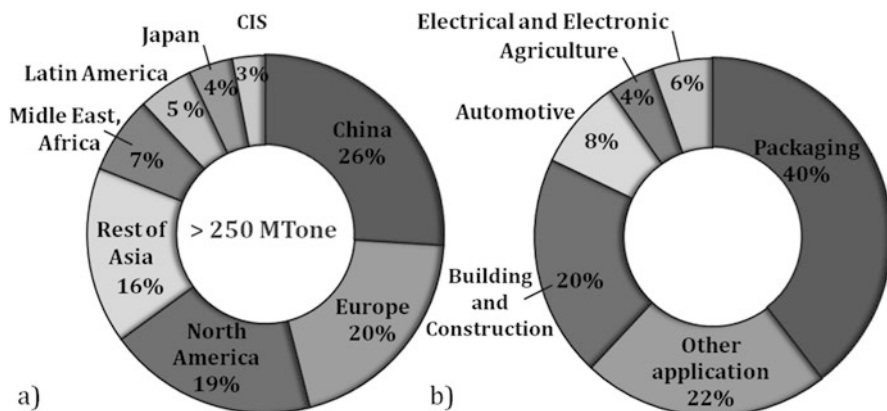


Fig. 1 (a) World plastic production and (b) plastic demand by sector in Europe in 2014 (Plastic Europe 2015)

The environmental problems derived from the plastic food packaging caused by both the petrochemical source consumption for their production and the accumulation of high amounts of plastic wastes have led to

a growing interest on the use of biobased and biodegradable polymers for food packaging. Poly(lactic acid) (PLA) is currently the most used biobased and biodegradable thermoplastic able to replace the petroleum-derived polymers for industrial applications (Auras et al. 2004). The industrial production of lactic acid is based on microbial carbohydrate fermentation which is able to produce optically pure lactic acid (Inkinen et al. 2011). PLA is processed at industrial scale with the processing technology frequently used for traditional petroleum-derived thermoplastics. Hence, nowadays PLA polymers have found a commercial application in single use disposal products due to its low price compared with other biodegradable polymers (Carrasco et al. 2014). PLA is biocompatible and biodegradable; thus it is used in biomedical and packaging sectors. It is classified as generally recognized as safe (GRAS) by the Food and Drug Administration (FDA), and it is safe for food packaging use (Jamshidian et al. 2010). Examples of PLA biomedical applications are bone implants (Turner II et al. 2004), fracture fixation devices, sutures, and nano-titration plates (Södergård and Stolt 2002), while as packaging, it is frequently used for short shelf-life products such as injection molded disposable cutlery and thermoformed containers such as trays and lids, bottles, cold drink cups, disposable salad cups, blister packages, and overwrap and flexible films (Auras et al. 2004; Bor et al. 2012; Jamshidian et al. 2010).

On the other hand, the wastes of PLA coming from packaging products can be composted, disposed in landfill, incinerated, and recycled (Chien et al. 2011). However, the introduction of PLA-based products and other biodegradable plastics into the packaging market chain implies another nature of plastic waste different than petrochemical plastics that has to be managed. On the other hand, nowadays

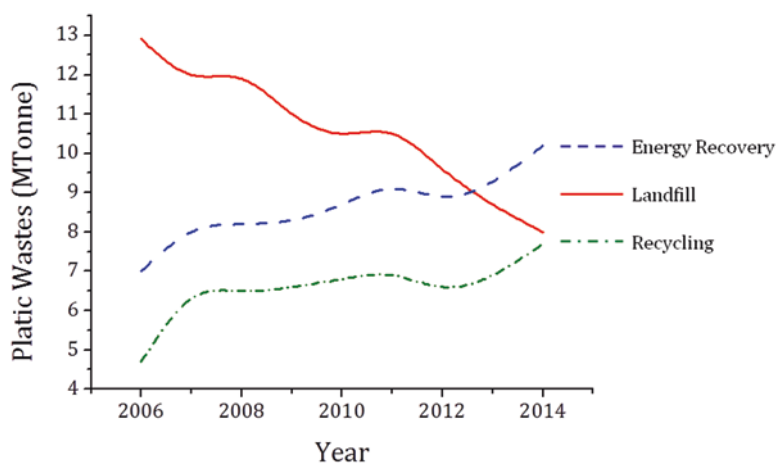


Fig. 2 Annual average of plastic postconsumer waste generation

consumers have low knowledge about where they have to throw away this kind of plastics after their use and they are commonly disposed with traditional packaging plastics (Samper et al. 2014). Therefore, PLA is possibly recycled with other plastics, resulting in contamination of plastics and thus interfering with plastic recycling efforts. Consequently, it seems that PLA is more suitable for disposal rather than recycling (Chien et al. 2011).

PLA is becoming increasingly popular owing to its high mechanical strength and easy processability compared to other biobased and biodegradable polymers such as poly(hydroxyalkanoates) (PHAs), poly(butylene succinate) (PBS), and poly(butylene adipate terephthalate) (PBAT). Nowadays PLA large-scale production is a reality, and another interesting point for the packaging plastic industry to prefer PLA among other biobased and biodegradable polymers is due to its relatively low price and commercial availability (Fiori 2015). However, one of the main drawbacks for PLA industrial processing is that it is sensitive to thermal degradation (Auras et al. 2004). The melt process has a debilitating effect on the integrity of PLA, which is shown by a decrease in both molecular weight and melt viscosity (Carlson et al. 1998).

Many efforts have been focused on improving not only PLA thermal properties but also its physical and mechanical properties which are still unacceptable and are hindering its practical exploitation (Armentano et al. 2013). This review aims to summarize the advantages of reinforcing PLA matrix with cellulose nanocrystals (CNCs) for the development of bionanocomposites for biodegradable food packaging applications. With this purpose, this chapter begins with a description of PLA properties, focusing on its processing and performance as food packaging material. Then the main characteristics for the melt processing of PLA-CNC bionanocomposites as well as their properties as food packaging materials are summarized. Finally, the chapter discusses the end-life options for PLA-CNC bionanocomposites that focus on compostability.

2 PLA Industrial Production

PLA is obtained from the lactic acid monomer which is produced by fermentation of renewable agricultural sources rich in carbohydrates, such as corn. After harvesting, the starch is separated from the other components of the corn kernel (proteins, fats, fibers, ash, and water) and converted via enzymatic hydrolysis into dextrose (Vink et al. 2003). The presence of hydroxyl and carboxyl groups in lactic acid enables it to be converted directly into polyester via a polycondensation reaction (Madhavan Nampoothiri et al. 2010). However, it is very difficult to obtain solvent-free high molecular weight PLA through the conventional condensation polymerization, and the polymerization time is very long (Auras et al. 2004; Madhavan Nampoothiri et al. 2010).

Industrial lactic acid production utilizes the homofermentative method of dextrose, commonly mediated by *Lactobacillus* (Madhavan Nampoothiri et al. 2010), to obtain the lactic acid monomers: *D*(-)-lactic acid and *L*(+)-lactic acid which are shown in Fig. 3a, b, respectively (Yu et al. 2003). Either *D*-lactic acid, *L*-lactic acid, or a mixture of both is pre-polymerized to obtain an intermediate low molecular mass poly(lactic acid) pre-polymer (Auras et al. 2004). In this step, water is removed under mild conditions and without the use of solvents (Vink et al. 2003). The low molecular mass pre-polymer is then catalytically converted into a mixture of lactide (the cyclic dimer of lactic acid) stereoisomers (Auras et al. 2004; Vink et al. 2003). Lactide is formed by the condensation of either two *L*-lactic acid (Fig. 3c), a *L*-lactic acid and a *D*-lactic acid (Fig. 3d), or two *D*-lactic acid (Fig. 3e) molecules (Auras et al. 2004).

The *L*-isomer constitutes the main fraction of PLA derived from renewable sources since the majority of lactic acid from biological sources exists in this form (Lim et al. 2008). Lactide is then purified to polymer grade by distillation and subsequently polymerized in a solvent-free ring-opening polymerization (ROP) to obtain high molecular weight PLA and finally processed into polylactide pellets

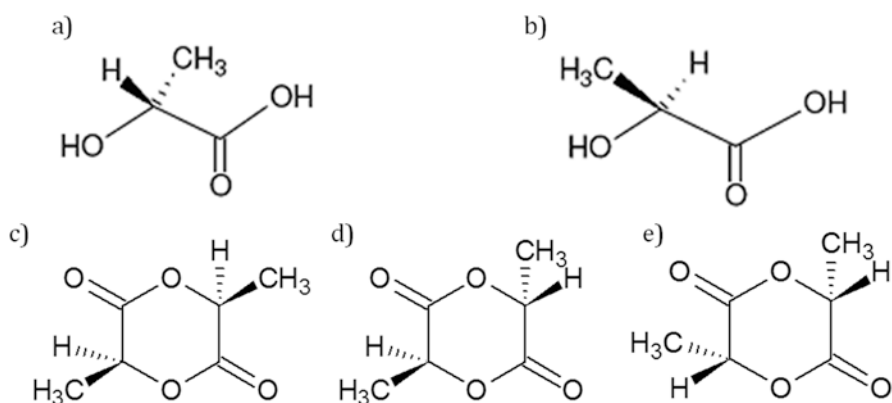


Fig. 3 Chemical structure of lactic acid stereoisomers: (a) *D*(-)-lactic acid and (b) *L*(+)-lactic acid. Chemical structures of cyclic dimer of lactic acid: (c) *L,L*-lactide, (d) *meso*-lactide, and (e) *DD*-lactide

for their commercial applications (Drumright et al. 2000; Inkinen et al. 2011; Vink et al. 2003). Figure 4 summarizes the steps involved in the industrial production of PLA. The most considered active initiator for the lactide ROP is stannous octoate bis(2-ethyl hexanoate) (SnOct₂), which causes good reaction rate and a

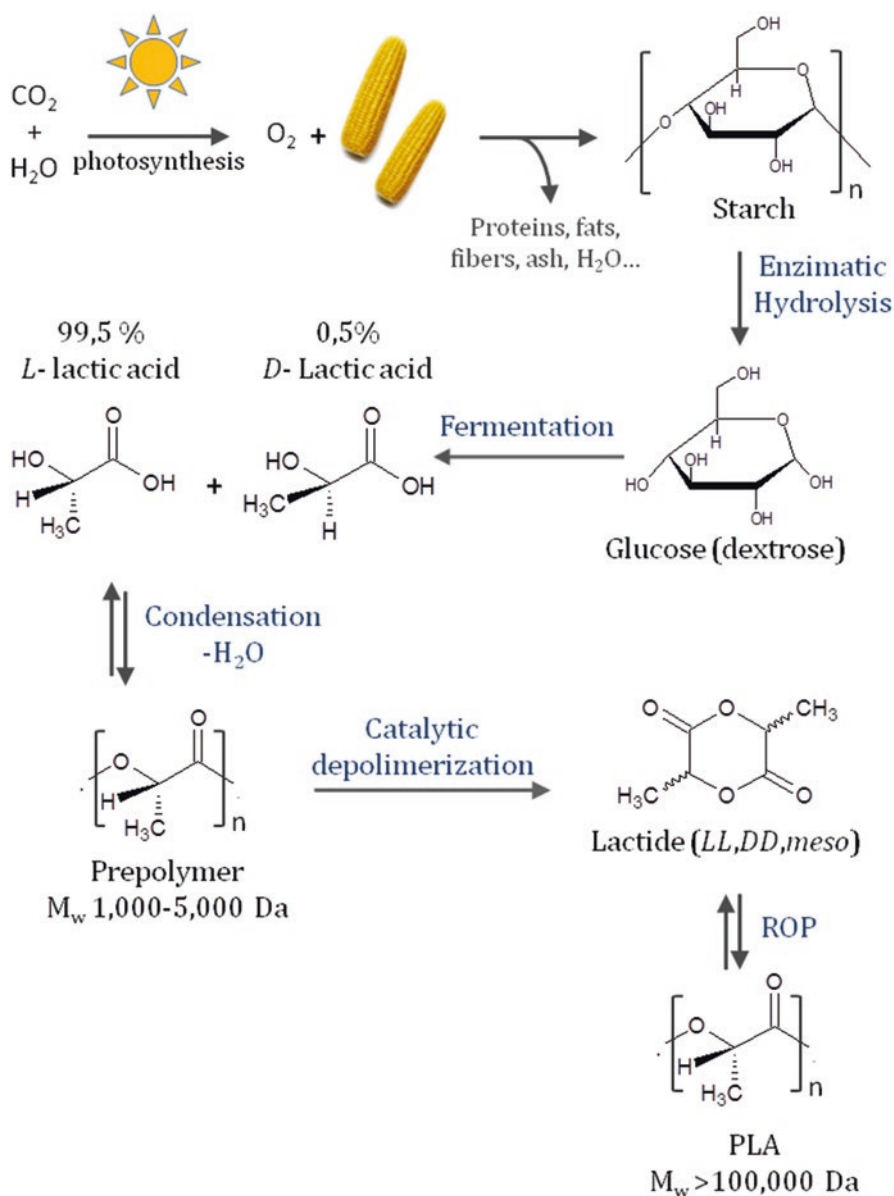


Fig. 4 Schematic representation of high molecular weight PLA industrial production

low level of racemization at high temperature and is accepted by FDA because it has low toxicity (Drumright et al. 2000). Poly(*L*-lactide) (PLLA) and poly(*D*-lactide) (PDLA) are prepared by incorporating 100% *L*-units or 100% *D*-units, respectively, while by incorporating the equimolar mixture of *L*-isomer and *D*-isomer at random, a stereocomplex crystalline structure (racemic poly(*L,D*-lactide), r-PLA) composed of optically pure macromolecular segments is obtained (Auras et al. 2004; Sarasua et al. 2005).

Commercial PLAs are copolymers of PLLA and PDLA (Carrasco et al. 2010). The properties of high molecular weight PLA, such as melting temperature and crystallinity, are determined by the ratio of *L*- and *D*-enantiomers and the molecular mass (Carrasco et al. 2010), which is controlled by the addition of hydroxylic compounds (Auras et al. 2004). PLAs with high *L*-lactide levels can be used to produce crystalline polymers, while the PLAs with higher *D*-lactide are more amorphous (Vink et al. 2003). The ability to control the stereochemical architecture of PLA allows controlling the speed of crystallization and finally the degree of crystallinity, the processing temperatures of the material, as well as the final mechanical properties (Auras et al. 2004).

The presence of impurities such as moisture; metals; free carboxylic acids, that is, lactic acid or lactic acid oligomers; and aldehydes can lead to a decrease on the molar masses in the ROP of lactide (Inkinen et al. 2011). D,L-Lactide has a higher melting point (116–119 °C) than *L*- and *D*-lactide (94–96 °C) as well as *meso*-lactide (43–47 °C), and thus, the differences on the melting points are used to estimate the purity of lactide for quality control purposes (Inkinen et al. 2011).

3 PLA Processing

PLA presents good processability in conventional industrial plastic transformation equipment (Carrasco et al. 2010). The main conversion methods for commercial grade PLA are based on melt processing (Armentano et al. 2013; Lim et al. 2008) such as injection molding, sheet extrusion, blow molding, thermoforming, film forming, etc. (Armentano et al. 2013; Auras et al. 2004). Prior to melting processing of PLA, the polymers have to be dried adequately to prevent excessive hydrolysis (molecular weight drop) which can then compromise the physical properties of the PLA-based materials (Lim et al. 2008). Amorphous PLA must be dried between 43 and 55 °C (below the T_g), meanwhile the typical drying conditions for semicrystalline PLA are 4 h at 80 °C (Jamshidian et al. 2010).

Melt processing approach involves heating PLA over its melting point, modeling it to the desired forms, and finally cooling to stabilize its dimensions (Carrasco et al. 2010). To ensure good homogeneity and optimal melt viscosity during PLA processing, the temperature is set up to 40–50 °C above the PLA melting temperature, that is, in the range between 180 and 210 °C (Fiori 2015). However, PLA undergoes thermal degradation at temperatures lower than the melting point of the polymer and then the degradation rate, and instability rapidly increases above the melting point (Yu et al. 2003), especially during processing (Arrieta et al. 2016a;

Carrasco et al. 2013). The resulting structural changes as a result of somewhat thermal degradation of PLA can affect the viscosity and rheology of PLA which consequently can cause processing-related problems (i.e., fuming) as well as PLA-based products with reduced mechanical properties (Inkinen et al. 2011).

To overcome the limited thermal stability of PLA, the main parameters that should be taken into account during melt processing are (i) processing temperature, (ii) residence time, and (iii) moisture content (Södergård and Stolt 2002). Thus, understanding the PLA thermal degradation is critical in order to optimize the PLA thermal processing conditions.

3.1 PLA Plasticization

Since PLA is highly brittle, one practical industrial strategy to facilitate its processing performance is the addition of plasticizers which will further improve the ductility of the final PLA-based materials. To obtain a fully biodegradable food packaging, the plasticizers should be not only admitted for food contact but also biodegradable. In this sense, PLA have been widely plasticized with several common plasticizers, mainly with glycerol (Martin and Averous 2001), poly(ethylene glycol) (PEG) (Arrieta et al. 2014f; Courgneau et al. 2011, 2013; Martin and Averous 2001; Paul et al. 2003), citrate esters such as acetyl-tri-n-butyl citrate (ATBC) (Arrieta et al. 2014a, 2015c, d, 2016b; Courgneau et al. 2011; Martin and Averous 2001), and oligomeric lactic acid (OLA) (Armentano et al. 2015a, b; Burgos et al. 2013, 2014; Martin and Averous 2001). Recently, the use of different renewable components derived from the agriculture or food industry has attracted interest as novel plasticizers such as D-limonene (Arrieta et al. 2013a, 2014d, 2015b; Fortunati et al. 2014a), β -carotene (López-Rubio and Lagaron 2010), vegetable oils (Ruellan et al. 2015), and epoxidized fatty acid esters (Ferri et al. 2016b), among others. The resulting plasticized PLA-based materials gained in flexibility and resilience at the expense of the reduction of the mechanical resistance.

4 PLA Thermal Transitions and Crystallinity

PLA's thermal transitions, glass transition temperature (T_g), crystallization temperature (T_c), and melting temperature (T_m) as well as the degree of crystallinity depend on its molecular characteristics such as the enantiomeric purity of the lactic acid stereocopolymers (ratio of *L*-lactide and *D*-lactide enantiomers), molecular weight, and the thermal history (Jamshidian et al. 2010; Södergård and Stolt 2002). The thermal transitions (T_g , T_c , and T_m) and the related enthalpies of PLA are determined by means of differential scanning calorimetry (DSC) technique (Inkinen et al. 2011). Enantiomerically pure 100% crystalline PLA made from pure *L*-lactide (PLLA) has the T_g at about 60 °C and an equilibrium melting point (T_{m0}) of 207 °C

(Drumright et al. 2000; Inkinen et al. 2011), and the theoretical melting enthalpy value commonly used to calculate the degree of crystallinity (χ_c) is 93 J/g (Inkinen et al. 2011; Södergård and Stolt 2002; Turner II et al. 2004) by means of the following equation:

$$\chi_c = 100\% \times \left[\frac{\Delta H_m - \Delta H_c}{\Delta H_m^c} \right] \times \frac{1}{W_{\text{PLA}}} \quad (1)$$

where ΔH_m is the melting enthalpy, ΔH_{cc} is the cold crystallization enthalpy, ΔH_m^c is the melting heat associated with pure crystalline PLA (93 J/g), and W_{PLA} is the weight fraction of PLA in the blend (Turner II et al. 2004). The glass transition temperature, crystallinity, and melting point can decrease with decreasing *L*-lactide isomer content (Lim et al. 2008). The introduction of stereochemical defects, *meso*-lactide or *D*-lactide, into poly(*L*-lactide) reduces the melting point, the rate of crystallization, and the degree of crystallinity of the resulting polymer (Auras et al. 2004) but has lower effect on the T_g (Drumright et al. 2000).

4.1 Melting Temperature

PLLA homopolymer shows the melting temperature at 207 °C. However, industrial grade PLA is not 100% pure PLLA. In fact, PLA derived from greater than 93% *L*-lactic acid can be semicrystalline, whereas PLA prepared from *meso*-lactide from between 50% and 93% *L*-lactic acid is strictly amorphous (Auras et al. 2004).

The maximum practical industrial obtainable melting point of semicrystalline stereochemically pure poly(lactide), either *L* or *D* (PLLA or PDLA), is around 180 °C with an enthalpy of melting of around 40–50 J/g (Drumright et al. 2000). Typical T_m values for semicrystalline PLA are in the range of 130–180 °C (Auras et al. 2004; Drumright et al. 2000; Lim et al. 2008). The melting temperature depression, due to *meso*-lactide or *D*-lactide introduction, has several important implications since it expands the PLA processing window, reduces the thermal and hydrolytic degradation, and decreases the lactide formation (Lim et al. 2008). Figure 5 shows the DSC curves of two semicrystalline PLAs with 2% and 4% of *D*-isomer in which it is possible to see that a higher amount of *D*-isomer produces a lower T_m value.

On the other hand, an increase in melting temperature occurs due to a estereo-complexation (Tsuji 2005), where intramolecular or intermolecular interactions of lactic units of opposite configurations, PLLA and PDLA, produce higher compaction (Sarasua et al. 2005). The T_{m0} of pure PLA stereocomplexes is at 279 °C, significantly above that of PLLA homopolymer (207 °C), with much higher enthalpy values (142 J/g) because of their different crystal structure. But, as a consequence of the introduction of impurities, the melting temperature of stereocomplex is typically in the range of 170–240 °C (Carlson et al. 1998). Additionally, the melting temperature also increases with molecular weight. However, while it shows a dramatic

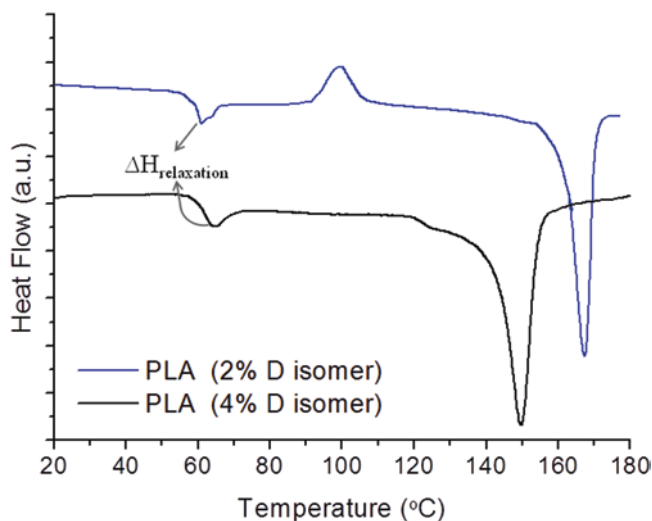


Fig. 5 DSC first heating scan of semicrystalline PLA with 2% and 4% of *D*-isomer

increase for low molecular weight, for instance, from 90 °C for oligomers up to 185 °C for PLA of about 100 Da, it then reaches an asymptotical value at higher PLA molecular weight values than 100 Da (Saeidlou et al. 2012). As a consequence of PLA low melting temperature and its deformation, it results better to use it for heat sealing and thermoforming applications (Jamshidian et al. 2010).

4.2 Glass Transition Temperature and Thermal History

PLA presents lower glass transition temperature (T_g) values (55–65 °C) (Gupta and Kumar 2007) than other plastics used in the food packaging sector, such as PET and PS, which makes PLA better for thermal processing and for heat sealing (Jamshidian et al. 2010). The T_g of PLA is more dependent on the molecular weight and the thermal history. The T_g value increases with molecular weight from about 54 °C in PLA with 50% *L*-lactide stereoisomer contents to maximum values of almost 60 °C at infinite molecular weight (Lim et al. 2008). Another influential parameter for T_g is the PLA chain architecture. Linear PLAs show higher T_g values than branched PLAs, in which the higher amount of chain ends produces crystal imperfections and branching points leading to a PLA matrix with higher free volume (Rodríguez et al. 2014; Saeidlou et al. 2012). Though, as a consequence of its deformation, the low glass transition temperature of PLA limits its usages in thermally processed packages (Jamshidian et al. 2010). Commercial applications of PLA are usually intended for its uses in ambient conditions, where PLA is at a temperature below, but close, to the T_g value. Thus, PLA products tend toward an equilibrium state through slow segmental rearrangements over time which is recognized as physical aging phenomenon (Cailloux et al. 2014).

The PLA physical aging induces changes in the crystallinity frequently evidenced during the first DSC heating of semicrystalline PLA as an endothermic relaxation superimposed on T_g (Fig. 5), due to a secondary molecular reordering in the amorphous phase (Auras et al. 2004, 2005). PLA with low crystallinity has a tendency to undergo rapid physical aging in a matter of days under storage temperature nearly to the PLA glass transition temperature (Jamshidian et al. 2010; Lim et al. 2008). The relaxation enthalpy (ΔH_r) of PLA increases with storage time because of the polymer structure spontaneously progress to a lower free-energy state (Burgos et al. 2013). The molecular weight has also influence on the physical aging of PLA. In this sense, it was observed that the decrease in molecular weight of PLLA increased the magnitude of the enthalpy of relaxation at the glass transition (Auras et al. 2004). The accelerated PLA physical aging leads to a remarkable decrease in final product toughness (Rodríguez et al. 2014). As a consequence, the physical aging is one of the most important drawbacks on the service life of PLA products and large-scale commercial applications (Cailloux et al. 2014). Quenching PLA from the melt at a high cooling rate (i.e., 500 °C/min), such as during injection molding process, will produce a highly amorphous PLA (Lim et al. 2008).

4.3 Crystallization and Crystal Structure

PLA crystallinity, the amount of crystalline regions with respect to amorphous content, also influences PLA melting point as well as many PLA final properties (i.e., mechanical and barrier properties). In isothermal conditions, PLLA can crystallize in the temperature range between 85 and 150 °C with a fastest rate of crystallization in the range of 95–115 °C (Courgneau et al. 2013). PLA can crystallize in the presence of either *meso*-lactide or *D*-lactide but increases the time for crystallization, and the size of the spherulites due to the structure becomes more disordered (Auras et al. 2004). For instance, an amount of just 4% of *D*-isomer, which is typical of commercial PLA grades, slows down its crystallization rate in normal processing conditions, leading to an almost 100% amorphous final material (Rodríguez et al. 2014).

PLA crystals can grow mainly in three structural positions called alpha (α), beta (β), and gamma (γ) forms (Zhang et al. 2008), which are dependent on the preparation conditions (Auras et al. 2004), even though from the melt PLA crystallizes only in the α -form (Jamshidian et al. 2010; Navarro-Baena et al. 2014a). When the crystallization takes place at temperatures higher than 120 °C, the PLA homopolymers crystallize in order α structure homocrystals with melting point at 185 °C (Auras et al. 2004; Lim et al. 2008). However, when PLLA crystallizes below 100 °C, there is a high rate of radial growth of the PLA spherulites (Jamshidian et al. 2010) leading to the formation of disorder α -structure crystals with lower thermodynamic stability, so-called α' (Zhang et al. 2008). Thus, when PLA crystallizes at temperatures below 100 °C, a small exotherm appears just before the melting peak due to the melting of these disordered α' crystals (Rodríguez et al. 2014). Nonetheless, at temperatures higher than 100 °C and

lower than 120 °C coexist both order and disorder crystals (α and α'), which then melt showing a double melting behavior (Burgos et al. 2013; Zhang et al. 2008). The β -structure grows upon mechanical stretching (Jamshidian et al. 2010) and shows the melting point at 175 °C (Auras et al. 2004), about 10 °C lower with respect to the α -crystal implying less thermal stability (Saeidlou et al. 2012). The γ -structure only develops on hexamethylbenzene substrate by epitaxial crystallization (Sarasua et al. 2005), when two chains are oriented antiparallel in the crystal cell (Saeidlou et al. 2012). In the case of homo-crystallization of PLLA and PDLA, the enantiomeric chains can co-crystallize together and form a stereocomplex, in which the crystal cell contains one PLLA and one PDLA chain (Saeidlou et al. 2012). As it was previously commented, PLA stereocomplexes melt at a significantly higher temperature than α - or β - crystals, and this stereocomplex crystal cell contains one PLLA and one PDLA chain, so-called η -form (Saeidlou et al. 2012; Sarasua et al. 2005).

The increase of PLA crystallinity may or may not be favorable depending on the end-use requirements of the PLA articles (Lim et al. 2008). For the food packaging field, the crystalline phase of PLA has an important impact on the mechanical and permeation performance. Consequently, considerable academic and industrial research efforts have been focused to increase the PLA crystallinity for food packaging proposes.

5 PLA Thermal Stability and Thermal Degradation

The thermal stability of polymers and their thermal degradation are relevant for their processing, potential applications as well as thermal recycling. Thus, the study of polymers thermal stability is particularly important (Arrieta et al. 2013b). As it was previously mentioned, PLA has a tendency to be affected by the melt processing conditions, and it also is affected by storage environments (Inkinen et al. 2011).

The ester carbon–oxygen linkages of PLA are easy to split under isothermal conditions (Södergård and Stolt 2002), such as those necessary to process PLA. Thus, the ester linkages tend to degrade during thermal processing (Carrasco et al. 2010; Yu et al. 2003). PLA also presents high hydrolysis rate that directly affects the final properties of the PLA-based products, such as the mechanical strength and the rate of hydrolytic degradation (Yu et al. 2003). The apparent activation energy (E_a) provides useful information of polymer thermal decomposition behavior (Arrieta et al. 2015b; Badía et al. 2010). The E_a decreases with weight loss of PLA at the initial stage of degradation and then increases remarkably with progress of degradation (Chien et al. 2011). In this sense, it is known that PLA is considerably less stable than other traditional thermoplastics such as PS, PP, and PET, showing an activation energy (E_a) for PLA weight loss between 186 and 257 °C of about 139 kJ/mol (Auras et al. 2004). Carrasco et al. studied the kinetic thermal degradation of PLA using several kinetic models (Friedman, Kissinger and Flynn-Wall-Ozawa) and found that all methods led to similar values of activation energy between 160 and 170 kJ/mol (Carrasco et al.

2013). Meanwhile, Chien et al. reported that the E_a of PLA between 250 and 300 °C is between 141 and 76 kJ/mol, using Doyle's and Reich's methods (Chien et al. 2011).

The thermal degradation of PLA seems to proceed by a very complicated mechanism (Aoyagi et al. 2002). It has been proposed that several reactions are involved in the degradation process of PLA during thermal treatments such as (i) hydrolysis process, (ii) depolymerization, (iii) thermooxidative random chain scission, and (iv) inter- and intramolecular transesterification reactions, resulting in the formation of lactide monomer and oligomers (Carrasco et al. 2010; Lim et al. 2008). The amount of residual monomer also has an important effect in inducing early degradation of the polymer; thus, the degradation of PLA is not only a consequence of its thermal degradation (Auras et al. 2004).

The processing of PLA pellets with trace amount of residual water, such as moisture, activates hydrolysis reactions (Fig. 6), leading to the cleavage of the ester linkage, with the production of acid and alcohol groups (Carrasco et al. 2010). The hydrolysis of the ester groups is autocatalyzed by carboxylic acid end groups (Khabbaz et al. 2000). The hydrolyzed monomers (lactic acids) also catalyze further PLA degradation (Auras et al. 2004). Thus, residual monomers and moisture favor the early molecular weight reduction (Armentano et al. 2013; Carrasco et al. 2010); this is why PLA pellets should be dried before processing, as it was previously commented in Sect. 3 (Armentano et al. 2013).

The presence of trace amount of catalysts used for the PLA synthesis may favor the depolymerization of PLA forming lactide (Aoyagi et al. 2002). Depolymerization reactions that take place during PLA melting are responsible for a thermal decomposition with lower energy barrier (Södergård and Stolt 2002). It should be taken into account that the depolymerization by-products, such as low molecular weight lactic polymers or acetaldehyde, must be avoided for food grade PLA-based materials because they can impart off-flavors to foodstuff and stay over the permitted migration level allowed by the food regulations (Fiori 2015). A retardation of the thermal degradation of PLA can be achieved through the purification of the polymer in order to reduce the not bound catalyst content, at the same time as other impurities and residual monomer can be also removed (Södergård and Stolt 2002).

Thermooxidative random chain scission of the ester groups has been proposed as one contributing mechanism of the PLA thermal degradation (Carrasco et al. 2013; Södergård and Stolt 2002).

The intermolecular transesterification would take place during PLA degradation in the melt, favoring the reaction between two ester molecules which exchange their radicals through chain cleavage along the polymer chain, leading to a variation of the distribution of molecular weights (Badia et al. 2011; Carrasco et al.

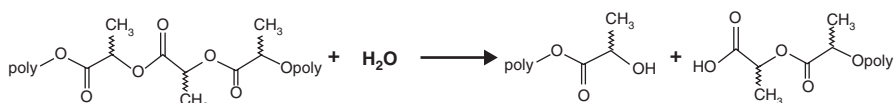


Fig. 6 PLA hydrolysis chain scission

2010). The intermolecular transesterification of PLA can be minimized by the addition of low amount of stabilizers during melt processing, such as 1,4-dianthraquinone (Carrasco et al. 2010), benzoyl peroxide (Carrasco et al. 2010; Södergård and Näsman 1994), tris(2,4-ditert-butylphenyl)-phosphate (Irgafos 168) (Arrieta et al. 2014a), and other stabilizers. For instance, Södergård and Näsman (1994) studied the stabilization of PLA by the addition of benzoyl peroxide and found that it was able to stabilize the polymer against thermal degradation even at 0.1 wt.% of stabilizer addition, while the addition of more than 0.5 wt.% had only a small additional retardant on the melt degradation effect of PLA (Södergård and Näsman 1994). At temperature less than 200 °C, conversion of PLLA into *meso*-lactide and oligomers is minimal. However, at temperature higher than 200 °C, the formation of *meso*-lactide increases, while oligomers are formed at temperatures higher than 230 °C (Lim et al. 2008).

The degradation of PLA during thermal processing is also caused by intramolecular transesterification (Carrasco et al. 2010), where ester units are interchanged between different chains. Kopinke et al. reported that intramolecular *trans*-esterification (Fig. 7a) and *cis*-elimination (Fig. 7b) are the two main thermal degradation mechanisms of PLA at temperatures above 200 °C, which leads to the formation of lactide and cyclic oligomers (by *trans*-esterification) (Fig. 7a), acrylic

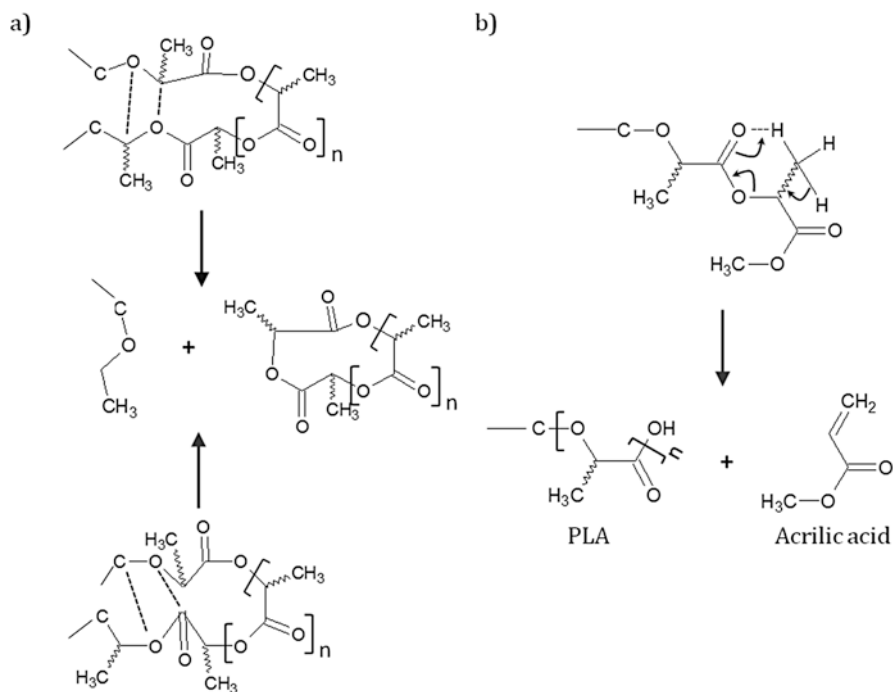


Fig. 7 Thermal degradation mechanisms of PLA: (a) *trans*-esterification, (b) *cis*-elimination (Adapted from Kopinke and Mackenzie 1997)

acid, and acyclic oligomers (by *cis*-elimination) (Fig. 7b) (Kopinke et al. 1996; Kopinke and Mackenzie 1997). But, the formation of cyclic compounds from the short-chain polymer is probably energetically more favorable than the longer ones during the pyrolysis (Westphal et al. 2001). Simultaneously, there is a recombination of the cyclic oligomers with linear polyesters through insertion reactions, while molecules with longer chain lengths are favored (Carrasco et al. 2010).

The degradation behavior strongly depends on the crystallinity of PLA and also on the polydispersity index (PDI) (Auras et al. 2004). When a material shows a high PDI, it contains some fraction of smaller molecules which are volatile, and the higher the PDI, the smaller the thermal stability (Carrasco et al. 2010). The PLA-based products that have suffered thermal degradation during processing, which reduces the PLA melt viscosity, can present reduced mechanical performance (Fiori 2015).

At significant temperatures higher than the recommended processing temperature of PLA (in the range of 180–210 °C), at above 300 °C, nonselective radical reactions occur (Rodríguez et al. 2014). Westphal et al. studied the degradation of PLA at the pyrolysis temperatures of 400 °C and 500 °C and identified the thermal degradation products by means of gas chromatography coupled with mass spectrometry (GC/MS). They found several degradation products of PLA, such as acetaldehyde, acrylic acid, lactoyl acrylic acid, two lactide isomers, and cyclic oligomers up to pentamers (Westphal et al. 2001). During the pyrolysis of PLA at even higher pyrolysis temperatures, 600 °C, it was observed that the thermal degradation products of PLA gave a dominant series of signals with $m/z = 56 + (n \times 72)$ in which n assumed different values according to the lactide oligomers formed: $n = 1$ for *meso*-lactide and lactide, $n = 2$ for the dimer, $n = 3$ for the formation of three different trimmers that shows very similar mass spectra, and $n = 4$ for the tetramer (Arrieta et al. 2013b).

6 PLA Mechanical Performance

The mechanical performance of PLA-based materials is mostly evaluated by tensile properties, that is, mainly the elastic modulus (E), yield strength (σ_y), tensile strength (TS), yield elongation (ϵ_y), and elongation at break (ϵ_b). PLA can show elastic modulus values between 1,200 and 3,500 MPa (Armentano et al. 2010; Jamshidian et al. 2010), yield strength between 20 and 70 MPa (Perego et al. 1996), tensile strength values between 40 and 70 MPa (Fiori 2015; Jamshidian et al. 2010; Södergård and Stolt 2002; Tsuji 2005), yield elongation of about 1.5% and 2.5% (Perego et al. 1996), and elongation at break between 2% and 10% (Fiori 2015). As many other PLA properties, its mechanical performance is dependent of controllable parameters such as chemical composition, degree of crystallinity, or molecular weight, among others (Nascimento et al. 2010). In fact, the polymer architecture plays an important role on the mechanical properties of the final product as well as on the processing conditions used to model it (Siracusa et al. 2008). Therefore, the mechanical properties of neat PLA also depend on the grade and stereochemistry, and they can varied to a large extent ranging from soft and elastic plastics to stiff and

high-strength material (Södergård and Stolt 2002). The crystallinity strongly influences PLA mechanical properties. In this sense, semicrystalline PLA, which has a tensile modulus of about 3,000 MPa, tensile strength of about 50–70 MPa, and poor elongation at break (around 4%), is preferred to the amorphous PLA when higher mechanical performance is desired (Södergård and Stolt 2002). Thus, semicrystalline PLA has the highest elastic modulus than PS, PP, and LDPE (Jamshidian et al. 2010). The higher content of L-lactide contributes to a higher PLA tensile strength (Auras et al. 2004). The tensile strength values of semicrystalline PLA are higher than LDPE (8–20 MPa) (Jamshidian et al. 2010), within the range of PS values (34–50 MPa) (Jamshidian et al. 2010), but are lower than PET (275 MPa) (Auras et al. 2004, 2005). However, the poor PLA elongation at break restricts its properties for some applications, such as film manufacturing (Fiori 2015). Amorphous PLA is a more ductile material ($E = 1,500\text{--}1,900$ MPa, TS = 40–50 MPa, and $\epsilon_b = 5\text{--}10\%$) (Perego et al. 1996). The annealing of PLA promotes an increase in the crystallinity with an increase in the elastic modulus and tensile strength values due to the increase in the stereoregularity of the chain (Nascimento et al. 2010), in addition to an increase in the impact resistance due to the cross-linking effect on the crystalline domains (Auras et al. 2004). Stereocomplexation improves the tensile properties of PLA-based materials (Tsuji 2005), whereas PLA plasticization increases the elongation at break. PLA of high molecular weight is needed to produce devices of high mechanical strength (Gupta and Kumar 2007). In fact, the mechanical properties of PLA can increase with an increase of molecular weight of PLA, from 50 to 100 Da (Gupta and Kumar 2007; Södergård and Stolt 2002). But, a further increment on the molecular weight will not significantly influence the mechanical performance of PLA (Södergård and Stolt 2002).

Although the PLA variation in stereochemistry, crystallinity, and molecular weight can improve its mechanical resistance and ductility, the resulting increase of toughness properties is usually insufficient to satisfy the requirement of most practical applications (Liu and Zhang 2011). Therefore, extensive research efforts have been focused on PLA modification to improve its mechanical performance for extending its use as packaging material, such as copolymerization (Navarro-Baena et al. 2015; Peponi et al. 2012, 2013), blending (Arrieta et al. 2014f; Ferri et al. 2016a), as well as the addition of modifiers such as plasticizers (Arrieta et al. 2013a; Burgos et al. 2014; Martino et al. 2009a; Ruellan et al. 2015) or fillers to develop composites (Balart et al. 2016) and nanocomposites (Fortunati et al. 2012a, c; Martino et al. 2011; Pantani et al. 2013). Particularly in the food packaging field, new strategies are focused on the development of PLA-based bionanocomposites with improved performance for food packaging applications.

7 PLA Barrier Properties

Food packaging materials should maintain foodstuff quality by controlling the mass transfer process, such as the loss of some food components (i.e., aroma, flavor, and fatty compounds) as well as the transfer of water vapor and gases (i.e., oxygen and/or carbon

dioxide) from the surrounding to the food packed. In this sense, the foremost drawback of PLA for food packaging proposes, as well as other biobased and biodegradable polymeric materials, is its relative permeability to small molecules (Auras et al. 2006).

Besides containing and protecting the foodstuff from physical damage, food packaging systems also should maintain their quality and shelf life by controlling the mass transfer of water vapor, oxygen, and/or carbon dioxide, which are responsible for numerous reactions involved in food degradation (oxidation, microbial growth, physiological reactions, etc.). The addition of nanoparticles to develop nanocomposites has proved to be an effective strategy to improve the barrier properties of polymer-based packaging materials (Sanchez-Garcia and Lagaron 2010).

7.1 PLA Surface Wettability and Water Vapor Permeability

In food packaging, the surface wettability gains importance since it directly influences many other properties of polymers such as the permeability toward water vapor, adhesion, selective adsorption, and the release of adsorbed molecules, among others (Fombuena et al. 2013, 2014). The wettability of the packaging material surfaces is frequently investigated by water contact angle (WCA) measurements (Hambleton et al. 2009). The static WCA will show values lower than 65° for hydrophilic surfaces, while it will increase to higher values than 65° for hydrophobic surfaces (Vogler 1998). Even though PLA is a relatively hydrophobic material, with a static water contact angle of approximately 80° (Rasal et al. 2010), it presents higher wetting properties than LDPE and PP (static water contact angle around 100°) (Balart et al. 2012; Fombuena et al. 2013). Although the water permeation model for PLA is not yet completely understood, it seems that the water molecules are not highly soluble in the polymer matrix. In fact, they are associated with each other, binding via hydrogen bonding, forming clusters which is the form in that the water diffuses through the polymer matrix (Auras et al. 2004). The water vapor permeability coefficients of PLA are around 1×10^{14} kg m/s m² Pa (Mattioli et al. 2013).

7.2 PLA Gas Barrier

PLA presents better carbon dioxide and oxygen barrier properties than PS but lower than PET (Auras et al. 2005). The carbon dioxide permeability coefficient for PLA is between 1.76×10^{-17} kg m/m²s Pa and 2.77×10^{-17} kg m/m²s Pa (at 25 °C and 0% RH) (Auras 2007; Lehermeier et al. 2001) which is lower than the crystalline PS carbon dioxide permeability (1.55×10^{-16} kg m/m²s Pa at 25 °C and 0% RH) but higher than that of PET (1.73×10^{-18} and 3.17×10^{-18} kg m/m²s Pa at 45 °C at 0% RH) (Auras et al. 2004).

The oxygen transmission rate (OTR^{*e}) of neat PLA is between 30 and 44 cm³ mm/m² day (Arrieta et al. 2013a; Burgos et al. 2013; Fortunati et al. 2012c; Martino et al. 2009a), which is considerably lower to that of LDPE (160 cm³ mm/m² day) but higher than that of PET (3 cm³ mm/m² day) (Burgos et al. 2013). PET contains an aromatic ring in the polymer chain backbone which leads to low gas permeation (Lehermeier et al. 2001). It has been reported that the molecular rearrangement during storage led to OTR^{*e} reductions due to the gradual decrease of the free volume available to gas diffusion as a consequence of the PLA physical aging (Burgos et al. 2013; Martino et al. 2009b).

8 PLA Visual Appearance and Optical Properties

Transparency is an essential issue to be considered for the industrial production of food packaging materials since seeing through the packaging is one of the most important requirements for the consumers to perceive the food packed aspect (Arrieta et al. 2013a). The control of UV light transmission through the packaging is also an important parameter to protect some food products until they reach the consumer, mainly when light-sensitive foods are involved (Arrieta et al. 2014c; Fiori 2015).

PLA is a highly transparent material, with a transparency degree similar to PS, LDPE, PET, or cellophane (Auras et al. 2004; Fiori 2015). Although the lower range of UV light (UV-C 190–220 nm) is not transmitted by PLA, nearly all the UV-B (315–280 nm) and UV-A (400–315 nm) light as well as the higher range of UV-C (between 220 and 280 nm) light is transmitted (Auras et al. 2004).

9 Improving PLA Through the Development of Bionanocomposites

Nanotechnology presents new opportunities to enhance material performance, and thus, nanocomposites have been considered as alternative novel materials across a wide range of industrial fields (Bumbudsanpharoke and Ko 2015; Peponi et al. 2014). In this context, a new approach is growing up in the food packaging sector focused on the development of biobased and biodegradable nanocomposites since the addition of nanoparticles leads to an enhancement in the thermomechanical performance of biobased polymers. By definition, nanoparticles are those materials having at least one dimension in the range of nanoscale, from approximately 1 to 100 nm (Raquez et al. 2013). The introduction of nanosized particles into the polymeric matrix can considerably improve some specific properties due to the strong and large polymer/nanoparticle interactions if good nanoparticle dispersion is achieved (Peponi et al. 2014). The addition of nanoparticles into polymer matrices not only improves the mechanical properties and thermal stability, but also it offers many additional advantages such as the reduction in raw materials and the

elimination of expensive lamination secondary processes, while the modification of the thermal properties of polymers leads to a reduction in machine cycle time and temperature (Silvestre et al. 2011).

The development of nanocomposites to improve the inherent shortcomings of PLA-based materials has proven to be a promising technology with particular interest in the food packaging field. For food safety reasons, the nanoreinforcement should be nontoxic and approved for food contact. Additionally, to guarantee the PLA-based packaging green nature and sustainable end of life option, the ideal nanoparticle should be also biobased and biodegradable. In this sense, those nanoparticles derived from agricultural-related industries, such as wood and plant fibers, have gained significant interest for the development of biobased and biodegradable nanocomposites. It is widely known that the high mechanical and nanomechanical performance of natural materials extracted from the agriculture is conferred by cellulosic hierarchical structures (Rayón et al. 2013, 2014). In fact, nanocellulose materials and especially its specific form of cellulose nanocrystals (CNCs) have shown that they are interesting filler as reinforcement for biobased and biodegradable materials. In fact, CNCs have shown to be effective nanofiller for various biobased and biodegradable polymer matrices with interest in the food packaging field including PLA (Fortunati et al. 2012a, b; Navarro-Baena et al. 2014b; Peltzer et al. 2014), PHB (Arrieta et al. 2014b, c, 2015a, c; Patrício et al. 2013), poly(hydroxybutyrate-co-hydroxyvalerate) (PHBV) (Martínez-Sanz et al. 2014), poly(vinyl alcohol) (PVA) (Fortunati et al. 2013b), and poly(butylene succinate) (PBS) (Luzi et al. 2016; Zhang and Zhang 2016), among others.

9.1 Cellulose Nanocrystal Obtainment, Properties, and Functionalization

Nanocellulose is used as reinforcing filler for biopolymer matrices intended for the biodegradable food packaging industry, due to its many advantages such as its high stiffness, excellent barrier properties, and low density (Arrieta et al. 2015a; Fortunati et al. 2013c; Peltzer et al. 2014; Sonseca et al. 2014). Additionally, the starting material, cellulose, is considered the most abundant renewable polymer in nature all around the world with an annual production of about 7.52×10^{10} tons, and it is also highly biodegradable (Brinchi et al. 2013; Habibi 2014). Although nanocellulose can be extracted from various natural raw materials, for the industrial production of CNC microcrystalline cellulose (MCC, dimensions ranging between 10 and 50 μm), it is a commonly commercially available material used as starting material in laboratories via sulfuric acid hydrolysis (45 °C for 30 min) (Arrieta et al. 2014b; Brinchi et al. 2013; Mujica-Garcia et al. 2016; Oksman et al. 2016).

As a structural component in plants, cellulose is found as assembly of individual crystalline cellulose chains linked to form cellulose fibers which are embedded in an amorphous matrix composed of hemicelluloses and lignin (Siqueira et al. 2010).

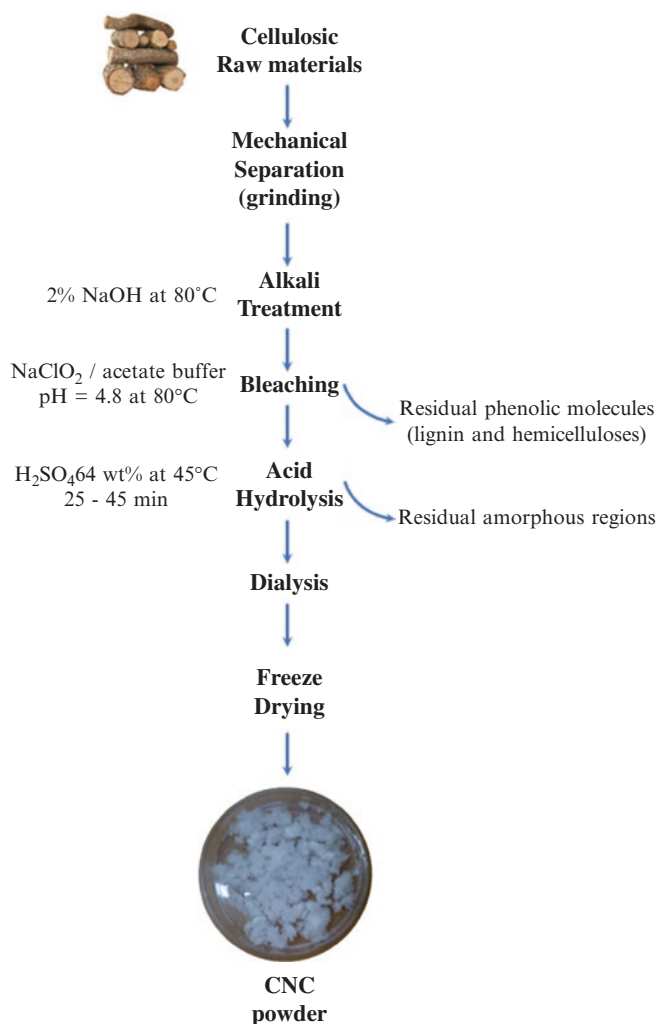


Fig. 8 Pretreatment, purification steps of the raw materials, and CNC obtainment

In fact, around 36 glucan chain assemblies are bounded through van der Waals forces, and due to the presence of many hydroxyl groups along the cellulose chain, it results in the formation of a network of intra- and hydrogen bonds into larger fibrils (30–100 cellulose molecules), which pack into larger microfibrils (20–50 nm), and these are assembled into the cellulose fibers (Habibi 2014; Mariano et al. 2014). Although the very basic chemical structure of all kinds of cellulose is identical, the supramolecular structures of cellulose from different sources and different processes can be significantly different (Li et al. 2015).

Classically, cellulose is isolated from its natural matrix with the removal of lignin, hemicelluloses, and resins using chemical treatments consisting of alkali extraction and bleaching. Some pretreatments and purification steps of the raw material are necessary (Fig. 8). Generally the extraction consists in an alkali treatment (2% NaOH at 80 °C) which allows the removal of soluble polysaccharides. The subsequent bleaching treatment (i.e., NaClO₂/acetate buffer pH = 4.8, 80 °C) removes most of the residual phenolic molecules like lignin or polyphenols (Brinchi et al. 2013; Mariano et al. 2014). Then, from the bleached fibers, nanocellulose is dissociated from the amorphous parts under acid hydrolysis conditions, generally sulfuric acid hydrolysis (H₂SO₄ 64 wt.% at 45 °C for 25–45 min), leading to the formation of high-purity single cellulose nanocrystals (CNCs) (Brinchi et al. 2013; Habibi 2014). Due to the fact that for the industrial melt processing of PLA-CNC nanocomposites, CNC powder is required, thus, CNC should be freeze-dried. However, during CNC freeze-drying process, the CNC tends to agglomerate into flakes (Fortunati et al. 2013a). Therefore, to promote the well dispersion of CNC into PLA matrix for melt processing, it is necessary to lower the surface energy of the CNC nanoparticles by means of the surface functionalization by either physical or chemical modifications (Arrieta et al. 2016a). A typical physical functionalization is coating CNC surface with a surfactant (s-CNC) (Arrieta et al. 2014b; Bonini et al. 2002; Fortunati et al. 2012b; Luzi et al. 2015), while for chemical surface functionalization, the most followed strategy is the grafting from reaction which consists of the use of the surface CNC hydroxyl groups as initiators for the ring-opening polymerization of PLLA (Lönnerberg et al. 2006; Navarro-Baena et al. 2014b; Peltzer et al. 2014).

10 PLA-CNC-Based Nanocomposites for Food Packaging

Despite the high potential of biobased and biodegradable plastics to substitute petroleum-based polymers, they still present a number of processing and performance shortcomings for the food packaging sector. This is related to their lower barrier properties, strong water sensitivity, lower thermal resistance, and lower shelf-life stability due to aging, migration, and some processability issues (Lagaron and Lopez-Rubio 2011).

10.1 PLA-CNC Processing

The low thermal stability of nanocellulose limits the choice of polymer matrices and processing technologies for the development of CNC-based nanocomposites (Oksman et al. 2016). In fact, since cellulose has a glass transition temperature in the range of 200–230 °C and thermal decomposition starts at around 260 °C, the compounding temperature is commonly restricted to about 200 °C in the extrusion of thermoplastic nanocomposites reinforced with CNC (Oksman et al. 2016). Hence, it results optimal for the reinforcement of several biopolymer matrices, including PLA which should be processed at temperatures at about 200 °C as it was commented in Sect. 3.

It is widely known that the polymer bionanocomposite properties are strongly dependent on a uniform dispersion of the nanoparticles in the polymer matrix and the resultant huge interfacial area developed (Peponi et al. 2014). The high amount of hydroxyl groups on the surface of CNC induces high attraction between them (Aranguren et al. 2013). Therefore, the surface properties of nanocellulose determine the CNC–CNC bonding within the cellulose network as well as the interfacial adhesion between the CNC and the polymer matrix, which ultimately determines the structure and properties of the final nanocomposites (Arrieta et al. 2016a; Oksman et al. 2016). Thus, the high polarity of CNC surface and the resultant low interfacial compatibility with hydrophobic polymer matrices, such as the case of PLA, make difficult the homogenous dispersion of nanocellulose in the polymer matrices (Arrieta et al. 2014c; Martínez-Sanz et al. 2013). However, the major challenger to obtain higher performance due to nanocellulose addition is not only the well dispersion of CNC in the polymer matrix but also the optimization of the CNC–polymer matrix interface (Oksman et al. 2016).

The processing conditions of PLA-CNC are of fundamental importance because the processes will ultimately affect the final nanocomposite performance as a consequence of the dispersion, distribution, and alignment of the reinforcing phase (Oksman et al. 2016). As it was already commented, the most followed strategies to improve the dispersion and consequently the interfacial adhesion of CNC with polymer matrices for the industrial processing of CNC are the physical or chemical surface modification of CNC for avoiding their agglomeration (Arrieta et al. 2016a).

The processing conditions of melt-extruded PLA reinforced with unmodified CNC and surface-modified CNC by means of a surfactant (s-CNC) were studied by Arrieta et al. They observed some changes in the force applied in the system with the addition of CNC due to the viscosity changes which increased with cellulose introduction. In fact, the force during melt extrusion increased from 1,000 N to around 1,200 N with the addition of CNC, while it increased from 1,000 N to around 1,400 N with the addition of surface-modified s-CNC (Arrieta et al. 2014b). The increment in the force of the system during processing was attributed to the viscosity changes that increased with cellulose introduction (Arrieta et al. 2014b, c).

10.2 PLA-CNC Bionanocomposite Properties

As it was already mentioned, PLA can be used widely in the packaging industry due to its heat formability, injection, and blow moldability as well as due to its properties like excellent transparency, good oil, and chemical and UV resistance also satisfying mechanical and thermal properties. However, PLA presents some drawbacks when it is used in liquid products where long shelf life is demanded, for products which are sensitive to moisture or for carbonated beverages as a consequence of the high water vapor and gas permeability. Therefore, in order to make PLA an appropriate packaging material for these kinds of products, improvement of its barrier properties is required (Halász et al. 2015). Petersson et al. studied the barrier

properties of composites of PLA with microcrystalline cellulose (MCC). However, they reported an increase in the oxygen permeability, due to the not efficient shape, loading, and dispersion of the MCC in blocking the gas molecule path in the matrix (Petersson and Oksman 2006). In this sense, the enhancement of the polymer barrier properties due to the creation of a tortuous pathway by means of the introduction of nanofillers may be the most obvious application of nanocomposites in the food packaging sector (Armentano et al. 2013; Peltzer and Beltrán-Sanahuja 2015). It is known that the well-dispersed nanoparticles through the polymer matrix can provoke certain tortuosity to diffusing molecules (Pantani et al. 2013). In fact, barrier properties are mainly controlled by the size and the morphology of the nanofillers as well as by their effective dispersion in the biopolymer matrix. Figure 9 shows a schematic representation of PLA-CNC bionanocomposite in which CNC forces the permeating low molecular weight molecules to follow a more tortuous path leading to an improvement on the barrier performance.

The addition of low amounts of CNC, between 1 and 3 wt.%, does not affect the wettability properties of PLA (Fortunati et al. 2014a). However, the addition of 5 wt.% of CNC causes an increase in the PLA surface wettability due to the high amount of hydroxyl groups of CNC (Arrieta et al. 2014c). Nevertheless, functionalized s-CNC did not significantly change the PLA wettability (Arrieta et al. 2014c), ascribed to the better dispersed s-CNC in PLA matrix that exposed lower OH groups on the film surface (Arrieta et al. 2015a). In fact, the hydrophilic part of the surfactant is adsorbed on the surface of CNC, while the hydrophobic part provides nanocrystals with nonpolar surface (Fortunati et al. 2012a; Petersson et al. 2007).

Sanchez-García et al. reported an improvement in the barrier properties of PLA biocomposites with alpha purified cellulose microfibrils. Although water and D-limonene direct permeability was seen to decrease to a significant extent in the biocomposites with 1 wt.% filler loading, higher fiber contents led to filler agglomeration and detrimental effects on permeability (Sanchez-Garcia et al. 2008). Sanchez-García and Lagaron focused the study on the impact of CNC derived from highly purified alpha cellulose fibers in the barrier properties of PLA bionanocomposites. They found that the CNCs were able to reduce the water permeability by up to 82% and the oxygen permeability by up to 90% with only 3 wt.% of nanocellulose content. This barrier enhancement was higher than expected by applying the most widely used models. The authors explained this behavior with the highly crystalline cellulose nanoparticles, PLA crystallinity development, and sorbed moisture filling the free volume. However, the mechanical performance was seen lower than that of neat PLA; this observation was ascribed to both the filler size, being below the percolation threshold, and most importantly to filler-induced plasticization by sorbed moisture. In spite of this, the authors concluded that purified CNCs were adequate for significant improvement in the barrier properties to gases and vapors of PLA, hence resulting in fully renewable bionanocomposites of interest in biopackaging and membrane

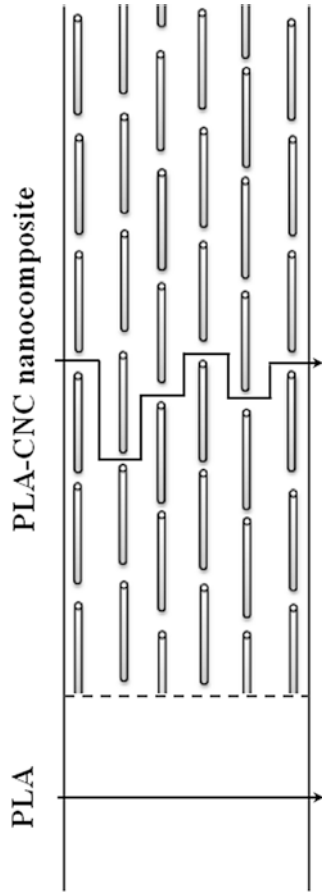


Fig. 9 Schematic representation of low molecular weight molecule pathway in PLA (*left* side) and the more tortuous pathway in PLA-CNC bionanocomposite (*right* side)

and coating applications (Sanchez-Garcia and Lagaron 2010). Meanwhile, Fortunati et al. performed several studies on bionanocomposites based on PLA and CNC. They recognized cellulose nanoparticles as important biobased fillers to enhance the biopolymer performance, in terms of mechanical, thermal, and barrier properties (Fortunati et al. 2012a, b, c, d). In their studies, they modified nanoparticle surface by means of the use of a surfactant to enhance compatibility of the nanoparticles and the polymer matrix (Fortunati et al. 2012c). The effect of CNC in the PLA matrix was investigated in terms of barrier properties against oxygen and water vapor and overall migration test in consideration of the intended application in food packaging. Results showed that reductions of 34% in water vapor permeability were obtained for films with 1 wt.% of s-CNC, and good oxygen barrier properties were obtained for all bionanocomposites, underlining the success of the reinforcement effect of the well-dispersed nanocellulose (Fortunati et al. 2014b, c). Other studies reported the development of multilayers, built up with the layer-by-layer electrostatic deposition of chitosan and ultrasonically green produced CNC. Barrier properties were well improved for PLA films and bottles due to the dense, well-packed, and well-absorbed biocoatings. These developments could increase in three times the product's shelf life (Halász et al. 2015). In addition, other functionalities can be provided to the material with chitosan and cellulose nanocrystals like antimicrobial or wear resistance (Fu et al. 2005; Hoeger et al. 2011; Sanchez-Garcia and Lagaron 2010). However, some migration studies should be performed to prove that no release of constituents to the food occurs and validate the usability of such coatings for food applications. Properties of PLA-CNC nanocomposites for food packaging will be described deeply in the following sections.

The absorption of visible and UV light by polymeric materials is one of the main factors affecting food quality, and thus, the transmission of visible and ultraviolet light is an important parameter for food packaging in order to preserve and protect products until they reach the consumer (Auras et al. 2005). Moreover, the UV radiation is increasingly utilized for sanitization in the food industry as an alternative method to chemical preservatives (Fiori 2015). For that reason, food packaging materials used as primary packaging are critical in minimizing food damage and should not be decomposed by radiation (Auras et al. 2004; Fiori 2015). PLA-CNC nanocomposites show good transparency, and it has been related with the good dispersion of CNC into PLA matrix (Armentano et al. 2013). Additionally, CNC and particularly s-CNC reduce the UV light transmission in the UV-C region (maximum at 275–280 nm) (Arrieta et al. 2015a, c; Fortunati et al. 2015), generally created from artificial light (Auras et al. 2004).

Regarding the mechanical properties of PLA-CNC-based nanocomposites, it has been shown that the addition of CNC enhances the mechanical performance of PLA due to the reinforcement effects induced by nanocellulose crystals. Table 1 summarizes the mechanical properties of several PLA-CNC bionano-

Table 1 Tensile test results of PLA and PLA-PHB bionanocomposite film formulations

Film formulations	E (MPa)	σ_Y (MPa)	ϵ_Y (%)	σ_B (MPa)	ϵ_B (%)	Reference
PLA	1,200–2,400	50–55	2.0–3.5	40–50	45–90	Arrieta et al. (2015a) and Fortunati et al. (2012a)
PLA-CNC1	2,000	43±3	3.9±1.0	25±2	61±3	Fortunati et al. (2014a)
PLA-CNC3	2,500	40±5	3.0±1.0	29±3	38±4	Fortunati et al. (2014a)
PLA-CNC5	1,700–2,930	39±1	2.3±0.2	30–55	30–35	Arrieta et al. (2014c) and Fortunati et al. (2012a)
PLA-s-CNC5	1,400–4,400	54±5	1.2±0.5	35–45	20–30	Arrieta et al. (2014c) and Fortunati et al. (2012a)
PLA-CNC1-TEC20	1,100±40	15±2	–	24±1	309±34	Herrera et al. (2016)
PLA-CNC1-Lim20	680±50	16±3	1.5±1.0	16±4	288±55	Fortunati et al. (2014a)
PLA-CNC3-Lim20	1050±50	22±3	2.6±1.0	23±6	272±70	Fortunati et al. (2014a)
PLA-CNC5-ATBC15	1,030±50	28±4	2.5±0.5	26±3	14.8±0.8	Arrieta et al. (2015a)
PLA-s-CNC5-ATBC15	590±60	26±3	3.1±0.9	25±3	48.2±2.9	Arrieta et al. (2015a)

composites processed by extrusion reported in the literature in which different amounts of CNC (1 wt.%, 3 wt.% and 5 wt.%) were used as well as plasticized PLA-CNC systems with different plasticizers: triethyl citrate (TEC), D-limonene (Lim), and acetyl tributyl citrate (ATBC).

11 PLA-CNC Migration in Food Contact

Food packaging is required to contain food products and protect them from the surroundings avoiding contamination, humidity, and oxidation process during transport, handling, and storage (Arrieta et al. 2015a) as well as to provide information to the consumer about ingredients and nutritional data of the product (Peltzer and Beltrán-Sanahuja 2015). All these functions are important to control the packaging performance and at the same time it is important to study the changes that can occur in the packaging material properties during their interaction with the packaged food (Peltzer and Beltrán-Sanahuja 2015).

The use of biodegradable polymers for food packaging applications is a trending topic, and new materials are emerging for such applications, due to the need to look for alternatives to synthetic- and petroleum-based materials or improve current materials. PLA is very suitable for the manufacture of cups, bottles, films, and

containers. Up to now, there are no specific regulations for biopolymers and biodegradable materials. But, when these materials are intended to be in contact with food, they are treated in exactly the same way as conventional plastics and lie on the scope of European regulations and good manufacturing practice guidelines for the compliance of any food contact material regulation, such as Regulation 1935/2004 and Regulation 10/2011 (European Commission 2009, 2011). However, due to differences in origin and properties between conventional and biobased materials, including PLA, some differences have been noticed (Gontard et al. 2011; Sipilainen-Malm et al. 2000). Differences are mainly due to the compliance tests that the materials are submitted to and food liquid simulants are used specially designed for water-resistant materials. Very few studies are referenced about the safety assessment of biopolymer-based packaging materials. PLA is the most studied biopolymer and very limited migration was found in food packed with PLA, within the fixed overall migration limit in all cases (Conn et al. 1995; Fortunati et al. 2012c). The potential migrants from PLA are lactic acid, lactoyllactic acid (linear dimer of lactic acid), other small oligomers of PLA, and the lactide dimer. All these compounds that migrate from PLA contacting food are known to hydrolyze in aqueous media into lactic acid, which is already authorized as a monomer and additive (Regulation No. 10/2011), with no restrictions or specifications (European Commission 2011).

The incorporation of nanoparticles adds further complexity in terms of safety concerns. Regarding the nanocomposites, an adequate toxicological data is not yet available, and safety nanotechnology assessments are still in progress (Bumbudsanpharoke and Ko 2015). The knowledge about the risks linked to the use of nanoparticles in food contact materials is very short. The European Food Safety Authority (EFSA) highlighted that suitable risk assessment approach should be done to the specific properties of the nanoparticles. The toxicity of nanoparticles depends on several factors such as aggregation, shape, and elemental composition. Therefore, an approach to determine nanoparticle migration levels and assess their toxicity should provide information on those parameters (at least size distribution, state of aggregation, and elemental composition), but analytical techniques still cannot achieve such analysis. In addition to health risk, there is the potential environmental contamination produced by nanoparticles. In the case of PLA, nano-biocomposites used in food packaging raise the issue of environmental contamination as the result of nanomaterials being released from the biopolymer bulk following polymer degradation. Ecotoxicity tests are required to determine the impact and risks of the nanomaterials to human health and the environment. In fact, the Novel Food Regulation EC No 258/97 concerns the commercial distribution and introduction to the market within the European Union of novel foods or novel food ingredients. Under this regulation, foods deemed to be novel must undergo a safety assessment prior to being placed on the market. This could be the piece of legislation where PLA bionanocomposites could be associated (Cushen et al. 2012; Peltzer and Beltrán-Sanahuja 2015). Therefore, the advantages of using biodegradable nanoparticles such as CNC would contribute to the environment protection, as it will be described in the next section.

Regarding PLA-CNC bionanocomposites, it has been shown that the migration level of bionanocomposites based on PLA-CNC as well as PLA/s-CNC was below the overall migration limits indicated in the current legislation in food stimulants, suggesting the possibility to use these systems in food packaging applications (Fortunati et al. 2012c, b).

12 PLA-CNC Nanocomposite End-Life Options

PLA-CNC bionanocomposites not only show higher thermal, mechanical, and gas barrier performance for their use as food packaging material but also are recyclable and biodegradable as additional advantages from an environmental point of view.

12.1 PLA-CNC Recycling

It has been suggested that since PLA undergoes thermal degradation when exposed to elevated temperatures, leading to the formation of lactide monomers, it can be leveraged for the feedstock recycling of PLA (Lim et al. 2008). However, the major problem of recycling PLA is the low thermal stability. Carasco et al. simulated recycling process of PLA by processing PLA by extrusion (residence time of 3 min and temperature profile between 145 and 195 °C) followed by a cooling process and then granulating the obtained material to be injected (temperature profile of 180 °C, 200 °C, and 210 °C). They observed a decrease in PLA viscosity, due to a decrease in molecular weight as a consequence of polymer degradation (Carrasco et al. 2010). Similarly, Badia et al. studied the thermomechanical degradation of PLA by means of successive injection cycles to simulate multiple processing stages that occurs during PLA recycling. They reported that the thermomechanical degradation of PLA occurs mainly via hydrolytic, homolytic chain scission, and intermolecular transesterifications, leading to the formation of mainly linear hydroxyl and carboxyl terminated species, especially after the third reprocessing stage (Badia et al. 2011). Even though specific studies of PLA-CNC nanocomposite recycling have not been carried out, concerning that CNCs increase the PLA thermal stability, it seems that it should be possible to increase the value of recycled PLA coming from PLA-CNC nanocomposites. For instance, PLA-CNC and PLA-s-CNC nanocomposites were studied by isothermal thermogravimetric analysis at 200 °C to simulate the extrusion conditions, and both CNC and s-CNC slightly improved the thermal stability of pure PLA, losing less than 1% of the initial weight exposed at the processing temperature during 20 min (Arrieta et al. 2014b). Nevertheless, the propensity for the lactide monomer to undergo racemization to form *meso*-lactide can impact the optical purity and, thus, the service performance of the resulting recycled PLA-based products (Lim et al. 2008). Accordingly, PLA seems more suitable for disposal rather than recycling (Chien et al. 2011).

12.2 PLA-CNC Biodegradation Under Composting Conditions

As it was previously commented, high amount of plastic wastes go to landfill every year. Landfill disposal is mediated by anaerobic fermentation producing hazardous methane. Even though methane produced in landfills could be used as an energy source, the huge amount of plastic wastes disposed in landfills have to be reduced (Arrieta et al. 2014e; Yagi et al. 2013). Thus, it is known that composting is the most adequate post-use waste treatment for food packaging biodegradable plastics (Arrieta et al. 2014e). Polyesters play a predominant role as biodegradable plastics due to their potentially hydrolyzable ester bonds (Madhavan Nampothiri et al. 2010). In fact, PLA polymers, by having -C-O- ester linkages in the polymer backbone which are hydrolyzable functional groups, are susceptible to hydrolysis (Kale et al. 2007). PLA biodegrades quickly under composting conditions and does not leave toxic residue (Shah et al. 2008). In this sense, PLA can be biodegraded to water and carbon dioxide under environmental conditions by microorganisms providing composting as a simple and sustainable disposal option (Kale et al. 2006, 2007). The initial step of PLA disintegration is the surface hydrolysis; the polymer is disintegrated in low molecular weight species (Fig. 10) (Kale et al. 2007; Song et al. 2009). The resultant breakdowns are suitable for the degradation by the microorganisms. Thus, random nonenzymatic chain scission of the ester groups leads to a reduction in molecular weight, which is further accelerated by acids or bases and is affected by temperature and moisture levels (Kale et al. 2006). Molecular weight variations are an indication of the degradation rate of the polymers and give information about when the main fragmentation occurs in a polymer (Kale et al. 2007). Firstly, the polymer amorphous phase is attacked by microorganisms at the initial stage of the disintegration process which leads to the loss of transparency (Arrieta et al. 2014e; Fortunati et al. 2012d). Meanwhile, the ordered structure in the crystalline fractions could retain the action of microorganisms and, thus, are the last part of the polymeric matrix to be disintegrated under composting (Arrieta et al. 2014e). PLA also changed the color during disintegration and became more opaque (Arrieta et al. 2014c). When the degradation process of the polymer matrices has started, a change in the refraction index of the materials is observed as a result of water absorption and/or presence of products formed by the hydrolytic degradation process (Fortunati et al. 2012d). During the first days of PLA disintegration under compost conditions, an immediate increase in thickness can be observed attributed mainly to the distortion of the material due to high temperature levels and the increased presence of a porous structure due to hydrolysis of the polymer (Kale et al. 2007). During the hydrolysis process, PLA decreases in size showed by a reduction of the thickness and in degradable film piece size reduction and increase in fragility (Arrieta et al. 2014b; Siracusa et al. 2008).

CNC not only suit very well in PLA but also maintain its biodegradability and compostability due to the nature of cellulosic material (Halász et al. 2015). The presence of CNC increased the disintegrability rate of PLA, and this behavior has been attributed to the hydrophilic nature of nanocellulose (Arrieta et al. 2014c; Fortunati et al. 2014b). Although s-CNC also speeds up the disintegration process of PLA, it

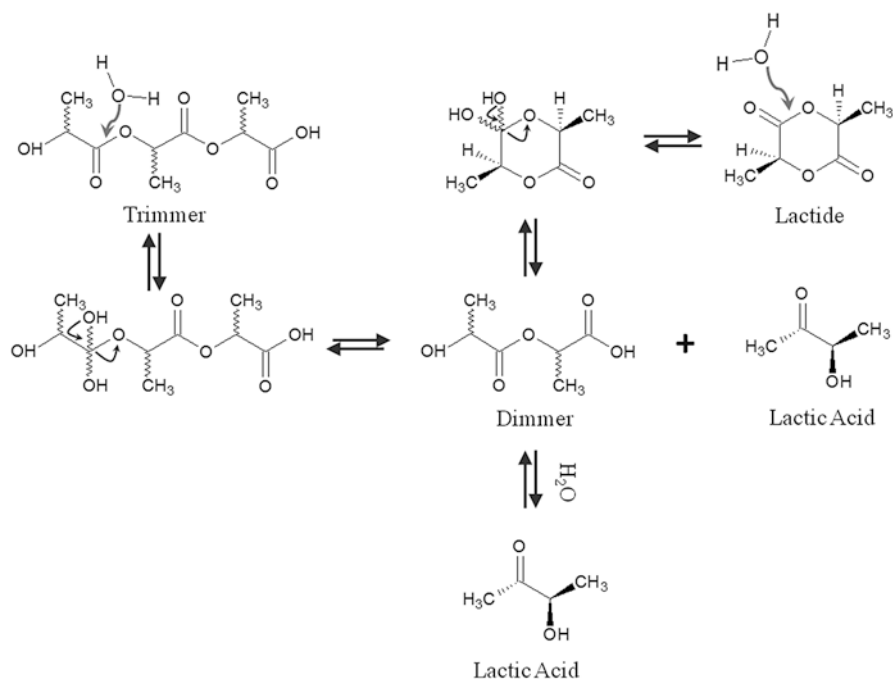


Fig. 10 Schematic representation of PLA hydrolysis and molecular weight loss (Adapted from Kale et al. 2006)

was found that the presence of s-CNC slightly limits the water diffusion by the increase in barrier properties and consequently delays the hydrolysis process and further degradation (Fortunati et al. 2014b). PLA-s-CNC systems present a more porous structure than PLA reinforced with un-functionalized CNC, which have been ascribed as the presence of the surfactant (Luzi et al. 2015). It is widely known that the disintegration of PLA in composting conditions is enhanced by the presence of plasticizers (Arrieta et al. 2014e, 2015a; Lemmouchi et al. 2009), which also speed up the disintegration of PLA-CNC- and PLA-s-CNC-plasticized nanocomposites.

13 Conclusions

The costs of biobased and biodegradable polymers are generally still much higher than that of their traditional polymer counterparts frequently used in the food packaging field. Although PLA is currently used in the market in several packaging applications, its potential to substitute petrochemical-based polymers has not yet been realized in full perspective. The reinforcing effect of CNC has a large potential in enhancing the crystallinity of PLA that could result in higher tortuosity of the transport path improving the typically low barrier properties of PLA. However, the high polarity of CNC surface should be reduced for the industrial melt processing of

PLA–nanocellulose-based materials. The surface functionalization by means of the use of a surfactant is an easy way to improve the dispersion of CNC into PLA matrix. The well dispersion of cellulosic nanoparticles achieved during nanocomposite processing has a large potential in improving the mechanical performance. Additionally, the CNC presence also accelerates the degradation rate of the PLA-based nanocomposites. These bionanocomposites are promising candidates for sustainable post-use waste treatments, such as composting, when short biodegradation times are required like the case of food packaging.

Acknowledgments Authors thank the Spanish Ministry of Science and Innovation (MAT2013-48059-C2-1-R and MAT2014-55778-REDT) as well as the Regional Government of Madrid (S2013/MIT-2862). M. P. Arrieta and L. Peponi are recipients of a Juan de la Cierva (FJCI-2014-20630) and a Ramon y Cajal (RYC-2014-15595) contracts from the MINECO, respectively.

References

- Aoyagi Y, Yamashita K, Doi Y (2002) Thermal degradation of poly[(R)-3-hydroxybutyrate], poly[ϵ -caprolactone], and poly[(S)-lactide]. *Polym Degrad Stab* 76(1):53–59
- Aranguren MI, Marcovich NE, Salgueiro W, Somoza A (2013) Effect of the nano-cellulose content on the properties of reinforced polyurethanes. A study using mechanical tests and positron annihilation spectroscopy. *Polym Test* 32(1):115–122
- Armentano I, Dottori M, Fortunati E, Mattioli S, Kenny JM (2010) Biodegradable polymer matrix nanocomposites for tissue engineering: a review. *Polym Degrad Stab* 95(11):2126–2146
- Armentano I, Bitinis N, Fortunati E, Mattioli S, Rescignano N, Verdejo R, Lopez-Manchado MA, Kenny JM (2013) Multifunctional nanostructured PLA materials for packaging and tissue engineering. *Prog Polym Sci* 38(10–11):1720–1747
- Armentano I, Fortunati E, Burgos N, Dominici F, Luzi F, Fiori S, Jiménez A, Yoon K, Ahn J, Kang S, Kenny JM (2015a) Bio-based PLA-PHB plasticized blend films: processing and structural characterization. *LWT Food Sci Technol* 64(2):980–988
- Armentano I, Fortunati E, Burgos N, Dominici F, Luzi F, Fiori S, Jiménez A, Yoon K, Ahn J, Kang S, Kenny JM (2015b) Processing and characterization of plasticized PLA/PHB blends for biodegradable multiphase systems. *Express Polym Lett* 9(7):583–596
- Arrieta MP, López J, Ferrándiz S, Peltzer MA (2013a) Characterization of PLA-limonene blends for food packaging applications. *Polym Test* 32(4):760–768
- Arrieta MP, Parres F, López J, Jiménez A (2013b) Development of a novel pyrolysis-gas chromatography/mass spectrometry method for the analysis of poly(lactic acid) thermal degradation products. *J Anal Appl Pyrolysis* 101:150–155
- Arrieta MP, Castro-López MDM, Rayón E, Barral-Losada LF, López-Vilariño JM, López J, González-Rodríguez MV (2014a) Plasticized poly(lactic acid)-poly(hydroxybutyrate) (PLA-PHB) blends incorporated with catechin intended for active food-packaging applications. *J Agric Food Chem* 62(41):10170–10180
- Arrieta MP, Fortunati E, Dominici F, Rayón E, López J, Kenny JM (2014b) Multifunctional PLA-PHB/cellulose nanocrystal films: processing, structural and thermal properties. *Carbohydr Polym* 107(0):16–24
- Arrieta MP, Fortunati E, Dominici F, Rayón E, López J, Kenny JM (2014c) PLA-PHB/cellulose based films: mechanical, barrier and disintegration properties. *Polym Degrad Stab* 107:139–149
- Arrieta MP, López J, Hernández A, Rayón E (2014d) Ternary PLA-PHB-limonene blends intended for biodegradable food packaging applications. *Eur Polym J* 50(0):255–270

- Arrieta MP, López J, Rayón E, Jiménez A (2014e) Disintegrability under composting conditions of plasticized PLA-PHB blends. *Polym Degrad Stab* 108:307–318
- Arrieta MP, Samper MD, López J, Jiménez A (2014f) Combined effect of poly(hydroxybutyrate) and plasticizers on polylactic acid properties for film intended for food packaging. *J Polym Environ* 22(4):460–470
- Arrieta MP, Fortunati E, Dominicci F, López J, Kenny JM (2015a) Bionanocomposite films based on plasticized PLA-PHB/cellulose nanocrystal blends. *Carbohydr Polym* 121:265–275
- Arrieta MP, López J, López D, Kenny JM, Peponi L (2015b) Biodegradable electrospun bionanocomposite fibers based on plasticized PLA-PHB blends reinforced with cellulose nanocrystals. *Ind Crop Prod* 93:290–301
- Arrieta MP, López J, López D, Kenny JM, Peponi L (2015c) Development of flexible materials based on plasticized electrospun PLA-PHB blends: structural, thermal, mechanical and disintegration properties. *Eur Polym J* 73:433–446
- Arrieta MP, López J, Ferrándiz S, Peltzer MA (2015d) Effect of D-limonene on the stabilization of poly(lactic acid). *Acta Horti*:719–725
- Arrieta MP, Fortunati E, Burgos N, Peltzer MA, López J, Peponi L (2016a) Nanocellulose-based polymeric blends for food packaging applications-chapter 7. In: Puglia D, Fortunati E, Kenny JM (eds) Multifunctional polymeric nanocomposites based on cellulosic reinforcements. William Andrew Publishing, Oxford, pp 205–252. Copyright © 2016 Elsevier
- Arrieta MP, López J, López D, Kenny JM, Peponi L (2016b) Effect of chitosan and catechin addition on the structural, thermal, mechanical and disintegration properties of plasticized electrospun PLA-PHB biocomposites. *Polym Degrad Stab* 132:157–168
- Auras RA (2007) Solubility of gases and vapors in polylactide polymers. In: Letcher TM (ed) Thermodynamics, solubility and environmental issues. Elsevier, Amsterdam, pp 343–368
- Auras R, Harte B, Selke S (2004) An overview of polylactides as packaging materials. *Macromol Biosci* 4(9):864
- Auras R, Harte B, Selke S (2005) Polylactides. A new era of biodegradable polymers for packaging application. *Ann Tech Conf – ANTEC Conf Proc* 8:320–324
- Auras R, Harte B, Selke S (2006) Sorption of ethyl acetate and d-limonene in poly(lactide) polymers. *J Sci Food Agric* 86(4):648–656
- Badía JD, Santonja-Blasco L, Moriana R, Ribes-Greus A (2010) Thermal analysis applied to the characterization of degradation in soil of polylactide: II. On the thermal stability and thermal decomposition kinetics. *Polym Degrad Stab* 95(11):2185–2191
- Badía JD, Stromberg E, Ribes-Greus A, Karlsson S (2011) Assessing the MALDI-TOF MS sample preparation procedure to analyze the influence of thermo-oxidative ageing and thermo-mechanical degradation on poly(lactide). *Eur Polym J* 47(7):1416–1428
- Balart J, Fombuena V, Boronat T, Reig MJ, Balart R (2012) Surface modification of polypropylene substrates by UV photografting of methyl methacrylate (MMA) for improved surface wettability. *J Mater Sci* 47(5):2375–2383
- Balart JF, Fombuena V, Fenollar O, Boronat T, Sánchez-Nacher L (2016) Processing and characterization of high environmental efficiency composites based on PLA and hazelnut shell flour (HSF) with biobased plasticizers derived from epoxidized linseed oil (ELO). *Compos Part B* 86:168–177
- Bonini C, Heux L, Cavaillé JY, Lindner P, Dewhurst C, Terech P (2002) Rodlike cellulose whiskers coated with surfactant: a small-angle neutron scattering characterization. *Langmuir* 18(8):3311–3314
- Bor Y, Alin J, Hakkarainen M (2012) Electrospray ionization-mass spectrometry analysis reveals migration of cyclic lactide oligomers from polylactide packaging in contact with ethanolic food simulat. *Packag Technol Sci* 25(7):427–433
- Brinchi L, Cotana F, Fortunati E, Kenny JM (2013) Production of nanocrystalline cellulose from lignocellulosic biomass: technology and applications. *Carbohydr Polym* 94(1):154–169
- Bumbudsanpharoke N, Ko S (2015) Nano-food packaging: an overview of market, migration research, and safety regulations. *J Food Sci* 80(5):R910–R923
- Burgos N, Martino VP, Jiménez A (2013) Characterization and ageing study of poly(lactic acid) films plasticized with oligomeric lactic acid. *Polym Degrad Stab* 98(2):651–658

- Burgos N, Tolaguera D, Fiori S, Jiménez A (2014) Synthesis and characterization of lactic acid oligomers: evaluation of performance as poly(lactic acid) plasticizers. *J Polym Environ* 22(2):227–235
- Cailloux J, Santana OO, Franco-Urquiza E, Bou JJ, Carrasco F, MasPOCH ML (2014) Sheets of branched poly(lactic acid) obtained by one-step reactive extrusion-calendering process: physical aging and fracture behavior. *J Mater Sci* 49(11):4093–4107
- Carlson D, Dubois P, Nie L, Narayan R (1998) Free radical branching of polylactide by reactive extrusion. *Polym Eng Sci* 38(2):311–321
- Carrasco F, Pages P, Gamez-Perez J, Santana OO, MasPOCH ML (2010) Processing of poly(lactic acid): characterization of chemical structure, thermal stability and mechanical properties. *Polym Degrad Stab* 95(2):116–125
- Carrasco F, Pérez-Maqueda LA, Sánchez-Jiménez PE, Perejón A, Santana OO, MasPOCH ML (2013) Enhanced general analytical equation for the kinetics of the thermal degradation of poly(lactic acid) driven by random scission. *Polym Test* 32(5):937–945
- Carrasco F, Cailloux J, Sánchez-Jiménez PE, MasPOCH ML (2014) Improvement of the thermal stability of branched poly(lactic acid) obtained by reactive extrusion. *Polym Degrad Stab* 104(1):40–49
- Chien YC, Liang C, Yang SH (2011) Exploratory study on the pyrolysis and PAH emissions of polylactic acid. *Atmos Environ* 45(1):123–127
- Conn RE, Kolstad JJ, Borzelleca JF, Dixler DS, Filer LJ Jr, Ladu BN Jr, Pariza MW (1995) Safety assessment of polylactide (PLA) for use as a food-contact polymer. *Food Chem Toxicol* 33(4):273–283
- Courgneau C, Domenek S, Guinault A, Averous L, Ducruet V (2011) Analysis of the structure-properties relationships of different multiphase systems based on plasticized poly(lactic acid). *J Polym Environ* 19(2):362–371
- Courgneau C, Ducruet V, Avérous L, Grenet J, Domenek S (2013) Nonisothermal crystallization kinetics of poly(lactide) – effect of plasticizers and nucleating agent. *Polym Eng Sci* 53(5):1085–1098
- Cushen M, Kerry J, Morris M, Cruz-Romero M, Cummins E (2012) Nanotechnologies in the food industry – recent developments, risks and regulation. *Trends Food Sci Technol* 24(1):30–46
- Drumright RE, Gruber PR, Henton DE (2000) Polylactic acid technology. *Adv Mater* 12(23):1841–1846
- European Commission (2009) Regulation No 1935/2004 of the European Parliament and of the Council of 27 October 2004 on materials and articles intended to come in contact with food and repealing Directives 80/590/EEC and 89/109/EEC
- European Commission (2011) On plastic materials and articles intended to come into contact with food. (Vol. COMMISSION REGULATION (EU) No 10/2011): Off J Eur Communities
- European Commission (2013) Green Paper. Eur Strategy Plast Waste Environ 123:1–20
- Ferri JM, Fenollar O, Jorda-Vilaplana A, García-Sanoguera D, Balart R (2016a) Effect of miscibility on mechanical and thermal properties of poly(lactic acid)/polycaprolactone blends. *Polym Int* 65(4):453–463
- Ferri JM, Samper MD, García-Sanoguera D, Reig MJ, Fenollar O, Balart R (2016b) Plasticizing effect of biobased epoxidized fatty acid esters on mechanical and thermal properties of poly(lactic acid). *J Mater Sci* 51(11):1–11
- Fiori S. (2015). Industrial uses of PLA. *RSC Polym Chem Ser*; 317–333
- Fombuena V, Balart J, Boronat T, Sánchez-Nácher L, Garcia-Sanoguera D (2013) Improving mechanical performance of thermoplastic adhesion joints by atmospheric plasma. *Mater Des* 47:49–56
- Fombuena V, García-Sanoguera D, Sánchez-Nácher L, Balart R, Boronat T (2014) Optimization of atmospheric plasma treatment of LDPE films: influence on adhesive properties and ageing behavior. *J Adhes Sci Technol* 28(1):97–113
- Fortunati E, Armentano I, Zhou Q, Iannoni A, Saino E, Visai L, Berglund LA, Kenny JM (2012a) Multifunctional bionanocomposite films of poly(lactic acid), cellulose nanocrystals and silver nanoparticles. *Carbohydr Polym* 87(2):1596–1605
- Fortunati E, Peltzer M, Armentano I, Torre L, Jiménez A, Kenny JM (2012b) Effects of modified cellulose nanocrystals on the barrier and migration properties of PLA nano-biocomposites. *Carbohydr Polym* 90(2):948–956
- Fortunati E, Puglia D, Santulli C, Sarasini F, Kenny JM (2012c) Biodegradation of *Phormium tenax*/poly(lactic acid) composites. *J Appl Polym Sci* 125(SUPPL. 2):E562–E572

- Fortunati E, Armentano I, Zhou Q, Puglia D, Terenzi A, Berglund LA, Kenny JM (2012d) Microstructure and nonisothermal cold crystallization of PLA composites based on silver nanoparticles and nanocrystalline cellulose. *Polym Degrad Stab* 97(10):2027–2036
- Fortunati E, Peltzer M, Armentano I, Jiménez A, Kenny JM (2013a) Combined effects of cellulose nanocrystals and silver nanoparticles on the barrier and migration properties of PLA nanobiocomposites. *J Food Eng* 118(1):117–124
- Fortunati E, Puglia D, Luzi F, Santulli C, Kenny JM, Torre L (2013b) Binary PVA bio-nanocomposites containing cellulose nanocrystals extracted from different natural sources: part I. *Carbohydr Polym* 97(2):825–836
- Fortunati E, Puglia D, Monti M, Peponi L, Santulli C, Kenny JM, Torre L (2013c) Extraction of cellulose nanocrystals from *Phormium tenax* fibres. *J Polym Environ* 21(2):319–328
- Fortunati E, Luzi F, Puglia D, Dominici F, Santulli C, Kenny JM, Torre L (2014a) Investigation of thermo-mechanical, chemical and degradative properties of PLA-limonene films reinforced with cellulose nanocrystals extracted from *Phormium tenax* leaves. *Eur Polym J* 56(1):77–91
- Fortunati E, Rinaldi S, Peltzer M, Bloise N, Visai L, Armentano I, Jiménez A, Latterini L, Kenny JM (2014b) Nano-biocomposite films with modified cellulose nanocrystals and synthesized silver nanoparticles. *Carbohydr Polym* 101(0):1122–1133
- Fortunati E, Luzi F, Puglia D, Petrucci R, Kenny JM, Torre L (2015) Processing of PLA nanocomposites with cellulose nanocrystals extracted from *Posidonia oceanica* waste: innovative reuse of coastal plant. *Ind Crop Prod* 67:439–447
- Fu J, Ji J, Yuan W, Shen J (2005) Construction of anti-adhesive and antibacterial multilayer films via layer-by-layer assembly of heparin and chitosan. *Biomaterials* 26(33):6684–6692
- Gontard N, Angellier-Coussy H, Chalier P, Gastaldi E, Guillard V, Guillaume C, Peyron S (2011) Food packaging applications of biopolymer-based films. In: *Biopolymers – new materials for sustainable films and coatings*. Wiley, Chichester, pp 211–232
- Gupta AP, Kumar V (2007) New emerging trends in synthetic biodegradable polymers – polylactide: a critique. *Eur Polym J* 43(10):4053–4074
- Habibi Y (2014) Key advances in the chemical modification of nanocelluloses. *Chem Soc Rev* 43(5):1519–1542
- Halász K, Hosakun Y, Csóka L (2015) Reducing water vapor permeability of poly(lactic acid) film and bottle through layer-by-layer deposition of green-processed cellulose nanocrystals and chitosan. *Int J Polym Sci*. ID 954290
- Hambleton A, Fabra MJ, Debeaufort F, Dury-Brun C, Voilley A (2009) Interface and aroma barrier properties of iota-carrageenan emulsion-based films used for encapsulation of active food compounds. *J Food Eng* 93(1):80–88
- Herrera N, Salaberria AM, Mathew AP, Oksman K (2016) Plasticized polylactic acid nanocomposite films with cellulose and chitin nanocrystals prepared using extrusion and compression molding with two cooling rates: effects on mechanical, thermal and optical properties. *Compos Part A Appl Sci Manuf* 83:89–97
- Hoeger I, Rojas OJ, Efimenko K, Velev OD, Kelley SS (2011) Ultrathin film coatings of aligned cellulose nanocrystals from a convective-shear assembly system and their surface mechanical properties. *Soft Matter* 7(5):1957–1967
- Inkinen S, Hakkarainen M, Albertsson A-C, Sodergard A (2011) From lactic acid to poly(lactic acid) (PLA): characterization and analysis of PLA and its precursors. *Biomacromolecules* 12(3):523–532
- Jamshidian M, Tehrani EA, Imran M, Jacquot M, Desobry S (2010) Poly-lactic acid: production, applications, nanocomposites, and release studies. *Compr Rev Food Sci Food Saf* 9(5):552–571
- Kale G, Auras R, Singh SP (2006) Degradation of commercial biodegradable packages under real composting and ambient exposure conditions. *J Polym Environ* 14(3):317–334
- Kale G, Kijchavengkul T, Auras R, Rubino M, Selke SE, Singh SP (2007) Compostability of bioplastic packaging materials: an overview. *Macromol Biosci* 7(3):255–277
- Khabbaz F, Karlsson S, Albertsson AC (2000) Py-GC/MS an effective technique to characterizing of degradation mechanism of poly (L-lactide) in the different environment. *J Appl Polym Sci* 78(13):2369–2378
- Kopinke FD, Mackenzie K (1997) Mechanistic aspects of the thermal degradation of poly(lactic acid) and poly(β -hydroxybutyric acid). *J Anal Appl Pyrolysis* 40–41:43–53

- Kopinke FD, Remmler M, Mackenzie K, Möder M, Wachsen O (1996) Thermal decomposition of biodegradable polyesters – II. Poly(lactic acid). *Polym Degrad Stab* 53(3):329–342
- Lagaron JM, Lopez-Rubio A (2011) Nanotechnology for bioplastics: opportunities, challenges and strategies. *Trends Food Sci Technol* 22(11):611–617
- Lehermeier HJ, Dorgan JR, Way JD (2001) Gas permeation properties of poly(lactic acid). *J Membr Sci* 190(2):243–251
- Lemmouchi Y, Murariu M, Dos Santos AM, Amass AJ, Schacht E, Dubois P (2009) Plasticization of poly(lactide) with blends of tributyl citrate and low molecular weight poly(D,L-lactide)-b-poly(ethylene glycol) copolymers. *Eur Polym J* 45(10):2839–2848
- Li F, Mascheroni E, Piergiovanni L (2015) The potential of nanocellulose in the packaging field: a review. *Packag Technol Sci* 28(6):475–508
- Lim LT, Auras R, Rubino M (2008) Processing technologies for poly(lactic acid). *Prog Polym Sci* 33(8):820–852
- Liu H, Zhang J (2011) Research progress in toughening modification of poly(lactic acid). *J Polym Sci B Polym Phys* 49(15):1051–1083
- Lönnerberg H, Zhou Q, Brumer Iii H, Teeri TT, Malmström E, Hult A (2006) Grafting of cellulose fibers with poly(ϵ -caprolactone) and poly(L-lactic acid) via ring-opening polymerization. *Biomacromolecules* 7(7):2178–2185
- López-Rubio A, Lagaron JM (2010) Improvement of UV stability and mechanical properties of biopolyesters through the addition of β -carotene. *Polym Degrad Stab* 95(11):2162–2168
- Luzi F, Fortunati E, Puglia D, Petrucci R, Kenny JM, Torre L (2015) Study of disintegrability in compost and enzymatic degradation of PLA and PLA nanocomposites reinforced with cellulose nanocrystals extracted from *Posidonia oceanica*. *Polym Degrad Stab* 121:105–115
- Luzi F, Fortunati E, Jiménez A, Puglia D, Pezzolla D, Gigliotti G, Kenny JM, Chiralt A, Torre L (2016) Production and characterization of PLA-PBS biodegradable blends reinforced with cellulose nanocrystals extracted from hemp fibres. *Ind Crops Prod* 93:276–289
- Madhavan Nampoothiri K, Nair NR, John RP (2010) An overview of the recent developments in polylactide (PLA) research. *Bioresour Technol* 101(22):8493–8501
- Mariano M, El Kissi N, Dufresne A (2014) Cellulose nanocrystals and related nanocomposites: review of some properties and challenges. *J Polym Sci B Polym Phys* 52(12):791–806
- Martin O, Averous L (2001) Poly(lactic acid): plasticization and properties of biodegradable multiphase systems. *Polymer* 42(14):6209–6219
- Martínez-Sanz M, Abdelwahab MA, Lopez-Rubio A, Lagaron JM, Chiellini E, Williams TG, Wood DF, Orts WJ, Imam SH (2013) Incorporation of poly(glycidylmethacrylate) grafted bacterial cellulose nanowhiskers in poly(lactic acid) nanocomposites: improved barrier and mechanical properties. *Eur Polym J* 49(8):2062–2072
- Martínez-Sanz M, Villano M, Oliveira C, Albuquerque MGE, Majone M, Reis M, Lopez-Rubio A, Lagaron JM (2014) Characterization of polyhydroxyalkanoates synthesized from microbial mixed cultures and of their nanobiocomposites with bacterial cellulose nanowhiskers. *New Biotechnol* 31(4):364–376
- Martino VP, Jiménez A, Ruseckaite RA (2009a) Processing and characterization of poly(lactic acid) films plasticized with commercial adipates. *J Appl Polym Sci* 112(4):2010–2018
- Martino VP, Ruseckaite RA, Jimenez A (2009b) Ageing of poly(lactic acid) films plasticized with commercial polyadipates. *Polym Int* 58(4):437–444
- Martino VP, Jiménez A, Ruseckaite RA, Avérous L (2011) Structure and properties of clay nanobiocomposites based on poly(lactic acid) plasticized with polyadipates. *Polym Adv Technol* 22(12):2206–2213
- Mattioli S, Peltzer M, Fortunati E, Armentano I, Jiménez A, Kenny JM (2013) Structure, gas-barrier properties and overall migration of poly(lactic acid) films coated with hydrogenated amorphous carbon layers. *Carbon* 63:274–282
- Mujica-García A, Hooshmand S, Skrifvars M, Kenny JM, Oksman K, Peponi L (2016) Poly(lactic acid) melt-spun fibers reinforced with functionalized cellulose nanocrystals. *RSC Adv* 6(11):9221–9231
- Nascimento L, Gamez-Perez J, Santana OO, Velasco JI, MasPOCH ML, Franco-Urquiza E (2010) Effect of the recycling and annealing on the mechanical and fracture properties of poly(lactic acid). *J Polym Environ* 18(4):654–660

- Navarro-Baena I, Kenny JM, Peponi L (2014a) Crystallization and thermal characterization of biodegradable tri-block copolymers and poly(ester-urethane)s based on PCL and PLLA. *Polym Degradation Stab*
- Navarro-Baena I, Kenny JM, Peponi L (2014b) Thermally-activated shape memory behaviour of bionanocomposites reinforced with cellulose nanocrystals. *Cellulose* 21(6):4231–4246
- Navarro-Baena I, Arrieta MP, Sonseca A, Torre L, López D, Giménez E, Kenny JM, Peponi L (2015) Biodegradable nanocomposites based on poly(ester-urethane) and nanosized hydroxyapatite: plasticant and reinforcement effects. *Polym Degrad Stab* 121:171–179
- Oksman K, Aitomäki Y, Mathew AP, Siqueira G, Zhou Q, Butylina S, Tanpichai S, Zhou X, Hooshmand S (2016) Review of the recent developments in cellulose nanocomposite processing. *Compos Part A Appl Sci Manuf* 83:2–18
- Pantani R, Gorrasi G, Vigliotta G, Murariu M, Dubois P (2013) PLA-ZnO nanocomposite films: water vapor barrier properties and specific end-use characteristics. *Eur Polym J* 49(11):3471–3482
- Patrício PSDO, Pereira FV, Dos Santos MC, De Souza PP, Roa JPB, Orefice RL (2013) Increasing the elongation at break of polyhydroxybutyrate biopolymer: effect of cellulose nanowhiskers on mechanical and thermal properties. *J Appl Polym Sci* 127(5):3613–3621
- Paul M-A, Alexandre M, Degée P, Henrist C, Rulmont A, Dubois P (2003) New nanocomposite materials based on plasticized poly(l-lactide) and organo-modified montmorillonites: thermal and morphological study. *Polymer* 44(2):443–450
- Peltzer MA, Beltrán-Sanahuja A (2015) Legislation related to PLA. In: Jiménez A, Peltzer M, Ruseckaite R (eds) *RSC polymer chemistry series*, vol 2015, pp 334–346
- Peltzer M, Pei A, Zhou Q, Berglund L, Jiménez A (2014) Surface modification of cellulose nanocrystals by grafting with poly(lactic acid). *Polym Int* 63(6):1056–1062
- Peponi L, Navarro-Baena I, Báez JE, Kenny JM, Marcos-Fernández A (2012) Effect of the molecular weight on the crystallinity of PCL-b-PLLA di-block copolymers. *Polymer (United Kingdom)* 53(21):4561–4568
- Peponi L, Navarro-Baena I, Sonseca A, Gimenez E, Marcos-Fernandez A, Kenny JM (2013) Synthesis and characterization of PCL-PLLA polyurethane with shape memory behavior. *Eur Polym J* 49(4):893–903
- Peponi L, Puglia D, Torre L, Valentini L, Kenny JM (2014) Processing of nanostructured polymers and advanced polymeric based nanocomposites. *Mater Sci Eng R* 85(1):1–46
- Perego G, Cella GD, Bastioli C (1996) Effect of molecular weight and crystallinity on poly(lactic acid) mechanical properties. *J Appl Polym Sci* 59(1):37–43
- Petersson L, Oksman K (2006) Biopolymer based nanocomposites: comparing layered silicates and microcrystalline cellulose as nanoreinforcement. *Compos Sci Technol* 66(13):2187–2196
- Petersson L, Kvien I, Oksman K (2007) Structure and thermal properties of poly(lactic acid)/cellulose whiskers nanocomposite materials. *Compos Sci Technol* 67(11–12):2535–2544
- Plastic Europe (2015) An analysis of European plastics production, demand and waste data. *Plastics – the facts*
- Raquez JM, Habibi Y, Murariu M, Dubois P (2013) Polylactide (PLA)-based nanocomposites. *Prog Polym Sci* 38(10–11):1504–1542
- Rasal RM, Janorkar AV, Hirt DE (2010) Poly(lactic acid) modifications. *Prog Polym Sci* 35(3):338–356
- Rayón E, López J, Arrieta MP (2013) Mechanical characterization of microlaminar structures extracted from cellulosic materials using nanoindentation technique. *Cellul Chem Technol* 47(5–6):345–351
- Rayón E, Ferrandiz S, Rico MI, López J, Arrieta MP (2014) Microstructure, mechanical and thermogravimetric characterization of cellulosic by-products obtained from the biomass seeds. *Int J Food Prop* 0(0):0
- Rodríguez C, Arencón D, Belzunce J, Maspoch ML (2014) Small punch test on the analysis of fracture behaviour of PLA-nanocomposite films. *Polym Test* 33:21–29
- Ruellan A, Guinault A, Sollogoub C, Chollet G, Ait-Mada A, Ducruet V, Domenek S (2015) Industrial vegetable oil by-products increase the ductility of polylactide. *Express Polym Lett* 9(12):1087–1103
- Saeidlou S, Huneault MA, Li H, Park CB (2012) Poly(lactic acid) crystallization. *Prog Polym Sci* 37(12):1657–1677

- Samper MD, Arrieta MP, Ferrándiz S, López J (2014) Influence of biodegradable materials in the recycled polystyrene. *J Appl Polym Sci* 131(23)
- Sanchez-García MD, Lagaron JM (2010) On the use of plant cellulose nanowhiskers to enhance the barrier properties of polylactic acid. *Cellulose* 17(5):987–1004
- Sanchez-García MD, Gimenez E, Lagaron JM (2008) Morphology and barrier properties of solvent cast composites of thermoplastic biopolymers and purified cellulose fibers. *Carbohydr Polym* 71(2):235–244
- Sarasua JR, Arraiza AL, Balerdi P, Maiza I (2005) Crystallization and thermal behaviour of optically pure polylactides and their blends. *J Mater Sci* 40(8):1855–1862
- Shah AA, Hasan F, Hameed A, Ahmed S (2008) Biological degradation of plastics: a comprehensive review. *Biotechnol Adv* 26(3):246–265
- Silvestre C, Duraccio D, Cimmino S (2011) Food packaging based on polymer nanomaterials. *Prog Polym Sci* 36(12):1766–1782
- Sipilainen-Malm T, Thoden van Velzen U, Leufven A (2000) Safety and food contact legislation. In: Weber CJ (ed) *Biobased packaging materials for the food industry*. KVL Department of Dairy and Food Science, Denmark
- Siqueira G, Bras J, Dufresne A (2010) Cellulosic bionanocomposites: a review of preparation, properties and applications. *Polymers* 2(4):728–765
- Siracusa V, Rocculi P, Romani S, Rosa MD (2008) Biodegradable polymers for food packaging: a review. *Trends Food Sci Technol* 19(12):634–643
- Södergård A, Näsman JH (1994) Stabilization of poly(L-lactide) in the melt. *Polym Degrad Stab* 46(1):25–30
- Södergård A, Stolt M (2002) Properties of lactic acid based polymers and their correlation with composition. *Prog Polym Sci* 27(6):1123–1163
- Song JH, Murphy RJ, Narayan R, Davies GBH (2009) Biodegradable and compostable alternatives to conventional plastics. *Phil Trans R Soc London* 364(1526):2127–2139
- Sonseca Á, Camarero-Espinosa S, Peponi L, Weder C, Foster EJ, Kenny JM, Giménez E (2014) Mechanical and shape-memory properties of poly(mannitol sebacate)/cellulose nanocrystal nanocomposites. *J Polym Sci, Part A: Polym Chem* 52(21):3123–3133
- Tsuji H (2005) Poly(lactide) stereocomplexes: formation, structure, properties, degradation, and applications. *Macromol Biosci* 5(7):569–597
- Turner JF II, Riga A, O'Connor A, Zhang J, Collis J (2004) Characterization of drawn and undrawn poly-L-lactide films by differential scanning calorimetry. *J Therm Anal Calorim* 75(1):257–268
- Vink ETH, Rábago KR, Glassner DA, Gruber PR (2003) Applications of life cycle assessment to NatureWorks™ polylactide (PLA) production. *Polym Degrad Stab* 80(3):403–419
- Vogler EA (1998) Structure and reactivity of water at biomaterial surfaces. *Adv Colloid Interf Sci* 74(1–3):69–117
- Westphal C, Perrot C, Karlsson S (2001) Py-GC/MS as a means to predict degree of degradation by giving microstructural changes modelled on LDPE and PLA. *Polym Degrad Stab* 73(2):281–287
- Yagi H, Ninomiya F, Funabashi M, Kunioka M (2013) Thermophilic anaerobic biodegradation test and analysis of eubacteria involved in anaerobic biodegradation of four specified biodegradable polyesters. *Polym Degrad Stab* 98(6):1182–1187
- Yu H, Huang N, Wang C, Tang Z (2003) Modeling of poly(L-lactide) thermal degradation: theoretical prediction of molecular weight and polydispersity index. *J Appl Polym Sci* 88(11):2557–2562
- Zhang X, Zhang Y (2016) Reinforcement effect of poly(butylene succinate) (PBS)-grafted cellulose nanocrystal on toughened PBS/polylactic acid blends. *Carbohydr Polym* 140:374–382
- Zhang J, Tashiro K, Tsuji H, Domb AJ (2008) Disorder-to-order phase transition and multiple melting behavior of poly(L-lactide) investigated by simultaneous measurements of WAXD and DSC. *Macromolecules* 41(4):1352–1357

Removal of Pollutants Using Electrospun Nanofiber Membranes

Laura G. Ribba, Jonathan D. Cimadoro, Norma Beatriz D'Accorso,
and Silvia Nair Goyanes

1 Introduction

There is an increasing worldwide concern about environmental issues. The quality of the environment has deteriorated due to different factors. In addition to natural sources of pollution, such as volcanic dust, sea salt particles, photochemically formed ozone, and products of forest fibers, among others, human sources of pollution (United Nations 1997), such as industrialization, processing of fossil fuels (which leads to emissions of greenhouse gases and accidental spills), and population growth, with a huge increase in waste production and natural resources demand, have grown strongly.

The two environmental systems with the most pressing environmental issues are water and air. Water pollution and shortage of freshwater are often cited as critical global problems. According to the environmental campaign organization WWF (World Wildlife Fund), "Pollution from toxic chemicals threatens life on this planet; every ocean and every continent, from the tropics to the once-pristine polar regions,

Norma Beatriz D'Accorso and Silvia Nair Goyanes contributed equally to this work.

L.G. Ribba • J.D. Cimadoro • S.N. Goyanes (✉)

Facultad de Ciencias Exactas y Naturales, Departamento de Física, Laboratorio de Polímeros y Materiales Compuestos (LPM&C), Universidad de Buenos Aires, Buenos Aires, Argentina

Consejo Nacional de Investigaciones Científicas y Técnicas (CONICET)-UBA, Instituto de Física de Buenos Aires (IFIBA), Buenos Aires, Argentina

e-mail: goyanes@df.uba.ar

N.B. D'Accorso (✉)

Facultad de Ciencias Exactas y Naturales, Departamento de Química Orgánica, Universidad de Buenos Aires, Buenos Aires, Argentina

Centro de Investigación en Hidratos de Carbono (CIHIDECAR), Consejo Nacional de Investigaciones Científicas y Técnicas (CONICET)-UBA, Buenos Aires, Argentina

e-mail: norma@qo.fcen.uba.ar

is contaminated.” World Health Organization stated that in 2013, 780 million people (11 percent of the world’s population) did not have access to safe drinking water (Kaur 2016). It is estimated that more than 50% of nations in the world will face freshwater stress or shortages by 2025. By 2075, it is further estimated that the number of nations facing these problems will increase to become 75% of all nations (Veleirinho et al. 2008).

Similarly, air is another environmental system that is of concern. Its pollution is a serious human health matter in many developing nations (Wang et al. 2014). An important source of human diseases in air is ultrafine particles, such as PM_{2.5} (2.5 μm in diameter or smaller), which are produced from all types of combustion, including motor vehicles, power plants, residential wood burning, forest fires, agricultural burning, and some industrial processes.

There is an enormous requirement for clean air and water around the world which has aroused immense interest in the development of high-efficiency devices for the detection and removal of pollutants. Different types of devices have been developed for the removal of contaminants. In that line, nanostructured filters have gained interest in recent years. Nanofibrous materials have attracted increasing attention in this field because of their unique properties such as high surface area, high aspect ratio, good mechanical properties, and the ability to incorporate different functionalities. Nanofibrous materials can be prepared by methods such as vapor-phase approach, template-directed synthesis, solution–liquid–solid technique, solution-phase growth based on capping reagents, self-assembly, solvothermal synthesis, and electrospinning (Thavasi et al. 2008). Among them, electrospinning has become more popular because of its easiness and low cost. It is one of the available inexpensive industry viable technologies, which can truly produce 1D fibers of micrometer to nanometer size ranges in diameter. While the range of applications of the materials produced by this technique is immense, the number of publications and patents related to its environmental applications in the last 10 years strongly increased, as it is shown in Fig. 1. The data clearly demonstrates that the electrospinning applied to environmental issues has attracted increasing attention recently. These literature data were obtained based on a search in Scopus system.

Different materials can be electrospun into nano-/microfibers. In particular, many biodegradable polymers offer this possibility (Persano et al. 2013). Fully or partially biodegradable devices for environmental control and remediation offer the added value of not further contributing to pollution after use.

This chapter highlights the potential and application of electrospun fibrous materials based on biodegradable polymers for environmental treatment, including pollutant detection, particle filtration, oil/water separation, and pollutant adsorption.

2 Electrospinning Process

Electrospinning is a simple method for producing a wide variety of materials composed of ultrathin fibers. In this technique, a droplet of dissolved polymer is exposed to an electric field, generating an electrical charge distribution. In these circumstances,

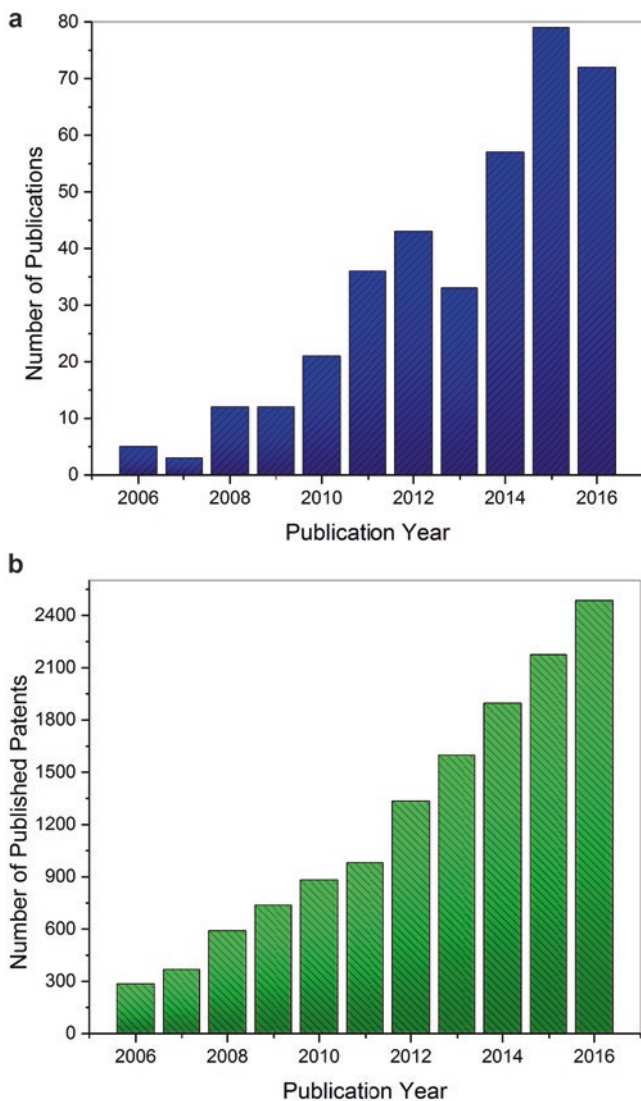


Fig. 1 (a) Comparison of the annual number of scientific publications about electrospinning for environmental remediation. (b) Comparison of the annual number of published patents about electrospinning for environmental remediation

two forces come into play: the surface tension of the solution and its electrostatic repulsion. Four main elements are required for a basic assembly of the electrospinning apparatus: a spinneret (typically a hypodermic syringe needle), a high-voltage current source (usually between 5 and 50 kV), an injector pump, and a grounded collector. Basically the syringe pump pushes the polymer solution through a conduit to the needle tip, where a drop is formed and, due to the high voltage, it is charged and deformed, forming a structure known as Taylor cone. From a given voltage value, the

electrostatic repulsion exceeds the surface tension, and a jet is ejected from the Taylor cone to the collector. Electrostatic repulsion causes bending instabilities to the jet during its path, deforming and stretching it, while the solvent is volatilized due to surface effects until it is finally deposited on the grounded collector.

This is a versatile process in at least two important aspects. On one hand, using it can generate ultrathin fibers of different materials like polymers, ceramics, and composite materials. In recent years, new methodologies have been investigated in order to allow other materials to be processed by this technique. On the other, it allows manipulating the type of fiber obtained, whereby different final materials can be generated, still using the same base material. The morphology of the obtained fibers depends on the characteristics of the electrospinning system, the process variables, and the ambient conditions. By changing these parameters, flattened, tapered, helical, branched, or hollow fibers with diameters ranging from submicrons to nanometers may be obtained, with interconnected pores and the possibility of generating surface porosity in the fiber itself (Ribba et al. 2014).

Besides, the electrospinning technique provides the ability to encapsulate or superficially deposit nanoparticles or nanofillers on the fibers (Yarin 2011). Introducing simple variations in the electrospinning equipment core-shell fibers, nanofibers with hollow interiors and nanofibers with internal porous structures can be obtained (Fig. 2). Furthermore, there are techniques that allow the introduction of specific functionalities on the fiber surface without modifying their morphology (Sánchez et al. 2016). The obtained nanofibers may be post-functionalized and the most usual methods are physical or chemical vapor deposition.

In the case of polymers, it is possible to cross-link the material before or after the nanofiber production (Bauguera et al. 2014). Before means that the polymers have already been cross-linked in the solution. In this case, special care must be taken to

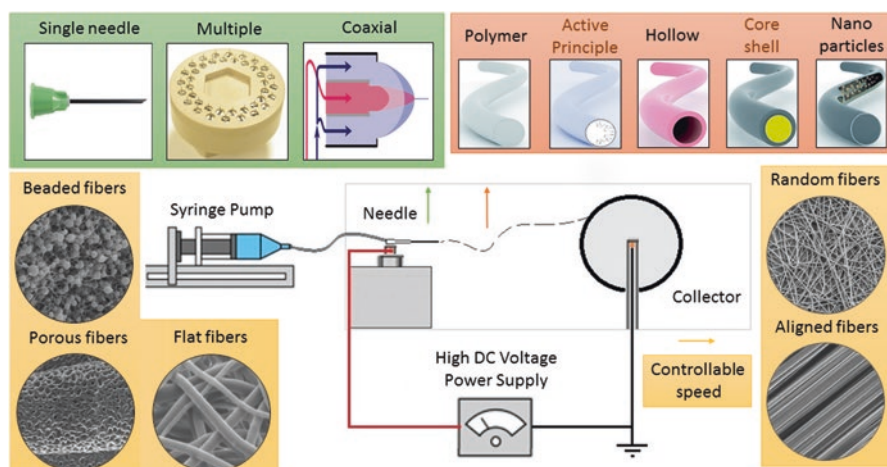


Fig. 2 Basic setup for electrospinning and some of the most interesting results that may be obtained

ensure that the solution continues to behave as a fluid at the operating temperature, or the technique cannot be used.

3 Biodegradable Polymers for Environmental Applications

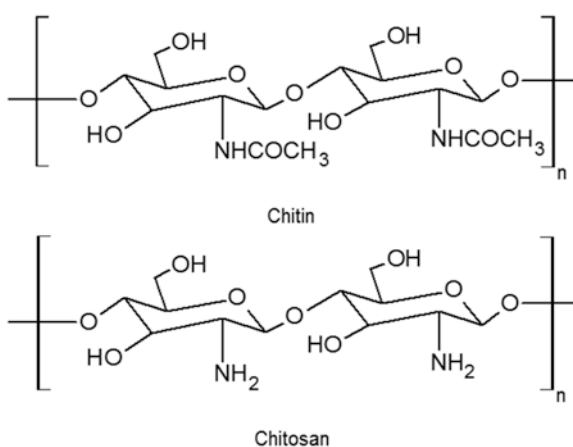
Biodegradable polymers are those that degrade upon disposal by the action of living organisms. Extraordinary progress has been made in the development of practical applications for materials based on this type of polymers. In particular, the property of biodegradability results very attractive in products for environmental remediation. The main features of biodegradable polymers that can be electrospun for environmental applications will be summarized in this section.

3.1 Chitosan

Chitosan is a linear polysaccharide composed of randomly distributed β -(1 \rightarrow 4)-linked D-glucosamine (deacetylated unit) and N-acetyl-D-glucosamine (acetylated unit). It is industrially produced by deacetylation of chitin, the second most abundant polysaccharide on earth, which is the structural element in the exoskeleton of crustaceans (such as crabs and shrimp) and cell walls of fungi. The criteria for distinguishing between chitin and chitosan are the solubilities of the polymers in dilute aqueous acid: chitin is insoluble, while chitosan forms viscous solutions. Figure 3 shows the chemical structure of chitin and chitosan.

Chitosan itself is a nontoxic biopolymer with a wide range of applications in the fields of biotechnological, biomedical, environmental, microbiological, and pharmaceutical studies (Logith et al. 2016). In particular, although it is complicated due

Fig. 3 Chemical structures of chitin and chitosan



to its poor solubility in water, it can be electrospun to form micro- and nanofibers. The most used solvents to dissolve chitosan are acetic acid, hydrochloric acid, formic acid, and trifluoroacetic acid (Huang et al. 2015). Many researchers investigated the optimal conditions for the obtaining of chitosan nanofibers. It has been found that increasing concentrations of chitosan cause the morphology of fibers to change from spherical beads to an interconnected fibrous network.

Electrospinning of chitosan nanofiber has also been accomplished using a blend of chitosan with another polymer, such as polyethylene oxide (PEO) (Rieger and Schiffman 2014), poly(vinyl alcohol) (PVA) (Abdelgawad et al. 2014), polyvinylpyrrolidone (PVP) (Zhang et al. 2012), and silk fibroin (Lai et al. 2014). Nevertheless, the obtained hybrid nanofibers normally have a large diameter.

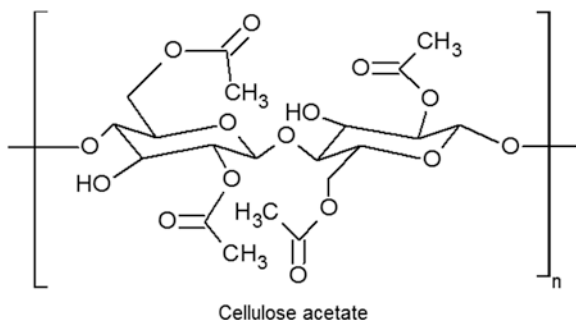
3.2 Cellulose Acetate (CA)

CA is a modified natural polymer with a wide range of properties. It is the acetate ester of cellulose, and its chemical structure is shown in Fig. 4. Although CA can be produced with a range of degrees of substitution (DS), the most common level is a DS of 2.5 due to good solubility in common solvents, molecular weights, and melt properties. It was first discovered in 1865, when Paul Schützenberger found that cellulose reacts with acetic anhydride to form cellulose acetate. The first soluble forms of CA were invented by Arthur Eichengrün and Theodore Becker in 1903 (Plastics Word 1968).

This polymer has been extensively investigated for its low cost and easy processability. However, its potential applications have been reduced by different limiting factors such as maximum operating temperature of about 40 °C, narrow pH range between 3 and 6, and high biodegradability (Guglielmi and Androttola 2010). Some of these drawbacks have recently been overcome by exploring the properties of cellulose acetate at nanoscale level. One possibility is nanofiber production by electrospinning method (Huang et al. 2003).

CA is a promising polymer with important applications for the electrospinning of permeable filtration systems, membranes, reverse osmosis, or aerosol treatments.

Fig. 4 Chemical structure of cellulose acetate



Its low absorption characteristics, thermal stability, easy-to-modify feature, and physical durability are some of the reasons of the wide utilization of the CA. In particular, electrospun nanofibrous mats of CA provide extremely chemical resistant platforms against most common organic solvents and are stable at very diverse pH values ranging from 3 to 12 (Tian et al. 2011).

The selection of appropriate electrospinning conditions has been conventionally based on trial and error or results from similar systems. CA has been successfully electrospun using different solvents, whether single, such as acetone, chloroform, *N,N*-dimethylformamide (DMF), dichloromethane (DCM), formic acid, methanol (MeOH), and pyridine, or in mixed solvent systems, such as acetone–dimethylacetamide, chloroform–MeOH, DCM–MeOH, and acetone/DMF/trifluoroethanol (Ma and Ramakrishna 2008).

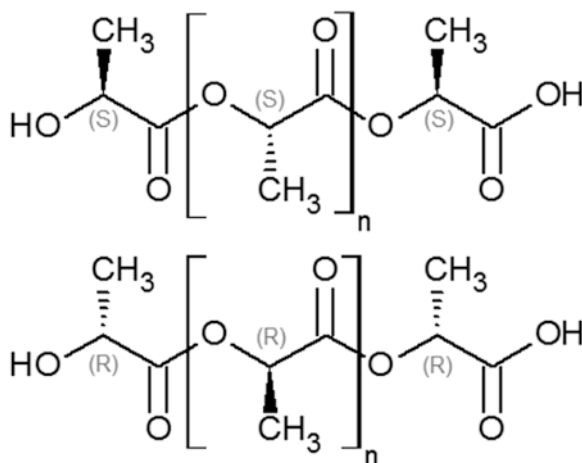
The influence of ambient parameters and electrospinning parameters on the nature of electrospun CA fibers has not been widely studied. Both humidity and temperature were found to have profound influence on the fiber diameter of electrospun CA (De Vrieze et al. 2009). While humidity trends to increase average diameter of nanofibers, temperature dictates the solvent evaporation rate and viscosity of the polymer solution.

3.3 Poly(lactic Acid) (PLA)

PLA is an aliphatic polyester made from α -hydroxy acids. It is a thermoplastic, high-strength, high-modulus polymer that can be made from annually renewable resources, and it is considered biodegradable and compostable. Its chemical structure is shown in Fig. 5.

The stereochemical structure of this polymer can be easily modified by polymerizing a controlled mixture of the L- or D-isomers to yield high molecular weight

Fig. 5 Chemical structures of poly(lactic acid)



amorphous or crystalline polymers that can be used for food contact and are generally recognized as safe (GRAS) (Conn et al. 1995). Besides, its degradation is conducted through simple hydrolysis of the ester bond and does not require the presence of enzymes to catalyze it, with lactic acid being a typical harmless by-product of decomposition.

Commercial PLA is readily soluble in organic solvents and can be cast into thin films, fibers, foams, or other forms. In particular, electrospinning is a common method of making PLA fibers. In order to prepare PLA solutions, different solvents such as dimethylformamide, methylene chloride, dichloromethane, and chloroform have been used (Casasola et al. 2014). Typically, the concentration required for the formation of fibers is above 8 wt.% (Picciani et al. 2009). Electrospun PLA membranes are highly hydrophobic (Yue et al. 2015), as a result of the increased surface roughness and its chemical composition. Thus, water cannot penetrate electrospun PLA membranes and only remains on the surfaces. In order to change its wettability to add new functionalities, different polymers, like poly(ϵ -caprolactone), poly(3-hydroxybutyrate-co-3-hydroxyvalerate), and chitosan, were blended with PLA to produce electrospun membranes.

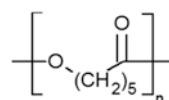
Due to its biodegradability and biocompatibility, added to the fact that it is mechanically robust and environmentally stable, PLA has attracted much attention in many applications. Membranes from PLA are mainly used as the scaffolds for drug delivery and tissue engineering (Valente et al. 2016), sensors (Picciani et al. 2016), and filters (Wang et al. 2015), between others.

3.4 Polycaprolactone (PCL)

Polycaprolactone is a hydrophobic semicrystalline polymer. It can be synthesized by ring-opening polymerization of ϵ -caprolactone using various anionic, cationic, and coordination catalysts or by free radical ring-opening polymerization of 2-methylene-1,2-dioxepane (Chasin et al. 1990). Its chemical structure is shown in Fig. 6. Normally, PCL can be degraded by hydrolysis of its ester linkages in physical condition and also by living organisms such as bacteria and fungi. However, it cannot be degraded in animal and human bodies because of deficiency of suitable enzymes in bodies, making it suitable for use in biomedical applications that require slow degradation (Vert 2009).

At room temperature, it can be soluble in chloroform, dichloromethane, benzene, toluene, carbon tetrachloride, 2-nitropropane, cyclohexanone, etc. (Coulembier et al. 2006). PCL can be formed as continuous ultrafine fibers by electrospinning to give excellent characteristics such as high porosity and surface area. Typically, the concentration required for the formation of fibers is above 8 wt.% (Suwantong

Fig. 6 Chemical structures of polycaprolactone



2016). Besides, PCL can be blended and modified with other polymers to improve its physical, chemical, and mechanical properties (Lee et al. 2012; Hartman et al. 2010; Zheng et al. 2014; Wutticharoenmongkol et al. 2006). As it is approved by the Food and Drug Administration for use in humans, it has promising potential for use in biomedical application (Kim 2008), but it is also used in other fields such as environmental remediation (Hota et al. 2008) and sensing (Low et al. 2014).

3.5 Poly(β -hydroxybutyrate) (PHB)

PHB is a biotechnologically produced polyester that constitutes a form of energy storage molecule to be metabolized when other common energy sources are not available. It is produced by microorganisms (such as *Ralstonia eutrophus*, *Methylobacterium rhodesianum*, or *Bacillus megaterium*) apparently in response to conditions of physiological stress (limited nutrients). Microbial biosynthesis of PHB starts with the condensation of two molecules of acetyl-CoA to give acetoacetyl-CoA which is subsequently reduced to hydroxybutyryl-CoA. This latter compound is then used as a monomer to polymerize PHB. An important characteristic of this polyester, which broadens the range of possible applications, is its biodegradability. It can be degraded to water and carbon dioxide under environmental conditions by a variety of bacteria and has much potential for applications of environmentally degradable plastics. However, it suffers from some disadvantages compared with conventional plastics, for example, brittleness and a narrow processability window. To improve such properties, various copolymers containing other hydroxyalkanoate units have been biosynthesized. PHB and the copolymer, poly(3-hydroxybutyrate-co-3-hydroxyvalerate) (PHBV), are produced by Monsanto® and sold under the trade name Biopolm®.

Biodegradable nanofibrous PHB and PHBV membranes have been prepared by electrospinning. Fibers were obtained by electrospinning from a chloroform solution, resulting in an average fiber diameter of 2.5 μm . In order to reduce the average fiber diameter, an organosoluble salt (benzyl trialkylammonium chloride, BTEAC) was added to the electrospinning solution (Choi et al. 2004). Sombatmankhong et al. (2006) studied the effect of electrospinning parameters on PHB, PHBV, and their blended fibers and obtained well-aligned, cross-sectionally round fibers by using a rotating cylindrical collector. The average diameter of the electrospun fibers from PHB and PHBV solutions ranged between 1.6 and 8.8 μm . Mechanically, much improvement in the tensile strength and the elongation at break was observed for the blended fiber membranes over those of the PHB and PHBV fiber ones.

4 Pollutant Detection

A key strategy for the control and remediation of the environment is threat detection. Sensors are important tools that allow pollutant detection in the environment. One of the main characteristics of electrospun nanofibers is their high surface area,

what results convenient for a large number of applications. In particular, they have a promising future in the field of industrial pollutant detection. Whether the fiber's reactive component is on its surface or inside it, the contaminant will easily find access to it and then be detected. Besides, electrospinning technology allows the development of nanofibrous mats in a broad range of complex architectures, ranging from porous, core-shell, and multicore to tubular or cable-like structures, expanding the range of possible new sensors.

As it was mentioned before, nanofibers from different raw materials can be obtained by electrospinning, but we are going to focus on those based on biodegradable polymers. Biodegradable sensors could be applied in a variety of circumstances without further contributing to pollution, such as in the monitoring of environmental conditions after ecological disasters or in sustainable agriculture by monitoring nutrients and water in soil.

Among the most investigated sensing systems, quartz crystal microbalance (QCM) has been widely used due to its accuracy, real-time detection, and inexpensiveness (Wang et al. 2012). It is a mass sensing platform with a sensitive coating capable to adsorb specific molecules. Considerable efforts have been devoted to develop electrospun nanofiber-based QCM sensors to enhance the sensing performance. Although the use of biodegradable polymers as a basis for these materials has not been widely studied, there are cases in the literature in which partially biodegradable sensors were successfully developed. Wang et al. developed a promising strategy to combine polyethyleneimine (PEI)-modified chitosan electrospun membrane and QCM to construct highly sensitive formaldehyde sensors. The chitosan fibrous substrate was uniformly modified with PEI, giving the structure abundant primary amine groups to interact with formaldehyde molecules. A QCM was coated with this nanostructure to give rise to a formaldehyde sensor with rapid response and low detection limit (5 ppm) at room temperature. Mass changes are directly related to the interaction between adsorption compounds and coating layers (Kimura et al. 2012), (Raza et al. 2014b), (Fang et al. 2016). Another example is the case of Jia et al. (2016) who fabricated novel cellulose acetate (CA)/PEI/poly(acrylic acid) (PAA) nanofibers/QCM sensor for ammonia gas detection, which is the main component of fertilizers, pharmaceuticals, surfactants, and coolants widely used in industry and agriculture, strongly irritating the human skin and mucosa as well as causing protein degeneration. They found that incorporated into QCM system, the CA/PEI/PAA nanofibers exhibited an outstanding and desirable sensing behavior, including high sensitivity, fast response, and good repeatability, making them a promising candidate as an ammonia gas detector.

Another possibility is the use of conductometric sensors, based on certain kinds of conducting materials which cause a change in their electrical resistance in response to an interaction with gases and vapors. Polyaniline (PANi) is a conductive polymer which can be used as sensing element. Different authors combined PANi with biodegradable polymers in order to develop conductometric sensors. Serrano et al. (2014) prepared conducting PLA/PANi nanofibers and used it to sense alcohol vapors of increasing molecular size enhancing the contribution of PLA in the sensor feature. Another example is the case of Ismail et al. (2014), who electrospun fibers

of silk and coated them by polyaniline, finding it suitable as sensing material for electrochemical sensors in liquids, capable of detecting an electrolyte (i.e., methanesulfonic acid) in solution. PCL blended with PANi was also utilized to develop these types of sensors by electrospinning. Low et al. (2014) found that fibers based on those polymers could act as gas sensors of water vapor, NH_3 , and NO_2 and the sensitivities to analytes could be modified changing the acid doping. Another biodegradable polymer that was used to develop conductometric sensors is PHB. Macagno et al. (2016) developed biodegradable electrospun nanofibrous scaffold based on the polymer blend PANi/PHB. The nanofibrous layers carried out directly on chemoresistors resulted in highly porous membranes, and the potentials of such blended scaffolds have been analyzed. They found that the nanofibrous layers were successful at sensing ammonia, triethylamine, and acetic acid. Figure 7 depicts the sensor transient responses when a defined concentration of ammonia (834 ppb) was cyclically flowed throughout a measurement chamber under 10% relative humidity (RH). The sensor showed both comparable responses and starting current recovery when the sensing gas was turned on. Moreover, they studied the influence of relative humidity in their performance, finding that water vapors hugely improved the chemical interactions with the selected analytes.

Another sensing strategy is the use of optical properties. One example is the detection of heavy metals such as mercuric ion, through the application of turn-on fluorescence sensing systems. Rhodamine is an excellent candidate for constructing off-on fluorescent sensors, as depending on surrounding conditions, its spirocyclic

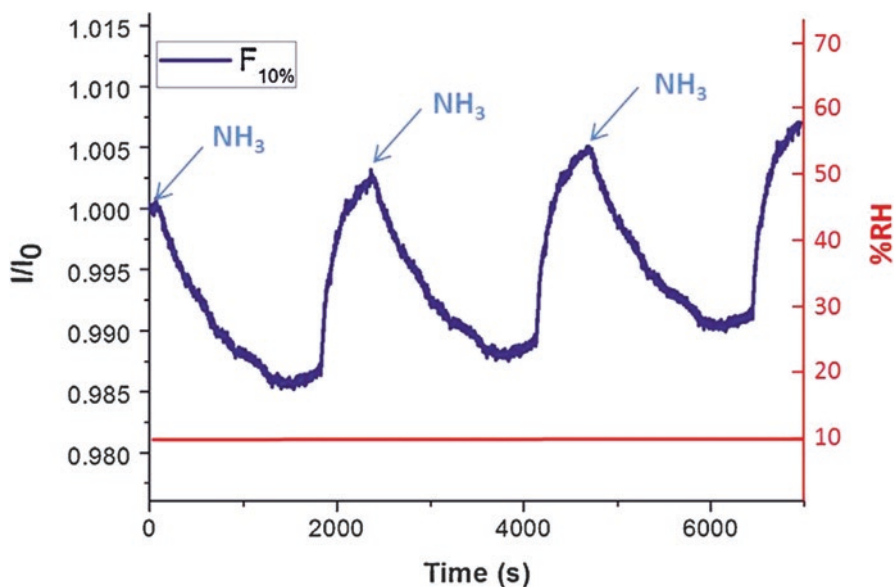


Fig. 7 Biplot of three consecutive responses of F (PANi 11%) sensor, reported as normalized current (I/I_0) to the same concentration of NH_3 (834 ppb) flowed throughout the measuring chamber (300 sccm) in 10% wet air (%RH) (Reproduced from Macagno et al. 2016)

derivatives can exist in two isomeric forms: one nonfluorescent and colorless and the other pink with strong fluorescence. Horzum et al. (2016) developed a turn-on fluorescence sensing system for mercuric ions (Hg^{2+}) by simultaneous electrospinning chitosan and rhodamine B hydrazide with phenylisothiocyanate functionality. Mats exhibited not only considerably enhanced fluorescence intensity in the presence of mercury ions but also a remarkably high sensitivity and selectivity toward Hg^{2+} . Another possibility is the use of optical probes for gas detection. Hu et al. (2016) developed a highly sensitive and fast sensor for gaseous hydrogen chloride using the optical probe 5,10,15,20-tetraphenylporphyrin in an electrospun poly(lactic acid) nanoporous fiber membrane. With its porous structure, the sensor overcomes the slow gas absorption and diffusion of other sensing materials. The exposure to HCl gas causes a color change from pink to green that is due to the protonation of the central nitrogen atoms of the porphyrin, and fluorescence is quenched. The largest increase in absorbance occurs at 442 nm. HCl gas could be detected in this way even at sub-ppm levels.

5 Particle Filtration

Nanofibrous systems are being strongly studied as filters of both water and air. Due to their higher porosities and interconnected pore structures, they offer a higher permeability to filtration over conventional materials being used.

Filtration modes can be divided by crossflow filtration and dead-end filtration depending on the flow direction on membrane surface as shown in Fig. 8. In crossflow filtration, feed moves parallel to the filter medium to generate shear stress to scour the surface. This filtration mode is particularly effective when feedwater carries high level of foulants such as suspended solids and macromolecules. In dead-end filtration, no crossflow exists and feed moves toward the filter medium. All the particles that can be filtered by filter settle on the filter surface. Since the filtration is not sustainable forever without removing accumulated solids, backwashing is performed periodically and/or filter medium is replaced. This filtration mode is particularly effective when feedwater carries low level of foulants.

There are two possible stages in the operating of a filter: the stable stage, during which filtration efficiency and resistance are unchanged with the time, and the unstable stage, during which filtration efficiency and resistance are independent of the particle properties and change with particle deposition and corrosion effects. For low particle concentration and high-efficiency filters, the stable stage is the main one for the filtration. Nanofiber filters belong to this stage (Qin and Wang 2006).

Filtration efficiency can be expressed by the particle concentration of inlet and outlet flow (Eq. 1).

$$\eta = \frac{G_1 - G_2}{G_1} = \frac{Q(N_1 - N_2)}{QN_1} = 1 - \frac{N_2}{N_1} \quad (1)$$

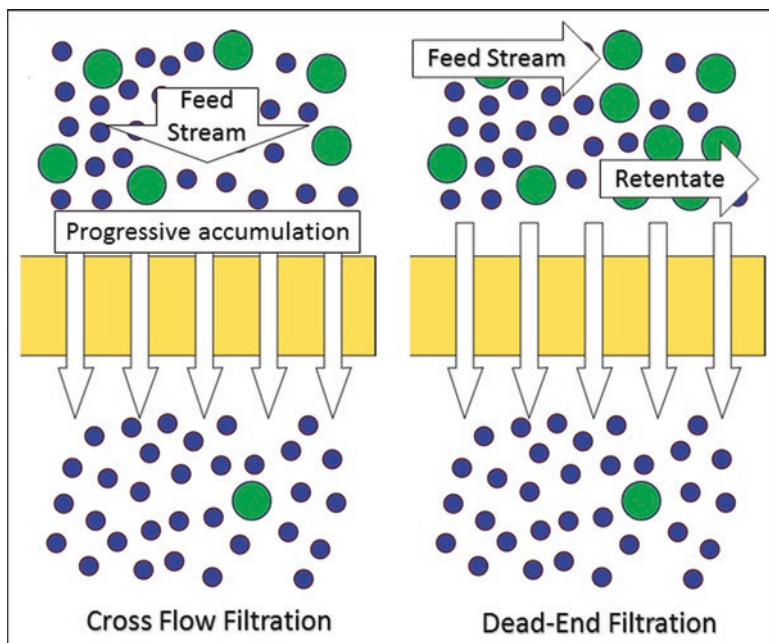


Fig. 8 Filtration membrane that separates a fluid from contaminating particles intercepting the feed flow

where G_1 and G_2 are the quantity of particles in inlet and outlet flow (mg/h), N_1 and N_2 are the particle concentration of inlet and outlet flow (mg/m³), and Q is the speed of particle suspension (m³/h).

There are different physical interaction mechanisms for separation and collection of particles, such as interception, inertial, diffusion, gravity, and static electricity effect. The total efficiency is resulted by collective contribution of individual efficiencies from the above interaction mechanisms. Figure 9 shows how these interaction mechanisms can be approximately assigned depending on particle sizes.

On the other hand, for nanometer-scale fibers, pressure drop can occur because of slip flow effect at the fiber surface. In case of air filters, Knudsen number is used to describe the importance of the molecular movements of gas molecules at the fiber surface to the overall flow field. The Knudsen number can be written as

$$K_n = \frac{\lambda}{R_f} \quad (2)$$

where “ λ ” is the gas mean free path (the dimension of the noncontinuous nature of the molecules) and R_f is the fiber mean radius. As K_n increases, the continuous flow theory starts to become less valid. Slip flow generally needs to be considered when $K_n > 0.1$ and definitely needs to be considered when K_n is around 0.25.

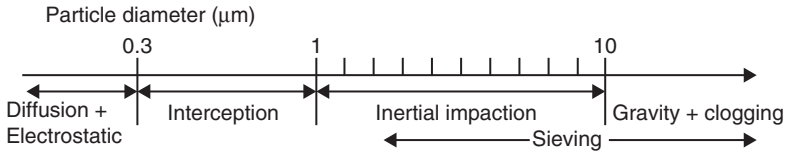


Fig. 9 Interaction mechanisms for separation and collection of particles

Both in water and wastewater treatment applications, the removal of micron-sized and other suspended solid particles such as flocs, bacteria, etc., is of utmost importance. At present, this is achieved thanks to membrane processes such as microfiltration and ultrafiltration. These membranes are usually obtained by the phase inversion method and by dry formed methods for fibrous membrane media such as spunbonded and melt-blown techniques. Electrospinning technique is another method through which these membranes can be obtained. Kaur et al. (2007) compared the filtration performance of a commercial microfiltration membrane with an electrospun nanofiber membrane of the same polymeric material. The surface of the electrospun membrane was exposed to argon plasma and subsequently graft-copolymerized with methacrylic acid, what reduces the pore size. The pore-size distribution obtained for the grafted electrospinning nanofibrous membrane had a similar profile to that of the commercial one but with a better flux throughput. The water flux of the grafted electrospun membrane resulted approximately 150–200% higher than the commercial membrane, showing that the electrospun nanofibrous membrane architecture is better than the phase inverted one and could result in energy-saving filters.

One of the main drawbacks of electrospun mats is their lack of integrity, which makes their management and disposal complex. One of the most commonly used collector covering materials is aluminum foil, due to its low thickness ($\sim 20 \mu\text{m}$) and good conductivity. It allows easy handling and continuous transport of the mats, but its high creasing affinity hinders the detachment step, with the risk of inducing microcracks. A good option for the development of filters is the use of a substrate on which nanofibers are electrospun to create a multilayer based on both the substrate and the electrospun mat. The substrate for this purpose should have the following properties: conductive (to be used as covering collector material), permeable (to be used as a filter), and able to allow a perfect adhesion with the polymer nanofibers. Nicosia et al. (2016) investigated different materials (glassine paper, lyocell, nylon grids) for use as substrates in the cellulose acetate membrane spinning process. They found that the support used to collect the nanofibers has a major influence on the final product and should not be neglected. In particular, a regular grid, made of nylon, was selected for the composition with CA nanofibers.

In order to add special features or improve the filter performance, composites, coatings, and functionalizations can be performed. The hydrophobic or hydrophilic nature of a membrane has a direct impact on its effectiveness. Goetz et al. (2016) electrospun CA random mats and coated them with chitin nanocrystals to obtain water filtration membranes with tailored surface characteristics. The flux through membranes coated with 5% of chitin nanocrystals was as high as $14,217 \text{ L} \cdot \text{m}^{-2} \cdot \text{h}^{-1}$ at 0.5 bar. Surface properties of the membranes significantly changed with

nanocrystal incorporation, changing from the original hydrophobic CA mats (contact angle 132°) to superhydrophilic membranes (contact angle 0°). Moreover, coated membranes also showed significant reduction in biofouling and biofilm formation.

An important feature that is very useful to add to filtration media is antimicrobial character. These can be done by a broad range of methodologies. One possibility is to add a component with antibacterial activity to the polymer solution before being electrospun and therefore create hybrid nanofibers. Fang et al. (2016) developed a biodegradable and multifunctional air filtration membrane by electrospinning of soy protein isolate (SPI)/PVA. SPI is known as renewable resource, intrinsically exhibiting biocompatibility, biodegradability, and even antibacterial activity after acid treatment, but it cannot be electrospun alone. The filtration efficiency of the nanofiber membrane reached 99.99% after test of 30 min for fine particles smaller than 2.5 nm in the case of small pressure drop. Besides, this kind of filtration membrane showed an antimicrobial activity to *Escherichia coli* in the study.

Another possibility is the addition of metal nanoparticles in the fibers or on their surface. Wang et al. (2016) produced chitosan fibers coated with Ag nanoparticles. The hybrid nanofibers exhibited a significant increase in filtration efficiency ($>99\%$) for removal of nanoparticle aerosol, compared to commercial high-efficiency particulate air filters, but with lower pressure drop and less mess. Besides, they showed excellent antibacterial activity, e.g., 97% of *E. coli* and 99% of *S. aureus* were killed within 2 h.

6 Oil/Water Separation

Oil pollution is one of the most important environmental concerns. It happens when oils are accidentally released to the environment, either in marine environment or in onshore activities such as from domestic household, industrial activity generating oily wastewater, oil terminal receiving oil, and docked ship oil tank cleaning.

Conventional techniques, such as skimming, ultrasonic separation, and flotation, are useful for the separation of oil/water-free mixtures but suffer from the limitations of low separation efficiency, high energy cost, and secondary pollution, and they are not applicable to oil/water emulsion separation. Separation using materials with selective oil/water affinities is a relatively recent area of development but is highly promising. Using their selective superwetting properties toward water and oil, special wettable surfaces (e.g., superhydrophobic/superoleophilic surfaces and underwater superoleophobic surfaces) for the separation of oil/water-free mixtures and emulsions can be fabricated using an appropriate surface structure and composition design. In this context, nanofiber mats with capabilities in oil/water separation, sorption, and oleophilic/hydrophobic surface can be used as a tool to combat both oily wastewater from domestic household and industrial activities and oily seawater due to the oil running down to the ocean.

Depending on the purpose of the materials, they can be separated into two categories: nanofibrous sorbents for oil spill cleanup and nanofibrous membranes for oil/water separation.

Oil extraction by sorbents involves using them to concentrate and transform oil from the spilled area to the semisolid or solid phase. Processes involved in oil sorption by fibrous porous sorbents are adsorption and capillary action (Zhu et al. 2011). The ideal characteristics of sorbent materials should include oleophilicity–hydrophobicity, high sorption rate and capacity, high buoyancy, and good reusability. Recently, electrospun nanofibers have shown great promise as sorbents for oil sorption compared to current oil sorbent materials, such as nonwoven polypropylene fibrous mats. The oil sorption capacity has been proven to be further enhanced because the nanofibrous sorbent can drive the oil not only into the voids between fibers but also into its multipores. Although the polymeric electrospun materials have shown to be very promising as oil sorbents, as far as authors know, there are no developments of biodegradable sorbents through this technique in literature.

On the other hand, membrane technology is considered the most promising approach to treat oily wastewater, due to its high separation efficiency and relatively simple operational process (Gao et al. 2014; Shi et al. 2013). Electrospun fibrous membranes with selective superwetting property can be obtained through manipulating both the surface geometrical structure and the chemical composition (Raza et al. 2014a). These separation membranes can be classified into three types: “water-removing,” “oil-removing,” and smart separation membranes.

Water-removing systems are basically water filters with high water permeability and oleophobicity. Zhang et al. (2015) developed membranes with complete water permeability by electrospinning a blend of PLA with a biodegradable and biocompatible polyester (P34HB). Water permeability is correlated with more hydrophilicity of P34HB than PLA and especially with structural porosity of the membranes. The developed membranes exhibit superior removal of water from the oil/water emulsion under gravity (Fig. 10). Another example is the case of Qi et al. (2006) who developed a three-tier membrane by placing a PVA electrospun nanofibrous scaffold onto a nonwoven microfibrillar substrate and then spincasted a hydrophilic layer (e.g., chitosan and PVA hydrogel) onto it. Because of the high porosity and thin, smooth barrier layer of the membrane, the “water-removing” membrane exhibited outstanding performance, including high flux and antifouling properties.

The “oil-removing” nanofibrous membranes allow oil to flow through freely repelling water completely. In order to obtain a membrane surface that simultaneously exhibits superhydrophobic and superoleophilic properties, construction of rough surfaces on a hydrophobic surface or surface modifiers with low surface energy methodologies can be used, according to the Wenzel and Cassie–Baxter model (Tsai et al. 2014; Zhang et al. 2013). Though biodegradable polymer electrospun membranes often do not meet the practical requirements for oil/water separation, to enhance membranes’ performance, modifications of the fibers, including the addition of other materials, are needed. For example, Shang et al. (2012) designed a superhydrophobic and superoleophilic fibrous membrane through a facile combination of electrospun CA nanofibers and an in situ polymerized fluorinated polybenzoxazine (F-PBZ) functional layer in which silica nanoparticles were incorporated. By employing this modification, the pristine hydrophilic CA nanofibrous membranes were endowed with a superhydrophobicity with the water contact angle of 161° and a

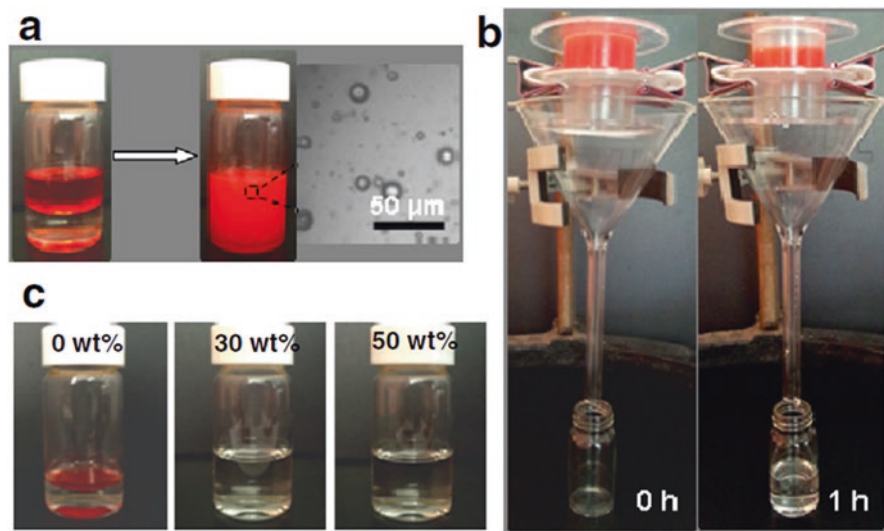


Fig. 10 (a) Formation of stable emulsion by vigorous stirring and corresponding optical micrographs of the emulsion, (b) optical photographs revealing separation of the emulsion by electrospun membranes with 50 wt.% P34HB under gravity, (c) optical photographs of the permeate obtained by electrospun membranes with the indicated P34HB content after separation for 1 h. Prior to separation, electrospun membranes were pre-wetted by water (Reproduced from Zhang et al. 2015)

superoleophilicity with the oil contact angle of 3° . Moreover, surface morphological studies indicated that the wettability of resultant membranes could be manipulated by tuning the surface composition as well as the hierarchical structures. The developed membranes exhibited fast and efficient separation for oil/water mixtures and excellent stability over a wide range of pH conditions.

In another study, Arslan et al. (2016) functionalized electrospun CA nanofibrous mats with 1H,1H,2H,2H-perfluorooctyltriethoxysilane (FS) via hydrolysis and condensation reactions to obtain CA/FS-NF. Perfluoro groups modified the hydrophilic CA nanofibers into superhydrophobic character with a water contact angle of $\sim 155^\circ$. Authors demonstrated that this novel oil/water nanofibrous separator functions effectively in hexane/oil and water separation experiments.

One of the main drawbacks of most modified electrospun membranes is that they remain fragile and highly sensitive to mechanical forces, which pose great restrictions on their industrial applications. In order to overcome this, Ma et al. (2016) coaxially electrospun CA and polyamide acid (PAA). The PAA core was then imidized at high temperature to obtain core-shell structured CA/polyimide (PI) electrospun fibrous membranes. The surface of the fibers was subsequently modified with fluorinated polybenzoxazine, in the presence or in the absence of silica nanoparticles. The modified membranes show a much higher critical tensile stress (130 MPa) and critical tensile strain (52%), when compared with CA fibrous membranes. Due to the use of the “heavily” fluorinated polybenzoxazine, the membranes

resulted superhydrophobic with a water contact angle of 162 and an oil contact angle which approaches 0. Interestingly, the newly designed membranes can effectively separate various oil/water mixtures, solely driven by gravity, with a high flux ($3,106.2 \pm 100 \text{ Lm}^{-2} \text{ h}^{-1}$) and a high separation efficiency (>99%), and thus possess great potential for oil/water separation.

Finally, membranes with stimuli-responsive wettability have attracted increasing interest because of their importance in fundamental studies and industrial applications. The controllable surface wettability can be achieved by applying an external stimulus, such as pH, light, temperature, electric fields, and even gas. Recently, Sun et al. (2004) developed smart stimuli-responsive poly(N-isopropylacrylamide) (PNIPAAm)-modified regenerated cellulose (RC) fibrous membranes which are capable of switching oil/water wettability as a response to different temperatures. Such switchable surface wettability allowed controllable oil/water separation.

7 Pollutant Adsorption

Adsorption is the ability of certain solids to selectively concentrate solute from solution onto their surface. Based on ionic interactions, this characteristic can be applied to successfully remove heavy metal ions from water, as positively charged metal ions and negatively charged matrices attract each other. Heavy metal pollutants in water can cause serious ailments such as dehydration, stomachache, nausea, dizziness, and/or lack of coordination in muscles, destroying the nervous systems of young children, lung irritation, eye irritation, skin rashes, vomiting, abdominal pain, lung insufficiency, and liver damage. For that reason, removal of heavy metal ions existing in water is an issue of utmost importance. Among all different techniques used to remove metal ions, adsorption is generally employed due to the availability of different adsorbents, high efficiency, easy handling, reversibility, and possible low cost.

Nanoscale materials are of great interests to be developed as efficient adsorbents for metal ions. Electrospun nanofibrous mats have a high porosity, high gas permeability, and high specific surface area per unit mass, which should lead to a high adsorption capacity if the material is chosen properly.

Among biodegradable polymers, chitosan is the main candidate to be used as adsorbent of metallic ions, due to the presence of very reactive amino(-NH₂) and hydroxyl(-OH) groups in its backbone. Adsorption depends on the pH values and chitosan is very sensitive to pH. Chemical modifications with cross-linking reagents, such as ethylene glycol diglycidyl ether, formaldehyde, glyoxal, epichlorohydrin, glutaraldehyde, and isocyanates, are performed to stabilize the chitosan in acidic solution, making it insoluble in acidic medium, and at the same time also enhance its mechanical properties (Chiou et al. 2004; Crini and Badot 2008).

Huang et al. (2015) developed composite nanofibers with chitosan and a thermo-responsive polymer (TRP), which provided the function of thermal cross-linking

of the nanofibrous mats to form water-stable nanofibers in aqueous solution. Subsequently, glutaraldehyde was used as a secondary cross-linking agent to increase the gel fraction of the nanofibrous mats. Comparing the nanofibrous mats and films of the same material, the fibrous mats showed significant increased adsorption of Cu (II). The adsorption amount of Cu (II) on the chitosan/TRP (50/50) nanofibrous mats could reach (79 ± 2) mg/g-mats, and its desorption was relatively effective. The incorporation of the TRP significantly improved the desorption of Cu (II) from the nanofibrous mats. The developed fibrous mats maintained the capacity of Cu (II) adsorption for four-time regeneration.

In order to improve some of the chitosan electrospun mat drawbacks, a blend with other polymers could be electrospun. It is the case of Habiba et al. (2017) who developed chitosan/PVA/zeolite nanofibrous composite membrane by electrospinning. PVA can be used to immobilize chitosan (Kumar et al. 2009), reduce its crystallinity (Kim et al. 1992), and help the formation of good nanofiber during electrospinning, thanks to the strong hydrogen bond of PVA with functional groups $-NH_2$ and $NH-R$ (Qi et al. 2010). However, slow heavy metal adsorption rate was reported for chitosan/PVA electrospun nanofiber (Esmaeili and Beni 2014). For that reason, the authors incorporated zeolite, a widely used adsorbent for removal of heavy metal ions. While its porous structure can accommodate heavy metal ions, they tend to aggregate during operation (Baybas and Ulusoy 2011). Authors synthesized chitosan/PVA/zeolite nanofibrous composite membrane to overcome the limitation of both chitosan and zeolite. They found that adsorption rate for Cr (VI), Fe (III), and Ni (II) ions was high, but the membrane's adsorption capacity at high concentration was reduced. The adsorption capacity of nanofiber was unaltered after five recycling runs, which indicated the reusability of chitosan/PVA/zeolite nanofibrous membrane.

Another possibility is the development of core-shell fibers. Lee et al. (2016) enhanced the mechanical strength of electrospun chitosan nanofibers, with the addition of PLA at the core. They measured the removal efficiency of the shell-core chitosan/PLA nanofibers and compared it with the efficiency of blended chitosan/PLA nanofibers. Their results suggested that the electrospun of core-shell nanofibers exhibited superior metal ion removal efficiency compared to the blended nanofibers.

Another biodegradable polymer employed for the development of electrospun membranes for the removal of metal ions is cellulose acetate. Taha et al. (2012) successfully prepared NH_2 -functionalized cellulose acetate (CA)/silica composite nanofibrous membranes by sol-gel combined with electrospinning technology. The membranes were used for Cr (VI) ion removal from aqueous solution through static and dynamic experiments. The maximum adsorption capacity for Cr (VI) was estimated to be 19.46 mg/g, and the membrane could be conveniently regenerated by alkalization, showing a potential application in the field of water treatment.

Similarly, Hota et al. (2008) incorporated nanoboehmite into PCL electrospun nanofibers to develop a composite electrospun fiber membrane with sorptive characteristics. This membrane showed a Cd^{2+} removal ability of 0.2 $\mu g/mg$. Because of

encapsulation of the functional nanoparticles within the nanofibers and less exposure to the heavy metal ions, the removal efficiency was not comparable with that of the nanofibers containing functional polymeric molecules.

8 Conclusions and Future Perspectives for Electrospun Nanofibers

Concern over the care of the planet and its resources has reached unprecedented levels. Issues such as energy and the environment are of great importance nowadays. Both in the field of clean energy (fuel cells, batteries, and solar cells) and in the environment (filtration membranes for water and air cleaning and substitution of nonbiodegradable materials), research on materials based on nanofibers has provided promising evidence on their potential applications.

Electrospinning can produce highly porous nanofibrous structures from a variety of polymers, both organic and inorganic in different configurations and assemblies. New materials are compatibilized with it yearly, what multiplies the possible applications. In particular, some biodegradable polymers, such as chitosan, CA, PLA, PCL, and PHB, can be processed into nano- or microfibers through this technique, adding to the outstanding characteristics of these meshes, the important property of biodegradability.

The nanofiber membranes provide a technology that will significantly reduce pollution in water and air but also represent a product of very high added value. Since the electrospinning technique has already been taken to industrial scales, a large number of internationally renowned companies have joined the research in order to perfect developments in nanofibers, as it can be seen in the increasing number of patents related to this field.

In this chapter, we have discussed the development of various special electrospun nanofibrous materials, fully or partially biodegradable, for environmental applications. The technique of electrospinning has been presented, as well as the biodegradable materials, most used for environmental applications. Successful materials for pollution detection, particulate filtration, oil/water separation, and pollution absorption applications have been developed.

While developed materials show a promising future, there is still a problem to solve. Current electrospinning processes involve the use of organic solvents, which are toxic, corrosive, and detrimental to the environment. Recovering the solvent vapors after processing is expensive and industrially unavailable. In this context, the next big challenge is to develop green electrospinning process, either using water-based solvents or water-soluble reagents to produce stable nanofibers with the same performance as those already in existence.

Acknowledgments The authors would like to thank the Consejo Nacional de Investigaciones Científicas y Técnicas, Argentina (CONICET, PIP 11220120100508CO), Universidad de Buenos Aires (UBACYT 20020130100495BA), and ANPCyT (PICT 2012- 1093) for their financial support.

References

- Abdelgawad AM, Hudson SM, Rojas OJ (2014) Antimicrobial wound dressing nanofiber mats from multicomponent (chitosan/silver-NPs/polyvinyl alcohol) systems. *Carbohydr Polym* 100:166–178
- Arslan O, Aytac Z, Uyar T (2016) Superhydrophobic, hybrid, electrospun cellulose acetate Nanofibrous Mats for oil/water separation by tailored surface modification. *ACS Appl Mater Interfaces* 8:19747–19754
- Baiguera S, Del Gaudio C, Bianco A, Macchiaroni P (2014) Crosslinked Electrospun Mats made of natural polymers: potential applications for tissue engineering
- Baybas D, Ulusoy U (2011) Polyacrylamide–clinoptilolite/Y-zeolite composites: characterization and adsorptive features for terbium. *J Hazard Mater* 187:241–249
- Casasola R, Thomas NL, Trybala A, Georgiadou S (2014) Electrospun poly lactic acid (PLA) fibers: effect of different solvent systems on fiber morphology and diameter. *Polymer* 55:4728–4737
- Chasin M, Domb A, Ron E, Mathiowitz E, Langer R, Leong K, Laurencin C, Brem H, Grossman S (1990) Polyanhydrides as drug delivery systems. *Biodegradable Polym Drug Deliv Syst* 45:43–70
- Chiou M-S, Ho P-Y, Li H-Y (2004) Adsorption of anionic dyes in acid solutions using chemically cross-linked chitosan beads. *Dyes Pigments* 60:69–84
- Choi JS, Lee SW, Jeong L, Bae SH, Min BC, Youk JH, Park WH (2004) Effect of organosoluble salts on the nanofibrous structure of electrospun poly (3-hydroxybutyrate-co-3-hydroxyvalerate). *Int J Biol Macromol* 34:249–256
- Conn R, Kolstad J, Borzelleca J, Dixler D, Filer L, LaDu B, Pariza M (1995) Safety assessment of polylactide (PLA) for use as a food-contact polymer. *Food Chem Toxicol* 33:273–283
- Coulebrier O, Degée P, Hedrick JL, Dubois P (2006) From controlled ring-opening polymerization to biodegradable aliphatic polyester: especially poly (β -malic acid) derivatives. *Prog Polym Sci* 31:723–747
- Crini G, Badot P-M (2008) Application of chitosan, a natural aminopolysaccharide, for dye removal from aqueous solutions by adsorption processes using batch studies: a review of recent literature. *Prog Polym Sci* 33:399–447
- De Vrieze S, Van Camp T, Nelvig A, Hagström B, Westbroek P, De Clerck K (2009) The effect of temperature and humidity on electrospinning. *J Mat Sci* 44:1357
- Esmaili A, Beni AA (2014) A novel fixed-bed reactor design incorporating an electrospun PVA/chitosan nanofiber membrane. *J Hazard Mater* 280:788–796
- Fang Q, Zhu M, Yu S, Sui G, Yang X (2016) Studies on soy protein isolate/polyvinyl alcohol hybrid nanofiber membranes as multi-functional eco-friendly filtration materials. *Mat Sci Eng: B* 214:1–10
- Gao X, Xu LP, Xue Z, Feng L, Peng J, Wen Y, Wang S, Zhang X (2014) Dual-scaled porous nitrocellulose membranes with underwater Superoleophobicity for highly efficient oil/water separation. *Adv Mater* 26:1771–1775
- Goetz LA, Jalvo B, Rosal R, Mathew AP (2016) Superhydrophilic anti-fouling electrospun cellulose acetate membranes coated with chitin nanocrystals for water filtration. *J Membrane Sci* 510:238–248
- Guglielmi G, Andreottola G (2010) Selection and design of membrane bioreactors in environmental bioengineering. *Environ Biotechnol*. Springer, pp 439–516
- Habiba U, Afifi AM, Salleh A, Ang BC (2017) Chitosan/(polyvinyl alcohol)/zeolite electrospun composite nanofibrous membrane for adsorption of Cr 6+, Fe 3+ and Ni 2+. *J Hazard Mater* 322:182–194
- Hartman O, Zhang C, Adams EL, Farach-Carson MC, Petrelli NJ, Chase BD, Rabolt JF (2010) Biofunctionalization of electrospun PCL-based scaffolds with perlecan domain IV peptide to create a 3-D pharmacokinetic cancer model. *Biomaterials* 31:5700–5718
- Horzum N, Mete D, Karakuş E, Üçüncü M, Emrullahoğlu M, Demir MM (2016) Rhodamine-Immobilised Electrospun chitosan Nanofibrous material as a fluorescence turn-on Hg²⁺ sensor. *Chem Sel* 1:896–900

- Hota G, Kumar BR, Ng W, Ramakrishna S (2008) Fabrication and characterization of a boehmite nanoparticle impregnated electrospun fiber membrane for removal of metal ions. *J Mater Sci* 43:212–217
- Hu M, Kang W, Cheng B, Li Z, Zhao Y, Li L (2016) Sensitive and fast optical HCl gas sensor using a nanoporous fiber membrane consisting of poly (lactic acid) doped with tetraphenylporphyrin. *Microchim Acta* 183:1713–1720
- Huang Z-M, Zhang Y-Z, Kotaki M, Ramakrishna S (2003) A review on polymer nanofibers by electrospinning and their applications in nanocomposites. *Compos Sci Technol* 63:2223–2253
- Huang C-H, Hsieh T-H, Chiu W-Y (2015) Evaluation of thermally crosslinkable chitosan-based nanofibrous mats for the removal of metal ions. *Carbohydr Polym* 116:249–254
- Ismail YA, Martínez JG, Otero TF (2014) Fibroin/Polyaniline microfibrinous mat. Preparation and electrochemical characterization as reactive sensor. *Electrochim Acta* 123:501–510
- Jia Y, Zhang Y, Yu H, Nie W, Dong F (2016) Fabrication of novel cellulose acetate/Polyethylenimine/poly(acrylic acid) nanofibers/quartz crystal microbalance sensor for ammonia gas detection. *J Nanosci Nanotechnol* 16:12351–12355
- Kaur K (2016) Water pollution and maintenance towards sustainable development. *ACADEMICIA: Int Multidiscip Res J* 6:431–436
- Kaur S, Ma Z, Gopal R, Singh G, Ramakrishna S, Matsuura T (2007) Plasma-induced graft copolymerization of poly (methacrylic acid) on electrospun poly (vinylidene fluoride) nanofiber membrane. *Langmuir* 23:13085–13092
- Kim GH (2008) Electrospun PCL nanofibers with anisotropic mechanical properties as a biomedical scaffold. *Biomed Mater* 3:025010
- Kim JH, Kim JY, Lee YM, Kim KY (1992) Properties and swelling characteristics of cross-linked poly (vinyl alcohol)/chitosan blend membrane. *J Appl Polym Sci* 45:1711–1717
- Kimura M, Sakai R, Sato S, Fukawa T, Ikehara T, Maeda R, Mihara T (2012) Sensing of vaporous organic compounds by TiO₂ porous films covered with polythiophene layers. *Adv Funct Mater* 22:469–476
- Kumar M, Tripathi BP, Shahi VK (2009) Crosslinked chitosan/polyvinyl alcohol blend beads for removal and recovery of Cd (II) from wastewater. *J Hazard Mater* 172:1041–1048
- Lai G-J, Shalumon K, Chen S-H, Chen J-P (2014) Composite chitosan/silk fibroin nanofibers for modulation of osteogenic differentiation and proliferation of human mesenchymal stem cells. *Carbohydr Polym* 111:288–297
- Lee J, Yoo J, Atala A, Lee S (2012) Controlled heparin conjugation on electrospun poly (ϵ -caprolactone)/gelatin fibers for morphology-dependent protein delivery and enhanced cellular affinity. *Acta Biomater* 8:2549–2558
- Lee D-M, Kao C-W, Huang T-W, You J-H, Liu S-J (2016) Electrospinning of sheath-Core structured chitosan/Poly lactide nanofibers for the removal of metal ions. *Int Polym Process* 31:533–540
- Logith Kumar R, Keshav Narayan A, Dhivya S, Chawla A, Saravanan S, Selvamurugan N (2016) A review of chitosan and its derivatives in bone tissue engineering. *Carbohydr Polym* 151:172–188
- Low K, Chartuprayoon N, Echeverria C, Li C, Bosze W, Myung NV, Nam J (2014) Polyaniline/poly (ϵ -caprolactone) composite electrospun nanofiber-based gas sensors: optimization of sensing properties by dopants and doping concentration. *Nanotechnology* 25:115501
- Ma Z, Ramakrishna S (2008) Electrospun regenerated cellulose nanofiber affinity membrane functionalized with protein A/G for IgG purification. *J Membr Sci* 319:23–28
- Ma W, Guo Z, Zhao J, Yu Q, Wang F, Han J, Pan H, Yao J, Zhang Q, Samal SK (2016) Polyimide/cellulose acetate Core/Shell electrospun fibrous membranes for oil-water separation. *Sep Purif Technol* 177:71–85
- Macagnano A, Perri V, Zampetti E, Bearzotti A, De Cesare F (2016) Humidity effects on a novel eco-friendly chemosensor based on electrospun PANi/PHB nanofibers. *Sensor Actuat B-Chem* 232:16–27
- Nations United (1997) Glossary of environment statistics, studies in methods. United Nations New York, NY

- Nicosia A, Keppler T, Müller F, Vazquez B, Ravegnani F, Monticelli P, Belosi F (2016) Cellulose acetate nanofiber electrospun on nylon substrate as novel composite matrix for efficient, heat-resistant, air filters. *Chem Eng Sci* 153:284–294
- Persano L, Camposo A, Tekmen C, Pisignano D (2013) Industrial upscaling of electrospinning and applications of polymer nanofibers: a review. *Macromol Mater Eng* 298:504–520
- Picciani PH, Medeiros ES, Pan Z, Orts WJ, Mattoso LH, Soares BG (2009) Development of conducting polyaniline/poly (lactic acid) nanofibers by electrospinning. *J Appl Polym Sci* 112:744–753
- Plastics World (1968) vol v. 26, pt. 2. Cahners Publishing Company, the University of California
- Qi H, Hu P, Xu J, Wang A (2006) Encapsulation of drug reservoirs in fibers by emulsion electrospinning: morphology characterization and preliminary release assessment. *Biomacromolecules* 7:2327–2330
- Qi B, Yu A, Zhu S, Chen B, Li Y (2010) The preparation and cytocompatibility of injectable thermosensitive chitosan/poly (vinyl alcohol) hydrogel. *J Huazhong Univ Sci Technol Med* 30:89–93
- Qin XH, Wang SY (2006) Filtration properties of electrospinning nanofibers. *J Appl Polym Sci* 102:1285–1290
- Raza A, Ding B, Zainab G, El-Newehy M, Al-Deyab SS, Yu J (2014a) In situ cross-linked superwetting nanofibrous membranes for ultrafast oil–water separation. *J Mater Chem A* 2:10137–10145
- Raza A, Wang J, Yang S, Si Y, Ding B (2014b) Hierarchical porous carbon nanofibers via electrospinning. *Carbon Lett* 15:1–14
- Ribba L, Parisi M, D'Accorso NB, Goyanes S (2014) Electrospun nanofibrous mats: from vascular repair to osteointegration. *J Biomed Nanotechnol* 10:3508–3535
- Rieger KA, Schiffman JD (2014) Electrospinning an essential oil: Cinnamaldehyde enhances the antimicrobial efficacy of chitosan/poly (ethylene oxide) nanofibers. *Carbohydr Polym* 113:561–568
- Sánchez LD, Brack N, Postma A, Pigram PJ, Meagher L (2016) Surface modification of electrospun fibers for biomedical applications: a focus on radical polymerization methods. *Biomaterials* 106:24–45
- Serrano W, Meléndez A, Ramos I, Pinto NJ (2014) Sensor response of electrospun poly (lactic acid)/polyaniline nanofibers to aliphatic alcohol vapors of varying sizes. In: *Sensors (IBERSENSOR)*, 2014 IEEE 9th Ibero-American congress on. IEEE, pp 1–4
- Shang Y, Si Y, Raza A, Yang L, Mao X, Ding B, Yu J (2012) An in situ polymerization approach for the synthesis of superhydrophobic and superoleophilic nanofibrous membranes for oil–water separation. *Nanoscale* 4:7847–7854
- Shi Z, Zhang W, Zhang F, Liu X, Wang D, Jin J, Jiang L (2013) Ultrafast separation of emulsified oil/water mixtures by ultrathin free-standing single-walled carbon nanotube network films. *Adv Mater* 25:2422–2427
- Sombatmankhong K, Suwantong O, Waleetorncheepsawat S, Supaphol P (2006) Electrospun fiber mats of poly (3-hydroxybutyrate), poly (3-hydroxybutyrate-co-3-hydroxyvalerate), and their blends. *J Polym Sci B Polym Phys* 44:2923–2933
- Sun T, Wang G, Feng L, Liu B, Ma Y, Jiang L, Zhu D (2004) Reversible switching between superhydrophilicity and superhydrophobicity. *Angew Chemie* 116:361–364
- Suwantong O (2016) Biomedical applications of electrospun polycaprolactone fiber mats. *Polym Adv Technol* 27(10):1264–1273
- Taha AA, Wu Y-n, Wang H, Li F (2012) Preparation and application of functionalized cellulose acetate/silica composite nanofibrous membrane via electrospinning for Cr (VI) ion removal from aqueous solution. *J Environ Manag* 112:10–16
- Thavasi V, Singh G, Ramakrishna S (2008) Electrospun nanofibers in energy and environmental applications. *Energy Environ Sci* 1:205–221
- Tian Y, Wu M, Liu R, Li Y, Wang D, Tan J, Wu R, Huang Y (2011) Electrospun membrane of cellulose acetate for heavy metal ion adsorption in water treatment. *Carbohydr Polym* 83:743–748

- Tsai M-H, Tseng I-H, Chiang J-C, Li J-J (2014) Flexible polyimide films hybrid with functionalized boron nitride and graphene oxide simultaneously to improve thermal conduction and dimensional stability. *ACS Appl Mater Interfaces* 6:8639–8645
- Valente T, Silva D, Gomes P, Fernandes M, Santos J, Sencadas V (2016) Effect of sterilization methods on electrospun poly (lactic acid) (PLA) fiber alignment for biomedical applications. *ACS Appl Mater Interfaces* 8:3241–3249
- Veleirinho B, Rei MF, Lopes-DA-Silva J (2008) Solvent and concentration effects on the properties of electrospun poly (ethylene terephthalate) nanofiber mats. *J Polym Sci Pol Phys* 46:460–471
- Vert M (2009) Degradable and bioresorbable polymers in surgery and in pharmacology: beliefs and facts. *J Mater Sci Med* 20:437–446
- Wang X, Cui F, Lin J, Ding B, Yu J, Al-Deyab SS (2012) Functionalized nanoporous TiO₂ fibers on quartz crystal microbalance platform for formaldehyde sensor. *Sensor Actuat B-Chem* 171:658–665
- Wang Y, Hu B, Ji D, Liu Z, Tang G, Xin J, Zhang H, Song T, Wang L, Gao W (2014) Ozone weekend effects in the Beijing–Tianjin–Hebei metropolitan area, China. *Atmos Chem Phys* 14:2419–2429
- Wang Z, Zhao C, Pan Z (2015) Porous bead-on-string poly (lactic acid) fibrous membranes for air filtration. *J Colloid Interface Sci* 441:121–129
- Wang L, Zhang C, Gao F, Pan G (2016) Needleless electrospinning for scaled-up production of ultrafine chitosan hybrid nanofibers used for air filtration. *RSC Adv* 6:105988–105995
- Wutticharoengmongkol P, Sanchavanakit N, Pavasant P, Supaphol P (2006) Preparation and characterization of novel bone scaffolds based on electrospun polycaprolactone fibers filled with nanoparticles. *Macromol Biosci* 6:70–77
- Yarin A (2011) Coaxial electrospinning and emulsion electrospinning of core–shell fibers. *Polymer Adv Tech* 22:310–317
- Yue M, Zhou B, Jiao K, Qian X, Xu Z, Teng K, Zhao L, Wang J, Jiao Y (2015) Switchable hydrophobic/hydrophilic surface of electrospun poly (l-lactide) membranes obtained by CF 4 microwave plasma treatment. *Appl Surf Sci* 327:93–99
- Zhang L, Bai X, Tian H, Zhong L, Ma C, Zhou Y, Chen S, Li D (2012) Synthesis of antibacterial film CTS/PVP/TiO₂/Ag for drinking water system. *Carbohydr Polym* 89:1060–1066
- Zhang F, Zhang WB, Shi Z, Wang D, Jin J, Jiang L (2013) Nanowire-haired inorganic membranes with Superhydrophilicity and underwater ultralow adhesive Superoleophobicity for high-efficiency oil/water separation. *Adv Mater* 25:4192–4198
- Zhang P, Tian R, Lv R, Na B, Liu Q (2015) Water-permeable polylactide blend membranes for hydrophilicity-based separation. *Chem Eng J* 269:180–185
- Zheng R, Duan H, Xue J, Liu Y, Feng B, Zhao S, Zhu Y, Liu Y, He A, Zhang W (2014) The influence of gelatin/PCL ratio and 3-D construct shape of electrospun membranes on cartilage regeneration. *Biomaterials* 35:152–164
- Zhu Y, Murali S, Stoller MD, Ganesh K, Cai W, Ferreira PJ, Pirkle A, Wallace RM, Cychosz KA, Thommes M (2011) Carbon-based supercapacitors produced by activation of graphene. *Science* 332:1537–1541

Index

A

Acetobacter xylinum, 65
Acrylamide (AM), 57, 243, 244
2-Acrylamido-2-methylpropane-sulfonic acid (AMPS), 244
Adenocystis utricularis, 92, 97
Advanced glycation end products (AGE), 141
Agar, 84
Agarans, 78, 79
Agarose, 84
Ahnfeltia, 83
Air pollution, 301
Alginate, 26–29, 64, 65
Alkaline phosphatase (ALP), 60
Alkylcyanoacrylate, 53
Alzheimer's disease (AD), 140, 141
AMARA PU, 11
Ammonium persulfate (APS), 244
8-Anilino-1-naphthalenesulfonate (ANS), 7
Anionic drugs, 11
Anionic starches, 237–239
Antimicrobials and antivirals, 141, 144
 bacteria, 142
 formulations, 144, 145
 GM-0111, 142
 polymeric implants, 143
 viruses, 143, 144
Arthropods, 29
Artificial polymer, 25, 26
Artroglycan®, 150
Ascophyllum nodosum, 64, 91, 93
Atomic force microscopy (AFM), 11
Azobisisobutyronitrile (AIBN), 28

B

Bacterial cellulose nanoribbons
 biomedical applications, 169–171
 in food, 171, 172
 in situ nanocomposites, 167–169
 mechanical properties, 173
Bacterial nanocellulose, 194, 195
Bioactive glass (BG), 56
Bioartificial polymeric materials, 25
Biobased additives, 186–190, 192–195
 cellulose, 185
 derivatives, 186, 187
 micro- and nanocellulose fibers, 188–190
 lignin, 190, 191
 microbial polysaccharides, 191, 192
 bacterial nanocellulose, 194, 195
 diutan gum, 193
 welan gum, 192, 193
 xanthan gum, 192
Biobased bicyclic diols, 11
Biocompatibility, 56–59, 61, 63–65, 67
Biodegradability, 50, 56–58, 61, 63–65, 266, 267, 271, 280–282, 284, 289–293
Biodegradable polymers, 305
 CA, 306, 307
 chitosan, 305, 306
 PHB, 309
 PLA, 307, 308
 PLC, 308, 309
Biomedical devices, 169
Biomedicine, 2, 37
Biopolymer-based hydrogels, 118
Biopolymers, 118, 121, 124, 127, 129, 131, 220

- Biphasic calcium phosphate (BCP), 67
 Bis(chloroformate) (BCF), 14
 Bis(ethylene carbonate), 23
 2,2-Bis(hydroxymethyl) propionic acid (DMPA), 50
 1,6-Bis-*O*-phenoxy carbonyl, 23
 Bleeding, 181
Bombyx mori, 62
 Bone marrow stromal cells (BMSCs), 60
 Bone tissue engineering
 alginate, 64, 65
 C—C structure, 57
 cell adhesion and proliferation, 48
 cellulose, 65, 66
 chitosan, 62–64
 collagen, 59–61
 definition, 47
 hyaluronic acid, 66, 67
 numerous materials, 48
 osteoblast and osteoclast activity, 47
 polyanhydrides, 56
 polyesters, 55, 56
 polyhydroxyalkanoates, 58, 59
 porous 3D scaffolds, 47
 scaffold, cells, and growth factors, 48
 silk fibroin, 61, 62
 synthetic polymers, 55
 Bovine serum albumin (BSA), 126
 Brown seaweeds
 alginates, 89, 90
 anticoagulant activity, 97
 antitumor activity and related activities, 97, 98
 antiviral activity, 95–97
 biomedical applications, 99
 fucoidans, 90–92
 industrial applications, 93–95
Bryopsis plumosa, 101
 β -tricalcium phosphate (β -TCP), 61
 1,4-Butanediol, 3
- C**
 C—C structure, 57
 Calcium alginate gel microspheres (CaA), 28
 Calcium methacrylate (CDMA), 57
 Calcium phosphates (CaPs), 62
 Cancer, 145–147
 Carbohydrate-based polyurethanes, 5
 biocompatibility, 1
 biodegradation, 1
 biological fluids, 2
 biomaterials, 1
 modern medicine and chemistry, 1
 petro-based monomers, 1
 petroleum feedstocks, 1
 thermoplastic/thermosetting, 2, 3
 urethane linkage, 3–25
 Carbohydrates, 199
 5(6)-Carboxyfluorescein (CF), 7
 Carboxymethyl and sulfonic groups, 237
 Carboxymethyl moieties, 238
 Carboxymethyl starch (CMS), 237
 Carboxymethylcellulose (CMC), 125
 λ -Carrageenan, 82
 κ -Carrageenans, 83, 86
 Carraguard[®], 86
 Casing, 179, 180
 Cationic starches, 231–237
Caulerpa spp., 102
 Cell adhesion molecules (CAM), 149
 Cellulose, 34–36, 65, 66
 Cellulose acetate (CA), 306, 307
 Cellulose ethers (CE), 186
 Cellulose nanocrystals (CNCs), 66, 267, 282, 284, 288
 Cellulose nanofibrils, 190
 Cellulose nanowhiskers (CNW), 189
 Cement paste, 179
 Cement slurry, 179, 184
 Ceric ammonium sulfate (CAS), 245
 Ceric sulfate (CS), 244
Champia feldmannii, 87
 Chemical stability, 207
 Chikungunya virus (CHIKV), 143
 Chitin nanocrystals (CHNCs), 29–32
 Chitosan, 29–32, 62–64, 305, 306
 biopolymer, 251
 drug delivery, 254, 255
 feasibility, 252
 food industries, 255, 256
 positively charged, 252
 tissue engineering, 253–254
 water treatment, 256–260
 wound dressing, 253
 3-Chloro-2-hydroxypropyltrimethylammonium chloride (CHPTAC), 231
 Chloromethyl styrene, 33
 Chondrocytes, 57
 Chondroitin sulfate (CS), 63, 136
Chondrophycus
 C. flagelliferus, 80
 C. papillosus, 80
Chondrus ocellatus, 87
Chorda filum, 91
 Click chemistry, 123–130

- copper-free
 - DA reaction, 126–129
 - Michael addition, 129, 130
 - radical-mediated thiol-ene chemistry, 125, 126
 - SPAAC, 123–125
 - CuAAC, 121–123
 - hydrogels, 119
 - Cluster of differentiation 44 (CD44), 146
 - Codium*, 100, 101
 - C. fragile*, 102
 - C. vermilara*, 101
 - C. yezoensis*, 101
 - Controlled-release formulations, 117
 - Copper(I)-catalyzed azide–alkyne cycloaddition (CuAAC) reaction, 121–123
 - Copper-free click chemistry
 - DA reaction, 126–129
 - Michael addition, 129, 130
 - radical-mediated thiol-ene chemistry, 125, 126
 - SPAAC, 123–125
 - CorMatrix ECM™, 154
 - Corneal keratan sulfate (KS), 138
 - Cross-linking, 118, 119, 121, 124, 125, 127–129
 - Cryptopleura ramosa*, 86
 - Cyclic carbonate, 20
- D**
- DADAPU, 15
 - DAMAPU, 14
 - Degrees of deacetylation (DD), 63
 - Dengue virus (DENV), 144
 - Dermatan sulfate (DS), 136
 - D-galacto, 10
 - D-galactono-1,4-lactone (GalL), 20
 - D-Galp, 76
 - D-glucamine, 21
 - D-gluco, 10, 19
 - Diacyl azides, 19
 - Dianhydroalditol diamines (DADA), 13
 - Dianhydroalditols, 13
 - Diels–alder reaction (DA), 126–129
 - Diethylene glycol (DEG), 28, 35
 - Differential scanning calorimetry (DSC), 271
 - 1,6-Diisocyanatohexane (HDI), 50
 - Dimethacrylate monomers, 7
 - Dimethyl sulfoxide (DMSO), 231, 238, 239
 - 2-(Dimethylamino)ethyl methacrylate (DMAEMA), 57
 - Dimethylolpropionic acid (DMPA), 18
 - Disaccharides, 26
 - 1,6-Di-*O*-phenylcarbonyl-2,3,4,6-tetra-*O*-methyl-*D*-mannitol (ManDPC), 21
 - 4,4'-Diphenylmethane diisocyanate (MDI), 3, 5
 - 1,4-Di-*S*-benzyl-*D,L*-dithiothreitol, 10, 11
 - D*-isosorbide, 13
 - Dispersants, 184
 - DiSTPU, 10
 - Di-*tert*-butyltricarbonate (DTBTC), 19
 - 2,2'-Dithiodiethanol (DiT), 10
 - Diutan gum, 193–195
 - D,L*-erythritol, 10
 - DL*-hybrids, 79–82, 86
 - D*-mannitol, 10, 21, 23
 - D*-manno, 10, 19
 - Drilling, 204–205
 - Drug delivery systems (DDS), 117
 - Durvillaea antarctica*, 90
 - Dye removal, 259, 260
- E**
- Ebola virus (EBOV), 144
 - Elastomers, 27
 - Electrospinning, 302–305
 - Electrospun cellulose/CNC nanocomposite nanofibers (ECCNN), 66
 - Electrospun nanofibers, 320
 - Electrostatic repulsion, 185
 - Endo* hydroxyl group, 13
 - Enhanced oil recovery (EOR)
 - anionic starches, 237–239
 - biopolymer, 228
 - cationic starches, 231–237
 - fluid flow behavior, 228
 - grafted starches, 242–245
 - heterogeneous, 227
 - non-homogeneity, 227
 - nonionic starches, 239–242
 - oil field applications, 229–231
 - polymer flooding, 228
 - water-soluble polymers, 228
 - Enteromorpha intestinalis*, 100, 102
 - Epichlorohydrin, 19
 - 2,3-Epoxypropyltrimethylammonium chloride (EPTAC), 231, 232
 - Ethyl ester *L*-lysine diisocyanate (EELDI), 17
 - 1,2-Ethylene diamine, 3
 - Ethylene glycol (EG), 50
 - The European Food Safety Authority (EFSA), 290
 - Exo*-oriented hydroxyl group, 13
 - Extracellular matrix (ECM), 135

F

- Fibers, 67
- Fibrous protein, 61
- Filtration efficiency, 312
- Floridean glycogen, 76
- Floridean starch, 76
- Flotation, 315
- Fluid loss control, 181–183, 188
- Foams, 67
- Food and Drug Administration (FDA), 266
- Food ingredients, 172
- Food packaging, 265–267, 271, 273, 275, 279–282, 284–294
- Free water control, 183, 184
- Fucoglucuronans, 90
- Fucoglucuronomannans, 90
- Fucoidans, 90–92, 95
- Fucus*
 - F. distichus*, 91
 - F. evanescens*, 91
 - F. serratus*, 91
 - F. vesiculosus*, 90

G

- Galactan, 86, 89
- Galactaric acid, 23
- Galaxaura rugosa*, 80
- Gaviscon®, 99
- Gelatin, 61, 127
- Gelidium*, 83
- Gel-type structures, 234
- Generally recognized as safe (GRAS), 171, 266
- Gigartinales seaweeds, 82
- Globular protein, 61
- Glucaric acid, 7
- Glucarodilactone (GlcDL), 7
- Glucarodilactone methacrylate (GDMA), 7
- Gluconacetobacter*
 - G. genera*, 165
 - G. medellinensis*, 166
- Glucuronic acid, 7
- Glucuronoxylorhamnans, 100
- Glucuronoxylorhamnogalactans, 100
- Glycidyltrimethylammonium chloride, 231
- Glycosaminoglycans (GAGs), 84, 135, 142–145
 - advances in production, 138–140
 - Alzheimer's disease, 140, 141
 - antimicrobials and antivirals, 141, 144
 - bacteria, 142
 - formulations, 144, 145
 - GM-0111, 142
 - polymeric implants, 143
 - viruses, 143, 144

- applications, 153, 154
- cancer, 145–147
- CS, 136
- DS, 136
- HA, 136
- heterogeneous GAGs extracts, 148
- HS, 138
- inflammation and immunity, 149–151
- KS, 138
- nanocarriers, 147, 148
- skin and cosmetics, 151, 152
- synthetic analogs or modified, 146
- tissue engineering, 152, 153
- tumor cells imaging, 148

Gracilaria lemaneiformis, 83, 87

Green seaweeds

- anticoagulant activity, 102
- antitumor activity and related activities, 102, 103
- antiviral activity, 102
- biomedical applications, 103
- structure, 100, 101

Guar gums

- history, 200–201
- structure, 201–202

Gymnogongrus torulosus, 86

H

- Hard segment (HS), 2
- Hendra virus (HEV), 144
- Henipavirus* Nipah virus (NIV), 144
- Heparan sulfate (HS), 138
- Heparanase, 146
- Heparin, 32, 34
- Hepatitis C virus (HCV), 143
- Hestrin–Schramm medium (HS), 3, 166
- Heteroatoms, 50
- Hexamethylene dicarbamate (HMDC), 22
- Hexamethylene diisocyanate (HMDI), 5, 10
- High-density poly(ethylene) (HDPE), 265
- Human cytomegalovirus (HCMV), 84
- Human immunodeficiency virus (HIV), 84
- Human mesenchymal stem cells (hMSCs), 57
- Human papillomavirus (HPV), 84, 143
- Hyaluronan, 57
- Hyaluronic acid (HA), 66, 67, 121, 136
- Hydration, 205
- Hydraulic fracturing application, 202–204
- Hydrogels, 67, 117–121
- Hydrolytic biodegradation, 49–52
- Hydrolytic stability, 10
- Hydrolyzable poly, 7, 8

Hydrolyzed polyacrylamides (HPAM),
228, 234

Hydroxides, 240

Hydroxyapatite (HA), 56, 61, 65

4-Hydroxybutyrate, 58

2-Hydroxyethyl acrylate (HEA), 57

2-Hydroxyethyl methacrylate (HEMA), 28

Hydroxyethyl starches (HES), 240

2-Hydroxy-3-(trimethylammonium)propyl
starch (HTPS), 232, 234, 237

Hydroxyl ions, 242

Hydroxypropyl groups, 240, 242

Hypnea musciformis, 80

I

In situ fermentation, 167, 168

Infrared spectroscopy (IR), 244

Injectivity, 218, 219

Interaction mechanisms, 314

Iridaea undulosa, 80

Isomannide (IM), 15

Isophorone diisocyanate (IPDI), 6, 28

Isopropanol (IP), 238

Isosorbide (IS), 13–15

J

Jania rubens, 79

K

Kappaphycus alvarezii, 80

Koltostat[®], 99

Komagataeibacter medellinensis, 166, 172

L

Laminaria, 93

L. cichorioides, 91

L. digitata, 64

L. hyperborea, 64

L. japonica, 64

L. thyrsoiflora, 79

L-arabinitol, 10, 11

Leathesia difformis, 96

Lessonia, 93

L-gulonolactone, 6

Liagora valida, 80

Lignin, 190, 191

Lignosulfonates, 190, 191

Lost circulation materials, 184, 185

Low molecular weight heparin (LMWH), 129

Low-density poly(ethylene) (LDPE), 265

M

Macrocystis pyrifera, 64, 93

Mannarodilactone (ManDL), 7

Mannarodilactone methacrylate (MDMA), 7

Marburg virus (MARV), 144

Mechanical properties, 167, 170, 173

Mechanical stability, 216

Mesenchymal stem cells (MSCs), 60

Meshes, 67

Metal removal, 257–259

Methacrylated glycol chitosan (MeGC), 60

Methacryloxypropyl trimethoxysilane, 57

Methyl (S)-2,6-diisocyanatohexanoate
(MELDI), 10

Methyl α -D-glucopyranoside derivatives, 9

Michael addition, 129, 130

Micro- and nanocellulose fibers, 188–190

Microbial polysaccharides, 191, 192, 199

bacterial nanocellulose, 194, 195

diutan gum, 193

welan gum, 192, 193

xanthan gum, 192

Microbiological stability, 215

Microcrystalline cellulose (MCC), 88

Molecular weights (MW), 240

Molecularly imprinted polymers (MIPs), 29

Monochloroacetic acid (MCAA), 238

Monostroma nitidum, 102

Murine leukemia virus, 144

N

Nanocellulose materials, 189

Nanocomposites, 284–286, 288

development, 282

for food packaging, 284

PLA-CNC bionanocomposite

properties, 285, 286, 288

PLA-CNC processing, 284, 285

in situ processing, 167

onset temperature, 168

PVA/BNC, 168

Nanocrystalline cellulose (NCC), 189

Nanofiber membranes, 314, 315, 320

Nanofibrous systems, 312

Nano-hydroxyapatite/gelatin (HA/gel), 61

Nemalion helminthoides, 80

O

Oilwell cement, 180, 182–195

additives

dispersants, 184

fluid loss control, 182, 183

- Oilwell cement (*cont.*)
 free water control, 183, 184
 lightweight, 185
 lost circulation materials, 184, 185
 retarders, 182
 biobased additives
 cellulose, 185–190
 lignin, 190, 191
 microbial polysaccharides, 191–195
 Oligomeric lactic acid (OLA), 271
 Osteoarthritis, 136, 149–151
 Osteogenic growth peptide (OGP), 66
 Oxidative biodegradation, 52–55
- P**
- Padina*
P. australis, 92
P. pavonica, 93
- PHARApu, 11
 Pharmaceutical industry, 117
 l-Phenyl carbonate, 21
 Phycocolloids, 94
 Phylloporaceae, 76
 Plastic postconsumer waste generation, 267
 Pollutants, removal, 305–309
 biodegradable polymers, 305
 CA, 306, 307
 chitosan, 305, 306
 PHB, 309
 PLA, 307, 308
 PLC, 308, 309
 electrospinning, 302–305
 oil/water separation, 315–318
 particle filtration, 312–315
 pollutant adsorption, 318, 319
 pollutant detection, 309–312
 Poly(1,8-octanediol-co-citrate) (POC), 56
 Poly(3-hydroxybutyrate) (P3HB), 58
 Poly(butylene adipate terephthalate) (PBAT), 267
 Poly(diisopropyl fumarate) (PDIPF), 57
 Poly(ethylene glycol) (PEG), 7, 60
 Poly(glycolic acid) (PGA), 55
 Poly(hydroxyalkanoates) (PHAs), 267
 Poly(lactic acid) (PLA), 55, 266, 272–275, 280–286, 288, 289, 291–293, 307, 308
 barrier properties, 279
 gas barrier, 280, 281
 surface wettability and water vapor permeability, 280
 bionanocomposites, development, 281, 282
 nanocellulose, 282–284
 CNC-based nanocomposites for food packaging, 284
 PLA-CNC bionanocomposite properties, 285, 286, 288, 289
 PLA-CNC processing, 284, 285
 hydrolysis chain scission, 276
 industrial production, 268–270
 mechanical performance, 278, 279
 PLA-CNC migration in food contact, 289–291
 PLA-CNC nanocomposite end-life options, 291
 biodegradation under composting conditions, 292, 293
 recycling, 291
 plasticization, 271
 processing, 270, 271
 thermal stability and degradation, 275–278
 thermal transitions and crystallinity, 271, 272
 crystallization and crystal structure, 274, 275
 glass transition temperature, 273, 274
 melting temperature, 272, 273
 visual appearance and optical properties, 281
 Poly(lactide-co-glycolide) (PLGA), 55, 60
 Poly(styrene) (PS), 265
 Poly(tetramethylene glycol) (PTMG), 15
 Poly(urethane urea) dispersions, 17
 Poly(β -hydroxybutyrate) (PHB), 309
 Poly(ϵ -caprolactone) (PCL), 2, 56, 60
 Polyamides, 56
 Poly(aniline) (PANI), 310
 Polycaprolactone (PCL), 30, 50, 51, 308, 309
 Polycarbonate (PC), 51
 Polycarbonate diol 2000 (PCD), 16
 Polydispersity index (PDI), 278
 Polyesters, 54–56
 polyethylene glycol (PEG), 51
 Polyethylene terephthalate (PET), 50, 265
 Polyglycolic acid (PGA), 49, 60
 Polyhydroxyalkanoates (PHAs), 56, 58, 59
 Polyhydroxyurethanes (PHUs), 5, 10
 Poly(lactic acid) (PLA), 49, 60
 Polymeric materials
 amorphous polymers, 49
 biodegradation, 49
 biological environment, 49
 hydrolytic biodegradation, 49–52
 hydrophobic polymers, 49
 oxidative biodegradation, 52–55
 synergic pathways, 49
 Polyolefins, 54
 Polypropylene fumarate (PPF), 56

- Polysaccharides, 25, 199, 229
Polysiphonia, 79
 polyurethane dispersions (PUDs), 17
 Polyurethane hard segment, 11
 Polyurethane-grafted calcium alginate gel
 microspheres (PU-g-ACa), 28, 29
 Polyurethane–heparin nanoparticles (PU-Hep-
 NPs), 34
 Polyurethanes (PU), 50
 Polyvinyl alcohol (PVA), 60, 167
Porphyra, 79
 Portland cement, 179
 Potassium-based starches (CMS-K), 239
 Protein-based hydrogels, 123
 P-selectin, 146
Pterocladia, 83
Punctaria plantaginea, 92
- Q**
 Quartz crystal microbalance (QCM), 310
- R**
 Radical polymerization, 153
 Radical-mediated thiol-ene chemistry, 125, 126
 RAW264.7 macrophages, 57
 Receptor for advanced glycation end products
 (RAGE), 145
 Red seaweeds
 anticoagulant activity, 86
 antitumor activity and related activities, 87
 antiviral activity, 84–86
 biomedical applications, 88, 89
 lipid synthesis, 87
 triglycerides, 87
 Respiratory syncytial virus (RSV), 143
 Retarders, 182
 Retention, 217, 218
 Rheological and flow properties, 228
 Rheology, 205–206
 Rhodamine, 311
- S**
Saccharina
 S. latissima, 91
 S. fusiformis, 91
Saccharomyces cerevisiae, 95
Sargassum
 S. crassifolium, 92
 S. fluitans, 90
 S. polycystum, 92
 S. stenophyllum, 92, 93
Schizymenia binderi, 86
Sebdenia polydactyla, 80
 Sebdeniales, 80
 Segmented thermoplastic polyurethane
 (STPU), 31
 Silk fibroin, 61, 62
 Skimming, 315
 Sodium alginate nanoparticles, 27
 Sodium carboxymethyl starch, 238
 Sodium chloride, 241
 Sodium monochloro acetate (SMCA), 238,
 239
 Sodium sulfate, 241
 Soft segment (SS), 2, 3
 Solieriaceae, 76
 Sorbsan®, 99
Spatoglossum schröderi, 92, 97
 Sphingan biopolymer, 193
 Starch, 34–36
 Starch-g-poly(acrylamide), 243
 Strain-promoted azide–alkyne cycloaddition
 (SPAAC), 123–125
Streptococcus zooepidemicus, 139
 Sulfated mannans, 80
 Sulfation, 136, 138, 140, 143, 147,
 150, 153
 Sulodexide, 154
- T**
 TAARA PU, 11
 Taylor cone, 303
 Thermal stability, 206
 Thermoplastic elastomer, 15
 Thermoplastic starch (TPS), 167
 Thermoresponsive biopolymer-based
 hydrogels, 124
 Thermo-responsive polymer (TRP), 318
 2,4-Toluene diisocyanates (TDI), 35
 Tissue engineering, 152, 153
 Tricalcium phosphate (TCP), 59
 2,3,4-Tri-O-allyl-L-arabinitol (TAARA), 11
- U**
 Ultrasonic separation, 315
Ulva
 U. conglobata, 102
 U. fasciata, 103
 U. pertusa, 103
 U. rigida, 100, 103
 U. reticulata, 103
 Ulvans, 75, 100, 102, 103
 Urethane linkage, 3–25

V

Vinyl alcohol, 243

W

Water contact angle (WCA) measurements, 280

Water pollution, 301

Water reducers, 184

Water treatment, 256–260

Weak chain, 25

Welan gum, 192, 193, 195

World plastic production, 265, 266

X

Xanthan gum, 192, 194, 195, 209

Xanthan vs. HPAM, 220

Xanthomonas campestris, 192

Xanthum

origin, 210–211

production, 211

properties, 211–213

thermal properties, 214, 215

Xylitol (Xil), 22

Xyloarabinogalactans, 100

Xylomannans, 80

Y

Young's modulus, 168, 169

Z

Zirconium propoxide, 57